

Decarboxylases and Dehydrogenases in Biocatalysis: Sustainable Production of Amines in Batch and Continuous Flow Systems

Inaugural dissertation
of the Faculty of Science,
University of Bern

presented by

Stefania Gianolio

from Bergamo, Italy

Supervisor of the doctoral thesis:

Dr. Prof. Francesca Paradisi

Department of Chemistry, Biochemistry and Pharmaceutical Sciences
University of Bern

Decarboxylases and Dehydrogenases in Biocatalysis: Sustainable Production of Amines in Batch and Continuous Flow Systems

Inaugural dissertation
of the Faculty of Science,
University of Bern

presented by

Stefania Gianolio

from Bergamo, Italy

Supervisor of the doctoral thesis :

Dr. Prof. Francesca Paradisi

Department of Chemistry, Biochemistry and Pharmaceutical Sciences
University of Bern

Accepted by the Faculty of Science.

Bern, 18th September 2023

The Dean
Prof. Marco Herwegh

Original document saved on the web server of the University Library of Bern



Creative Commons Attribution-Non-Commercial-No derivative works 2.5 Switzerland license. To see the license go to <http://creativecommons.org/licenses/by-nc-nd/2.5/ch/deed.en> or write to Creative Commons, 171 Second Street, Suite 300, San Francisco, California 94105,USA.

Table of Contents

Abstract	7
Abbreviations	8
1. Introduction	13
1.1 Biocatalysis.....	13
1.3 Biocatalysis in amines synthesis	16
1.3.1 Amino acids from bacterial fermentation as process feedstock: L-DOPA production.....	17
1.3.2 Biocatalytic decarboxylation of amino acids.....	20
1.4 Amino acid decarboxylases, amino acid dehydrogenases, and amine dehydrogenases in the production of amines	23
1.4.1 Amino acid decarboxylase: L-tyrosine decarboxylase and L-valine decarboxylase.....	23
1.4.1 Amino acid dehydrogenases and amine dehydrogenases	27
1.5 Biocatalyst immobilization and flow applications advantages.....	35
1.5.1 Advantages of immobilized biocatalysts.....	36
1.5.2 Immobilization of cell-free enzymes and whole cells	37
1.5.3 Immobilization strategies.....	38
1.5.4 Immobilized amino acid decarboxylases and amine dehydrogenases.....	40
1.5.4.1 Amino acid decarboxylases	40
1.5.4.2 Amine dehydrogenase.....	43
1.6 Bibliography	48
2. Aims and objectives	64
3. Materials and methods	65
3.1 Materials	65
3.2 General methods	66
3.2.1 Culture media.....	66
3.2.2 Preparation of chemically competent cells.....	67
3.2.3 Preparation of agarose gel for DNA assay	67
3.2.4 Transformation of competent <i>E. coli</i> cells	67
3.2.5 Expression of proteins.....	67
3.2.6 Protein purification	68
3.2.7 SDS-PAGE preparation and execution	71
3.2.8 Protein quantification	71

3.2.9 Sample preparation and HPLC analysis.....	71
3.2.10 Enzymatic activity measurements	72
3.2.10.1 Activity assay of <i>LbTDC</i>	72
3.2.10.2 Activity assay for <i>HeWT and TsRTA</i>	73
3.2.10.3 Activity of amino acid dehydrogenases and amine dehydrogenases.....	73
3.2.10.4 Activity of <i>VImD</i>	74
3.2.10.5 Activity of <i>HLADH</i>	74
3.2.11 Enzyme immobilization	75
3.2.12 Agarose epoxy functionalization.....	76
3.2.13 Support aldehyde functionalization.....	77
3.2.14 Covalent immobilization on glyoxyl support	77
3.2.15 Covalent immobilization on epoxy support with directionality	77
3.2.16 Polyethyleneimine coating of epoxy supports.....	77
3.2.17 Stability assay for immobilized enzyme against apolar organic solvents.....	77
3.2.18 Alginate beads production	78
3.2.19 Biotransformations in batch	78
3.2.19.1 <i>LbTDC</i> biotransformations.....	78
3.2.19.2 <i>HeWT</i> and <i>TsRTA</i> biotransformations with <i>HLADH</i>	79
3.2.19.4 Biotransformations with <i>VImD</i> in whole cell alginates	79
3.2.19.5 Biotransformations with <i>VImD</i> in purified enzyme alginates	80
3.2.19.6 Scale up of <i>VImD</i> decarboxylation reactions in SpinChem® system	80
3.2.20 Distillation of isobutylamine from the decarboxylation of L-valine	80
3.2.21 Liquid-liquid extraction of 1-amino-2-propanol and 3-(methylthio)propylamine	80
3.2.22 Continuous flow biotransformation process	81
3.2.22.1 Continuous flow decarboxylation with <i>LbTDC</i>	81
3.2.22.2 Continuous flow reactions with <i>HeWT</i> , <i>TsRTA</i> and <i>HLADH</i>	82
3.2.22.3 Continuous flow decarboxylation with <i>VImD</i>	82
3.2.23 L-DOPA fermentation.....	82
3.2.23.1 Storage of the strain <i>VH33ΔtyrR_DOPA</i>	82
3.2.23.2 M9 medium preparation	83
3.2.23.3 L-DOPA fermentation in flask.....	83
3.2.23.4 L-DOPA fermentation in bioreactor	83

3.2.23.5 Glucose quantification.....	84
3.2.24 Cloning PheDH.....	84
3.2.25 Phenylalanine dehydrogenase in solid screening design	85
3.2.26 Hordenine production with reductive amination reaction of tyramine.....	86
3.2.27 Continuous flow chemo enzymatic system for hordenine production with homogeneous operation conditions.....	87
3.2.28 Continuous flow chemo enzymatic system for hordenine production with heterogenous operation conditions	87
3.2.29 Hordenine isolation and purification	87
3.3 Bibliography	88
4. Tailoring minimal medium composition for enhanced L-DOPA microbial fermentation	104
4.1 Introduction	105
4.2 Results and discussion	106
4.2.1 Carbon flow for the production of L-dopa in VH33ΔtyrR_DOPA.....	106
4.2.2 Bacterial strain: transformed plasmids.....	107
4.2.3 Batch flask fermentation.....	110
4.2.4 Fermentation in bioreactor.....	112
4.2.4.1 Optimization of fermentation conditions: airflow and working volume .	112
4.2.4.2 Three phases optimization to tackle induction time and carbon source loading	113
4.2.4.3 Stabilizing L-DOPA concentration in the fermentation broth.....	116
4.3 Conclusion.....	116
4.4 Bibliography	118
5. Combined chemoenzymatic strategy for sustainable continuous synthesis of hordenine	134
5.1 Introduction	135
5.2 Results and discussion	137
5.2.1 Chemoenzymatic approach for Hordenine production.....	137
5.2.2 Identification of the optimal biocatalyst.....	137
5.2.3 Activity assay of <i>LbTDC</i>	138
5.2.4 Immobilization of <i>LbTDC</i>	139
5.2.5 Biocatalytic decarboxylation of L-tyrosine with immobilized <i>LbTDC</i> in batch141	

5.2.6 Batch test with immobilized enzyme and surfactant for process intensification	142
5.2.7 Immobilized enzyme integration into the continuous flow system	144
5.2.8 Optimization of the reductive amination step to convert tyramine to hordenine	145
5.2.9 Continuous flow reductive amination of tyramine in homogeneous mode .	146
5.2.10 Continuous flow reductive amination of tyramine in heterogeneous mode	148
5.3 Conclusion.....	151
5.4 Bibliography	153
6. Production of short chain primary amines with immobilized valine decarboxylase	169
6.1 Introduction	170
6.2 Results and discussion	170
6.2.1 VImD expression and purification	170
6.2.3 Covalent immobilization on inert supports	175
6.2.4 Alginates production with Ca ⁺² and Ba ⁺²	177
6.2.5 Small batch biotransformations (0.1 M scale)	180
6.2.6 Reusability and stability of free purified enzyme and whole cell alginate bead systems.....	182
6.2.7 Scale-up of whole cell alginate bead biotransformations	183
6.2.8 SpinChem [®] system with whole cell alginate beads	184
6.2.9 Purified VImD barium alginate beads	186
6.2.10 SpinChem [®] system with cell crude extract in dialysis membrane.....	187
6.2.11 Downstream for the isolation of the products	188
6.2.11.1 Isobutylamine isolation	188
6.2.11.2 Liquid-liquid extraction for 1-amino-2-propanol and 3-(methylthio)-propylamine.....	189
6.2.11.3 Trituration of 1-amino-2-propanol.....	191
6.2.12 Quantification of the leaked protein in the SpinChem [®] product solution ..	191
6.3 Conclusion.....	192
6.4 Bibliography	193
7. Exploring the potential of amine dehydrogenases in oxidative deamination for aldehyde production	209
7.1 Introduction	210

7.2 Results and discussion	214
7.2.1 AmDHs expression and purification.....	214
7.2.2 AmDHs screening for oxidative deamination activity.....	215
7.2.3 Optimization of expression and purification for <i>Cfus</i> AmDH W145A mutant	222
7.2.4 Screening of <i>Cfus</i> AmDH W145A activity.....	223
7.3 Conclusion.....	223
7.4 Bibliography.....	224
Appendix A: Additional related studies	239
A.1 Screening of engineered amino acid dehydrogenases for oxidative deamination reaction.....	240
A.1.1 Background.....	241
A1.2 Findings.....	243
A.2 Hydroxytyrosol multi-enzymatic cascade.....	270
A.2.1 Background.....	271
A.2.2 Findings.....	272
Appendix B: NMR spectra.....	297
Acknowledgements	301

Abstract

Nowadays the urgent need for sustainable and greener production processes is driving considerable interest towards the continuously progressing field of biocatalysis. Enzymes, the essential components of biocatalysis, provide an environmentally friendly approach to chemical transformations, presenting cleaner and more selective synthesis pathways compared to conventional, potentially hazardous, chemical methods. However, to truly unlock the potential of enzymes and apply them effectively at an industrial level, a great level of optimization is often required.

This research introduces a set of biocatalytic tools specifically tailored to overcome the challenges associated with chemical amine production. The explored approach was the decarboxylation of natural amino acids. These precursors represent a sustainable feedstock source since they can be obtained via microbial fermentation in a circular economy, from natural and readily available substrates. The aim is to propose a green, eco-conscious alternative to traditional amine production, which often involves the generation of waste and the use of dangerous reagents. The practicality and efficiency of these novel biocatalytic instruments are validated through direct application, thereby showcasing their potential for implementation in industry.

A significant aspect of the study revolves around not just the development of these biocatalytic tools, but also enhancing their resilience for industrial scale-up. The central strategy to augment the robustness of the biocatalysts, and thereby widen their application field, is the immobilization of the biocatalyst. By doing so, the biocatalyst can be integrated in an easier manner inside the chemical synthesis and can become a reliable co-actor, addressing the most environmentally problematic steps in the chemical process. This collaborative method allows biocatalysts to complement traditional chemical stages, providing an inclusive and comprehensive strategy for sustainable chemical production.

Moreover, it is essential to note that the versatility of enzymes should be explored further. Out-of-the-box applications for these biological catalysts must be considered, keeping in mind that enzymatic reactions often occur under equilibrium, hence influencing the reaction directionality. In this study, an effort was made to harness the capabilities of amino acid dehydrogenases and amine dehydrogenase to catalyse the oxidative deamination reaction expanding their substrate scope. The aim is to generate aldehydes or ketones from amines, which hold promising potential in the field of chemical applications.

Abbreviations

AADHs	Amino acid dehydrogenases
<i>Apau</i> AmDH	Amine dehydrogenase from <i>Aminomonas</i>
<i>Bs</i> LeuDH	Leucine dehydrogenase from <i>Bacillus stereothermophilus</i>
CCK-8	Cell Counting Kit-8
<i>Cfus</i> AmDH	Amine dehydrogenase from <i>Cystobacter fuscus</i>
CLEAs	Cross-linked enzyme aggregates
DCM	Dichloromethane
<i>E. coli</i>	<i>Escherichia coli</i>
FDH	Formate dehydrogenase
FITC	Fluorescein isothiocyanate
FMOc	Fluorenylmethyloxycarbonyl
Fwd	Forward
GAD	Glutamate decarboxylase
GC	Guanine-Cytosine
GDH	Glucose dehydrogenase
HCl	Hydrochloric acid
<i>He</i> WT	ω -Transaminase from <i>Halomonas elongata</i>
HPLC	High Performance Liquid Chromatography
IDA	Iminodiacetic acid
IMAC	Immobilized metal affinity chromatography
IPTG	Isopropyl β -D-1-thiogalactopyranoside
K_M	Michaelis constant
L-DOPA	L-3,4-dihydroxyphenylalanine

LB	Luria Bertani (broth or agar)
LDC	Lysine decarboxylase
LE-AmDH-v1	Engineered amine dehydrogenase variant from LysEDH
<i>Lb</i> TDC	L-tyrosine decarboxylase from <i>Lactobacillus brevis</i>
LysEDH	Lysine dehydrogenase from <i>Geobacillus stearothermophilus</i>
MATOUAmDH2	Amine dehydrogenase from the Marine Atlas of Tara Oceans Unigenes database
M.c.	Molar conversion
MeCN	Acetonitrile
<i>Micro</i> AmDH	Amine dehydrogenase from <i>Microbacterium sp.</i>
MIBK	Methyl isobutyl ketone
MNPs	Magnetic nanoparticles
<i>Msm</i> eAmDH	Amine dehydrogenase from <i>Mycobacterium smegmatis</i>
MTBE	Methyl tert-butyl ether
MTT	3-(4,5-dimethylthiazol-2-yl)-2,5-diphenyltetrazolium bromide
<i>Mvac</i> AmDH	Amine dehydrogenase from <i>Mycobacterium vaccae</i>
NAD ⁺	Nicotinamide adenine dinucleotide (oxidized)
NADH	Nicotinamide adenine dinucleotide (reduced)
nat-AmDHs	Natural amine dehydrogenases
NMR	Nuclear Magnetic Resonance
NTA	Nitrilotriacetic acid
PA510	Polyamide PA510
PCR	Polymerase Chain Reaction
PBR	Packed bed reactor
PheDH	Phenylalanine dehydrogenase

pic-BH ₃	Picoline borane
PLP	Pyridoxal-5'-phosphate
PMS	Phenazine methosulfate
Rev	Reverse
T _R	Residence time
SALLE	Salting-Out Assisted Liquid-Liquid Extraction
SCPAs	Short-chain primary amines
SDMS	Site-directed saturation mutagenesis
STAB	Sodium triacetoxyborohydride
TA	Transaminase
TB	Terrific broth
TLC	Thin layer chromatography
T _m	Melting Temperature
TM_PheDH	Engineered amine dehydrogenase variant from PheDH from <i>Rhodococcus</i> sp. M4
Tpl	Tyrosine phenol-lase
VImD	L-valine decarboxylase from <i>Streptomyces viridifaciens</i>
TsRTA	(R)-Selective Transaminase from <i>Thermomyces stellatus</i>
WST-1	2-(4-Iodophenyl)-3-(4-nitrophenyl)-5-(2,4-disulfophenyl)-2H-tetrazolium
wt	Wild-type

Amino acids

A - Ala	Alanine
C - Cys	Cysteine
D - Asp	Aspartic acid

E - Glu	Glutamic acid
F - Phe	Phenylalanine
G - Gly	Glycine
H - His	Histidine
I - Ile	Isoleucine
K - Lys	Lysine
L - Leu	Leucine
M - Met	Methionine
N - Asn	Asparagine
P - Pro	Proline
Q - Gln	Glutamine
R - Arg	Arginine
S - Ser	Serine
T - Thr	Threonine
V - Val	Valine
W - Trp	Tryptophan
Y - Tyr	Tyrosine

DNA nucleotides

A	Adenine
C	Cytosine
T	Thymine
G	Guanine

Units of measure /symbols

%	Percentage
bp	Base pair
°C	Celsius
CV	Column Volume
Da	Dalton
ee	enantiomeric excess
ϵ	Extinction coefficient
g	Gram
h	Hour
L	Litre
M	Molarity
m	meter
min	Minute
mol	Mole
rpm	Rotation per minute
Rt	Resident Time
s	Second
U	Units of activity
V	Volume
λ	wavelength

1. Introduction

1.1 Biocatalysis

Biocatalysis, an evolving field in synthetic chemistry, harnesses enzymes to perform chemical transformations.(Alcántara et al., 2022; Sheldon & Brady, 2019; Sheldon & Woodley, 2018) The utilization of biocatalysis aligns with Green Chemistry principles,(Roschangar et al., 2015) a framework aimed at minimizing or eradicating the use and generation of hazardous and environmentally detrimental substances in chemical processes.

Enzymes are macromolecules that accelerate chemical reactions by lowering the activation energy barrier required to perform molecular transformations. The high selectivity of enzymes enables them to catalyze specific reactions efficiently, reducing waste, and producing desired products. This feature proves exceptionally beneficial across various sectors, including chemical and pharmaceutical manufacturing, as well as the food and cosmetics industries, where complex and chiral molecules are synthesized. Recent advancements in synthetic biology and bioinformatic technologies, including metagenomics, genome sequencing, protein engineering, directed evolution, and high-throughput screening, have propelled the growth of biocatalysis. These techniques facilitate the biocatalysts discovery, expanding their substrate scope and enabling new reaction chemistries.(Bell et al., 2021)

Enzymes align with several principles of Green Chemistry due to their low toxicity, high efficiency, renewable nature, and ability to operate under mild conditions. For example, enzymatic reactions are commonly run in water or low-hazard organic solvents, adhering to the principle of using benign solvents. As industries face increasing pressure to adopt environmentally friendly and sustainable methods, biocatalysis is set to play a significant role and continuous advancements in technology are likely to further enhance the discovery, development, and application of biocatalysts, contributing to greener and more sustainable chemical processes. A recent example of the practical application of biocatalysis in pharmaceutical synthesis is showcased by Novartis in 2020.(B. Wu et al., 2020) In this case, biocatalysis was employed in the synthesis of an FXI (Factor XI) inhibitor, which is being studied for potential applications in treating or preventing thrombosis and related diseases.

By employing an enzyme, Novartis was able to shorten the synthetic route, reducing five steps with just to one, starting from a different intermediate **9** rather than **1** (Figure 1.1). This enabled the synthesis of the corresponding chiral product **8** in very high conversion and enantiomeric excess.

During the enzymes screening, hits were identified to produce either the desired (*S*)-alcohol or the undesired (*R*)-alcohol. Ultimately, the ketoreductase enzyme KRED-NADH-110 was selected for the stereoselective reduction of the α -chloroketone **9** to the (*S*)-

alcohol (**10**). This selection was based on the enzyme activity, enantioselectivity, and compatibility with utilizing isopropanol to recycle NADH.

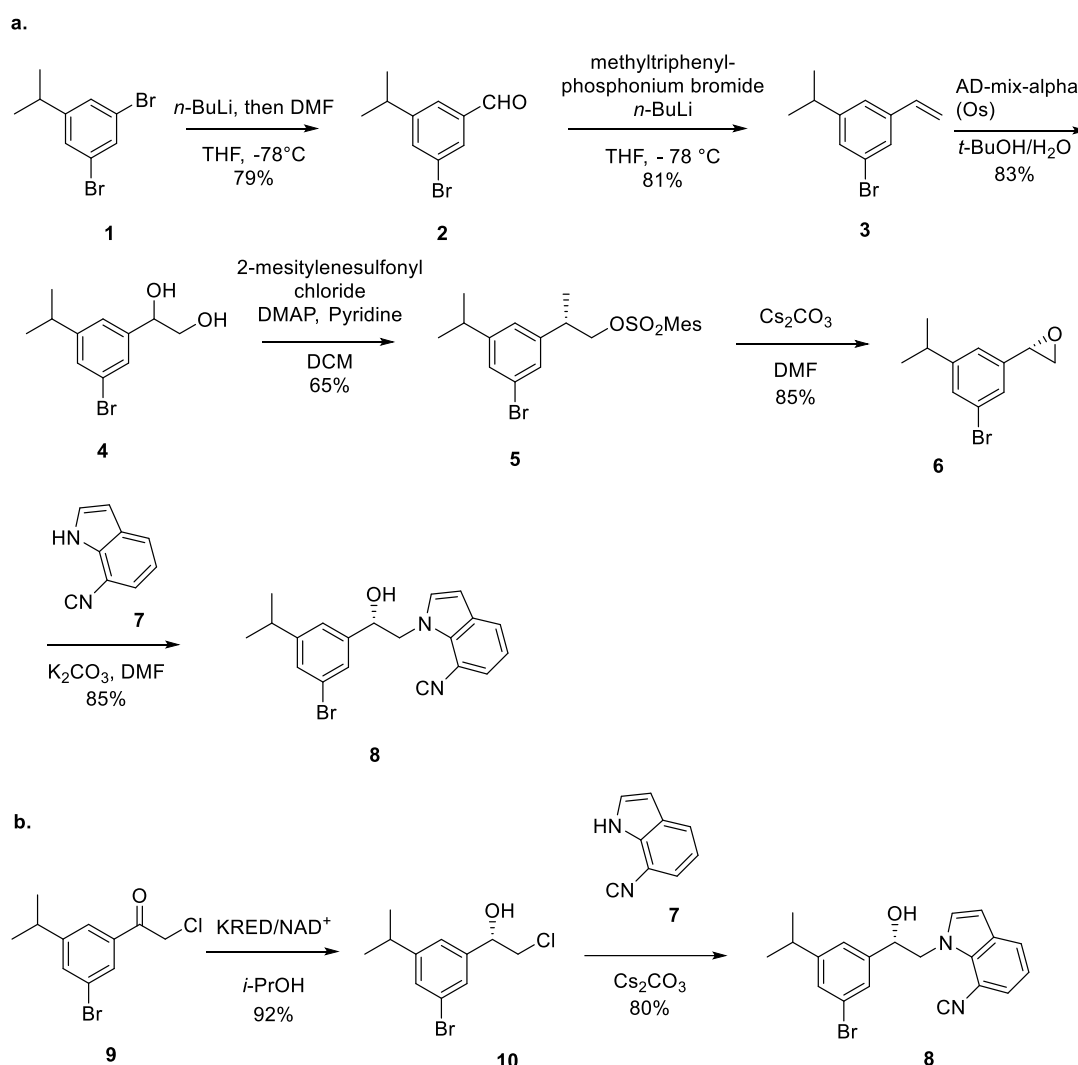


Figure 1.1: (*S*)-1-(3-Bromo-5-isopropylphenyl)-2-chloroethan-1-ol (**10**) is a key intermediate, and the enzymatic reduction of 1-(3-bromo-5-isopropylphenyl)-2-chloroethan-1-one (**9**) to the chiral alcohol was investigated using ketoreductase (KRED) screening kits manufactured by Codexis. **a.** Chemical synthesis for FXI inhibitor till the intermediate **8**. **b.** Biocatalytic alternative with KRED application.

In fact, with an ingeniously process optimization, the cofactor regeneration was realized by the oxidation of isopropanol to propionaldehyde, exploiting the capability of the KRED-NADH-110 to directly use NAD⁺ in the oxidation reaction. Therefore, this process set up avoided implementing a coenzyme recycling system, sparing the addition of another biocatalyst to the system.

Moreover, the biocatalytic alternative effectively addressed the scalability and safety challenges linked with traditional chemical synthesis, wherein the use of toxic OsO₄, in AD-mix-alpha, was required in the asymmetric dihydroxylation step to yield **4**. By

shortening the process, it avoided harmful reagents like *n*-BuLi, DMF, and the aforementioned AD-mix- α , reducing both environmental impact and health risks. The biocatalytic route also circumvented the need for extremely low temperatures and unstable intermediates, like epoxide intermediate **6**, enhancing energy efficiency, reliability, and cost-effectiveness. In summary, this example proves that the greenest solutions can also be the most convenient ones, making them a good choice for businesses.

1.2 Amines production and environmental implications

Categorized by their distinctive chemical structure that includes one or more nitrogen atoms bonded to carbon, amines have a crucial role in both biological and industrial contexts. In the biological sphere, these compounds are essential, forming the core components of amino acids and nucleotides of proteins and DNA, respectively. On an industrial scale, amines simultaneously play an important role, both as invaluable building blocks and as valuable products across a wide range of sectors, including agriculture, pharmaceuticals, textiles, polymers, cleaning industries, and cosmetics. (Froidevaux et al., 2016; Lawrence, 2004; Nasri, 2017a)

Regrettably, the production of many commercially available amines relies on the Haber–Bosch procedure, a process that harnesses nitrogen and hydrogen to produce ammonia, which is then incorporated into hydrocarbons derived from fossil fuels. Nitrogen, the elemental constituent in amines, is present in 84% of FDA-approved medicines, highlighting the critical role of nitrogen-inclusive materials substances in drug discovery programs and chemical libraries. (Vitaku et al., 2014).

Despite significant advancements since the onset of the Haber-Bosch process in the early 1900s, this procedure still consumes a considerable amount of energy. It is responsible for 1-2 % of the world's total annual energy usage and half of the yearly global hydrogen output. (M. Wang et al., 2021)

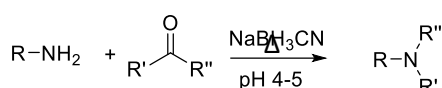
Crucially, the dependence on fossil resources for the synthesis of industrially relevant amines, including aliphatic amines such as alkylamines and diamines, aromatic amines like anilines, and aminoalcohols such as ethanolamines and propanolamines, presents substantial environmental challenges. (Pelckmans et al., 2017; Pilkington et al., 2021) Indeed the production of light olefins, a critical raw material for these processes, typically employs methods like steam or catalytic cracking, which are not only energy-intensive but also contribute significantly to global CO₂ emissions, producing millions of tons annually.

Conventional synthetic methods for amine production (Figure 1.2), like ammonolysis of alkyl halides, reduction of alkyl azides, nitriles, and amides, and hydroamination of alkenes, are all hampered by a set of limitations, (Truong et al., 2023) including the need for costly reagents, poor selectivity, use of harsh reaction conditions, and low compatibility with sensitive functional groups. Despite their prevalent use, these

methods come with significant environmental implications. They often require an overabundance of reagents, rely on hazardous reducing agents, necessitate energy-intensive conditions, and produce waste products detrimental to both human health and the environment. Furthermore, the reliance on non-renewable resources for these reactions intensifies their environmental footprint.

With these sustainability concerns, innovative and more environmentally friendly alternatives are urgently required.

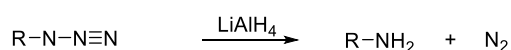
Reductive amination



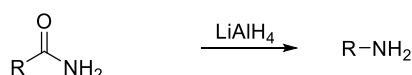
Ammonolysis of alkyl halides



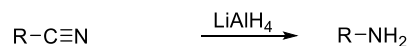
Reduction of alkyl azides



Reduction of amides



Reduction of nitriles



Hydroamination of alkenes

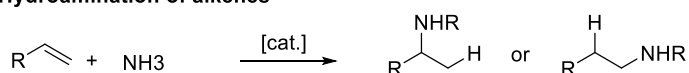


Figure 1.2: Traditional synthetic routes for the production of amines, including reductive amination, ammonolysis of alkyl halides, reduction of alkyl azides, nitriles, and amides, and hydroamination of alkenes.

1.3 Biocatalysis in amines synthesis

The transformation towards a sustainable chemical industry is intrinsically tied to the effective conversion of renewable resources into valuable compounds and energy sources. Concurrently, the development and implementation of innovative strategies that, not only mitigate waste production and environmental pollution, but also avoid the depletion of non-renewable resources, are absolutely critical. Consequently, the scientific research community has made significant achievements in the development of renewable feedstock production, such as the generation of amino acids through microbial fermentation processes, to directly recycle carbon and nitrogen from biomass into

nitrogenous compounds like amines, amides, or nitriles. It is important to mention, however, that despite the fact that natural amino acids hold significant potential for further processing (Song et al., 2020) (Figure 1.3), they of course possess intrinsic value across diverse fields.

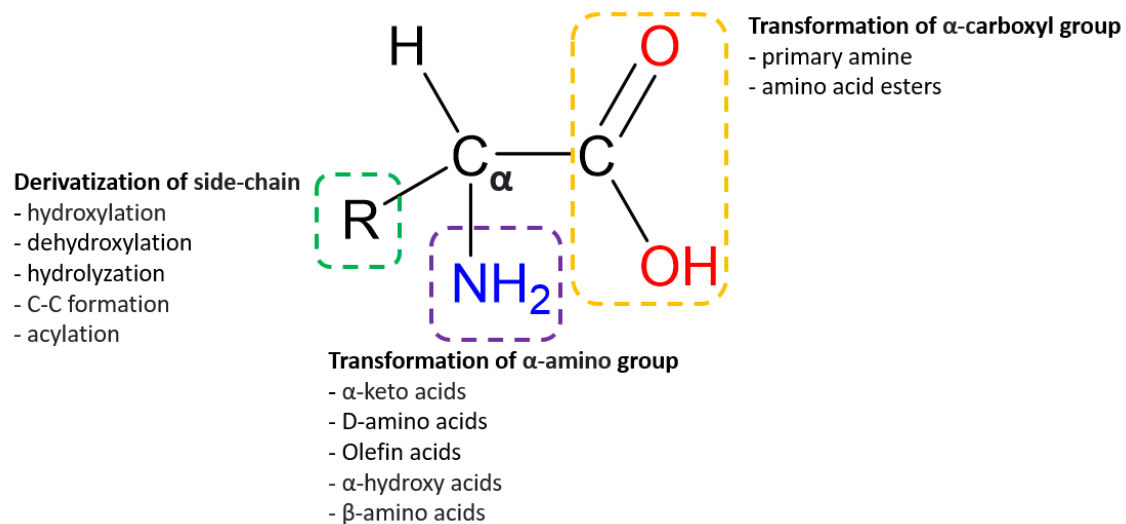


Figure 1.3: Visual representation of the multiple potential chemical modifications of amino acid functionalities. This figure highlights the versatility and complexity of structural alterations possible, underscoring the broad utility and adaptability of amino acids in various fields of study and application.

1.3.1 Amino acids from bacterial fermentation as process feedstock: L-DOPA production

The synthesis of L-3,4-dihydroxyphenylalanine (L-DOPA), an important amino acid for treating Parkinson's disease, illustrates a perfect example for this perspective. The biotechnological method, which has been a subject of interest in the last decade, overcomes issues, such as poor conversion rates and low enantioselectivity, typical of the commercial process of L-DOPA synthesis through asymmetric hydrogenation, developed by Monsanto (Figure 1.4). (Knowles, n.d.) These alternative biotechnological approaches exploit microorganisms with tyrosinase, tyrosine phenol-lase (Tpl), or *p*-hydroxyphenylacetate 3-hydroxylase (PHAH) activity (Figure 1.5).

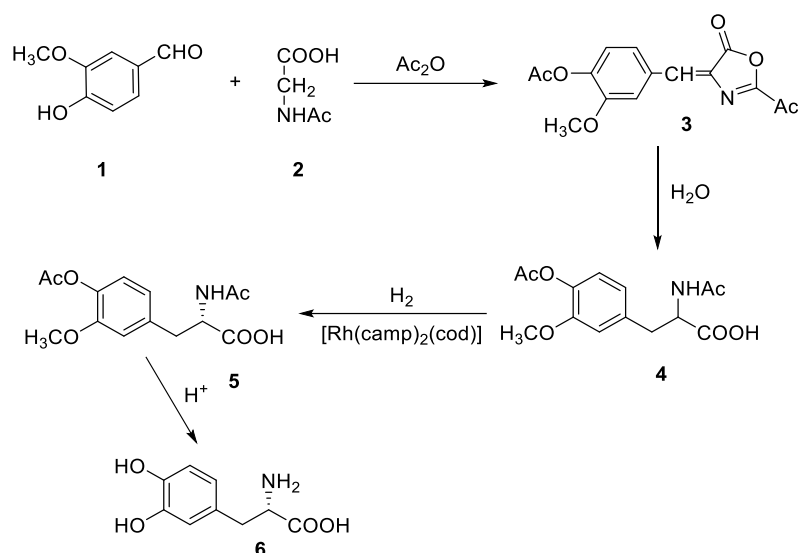


Figure 1.4 : Monsanto L-DOPA (6) process starting from vanillin (1).

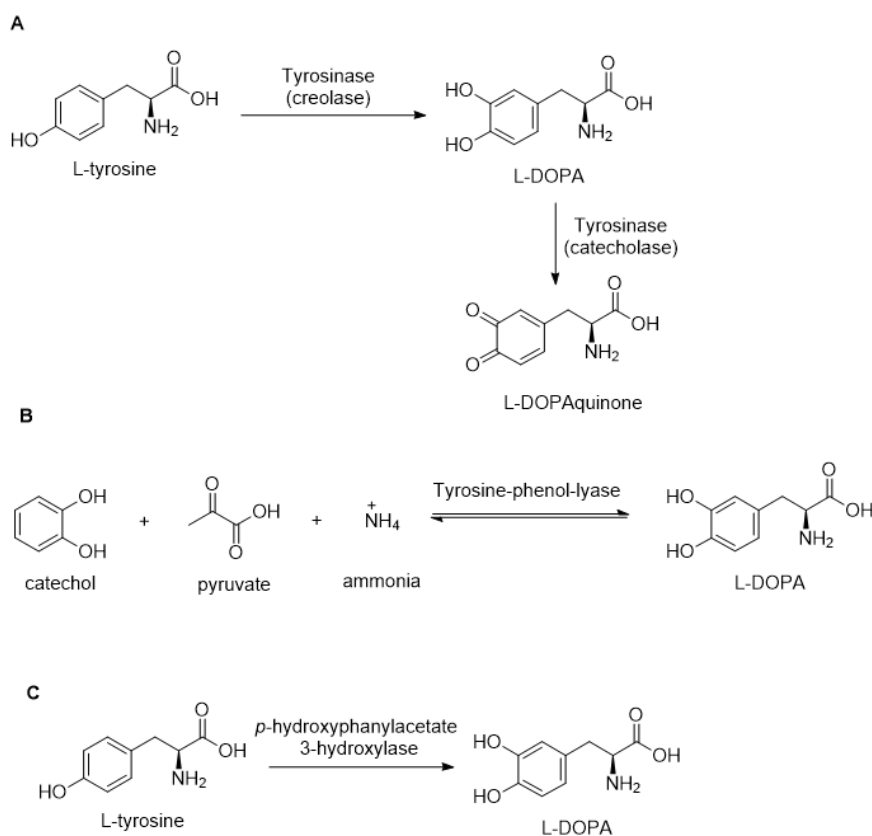


Figure 1.5: Different enzymes application for the biocatalytic production of L-DOPA. (A) Tyrosinase; (B) Tyrosine-phenol-lyase (Tpl); (C) *p*-hydroxyphenylacetate 3-hydroxylase (PHAH).

While each approach has proven efficient for L-DOPA production, it is important to note that each one has its own drawbacks to overcome (Table 1.1). (Kurpejović et al., 2021)

Enzyme	Substrate	Drawbacks	L-DOPA (g/L)
Tyrosine phenolase	catechol, pyruvate, ammonia	<ul style="list-style-type: none"> • Toxic precursor catechol is required 	20.7(Foor et al., 1993)
Tyrosinase	L-tyrosine	<ul style="list-style-type: none"> • The catecholase activity reduces L-DOPA yield <i>via</i> oxidation • Difficult heterologous expression because of the requirement of adaptor proteins 	3.81(Surwase et al., 2012)
PHAH	D-glucose	<ul style="list-style-type: none"> • Require L-tyrosine as precursor or complex and high-cost nutrients in production media • NADH and FADH₂ cofactor dependence 	8.67(T. Wei et al., 2016)

Table 1.1: L-DOPA production with different biocatalytic approaches and their related drawbacks.

In the latest study by Kurpejović *et al.* for L-DOPA production, a novel approach was adopted with a new microorganism (*Corynebacterium glutamicum*) expressing the tyrosinase from *Ralstonia solanacearum*.(Kurpejović et al., 2021) In this case, the additional overexpression of xylose utilization genes (namely xylAXc and xylBCg) in *C. glutamicum* allowed the exploitation of lignocellulosic biomass (LCB) as a carbon and energy source for sustainable L-DOPA production. In fact, xylose is the second most abundant sugar in LCB wastes,(Narisetty et al., 2022) as it is a more eco-friendly and cost-effective choice compared to the define and pure carbon source such as D-glucose.

These considerable efforts which have been made to enhance and optimize the production of L-DOPA, are driven by the substantial value of the non-proteogenic amino acid. In fact, aside from being a key medication in the treatment of Parkinson disease, L-DOPA utility extends beyond this application. For instance, it is utilized as a supplement in fermentation media for the production of (S)-Norcoclaurine in yeast.(Payne et al., 2021; Pyne et al., 2020) This compound is important as it acts as a precursor in the biosynthesis of benzyloquinoline alkaloids (BIAs). BIAs are a broad category of plant secondary metabolites with varying structures and biological functions. Among them, significant pharmaceutical compounds are morphine, an analgesic; berberine, an antibacterial agent; and noscapine, an anti-cancer compound. In BIAs biosynthesis, the first crucial step involves the enzymatic transformation of dopamine, derived from the

decarboxylation of L-DOPA, and 4-hydroxyphenylacetaldehyde (4-HPAA) into (S)-norcoclaurine, catalyzed by norcoclaurine synthase (NCS) (Figure 1.6). Therefore, L-DOPA role in this process underscores its importance in the biotechnological production of these compounds.

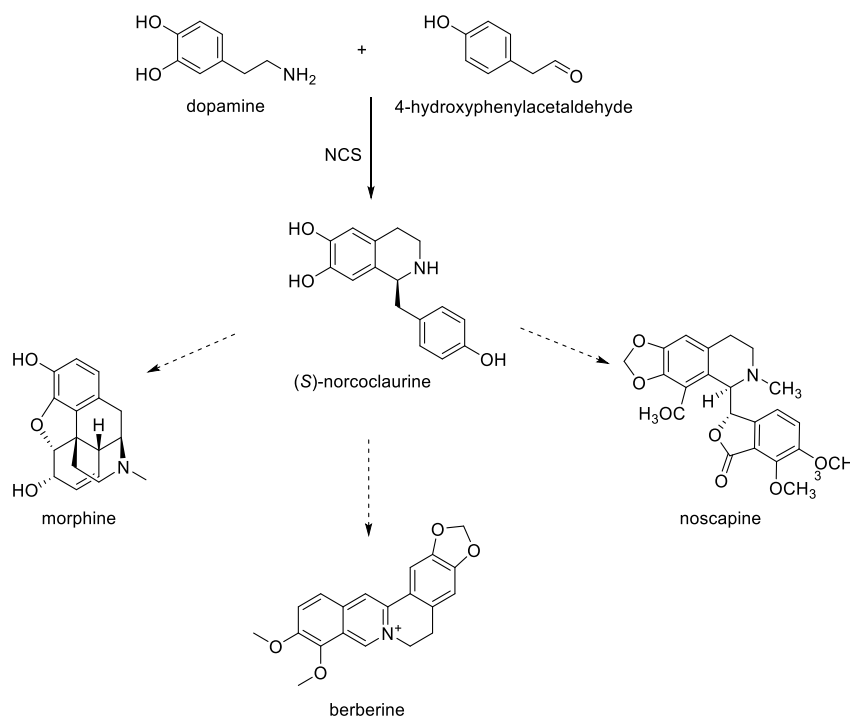


Figure 1.6: The biosynthesis of diverse benzylisoquinoline alkaloids such as berberine, morphine, and noscapine hinges on the condensation of dopamine and 4-hydroxyphenylacetaldehyde by norcoclaurine synthase (NCS), producing (S)-norcoclaurine as a crucial intermediate.

1.3.2 Biocatalytic decarboxylation of amino acids

The engineering of bacterial strains capable of fermenting various amino acids from sustainable carbon sources, such as agricultural or industrial waste, has emerged as a particularly promising strategy. (Kumar et al., 2014; Leuchtenberger et al., 2005; Wieschalka et al., 2013) A significant amount of attention has been directed to ensure that these advancements do not interfere with the demands of the food industry, thus balancing our environmental objectives with the sustained delivery of essential goods and services. (B. Zhang et al., 2020) Moreover, the utilization of protein-rich biomass waste offers another avenue for sustainable production. (Gupte et al., 2022; Nasri, 2017b) Indeed, proteins and amino acids hold considerable promise for generating nitrogen-containing chemicals in a bio-refinery, given that there is no conflict with food production. For example, the decarboxylation of amino acids can yield valuable amine products, turning what would otherwise be discarded into valuable chemical precursors. (Li et al., 2016; Teng et al., 2011; H. Zhang et al., 2016)

The case study of bio-based nylon production from the natural amine, cadaverine, illustrates an inspiring example of harnessing amino acid decarboxylases for the generation of high-value materials from a readily available and renewable carbon source, such as D-glucose (Figure 1.7). In this instance, *Corynebacterium glutamicum* GH30HaLDC, a microbial strain engineered for the expression of lysine decarboxylase from *Hafnia alvei*, (Kim et al., 2019) was exploited to decarboxylate L-lysine, yielding cadaverine - a key precursor in the production of nylon. The resultant cadaverine was then chemically co-polymerized with sebacic acid to form polyamide PA510, a type of nylon.

This example stands out not just for the application of biocatalysis in the initial stages, but for the convenient integration of biological and chemical strategies towards the production of a commercially significant product. The introduction of a biocatalyst in the process ensures a renewable and eco-friendly generation of the valuable precursor cadaverine, while the subsequent chemical polymerization transforms this bio-derived intermediate into a robust and functional material. Consequently, this process exemplifies how strategic integration of bio-based processes with traditional chemical reactions can lead to a more sustainable and environmentally conscious production of industrially important materials.

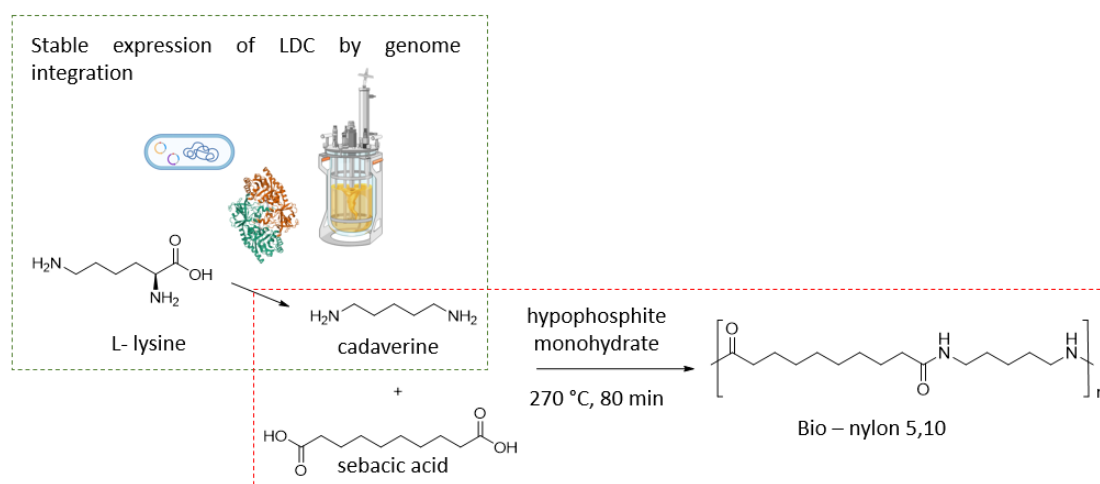


Figure 1.7: Production of bio-based nylon. The engineered microbial strain, *C. glutamicum* GH30HaLDC, was utilized to produce 125 g/L of cadaverine through fed-batch culture, resulting in a 20% increase in yield compared to previous methods. Cadaverine, obtained by L-lysine decarboxylation by lysine decarboxylase (LDC) from *Hafnia alvei* (Kim et al., 2019), is then recovered, purified, and co-polymerized with sebacic acid to synthesize polyamide PA510, a bio-based nylon with thermal and material properties comparable to those of traditionally produced PA510. Indeed, the evaluation of both biological and chemical methodologies is essential in the field of industrial biotechnology, given its multidisciplinary nature. To decide which approach is most suitable, a systematic comparison must be carried out (Table 1.2).

Method	Advantages	Limitations
Biological	<ul style="list-style-type: none"> • Renewable and sustainable by using biomass feedstocks • Environmentally beneficial due to less harmful reagents • Highly regio- and stereoselective • Safer because of milder reaction conditions (<i>e.g.</i> pressure and temperature) 	<ul style="list-style-type: none"> • Lower reproducibility due to many variables to optimize (<i>e.g.</i> cell status and cultivation media) • Primarily operated on organic molecules • More sensitive to the toxicity of a target product or intermediates
Chemical	<ul style="list-style-type: none"> • Capable of producing a wider variety of chemicals • Broader range of optimal conditions (<i>e.g.</i> temperature and pressure) for catalysts 	<ul style="list-style-type: none"> • Issues with selectivity • Harsher reaction conditions (<i>e.g.</i> high temperature and pressure) • Generation of a greater amount of toxic, non-degradable/recyclable by-products
Integrated	<ul style="list-style-type: none"> • Potential to build the most efficient path for a target chemical synthesis by leveraging the strengths of both biological and chemical processes 	<ul style="list-style-type: none"> • Specific limitations will depend on the particular integrated methods used, and could potentially involve limitations from both biological and chemical methods

Table 1.2: Competitive strengths and limitations of biological, chemical, and integrated processes

This comparison should also take into account economically relevant factors, including the cost of raw materials, operational costs, and the technical feasibility of each method. Through this so-called technoeconomic analysis, one can discern which method, biological or chemical, might serve as the most efficient and optimal route for a particular process.(S. Y. Lee et al., 2019)

1.4 Amino acid decarboxylases, amino acid dehydrogenases, and amine dehydrogenases in the production of amines

The scientific community agrees that a variety of biocatalysts, originating from five major enzyme classes - oxidoreductases (EC 1.), transferases (EC 2.), hydrolases (EC 3.), lyases (EC 4.) and isomerases (EC 5.) - play a significant role in the formation of amines.(Mutti & Knaus, 2021)

In the following paragraphs, the specific role of amino acid decarboxylases (EC 4.1.1.X), amino acid dehydrogenases (E.C. 1.4.1.X) and amine dehydrogenases is discussed.

1.4.1 Amino acid decarboxylase: L-tyrosine decarboxylase and L-valine decarboxylase

Amino acid decarboxylases (EC 4.1.1) are a class of biological catalysts commonly present in various life forms, such as microorganisms, animals, and plants. These enzymes catalyse the reaction that converts amino acids into the corresponding amine and carbon dioxide (Figure 1.8).

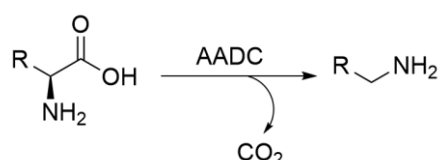


Figure 1.8: L-amino acid decarboxylation reaction

The multifunctionality of amino acid decarboxylases originates from the fact that their roles diverge according to their specific type and the organisms in which they are found. In animals, they are involved in the biosynthesis of biogenic amines and polyamines. On the other hand, in bacteria, certain inducible biodegradative enzymes that decarboxylate amino acids have been suggested to play a role in pH regulation within the bacterial cell and its environment. One example of such functionality is the glutamate decarboxylase (GAD), which assists in maintaining the stability of pH levels in the organism growth environment through the production of amines.(Gut et al., 2006)

The majority of amino acid decarboxylases employ pyridoxal-5'-phosphate (PLP) as their coenzyme(SANDMEIER et al., 1994a) and can be generally classified in two Fold Types, I and III.(Eliot & Kirsch, 2004; Jansonius, 1998)

A further classification distinguishes Group I, Group II, and Group III, for the Fold Type I enzymes, whereas Fold Type III enzymes comprise Group IV. (SANDMEIER et al., 1994b)

This classification has been possible thanks to the crystal structures of numerous amino acid decarboxylases which have been to date successfully elucidated. Group I solely consists of glycine decarboxylase. (Nakai et al., 2005) Group II consists in several decarboxylases, including histidine decarboxylase (HisDC), (Komori et al., 2012) glutamate decarboxylase (GAD), (Capitani, 2003) L-tyrosine decarboxylase (TDC), (Zhu et al., 2016a) L-lysine decarboxylase, (Sagong et al., 2016) and aromatic-L-amino acid decarboxylase. (Giardina et al., 2011) Group III includes bacterial L-ornithine decarboxylase. (J. Lee et al., 2007) and biodegradative L-arginine decarboxylase. (Andréll et al., 2009) Lastly, Group IV contains eukaryotic L-ornithine decarboxylase, (Almud et al., 2000) L-arginine decarboxylase, (Tolbert et al., 2003) and diaminopimelate decarboxylase. (Ray et al., 2002)

The catalytic cycle of PLP-dependent decarboxylases involves nucleophilic attacks, transaldimination reaction, and proton transfer reactions, leading to product formation and enzyme regeneration.

As shown in Figure 1.9, the single steps in the mechanism of action are:

1. Formation of the external aldimine (transaldimination): The catalytic cycle initiates when the incoming substrate amino group performs a nucleophilic attack on the C4' of the internal aldimine (the original PLP-enzyme complex). This transaldimination reaction results in the formation of an external aldimine where a new Schiff base linkage is established between the PLP and the amino acid substrate.
2. Decarboxylation and quinonoid intermediate formation: The σ bond between the α -carbon ($C\alpha$) and the carboxylate group of the amino acid substrate is then broken. The electron rearrangement in the resulting carbanionic intermediate leads to the formation of a quinonoid intermediate, which is a significant stabilizing contributor among resonance structures.
3. Protonation of the external aldimine: The quinonoid intermediate undergoes protonation on $C\alpha$ by abstracting a proton from an active-site tyrosine residue that acts as a catalytic acid.
4. Enzyme regeneration (transaldimination): The second round of transaldimination occurs through the nucleophilic attack by a catalytic lysine. This leads to the regeneration of the internal aldimine (restoring the original PLP-enzyme complex) and releases the decarboxylated product, an amine.

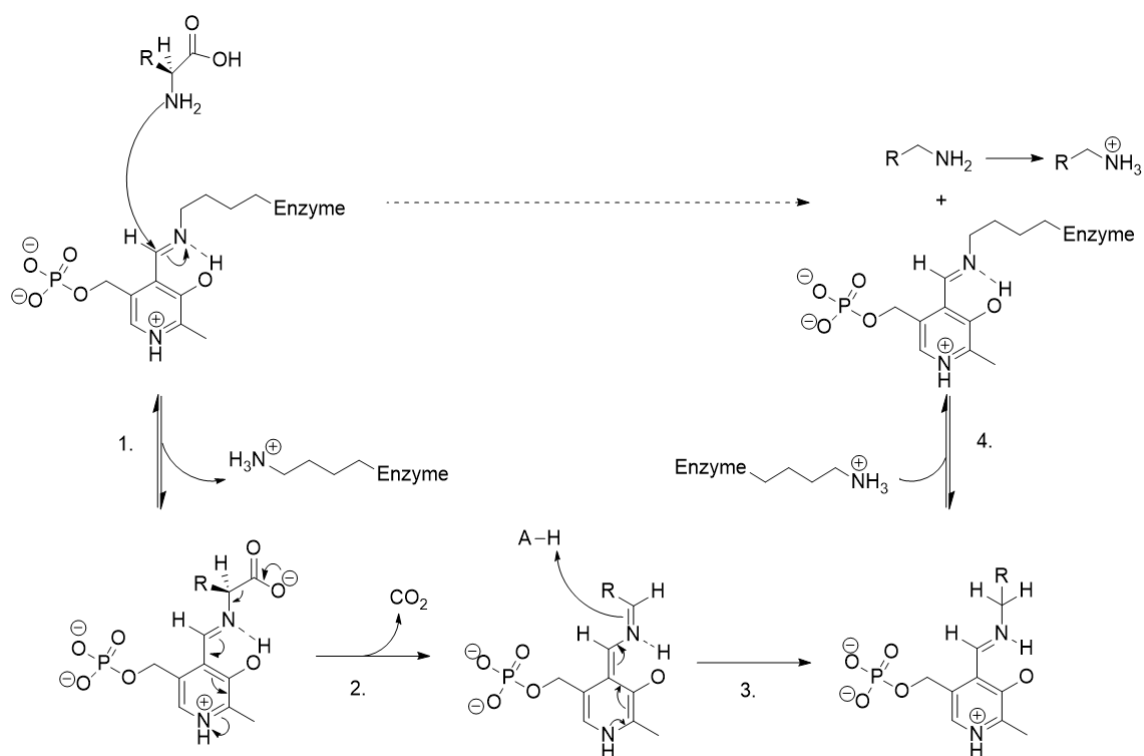


Figure 1.9: Mechanism for the PLP-catalyzed decarboxylation of L-amino acids in enzymes. The crucial function of PLP in the decarboxylation reaction lies in its electron-withdrawing properties and electron sink capability. This is achieved through the pyridine ring of PLP participating in the formation of resonance structures, which are essential for stabilizing the carbanionic intermediate created during the carbon-carbon bond cleavage process.

Among various amino acid decarboxylases, L-tyrosine decarboxylase from *Lactobacillus brevis* (*LbTDC*) (K. Zhang & Ni, 2014) stands out. It displays significant potential due to its elevated activity levels towards L-tyrosine, which, as per previous studies, are considerably higher than those of plant or insect TDCs. Successful heterologous expression of this enzyme in *E. coli* has been achieved, (K. Zhang & Ni, 2014) furthering its research potential.

Previous studies attempted to chemically decarboxylate L-tyrosine using isophorone, as organocatalyst, at 150 °C in 2-propanol over the course of 24 hours (Figure 1.10 A). However, due to the poor solubility of the amino acid in this solvent, the method was ineffective, resulting in a limited conversion of only 2%. (Claes et al., 2019) An alternative strategy, involving the decarboxylation of L-tyrosine with a different enone catalyst, *R*-carvone, at a higher temperature of 190 °C in *n*-propanol for 40 minutes, achieved better conversion and 67 % yield (Figure 1.10 B). (Jackson et al., 2015)

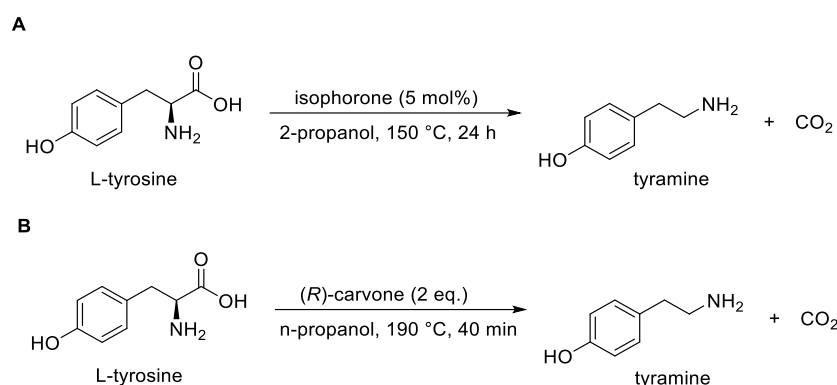


Figure 1.10: Organocatalytic decarboxylation of L-tyrosine with **(A)** isophorone and **(B)** *(R)*-carvone.

Compared to these traditional chemical methods, employing *LbTDC* presents a more efficient solution for the decarboxylation process (Figure 1.11). (Gianolio et al., 2022)

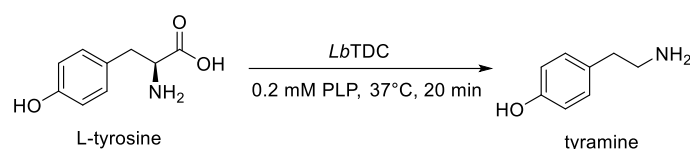


Figure 1.11: Enzymatic decarboxylation of L-tyrosine at 2.5 mM scale with *LbTDC*.

The enzymatic approach allows the reaction to be conducted under significantly milder conditions, specifically at 37 °C, using a biodegradable catalyst, and achieving complete conversion of the starting material. Although the solubility of L-tyrosine in water is better than its solubility in organic solvents, it still poses a challenge at a pH of 5, where *LbTDC* catalyzes optimally the reaction. (K. Zhang & Ni, 2014) Improving the amino acid solubility beyond 5 mM, even with the use of surfactants or solubilizing agents, remains a considerable challenge. (Jiang et al., 2019a)

Typically, amino acid decarboxylases demonstrate a high degree of substrate specificity. However, *LbTDC* is active not only towards its natural substrate, L-tyrosine, but has also activity towards L-DOPA. This ability of *LbTDC* to accept L-DOPA as an alternate substrate highlights the enzyme catalytic versatility for different applications.

Another particularly remarkable case of substrate promiscuity has been highlighted with the use of L-valine decarboxylase from *Streptomyces viridifaciens* (VImD). (Garg et al., 2002a) This enzyme displays an exceptional degree of substrate versatility and does not only act on its natural substrate, but also catalyzes the decarboxylation of a broad range of amino acids (Table 1.3), including L-alanine (**2**), L-2-aminobutyrate (**3**), 2-aminoisobutyrate (**4**), L-norvaline (**5**), L-isovaline (**6**), L-norleucine (**7**), L-leucine (**8**), L-isoleucine (**9**), 1-aminocyclopentanecarboxylic acid (**10**), 1-aminocyclohexanecarboxylic acid (**11**), and L-2-phenylglycine (**12**). (D. I. Kim et al., 2021) The products of these reactions range from ethylamine to benzylamine.

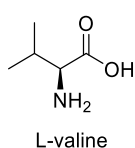
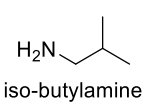
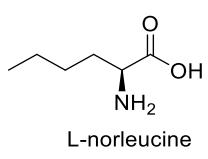
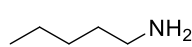
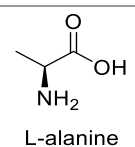
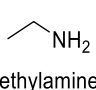
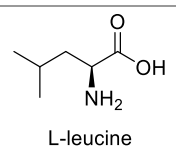
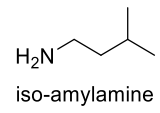
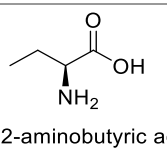
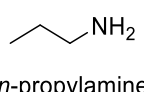
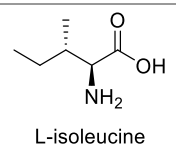
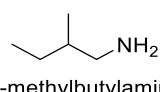
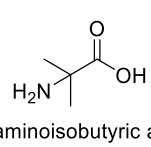
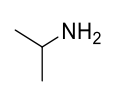
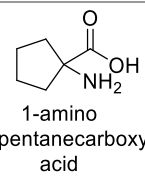
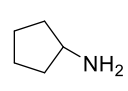
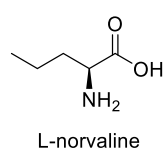
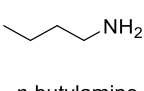
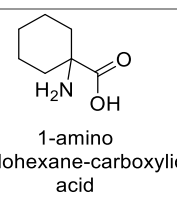
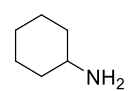
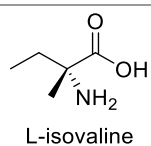
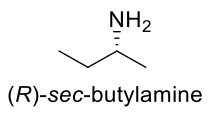
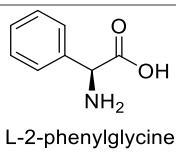
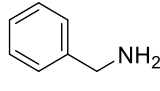
n°	Substrate	Product	n°	Substrate	Product
1	 L-valine	 iso-butylamine	7	 L-norleucine	 <i>n</i> -amylamine
2	 L-alanine	 ethylamine	8	 L-leucine	 iso-amylamine
3	 L-2-aminobutyric acid	 <i>n</i> -propylamine	9	 L-isoleucine	 2-methylbutylamine
4	 2-aminoisobutyric acid	 iso-propylamine	10	 1-amino cyclopentanecarboxylic acid	 cyclopentylamine
5	 L-norvaline	 <i>n</i> -butylamine	11	 1-amino cyclohexane-carboxylic acid	 cyclohexylamine
6	 L-isovaline	 (<i>R</i>)-sec-butylamine	12	 L-2-phenylglycine	 benzylamine

Table 1.3 : VImD Substrate scope.

The substrates which VImD can accept and transform with actually more than 80% conversion to their respective short-chain primary amines (SCPAs) were L-valine (**1**), L-2-aminobutyrate (**3**), L-norvaline (**5**), L-isovaline (**6**), L-isoleucine (**9**), and 1-aminocyclopentanecarboxylic acid (**10**). These reactions were also catalyzed at mild conditions and offer a valid alternative to the chemical approach, effectively providing a platform strain that has the capacity to generate a wide range of bio-derived products.

1.4.1 Amino acid dehydrogenases and amine dehydrogenases

Amine dehydrogenases (AmDHs) are becoming increasingly recognized for their potential in chiral amine synthesis, outperforming traditional chemical methodologies.

What importantly distinguishes them are their atomic efficiency and broad versatility, and particularly their ability to catalyze the asymmetric reductive amination of ketones

to their corresponding chiral amines (Figure 1.12). This process, which utilizes ammonia as the amino donor and NAD(P)H as cofactors, is highly efficient, producing only water as a by-product. Given the environmental and economic advantages, this method is of considerable importance in the pharmaceutical industry.

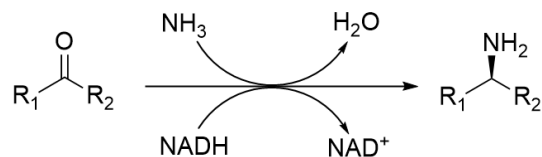


Figure 1.12: Asymmetric reduction of ketones by amine dehydrogenases

There are two primary sources of AmDHs: engineered amino acid dehydrogenases (AADHs) and naturally occurring AmDHs.

As far as AADHs, they are engaged in the oxidation of L-amino acids and the reversible reductive amination of corresponding α -keto acids (Figure 1.13). The presence of the carboxylic acid group in the keto acids or amino acids is a prerequisite for their catalytic activity, consequently restricting their substrate range to molecules with this specific structural attribute.

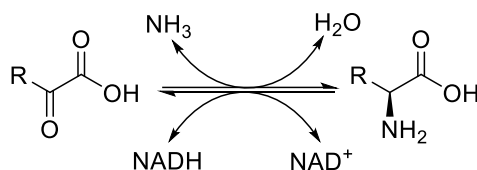


Figure 1.13: General AADHs reaction scheme.

To extend the range of AADHs applications, a great focus was dedicated to the directed evolution of these enzymes, leading to the generation of engineered amine dehydrogenases.

The first engineered AmDH, reported in 2012 (Abrahamson et al., 2012), had leucine dehydrogenase from *Bacillus stercorophilus* (*BsLeuDH*) as the initial protein scaffold (1LEH). (Baker et al., 1995) With 11 rounds of protein engineering, *via* combinatorial active-site saturation testing (CASTing) and site-directed saturation mutagenesis (SDSM), a novel variant (K68S, E114V, N261L, V291C) was generated with completely inverted enzyme specificity and an amination activity of 0.69 U/mg towards methyl isobutyl ketone (MIBK) (Figure 1.14). MIBK, as novel substrate, is the corresponding molecule when the carboxyl moiety is removed from α -ketoisocaproate.

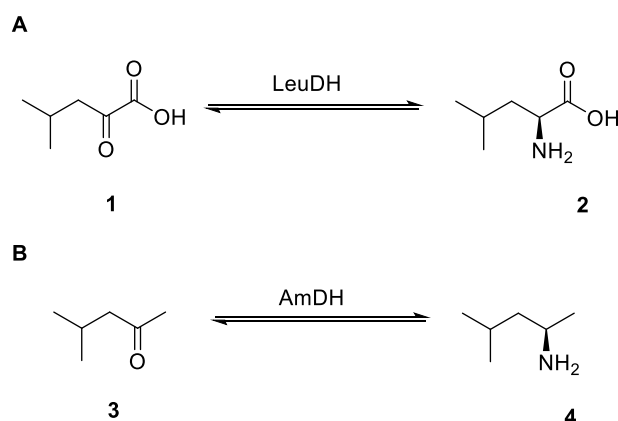


Figure 1.14: **A.** Wild-type leucine dehydrogenase (LeuDH) reaction for the symmetric reductive amination of α -ketoisocaproate (**1**) to L-leucine (**2**); **B.** Novel amine dehydrogenase reaction for the symmetric reductive amination of MIBK (**3**) to (*R*)-4-methylpentan-2-amine (**4**) .

The K68S/E114V/N261L/V291C variant demonstrated both amination and deamination activities. As far as the deamination, it was shown to be active against (*R*)-methylbenzylamine (586.3 mU/mg) and cyclohexylamine (56 mU/mg). In addition, effective amination activity was measured against cyclohexanone (123.4 mU/mg) and acetophenone (58.8 mU/mg).

With a similar mechanism as LeuDHs, PheDHs are also members of the larger AADH family, but they typically exhibit a substrate preference toward aromatic ketones. (Sharma et al., 2017) Corresponding mutations at positions analogous to K68 and N261 in *Bs*LeuDH led to similar developments of AmDH activity in PheDHs (Figure 1.15).

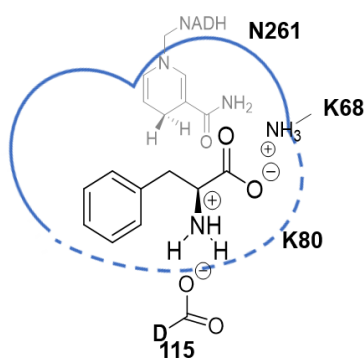


Figure 1.15: Exemplified catalytic pocket of LeuDH and PheDH illustrating the catalytic residues D115 and K80. The amino acid residues targeted successfully for the amination activity towards ketones were N261 and K68, which are responsible for the coordination of the carboxylic group of the natural amino acidic substrate. The sequence numbering used is that of *Bs*LeuDH.

Bommarius *et al.* also applied similar mutations to the PheDH derived from *Bacillus badius*. This mutant, termed PheDH-AmDH (K77S/N276L), was able to carry out the asymmetric reductive amination of 4-fluorophenyl acetone to (*R*)-4-fluoro- α -

methylphenylethylamine, achieving a high enantiomeric excess of 99 %.(Abrahamson et al., 2013) Similarly, Ye *et al.* managed to create a triple mutant PheDH (TM_PheDH K66Q/S149G/N262C) using PheDH from *Rhodococcus* sp. M4 (Figure 1.16). The variant was active towards phenylacetone and 4-phenyl-2-butanone (with 5 and 8.8 mU/mg respectively), giving (*R*)-amphetamine and (*R*)-1-methyl-3-phenylpropylamine in >98% ee, respectively.(Ye et al., 2015)

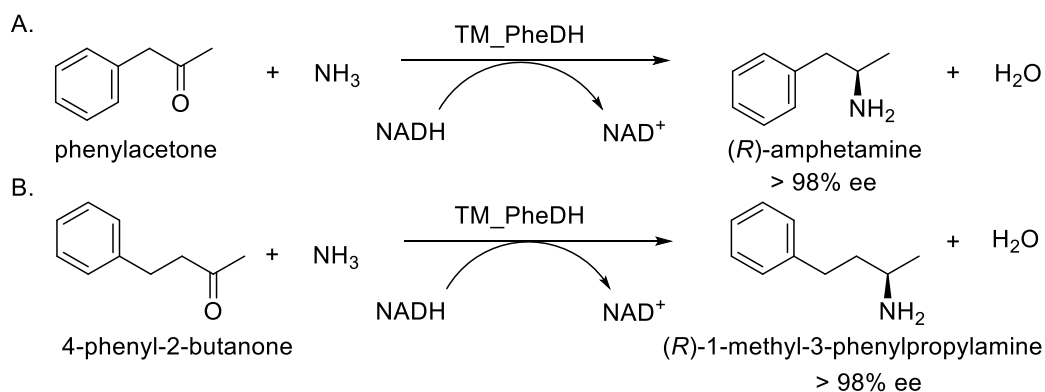


Figure 1.16: The evolved amine dehydrogenase TM_pheDH, originated from *Rhodococcus* sp. M4 PheDH, has been employed for the asymmetric amination of (A) phenylacetone and; (B) 4-phenyl-2-butanone. This results in the production of (*R*)-Amphetamine and (*R*)-1-methyl-3-phenylpropylamine, respectively.

In contrast to the previously mentioned enzymes which were engineered from closely related α -AADHs scaffolds (LeuDH, PDB 1LEH and PheDH, PDB 1C1D), lysine ϵ -dehydrogenases (LysEDHs) have also been utilized.(Tseliou et al., 2019) Although the LysEDH does not naturally catalyze an asymmetric transformation, acting in fact on the primary ϵ -amino group of L-lysine, it has been strategically exploited in attempts to generate AmDHs that carry out the reductive amination of prochiral ketones. *Via* computational analyses, a number of potential mutagenesis targets (V130, A131, V172, F173, H181, Y238, T240, and R242) were identified. Among them, only the variant F173 (LE-AmDH-v1) proved to be able to convert the target ketone, acetophenone to the corresponding amine (Figure 1.17). The residue F173 had an important role for the orientation of natural substrate and for the active site hydrophobicity. When mutated to alanine, the binding pocket expands, reducing the residue size by 4.3 Å and allowing the binding of bulky aromatic ketones such acetophenone.

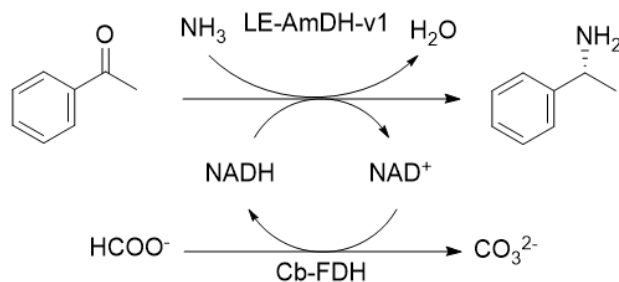


Figure 1.17: Reductive amination of acetophenone by LE-AmDH-v1 with cofactor recycling system. After 48 h at 50 °C, the conversion was 82 % with >99 % ee, at a 5 mM scale.

Adding to its new substrate specificity, LE-AmDH-v1 also proved effective in the kinetic resolution of racemic amines, working in the enantioselective oxidative deamination direction. (Tseliou et al., 2020) Notably, the previously discovered AmDHs did not exhibit such a property. Indeed LE-AmDH-v1 showcased exceptional activity and stereoselectivity in the asymmetric synthesis of pharmaceutically relevant *R*-configured α -chiral amines, including (*R*)- α -methylbenzylamines, (*R*)-1-amino-tetraline, and (*R*)-4-aminochromane.

Conversely, natural AmDHs have been discovered in diverse bacteria and eukaryotes, aided by genome mining and metagenomic technology. (Caparco, Pelletier, et al., 2020) Although they differ in sequence identities and structural similarities compared to engineered AmDHs, these naturally occurring variants provide more options for the synthesis of chiral amines and serve as valuable templates for protein engineering of AmDHs.

The 2019 study, (Mayol et al., 2019a) by the group of G. Grogan and C. Vergne-Vaxelaire, unveiled a series of novel native AmDHs (nat-AmDHs). The new AmDHs were identified from various microorganisms and were annotated in the Uniprot database, often as a dihydrodipicolinate reductase or as an uncharacterized protein. However, in this study, these enzymes were revealed to have AmDH activity. The wide substrate scope was made up by diverse aliphatic ketones and aldehydes, and three non-functionalized amines (pentan-2-amine, α -methylbenzylamine, and cyclohexylamine).

The novel nat-AmDHs included *MsmAmDH* (A0A0D6I8P6), derived from *Mycobacterium smegmatis*, *MvacAmDH* (K0UKT5), isolated from *Mycobacterium vaccae*, *ApauAmDH* (E3CZE3), derived from *Aminomonas*, *MicroAmDH* (C3UMY1), found in *Microbacterium* sp., and lastly, *CfusAmDH* (S9Q235), isolated from *Cystobacter fuscus*. Among these proteins when *MsmAmDH* is used as protein sequence reference, the percentage of identity range from 38 up to 89 %. (Mayol et al., 2019a)

From this screening, in the reductive amination direction, the reported highest activities with *MicroAmDH* were 614.5 mU/mg for cyclohexanone with ammonia, and 851.3 mU/mg for isobutyraldehyde with methylamine as the amine donor. However, for

the oxidative deamination, only *Msm*eAmDH displayed an activity of 6 mU/mg against cyclohexylamine.

After biochemical characterization and substrate spectrum testing, it was not possible to determinate the cofactor preference (NADH or NADPH) for each enzyme, in fact this specificity appeared to be substrate dependent. Similarly, to engineered AADHs, these enzymes exhibit a high K_M for ammonia, necessitating the use of an ammonia buffer at high concentrations, typically between 1-2 M, at a pH of 8.0-9.5. The hypothetical mechanism of nat-AmDH is described in Figure 1.18.

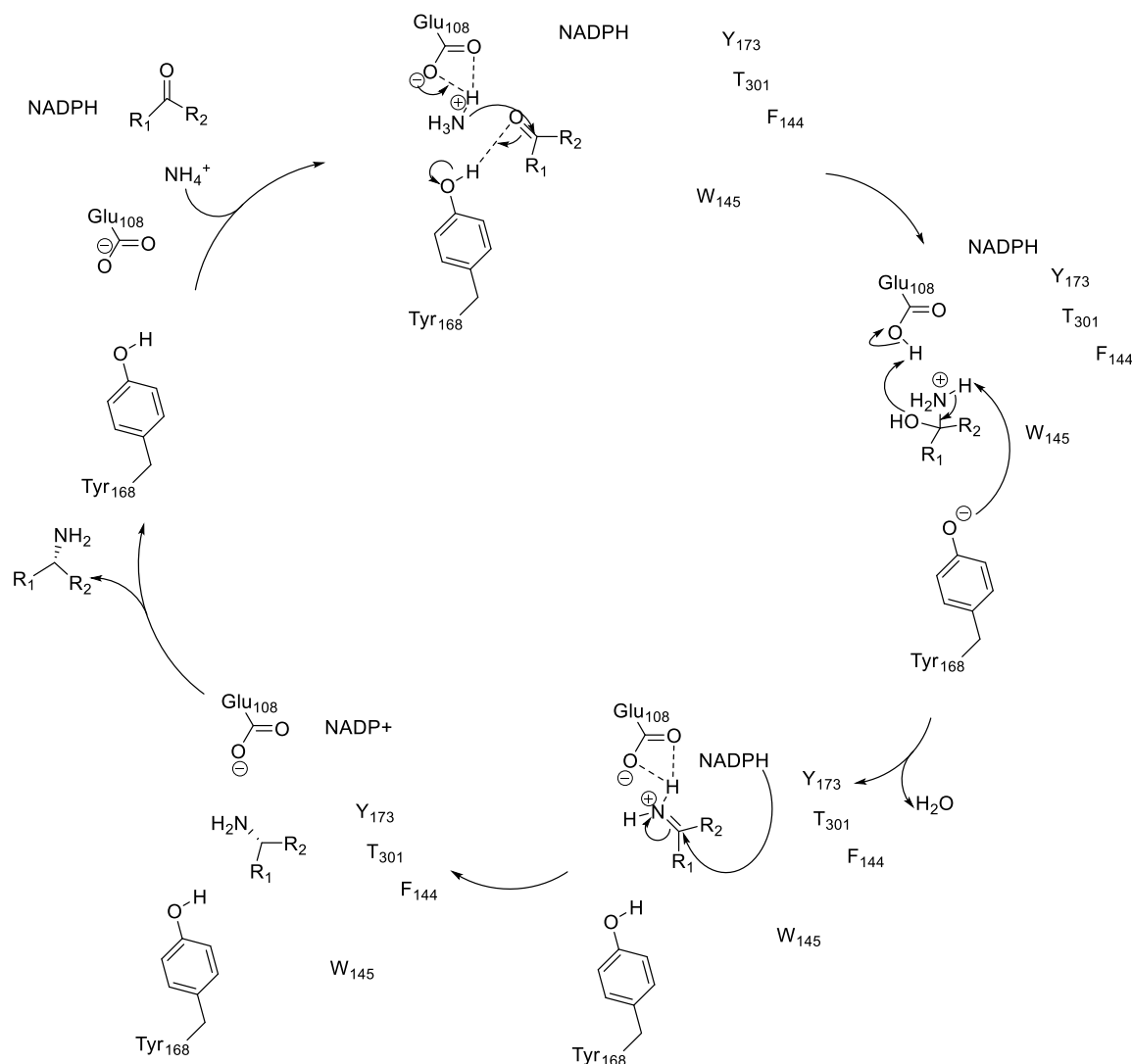


Figure 1.18: Putative mechanism of nat-AmDHs. The sequence numbering used is that of *Cfus*AmDH. In the process, the glutamate (E108) triggers the activation of ammonia. The ammonia subsequently targets the electrophilic carbon of the substrate's carbonyl group. As a result, carbinolamine is produced which, upon undergoing dehydration, leads to the formation of the imine product, after its reduction by the hydride sourced from the nicotinamide cofactor. In *Cfus*AmDH, for the substrate binding, a hydrophobic cage is formed between the cofactor and the aromatic rings of the aromatic residues in the first layer of the pocket.

In 2020, a new enzyme, MATOUAmDH2, (Bennett et al., 2022; Caparco, Pelletier, et al., 2020) which was discovered in an eukaryotic organism, demonstrated unprecedented activity among nat-AmDHs for aliphatic aldehydes like isobutyraldehyde and pentanal. Notably, this biocatalyst showed low homology with already characterized nat-AmDHs (< 34%).

In 2021, a new study for the production of small optically active molecules, involving *CfusAmDH*, *MsmAmDH*, *MicroAmDH*, and MATOUAmDH2 was reported. These enzymes demonstrated indeed efficiency in synthesizing hydroxylated or unfunctionalized small 2-aminoalkanes, with moderate to high enantioselectivities, without requiring any protein engineering (Figure 1.19). (Ducrot et al., 2021)

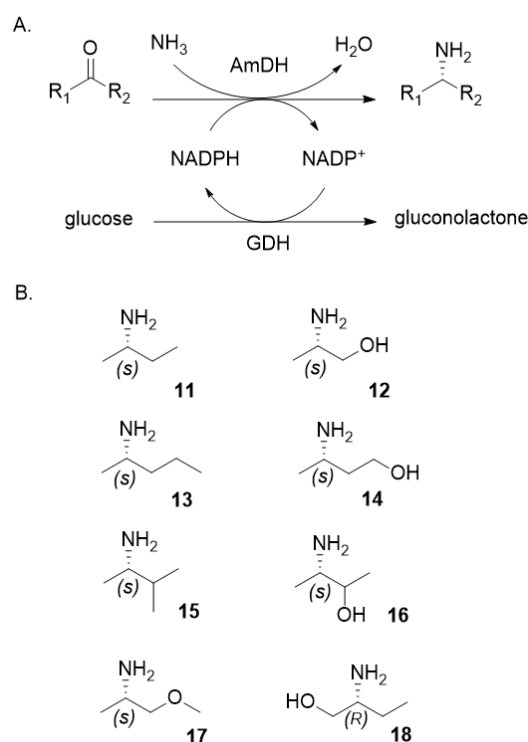


Figure 1.19: Reductive amination reactions catalyzed by nat-AmDHs *CfusAmDH*, *MsmAmDH*, *MicroAmDH*, and MATOUAmDH2. A. Reductive amination system with recycling of the cofactor by glucose dehydrogenase (GDH). B. Chiral hydroxylated or unfunctionalized 2-aminoalkanes produced by the system: **11.** (*S*)-butan-2-amine; **12.** Alaninol; **13.** (*S*)-pentan-2-amine; **14.** 3-aminobutan-1-ol; **15.** (*S*)-3-methylbutan-2-amine; **16.** 3-aminobutan-2-ol; **17.** (*S*)-1-methoxypropan-2-amine; **18.** (*S*)-2-aminobutan-1-ol.

Despite the great potential for nat-AmDHs, clear issues can still be identified, including a narrow substrate scope and low catalytic activity. Therefore, research in the field of AmDH-catalyzed reactions has put action to advance and innovate, leading to efforts in engineering AmDH systems to overcome their typical limitations.

The issue of the limited substrate scope of nat-AmDHs was addressed by primarily focusing on enlarging the active site. An *in silico* analysis of the amino acid residues in the

active sites of the nat-AmDH family revealed it to be predominantly composed of the sterically demanding aromatic amino acids, which resulted in a notably small active site. For improved functionality, expansion of this active site was then necessary.

A significant example is the obtained variant of *CfusAmDH*, based on *in silico* findings, where a W145A mutation allowed the integration in the enzyme substrate scope of long chain aldehydes (Figure 1.20).^(Ducrot et al., 2022) The mutant showed activities of 401, 405, and 483 mU/mg towards hexanal, heptanal, and octanal, respectively. The wild-type version of *CfusAmDH* demonstrated little to no activity for substrates larger than pentanal (< 20 mU/mg), in contrast to the engineered variant. Interestingly, this *CfusAmDH* W145A showed instead lesser activity than the wild-type enzyme towards the smaller substrate, pentanal.

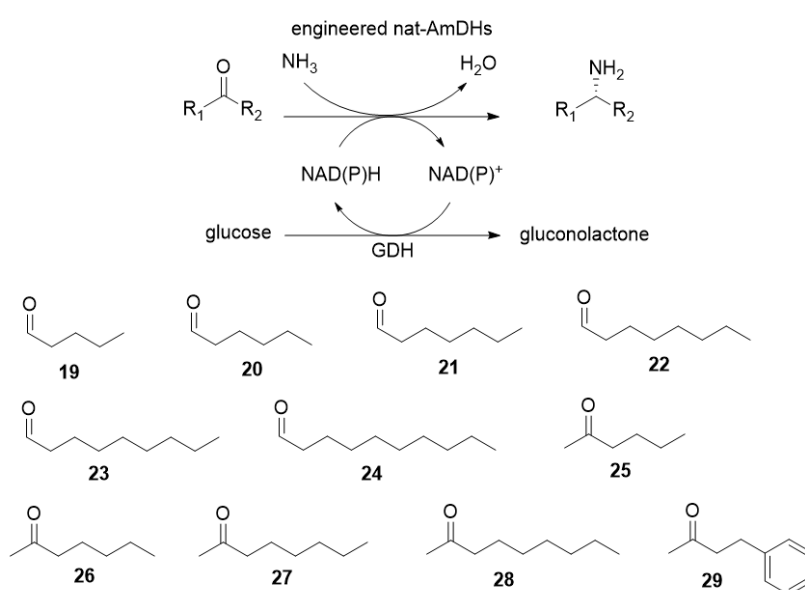


Figure 1.20: Engineered nat-AmDHs catalyzed the reductive amination of ketones and aldehydes, leading to the corresponding amines. Substrate: **19.** pentanal; **20.** hexanal; **21.** heptanal; **22.** octanal, **23.** nonanal; **24.** decanal; **25.** hexan-2-one; **26.** heptan-2-one; **27.** octan-2-one; **28.** nonan-2-one; **29.** 4-phenylbutan-2-one.

Among nine different AmDHs, considering wt and engineered versions, not only *CfusAmDH* W145A, but also the corresponding mutants of *ApauAmDH*, *PortiAmDH*, and MATOUAmDH2 performed well, with decent conversions for the synthesis of the corresponding amines.^(Ducrot et al., 2022) The reaction involving the conversion of 4-phenylbutan-2-one was of particular interest. In this case, *CfusAmDH* W145 demonstrated exceptional performance, achieving a conversion of 52.5 % and an enantiomeric excess of 99.6 % after 24 hours. This significantly outperformed the wild-type version, which was reported to have a conversion of less than 1 %.

As previously noted, AmDHs have been mainly utilized for the production of small chiral amines and also for kinetic resolution. However, their applications extend beyond these

uses, demonstrating versatility in enzymatic cascades for the deracemization of racemic amines (Jeon et al., 2017; Patil et al., 2019; Yoon et al., 2019) and in their coupling with other catalytic steps to synthesize desired products from more cost-effective and readily available starting materials. (Cai et al., 2020) A particularly noteworthy application involves coupling AmDHs with alcohol dehydrogenases (ADH), thus creating a hydrogen borrowing system (Figure 1.21) allowing for efficient cofactor recycling. (Böhmer et al., 2018a; Houwman et al., 2019; Montgomery et al., 2017; Mutti et al., 2015; Thompson & Turner, 2017a)

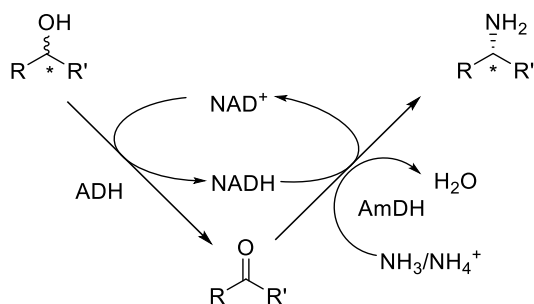


Figure 1.21: Representation of the hydrogen borrowing strategy utilizing both alcohol dehydrogenase (ADH) and amine dehydrogenase (AmDH). This innovative approach, predominantly used with engineered AADHs, offers a smart solution for cofactor recycling. The pioneering work of Mutti *et al.* in 2015 first showcased the successful application of this strategy in the literature.

Ultimately, it is outstanding to see how AmDHs have become important tools, especially in using aldehydes or ketones, to make amine products through reductive amination chemistries in an environmentally friendly way. Intriguingly, the exploration of the reverse reaction - oxidative deamination - has not generated the same level of attention and remains a largely unexplored territory. In this potential research direction, the production of valuable carbonyl compounds could be the main objective, thereby opening new avenues for sustainable chemical synthesis.

Specifically, using AmDHs in the well-documented hydrogen-borrowing strategy, where they are coupled with ADHs, could, starting this time from primary amines, facilitate the production of valuable alcohols. This approach circumvents issues associated with the instability and reactivity of certain aldehydes, which would be promptly reduced to alcohols by the effectively coupled ADH.

1.5 Biocatalyst immobilization and flow applications advantages

The use of enzymes, especially in aqueous environments, is typically restricted to one-time and single-shot applications, which is neither economically feasible nor aligned with principles of a circular economy. This limitation can be mitigated by immobilizing the

enzyme on an insoluble and recyclable solid, transforming it into a heterogeneous catalyst that can be used multiple times.(Sheldon et al., 2021)

With a straightforward definition, enzyme immobilization can be described as the process where an enzyme is physically confined or localized in a certain defined region of space with retention of its catalytic activity, and can be used repeatedly or in continuous. This technique offers a wide array of advantages that can significantly enhance the feasibility and efficiency of enzymatic processes.

1.5.1 Advantages of immobilized biocatalysts

One of the most prominent benefits is the improved stability that immobilized enzymes exhibit. They are more resistant to changes in temperature, pH, and other environmental conditions compared to their free version. This elevated stability can even lead to a prolonged enzyme lifespan, permitting repeated usage over time. Consequently, the ability to reuse the biocatalyst substantially reduces costs, contributing to the sustainability of the process.

Another significant advantage lies in the convenience of product separation. Immobilized enzymes streamline the process of separating products from the catalyst, allowing the avoidance of complex recovery steps and thereby enhancing efficiency while lowering production costs.

Moreover, when enzymes are immobilized, they can be integrated into continuous operations of enzymatic reactors, using different type and size of reactors, according to the reaction scale. The enzymes, held in place, allow for a continuous flow of substrates and products, opening opportunities for automated and large-scale production.

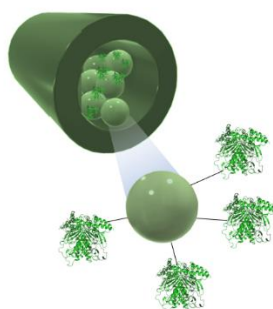


Figure 1.22: 3D cross-section view of a packed bed reactor (PBR). The visual representation highlights the densely packed biocatalyst-coated support beads within the reactor.

Upon closer observation of a packed bed reactor (Figure 1.22), it is evident that the substantial concentration of enzymes compacted into a relatively small volume generate a high catalytic density, considerably boosting the reaction rate and increasing the process efficiency. Bringing these benefits together, the immense potential of enzyme immobilization is greatly relevant in diverse fields and applications.(DiCosimo et al., 2013)

Taking this into account, the decision to immobilize a biocatalyst still requires a careful evaluation of factors such as process economics, enzyme activity, stability, recyclability, and flow conditions, as it is an approach which can require compromises, as it is an approach which can require compromises.

Despite the multiple advantages this strategy offers, there are also significant drawbacks that may discourage its use under certain circumstances. One of the most notable challenges arises from the potential deactivation of the biocatalyst during the immobilization process. This occurs due to the conformational changes that the enzyme might undergo when it is bound to the support, which can impact its catalytic activity. Moreover, activity loss can also be attributed to diffusion limitations, especially with macromolecular substrates and with big solid support particle sizes. Physical damage to the immobilized enzyme, caused by abrasive forces, for example from a mechanical stirrer, can also lead to a decrease in activity.

The costs and the time for the immobilization process could also represent a limitation or a disadvantage compared to the use of a liquid enzymatic preparation but, in general and despite these issues, the ability to recycle the immobilized enzyme can often counterbalance them.

Therefore, it is important to perform a careful evaluation of the process feasibility with the immobilized biocatalyst, calculating the minimum number of cycles required to reach the targeted production profit, given the potential activity loss and the investments in time and process design.

1.5.2 Immobilization of cell-free enzymes and whole cells

Another important aspect to consider is that the act of immobilizing a biocatalyst is not restricted solely to purified proteins. In fact, the process can also be used on whole cells, expanding the possibilities for creating efficient biocatalytic systems. (Lapponi et al., 2022) There are several reasons why the immobilization of whole cells may be more preferable, but as mentioned before, this decision should also be considered with a case-by-case approach. Indeed, where multiple enzymes are required for a series of reactions, whole cells have an important advantage because the entire enzymatic pathway would proceed in one step, bypassing the need for individual enzyme isolation and purification. Moreover, whole cells offer a more stable environment, potentially enhancing enzyme resilience to environmental fluctuations, such as temperature and pH changes.

From an economic point of view, using whole cells often eliminates the expensive and labor-intensive enzyme purification process. Whole cells also have the capacity to regenerate enzyme cofactors, augmenting process efficiency and eliminating the exogenous cofactors addition. However, whole-cell immobilization is not without its challenges. Potential hindrances include reduced activity due to the cell wall impeding

substrate access, side reaction from endogenous cellular metabolism and issues related to cell growth and viability.

1.5.3 Immobilization strategies

Methods of immobilisation of enzymes can be broadly categorized based on the stability and strength of the enzyme-support interaction, which might be reversible or irreversible, and whether the process is of a physical or chemical nature (Figure 1.23). Physical immobilization involves the adsorption of enzymes or cells onto the surface of a support material or their entrapment within a matrix, without the formation of strong chemical bonds. These methods often retain the enzyme or cell native conformation and activity better, but the biocatalyst can also desorb under certain conditions leaking in the reaction environment. In contrast, chemical immobilization methods involve forming covalent bonds, cross-links, or ionic bonds between the enzyme or cell and the support. These bonds are stronger and can improve the stability of the enzyme or cell, but they may also affect the enzyme conformation and activity or the cell viability.

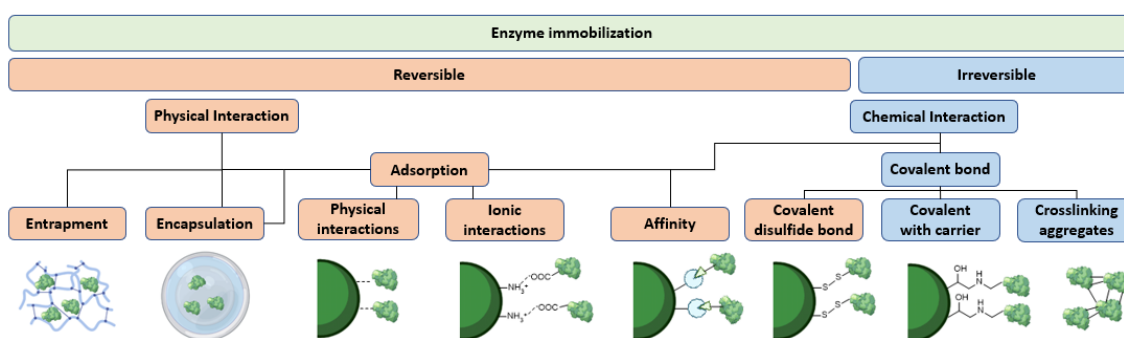
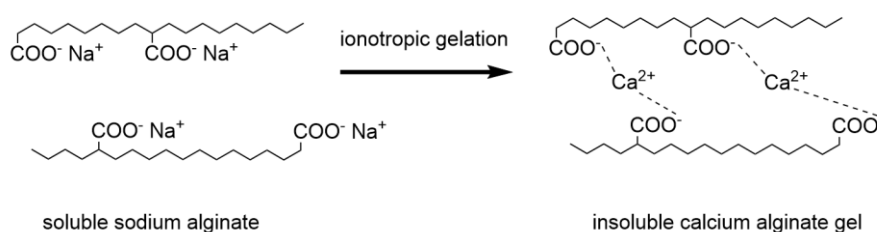


Figure 1.23: Different type of immobilization strategies.

Covalent immobilization strategies, by their very nature, result in a more stable immobilized biocatalyst due to the minimized risk of leakage during the reaction cycle. Few examples from the literature show how covalent cell immobilization, especially using agents like glutaraldehyde (GA), ensures robust and stable attachment of cells to surfaces, thus mitigating the issues of cell detachment coming from adsorbed cell systems. (Bai et al., 2019; P. Wu et al., 2020) Despite these advantages, the use of cross-linking agents can result in cytotoxicity and cell viability loss and consequently, covalent support binding is typically more suited for enzyme immobilization rather than whole cell immobilization.

The selection of the support material, to which the enzyme or cell is attached, also plays an important role in the immobilization process. The options range from synthetic resins, recognized for their durability and practicality, to inorganic materials, such as silica or magnetic nanoparticles. Hydrogels and biopolymers (such as polysaccharides as alginate, pectate, carrageenan or chitosan) in particular, offer unique advantages for whole cell immobilization. (Lapponi et al., 2022; Sheldon et al., 2021) Hydrogels present a soft,

water-rich environment similar to the natural habitat of the cell, while biopolymers furnish a biocompatible setting that can often be tailored for specific applications (Figure 1.24).



Polyelectrolyte	Gelating ion
-COO ⁻ Alginate	Ca ²⁺ , Ba ²⁺ , Co ²⁺
Pectinate	Mg ²⁺ , Ca ²⁺
-SO ₃ ⁻ Carrageenan	Ca ²⁺
-NH ₃ ⁺ Chitosan	Polyphosphate

Figure 1.24: Ionotropic gelation mechanism and outline for the support choice in terms of hydrogel and biopolymers based on natural polyelectrolyte. Other natural biopolymers could be exploit with similar strategy upon derivatization with ionizable groups.

Eventually, each method and support type offer unique advantages and challenges, and the optimal choice depends on the specific application and the properties of the biocatalyst to be immobilized. Ideally, the designed strategy should maximize the stability and activity of the immobilized enzyme or cell, while also considering all practical factors like cost and ease of use.

1.5.4 Immobilized amino acid decarboxylases and amine dehydrogenases

1.5.4.1 Amino acid decarboxylases

The utilization of amino acid decarboxylases and amine dehydrogenases as immobilized biocatalysts, particularly in continuous flow operations, has been innovatively documented in literature.

Given their potential in industrial applications, amino acid decarboxylases, particularly those acting on Lysine (LDC) and Glutamate (GDC), have attracted a significant amount of attention. There are multiple examples of successful strategies for their immobilization. Indeed, one of the first examples of amino acid decarboxylase immobilization dates back to 1995, and it involves the decarboxylation of L-tyrosine and L-DOPA by the *Papaver somniferum* cells. (Stano et al., 1995) These cells naturally express L-tyrosine decarboxylase (EC 4.1.1.25, TDC) and L-DOPA decarboxylase (EC 4.1.1.26, DOPADC). The immobilization process in this case involved the creation of cross-linked enzyme aggregates (CLEAs) post-permeabilization in Tween 80, with glutaraldehyde as the cross-linking agent.

Though this method presents several challenges, including the fragility of the resultant particles, issues with substrate/product diffusion, and activity loss due to conformational changes during covalent bond formation. Nevertheless, the process eliminates the need for a support, as the enzyme itself fulfills this role.

A 2017 study employed a similar approach for the immobilization of lysine decarboxylase from *E. coli*, but using a cell-free extract and glutaraldehyde (GA) as the immobilization agent (Figure 1.25). (S. H. Park et al., 2017) Despite a low recovered activity of just 8 % and an immobilization yield of 30%, the enzyme aggregates were rapidly recovered and the residual activity was 53 % after the 10th recycle.

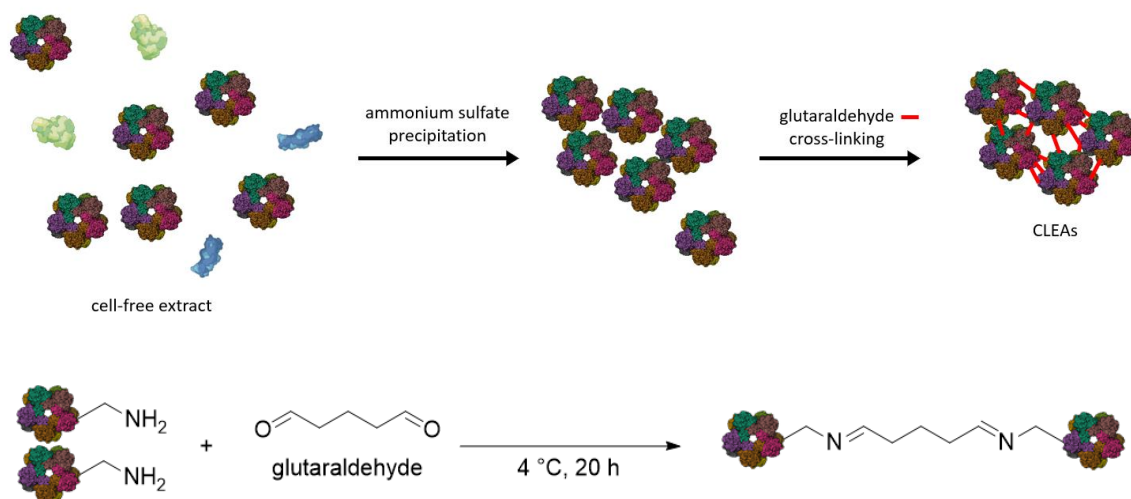
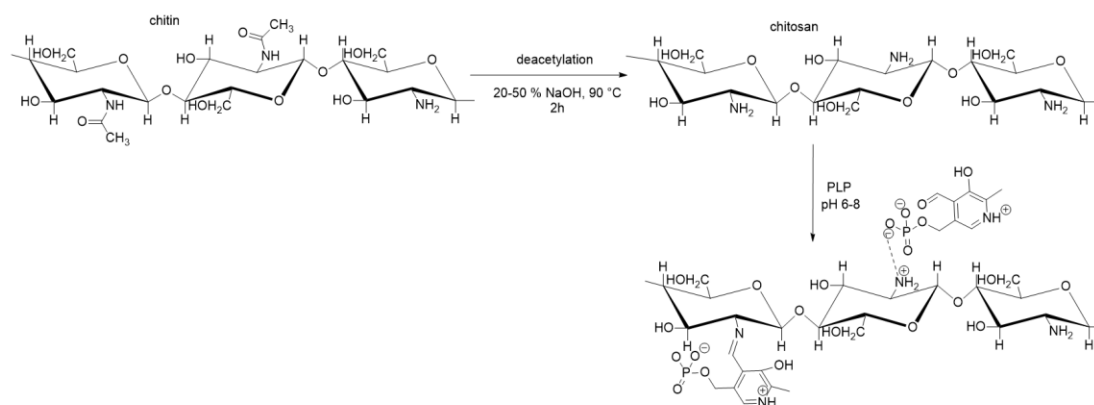


Figure 1.25: Scheme flow for CLEAs preparation. Glutaraldehyde is a bi-functionalized cross-linker and can be used to consolidate the precipitated enzyme forming aggregates *via* imine bonds.

More recent studies have extended the approach to co-immobilization of lysine decarboxylase along with its cofactor, Pyridoxal 5'-Phosphate (PLP). In one case, the enzyme was fused with a chitin-binding domain and then immobilized on chitin *via* affinity immobilization. (G. Wei et al., 2022) Experimenting with the chitin degree of deacetylation (DDA), this approach offered an intriguing strategy to secure both the enzyme and its cofactor on the same support (Figure 1.26).

A



B

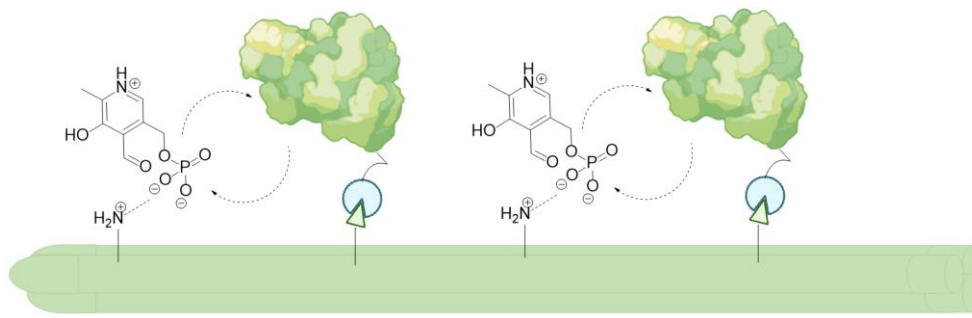
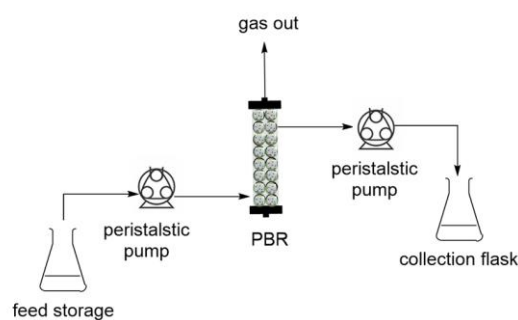


Figure 1.26: A. Deacetylation of chitin to yield free amino group where to anchor *via* ionic bond or Schiff case the PLP cofactor; **B.** Co-immobilization of Lysine decarboxylase, fused with a linker to the chitin-binding domain (ChBD), *via* affinity immobilization, and PLP cofactor. In virtue of the reversibility of the cofactor immobilization, PLP can move between the enzyme active site and the support surface.

In another experiment, the enzyme and PLP were co-immobilized on barium alginate beads using polyethyleneimine (PEI), exploiting the ionic interaction between the PLP and the activated support. (Mi et al., 2022) In this case, alginate beads were used in a continuous flow reactor (Figure 1.27). This 10 mL column reactor, with a diameter of 1.5 cm and a height of 7 cm, was fed by a peristaltic pump that continuously transported a 1 M lysine solution into the reactor at a flow rate of 0.07 mL/min, achieving a productivity of cadaverine of 14.28 g/(L·h). However, with the progression of the reaction time, there was a minor decrease in catalytic efficiency. This decrease was attributed to the gradual loss of enzyme and coenzyme, present also when higher flow rates were trialed. Moreover, an important component of this experimental setup was the inclusion of an outlet to allow the generated CO₂ to escape the reactor without causing an increase in pressure. Pressure build-up from the production of gaseous by-products such as CO₂ during decarboxylation in a closed packed bed reactor can indeed lead to reactor failure and disrupt the reaction. Consequently, the reactor design should include, if possible, an effective venting system to regulate pressure. Nevertheless, creating such a setup is not straightforward and, for this reason, batch processing tends to be the preferred option at larger scales.

A



B

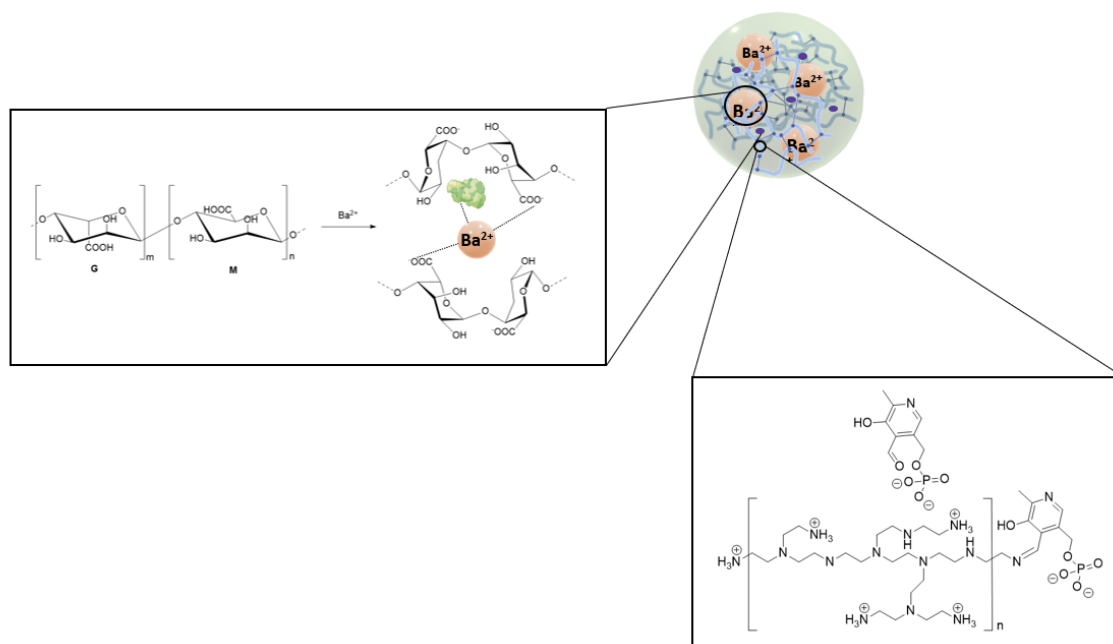


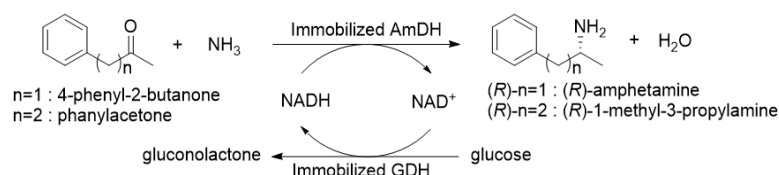
Figure 1.27: A. System set up for barium alginate beads with co-immobilized Lysine decarboxylase and PLP in continuous flow; **B.** In the beads, the His-tagged biocatalyst is adsorbed in the matrix and immobilized by ionic interaction with Ba^{2+} . PLP is co-immobilized on PEI through ionic bridges and reversible imine bonds (Schiff's bases).

1.5.4.2 Amine dehydrogenase

As described previously, the exploitation of AmDHs for reductive amination reactions has great potential in the synthesis of α -chiral amines. If for transaminases (TAs), an excess of amine donors such as isopropylamine and alanine is needed, for AmDHs this is replaced by the use of cost-effective ammonia salts as the amine source. On the other end, as far as the cofactor dependency, to sidestep the problem of its cost, AmDHs are always utilized in a dual-enzyme biotransformation, coupled with the cofactor recycling system, either *Candida boidinii* FDH (*Cb*FDH) or microbial GDH. However, despite their potential, AmDHs are hindered by product and substrate inhibition, as well as low productivity, even under intensified conditions. (Thompson et al., 2019) To mitigate these issues, continuous flow reactions can be used wherein the substrate and product are constantly removed. Yet to execute this, advanced research into immobilization techniques is crucial.

In the context of biotransformations using immobilized AmDHs, several advances have been made. In 2017, an innovative methodology was applied to immobilize an engineered version of AmDH, which was derived from the phenylalanine dehydrogenase of *Rhodococcus* sp. M4. (J. Liu et al., 2017) This process, based on affinity immobilization, utilized magnetic nanoparticles (MNPs) as support (Figure 1.28). A cell-free extract with a His-tagged version of the enzyme was used for this purpose, allowing selective fixation on the carrier and enhancing enzyme loading. The result was a highly efficient biocatalyst with an immobilization yield of over 90% even with high enzyme loading of over 100 mg/g. This immobilized biocatalyst, used in combination with an immobilized GDH, exhibited excellent performance in the asymmetric reductive amination of 4-phenyl-2-butanone, resulting in an (*R*)-enantiomer with 99 % ee and a 74% conversion from the batch reaction with a working scale of 4 mM in 2 mL final volume.

A



B

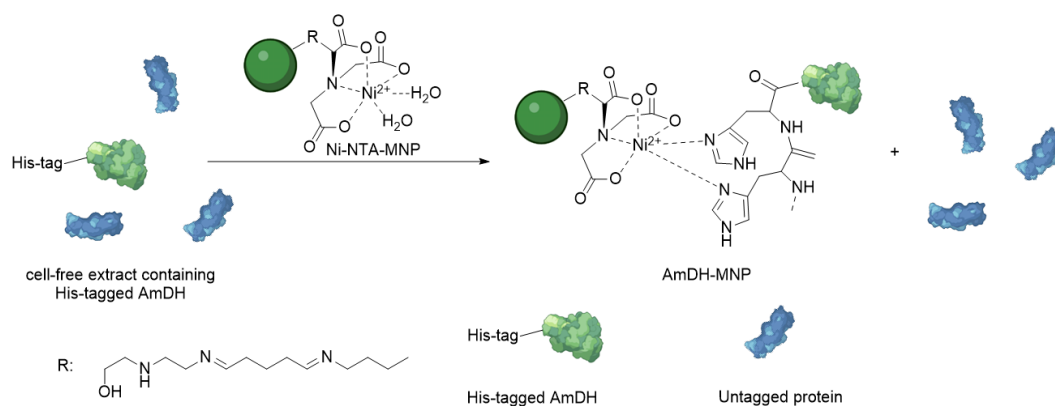


Figure 1.28: A. Co-immobilization of AmDH and GDH for the asymmetric reductive amination to yield (*R*)-amphetamine and (*R*)-1-methyl-3-propylamine with the mechanism for cofactor recycling.; **B.** Process of immobilizing his-tagged AmDH on Ni-NTA MNPs is facilitated directly from the cell-free extract, utilizing a highly specific affinity attachment approach.

Subsequently, in 2018, Böhmer *et al.* introduced a revolutionary immobilized system that incorporated two purified enzymes alcohol dehydrogenase from *Aromatoleum aromaticum* (AA-ADH) and a chimeric amine dehydrogenase (Ch1-AmDH). The co-immobilization of both dehydrogenases on controlled porosity glass Fe(III)-ion-affinity beads (EziG) was performed, thereby improving the hydrogen-borrowing biocatalytic amination process effectiveness (Figure 1.29). (Böhmer *et al.*, 2018b) This method exploited metal-ion affinity for selective binding of His-tagged enzymes as the one reported before. The dual-enzyme system showcased good recyclability, maintaining performance over five cycles and was employed for the preparative scale amination of (*S*)-phenylpropan-2-ol yielding a 90% conversion in 24 hours. Yet again, these reactions were conducted in batch.

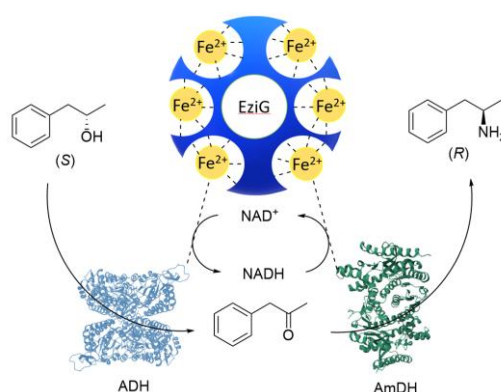


Figure 1.29: Co-immobilization of ADH and AmDH *via* ionic interaction on controlled porosity glass Fe(III)-ion-affinity beads (EziG) for the hydrogen-borrowing alcohol bioamination.

By 2020, a novel strategy emerged in which calcium-phosphate-protein supraparticles saturated with a leucine zipper binding domain (Z_R) were used as a modular

immobilization platform.(Caparco, Bommarius, et al., 2020) These supraparticles were employed for the immobilization of cFL1-AmDH and *Cb*-FDH, each of which was fused to a complementary leucine zipper domain (Z_E) (Figure 1.30). Prior work had already integrated Z_R directly into porous calcium-phosphate supraparticles, but this study took the concept further by demonstrating Z_E/Z_R immobilization of enzymes on a heterogeneous solid phase, with minimal interference with the enzymes structure or functionality, as the unchanged kinetic constants for both AmDH Z_E and FDH Z_E showed. In order to adjust the ratio between AmDH Z_E and FDH Z_E , different fluorescent model proteins, fused with Z_E , were used to correlate fluorescence count to protein loading. Not only their fluorescence provided a clear visualization of protein immobilization on supraparticles, but it proved also close correlation between the fluorescence count and the loading solution concentration. The linear trend of enzyme loadings and fluorescence was also proved using single-enzyme FITC-conjugation experiments, with AmDH Z_E -FITC and FDH Z_E -FITC . The fluorescent uptake of the FITC-enzyme- Z_E complexes displayed a near-identical relative affinity for the supra-particles, confirming the effectiveness of this strategy.

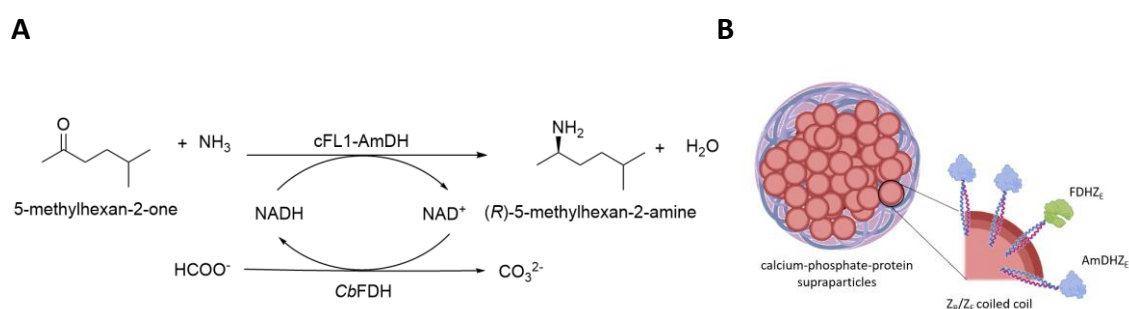
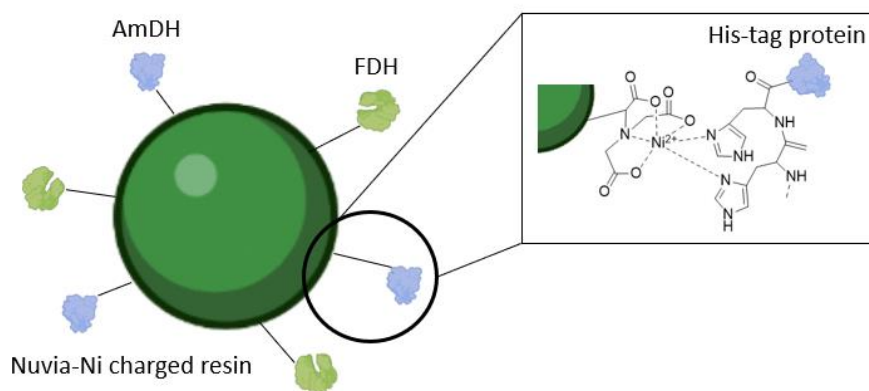


Figure 1.30: A. Co-immobilization of cFL1-AmDH and *Cb*FDH for the asymmetric reductive amination of 5-methylhexan-2-one. **B.** Reversible immobilization of the biocatalysts through affinity binding domains with Leucine zipper heterodimers Z_E and Z_R (glutamate- and arginine-rich, respectively) on calcium-phosphate-protein supraparticles.

In 2021, Franklin and colleagues pioneered the creation of a continuous flow packed bed reactor system (Figure 1.31 B).(Franklin et al., 2021) This system was designed for the asymmetric reductive amination of 5-methyl-2-hexanone using the same chimeric amine dehydrogenase (cFL1-AmDH) and *Cb*-FDH (Figure 1.31 A). As in the case of EziG, a commercial resin (Nuvia IMAC from BioRad) was also chosen as a support, leveraging the

ionic interaction between the His-tag on the proteins and the nickel ions on the resin. In fact, the support is composed of a base structure to which NTA (nitrilotriacetic acid) groups are attached. These NTA groups can bind metal ions that, in turn, bind his-tagged proteins. This was the first example of a continuous flow reaction system capable of generating enantiomerically pure (*R*)-amines with co-immobilized AmDH and FDH, demonstrating a substantial improvement in operational stability by lasting over 24 hours. However, even after the optimization of the ratio of AmDH to FDH, the packed immobilized resin in the reactor had a significantly higher AmDH concentration. This resulted in a portion of the AmDH remaining unexploited and in sub-optimal operating conditions. A drop in conversion efficiency also arose from the competitive product inhibition by (*R*)-amine on the ketone, which, despite the in-continuous mode, could not be successfully avoided.

A



B

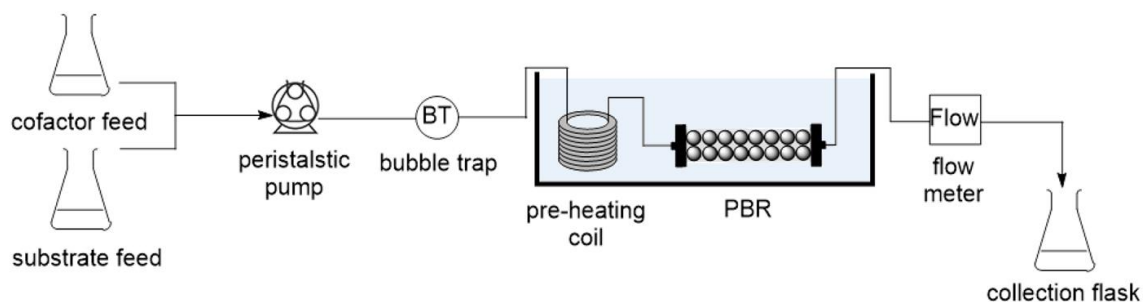


Figure 1.31: **A.** Co-immobilization on commercial immobilized metal affinity chromatography (IMAC) resin; **B.** Flowchart illustrating the continuous operation of the packed bed reactor system.

1.6 Bibliography

- Abrahamson, M. J., Vázquez-Figueroa, E., Woodall, N. B., Moore, J. C., & Bommaris, A. S. (2012). Development of an Amine Dehydrogenase for Synthesis of Chiral Amines. *Angewandte Chemie International Edition*, 51(16), 3969–3972. <https://doi.org/10.1002/anie.201107813>
- Abrahamson, M. J., Wong, J. W., & Bommaris, A. S. (2013). The Evolution of an Amine Dehydrogenase Biocatalyst for the Asymmetric Production of Chiral Amines. *Advanced Synthesis & Catalysis*, 355(9), 1780–1786. <https://doi.org/10.1002/adsc.201201030>
- Alcántara, A. R., Domínguez de María, P., Littlechild, J. A., Schürmann, M., Sheldon, R. A., & Wohlgemuth, R. (2022). Biocatalysis as Key to Sustainable Industrial Chemistry. *ChemSusChem*, 15(9). <https://doi.org/10.1002/cssc.202102709>

- Almrud, J. J., Oliveira, M. A., Kern, A. D., Grishin, N. V., Phillips, M. A., & Hackert, M. L. (2000). Crystal structure of human ornithine decarboxylase at 2.1 Å resolution: structural insights to antizyme binding. *Journal of Molecular Biology*, 295(1), 7–16. <https://doi.org/10.1006/jmbi.1999.3331>
- Andréll, J., Hicks, M. G., Palmer, T., Carpenter, E. P., Iwata, S., & Maher, M. J. (2009). Crystal Structure of the Acid-Induced Arginine Decarboxylase from *Escherichia coli*: Reversible Decamer Assembly Controls Enzyme Activity. *Biochemistry*, 48(18), 3915–3927. <https://doi.org/10.1021/bi900075d>
- Anwar, S., Mohammad, T., Shamsi, A., Queen, A., Parveen, S., Luqman, S., Hasan, G. M., Alamry, K. A., Azum, N., Asiri, A. M., & Hassan, M. I. (2020). Discovery of hordenine as a potential inhibitor of pyruvate dehydrogenase kinase 3: Implication in lung cancer therapy. *Biomedicines*, 8(5), 32–228.
- Asano, Y., Nakazawa, A., & Endo, K. (1987). Novel phenylalanine dehydrogenases from *Sporosarcina ureae* and *Bacillus sphaericus*. Purification and characterization. *The Journal of Biological Chemistry*, 262(21), 10346–10354. <http://www.ncbi.nlm.nih.gov/pubmed/3112142>
- Báez, J. L., Bolívar, F., & Gosset, G. (2001). Determination of 3-deoxy-D- *arabino* -heptulosonate 7-phosphate productivity and yield from glucose in *Escherichia coli* devoid of the glucose phosphotransferase transport system. *Biotechnology and Bioengineering*, 73(6), 530–535. <https://doi.org/10.1002/bit.1088>
- Bai, Z., Sun, X., Yu, X., & Li, L. (2019). Chitosan Microbeads as Supporter for *Pseudomonas putida* with Surface Displayed Laccases for Decolorization of Synthetic Dyes. *Applied Sciences*, 9(1), 138. <https://doi.org/10.3390/app9010138>
- Baker, P. J., Turnbull, A. P., Sedelnikova, S. E., Stillman, T. J., & Rice, D. W. (1995). A role for quaternary structure in the substrate specificity of leucine dehydrogenase. *Structure*, 3(7), 693–705. [https://doi.org/10.1016/S0969-2126\(01\)00204-0](https://doi.org/10.1016/S0969-2126(01)00204-0)
- Barwell, C. J., Basma, A. N., Lafi, M. A. K., & Leake, L. D. (2011). Deamination of hordenine by monoamine oxidase and its action on vasa deferentia of the rat. *Journal of Pharmacy and Pharmacology*, 41(6), 421–423. <https://doi.org/10.1111/j.2042-7158.1989.tb06492.x>
- Bell, E. L., Finnigan, W., France, S. P., Green, A. P., Hayes, M. A., Hepworth, L. J., Lovelock, S. L., Niihura, H., Osuna, S., Romero, E., Ryan, K. S., Turner, N. J., & Flitsch, S. L. (2021). Biocatalysis. *Nature Reviews Methods Primers*, 1(1), 46. <https://doi.org/10.1038/s43586-021-00044-z>
- Benítez-Mateos, A. I., Roura Padrosa, D., & Paradisi, F. (2022). Multistep enzyme cascades as a route towards green and sustainable pharmaceutical syntheses. *Nature Chemistry*, 14(5), 489–499. <https://doi.org/10.1038/s41557-022-00931-2>
- Bennett, M., Ducrot, L., Vergne-Vaxelaire, C., & Grogan, G. (2022). Structure and Mutation of the Native Amine Dehydrogenase MATOUAmDH2. *ChemBioChem*, 23(10). <https://doi.org/10.1002/cbic.202200136>
- Berridge, M. V., Herst, P. M., & Tan, A. S. (2005). *Tetrazolium dyes as tools in cell biology: New insights into their cellular reduction* (pp. 127–152). [https://doi.org/10.1016/S1387-2656\(05\)11004-7](https://doi.org/10.1016/S1387-2656(05)11004-7)

- Bertelli, M., Kiani, A. K., Paolacci, S., Manara, E., Kurti, D., Dhuli, K., Bushati, V., Miertus, J., Pangallo, D., Baglivo, M., Beccari, T., & Michelini, S. (2020). Hydroxytyrosol: A natural compound with promising pharmacological activities. *Journal of Biotechnology*, *309*, 29–33. <https://doi.org/10.1016/j.jbiotec.2019.12.016>
- Bhatia, S. K., Kim, Y. H., Kim, H. J., Seo, H.-M., Kim, J.-H., Song, H.-S., Sathiyarayanan, G., Park, S.-H., Park, K., & Yang, Y.-H. (2015). Biotransformation of lysine into cadaverine using barium alginate-immobilized *Escherichia coli* overexpressing CadA. *Bioprocess and Biosystems Engineering*, *38*(12), 2315–2322. <https://doi.org/10.1007/s00449-015-1465-9>
- Bloch, D. N., Sandre, M., Ben Zichri, S., Masato, A., Kolusheva, S., Bubacco, L., & Jelinek, R. (2023). Scavenging neurotoxic aldehydes using lysine carbon dots. *Nanoscale Advances*, *5*(5), 1356–1367. <https://doi.org/10.1039/D2NA00804A>
- Böhmer, W., Knaus, T., & Mutti, F. G. (2018a). Hydrogen-Borrowing Alcohol Bioamination with Coimmobilized Dehydrogenases. *ChemCatChem*, *10*(4), 731–735. <https://doi.org/10.1002/cctc.201701366>
- Böhmer, W., Knaus, T., & Mutti, F. G. (2018b). Hydrogen-Borrowing Alcohol Bioamination with Coimmobilized Dehydrogenases. *ChemCatChem*, *10*(4), 731–735. <https://doi.org/10.1002/cctc.201701366>
- Cai, R.-F., Liu, L., Chen, F.-F., Li, A., Xu, J.-H., & Zheng, G.-W. (2020). Reductive Amination of Biobased Levulinic Acid to Unnatural Chiral γ -Amino Acid Using an Engineered Amine Dehydrogenase. *ACS Sustainable Chemistry & Engineering*, *8*(46), 17054–17061. <https://doi.org/10.1021/acssuschemeng.0c04647>
- Caparco, A. A., Bommarius, B. R., Bommarius, A. S., & Champion, J. A. (2020). Protein-inorganic calcium-phosphate supraparticles as a robust platform for enzyme co-immobilization. *Biotechnology and Bioengineering*, *117*(7), 1979–1989. <https://doi.org/10.1002/bit.27348>
- Caparco, A. A., Pelletier, E., Petit, J. L., Jouenne, A., Bommarius, B. R., Berardinis, V., Zapparucha, A., Champion, J. A., Bommarius, A. S., & Vergne-Vaxelaire, C. (2020). Metagenomic Mining for Amine Dehydrogenase Discovery. *Advanced Synthesis & Catalysis*, *362*(12), 2427–2436. <https://doi.org/10.1002/adsc.202000094>
- Capitani, G. (2003). Crystal structure and functional analysis of *Escherichia coli* glutamate decarboxylase. *The EMBO Journal*, *22*(16), 4027–4037. <https://doi.org/10.1093/emboj/cdg403>
- Cerioli, L., Planchestainer, M., Cassidy, J., Tessaro, D., & Paradisi, F. (2015). Characterization of a novel amine transaminase from *Halomonas elongata*. *Journal of Molecular Catalysis B: Enzymatic*, *120*, 141–150. <https://doi.org/10.1016/j.molcatb.2015.07.009>
- Chen, W., Yao, J., Meng, J., Han, W., Tao, Y., Chen, Y., Guo, Y., Shi, G., He, Y., Jin, J.-M., & Tang, S.-Y. (2019). Promiscuous enzymatic activity-aided multiple-pathway network design for metabolic flux rearrangement in hydroxytyrosol biosynthesis. *Nature Communications*, *10*(1), 960. <https://doi.org/10.1038/s41467-019-08781-2>
- Claes, L., Janssen, M., & De Vos, D. E. (2019). Organocatalytic Decarboxylation of Amino Acids as a Route to Bio-based Amines and Amides. *ChemCatChem*, *11*(17), 4297–4306. <https://doi.org/10.1002/cctc.201900800>

- Contente, M. L., & Paradisi, F. (2018). Self-sustaining closed-loop multienzyme-mediated conversion of amines into alcohols in continuous reactions. *Nature Catalysis*, *1*(6), 452–459. <https://doi.org/10.1038/s41929-018-0082-9>
- Cosenza, V. A., Navarro, D. A., & Stortz, C. A. (2011). Usage of α -picoline borane for the reductive amination of carbohydrates. *Arkivoc*, *2011*(7), 182–194. <https://doi.org/10.3998/ark.5550190.0012.716>
- Coyle, J. P., Johnson, C., Jensen, J., Farcas, M., Derk, R., Stueckle, T. A., Kornberg, T. G., Rojanasakul, Y., & Rojanasakul, L. W. (2023). Variation in pentose phosphate pathway-associated metabolism dictates cytotoxicity outcomes determined by tetrazolium reduction assays. *Scientific Reports*, *13*(1), 8220. <https://doi.org/10.1038/s41598-023-35310-5>
- DiCosimo, R., McAuliffe, J., Poulouse, A. J., & Bohlmann, G. (2013). Industrial use of immobilized enzymes. *Chemical Society Reviews*, *42*(15), 6437. <https://doi.org/10.1039/c3cs35506c>
- Ducrot, L., Bennett, M., André-Leroux, G., Elisée, E., Marynberg, S., Fossey-Jouenne, A., Zaparucha, A., Grogan, G., & Vergne-Vaxelaire, C. (2022). Expanding the Substrate Scope of Native Amine Dehydrogenases through *In Silico* Structural Exploration and Targeted Protein Engineering. *ChemCatChem*, *14*(22). <https://doi.org/10.1002/cctc.202200880>
- Ducrot, L., Bennett, M., Caparco, A. A., Champion, J. A., Bommarius, A. S., Zaparucha, A., Grogan, G., & Vergne-Vaxelaire, C. (2021). Biocatalytic Reductive Amination by Native Amine Dehydrogenases to Access Short Chiral Alkyl Amines and Amino Alcohols. *Frontiers in Catalysis*, *1*. <https://doi.org/10.3389/fctls.2021.781284>
- Eliot, A. C., & Kirsch, J. F. (2004). Pyridoxal Phosphate Enzymes: Mechanistic, Structural, and Evolutionary Considerations. *Annual Review of Biochemistry*, *73*(1), 383–415. <https://doi.org/10.1146/annurev.biochem.73.011303.074021>
- Eller, K., Henkes, E., Rossbacher, R., & Höke, H. (2000). Amines, Aliphatic. In *Ullmann's Encyclopedia of Industrial Chemistry*. Wiley-VCH Verlag GmbH & Co. KGaA. https://doi.org/10.1002/14356007.a02_001
- Escalante, A., Calderón, R., Valdivia, A., de Anda, R., Hernández, G., Ramírez, O. T., Gosset, G., & Bolívar, F. (2010). Metabolic engineering for the production of shikimic acid in an evolved *Escherichia coli* strain lacking the phosphoenolpyruvate: carbohydrate phosphotransferase system. *Microbial Cell Factories*, *9*(1), 21. <https://doi.org/10.1186/1475-2859-9-21>
- Foor, F., Morin, N., & Bostian, K. A. (1993). Production of L-dihydroxyphenylalanine in *Escherichia coli* with the tyrosine phenol-lyase gene cloned from *Erwinia herbicola*. *Applied and Environmental Microbiology*, *59*(9), 3070–3075. <https://doi.org/10.1128/aem.59.9.3070-3075.1993>
- Fordjour, E., Adipah, F. K., Zhou, S., Du, G., & Zhou, J. (2019). Metabolic engineering of *Escherichia coli* BL21 (DE3) for de novo production of l-DOPA from d-glucose. *Microbial Cell Factories*, *18*(1). <https://doi.org/10.1186/s12934-019-1122-0>
- Franklin, R. D., Whitley, J. A., Caparco, A. A., Bommarius, B. R., Champion, J. A., & Bommarius, A. S. (2021). Continuous production of a chiral amine in a packed bed reactor with co-immobilized amine dehydrogenase and formate dehydrogenase. *Chemical Engineering Journal*, *407*, 127065. <https://doi.org/10.1016/j.cej.2020.127065>

- Froidevaux, V., Negrell, C., Caillol, S., Pascault, J.-P., & Boutevin, B. (2016). Biobased Amines: From Synthesis to Polymers; Present and Future. *Chemical Reviews*, *116*(22), 14181–14224. <https://doi.org/10.1021/acs.chemrev.6b00486>
- Garg, R. P., Ma, Y., Hoyt, J. C., & Parry, R. J. (2002a). Molecular characterization and analysis of the biosynthetic gene cluster for the azoxy antibiotic valanimycin. *Molecular Microbiology*, *46*(2), 505–517. <https://doi.org/10.1046/j.1365-2958.2002.03169.x>
- Garg, R. P., Ma, Y., Hoyt, J. C., & Parry, R. J. (2002b). Molecular characterization and analysis of the biosynthetic gene cluster for the azoxy antibiotic valanimycin. *Molecular Microbiology*, *46*(2), 505–517. <https://doi.org/10.1046/j.1365-2958.2002.03169.x>
- Ghislieri, D., & Turner, N. J. (2014). Biocatalytic Approaches to the Synthesis of Enantiomerically Pure Chiral Amines. *Topics in Catalysis*, *57*(5), 284–300. <https://doi.org/10.1007/s11244-013-0184-1>
- Gianolio, S., Roura Padrosa, D., & Paradisi, F. (2022). Combined chemoenzymatic strategy for sustainable continuous synthesis of the natural product hordenine. *Green Chemistry*, *24*(21), 8434–8440. <https://doi.org/10.1039/D2GC02767D>
- Giardina, G., Montioli, R., Gianni, S., Cellini, B., Paiardini, A., Voltattorni, C. B., & Cutruzzolà, F. (2011). Open conformation of human DOPA decarboxylase reveals the mechanism of PLP addition to Group II decarboxylases. *Proceedings of the National Academy of Sciences*, *108*(51), 20514–20519. <https://doi.org/10.1073/pnas.1111456108>
- Gong, X., Tao, J., Wang, Y., Wu, J., An, J., Meng, J., Wang, X., Chen, Y., & Zou, J. (2021). Total barley maiya alkaloids inhibit prolactin secretion by acting on dopamine D2 receptor and protein kinase A targets. *Journal of Ethnopharmacology*, *273*, 113994. <https://doi.org/10.1016/j.jep.2021.113994>
- Gosset, G., Yong-Xiao, J., & Berry, A. (1996). A direct comparison of approaches for increasing carbon flow to aromatic biosynthesis in *Escherichia coli*. *Journal of Industrial Microbiology*, *17*(1), 47–52. <https://doi.org/10.1007/BF01570148>
- Guisán, José M. (1988). Aldehyde-agarose gels as activated supports for immobilization-stabilization of enzymes. *Enzyme and Microbial Technology*, *10*(6), 375–382. [https://doi.org/10.1016/0141-0229\(88\)90018-X](https://doi.org/10.1016/0141-0229(88)90018-X)
- Guo, K., Ji, C., & Li, L. (2007). Stable-Isotope Dimethylation Labeling Combined with LC-ESI MS for Quantification of Amine-Containing Metabolites in Biological Samples. *Analytical Chemistry*, *79*(22), 8631–8638. <https://doi.org/10.1021/ac0704356>
- Guo, Z., Yan, N., & Lapkin, A. A. (2019). Towards circular economy: integration of bio-waste into chemical supply chain. *Current Opinion in Chemical Engineering*, *26*, 148–156. <https://doi.org/10.1016/j.coche.2019.09.010>
- Gupte, A. P., Basaglia, M., Casella, S., & Favaro, L. (2022). Rice waste streams as a promising source of biofuels: feedstocks, biotechnologies and future perspectives. *Renewable and Sustainable Energy Reviews*, *167*, 112673. <https://doi.org/10.1016/j.rser.2022.112673>
- Gut, H., Pennacchiotti, E., John, R. A., Bossa, F., Capitani, G., De Biase, D., & Grütter, M. G. (2006). *Escherichia coli* acid resistance: pH-sensing, activation by chloride and

- autoinhibition in GadB. *The EMBO Journal*, 25(11), 2643–2651.
<https://doi.org/10.1038/sj.emboj.7601107>
- H. Orrego, A., Romero-Fernández, M., Millán-Linares, M., Yust, M., Guisán, J., & Rocha-Martin, J. (2018). Stabilization of Enzymes by Multipoint Covalent Attachment on Aldehyde-Supports: 2-Picoline Borane as an Alternative Reducing Agent. *Catalysts*, 8(8), 333.
<https://doi.org/10.3390/catal8080333>
- Hamid, M. H. S. A., Slatford, P. A., & Williams, J. M. J. (2007). Borrowing Hydrogen in the Activation of Alcohols. *Advanced Synthesis & Catalysis*, 349(10), 1555–1575.
<https://doi.org/10.1002/adsc.200600638>
- Hapke, H. J., & Strathmann, W. (1995). [Pharmacological effects of hordenine]. *DTW. Deutsche Tierärztliche Wochenschrift*, 102(6), 228–232.
<http://www.ncbi.nlm.nih.gov/pubmed/8582256>
- Harper, B. A., Barbut, S., Lim, L.-T., & Marcone, M. F. (2014). Effect of Various Gelling Cations on the Physical Properties of “Wet” Alginate Films. *Journal of Food Science*, 79(4), E562–E567.
<https://doi.org/10.1111/1750-3841.12376>
- Heckmann, C. M., Gourlay, L. J., Dominguez, B., & Paradisi, F. (2020). An (R)-Selective Transaminase From *Thermomyces stellatus*: Stabilizing the Tetrameric Form. *Frontiers in Bioengineering and Biotechnology*, 8. <https://doi.org/10.3389/fbioe.2020.00707>
- Heffter, A. (1898). Ueber Pellote. *Archiv Für Experimentelle Pathologie Und Pharmakologie*, 40(5–6), 385–429. <https://doi.org/10.1007/BF01825267>
- Heydari, M., Ohshima, T., Nunoura-Kominato, N., & Sakuraba, H. (2004). Highly Stable Lysine 6-Dehydrogenase from the Thermophile *Geobacillus stearothermophilus* Isolated from a Japanese Hot Spring: Characterization, Gene Cloning and Sequencing, and Expression. *Applied and Environmental Microbiology*, 70(2), 937–942.
<https://doi.org/10.1128/AEM.70.2.937-942.2004>
- Holbrook, O. T., Molligoda, B., Bushell, K. N., & Gobrogge, K. L. (2022). Behavioral consequences of the downstream products of ethanol metabolism involved in alcohol use disorder. *Neuroscience & Biobehavioral Reviews*, 133, 104501.
<https://doi.org/10.1016/j.neubiorev.2021.12.024>
- Houwman, J. A., Knaus, T., Costa, M., & Mutti, F. G. (2019). Efficient synthesis of enantiopure amines from alcohols using resting *E. coli* cells and ammonia. *Green Chemistry*, 21(14), 3846–3857. <https://doi.org/10.1039/C9GC01059A>
- Huang, J., Mei, L., Wu, H., & Lin, D. (2007). Biosynthesis of γ -aminobutyric acid (GABA) using immobilized whole cells of *Lactobacillus brevis*. *World Journal of Microbiology and Biotechnology*, 23(6), 865–871. <https://doi.org/10.1007/s11274-006-9311-5>
- Huang, R., Chen, H., Zhong, C., Kim, J. E., & Zhang, Y.-H. P. (2016). High-Throughput Screening of Coenzyme Preference Change of Thermophilic 6-Phosphogluconate Dehydrogenase from NADP⁺ to NAD⁺. *Scientific Reports*, 6(1), 32644. <https://doi.org/10.1038/srep32644>
- Hwang, E. T., & Lee, S. (2019). Multienzymatic Cascade Reactions via Enzyme Complex by Immobilization. *ACS Catalysis*, 9(5), 4402–4425. <https://doi.org/10.1021/acscatal.8b04921>

- Jackson, D. M., Ashley, R. L., Brownfield, C. B., Morrison, D. R., & Morrison, R. W. (2015). Rapid Conventional and Microwave-Assisted Decarboxylation of L-Histidine and Other Amino Acids via Organocatalysis with R-Carvone Under Superheated Conditions. *Synthetic Communications*, 45(23), 2691–2700. <https://doi.org/10.1080/00397911.2015.1100745>
- Jansonius, J. N. (1998). Structure, evolution and action of vitamin B6-dependent enzymes. *Current Opinion in Structural Biology*, 8(6), 759–769. [https://doi.org/10.1016/S0959-440X\(98\)80096-1](https://doi.org/10.1016/S0959-440X(98)80096-1)
- Jeon, H., Yoon, S., Ahsan, M., Sung, S., Kim, G.-H., Sundaramoorthy, U., Rhee, S.-K., & Yun, H. (2017). The Kinetic Resolution of Racemic Amines Using a Whole-Cell Biocatalyst Co-Expressing Amine Dehydrogenase and NADH Oxidase. *Catalysts*, 7(9), 251. <https://doi.org/10.3390/catal7090251>
- Jiang, M., Xu, G., Ni, J., Zhang, K., Dong, J., Han, R., & Ni, Y. (2019a). Improving Soluble Expression of Tyrosine Decarboxylase from *Lactobacillus brevis* for Tyramine Synthesis with High Total Turnover Number. *Applied Biochemistry and Biotechnology*, 188(2), 436–449. <https://doi.org/10.1007/s12010-018-2925-x>
- Jiang, M., Xu, G., Ni, J., Zhang, K., Dong, J., Han, R., & Ni, Y. (2019b). Improving Soluble Expression of Tyrosine Decarboxylase from *Lactobacillus brevis* for Tyramine Synthesis with High Total Turnover Number. *Applied Biochemistry and Biotechnology*, 188(2), 436–449. <https://doi.org/10.1007/s12010-018-2925-x>
- Jones, J. A., Collins, S. M., Vernacchio, V. R., Lachance, D. M., & Koffas, M. A. G. (2016). Optimization of naringenin and *p*-coumaric acid hydroxylation using the native *E. coli* hydroxylase complex, HpaBC. *Biotechnology Progress*, 32(1), 21–25. <https://doi.org/10.1002/btpr.2185>
- Khorsand, F., Murphy, C. D., Whitehead, A. J., & Engel, P. C. (2017). Biocatalytic stereoinversion of *p*-para-bromophenylalanine in a one-pot three-enzyme reaction. *Green Chemistry*, 19(2), 503–510. <https://doi.org/10.1039/C6GC01922F>
- Kim, Baritugo, Oh, Kang, Jung, Jang, Song, Kim, Lee, Hwang, Park, Park, & Joo. (2019). High-Level Conversion of L-lysine into Cadaverine by *Escherichia coli* Whole Cell Biocatalyst Expressing *Hafnia alvei* L-lysine Decarboxylase. *Polymers*, 11(7), 1184. <https://doi.org/10.3390/polym11071184>
- Kim, D. I., Chae, T. U., Kim, H. U., Jang, W. D., & Lee, S. Y. (2021). Microbial production of multiple short-chain primary amines via retrobiosynthesis. *Nature Communications*, 12(1), 173. <https://doi.org/10.1038/s41467-020-20423-6>
- Kim, S.-C., Lee, J.-H., Kim, M.-H., Lee, J.-A., Kim, Y. B., Jung, E., Kim, Y.-S., Lee, J., & Park, D. (2013). Hordenine, a single compound produced during barley germination, inhibits melanogenesis in human melanocytes. *Food Chemistry*, 141(1), 174–181. <https://doi.org/10.1016/j.foodchem.2013.03.017>
- Knaus, T., Böhmer, W., & Mutti, F. G. (2017). Amine dehydrogenases: efficient biocatalysts for the reductive amination of carbonyl compounds. *Green Chemistry*, 19(2), 453–463. <https://doi.org/10.1039/C6GC01987K>

- Knowles, W. S. (n.d.). Asymmetric Hydrogenations– The MonsantoL-Dopa Process. In *Asymmetric Catalysis on Industrial Scale* (pp. 21–38). Wiley-VCH Verlag GmbH & Co. KGaA. <https://doi.org/10.1002/3527602151.ch1>
- Komori, H., Nitta, Y., Ueno, H., & Higuchi, Y. (2012). Structural Study Reveals That Ser-354 Determines Substrate Specificity on Human Histidine Decarboxylase. *Journal of Biological Chemistry*, *287*(34), 29175–29183. <https://doi.org/10.1074/jbc.M112.381897>
- Kugler, P. (1979). A gel-sandwich technique for the qualitative and quantitative determination of dehydrogenases in the enzyme histochemistry. *Histochemistry*, *60*(3), 265–293. <https://doi.org/10.1007/BF00500656>
- Kumar, R., Vikramachakravarthi, D., & Pal, P. (2014). Production and purification of glutamic acid: A critical review towards process intensification. *Chemical Engineering and Processing: Process Intensification*, *81*, 59–71. <https://doi.org/10.1016/j.cep.2014.04.012>
- Kurpejović, E., Wendisch, V. F., & Sariyar Akbulut, B. (2021). Tyrosinase-based production of L-DOPA by *Corynebacterium glutamicum*. *Applied Microbiology and Biotechnology*, *105*(24), 9103–9111. <https://doi.org/10.1007/s00253-021-11681-5>
- Lapponi, M. J., Méndez, M. B., Trelles, J. A., & Rivero, C. W. (2022). Cell immobilization strategies for biotransformations. *Current Opinion in Green and Sustainable Chemistry*, *33*, 100565. <https://doi.org/10.1016/j.cogsc.2021.100565>
- Lawrence, S. A. (2004). *Amines: synthesis, properties and applications*. Cambridge University Press.
- Lee, J., Michael, A. J., Martynowski, D., Goldsmith, E. J., & Phillips, M. A. (2007). Phylogenetic Diversity and the Structural Basis of Substrate Specificity in the β/α -Barrel Fold Basic Amino Acid Decarboxylases. *Journal of Biological Chemistry*, *282*(37), 27115–27125. <https://doi.org/10.1074/jbc.M704066200>
- Lee, S. Y., Kim, H. U., Chae, T. U., Cho, J. S., Kim, J. W., Shin, J. H., Kim, D. I., Ko, Y.-S., Jang, W. D., & Jang, Y.-S. (2019). A comprehensive metabolic map for production of bio-based chemicals. *Nature Catalysis*, *2*(1), 18–33. <https://doi.org/10.1038/s41929-018-0212-4>
- Leuchtenberger, W., Huthmacher, K., & Drauz, K. (2005). Biotechnological production of amino acids and derivatives: current status and prospects. *Applied Microbiology and Biotechnology*, *69*(1), 1–8. <https://doi.org/10.1007/s00253-005-0155-y>
- Li, N., Chou, H., & Xu, Y. (2016). Improved cadaverine production from mutant *Klebsiella oxytoca* lysine decarboxylase. *Engineering in Life Sciences*, *16*(3), 299–305. <https://doi.org/10.1002/elsc.201500037>
- Liu, G., Zhou, N., Zhang, M., Li, S., Tian, Q., Chen, J., Chen, B., Wu, Y., & Yao, S. (2010). Hydrophobic solvent induced phase transition extraction to extract drugs from plasma for high performance liquid chromatography–mass spectrometric analysis. *Journal of Chromatography A*, *1217*(3), 243–249. <https://doi.org/10.1016/j.chroma.2009.11.037>
- Liu, J., Pang, B. Q. W., Adams, J. P., Snajdrova, R., & Li, Z. (2017). Coupled Immobilized Amine Dehydrogenase and Glucose Dehydrogenase for Asymmetric Synthesis of Amines by Reductive Amination with Cofactor Recycling. *ChemCatChem*, *9*(3), 425–431. <https://doi.org/10.1002/cctc.201601446>

- Liu, Y., Liu, P., Gao, S., Wang, Z., Luan, P., González-Sabín, J., & Jiang, Y. (2021). Construction of chemoenzymatic cascade reactions for bridging chemocatalysis and Biocatalysis: Principles, strategies and prospective. *Chemical Engineering Journal*, *420*, 127659. <https://doi.org/10.1016/j.cej.2020.127659>
- Ma, J., Wang, S., Huang, X., Geng, P., Wen, C., Zhou, Y., Yu, L., & Wang, X. (2015). Validated UPLC–MS/MS method for determination of hordenine in rat plasma and its application to pharmacokinetic study. *Journal of Pharmaceutical and Biomedical Analysis*, *111*, 131–137. <https://doi.org/10.1016/j.jpba.2015.03.032>
- Mateo, C., Grazú, V., Pessela, B. C. C., Montes, T., Palomo, J. M., Torres, R., López-Gallego, F., Fernández-Lafuente, R., & Guisán, J. M. (2007a). Advances in the design of new epoxy supports for enzyme immobilization–stabilization. *Biochemical Society Transactions*, *35*(6), 1593–1601. <https://doi.org/10.1042/BST0351593>
- Mateo, C., Grazú, V., Pessela, B. C. C., Montes, T., Palomo, J. M., Torres, R., López-Gallego, F., Fernández-Lafuente, R., & Guisán, J. M. (2007b). Advances in the design of new epoxy supports for enzyme immobilization–stabilization. *Biochemical Society Transactions*, *35*(6), 1593–1601. <https://doi.org/10.1042/BST0351593>
- Mayol, O., Bastard, K., Beloti, L., Frese, A., Turkenburg, J. P., Petit, J.-L., Mariage, A., Debard, A., Pellouin, V., Perret, A., de Berardinis, V., Zaparucha, A., Grogan, G., & Vergne-Vaxelaire, C. (2019a). A family of native amine dehydrogenases for the asymmetric reductive amination of ketones. *Nature Catalysis*, *2*(4), 324–333. <https://doi.org/10.1038/s41929-019-0249-z>
- Mayol, O., Bastard, K., Beloti, L., Frese, A., Turkenburg, J. P., Petit, J.-L., Mariage, A., Debard, A., Pellouin, V., Perret, A., de Berardinis, V., Zaparucha, A., Grogan, G., & Vergne-Vaxelaire, C. (2019b). A family of native amine dehydrogenases for the asymmetric reductive amination of ketones. *Nature Catalysis*, *2*(4), 324–333. <https://doi.org/10.1038/s41929-019-0249-z>
- Meyer, E. (1982). Separation of two distinct S-adenosylmethionine dependent N-methyltransferases involved in hordenine biosynthesis in *Hordeum vulgare*. *Plant Cell Reports*, *1*(6), 236–239. <https://doi.org/10.1007/BF00272627>
- Mi, J., Liu, S., Du, Y., Qi, H., & Zhang, L. (2022). Cofactor self-sufficient by co-immobilization of pyridoxal 5'-phosphate and lysine decarboxylase for cadaverine production. *Bioresource Technology Reports*, *17*, 100939. <https://doi.org/10.1016/j.biteb.2021.100939>
- Montgomery, S. L., Mangas-Sanchez, J., Thompson, M. P., Aleku, G. A., Dominguez, B., & Turner, N. J. (2017). Direct Alkylation of Amines with Primary and Secondary Alcohols through Biocatalytic Hydrogen Borrowing. *Angewandte Chemie*, *129*(35), 10627–10630. <https://doi.org/10.1002/ange.201705848>
- Mørch, Y. A., Donati, I., Strand, B. L., & Skjåk-Bræk, G. (2006). Effect of Ca²⁺, Ba²⁺, and Sr²⁺ on Alginate Microbeads. *Biomacromolecules*, *7*(5), 1471–1480. <https://doi.org/10.1021/bm060010d>
- Muñoz, A. J., Hernández-Chávez, G., De Anda, R., Martínez, A., Bolívar, F., & Gosset, G. (2011). Metabolic engineering of *Escherichia coli* for improving l-3,4-dihydroxyphenylalanine (l-DOPA) synthesis from glucose. *Journal of Industrial Microbiology and Biotechnology*, *38*(11), 1845–1852. <https://doi.org/10.1007/s10295-011-0973-0>

- Mutti, F. G., & Knaus, T. (2021). Enzymes Applied to the Synthesis of Amines. In *Biocatalysis for Practitioners* (pp. 143–180). Wiley. <https://doi.org/10.1002/9783527824465.ch6>
- Mutti, F. G., Knaus, T., Scrutton, N. S., Breuer, M., & Turner, N. J. (2015). Conversion of alcohols to enantiopure amines through dual-enzyme hydrogen-borrowing cascades. *Science*, *349*(6255), 1525–1529. <https://doi.org/10.1126/science.aac9283>
- Nakai, T., Nakagawa, N., Maoka, N., Masui, R., Kuramitsu, S., & Kamiya, N. (2005). Structure of P-protein of the glycine cleavage system: implications for nonketotic hyperglycinemia. *The EMBO Journal*, *24*(8), 1523–1536. <https://doi.org/10.1038/sj.emboj.7600632>
- Narisetty, V., Cox, R., Bommareddy, R., Agrawal, D., Ahmad, E., Pant, K. K., Chandel, A. K., Bhatia, S. K., Kumar, D., Binod, P., Gupta, V. K., & Kumar, V. (2022). Valorisation of xylose to renewable fuels and chemicals, an essential step in augmenting the commercial viability of lignocellulosic biorefineries. *Sustainable Energy & Fuels*, *6*(1), 29–65. <https://doi.org/10.1039/D1SE00927C>
- Nasri, M. (2017a). *Protein Hydrolysates and Biopeptides* (pp. 109–159). <https://doi.org/10.1016/bs.afnr.2016.10.003>
- Nasri, M. (2017b). *Protein Hydrolysates and Biopeptides* (pp. 109–159). <https://doi.org/10.1016/bs.afnr.2016.10.003>
- Natte, K., Neumann, H., Jagadeesh, R. v., & Beller, M. (2017). Convenient iron-catalyzed reductive aminations without hydrogen for selective synthesis of N-methylamines. *Nature Communications*, *8*(1), 1344. <https://doi.org/10.1038/s41467-017-01428-0>
- Nguyen, N. H., Truong-Thi, N.-H., Nguyen, D. T. D., Ching, Y. C., Huynh, N. T., & Nguyen, D. H. (2022). Non-ionic surfactants As co-templates to control the mesopore diameter of hollow mesoporous silica nanoparticles for drug delivery applications. *Colloids and Surfaces A: Physicochemical and Engineering Aspects*, *655*, 130218. <https://doi.org/10.1016/j.colsurfa.2022.130218>
- Ohta, H., Murakami, Y., Takebe, Y., Murasaki, K., Oshima, K., Yoshihara, H., & Morimura, S. (2020). <i>N</i>-Methyltyramine, a Gastrin-releasing Factor in Beer, and Structurally Related Compounds as Agonists for Human Trace Amine-associated Receptor 1. *Food Science and Technology Research*, *26*(2), 313–317. <https://doi.org/10.3136/fstr.26.313>
- PARADISI, F., COLLINS, S., MAGUIRE, A., & ENGEL, P. (2007). Phenylalanine dehydrogenase mutants: Efficient biocatalysts for synthesis of non-natural phenylalanine derivatives. *Journal of Biotechnology*, *128*(2), 408–411. <https://doi.org/10.1016/j.jbiotec.2006.08.008>
- Park, J.-Y., Choi, M.-J., Yu, H., Choi, Y., Park, K.-M., & Chang, P.-S. (2022). Multi-functional behavior of food emulsifier erythorbyl laurate in different colloidal conditions of homogeneous oil-in-water emulsion system. *Colloids and Surfaces A: Physicochemical and Engineering Aspects*, *636*, 128127. <https://doi.org/10.1016/j.colsurfa.2021.128127>
- Park, S. H., Soetyono, F., & Kim, H. K. (2017). Cadaverine Production by Using Cross-Linked Enzyme Aggregate of Escherichia coli Lysine Decarboxylase. *Journal of Microbiology and Biotechnology*, *27*(2), 289–296. <https://doi.org/10.4014/jmb.1608.08033>

- Patil, M. D., Grogan, G., Bommarius, A., & Yun, H. (2018). Oxidoreductase-Catalyzed Synthesis of Chiral Amines. *ACS Catalysis*, *8*(12), 10985–11015. <https://doi.org/10.1021/acscatal.8b02924>
- Patil, M. D., Yoon, S., Jeon, H., Khobragade, T. P., Sarak, S., Pagar, A. D., Won, Y., & Yun, H. (2019). Kinetic Resolution of Racemic Amines to Enantiopure (S)-amines by a Biocatalytic Cascade Employing Amine Dehydrogenase and Alanine Dehydrogenase. *Catalysts*, *9*(7), 600. <https://doi.org/10.3390/catal9070600>
- Payne, J. T., Valentic, T. R., & Smolke, C. D. (2021). Complete biosynthesis of the bisbenzylisoquinoline alkaloids guattegaumerine and berbaminine in yeast. *Proceedings of the National Academy of Sciences*, *118*(51). <https://doi.org/10.1073/pnas.2112520118>
- Pelckmans, M., Renders, T., Van de Vyver, S., & Sels, B. F. (2017). Bio-based amines through sustainable heterogeneous catalysis. *Green Chemistry*, *19*(22), 5303–5331. <https://doi.org/10.1039/C7GC02299A>
- Pilkington, R. L., Dallaston, M. A., Savage, G. P., Williams, C. M., & Polyzos, A. (2021). Enone-promoted decarboxylation of *trans*-4-hydroxy-*l*-proline in flow: a side-by-side comparison to batch. *Reaction Chemistry & Engineering*, *6*(3), 486–493. <https://doi.org/10.1039/D0RE00442A>
- Planchestainer, M., Hegarty, E., Heckmann, C. M., Gourlay, L. J., & Paradisi, F. (2019). Widely applicable background depletion step enables transaminase evolution through solid-phase screening. *Chemical Science*, *10*(23), 5952–5958. <https://doi.org/10.1039/C8SC05712E>
- Prieto, M. A., & Garcia, J. L. (1994). Molecular characterization of 4-hydroxyphenylacetate 3-hydroxylase of *Escherichia coli*. A two-protein component enzyme. *Journal of Biological Chemistry*, *269*(36), 22823–22829. [https://doi.org/10.1016/S0021-9258\(17\)31719-2](https://doi.org/10.1016/S0021-9258(17)31719-2)
- Pyne, M. E., Kevvai, K., Grewal, P. S., Narcross, L., Choi, B., Bourgeois, L., Dueber, J. E., & Martin, V. J. J. (2020). A yeast platform for high-level synthesis of tetrahydroisoquinoline alkaloids. *Nature Communications*, *11*(1), 3337. <https://doi.org/10.1038/s41467-020-17172-x>
- Quaglia, D., Irwin, J. A., & Paradisi, F. (2012a). Horse Liver Alcohol Dehydrogenase: New Perspectives for an Old Enzyme. *Molecular Biotechnology*, *52*(3), 244–250. <https://doi.org/10.1007/s12033-012-9542-7>
- Quaglia, D., Irwin, J. A., & Paradisi, F. (2012b). Horse Liver Alcohol Dehydrogenase: New Perspectives for an Old Enzyme. *Molecular Biotechnology*, *52*(3), 244–250. <https://doi.org/10.1007/s12033-012-9542-7>
- Ray, S. S., Bonanno, J. B., Rajashankar, K. R., Pinho, M. G., He, G., De Lencastre, H., Tomasz, A., & Burley, S. K. (2002). Cocrystal Structures of Diaminopimelate Decarboxylase. *Structure*, *10*(11), 1499–1508. [https://doi.org/10.1016/S0969-2126\(02\)00880-8](https://doi.org/10.1016/S0969-2126(02)00880-8)
- Reetz, M. T. (2013). Biocatalysis in Organic Chemistry and Biotechnology: Past, Present, and Future. *Journal of the American Chemical Society*, *135*(34), 12480–12496. <https://doi.org/10.1021/ja405051f>
- Roschangar, F., Sheldon, R. A., & Senanayake, C. H. (2015). Overcoming barriers to green chemistry in the pharmaceutical industry – the Green Aspiration Level™ concept. *Green Chemistry*, *17*(2), 752–768. <https://doi.org/10.1039/C4GC01563K>

- Ruhaak, L. R., Steenvoorden, E., Koeleman, C. A. M., Deelder, A. M., & Wuhrer, M. (2010). 2-Picoline-borane: A non-toxic reducing agent for oligosaccharide labeling by reductive amination. *Proteomics*, *10*(12), 2330–2336. <https://doi.org/10.1002/pmic.200900804>
- Sagong, H.-Y., Son, H. F., Kim, S., Kim, Y.-H., Kim, I.-K., & Kim, K.-J. (2016). Crystal Structure and Pyridoxal 5-Phosphate Binding Property of Lysine Decarboxylase from *Selenomonas ruminantium*. *PLOS ONE*, *11*(11), e0166667. <https://doi.org/10.1371/journal.pone.0166667>
- Said, A. A. E., Ali, T. F. S., Attia, E. Z., Ahmed, A.-S. F., Shehata, A. H., Abdelmohsen, U. R., & Fouad, M. A. (2021). Antidepressant potential of *Mesembryanthemum cordifolium* roots assisted by metabolomic analysis and virtual screening. *Natural Product Research*, *35*(23), 5493–5497. <https://doi.org/10.1080/14786419.2020.1788019>
- SANDMEIER, E., HALE, T. I., & CHRISTEN, P. (1994a). Multiple evolutionary origin of pyridoxal-5'-phosphate-dependent amino acid decarboxylases. *European Journal of Biochemistry*, *221*(3), 997–1002. <https://doi.org/10.1111/j.1432-1033.1994.tb18816.x>
- SANDMEIER, E., HALE, T. I., & CHRISTEN, P. (1994b). Multiple evolutionary origin of pyridoxal-5'-phosphate-dependent amino acid decarboxylases. *European Journal of Biochemistry*, *221*(3), 997–1002. <https://doi.org/10.1111/j.1432-1033.1994.tb18816.x>
- Sato, S., Sakamoto, T., Miyazawa, E., & Kikugawa, Y. (2004). One-pot reductive amination of aldehydes and ketones with α -picoline-borane in methanol, in water, and in neat conditions. *Tetrahedron*, *60*(36), 7899–7906. <https://doi.org/10.1016/j.tet.2004.06.045>
- Schoenmakers, H., & Spiegel, L. (2014). Laboratory Distillation and Scale-up. In *Distillation* (pp. 319–339). Elsevier. <https://doi.org/10.1016/B978-0-12-386878-7.00010-3>
- Seah, S. Y. K., Britton, K. L., Rice, D. W., Asano, Y., & Engel, P. C. (2002). Single Amino Acid Substitution in *Bacillus sphaericus* Phenylalanine Dehydrogenase Dramatically Increases Its Discrimination between Phenylalanine and Tyrosine Substrates. *Biochemistry*, *41*(38), 11390–11397. <https://doi.org/10.1021/bi020196a>
- Seah, S. Y. K., Linda Britton, K., Baker, P. J., Rice, D. W., Asano, Y., & Engel, P. C. (1995). Alteration in relative activities of phenylalanine dehydrogenase towards different substrates by site-directed mutagenesis. *FEBS Letters*, *370*(1–2), 93–96. [https://doi.org/10.1016/0014-5793\(95\)00804-I](https://doi.org/10.1016/0014-5793(95)00804-I)
- Sen, K. Y., & Baidurah, S. (2021). Renewable biomass feedstocks for production of sustainable biodegradable polymer. *Current Opinion in Green and Sustainable Chemistry*, *27*, 100412. <https://doi.org/10.1016/j.cogsc.2020.100412>
- Sharma, M., Mangas-Sanchez, J., Turner, N. J., & Grogan, G. (2017). NAD(P)H-Dependent Dehydrogenases for the Asymmetric Reductive Amination of Ketones: Structure, Mechanism, Evolution and Application. *Advanced Synthesis & Catalysis*, *359*(12), 2011–2025. <https://doi.org/10.1002/adsc.201700356>
- Sheldon, R. A., Basso, A., & Brady, D. (2021). New frontiers in enzyme immobilisation: robust biocatalysts for a circular bio-based economy. *Chemical Society Reviews*, *50*(10), 5850–5862. <https://doi.org/10.1039/D1CS00015B>

- Sheldon, R. A., & Brady, D. (2019). Broadening the Scope of Biocatalysis in Sustainable Organic Synthesis. *ChemSusChem*, *12*(13), 2859–2881. <https://doi.org/10.1002/cssc.201900351>
- Sheldon, R. A., & Woodley, J. M. (2018). Role of Biocatalysis in Sustainable Chemistry. *Chemical Reviews*, *118*(2), 801–838. <https://doi.org/10.1021/acs.chemrev.7b00203>
- Sommer, T., Göen, T., Budnik, N., & Pischetsrieder, M. (2020). Absorption, Biokinetics, and Metabolism of the Dopamine D2 Receptor Agonist Hordenine (*N,N*-Dimethyltyramine) after Beer Consumption in Humans. *Journal of Agricultural and Food Chemistry*, *68*(7), 1998–2006. <https://doi.org/10.1021/acs.jafc.9b06029>
- Song, W., Chen, X., Wu, J., Xu, J., Zhang, W., Liu, J., Chen, J., & Liu, L. (2020). Biocatalytic derivatization of proteinogenic amino acids for fine chemicals. *Biotechnology Advances*, *40*, 107496. <https://doi.org/10.1016/j.biotechadv.2019.107496>
- Stano, J., Nemeč, P., Weissová, K., Kovács, P., Kákoniová, D., & Lisková, D. (1995). Decarboxylation of l-tyrosine and l-dopa by immobilized cells of *Papaver somniferum*. *Phytochemistry*, *38*(4), 859–860. [https://doi.org/10.1016/0031-9422\(94\)00768-O](https://doi.org/10.1016/0031-9422(94)00768-O)
- Stockert, J. C., Horobin, R. W., Colombo, L. L., & Blázquez-Castro, A. (2018). Tetrazolium salts and formazan products in Cell Biology: Viability assessment, fluorescence imaging, and labeling perspectives. *Acta Histochemica*, *120*(3), 159–167. <https://doi.org/10.1016/j.acthis.2018.02.005>
- Su, Y., Liu, Y., He, D., Hu, G., Wang, H., Ye, B., He, Y., Gao, X., & Liu, D. (2022). Hordenine inhibits neuroinflammation and exerts neuroprotective effects via inhibiting NF- κ B and MAPK signaling pathways in vivo and in vitro. *International Immunopharmacology*, *108*, 108694. <https://doi.org/10.1016/j.intimp.2022.108694>
- Surwase, S. N., Patil, S. A., Apine, O. A., & Jadhav, J. P. (2012). Efficient Microbial Conversion of l-Tyrosine to l-DOPA by *Brevundimonas* sp. SGJ. *Applied Biochemistry and Biotechnology*, *167*(5), 1015–1028. <https://doi.org/10.1007/s12010-012-9564-4>
- Tang, Y. Q., & Weng, N. (2013). Salting-out assisted liquid–liquid extraction for bioanalysis. *Bioanalysis*, *5*(12), 1583–1598. <https://doi.org/10.4155/bio.13.117>
- Teng, Y., Scott, E. L., van Zeeland, A. N. T., & Sanders, J. P. M. (2011). The use of l-lysine decarboxylase as a means to separate amino acids by electrodialysis. *Green Chemistry*, *13*(3), 624. <https://doi.org/10.1039/c0gc00611d>
- Thompson, M. P., Derrington, S. R., Heath, R. S., Porter, J. L., Mangas-Sanchez, J., Devine, P. N., Truppo, M. D., & Turner, N. J. (2019). A generic platform for the immobilisation of engineered biocatalysts. *Tetrahedron*, *75*(3), 327–334. <https://doi.org/10.1016/j.tet.2018.12.004>
- Thompson, M. P., & Turner, N. J. (2017a). Two-Enzyme Hydrogen-Borrowing Amination of Alcohols Enabled by a Cofactor-Switched Alcohol Dehydrogenase. *ChemCatChem*, *9*(20), 3833–3836. <https://doi.org/10.1002/cctc.201701092>
- Thompson, M. P., & Turner, N. J. (2017b). Two-Enzyme Hydrogen-Borrowing Amination of Alcohols Enabled by a Cofactor-Switched Alcohol Dehydrogenase. *ChemCatChem*, *9*(20), 3833–3836. <https://doi.org/10.1002/cctc.201701092>

- Tolbert, W. D., Graham, D. E., White, R. H., & Ealick, S. E. (2003). Pyruvoyl-Dependent Arginine Decarboxylase from *Methanococcus jannaschii*. *Structure*, *11*(3), 285–294. [https://doi.org/10.1016/S0969-2126\(03\)00026-1](https://doi.org/10.1016/S0969-2126(03)00026-1)
- Truong, C. C., Mishra, D. K., & Suh, Y. (2023). Recent Catalytic Advances on the Sustainable Production of Primary Furanic Amines from the One-Pot Reductive Amination of 5-Hydroxymethylfurfural. *ChemSusChem*, *16*(1). <https://doi.org/10.1002/cssc.202201846>
- Tseliou, V., Knaus, T., Masman, M. F., Corrado, M. L., & Mutti, F. G. (2019). Generation of amine dehydrogenases with increased catalytic performance and substrate scope from ϵ -deaminating L-Lysine dehydrogenase. *Nature Communications*, *10*(1), 3717. <https://doi.org/10.1038/s41467-019-11509-x>
- Tseliou, V., Knaus, T., Vilím, J., Masman, M. F., & Mutti, F. G. (2020). Kinetic Resolution of Racemic Primary Amines Using *Geobacillus stearotherophilus* Amine Dehydrogenase Variant. *ChemCatChem*, *12*(8), 2184–2188. <https://doi.org/10.1002/cctc.201902085>
- Tsukatani, T., Suenaga, H., Higuchi, T., Akao, T., Ishiyama, M., Ezo, K., & Matsumoto, K. (2008). Colorimetric cell proliferation assay for microorganisms in microtiter plate using water-soluble tetrazolium salts. *Journal of Microbiological Methods*, *75*(1), 109–116. <https://doi.org/10.1016/j.mimet.2008.05.016>
- Viejo, C. G., Villarreal-Lara, R., Torrico, D. D., Rodríguez-Velazco, Y. G., Escobedo-Avellaneda, Z., Ramos-Parra, P. A., Mandal, R., Singh, A. P., Hernández-Brenes, C., & Fuentes, S. (2020). Beer and consumer response using biometrics: Associations assessment of beer compounds and elicited emotions. *Foods*, *9*(6), 821.
- Vitaku, E., Smith, D. T., & Njardarson, J. T. (2014). Analysis of the Structural Diversity, Substitution Patterns, and Frequency of Nitrogen Heterocycles among U.S. FDA Approved Pharmaceuticals. *Journal of Medicinal Chemistry*, *57*(24), 10257–10274. <https://doi.org/10.1021/jm501100b>
- Wang, M., Khan, M. A., Mohsin, I., Wicks, J., Ip, A. H., Sumon, K. Z., Dinh, C.-T., Sargent, E. H., Gates, I. D., & Kibria, M. G. (2021). Can sustainable ammonia synthesis pathways compete with fossil-fuel based Haber–Bosch processes? *Energy & Environmental Science*, *14*(5), 2535–2548. <https://doi.org/10.1039/D0EE03808C>
- Wang, Q., Xin, Y., Zhang, F., Feng, Z., Fu, J., Luo, L., & Yin, Z. (2011). Enhanced γ -aminobutyric acid-forming activity of recombinant glutamate decarboxylase (gadA) from *Escherichia coli*. *World Journal of Microbiology and Biotechnology*, *27*(3), 693–700. <https://doi.org/10.1007/s11274-010-0508-2>
- Watanabe, Y., Tsuji, Y., Ige, H., Ohsugi, Y., & Ohta, T. (1984). Ruthenium-catalyzed N-alkylation and N-benzylation of aminoarenes with alcohols. *The Journal of Organic Chemistry*, *49*(18), 3359–3363. <https://doi.org/10.1021/jo00192a021>
- Weber, R. E. (1992). Use of ionic and zwitterionic (Tris/BisTris and HEPES) buffers in studies on hemoglobin function. *Journal of Applied Physiology*, *72*(4), 1611–1615. <https://doi.org/10.1152/jappl.1992.72.4.1611>
- Wei, G., Chen, Y., Zhou, N., Lu, Q., Xu, S., Zhang, A., Chen, K., & Ouyang, P. (2022). Chitin biopolymer mediates self-sufficient biocatalyst of pyridoxal 5'-phosphate and L-lysine

- decarboxylase. *Chemical Engineering Journal*, 427, 132030.
<https://doi.org/10.1016/j.cej.2021.132030>
- Wei, T., Cheng, B. Y., & Liu, J. Z. (2016). Genome engineering *Escherichia coli* for L-DOPA overproduction from glucose. *Scientific Reports*, 6. <https://doi.org/10.1038/srep30080>
- Wieschalka, S., Blombach, B., Bott, M., & Eikmanns, B. J. (2013). Bio-based production of organic acids with *Corynebacterium glutamicum*. *Microbial Biotechnology*, 6(2), 87–102.
<https://doi.org/10.1111/1751-7915.12013>
- Wohlgemuth, R. (2021). Biocatalysis-Key enabling tools from biocatalytic one-step and multi-step reactions to biocatalytic total synthesis. *New Biotechnol*, 60, 113–123.
- Wu, B., Zhang, S., Hong, T., Zhou, Y., Wang, H., Shi, M., Yang, H., Tian, X., Guo, J., Bian, J., Roache, J., Delgado, P., Mo, R., Fridrich, C., Gao, F., & Wang, J. (2020). Merging Biocatalysis, Flow, and Surfactant Chemistry: Innovative Synthesis of an FXI (Factor XI) Inhibitor. *Organic Process Research & Development*, 24(11), 2780–2788.
<https://doi.org/10.1021/acs.oprd.0c00412>
- Wu, P., Li, G., He, Y., Luo, D., Li, L., Guo, J., Ding, P., & Yang, F. (2020). High-efficient and sustainable biodegradation of microcystin-LR using *Sphingopyxis* sp. YF1 immobilized Fe₃O₄@chitosan. *Colloids and Surfaces B: Biointerfaces*, 185, 110633.
<https://doi.org/10.1016/j.colsurfb.2019.110633>
- Ye, L. J., Toh, H. H., Yang, Y., Adams, J. P., Snajdrova, R., & Li, Z. (2015). Engineering of Amine Dehydrogenase for Asymmetric Reductive Amination of Ketone by Evolving *Rhodococcus* Phenylalanine Dehydrogenase. *ACS Catalysis*, 5(2), 1119–1122.
<https://doi.org/10.1021/cs501906r>
- Yoon, S., Patil, M. D., Sarak, S., Jeon, H., Kim, G., Khobragade, T. P., Sung, S., & Yun, H. (2019). Deracemization of Racemic Amines to Enantiopure (R)- and (S)-amines by Biocatalytic Cascade Employing ω -Transaminase and Amine Dehydrogenase. *ChemCatChem*, 11(7), 1898–1902. <https://doi.org/10.1002/cctc.201900080>
- Yoshitaka Hashitani, B. (1925). On the chemical constituents of malt-rootlets with special reference to Hordenine. *Journal of the College of Agriculture*, 14, 1–56.
- Zhang, B., Jiang, Y., Li, Z., Wang, F., & Wu, X.-Y. (2020). Recent Progress on Chemical Production From Non-food Renewable Feedstocks Using *Corynebacterium glutamicum*. *Frontiers in Bioengineering and Biotechnology*, 8. <https://doi.org/10.3389/fbioe.2020.606047>
- Zhang, H., Wei, Y., Lu, Y., Wu, S., Liu, Q., Liu, J., & Jiao, Q. (2016). Three-step biocatalytic reaction using whole cells for efficient production of tyramine from keratin acid hydrolysis wastewater. *Applied Microbiology and Biotechnology*, 100(4), 1691–1700.
<https://doi.org/10.1007/s00253-015-7054-7>
- Zhang, K., & Ni, Y. (2014). Tyrosine decarboxylase from *Lactobacillus brevis*: Soluble expression and characterization. *Protein Expression and Purification*, 94, 33–39.
<https://doi.org/10.1016/j.pep.2013.10.018>
- Zhang, X., Du, L., Zhang, J., Li, C., Zhang, J., & Lv, X. (2021). Hordenine Protects Against Lipopolysaccharide-Induced Acute Lung Injury by Inhibiting Inflammation. *Frontiers in Pharmacology*, 12, 712232. <https://doi.org/10.3389/fphar.2021.712232>

- Zhao, W., Hu, S., Huang, J., Ke, P., Yao, S., Lei, Y., Mei, L., & Wang, J. (2016). Permeabilization of *Escherichia coli* with ampicillin for a whole cell biocatalyst with enhanced glutamate decarboxylase activity. *Chinese Journal of Chemical Engineering*, *24*(7), 909–913. <https://doi.org/10.1016/j.cjche.2016.02.001>
- Zhou, F., Xu, Y., Nie, Y., & Mu, X. (2022). Substrate-Specific Engineering of Amino Acid Dehydrogenase Superfamily for Synthesis of a Variety of Chiral Amines and Amino Acids. *Catalysts*, *12*(4), 380. <https://doi.org/10.3390/catal12040380>
- Zhou, J.-W., Ruan, L.-Y., Chen, H.-J., Luo, H.-Z., Jiang, H., Wang, J.-S., & Jia, A.-Q. (2019). Inhibition of Quorum Sensing and Virulence in *Serratia marcescens* by Hordenine. *Journal of Agricultural and Food Chemistry*, *67*(3), 784–795. <https://doi.org/10.1021/acs.jafc.8b05922>
- Zhu, H., Xu, G., Zhang, K., Kong, X., Han, R., Zhou, J., & Ni, Y. (2016a). Crystal structure of tyrosine decarboxylase and identification of key residues involved in conformational swing and substrate binding. *Scientific Reports*, *6*(1), 27779. <https://doi.org/10.1038/srep27779>
- Zhu, H., Xu, G., Zhang, K., Kong, X., Han, R., Zhou, J., & Ni, Y. (2016b). Crystal structure of tyrosine decarboxylase and identification of key residues involved in conformational swing and substrate binding. *Scientific Reports*, *6*(1), 27779. <https://doi.org/10.1038/srep27779>
- Zhuang, W., Liu, H., Zhang, Y., He, J., & Wang, P. (2021). Effective asymmetric preparation of (R)-1-[3-(trifluoromethyl)phenyl]ethanol with recombinant *E. coli* whole cells in an aqueous Tween-20/natural deep eutectic solvent solution. *AMB Express*, *11*(1), 118. <https://doi.org/10.1186/s13568-021-01278-6>

2. Aims and objectives

The core focus of this thesis is the design and development of several strategies that enable the use of enzymes, frequently in an immobilized state, for the synthesis of both valuable end-products and flexible reaction intermediates through a sustainable biocatalytic approach. The specific goals of this study can be outlined as follows:

1. The production of L-dopa using microbial fermentation within a bioreactor, followed by pairing the fermented product with a continuous flow system. Using an engineered *E. coli* strain acquired through a collaboration with Professor Gosset, the aim is to produce a fermentation broth rich in the aromatic amino acid, expected to function as a sustainable feedstock for an enzymatic cascade in a continuous flow. A potential application is the production of a range of interesting aromatic derivatives such as hydroxytyrosol, a valuable antioxidant.
2. Harnessing the decarboxylation of L-tyrosine in a continuous flow module by incorporating the immobilized tyrosine decarboxylase derived from *Lactobacillus brevis*. The immobilized biocatalyst, strengthened through covalent immobilization, will find its place in various cascades, benefiting from the enzyme promiscuity towards L-tyrosine and L-dopa. Chemical steps will be combined within the continuous flow system in order to leverage the decarboxylation product, tyramine. This biogenic amine will then serve as a natural precursor for the synthesis of amino compounds, such as the valuable phytochemical hordenine.
3. Generation of a biocatalytic platform for the synthesis of short-chain primary amines, employing a cost-effective and accessible strategy, based on the use of valine decarboxylase for *Streptomyces viridifaciens*. This system offers a sustainable alternative to the present amine production methods, which depend heavily on petroleum cracking. The enzymatic tool in question, composed of the highly promiscuous VImD, could prove versatile and effective for the eco-friendly production of varied amino products. Moreover, through its immobilization, the sustainability of the process will be enhanced by enabling the biocatalyst reuse.
4. Investigate amino acid and amine dehydrogenases for carrying out oxidative deamination, especially from primary amines such as catecholamines. This will

broaden the scope of these biocatalysts, which are typically employed in the reverse direction for the production of chiral amines *via* reductive amination. The hypothesized coupling of an amine dehydrogenase with an alcohol dehydrogenase in a hydrogen-borrowing system will be a novel approach which can be integrated within continuous-flow enzymatic cascades, such as the one for hydroxytyrosol, facilitating the convenient regeneration of the NAD(P)H cofactor in one module.

3. Materials and methods

3.1 Materials

Used materials included a Q5 High-fidelity DNA polymerase, 5x Q5 reaction buffer, dNTPs were purchased from New England Biolabs (NEB). Restriction enzymes (BamHI, HindIII), CutSmart buffer, 6x gel loading dye and unstained protein standard (broad range 10-200 kDa) were also sourced from NEB. The primers were synthesized by Microsynth. The NADH, NAD⁺, NADPH, and NADP⁺ were acquired from Apollo Scientific.

The following materials were purchased from Fisher Scientific: LB broth, LB broth with Agar, imidazole, ampicillin sodium salt, kanamycin sulfate, sodium chloride, sodium hydroxide, tris base, HEPES buffer, sodium borohydride, SYBR Safe DNA gel stain, agarose, GeneJET Plasmid Miniprep kit, GeneJET Gel Extraction kit, N,N,N',N'-tetramethylethylenediamine (TEMED), bromophenol blue, magnesium sulfate, potassium iodide, and polyethyleneimine 50 % aqueous solutions (branched, MN 60'000). Additionally, acetonitrile, isopropanol, and chloroform were sourced from the same supplier.

Yeast extract, N-Z-amine, glycerol, D-sorbitol, potassium phosphate dibasic and monobasic, ammonium sulfate, α -lactose monohydrate, isopropyl β -D-thiogalactoside, glycine, D-glucose, ethylenediaminetetraacetic acid, calcium chloride, magnesium chloride hexahydrate, nickel (II) chloride hexahydrate, cobalt (II) chloride, copper (II) chloride dihydrate, iron (III) chloride hexahydrate, manganese (II) chloride tetrahydrate, sodium pyruvate, L-phenylalanine, sodium dodecyl sulfate, 2-mercaptoethanol, acetic anhydride, acrylamide/bis-acrylamide 30% solution, ammonium persulfate, Instant blue, Bradford reagent, sodium periodate, boric acid, sodium tetraborate decahydrate, sodium bicarbonate, trifluoroacetic acid, iminodiacetic acid, sodium phenylpyruvate, tyramine, L-tyrosine disodium salt dihydrate, Cell Counting Kit - 8, MTT, PMS, WST-1 were acquired from Sigma Aldrich.

The compounds L-valine, L-isoleucine, L-leucine, L-threonine, L-methionine, L-alanine, L-2-phenylglycine, isobutylamine, and 1-amino-2-propanol, ethylamine, isoamylamine, 3-(methylthio)propanamine were sourced from Chemie Brunschwig AG.

Enzyme carrier ReliSorb EP400/SS, EP403/S and HFA403/S were kindly donated by Resindion S.R.L..

Ethanol absolute was acquired from VWR, while hydrochloric acid (37 %) from Fluka. Acetic acid was bought by Hanseler.

All reagents were of analytical grade unless otherwise specified.

E. coli strain for the production of L-DOPA was supplied by Prof. G. Gosset (Departamento de Ingenieria Celular y Biocatalisis, Instituto de Biotecnologıa, Universidad Nacional Autonoma de Mexico),(Munoz et al., 2011) while plasmids of tyrosine decarboxylase (*LbTDC-pRSETb*) and phenylalanine dehydrogenase (*PheDH-ptac85*)(PARADISI et al., 2007) were belonging to the plasmid library in the University of Nottingham. The amine dehydrogenases *CfusAmDH*, *MicroAmDH*, *MATOUAmDH* were supplied by Prof. C. Vergne-Vaxelaire (Universite Paris-Saclay).(Mayol et al., 2019a) The plasmid of the lysine dehydrogenase (*LysEDH-pET28b*) was supplied by Prof. F. Mutti (Amsterdam University).(Tseliou et al., 2019) The plasmid of *VImD* (*VImD-pET22b(+)*) was ordered through GenScript.

3.2 General methods

3.2.1 Culture media

LB medium: 25 g/L of pre-mix LB powder dissolved in dH₂O. Premix powder consists of yeast extract (5 g/L), tryptone (10 g/L) and NaCl (10 g/L).

LB agar plates: 40 g/L of pre-mix LB Agar powder dissolved in dH₂O. Premix powder consists of yeast extract (5 g/L), tryptone (10 g/L), NaCl (10 g/L) and 15 g/L agar.

ZYP-5052 Autoinduction media: solution consisting of N-Z-Amine (10 g/L), yeast extract (5 g/L), (NH₄)₂SO₄ 1M (25 mL/L), KH₂PO₄ 1M (50 mL/L), K₂HPO₄ 1M (50 mL/L) was firstly autoclaved. Then MgSO₄ 1M (2 mL/L), 1000x trace elements solution (2 mL/L) and 50x 5052 solution (20 mL/L; made with 250 g/L glycerol, 25 g/L glucose and 100 g/L α -lactose monohydrate in dH₂O) were added in sterile conditions. Trace elements solution contains FeCl₂ (50 mM), CaCl₂ (20 mM), MnCl₂ (10 mM), ZnSO₄ (10 mM), CoCl₂ (2 mM), CuCl₂ (2 mM), NiCl₂ (2 mM), HCl (60 mM), Na₂MoO₄ (2 mM), Na₂SeO₄ (2 mM) and H₃BO₃ (2 mM).

TB medium: N-Z amine (12 g), yeast extract (24 g), glycerol (5 g), K₂HPO₄ (2.2 g) and KH₂PO₄ (9.4 g) and distilled H₂O (1L).

SOB medium: N-Z amine (5 g), yeast extract (1.25 g), NaCl (0.25 g), KCl (0.05 g), MgCl₂ 6H₂O (0.5 g), MgSO₄ 6H₂O (0.6 g) and distilled H₂O (250 mL).

M9 L-DOPA Fermentation Medium: five stock solutions (5X) for M9 salts, D-glucose, MgSO₄, CaCl₂, and ascorbic acid were prepared and then filtered with 0.2 μ m filters under the laminar flow hood. Final medium composition: 6 g/L Na₂HPO₄, 0.5 g/L NaCl, 3 g/L KH₂PO₄, 1 g/L NH₄Cl, 10 g/L glucose, 0.247 g/L MgSO₄, 0.0147 g/L CaCl₂.

Optimized M9Y Fermentation Medium: Based on M9 medium. Final composition: 6 g/L Na₂HPO₄, 0.5 g/L NaCl, 3 g/L KH₂PO₄, 1 g/L NH₄Cl, 0.247 g/L MgSO₄, 0.0147 g/L CaCl₂, 50 g/L glucose, 2 g/L yeast extract, 0.45 g/L ascorbic acid.

3.2.2 Preparation of chemically competent cells

A colony of desired *E. coli* strain was inoculated in 10 mL of LB media and grown at 37 °C and 150 rpm overnight. 1 mL of this cell culture was employed to inoculate 100 mL of LB, which were then incubated at 37 °C, 150 rpm until they reached OD 0.4. The culture was chilled then for 30 minutes and centrifuged at 3000 g for 15 minutes at 4 °C to harvest the cells. The supernatant was discarded, and the pellet resuspended in 50 mL of 100 mM magnesium chloride on ice. After centrifugating at 2000 g for 15 minutes at 4 °C, the pellet was resuspended in 25 mL of 100 mM calcium chloride and incubated on ice for 30 minutes. The final step involved the centrifugation at 2000 g for 15 minutes at 4 °C, followed by resuspension of the pellet in 0.5 mL of a solution containing 85 mM calcium chloride and 15 % glycerol. 40 µL of the suspension were then aliquoted into 1.5 mL microcentrifuge tubes and stored at - 80 °C.

3.2.3 Preparation of agarose gel for DNA assay

DNA gel electrophoresis was conducted using 0.8 % (w/v) agarose. To make the solution, 0.32 g of agarose was dissolved in 40 mL of TAE buffer by heating in a microwave until clear. After cooling, 2 µL of SYBR Safe DNA gel staining were added. The solution was loaded into the gel cassette, allowed to solidify, and the rack removed. Samples were mixed with gel loading dye (purple 6x), usually 25 µL of sample and 5 µL of dye. TAE buffer was added to the gel cassette and samples loaded into the wells, along with the DNA ladder. Electrophoresis was performed at 75 V and 150 mA for 50 minutes. The gel was visualized using a UV lamp to observe the DNA bands.

3.2.4 Transformation of competent *E. coli* cells

0.5-1 µL (100 ng) of plasmid was added to 40 µL of chemically competent cells in a microcentrifuge tube. The cells were left on ice for 30 minutes and then subjected to heat-shock at 42 °C for 90 seconds. After cooling on ice for 5 minutes, 250 µL of SOB or LB media was added to the tube and incubated for 1 hour at 37 °C (150 rpm). 50-150 µL of the solution was spread onto a LB-agar plate with the appropriate antibiotic and grown overnight at 37 °C.

3.2.5 Expression of proteins

A single colony was taken from a LB-agar plate containing transformed cells and used to inoculate 5 mL of LB media with the appropriate antibiotic. The starting culture was incubated overnight (37 °C, 150 rpm) and then diluted to 0.1 OD in either LB or TB media (300 mL) containing the suitable antibiotic. Incubation was continued until the OD₆₀₀

reached the desired target value (0.6 - 1.2), while shaking at 150 rpm. Cells were then induced with 0.1-1 mM IPTG, then grown overnight, otherwise specified, at the specific temperature. Just in the case of HLDH the induction was performed with 0.4 μ M of tetracycline. The cells were harvested by centrifugation at 2500 rpm for 20 minutes at 4 °C and the supernatant was removed, and the cells washed with water to then be pelleted down. In the Table 3.1 the conditions for protein expression are reported specifically for each biocatalysts.

The resulting cell pellet was stored at -20 °C. For the ZYP-5052 autoinduction media, 300 mL of the medium with appropriate antibiotic was inoculated with a single colony and grown at 37°C with shaking at 150 rpm. After 16 hours, cells were harvested by centrifugation at 4500 rpm for 20 minutes at 4 °C, and the resulting dry cell paste was stored at -20 °C.

Enzyme	Plasmid	Medium	Temperature after induction	Time of expression (h)	Antibiotic
<i>LbTDC</i>	pRSETb	LB, 1 % glucose	25	5	ampicillin
<i>TsRTA</i>	pET22b(+)	TB, 5 g/L lactose	25	16	ampicillin
<i>HeWT</i>	pRSETb	Autoinduction ZYP	37	16	ampicillin
<i>BsPheDH</i>	pRSETb	Autoinduction ZYP	37	16	ampicillin
<i>LysEDH</i>	pET28b	LB	25	16	kanamycin
<i>CfusAmDH</i>	pET22b-LIC	LB	16	16	ampicillin
<i>MATOUAmDH2</i>	pET22b-LIC	LB	16	16	ampicillin
<i>MicroAmDH</i>	pET22b-LIC	LB	16	16	ampicillin
<i>VImD</i>	pET22b(+)	LB	37	5	ampicillin
<i>HLADH</i>	pASK_IBA	TB	20	16	ampicillin

Table 3.1: Proteins expression conditions

3.2.6 Protein purification

The procedure for cell lysis involved the thawing of the frozen cell pellet (1-3 g) on ice and resuspension in loading buffer as outlined in Table 3.2. The volume of loading buffer used was approximately 2 mL per gram of dry cells. The resulting suspension underwent sonication to disrupt the cells, utilizing a 5-second pulse on and 5-second pulse off sequence for a minimum of 8 minutes with an amplitude ranging from 40-60 %. The subsequent removal of cell debris was achieved through centrifugation at 14'500 rpm for 45 minutes at 4 °C. This resulted in a cell-free extract that was filtered through a 0.45 μ m pore size syringe filter.

Purification of the crude protein from the cell lysate was accomplished through loading onto a His-trap FF crude Ni-affinity column on the ÄKTA start Protein Purification System, utilizing the UNICORN start software and Frac30 fraction collector from GE Healthcare. The column (1 or 5 mL) was initially equilibrated with loading buffer and then loaded with the crude extract. Non-specific proteins were removed through washing with loading buffer (5 column volumes) followed by an isocratic step with a 10 % elution buffer/ 90 % loading buffer mixture (5 column volumes).

The recombinant proteins were finally eluted using 100 % elution buffer as outlined in Table 3.2, in 1 or 2 mL fractions. The fractions containing the purified protein were subjected to dialysis at 4°C with mild stirring, using a cellulose membrane with a 14 kDa MWCO (Sigma Aldrich) inserted into 800 mL of storage buffer. The initial dialysis stage was conducted for 1 hour, followed by changing the buffer and allowing it to dialyze overnight at 4 °C. The following day, the proteins were identified through SDS-PAGE analysis, and their concentration was determined at 280 nm.

Enzyme	Loading buffer	Elution buffer	Storage buffer
<i>LbTDC</i>	25 mM Tris buffer, 300 mM NaCl, 20 mM imidazole, 0.2 mM PLP, pH 7.4	25 mM Tris buffer, 300 mM NaCl, 280 mM imidazole, 0.2 mM PLP, pH 7.4	25 mM potassium phosphate buffer, 150 mM NaCl, 0.2 mM PLP, pH 7.4
<i>TsRTA</i>	50 mM potassium phosphate buffer, 100 mM NaCl, 20 mM imidazole, 0.1 mM PLP, pH 8	50 mM potassium phosphate buffer, 100 mM NaCl, 280 mM imidazole, 0.1 mM PLP, pH 8	50 mM potassium phosphate buffer, 0.1 mM PLP, pH 8
<i>HeWT</i>	50 mM potassium phosphate buffer, 100 mM NaCl, 20 mM imidazole, 0.1 mM PLP, pH 8	50 mM potassium phosphate buffer, 100 mM NaCl, 280 mM imidazole, 0.1 mM PLP, pH 8	50 mM potassium phosphate buffer, 0.1 mM PLP, pH 8

<i>BsPheDH</i>	50 mM potassium phosphate buffer, 100 mM NaCl, 30 mM imidazole, pH 8	50 mM potassium phosphate buffer, 100 mM NaCl, 300 mM imidazole, pH 8	50 mM potassium phosphate buffer, 100 mM KCl, pH 8
<i>LysEDH</i>	50 mM potassium phosphate buffer, 100 mM NaCl, 30 mM imidazole, pH 8	50 mM potassium phosphate buffer, 100 mM NaCl, 300 mM imidazole, pH 8	50 mM potassium phosphate buffer, pH 8
<i>CfusAmDH</i>	100 mM potassium phosphate buffer, 50 mM NaCl, 10 % glycerol, 30 mM imidazole, pH 7.5	100 mM potassium phosphate buffer, 50 mM NaCl, 10 % glycerol, 250 mM imidazole, pH 7.5	100 mM potassium phosphate buffer, 10 % glycerol, pH 7.5
<i>MATOUAmDH2</i>	100 mM potassium phosphate buffer, 50 mM NaCl, 10 % glycerol, 30 mM imidazole, pH 7.5	100 mM potassium phosphate buffer, 50 mM NaCl, 10 % glycerol, 250 mM imidazole, pH 7.5	100 mM potassium phosphate buffer, 10 % glycerol, pH 7.5
<i>MicroAmDH</i>	100 mM potassium phosphate buffer, 50 mM NaCl, 10 % glycerol, 30 mM imidazole, pH 7.5	100 mM potassium phosphate buffer, 50 mM NaCl, 10 % glycerol, 250 mM imidazole, pH 7.5	100 mM potassium phosphate buffer, 10 % glycerol, pH 7.5

VImD	50 mM potassium phosphate buffer, 300 mM NaCl, 7.5 mM imidazole, pH 7.5w	50 mM potassium phosphate buffer, 300 mM NaCl, 150 mM imidazole, pH 7.5	50 mM potassium phosphate buffer, pH 7.5
HLDH	20 mM potassium phosphate buffer, 280 mM NaCl, 6m M KCl, pH 7.4	20 mM potassium phosphate buffer, 280 mM NaCl, 6m M KCl, 2.5 mM <i>d</i> -desthiobiotin, pH 7.4	50 mM potassium phosphate buffer, pH 8.5

Table 3.2: Proteins purification conditions

3.2.7 SDS-PAGE preparation and execution

To prepare and execute SDS-PAGE, a 12 % polyacrylamide resolving gel was first prepared and positioned between two glass plates. The stacking gel was then loaded with a rack to shape the wells. Meanwhile, samples were diluted with 2x loading dye and heated at 90 °C for 10 minutes. Once both layers of the gel had polymerized, running buffer was poured into the gel holder. Next, 5-10 μ L of sample was added to each gel well, including one containing the protein ladder (an unstained protein standard with a broad range of 10-200 kDa). The gel was then run at 200 mV and 30 mA in SDS running buffer for approximately 80 minutes. Finally, the gel was stained using Instant Blue (Expedeon®).

3.2.8 Protein quantification

Protein concentration was measured at 280 nm. 2 μ L of the protein sample were pipetted into a clean EPOC sample well. The absorbance of the protein sample was measured at 280 nm using the EPOC spectrophotometer (BioTek Epoch 2 Microplate Spectrophotometer). The protein concentration was then calculated using the molar extinction coefficient (ϵ) and molecular weight (MW) of the protein. The specific values for these parameters varied depending on the protein being measured.

3.2.9 Sample preparation and HPLC analysis

If the monitored compound was detectable by UV-Vis, a 50 μ L sample was taken and quenched by adding 175 μ L of 0.2 % HCl and 175 μ L of acetonitrile. The prepared sample

was then analyzed using High-Performance Liquid Chromatography (HPLC) to determine the conversion.

For aliphatic amino compound, the reaction was followed by the derivatization of the amino group using 9-Fluorenylmethoxycarbonyl chloride (Fmoc-Cl). To prepare the samples, 50 μL of the appropriately diluted reaction mixture (ensuring a maximum of 25 mM of the compound to be derivatized) was added to 100 μL of a 100 mM borate buffer solution (pH 9), followed by the addition of 200 μL of 15 mM Fmoc-Cl in acetonitrile. The samples were then resuspended in the mobile phase (0.2 % HCl and acetonitrile and analyzed with HPLC. Calibration curves from standard solutions of each compound were used for quantification of substrate and product concentration.

The HPLC (UltiMate 3000 UHPLC Thermo Fisher Scientific) used a C18 column (Waters X-Bridge specifications). The flow rate was 0.8 mL/min and the oven was set at 45 °C. The samples were analyzed using a gradient method, which involved an initial solvent composition of 5 % acetonitrile (B) in 0.1 % trifluoroacetic acid (TFA) in milliQ water (A), gradually increasing to 95 % acetonitrile over a span of 4 minutes. Alternatively, if peaks could not be resolved, a water-methanol phase was used with the following method: water 0.1 % TFA (A), methanol (B), 0-1 min 1 % B, 1-7 min 40 % B, 7-9 min 45 % B, 9-10 min 1 % B, and the flow rate was set to 1 mL/min. In this case, the sample was resuspended in the HPLC vial in 0.2 % HCl.

3.2.10 Enzymatic activity measurements

To determine the specific activity of an enzyme, either the depletion of substrate or the formation of product were measured at a specific wavelength.

For oxidoreductases, the activity was assessed by monitoring the production or consumption of the cofactor NADH during the catalytic reaction at a wavelength of 340 nm (with a molar extinction coefficient of $6.22 \text{ mM}^{-1} \text{ cm}^{-1}$). One unit of enzyme activity was defined as the amount of enzyme required to catalyze the formation or depletion of 1 μmol of product, substrate, or cofactor per minute.

When working in acrylic 96 well-plates, Biotek Epoch 2 Microplate Spectrophotometer was used to measure changes in absorbance over time. However, when using cuvettes, a Cary 60 UV-Vis spectrophotometer (Agilent) was employed. Working with decarboxylases, HPLC was used to monitor the enzyme activity. The change in absorbance per minute was then converted into a change in concentration per minute using a calibration curve.

3.2.10.1 Activity assay of *LbTDC*

LbTDC (K. Zhang & Ni, 2014) activity measurements were performed using HPLC, specifically by measuring the conversion of tyrosine to tyramine at 280 nm. One unit (U) of activity was defined as the amount of enzyme required to catalyze the consumption of 1 μmol of

L-tyrosine per minute under reference conditions, namely 2.5 mM tyrosine, 0.2 mM PLP, and 30 μL of *LbTDC* (from a dilution of 100 folds) in 200 mM sodium acetate buffer, pH 5.0, in a 1 mL Eppendorf. The activity measurements were performed up to 20 minutes at 5-minute intervals, with the temperature set at 37 °C.

Successful resolution of the peaks was obtained with the elution phase water 0.1 % TFA - methanol.

3.2.10.2 Activity assay for *HeWT* and *TsRTA*

To measure the activity of the enzymes, *HeWT* (Cerioli et al., 2015) and *TsRTA* (Heckmann et al., 2020) spectrophotometric activity measurements were performed by determining the production of acetophenone at 245 nm at 25 °C in a 1.5 mL cuvette (total volume 1 mL) for a duration of 5 minutes. One unit (U) of activity was defined as the amount of enzyme required to produce 1 μmol of acetophenone (with an extinction coefficient of $12.6 \text{ mM}^{-1} \text{ cm}^{-1}$) per minute under reference conditions: 2.5 mM (*S*)-MBA, 2.5 mM pyruvate, 0.25 % DMSO, 0.1 mM PLP, and an appropriate amount of enzyme in 50 mM potassium phosphate buffer at pH 8.0. For *TsRTA*, (*R*)-methylbenzylamine was employed.

3.2.10.3 Activity of amino acid dehydrogenases and amine dehydrogenases

To measure the activity of amino acid dehydrogenases and amine dehydrogenases the Cary 60 or the fluorescence spectrophotometer were used.

To measure the activity of PheDH (PARADISI et al., 2007) a reaction mixture was prepared by combining 5 μL of enzyme solution with 5 mM substrate and 1 mM NAD^+ in 0.1 M glycine-KOH buffer, 100 mM KCl, 10.4 pH, inside a UV cuvette with total volume of 1 mL. The formation of NADH was measured spectrophotometrically at 340 nm using the Cary 60, at 25 °C. For the mutants of PheDH, the enzyme concentration in the activity assay was increased and the activity was monitored over 10 minutes.

The activity of LysEDH (Heydari et al., 2004) was measured introducing 5 μL of soluble enzyme into the reaction mixture, which was composed of 10 mM L-lysine and 1 mM NAD^+ in a total volume of 1 mL solution of 50 mM phosphate buffer at pH 8. The formation of NADH absorbance at 340 nm was observed over 2 minutes at 25 °C.

With amine dehydrogenases (AmDHs) the fluorescence of the NADH cofactor was measured using a fluorescence spectrophotometer or the Cary 60. The fluorescence of the cofactor was excited at a wavelength of $351 \pm 9 \text{ nm}$ and the emission was measured at $450 \pm 30 \text{ nm}$. The change in the fluorescence was monitored in 96 well plates, over a period of time of 10 minutes, recording the fluorescence value every 30 seconds, and the rate of NADH formation was calculated using the Lambert-Beer law and the molar extinction coefficient of NADH ($6.22 \text{ mM}^{-1} \text{ cm}^{-1}$). Similarly, the cofactor formation was monitored also at the Cary 60, at 340 nm, in continuous for 10 minutes in cuvette. The activity of AmDHs was calculated based on the rate of NADH formation

under these specific conditions: 100 μL of enzyme dilution, 50 mM substrate, 0.1 mM NAD^+ , 100 mM sodium carbonate buffer in a final volume of 200 μl for 96 well plates or 1 mL for cuvettes.

3.2.10.4 Activity of VImD

To measure the activity of VImD, (Garg et al., 2002a) 0.025 mg of enzyme were mixed with a reaction mixture of 5 mM L-valine and 0.1 mM PLP, in 50 mM phosphate buffer, pH 7.5. The total volume of the reaction mixture was 1 mL, and it was incubated for 20 minutes at 37 $^{\circ}\text{C}$ with 150 rpm orbital shaking. Every 5 minutes, a 50 μL sample was taken from the reaction mixture and derivatized with FMOC by mixing with 100 μL borate buffer at pH 9 and 200 μL of 15 mM FMOC in acetonitrile. The resulting solution was then mixed with 175 μL of 0.2 % HCl and 175 μL of acetonitrile, filtered and submitted to HPLC analysis at 265 nm.

The activity of VImD was calculated based on the rate of decarboxylation of L-valine with the calibration curve of isobutylamine (reaction product).

3.2.10.5 Activity of HLADH

To measure the activity of HLADH, (Quaglia et al., 2012a) a solution containing 1 mM NAD^+ and 40 mM ethanol in 50 mM phosphate buffer at pH 8.5 was prepared. The solution was added to a 1 mL UV cuvette and placed in the Cary 60 spectrophotometer. The temperature was set to 25 $^{\circ}\text{C}$. 2 μl of HLADH were then added to the solution to initiate the reaction. The formation of NADH was monitored by measuring the increase in absorbance at 340 nm over time. The specific activity was calculated using the molar extinction coefficient of NADH at 340 nm ($6.22 \text{ mM}^{-1} \text{ cm}^{-1}$).

3.2.11 Enzyme immobilization

To conduct an immobilization study, critical steps must be considered, including the selection of the optimal support, the appropriate immobilization chemistry, and the optimal protein loading.

Different immobilization carrier for covalently immobilization have been trialed (Table 3.3).

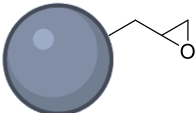
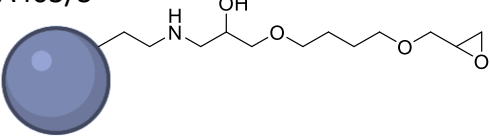
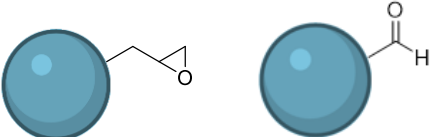
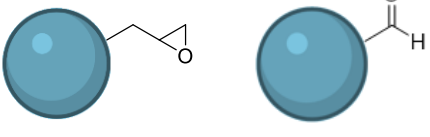
Epoxydic resin	Characteristics
EP4003/S 	
HFA403/S 	Particle size: 100-300 μm \emptyset Pores: 40-60 nm
EP400/SS 	Particle size: 50-150 μm \emptyset Pores: 40-50 nm Hydrophilic
Agarose 	Particle size : 50-150 μm \emptyset pores : ~200 nm Hydrophilic

Table 3.3: Supports involved in the biocatalysts immobilization.

For the immobilization chemistry on the supports described above, covalent immobilization was the strategy of choice. The handle, decorating the carriers involved in the immobilization study, were epoxy groups (in epoxy-supports) or aldehyde groups (glyoxyl supports). In most of the case the immobilization of His-tagged enzymes was performed using cobalt-IDA-functionalized epoxy resin as an efficient method that exploits the strong affinity between histidine residues and chelated cobalt ions on the support.

The optimal protein loading, as crucial parameter for enzyme recovered activity, were evaluated with a case-by-case approach. Practically, the immobilization process involved preparing the enzyme solution in an appropriate buffer and incubating it with the selected support under mild agitation at room temperature or at 4 °C for overnight immobilization.

Enzyme immobilization was monitored by periodically taking supernatant samples and comparing them to the initial enzyme solution concentration (control sample). Protein concentration was assessed at 280 nm by EPOC and SDS-PAGE to confirm complete immobilization.

Upon reaching the maximum achievable immobilization yield, the support was washed with water and desorption buffer in case cobalt was present (50 mM EDTA, 500 mM NaCl in 50 mM phosphate buffer pH 7), and incubated in blocking buffer (3 M glycine in 20 mM phosphate buffer pH 8.5) overnight. In the end the support was washed again with water before storing it at 4 °C.

3.2.12 Agarose epoxy functionalization

To prepare the support, agarose (10 g) was mixed with water and acetone, followed by the addition of NaOH (3.38 g) and NaBH₄ (0.4 g). Epichloridrine (11 mL) was then slowly added while maintaining low temperatures to prevent epoxide oxidation. The mixture was incubated overnight at room temperature with gentle agitation. Agarose was then filtered and washed thoroughly with water. To quantify epoxy groups, the resin (50 mg) was incubated with 0.5 M H₂SO₄ for 1 hour. After washing with water, it was then incubated with 0.5 mL of 10 mM NaIO₄ for an additional hour. The supernatant (100 µL) absorbance was finally measured in a 96-well plate at 405 nm after mixing the solution with 500 µL of saturated bicarbonate solution and 500 µL of 10 % (w/v) KI solution. Calculations were performed to determine the epoxy group concentration on the agarose support. Control samples, including a blank, initial solution, and control support, were also tested to ensure accuracy in the quantification process. In general 1 g of 6BCL agarose contains 70-75 µmols of diols that can be oxidised.

3.2.13 Support aldehyde functionalization

1 g of epoxy support was mixed with 10 mL of 100 mM H₂SO₄ and incubated overnight. After washing with deionized water, the resin was treated with 10 mL of 30 mM NaIO₄ for 2 hours, followed by washing with water. (Guisán, 1988) For the quantification of the aldehyde groups at 405 nm, the aforementioned procedure for the quantification of epoxy group was followed.

3.2.14 Covalent immobilization on glyoxyl support

The protein solution was prepared in a 100 mM NaHCO₃ buffer, pH 10. After washing the support with the same buffer, the protein solution was added. After incubation, the Schiff bases were reduced by adding 10 mg of NaBH₄ to the suspension, left then under mild agitation for 30 minutes at 4 °C.

3.2.15 Covalent immobilization on epoxy support with directionality

First, 1 g of epoxy resin was incubated with 2 mL of modification buffer (100 mM sodium borate, 2 M iminodiacetic acid, 50 mM phosphate buffer, pH 8) under gentle agitation for 2 hours. After washing, the modified support was incubated with 5 mL of metal buffer (1 M NaCl, 5 mg/mL CoCl₂ in 50 mM phosphate buffer, pH 6) for 2 hours. The support was then washed and incubated with the protein solution. After immobilization, the support was washed with 3 mL of desorption buffer (50 mM EDTA, 500 mM NaCl in 50 mM phosphate buffer, pH 7) to remove the metal and rinsed with deionized water. The support was then incubated in 4 mL blocking buffer (3 M glycine in 20 mM phosphate buffer, pH 8.5) overnight, followed by a final wash. (Mateo et al., 2007a)

3.2.16 Polyethyleneimine coating of epoxy supports

To prepare the coating solution, 10 mg/mL of polyethyleneimine was dissolved in 100 mM NaHCO₃ buffer (pH 10). Subsequently, 10 mL of the prepared solution was combined with 1 g of the chosen epoxy-support (EP400/SS or agarose) and incubated overnight. Post-incubation, the epoxy resin was extensively washed with deionized water and stored at 4°C. The protein solution in 5 mM phosphate buffer (pH 7) was incubated with the support.

3.2.17 Stability assay for immobilized enzyme against apolar organic solvents

An assay was conducted to evaluate the stability of immobilized enzymes in the presence of apolar organic solvents. For this experiment, a sample of the immobilized support, ranging between 20 to 50 mg, was placed in a glass vial. The vial contained a mixture of an aqueous phase, consisting of the buffer used during the catalysis of the reaction, and an organic phase, typically toluene. The enzyme-bound support was incubated for specific time intervals, including 1, 2, 4, and 6 hours. Following each incubation period,

the resin was thoroughly washed, and an enzyme activity test was performed to determine the stability of the immobilized enzyme under these conditions. This approach provided crucial insights into the enzyme's resilience when exposed to apolar organic solvents.

3.2.18 Alginate beads production

The formation of alginate beads containing whole cells expressing VImd or purified enzyme was achieved through an extrusion process using a peristaltic pump. A mixture of 5 % sodium alginate and *E. coli* cells expressing VImd was prepared to yield 60 or 120 OD in the alginate mixture. Alternatively, for encapsulating purified enzyme, a solution of 10 mg/mL of VImD was mixed with 5 % sodium alginate in a 2:1 proportion (enzyme solution : sodium alginate). This mixture was then pumped through a PTFE tube with 3 mm diameter, and at the end of the tube, a pipette tip was placed to generate a continuous flow of droplets. The flow rate was 3 mL/min. These droplets were dropped into a solution of either CaCl₂ or BaCl₂, which caused the sodium alginate to crosslink and solidify, forming beads containing the whole cells or purified enzyme. This method allowed for the efficient encapsulation of the cells or enzyme within the alginate beads, creating a biocatalyst suitable for use in biotransformation reactions.

3.2.19 Biotransformations in batch

Enzymatic reactions were performed in 1.5 or 2 mL microcentrifuge tubes, where a mixture of substrate(s), cofactor (if needed), and biocatalyst(s), either in a free or immobilized form, were added. The reaction mixture was then incubated at the preferred temperature for a specified amount of time. After the incubation period, the reaction was stopped, and samples were taken to analyze the conversion to the product(s).

3.2.19.1 *LbTDC* biotransformations

For batch reactions using *LbTDC*, either free or immobilized biocatalysts were used. In the case of free enzyme, the reaction was performed in 2 mL Eppendorf tubes. The reaction mixture contained 2.5 mM of substrate (L-tyrosine or L-DOPA), which was suspended in 200 mM sodium acetate buffer pH 5.0, along with 0.2 mM PLP. The free enzyme concentration in the biotransformation was 0.03 mg/mL. The reaction mixture was then incubated at 37 °C with constant shaking at 150 rpm. The final reaction volume was 1 mL, and 100 µL aliquots were collected at different reaction times. To stop the reaction, 0.2 % HCl was added to all samples, which were then submitted for HPLC analysis.

In the case of immobilized *LbTDC*, the reaction was performed using 20 mg of the immobilized biocatalyst instead of free enzyme. The reaction mixture contained 5 mM of substrate, which was suspended in 200 mM sodium acetate buffer pH 5.0, 0.2 mM PLP. The reaction mixture was left under mixing at 37 °C with constant shaking at 150 rpm. The final reaction volume was 2 mL, and 50 µL aliquots were collected at different

reaction. To stop the reaction, 0.2 % HCl was added to all samples, which were then submitted for HPLC analysis.

3.2.19.2 *He*WT and *Ts*RTA biotransformations with HLADH

Biotransformations using *He*WT and *Ts*RTA (free or immobilized) together with HLADH (free or immobilized) were performed in 2 mL Eppendorf tubes. Substrate (tyramine, dopamine or 2- phenylethylamine) was suspended in 100 mM sodium phosphate buffer pH 8.5. When dopamine was chosen, 2.5 mM ascorbic acid was added in the reaction mixture. The reaction solution was prepared by mixing 5 mM, 10 mM, or 20 mM of substrate (1 equivalent) with 0.1 mM PLP, NADH and pyruvate (2, 10 or 50 equivalents). Different ratios of units of activity (U:U) of *He*WT:HLADH (1:1, 1:2, 1:3, 1:10) and *Ts*RTA:HLADH (1:1, 1:2, 1:3, 1:10) were trailed in biotransformations.

The reaction mixtures were incubated at 37 °C, 150 rpm, with a final reaction volume of 1 mL. Aliquots (50 µL) were collected at different time points (0, 1, 2, 3, 4, 6, 24 hours) and added to 350 µL of the 0.2 % HCl for HPLC analysis.

3.2.19.3 Biotransformation of VImD

Biotransformations using VImD were performed with different enzyme and substrate concentrations. In particular, the biocatalyst concentrations trialed were 0.5, 1, or 1.5 mg/mL of VImD, added to a reaction mixture containing the substrate, at a concentration depending on the substrate solubility, in buffer phosphate buffer, with 0.1 mM PLP, pH 7.5. The reaction mixture was then incubated at 37 °C and 150 rpm. The reaction was then sampled over time up to 24 hours, and the collected aliquots were derivatized with FMOc (in all cases of aliphatic substrates) to determine the maximum conversion of the product using HPLC. After FMOc derivatization, the sample was mixed with 0.2 % HCl and acetonitrile and submitted for HPLC analysis.

3.2.19.4 Biotransformations with VImD in whole cell alginates

Biotransformations using alginate beads containing whole cells expressing VImD were carried out in 2 mL Eppendorf. The batch reaction mixtures were prepared with different substrates concentrated according to their respective solubilities. 200 mg of alginate beads were added to 1 mL of reaction mixtures in 100 mM HEPES buffer, pH 7.5. The biotransformations were then incubated at 37 °C with constant shaking at 150 rpm. Aliquots were collected at different reaction times to monitor the progress of the biotransformation. After FMOc derivatization, a mix of 0.2 % HCl and acetonitrile was added to all samples, which were then submitted for HPLC analysis to determine the conversion of the substrates and the formation of the desired products.

3.2.19.5 Biotransformations with VImD in purified enzyme alginates

Biotransformations using alginate beads containing encapsulated free enzyme were performed in 2 mL Eppendorf where 200 mg of alginate beads with the encapsulated enzyme were added to a 1 mL reaction mixture. This mixture contained 0.1 M substrate and 0.1 mM PLP in 0.1 M HEPES buffer, pH 7.5. The biotransformations were incubated at 37 °C, and agitated at 150 rpm to ensure proper mixing. Aliquots were collected at different time points during the reaction to monitor the progress and determine the conversions to product. The samples were prepared for further HPLC analysis, after FMOC derivatization, in 0.2 % HCl and acetonitrile solution.

3.2.19.6 Scale up of VImD decarboxylation reactions in SpinChem® system

In the SpinChem® system, the VImD decarboxylation reactions were carried out starting with the preparation of the amino acid starting material, which was solubilized in HEPES buffer (pH 7.5) containing 0.1 mM PLP, to reach a final volume of 0.2 L. For the set up of the rotating packed bed reactor, 20 g of whole cell barium alginate beads, prepared as previously described, were placed into the reactor. The SpinChem® vessel glass jacket was then connected with tubes to a water bath, which was used to maintain a reaction temperature of 37 °C. The heating was facilitated by circulating the heated water using a peristaltic pump. Upon setting the reactor within the SpinChem® vessel, the starting material solution was added. The reaction was initiated by rotating the reactor at a speed of 340 rpm. The reaction progress was carefully monitored and the total reaction time did not exceed 24 hours.

3.2.20 Distillation of isobutylamine from the decarboxylation of L-valine

The L-valine decarboxylation reaction conducted in the SpinChem® system was processed further for product isolation. The resulting isobutylamine solution was transferred to a 500 mL round bottom flask, which was then connected to a distillation column and placed in an oil bath for its heating and evaporation. A T-shaped tube was installed at the top of the distillation column, which accommodated the thermometer and also provided a connection to the condenser. The condenser, set up for the transformation of vapor into liquid, was linked with a water stream. Once the vapour began to condense at 50°C, it was collected as distillate in a series of pre-weighed round bottom flasks arranged in a spider fraction collector. The distillate from this process was subsequently identified as pure isobutylamine via NMR analysis.

3.2.21 Liquid-liquid extraction of 1-amino-2-propanol and 3-(methylthio)propylamine

To isolate 1-amino-2-propanol and 3-(methylthio)propylamine, a liquid-liquid extraction methodology was implemented. The process was initiated by adjusting the pH of the

product solutions to pH 10, followed by a centrifugation step to eliminate protein precipitate from the solution. Different organic phases were trailed for the extraction: dichloromethane (DCM), ethyl acetate, heptane, methyl tert-butyl ether (MTBE), and diethyl ether.

Salting-Out Assisted Liquid-Liquid Extraction (SALLE)(Tang & Weng, 2013) was also attempted. With this approach, NaCl was added until saturation of the basified aqueous phase. This solution was then transferred to a separatory funnel and was extracted twice using the same volume of acetonitrile. To facilitate phase separation, hexane was added to the acetonitrile phase in a volume ratio of 1:20. The acetonitrile phase was collected, dried using sodium sulphate, and subsequently filtered using a paper filter. The filtrate was collected into a pre-weighed round-bottom flask, evaporated, and then analyzed via NMR.

3.2.22 Continuous flow biotransformation process

For enzymatic biotransformations, the employed continuous flow system comprised a commercially available R2S pumping module and R-4 reactor heater, both sourced from Vapourtec®. The meso-reactors utilized were Omnifit glass columns (6.6 mm bore x 150 mm length), incorporating glass heat exchangers in the setup. The packed bed reactor (PBR) was filled with the immobilized biocatalyst before being integrated into the continuous flow system. When necessary, a T-tube connection was used to allow the mixing of reagents. Flow rates were adjusted and optimized for each reaction, taking into account the length of the bed reactor and the required residence time ($\text{length [cm]} \times 0.3421 = \text{total volume [mL]}$. $\text{Total volume [mL]} / \text{residence time [min]} = \text{flow [mL/min]}$). To ensure accuracy, the exiting flow stream was collected in separate vials for each reaction cycle, with a collection time corresponding to the residence time.

3.2.22.1 Continuous flow decarboxylation with *LbTDC*

The continuous flow decarboxylation was carried out using *LbTDC* to convert L-tyrosine to tyramine or L-DOPA to dopamine. The packed bed reactor (PBR) employed in this experiments had a volume of 1.3 mL. Two protein loadings were tested, 1 mg/g and 5 mg/g.

The stock solutions for the continuous flow reaction were prepared in a 200 mM sodium acetate buffer at pH 5, with 0.1 mM PLP. In the case of L-DOPA, the buffer was supplemented with 0.45 mg/mL ascorbic acid. To ensure the complete solubilization of the substrates in the solution, the maximum concentration in the stock solution was kept at 5 mM, given the working pH of 5.0. The residence times tested in the experiment were 2.5, 5, 10, and 15 minutes. *LbTDC* was tested in a continuous flow system using only the EP400/SS support as immobilized biocatalyst. The temperature of the PBR was set at 37°C.

3.2.22.2 Continuous flow reactions with *HeWT*, *TsRTA* and *HLADH*

The continuous flow reactions involved transamination followed by hydrogenation, starting from 2-phenylethylamine or tyramine or dopamine substrates. An immobilized transaminase, *HeWT* or *TsRTA*, and an alcohol dehydrogenase, *HLADH*, were employed as biocatalysts. The substrate concentration in the initial stock solution was trialed with different values as 2.5, 5, or 10 mM. In addition to the aqueous phase, which contained the substrate, the cofactors and the amino-acceptor (100 mM phosphate buffer, pH 8, 0.1 mM PLP, 1 equivalent of dopamine or tyramine, 2,10 or 50 equivalents of pyruvate, 1 equivalent of NADH), an organic phase was introduced before the packed bed reactor (PBR) through a T-tube connection. Toluene was used as the organic phase, creating a segmented continuous flow system. A Zaiput liquid-liquid separator was placed at the end of the flow stream to separate the two phases, allowing for efficient product recovery and analysis. The PBR volume was 3.5 mL and the residence time was 30 minutes. The ration between aqueous phase and toluene was 7:3. The temperature of the PBR was set at 37°C or 28 °C.

3.2.22.3 Continuous flow decarboxylation with *VImD*

The continuous flow decarboxylation process utilized alginates containing the immobilized *VImD* enzyme, or in whole cells or as purified enzyme. In the packed bed reactor (PBR), alginates were carefully placed alongside celite, with the celite-to-alginate ratio optimized to provide the best biocatalyst stability while minimizing celite usage (ratio 1:25, celite : alginate). The PBR had a volume of 4 mL, and various residence times were tested to determine optimal reaction conditions. The stock solution contained the substrate and PLP cofactor (0.1 mM), prepared in 100 mM HEPES buffer, pH 7.5. To maintain optimal enzyme activity, the temperature of the PBR was set at 37°C.

3.2.23 L-DOPA fermentation

The *VH33ΔtyrR_DOPA* preculture in LB medium with 100 µg/ml ampicillin, 30 µg/ml tetracycline, and 30 µg/mL kanamycin was incubated overnight at 37°C and 150 rpm. Subsequently, 300 mL of LB medium, supplemented with 100 µg/ml ampicillin, 30 µg/ml tetracycline, and 30 µg/mL kanamycin, were inoculated with the preculture to achieve an OD₆₀₀ of 0.1. The cells were then incubated overnight at 37 °C and 150 rpm. The overnight preculture, with an OD₆₀₀ of 3.8, was used as the starting point for flask fermentation and bioreactor.

3.2.23.1 Storage of the strain *VH33ΔtyrR_DOPA*

VH33ΔtyrR_DOPA is an *E. coli* cell strain transformed with *pJLBaroG^{fbr}tktA* (*aroG^{fbr}* under control of the *lacUV5* promoter; and *tktA* under its native promoter) and

pTrchpaBCTrctyrCphea_{CM} (*hpaBC*, *tyrC* and *phea_{CM}* under control of the *trc* promoter).(Muñoz et al., 2011)

Glycerol stocks were used for long-term storage of VH33Δ*tyrR*_DOPA. To prepare a glycerol stock, an overnight cell culture was first grown in LB with 100 µg/ml ampicillin, 30 µg/ml tetracycline, and 30 µg/ml kanamycin. An aliquot of cell culture was then mixed with a solution containing 40% glycerol, creating a 50:50 (v/v) mixture in 1.5 mL Eppendorf tubes. Glycerol, a cryoprotector, helps to protect the cells from damage during the freezing process. The tubes were placed at - 80°C for long-term storage. When needed, the cells were taken from the freezer and thrown into dry ice in order to keep the glycerol stock frozen. The glycerol stock was used to streak an agar plate for the subsequent inoculation of LB medium for the overnight culture.

3.2.23.2 M9 medium preparation

The Minimal salt medium M9 for L-DOPA fermentation in flask was prepared mixing 6 g/L Na₂HPO₄, 0.5 g/L NaCl, 3 g/L KH₂PO₄ and 1 g/L NH₄Cl. To this solution 10 g/L glucose, 0.247 g/L MgSO₄, 0.0147 g/L CaCl₂ were then added. Typically, five stocks solutions (5X) for M9 salts, D-glucose, MgSO₄, CaCl₂ and ascorbic acid were prepared and filtered with 0.2 µm filter under the laminar flow hood, where the final fermentation medium was set up.

The optimized composition of the fermentation medium (M9Y) used in the bioreactor comprised 6 g/L Na₂HPO₄, 0.5 g/L NaCl, 3 g/L KH₂PO₄, 1 g/L NH₄Cl, 0.247 g/L MgSO₄, 0.0147 g/L CaCl₂, 50 g/L D-glucose, 2 g/L yeast extract, 0.45 g/L ascorbic acid.

3.2.23.3 L-DOPA fermentation in flask

The flask fermentation of L-DOPA from glucose started by using cells from the overnight preculture of VH33Δ*tyrR*_DOPA strain. The cells were inoculated into 250 mL flasks containing 100 mL of LB medium supplemented with 10 g/L D-glucose with 100 µg/mL ampicillin, 30 µg/mL tetracycline, and 30 µg/mL kanamycin at the initial OD₆₀₀ of 0.1. The shaking flasks were then incubated at 37 C, 150 rpm. After 1.5 h, 0.1 mM IPTG was added, and the cells were further incubated for another 3 h. After that, the cells were harvested by centrifugation (2500 rpm, 20 minutes), washed twice with M9 medium, and resuspended at a wet cell weight concentration of 28 g/L in 250 mL flasks containing 35 mL of M9 medium supplemented with 10 g/L D-glucose and 0.1 mM IPTG. The flasks were incubated at 37°C with 150 rpm shaking. After 24, 42 and 48 hours the biotransformations were sampled and the filtered aliquots submitted for HPLC analysis.

3.2.23.4 L-DOPA fermentation in bioreactor

The bioreactor for L-DOPA fermentation from glucose was performed at 0.65 L volume. The fermenter used was a 2 L volume vessel BiostatA (Sartorius), which was autoclaved along with the medium, a pH probe (Hamilton), an oxygen probe (Hamilton), the stirrer,

the cooling finger, the exhauster, and the necessary tubes. The base (NH₄OH 3 % v/v) and acid (H₃PO₄ 3 N) stock bottles, together with the one for the antifoam 204, were also autoclaved connected and clamped to the vessel lid ports. The selected optimal fermentation medium was M9Y, whose composition is described in the section 3.2.1 Culture media. The air flow system, measured in cubic centimeters per minute (ccm), was set at 250 ccm. The stirring was started at 800 rpm and the heating jacket was activated to keep the temperature of 37°C. The inoculum was then performed through a septum on the top of the vessel lid using a sterile syringe. An oxygen cascade was implemented to ensure 60% oxygen saturation. To ensure efficient oxygen transfer to the culture, the agitation speed was automatically adjusted, minimizing the usage of compressed air. Samples were taken to measure the OD₆₀₀, the glucose consumption and the L-tyrosine or L-DOPA production. The fermentation was performed for 68 hours, when the broth was finally harvested. After the biomass was discarded, the broth was stored at -20° C with the addition of 0.45 g/L ascorbic acid or adjusting the pH to 2 with 2 M HCl, to prevent the oxidation of L-DOPA.

3.2.23.5 Glucose quantification

The Megazyme D-Glucose (glucose oxidase/peroxidase; GOPOD) Assay Kit employs high purity glucose oxidase and peroxidase and was used for the measurement of D-glucose in the fermentation broth. In principle, in the kit-assay, the first reaction involved is the oxidation of glucose by a glucose oxidase, which convert D-glucose and water into D-gluconate and hydrogen peroxide. Hydrogen peroxide is then exploited from a peroxidase to form, from *p*-hydroxybenzoic acid and 4-aminoantipyrine, the quinoneimine dye. To perform the assay, 3 mL of GOPOD reagent (*p*-hydroxybenzoic acid and sodium azide, 0.095 % w/v, pH 7.4) were mixed with 100 µl of sample solution from the fermenter broth and incubated at 45 °C for 20 minutes in a thermomixer. The absorbance was measured in a 1 mL cuvette at 510 nm. The blank was set up with water, used instead of the fermentation broth. The concentration of D-glucose could be calculated from the ratio between the absorbance values from the sample analysis and the D-glucose standard from the kit.

3.2.24 Cloning PheDH

The PheDH gene (pTac85-*BsPheDH*) was cloned into the pRSETb vector, which contains a poly-histidine tag. PCR primers listed in Table 3.4 were designed for amplification, using Q5 High Fidelity DNA Polymerase and following the recommended procedure. The BamHI and HindIII restriction sites were used for cloning.

Primer Name	Sequence	Length (bp)	Tm (°C)	GC content (%)	Secondary structure
-------------	----------	-------------	---------	----------------	---------------------

Fwd_HisTag-PheDH	GTAGGATCCAATGGCA AAACAGCTTGAAAAG	31	73.5	41.9	Very weak
Rev_HisTag-PheDH	GCGAAGCTTTTACTCTT TTATGTTCCACTTCG	32	71.9	40.6	Moderate

Table 3.4: PheDH cloning primers

After thermocycling, the sample was loaded onto a 0.8 % (w/v) electrophoresis agarose gel, and the DNA fragment was purified with the GeneJET Gel Extraction kit. The purified PCR product (DNA insert) was digested with BamHI and HindIII restriction enzymes, along with the vector backbone. The resulting insert fragments and pRSETb backbone were purified and ligated with T4 Ligase. The reaction was incubated overnight at 16 °C, followed by ethanol precipitation using sodium acetate as salt.

The *BsPheDH*-pRSETb plasmid was transformed into electrocompetent *E. coli* XL10-GOLD cells, and a single colony was grown in 5 mL LB supplemented with ampicillin overnight to propagate the plasmid. The plasmid was then collected using the GeneJET Plasmid Miniprep kit. The obtained purified plasmid was sent for sequencing to confirm the success of the cloning.

3.2.25 Phenylalanine dehydrogenase in solid screening design

To engineer PheDH in order to obtain amine dehydrogenase activity towards catecholamines, a screening assay was needed. To identify the active mutant, the measurement of NADH generated through the conversion of the amino substrate to the oxidative deamination product was attempted directly on the culture agar plate with colonies, exploiting different dyes such as MTT (3-(4,5-dimethylthiazol-2-yl)-2,5-diphenyltetrazolium bromide) and WST-1 (2-(4-Iodophenyl)-3-(4-nitrophenyl)-5-(2,4-disulfophenyl)-2H-tetrazolium) (Figure 3.1). To set up the method, the natural substrate of PheDH, L-phenylalanine, was adopted to be converted into phenylpyruvate.

The screening assay procedure started plating the transformed cells onto a nitrocellulose membrane placed on an agar plate. After the growth of the colonies overnight, the induction of the protein expression was performed by placing the membrane with colonies on an agar plate where IPTG was added at 1 mM concentration for 16 hours at 37°C. (Planchestainer et al., 2019)

The depletion of the endogenous cofactor was attempted exposing the cells to WST-1 and PMS (phenazine methosulfate), using the kit CCK-8 (Sigma Aldrich), with the development of an orange dye coming from the conversion of the endogenous NADH to NAD⁺.

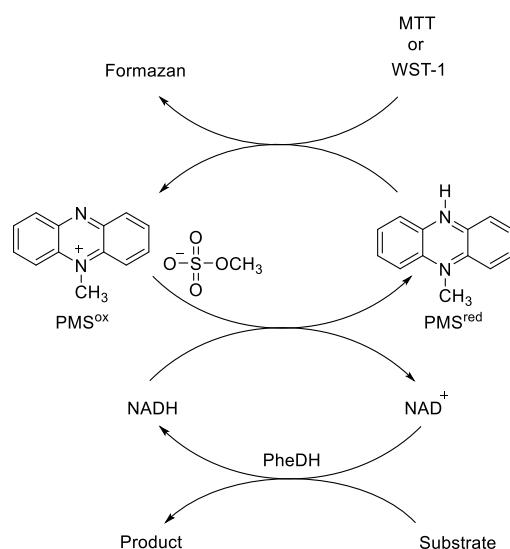


Figure 3.1 : Mechanism of action of MTT or WST-1 with PMS for the formation of colored formazan salts from NADH.

After washing the membrane with buffer, it was placed on a fresh agar plate and 1 mM NAD⁺ and 10 mM L-phenylalanine were offered to the cells, along with MTT and PMS. In this step, different conditions were trialed with 50 μ M MTT and 10 μ M PMS, and with 100 μ M MTT and 20 μ M PMS. The colorimetric reaction given by the MTT dye, precipitating inside the cells, should have allowed to identify by eye the active mutant colonies, which should have turned dark. The incubation for the colorimetric reaction was performed in absence of light for 2-4 hours.

Following a different strategy, MTT and PMS were also added afterwards the exposure of the cells to the substrate and the cofactor, allowing the oxidative deamination reaction to be catalysed before adding, after 1 or 2 hours, the selected reagents. A negative control with cell not expressing *PheDH* was always performed in parallel.

3.2.26 Hordenine production with reductive amination reaction of tyramine

Batch reactions were carried out in 15 mL Falcon tubes. A 2 mL solution of 10 mM tyramine in 200 mM sodium acetate buffer was combined with the desired volume of 37 % formaldehyde solution. In the initial screening, sodium triacetoxyborohydride (STAB), cyanoborohydride and sodium borohydride were tested mixing 50 mg each reducing agent with the tyramine solution to which 200 μ L of acetic acid were added. For the optimization experiments, in the case of STAB, 200 μ L of acetic acid and 2 mL of acetonitrile were mixed with the solution of tyramine and formaldehyde before the final addition of the reducing agent. For pic-BH₃, reactions were conducted with the same volume of acetic acid for the acidic pH tests or by diluting formaldehyde in 250 mM sodium carbonate for the experiments at basic pH. The reaction mixture was agitated, and 50 μ L aliquots from the batch reductive amination reactions were collected, mixed with 0.2 % HCl, and subjected to HPLC analysis. (Gianolio et al., 2022)

3.2.27 Continuous flow chemo enzymatic system for hordenine production with homogeneous operation conditions

Feedstock solutions were prepared in 50 mL Falcon tubes. The tyrosine stock solution consisted of 5 mM L-tyrosine disodium salt hydrate and 0.2 mM PLP in 200 mM sodium acetate buffer at pH 5. A 62.5 mM formaldehyde solution with 2.5 % v/v acetic acid in acetonitrile was prepared by diluting the commercial 37 % formaldehyde solution. The reducing agent STAB was dissolved in acetonitrile at a concentration of 60 mM, and the suspension was maintained homogeneous with magnetic stirring at 1500 rpm during the experiment. 1.3 mL PBR with immobilized *LbTDC* was connected to two T-tubes, corresponding to the inlets for formaldehyde (62.5 mM formaldehyde, 2.5 % v/v acetic acid in acetonitrile) and STAB (60 mM STAB in acetonitrile). The feeding flow rate for the PBR was 0.54 mL/min, the same as for the formaldehyde inlet and exactly half of the reducing agent feed. In line, a 10 mL flow coil reactor was connected and fed, at the resulting flow rate of 2.16 mL/min, with the mixed solutions, achieving a residence time of 5 minutes.(Gianolio et al., 2022)

3.2.28 Continuous flow chemo enzymatic system for hordenine production with heterogenous operation conditions

The feedstock for the L-tyrosine starting material was created as aforementioned. A 202.5 mM formaldehyde solution was prepared in 250 mM sodium carbonate (pH 11.5) from the commercial 37 % formaldehyde solution. 1.3 mL PBR with immobilized biocatalyst was connected to one T-tube, corresponding to the inlet for formaldehyde (202.5 mM formaldehyde, 250 mM sodium carbonate). The feeding flow rate for the immobilized *LbTDC* PBR was maintained at 0.54 mL/min, while the formaldehyde solution was pumped with a flow rate set at 0.1 mL/min. In line, the first PBR with immobilized enzyme was connected with a second PBR, containing 300 mg pic-BH₃ homogeneously mixed with 300 mg celite. The final flow rate was 0.64 mL/min, and the residence time in the PBR was 2.5 minutes.(Gianolio et al., 2022)

3.2.29 Hordenine isolation and purification

A 300 mL aliquot of the final product solution obtained using the STAB system was extracted once with an equal volume of ethyl acetate after adjusting the pH to 9.6. The aqueous phase was then washed twice with the same volume of ethyl acetate, and the organic phases were combined in a single flask. Sodium sulfate anhydrous was added to the mixture, which was subsequently filtered. The ethyl acetate was evaporated, leaving behind the crude product, which was resuspended in 5 mL of acetonitrile. An equimolar amount of 37 % HCl solution was added to the suspension to form hordenine hydrochloride, and the resulting precipitate was dried and submitted for NMR analysis. For the pic-BH₃ alternative process, 130 mL of the hordenine solution was extracted with

ethyl acetate (5 × 30 mL organic phase). After drying with sodium sulfate anhydrous, the solution was filtered, and the precipitation of hordenine hydrochloride was carried out in ethyl acetate as previously described. The precipitate was dried and submitted for NMR analysis.(Gianolio et al., 2022)

3.3 Bibliography

Abrahamson, M. J., Vázquez-Figueroa, E., Woodall, N. B., Moore, J. C., & Bommaris, A. S. (2012). Development of an Amine Dehydrogenase for Synthesis of Chiral Amines.

Angewandte Chemie International Edition, 51(16), 3969–3972.
<https://doi.org/10.1002/anie.201107813>

- Abrahamson, M. J., Wong, J. W., & Bommaris, A. S. (2013). The Evolution of an Amine Dehydrogenase Biocatalyst for the Asymmetric Production of Chiral Amines. *Advanced Synthesis & Catalysis*, 355(9), 1780–1786. <https://doi.org/10.1002/adsc.201201030>
- Alcántara, A. R., Domínguez de María, P., Littlechild, J. A., Schürmann, M., Sheldon, R. A., & Wohlgenuth, R. (2022). Biocatalysis as Key to Sustainable Industrial Chemistry. *ChemSusChem*, 15(9). <https://doi.org/10.1002/cssc.202102709>
- Almrud, J. J., Oliveira, M. A., Kern, A. D., Grishin, N. V., Phillips, M. A., & Hackert, M. L. (2000). Crystal structure of human ornithine decarboxylase at 2.1 Å resolution: structural insights to antizyme binding. *Journal of Molecular Biology*, 295(1), 7–16. <https://doi.org/10.1006/jmbi.1999.3331>
- Andréll, J., Hicks, M. G., Palmer, T., Carpenter, E. P., Iwata, S., & Maher, M. J. (2009). Crystal Structure of the Acid-Induced Arginine Decarboxylase from *Escherichia coli* : Reversible Decamer Assembly Controls Enzyme Activity. *Biochemistry*, 48(18), 3915–3927. <https://doi.org/10.1021/bi900075d>
- Anwar, S., Mohammad, T., Shamsi, A., Queen, A., Parveen, S., Luqman, S., Hasan, G. M., Alamry, K. A., Azum, N., Asiri, A. M., & Hassan, M. I. (2020). Discovery of hordenine as a potential inhibitor of pyruvate dehydrogenase kinase 3: Implication in lung cancer therapy. *Biomedicines*, 8(5), 32–228.
- Asano, Y., Nakazawa, A., & Endo, K. (1987). Novel phenylalanine dehydrogenases from *Sporosarcina ureae* and *Bacillus sphaericus*. Purification and characterization. *The Journal of Biological Chemistry*, 262(21), 10346–10354. <http://www.ncbi.nlm.nih.gov/pubmed/3112142>
- Báez, J. L., Bolívar, F., & Gosset, G. (2001). Determination of 3-deoxy-D- *arabino* -heptulosonate 7-phosphate productivity and yield from glucose in *Escherichia coli* devoid of the glucose phosphotransferase transport system. *Biotechnology and Bioengineering*, 73(6), 530–535. <https://doi.org/10.1002/bit.1088>
- Bai, Z., Sun, X., Yu, X., & Li, L. (2019). Chitosan Microbeads as Supporter for *Pseudomonas putida* with Surface Displayed Laccases for Decolorization of Synthetic Dyes. *Applied Sciences*, 9(1), 138. <https://doi.org/10.3390/app9010138>
- Baker, P. J., Turnbull, A. P., Sedelnikova, S. E., Stillman, T. J., & Rice, D. W. (1995). A role for quaternary structure in the substrate specificity of leucine dehydrogenase. *Structure*, 3(7), 693–705. [https://doi.org/10.1016/S0969-2126\(01\)00204-0](https://doi.org/10.1016/S0969-2126(01)00204-0)
- Barwell, C. J., Basma, A. N., Lafi, M. A. K., & Leake, L. D. (2011). Deamination of hordenine by monoamine oxidase and its action on vasa deferentia of the rat. *Journal of Pharmacy and Pharmacology*, 41(6), 421–423. <https://doi.org/10.1111/j.2042-7158.1989.tb06492.x>
- Bell, E. L., Finnigan, W., France, S. P., Green, A. P., Hayes, M. A., Hepworth, L. J., Lovelock, S. L., Niiikura, H., Osuna, S., Romero, E., Ryan, K. S., Turner, N. J., & Flitsch, S. L. (2021). Biocatalysis. *Nature Reviews Methods Primers*, 1(1), 46. <https://doi.org/10.1038/s43586-021-00044-z>

- Benítez-Mateos, A. I., Roura Padrosa, D., & Paradisi, F. (2022). Multistep enzyme cascades as a route towards green and sustainable pharmaceutical syntheses. *Nature Chemistry*, *14*(5), 489–499. <https://doi.org/10.1038/s41557-022-00931-2>
- Bennett, M., Ducrot, L., Vergne-Vaxelaire, C., & Grogan, G. (2022). Structure and Mutation of the Native Amine Dehydrogenase MATOUAmDH2. *ChemBioChem*, *23*(10). <https://doi.org/10.1002/cbic.202200136>
- Berridge, M. V., Herst, P. M., & Tan, A. S. (2005). *Tetrazolium dyes as tools in cell biology: New insights into their cellular reduction* (pp. 127–152). [https://doi.org/10.1016/S1387-2656\(05\)11004-7](https://doi.org/10.1016/S1387-2656(05)11004-7)
- Bertelli, M., Kiani, A. K., Paolacci, S., Manara, E., Kurti, D., Dhuli, K., Bushati, V., Miertus, J., Pangallo, D., Baglivo, M., Beccari, T., & Michelini, S. (2020). Hydroxytyrosol: A natural compound with promising pharmacological activities. *Journal of Biotechnology*, *309*, 29–33. <https://doi.org/10.1016/j.jbiotec.2019.12.016>
- Bhatia, S. K., Kim, Y. H., Kim, H. J., Seo, H.-M., Kim, J.-H., Song, H.-S., Sathiyarayanan, G., Park, S.-H., Park, K., & Yang, Y.-H. (2015). Biotransformation of lysine into cadaverine using barium alginate-immobilized *Escherichia coli* overexpressing CadA. *Bioprocess and Biosystems Engineering*, *38*(12), 2315–2322. <https://doi.org/10.1007/s00449-015-1465-9>
- Bloch, D. N., Sandre, M., Ben Zichri, S., Masato, A., Kolusheva, S., Bubacco, L., & Jelinek, R. (2023). Scavenging neurotoxic aldehydes using lysine carbon dots. *Nanoscale Advances*, *5*(5), 1356–1367. <https://doi.org/10.1039/D2NA00804A>
- Böhmer, W., Knaus, T., & Mutti, F. G. (2018a). Hydrogen-Borrowing Alcohol Bioamination with Coimmobilized Dehydrogenases. *ChemCatChem*, *10*(4), 731–735. <https://doi.org/10.1002/cctc.201701366>
- Böhmer, W., Knaus, T., & Mutti, F. G. (2018b). Hydrogen-Borrowing Alcohol Bioamination with Coimmobilized Dehydrogenases. *ChemCatChem*, *10*(4), 731–735. <https://doi.org/10.1002/cctc.201701366>
- Cai, R.-F., Liu, L., Chen, F.-F., Li, A., Xu, J.-H., & Zheng, G.-W. (2020). Reductive Amination of Biobased Levulinic Acid to Unnatural Chiral γ -Amino Acid Using an Engineered Amine Dehydrogenase. *ACS Sustainable Chemistry & Engineering*, *8*(46), 17054–17061. <https://doi.org/10.1021/acssuschemeng.0c04647>
- Caparco, A. A., Bommarius, B. R., Bommarius, A. S., & Champion, J. A. (2020). Protein-inorganic calcium-phosphate supraparticles as a robust platform for enzyme co-immobilization. *Biotechnology and Bioengineering*, *117*(7), 1979–1989. <https://doi.org/10.1002/bit.27348>
- Caparco, A. A., Pelletier, E., Petit, J. L., Jouenne, A., Bommarius, B. R., Berardinis, V., Zapparucha, A., Champion, J. A., Bommarius, A. S., & Vergne-Vaxelaire, C. (2020). Metagenomic Mining for Amine Dehydrogenase Discovery. *Advanced Synthesis & Catalysis*, *362*(12), 2427–2436. <https://doi.org/10.1002/adsc.202000094>
- Capitani, G. (2003). Crystal structure and functional analysis of *Escherichia coli* glutamate decarboxylase. *The EMBO Journal*, *22*(16), 4027–4037. <https://doi.org/10.1093/emboj/cdg403>

- Cerioli, L., Planchestainer, M., Cassidy, J., Tessaro, D., & Paradisi, F. (2015). Characterization of a novel amine transaminase from *Halomonas elongata*. *Journal of Molecular Catalysis B: Enzymatic*, *120*, 141–150. <https://doi.org/10.1016/j.molcatb.2015.07.009>
- Chen, W., Yao, J., Meng, J., Han, W., Tao, Y., Chen, Y., Guo, Y., Shi, G., He, Y., Jin, J.-M., & Tang, S.-Y. (2019). Promiscuous enzymatic activity-aided multiple-pathway network design for metabolic flux rearrangement in hydroxytyrosol biosynthesis. *Nature Communications*, *10*(1), 960. <https://doi.org/10.1038/s41467-019-08781-2>
- Claes, L., Janssen, M., & De Vos, D. E. (2019). Organocatalytic Decarboxylation of Amino Acids as a Route to Bio-based Amines and Amides. *ChemCatChem*, *11*(17), 4297–4306. <https://doi.org/10.1002/cctc.201900800>
- Contente, M. L., & Paradisi, F. (2018). Self-sustaining closed-loop multienzyme-mediated conversion of amines into alcohols in continuous reactions. *Nature Catalysis*, *1*(6), 452–459. <https://doi.org/10.1038/s41929-018-0082-9>
- Cosenza, V. A., Navarro, D. A., & Stortz, C. A. (2011). Usage of α -picoline borane for the reductive amination of carbohydrates. *Arkivoc*, *2011*(7), 182–194. <https://doi.org/10.3998/ark.5550190.0012.716>
- Coyle, J. P., Johnson, C., Jensen, J., Farcas, M., Derk, R., Stueckle, T. A., Kornberg, T. G., Rojanasakul, Y., & Rojanasakul, L. W. (2023). Variation in pentose phosphate pathway-associated metabolism dictates cytotoxicity outcomes determined by tetrazolium reduction assays. *Scientific Reports*, *13*(1), 8220. <https://doi.org/10.1038/s41598-023-35310-5>
- DiCosimo, R., McAuliffe, J., Poulou, A. J., & Bohlmann, G. (2013). Industrial use of immobilized enzymes. *Chemical Society Reviews*, *42*(15), 6437. <https://doi.org/10.1039/c3cs35506c>
- Ducrot, L., Bennett, M., André-Leroux, G., Elisée, E., Marynberg, S., Fossey-Jouenne, A., Zaparucha, A., Grogan, G., & Vergne-Vaxelaire, C. (2022). Expanding the Substrate Scope of Native Amine Dehydrogenases through *In Silico* Structural Exploration and Targeted Protein Engineering. *ChemCatChem*, *14*(22). <https://doi.org/10.1002/cctc.202200880>
- Ducrot, L., Bennett, M., Caparco, A. A., Champion, J. A., Bommarius, A. S., Zaparucha, A., Grogan, G., & Vergne-Vaxelaire, C. (2021). Biocatalytic Reductive Amination by Native Amine Dehydrogenases to Access Short Chiral Alkyl Amines and Amino Alcohols. *Frontiers in Catalysis*, *1*. <https://doi.org/10.3389/fctls.2021.781284>
- Eliot, A. C., & Kirsch, J. F. (2004). Pyridoxal Phosphate Enzymes: Mechanistic, Structural, and Evolutionary Considerations. *Annual Review of Biochemistry*, *73*(1), 383–415. <https://doi.org/10.1146/annurev.biochem.73.011303.074021>
- Eller, K., Henkes, E., Rossbacher, R., & Höke, H. (2000). Amines, Aliphatic. In *Ullmann's Encyclopedia of Industrial Chemistry*. Wiley-VCH Verlag GmbH & Co. KGaA. https://doi.org/10.1002/14356007.a02_001
- Escalante, A., Calderón, R., Valdivia, A., de Anda, R., Hernández, G., Ramírez, O. T., Gosset, G., & Bolívar, F. (2010). Metabolic engineering for the production of shikimic acid in an evolved *Escherichia coli* strain lacking the phosphoenolpyruvate: carbohydrate phosphotransferase system. *Microbial Cell Factories*, *9*(1), 21. <https://doi.org/10.1186/1475-2859-9-21>

- Foor, F., Morin, N., & Bostian, K. A. (1993). Production of L-dihydroxyphenylalanine in *Escherichia coli* with the tyrosine phenol-lyase gene cloned from *Erwinia herbicola*. *Applied and Environmental Microbiology*, *59*(9), 3070–3075. <https://doi.org/10.1128/aem.59.9.3070-3075.1993>
- Fordjour, E., Adipah, F. K., Zhou, S., Du, G., & Zhou, J. (2019). Metabolic engineering of *Escherichia coli* BL21 (DE3) for de novo production of l-DOPA from d-glucose. *Microbial Cell Factories*, *18*(1). <https://doi.org/10.1186/s12934-019-1122-0>
- Franklin, R. D., Whitley, J. A., Caparco, A. A., Bommarius, B. R., Champion, J. A., & Bommarius, A. S. (2021). Continuous production of a chiral amine in a packed bed reactor with co-immobilized amine dehydrogenase and formate dehydrogenase. *Chemical Engineering Journal*, *407*, 127065. <https://doi.org/10.1016/j.cej.2020.127065>
- Froidevaux, V., Negrell, C., Caillol, S., Pascault, J.-P., & Boutevin, B. (2016). Biobased Amines: From Synthesis to Polymers; Present and Future. *Chemical Reviews*, *116*(22), 14181–14224. <https://doi.org/10.1021/acs.chemrev.6b00486>
- Garg, R. P., Ma, Y., Hoyt, J. C., & Parry, R. J. (2002a). Molecular characterization and analysis of the biosynthetic gene cluster for the azoxy antibiotic valanimycin. *Molecular Microbiology*, *46*(2), 505–517. <https://doi.org/10.1046/j.1365-2958.2002.03169.x>
- Garg, R. P., Ma, Y., Hoyt, J. C., & Parry, R. J. (2002b). Molecular characterization and analysis of the biosynthetic gene cluster for the azoxy antibiotic valanimycin. *Molecular Microbiology*, *46*(2), 505–517. <https://doi.org/10.1046/j.1365-2958.2002.03169.x>
- Ghislieri, D., & Turner, N. J. (2014). Biocatalytic Approaches to the Synthesis of Enantiomerically Pure Chiral Amines. *Topics in Catalysis*, *57*(5), 284–300. <https://doi.org/10.1007/s11244-013-0184-1>
- Gianolio, S., Roura Padrosa, D., & Paradisi, F. (2022). Combined chemoenzymatic strategy for sustainable continuous synthesis of the natural product hordenine. *Green Chemistry*, *24*(21), 8434–8440. <https://doi.org/10.1039/D2GC02767D>
- Giardina, G., Montioli, R., Gianni, S., Cellini, B., Paiardini, A., Voltattorni, C. B., & Cutruzzolà, F. (2011). Open conformation of human DOPA decarboxylase reveals the mechanism of PLP addition to Group II decarboxylases. *Proceedings of the National Academy of Sciences*, *108*(51), 20514–20519. <https://doi.org/10.1073/pnas.1111456108>
- Gong, X., Tao, J., Wang, Y., Wu, J., An, J., Meng, J., Wang, X., Chen, Y., & Zou, J. (2021). Total barley maiya alkaloids inhibit prolactin secretion by acting on dopamine D2 receptor and protein kinase A targets. *Journal of Ethnopharmacology*, *273*, 113994. <https://doi.org/10.1016/j.jep.2021.113994>
- Gosset, G., Yong-Xiao, J., & Berry, A. (1996). A direct comparison of approaches for increasing carbon flow to aromatic biosynthesis in *Escherichia coli*. *Journal of Industrial Microbiology*, *17*(1), 47–52. <https://doi.org/10.1007/BF01570148>
- Guisán, JoséM. (1988). Aldehyde-agarose gels as activated supports for immobilization-stabilization of enzymes. *Enzyme and Microbial Technology*, *10*(6), 375–382. [https://doi.org/10.1016/0141-0229\(88\)90018-X](https://doi.org/10.1016/0141-0229(88)90018-X)

- Guo, K., Ji, C., & Li, L. (2007). Stable-Isotope Dimethylation Labeling Combined with LC-ESI MS for Quantification of Amine-Containing Metabolites in Biological Samples. *Analytical Chemistry*, 79(22), 8631–8638. <https://doi.org/10.1021/ac0704356>
- Guo, Z., Yan, N., & Lapkin, A. A. (2019). Towards circular economy: integration of bio-waste into chemical supply chain. *Current Opinion in Chemical Engineering*, 26, 148–156. <https://doi.org/10.1016/j.coche.2019.09.010>
- Gupte, A. P., Basaglia, M., Casella, S., & Favaro, L. (2022). Rice waste streams as a promising source of biofuels: feedstocks, biotechnologies and future perspectives. *Renewable and Sustainable Energy Reviews*, 167, 112673. <https://doi.org/10.1016/j.rser.2022.112673>
- Gut, H., Pennacchiotti, E., John, R. A., Bossa, F., Capitani, G., De Biase, D., & Grütter, M. G. (2006). Escherichia coli acid resistance: pH-sensing, activation by chloride and autoinhibition in GadB. *The EMBO Journal*, 25(11), 2643–2651. <https://doi.org/10.1038/sj.emboj.7601107>
- H. Orrego, A., Romero-Fernández, M., Millán-Linares, M., Yust, M., Guisán, J., & Rocha-Martin, J. (2018). Stabilization of Enzymes by Multipoint Covalent Attachment on Aldehyde-Supports: 2-Picoline Borane as an Alternative Reducing Agent. *Catalysts*, 8(8), 333. <https://doi.org/10.3390/catal8080333>
- Hamid, M. H. S. A., Slatford, P. A., & Williams, J. M. J. (2007). Borrowing Hydrogen in the Activation of Alcohols. *Advanced Synthesis & Catalysis*, 349(10), 1555–1575. <https://doi.org/10.1002/adsc.200600638>
- Hapke, H. J., & Strathmann, W. (1995). [Pharmacological effects of hordenine]. *DTW. Deutsche Tierärztliche Wochenschrift*, 102(6), 228–232. <http://www.ncbi.nlm.nih.gov/pubmed/8582256>
- Harper, B. A., Barbut, S., Lim, L.-T., & Marcone, M. F. (2014). Effect of Various Gelling Cations on the Physical Properties of “Wet” Alginate Films. *Journal of Food Science*, 79(4), E562–E567. <https://doi.org/10.1111/1750-3841.12376>
- Heckmann, C. M., Gourlay, L. J., Dominguez, B., & Paradisi, F. (2020). An (R)-Selective Transaminase From *Thermomyces stellatus*: Stabilizing the Tetrameric Form. *Frontiers in Bioengineering and Biotechnology*, 8. <https://doi.org/10.3389/fbioe.2020.00707>
- Heffter, A. (1898). Ueber Pellote. *Archiv Für Experimentelle Pathologie Und Pharmakologie*, 40(5–6), 385–429. <https://doi.org/10.1007/BF01825267>
- Heydari, M., Ohshima, T., Nunoura-Kominato, N., & Sakuraba, H. (2004). Highly Stable Lysine 6-Dehydrogenase from the Thermophile *Geobacillus stearothermophilus* Isolated from a Japanese Hot Spring: Characterization, Gene Cloning and Sequencing, and Expression. *Applied and Environmental Microbiology*, 70(2), 937–942. <https://doi.org/10.1128/AEM.70.2.937-942.2004>
- Holbrook, O. T., Molligoda, B., Bushell, K. N., & Gobrogge, K. L. (2022). Behavioral consequences of the downstream products of ethanol metabolism involved in alcohol use disorder. *Neuroscience & Biobehavioral Reviews*, 133, 104501. <https://doi.org/10.1016/j.neubiorev.2021.12.024>

- Houwman, J. A., Knaus, T., Costa, M., & Mutti, F. G. (2019). Efficient synthesis of enantiopure amines from alcohols using resting *E. coli* cells and ammonia. *Green Chemistry*, *21*(14), 3846–3857. <https://doi.org/10.1039/C9GC01059A>
- Huang, J., Mei, L., Wu, H., & Lin, D. (2007). Biosynthesis of γ -aminobutyric acid (GABA) using immobilized whole cells of *Lactobacillus brevis*. *World Journal of Microbiology and Biotechnology*, *23*(6), 865–871. <https://doi.org/10.1007/s11274-006-9311-5>
- Huang, R., Chen, H., Zhong, C., Kim, J. E., & Zhang, Y.-H. P. (2016). High-Throughput Screening of Coenzyme Preference Change of Thermophilic 6-Phosphogluconate Dehydrogenase from NADP⁺ to NAD⁺. *Scientific Reports*, *6*(1), 32644. <https://doi.org/10.1038/srep32644>
- Hwang, E. T., & Lee, S. (2019). Multienzymatic Cascade Reactions via Enzyme Complex by Immobilization. *ACS Catalysis*, *9*(5), 4402–4425. <https://doi.org/10.1021/acscatal.8b04921>
- Jackson, D. M., Ashley, R. L., Brownfield, C. B., Morrison, D. R., & Morrison, R. W. (2015). Rapid Conventional and Microwave-Assisted Decarboxylation of L-Histidine and Other Amino Acids via Organocatalysis with R-Carvone Under Superheated Conditions. *Synthetic Communications*, *45*(23), 2691–2700. <https://doi.org/10.1080/00397911.2015.1100745>
- Jansonius, J. N. (1998). Structure, evolution and action of vitamin B6-dependent enzymes. *Current Opinion in Structural Biology*, *8*(6), 759–769. [https://doi.org/10.1016/S0959-440X\(98\)80096-1](https://doi.org/10.1016/S0959-440X(98)80096-1)
- Jeon, H., Yoon, S., Ahsan, M., Sung, S., Kim, G.-H., Sundaramoorthy, U., Rhee, S.-K., & Yun, H. (2017). The Kinetic Resolution of Racemic Amines Using a Whole-Cell Biocatalyst Co-Expressing Amine Dehydrogenase and NADH Oxidase. *Catalysts*, *7*(9), 251. <https://doi.org/10.3390/catal7090251>
- Jiang, M., Xu, G., Ni, J., Zhang, K., Dong, J., Han, R., & Ni, Y. (2019a). Improving Soluble Expression of Tyrosine Decarboxylase from *Lactobacillus brevis* for Tyramine Synthesis with High Total Turnover Number. *Applied Biochemistry and Biotechnology*, *188*(2), 436–449. <https://doi.org/10.1007/s12010-018-2925-x>
- Jiang, M., Xu, G., Ni, J., Zhang, K., Dong, J., Han, R., & Ni, Y. (2019b). Improving Soluble Expression of Tyrosine Decarboxylase from *Lactobacillus brevis* for Tyramine Synthesis with High Total Turnover Number. *Applied Biochemistry and Biotechnology*, *188*(2), 436–449. <https://doi.org/10.1007/s12010-018-2925-x>
- Jones, J. A., Collins, S. M., Vernacchio, V. R., Lachance, D. M., & Koffas, M. A. G. (2016). Optimization of naringenin and *p*-coumaric acid hydroxylation using the native *E. coli* hydroxylase complex, HpaBC. *Biotechnology Progress*, *32*(1), 21–25. <https://doi.org/10.1002/btpr.2185>
- Khorsand, F., Murphy, C. D., Whitehead, A. J., & Engel, P. C. (2017). Biocatalytic stereoinversion of *p*-para-bromophenylalanine in a one-pot three-enzyme reaction. *Green Chemistry*, *19*(2), 503–510. <https://doi.org/10.1039/C6GC01922F>
- Kim, Baritugo, Oh, Kang, Jung, Jang, Song, Kim, Lee, Hwang, Park, Park, & Joo. (2019). High-Level Conversion of L-lysine into Cadaverine by *Escherichia coli* Whole Cell Biocatalyst Expressing *Hafnia alvei* L-lysine Decarboxylase. *Polymers*, *11*(7), 1184. <https://doi.org/10.3390/polym11071184>

- Kim, D. I., Chae, T. U., Kim, H. U., Jang, W. D., & Lee, S. Y. (2021). Microbial production of multiple short-chain primary amines via retrobiosynthesis. *Nature Communications*, *12*(1), 173. <https://doi.org/10.1038/s41467-020-20423-6>
- Kim, S.-C., Lee, J.-H., Kim, M.-H., Lee, J.-A., Kim, Y. B., Jung, E., Kim, Y.-S., Lee, J., & Park, D. (2013). Hordenine, a single compound produced during barley germination, inhibits melanogenesis in human melanocytes. *Food Chemistry*, *141*(1), 174–181. <https://doi.org/10.1016/j.foodchem.2013.03.017>
- Knaus, T., Böhmer, W., & Mutti, F. G. (2017). Amine dehydrogenases: efficient biocatalysts for the reductive amination of carbonyl compounds. *Green Chemistry*, *19*(2), 453–463. <https://doi.org/10.1039/C6GC01987K>
- Knowles, W. S. (n.d.). Asymmetric Hydrogenations– The MonsantoL-Dopa Process. In *Asymmetric Catalysis on Industrial Scale* (pp. 21–38). Wiley-VCH Verlag GmbH & Co. KGaA. <https://doi.org/10.1002/3527602151.ch1>
- Komori, H., Nitta, Y., Ueno, H., & Higuchi, Y. (2012). Structural Study Reveals That Ser-354 Determines Substrate Specificity on Human Histidine Decarboxylase. *Journal of Biological Chemistry*, *287*(34), 29175–29183. <https://doi.org/10.1074/jbc.M112.381897>
- Kugler, P. (1979). A gel-sandwich technique for the qualitative and quantitative determination of dehydrogenases in the enzyme histochemistry. *Histochemistry*, *60*(3), 265–293. <https://doi.org/10.1007/BF00500656>
- Kumar, R., Vikramachakravarthi, D., & Pal, P. (2014). Production and purification of glutamic acid: A critical review towards process intensification. *Chemical Engineering and Processing: Process Intensification*, *81*, 59–71. <https://doi.org/10.1016/j.cep.2014.04.012>
- Kurpejović, E., Wendisch, V. F., & Sariyar Akbulut, B. (2021). Tyrosinase-based production of L-DOPA by *Corynebacterium glutamicum*. *Applied Microbiology and Biotechnology*, *105*(24), 9103–9111. <https://doi.org/10.1007/s00253-021-11681-5>
- Lapponi, M. J., Méndez, M. B., Trelles, J. A., & Rivero, C. W. (2022). Cell immobilization strategies for biotransformations. *Current Opinion in Green and Sustainable Chemistry*, *33*, 100565. <https://doi.org/10.1016/j.cogsc.2021.100565>
- Lawrence, S. A. (2004). *Amines: synthesis, properties and applications*. Cambridge University Press.
- Lee, J., Michael, A. J., Martynowski, D., Goldsmith, E. J., & Phillips, M. A. (2007). Phylogenetic Diversity and the Structural Basis of Substrate Specificity in the β/α -Barrel Fold Basic Amino Acid Decarboxylases. *Journal of Biological Chemistry*, *282*(37), 27115–27125. <https://doi.org/10.1074/jbc.M704066200>
- Lee, S. Y., Kim, H. U., Chae, T. U., Cho, J. S., Kim, J. W., Shin, J. H., Kim, D. I., Ko, Y.-S., Jang, W. D., & Jang, Y.-S. (2019). A comprehensive metabolic map for production of bio-based chemicals. *Nature Catalysis*, *2*(1), 18–33. <https://doi.org/10.1038/s41929-018-0212-4>
- Leuchtenberger, W., Huthmacher, K., & Drauz, K. (2005). Biotechnological production of amino acids and derivatives: current status and prospects. *Applied Microbiology and Biotechnology*, *69*(1), 1–8. <https://doi.org/10.1007/s00253-005-0155-y>

- Li, N., Chou, H., & Xu, Y. (2016). Improved cadaverine production from mutant *Klebsiella oxytoca* lysine decarboxylase. *Engineering in Life Sciences*, 16(3), 299–305. <https://doi.org/10.1002/elsc.201500037>
- Liu, G., Zhou, N., Zhang, M., Li, S., Tian, Q., Chen, J., Chen, B., Wu, Y., & Yao, S. (2010). Hydrophobic solvent induced phase transition extraction to extract drugs from plasma for high performance liquid chromatography–mass spectrometric analysis. *Journal of Chromatography A*, 1217(3), 243–249. <https://doi.org/10.1016/j.chroma.2009.11.037>
- Liu, J., Pang, B. Q. W., Adams, J. P., Snajdrova, R., & Li, Z. (2017). Coupled Immobilized Amine Dehydrogenase and Glucose Dehydrogenase for Asymmetric Synthesis of Amines by Reductive Amination with Cofactor Recycling. *ChemCatChem*, 9(3), 425–431. <https://doi.org/10.1002/cctc.201601446>
- Liu, Y., Liu, P., Gao, S., Wang, Z., Luan, P., González-Sabín, J., & Jiang, Y. (2021). Construction of chemoenzymatic cascade reactions for bridging chemocatalysis and Biocatalysis: Principles, strategies and prospective. *Chemical Engineering Journal*, 420, 127659. <https://doi.org/10.1016/j.cej.2020.127659>
- Ma, J., Wang, S., Huang, X., Geng, P., Wen, C., Zhou, Y., Yu, L., & Wang, X. (2015). Validated UPLC–MS/MS method for determination of hordenine in rat plasma and its application to pharmacokinetic study. *Journal of Pharmaceutical and Biomedical Analysis*, 111, 131–137. <https://doi.org/10.1016/j.jpba.2015.03.032>
- Mateo, C., Grazú, V., Pessela, B. C. C., Montes, T., Palomo, J. M., Torres, R., López-Gallego, F., Fernández-Lafuente, R., & Guisán, J. M. (2007a). Advances in the design of new epoxy supports for enzyme immobilization–stabilization. *Biochemical Society Transactions*, 35(6), 1593–1601. <https://doi.org/10.1042/BST0351593>
- Mateo, C., Grazú, V., Pessela, B. C. C., Montes, T., Palomo, J. M., Torres, R., López-Gallego, F., Fernández-Lafuente, R., & Guisán, J. M. (2007b). Advances in the design of new epoxy supports for enzyme immobilization–stabilization. *Biochemical Society Transactions*, 35(6), 1593–1601. <https://doi.org/10.1042/BST0351593>
- Mayol, O., Bastard, K., Beloti, L., Frese, A., Turkenburg, J. P., Petit, J.-L., Mariage, A., Debard, A., Pellouin, V., Perret, A., de Berardinis, V., Zaparucha, A., Grogan, G., & Vergne-Vaxelaire, C. (2019a). A family of native amine dehydrogenases for the asymmetric reductive amination of ketones. *Nature Catalysis*, 2(4), 324–333. <https://doi.org/10.1038/s41929-019-0249-z>
- Mayol, O., Bastard, K., Beloti, L., Frese, A., Turkenburg, J. P., Petit, J.-L., Mariage, A., Debard, A., Pellouin, V., Perret, A., de Berardinis, V., Zaparucha, A., Grogan, G., & Vergne-Vaxelaire, C. (2019b). A family of native amine dehydrogenases for the asymmetric reductive amination of ketones. *Nature Catalysis*, 2(4), 324–333. <https://doi.org/10.1038/s41929-019-0249-z>
- Meyer, E. (1982). Separation of two distinct S-adenosylmethionine dependent N-methyltransferases involved in hordenine biosynthesis in *Hordeum vulgare*. *Plant Cell Reports*, 1(6), 236–239. <https://doi.org/10.1007/BF00272627>
- Mi, J., Liu, S., Du, Y., Qi, H., & Zhang, L. (2022). Cofactor self-sufficient by co-immobilization of pyridoxal 5'-phosphate and lysine decarboxylase for cadaverine production. *Bioresource Technology Reports*, 17, 100939. <https://doi.org/10.1016/j.biteb.2021.100939>

- Montgomery, S. L., Mangas-Sanchez, J., Thompson, M. P., Aleku, G. A., Dominguez, B., & Turner, N. J. (2017). Direct Alkylation of Amines with Primary and Secondary Alcohols through Biocatalytic Hydrogen Borrowing. *Angewandte Chemie*, *129*(35), 10627–10630. <https://doi.org/10.1002/ange.201705848>
- Mørch, Ý. A., Donati, I., Strand, B. L., & Skjåk-Bræk, G. (2006). Effect of Ca²⁺, Ba²⁺, and Sr²⁺ on Alginate Microbeads. *Biomacromolecules*, *7*(5), 1471–1480. <https://doi.org/10.1021/bm060010d>
- Muñoz, A. J., Hernández-Chávez, G., De Anda, R., Martínez, A., Bolívar, F., & Gosset, G. (2011). Metabolic engineering of *Escherichia coli* for improving l-3,4-dihydroxyphenylalanine (l-DOPA) synthesis from glucose. *Journal of Industrial Microbiology and Biotechnology*, *38*(11), 1845–1852. <https://doi.org/10.1007/s10295-011-0973-0>
- Mutti, F. G., & Knaus, T. (2021). Enzymes Applied to the Synthesis of Amines. In *Biocatalysis for Practitioners* (pp. 143–180). Wiley. <https://doi.org/10.1002/9783527824465.ch6>
- Mutti, F. G., Knaus, T., Scrutton, N. S., Breuer, M., & Turner, N. J. (2015). Conversion of alcohols to enantiopure amines through dual-enzyme hydrogen-borrowing cascades. *Science*, *349*(6255), 1525–1529. <https://doi.org/10.1126/science.aac9283>
- Nakai, T., Nakagawa, N., Maoka, N., Masui, R., Kuramitsu, S., & Kamiya, N. (2005). Structure of P-protein of the glycine cleavage system: implications for nonketotic hyperglycinemia. *The EMBO Journal*, *24*(8), 1523–1536. <https://doi.org/10.1038/sj.emboj.7600632>
- Narisetty, V., Cox, R., Bommareddy, R., Agrawal, D., Ahmad, E., Pant, K. K., Chandel, A. K., Bhatia, S. K., Kumar, D., Binod, P., Gupta, V. K., & Kumar, V. (2022). Valorisation of xylose to renewable fuels and chemicals, an essential step in augmenting the commercial viability of lignocellulosic biorefineries. *Sustainable Energy & Fuels*, *6*(1), 29–65. <https://doi.org/10.1039/D1SE00927C>
- Nasri, M. (2017a). *Protein Hydrolysates and Biopeptides* (pp. 109–159). <https://doi.org/10.1016/bs.afnr.2016.10.003>
- Nasri, M. (2017b). *Protein Hydrolysates and Biopeptides* (pp. 109–159). <https://doi.org/10.1016/bs.afnr.2016.10.003>
- Natte, K., Neumann, H., Jagadeesh, R. v., & Beller, M. (2017). Convenient iron-catalyzed reductive aminations without hydrogen for selective synthesis of N-methylamines. *Nature Communications*, *8*(1), 1344. <https://doi.org/10.1038/s41467-017-01428-0>
- Nguyen, N. H., Truong-Thi, N.-H., Nguyen, D. T. D., Ching, Y. C., Huynh, N. T., & Nguyen, D. H. (2022). Non-ionic surfactants As co-templates to control the mesopore diameter of hollow mesoporous silica nanoparticles for drug delivery applications. *Colloids and Surfaces A: Physicochemical and Engineering Aspects*, *655*, 130218. <https://doi.org/10.1016/j.colsurfa.2022.130218>
- Ohta, H., Murakami, Y., Takebe, Y., Murasaki, K., Oshima, K., Yoshihara, H., & Morimura, S. (2020). <i>N</i>-Methyltyramine, a Gastrin-releasing Factor in Beer, and Structurally Related Compounds as Agonists for Human Trace Amine-associated Receptor 1. *Food Science and Technology Research*, *26*(2), 313–317. <https://doi.org/10.3136/fstr.26.313>

- PARADISI, F., COLLINS, S., MAGUIRE, A., & ENGEL, P. (2007). Phenylalanine dehydrogenase mutants: Efficient biocatalysts for synthesis of non-natural phenylalanine derivatives. *Journal of Biotechnology*, *128*(2), 408–411. <https://doi.org/10.1016/j.jbiotec.2006.08.008>
- Park, J.-Y., Choi, M.-J., Yu, H., Choi, Y., Park, K.-M., & Chang, P.-S. (2022). Multi-functional behavior of food emulsifier erythorbyl laurate in different colloidal conditions of homogeneous oil-in-water emulsion system. *Colloids and Surfaces A: Physicochemical and Engineering Aspects*, *636*, 128127. <https://doi.org/10.1016/j.colsurfa.2021.128127>
- Park, S. H., Soetyono, F., & Kim, H. K. (2017). Cadaverine Production by Using Cross-Linked Enzyme Aggregate of Escherichia coli Lysine Decarboxylase. *Journal of Microbiology and Biotechnology*, *27*(2), 289–296. <https://doi.org/10.4014/jmb.1608.08033>
- Patil, M. D., Grogan, G., Bommarius, A., & Yun, H. (2018). Oxidoreductase-Catalyzed Synthesis of Chiral Amines. *ACS Catalysis*, *8*(12), 10985–11015. <https://doi.org/10.1021/acscatal.8b02924>
- Patil, M. D., Yoon, S., Jeon, H., Khobragade, T. P., Sarak, S., Pagar, A. D., Won, Y., & Yun, H. (2019). Kinetic Resolution of Racemic Amines to Enantiopure (S)-amines by a Biocatalytic Cascade Employing Amine Dehydrogenase and Alanine Dehydrogenase. *Catalysts*, *9*(7), 600. <https://doi.org/10.3390/catal9070600>
- Payne, J. T., Valentic, T. R., & Smolke, C. D. (2021). Complete biosynthesis of the bisbenzylisoquinoline alkaloids guattegaumerine and berbamunine in yeast. *Proceedings of the National Academy of Sciences*, *118*(51). <https://doi.org/10.1073/pnas.2112520118>
- Pelckmans, M., Renders, T., Van de Vyver, S., & Sels, B. F. (2017). Bio-based amines through sustainable heterogeneous catalysis. *Green Chemistry*, *19*(22), 5303–5331. <https://doi.org/10.1039/C7GC02299A>
- Pilkington, R. L., Dallaston, M. A., Savage, G. P., Williams, C. M., & Polyzos, A. (2021). Enone-promoted decarboxylation of *trans*-4-hydroxy-*l*-proline in flow: a side-by-side comparison to batch. *Reaction Chemistry & Engineering*, *6*(3), 486–493. <https://doi.org/10.1039/D0RE00442A>
- Planchestainer, M., Hegarty, E., Heckmann, C. M., Gourlay, L. J., & Paradisi, F. (2019). Widely applicable background depletion step enables transaminase evolution through solid-phase screening. *Chemical Science*, *10*(23), 5952–5958. <https://doi.org/10.1039/C8SC05712E>
- Prieto, M. A., & Garcia, J. L. (1994). Molecular characterization of 4-hydroxyphenylacetate 3-hydroxylase of Escherichia coli. A two-protein component enzyme. *Journal of Biological Chemistry*, *269*(36), 22823–22829. [https://doi.org/10.1016/S0021-9258\(17\)31719-2](https://doi.org/10.1016/S0021-9258(17)31719-2)
- Pyne, M. E., Kevvai, K., Grewal, P. S., Narcross, L., Choi, B., Bourgeois, L., Dueber, J. E., & Martin, V. J. J. (2020). A yeast platform for high-level synthesis of tetrahydroisoquinoline alkaloids. *Nature Communications*, *11*(1), 3337. <https://doi.org/10.1038/s41467-020-17172-x>
- Quaglia, D., Irwin, J. A., & Paradisi, F. (2012a). Horse Liver Alcohol Dehydrogenase: New Perspectives for an Old Enzyme. *Molecular Biotechnology*, *52*(3), 244–250. <https://doi.org/10.1007/s12033-012-9542-7>

- Quaglia, D., Irwin, J. A., & Paradisi, F. (2012b). Horse Liver Alcohol Dehydrogenase: New Perspectives for an Old Enzyme. *Molecular Biotechnology*, *52*(3), 244–250. <https://doi.org/10.1007/s12033-012-9542-7>
- Ray, S. S., Bonanno, J. B., Rajashankar, K. R., Pinho, M. G., He, G., De Lencastre, H., Tomasz, A., & Burley, S. K. (2002). Cocrystal Structures of Diaminopimelate Decarboxylase. *Structure*, *10*(11), 1499–1508. [https://doi.org/10.1016/S0969-2126\(02\)00880-8](https://doi.org/10.1016/S0969-2126(02)00880-8)
- Reetz, M. T. (2013). Biocatalysis in Organic Chemistry and Biotechnology: Past, Present, and Future. *Journal of the American Chemical Society*, *135*(34), 12480–12496. <https://doi.org/10.1021/ja405051f>
- Roschangar, F., Sheldon, R. A., & Senanayake, C. H. (2015). Overcoming barriers to green chemistry in the pharmaceutical industry – the Green Aspiration Level™ concept. *Green Chemistry*, *17*(2), 752–768. <https://doi.org/10.1039/C4GC01563K>
- Ruhaak, L. R., Steenvoorden, E., Koeleman, C. A. M., Deelder, A. M., & Wuhrer, M. (2010). 2-Picoline-borane: A non-toxic reducing agent for oligosaccharide labeling by reductive amination. *Proteomics*, *10*(12), 2330–2336. <https://doi.org/10.1002/pmic.200900804>
- Sagong, H.-Y., Son, H. F., Kim, S., Kim, Y.-H., Kim, I.-K., & Kim, K.-J. (2016). Crystal Structure and Pyridoxal 5-Phosphate Binding Property of Lysine Decarboxylase from *Selenomonas ruminantium*. *PLOS ONE*, *11*(11), e0166667. <https://doi.org/10.1371/journal.pone.0166667>
- Said, A. A. E., Ali, T. F. S., Attia, E. Z., Ahmed, A.-S. F., Shehata, A. H., Abdelmohsen, U. R., & Fouad, M. A. (2021). Antidepressant potential of *Mesembryanthemum cordifolium* roots assisted by metabolomic analysis and virtual screening. *Natural Product Research*, *35*(23), 5493–5497. <https://doi.org/10.1080/14786419.2020.1788019>
- SANDMEIER, E., HALE, T. I., & CHRISTEN, P. (1994a). Multiple evolutionary origin of pyridoxal-5'-phosphate-dependent amino acid decarboxylases. *European Journal of Biochemistry*, *221*(3), 997–1002. <https://doi.org/10.1111/j.1432-1033.1994.tb18816.x>
- SANDMEIER, E., HALE, T. I., & CHRISTEN, P. (1994b). Multiple evolutionary origin of pyridoxal-5'-phosphate-dependent amino acid decarboxylases. *European Journal of Biochemistry*, *221*(3), 997–1002. <https://doi.org/10.1111/j.1432-1033.1994.tb18816.x>
- Sato, S., Sakamoto, T., Miyazawa, E., & Kikugawa, Y. (2004). One-pot reductive amination of aldehydes and ketones with α -picoline-borane in methanol, in water, and in neat conditions. *Tetrahedron*, *60*(36), 7899–7906. <https://doi.org/10.1016/j.tet.2004.06.045>
- Schoenmakers, H., & Spiegel, L. (2014). Laboratory Distillation and Scale-up. In *Distillation* (pp. 319–339). Elsevier. <https://doi.org/10.1016/B978-0-12-386878-7.00010-3>
- Seah, S. Y. K., Britton, K. L., Rice, D. W., Asano, Y., & Engel, P. C. (2002). Single Amino Acid Substitution in *Bacillus sphaericus* Phenylalanine Dehydrogenase Dramatically Increases Its Discrimination between Phenylalanine and Tyrosine Substrates. *Biochemistry*, *41*(38), 11390–11397. <https://doi.org/10.1021/bi020196a>
- Seah, S. Y. K., Linda Britton, K., Baker, P. J., Rice, D. W., Asano, Y., & Engel, P. C. (1995). Alteration in relative activities of phenylalanine dehydrogenase towards different

- substrates by site-directed mutagenesis. *FEBS Letters*, 370(1–2), 93–96.
[https://doi.org/10.1016/0014-5793\(95\)00804-1](https://doi.org/10.1016/0014-5793(95)00804-1)
- Sen, K. Y., & Baidurah, S. (2021). Renewable biomass feedstocks for production of sustainable biodegradable polymer. *Current Opinion in Green and Sustainable Chemistry*, 27, 100412.
<https://doi.org/10.1016/j.cogsc.2020.100412>
- Sharma, M., Mangas-Sanchez, J., Turner, N. J., & Grogan, G. (2017). NAD(P)H-Dependent Dehydrogenases for the Asymmetric Reductive Amination of Ketones: Structure, Mechanism, Evolution and Application. *Advanced Synthesis & Catalysis*, 359(12), 2011–2025. <https://doi.org/10.1002/adsc.201700356>
- Sheldon, R. A., Basso, A., & Brady, D. (2021). New frontiers in enzyme immobilisation: robust biocatalysts for a circular bio-based economy. *Chemical Society Reviews*, 50(10), 5850–5862. <https://doi.org/10.1039/D1CS00015B>
- Sheldon, R. A., & Brady, D. (2019). Broadening the Scope of Biocatalysis in Sustainable Organic Synthesis. *ChemSusChem*, 12(13), 2859–2881. <https://doi.org/10.1002/cssc.201900351>
- Sheldon, R. A., & Woodley, J. M. (2018). Role of Biocatalysis in Sustainable Chemistry. *Chemical Reviews*, 118(2), 801–838. <https://doi.org/10.1021/acs.chemrev.7b00203>
- Sommer, T., Göen, T., Budnik, N., & Pischetsrieder, M. (2020). Absorption, Biokinetics, and Metabolism of the Dopamine D2 Receptor Agonist Hordenine (*N*, *N*-Dimethyltyramine) after Beer Consumption in Humans. *Journal of Agricultural and Food Chemistry*, 68(7), 1998–2006. <https://doi.org/10.1021/acs.jafc.9b06029>
- Song, W., Chen, X., Wu, J., Xu, J., Zhang, W., Liu, J., Chen, J., & Liu, L. (2020). Biocatalytic derivatization of proteinogenic amino acids for fine chemicals. *Biotechnology Advances*, 40, 107496. <https://doi.org/10.1016/j.biotechadv.2019.107496>
- Stano, J., Nemeč, P., Weissová, K., Kovács, P., Kákoniová, D., & Lisková, D. (1995). Decarboxylation of l-tyrosine and l-dopa by immobilized cells of *Papaver somniferum*. *Phytochemistry*, 38(4), 859–860. [https://doi.org/10.1016/0031-9422\(94\)00768-0](https://doi.org/10.1016/0031-9422(94)00768-0)
- Stockert, J. C., Horobin, R. W., Colombo, L. L., & Blázquez-Castro, A. (2018). Tetrazolium salts and formazan products in Cell Biology: Viability assessment, fluorescence imaging, and labeling perspectives. *Acta Histochemica*, 120(3), 159–167.
<https://doi.org/10.1016/j.acthis.2018.02.005>
- Su, Y., Liu, Y., He, D., Hu, G., Wang, H., Ye, B., He, Y., Gao, X., & Liu, D. (2022). Hordenine inhibits neuroinflammation and exerts neuroprotective effects via inhibiting NF-κB and MAPK signaling pathways in vivo and in vitro. *International Immunopharmacology*, 108, 108694.
<https://doi.org/10.1016/j.intimp.2022.108694>
- Surwase, S. N., Patil, S. A., Apine, O. A., & Jadhav, J. P. (2012). Efficient Microbial Conversion of l-Tyrosine to l-DOPA by *Brevundimonas* sp. SGJ. *Applied Biochemistry and Biotechnology*, 167(5), 1015–1028. <https://doi.org/10.1007/s12010-012-9564-4>
- Tang, Y. Q., & Weng, N. (2013). Salting-out assisted liquid–liquid extraction for bioanalysis. *Bioanalysis*, 5(12), 1583–1598. <https://doi.org/10.4155/bio.13.117>

- Teng, Y., Scott, E. L., van Zeeland, A. N. T., & Sanders, J. P. M. (2011). The use of l-lysine decarboxylase as a means to separate amino acids by electro dialysis. *Green Chemistry*, *13*(3), 624. <https://doi.org/10.1039/c0gc00611d>
- Thompson, M. P., Derrington, S. R., Heath, R. S., Porter, J. L., Mangas-Sanchez, J., Devine, P. N., Truppo, M. D., & Turner, N. J. (2019). A generic platform for the immobilisation of engineered biocatalysts. *Tetrahedron*, *75*(3), 327–334. <https://doi.org/10.1016/j.tet.2018.12.004>
- Thompson, M. P., & Turner, N. J. (2017a). Two-Enzyme Hydrogen-Borrowing Amination of Alcohols Enabled by a Cofactor-Switched Alcohol Dehydrogenase. *ChemCatChem*, *9*(20), 3833–3836. <https://doi.org/10.1002/cctc.201701092>
- Thompson, M. P., & Turner, N. J. (2017b). Two-Enzyme Hydrogen-Borrowing Amination of Alcohols Enabled by a Cofactor-Switched Alcohol Dehydrogenase. *ChemCatChem*, *9*(20), 3833–3836. <https://doi.org/10.1002/cctc.201701092>
- Tolbert, W. D., Graham, D. E., White, R. H., & Ealick, S. E. (2003). Pyruvoyl-Dependent Arginine Decarboxylase from *Methanococcus jannaschii*. *Structure*, *11*(3), 285–294. [https://doi.org/10.1016/S0969-2126\(03\)00026-1](https://doi.org/10.1016/S0969-2126(03)00026-1)
- Truong, C. C., Mishra, D. K., & Suh, Y. (2023). Recent Catalytic Advances on the Sustainable Production of Primary Furanic Amines from the One-Pot Reductive Amination of 5-Hydroxymethylfurfural. *ChemSusChem*, *16*(1). <https://doi.org/10.1002/cssc.202201846>
- Tseliou, V., Knaus, T., Masman, M. F., Corrado, M. L., & Mutti, F. G. (2019). Generation of amine dehydrogenases with increased catalytic performance and substrate scope from ϵ -deaminating L-Lysine dehydrogenase. *Nature Communications*, *10*(1), 3717. <https://doi.org/10.1038/s41467-019-11509-x>
- Tseliou, V., Knaus, T., Vilím, J., Masman, M. F., & Mutti, F. G. (2020). Kinetic Resolution of Racemic Primary Amines Using *Geobacillus stearothermophilus* Amine Dehydrogenase Variant. *ChemCatChem*, *12*(8), 2184–2188. <https://doi.org/10.1002/cctc.201902085>
- Tsukatani, T., Suenaga, H., Higuchi, T., Akao, T., Ishiyama, M., Ezo, K., & Matsumoto, K. (2008). Colorimetric cell proliferation assay for microorganisms in microtiter plate using water-soluble tetrazolium salts. *Journal of Microbiological Methods*, *75*(1), 109–116. <https://doi.org/10.1016/j.mimet.2008.05.016>
- Viejo, C. G., Villarreal-Lara, R., Torrico, D. D., Rodríguez-Velazco, Y. G., Escobedo-Avellaneda, Z., Ramos-Parra, P. A., Mandal, R., Singh, A. P., Hernández-Brenes, C., & Fuentes, S. (2020). Beer and consumer response using biometrics: Associations assessment of beer compounds and elicited emotions. *Foods*, *9*(6), 821.
- Vitaku, E., Smith, D. T., & Njardarson, J. T. (2014). Analysis of the Structural Diversity, Substitution Patterns, and Frequency of Nitrogen Heterocycles among U.S. FDA Approved Pharmaceuticals. *Journal of Medicinal Chemistry*, *57*(24), 10257–10274. <https://doi.org/10.1021/jm501100b>
- Wang, M., Khan, M. A., Mohsin, I., Wicks, J., Ip, A. H., Sumon, K. Z., Dinh, C.-T., Sargent, E. H., Gates, I. D., & Kibria, M. G. (2021). Can sustainable ammonia synthesis pathways compete with fossil-fuel based Haber–Bosch processes? *Energy & Environmental Science*, *14*(5), 2535–2548. <https://doi.org/10.1039/D0EE03808C>

- Wang, Q., Xin, Y., Zhang, F., Feng, Z., Fu, J., Luo, L., & Yin, Z. (2011). Enhanced γ -aminobutyric acid-forming activity of recombinant glutamate decarboxylase (*gadA*) from *Escherichia coli*. *World Journal of Microbiology and Biotechnology*, 27(3), 693–700. <https://doi.org/10.1007/s11274-010-0508-2>
- Watanabe, Y., Tsuji, Y., Ige, H., Ohsugi, Y., & Ohta, T. (1984). Ruthenium-catalyzed N-alkylation and N-benylation of aminoarenes with alcohols. *The Journal of Organic Chemistry*, 49(18), 3359–3363. <https://doi.org/10.1021/jo00192a021>
- Weber, R. E. (1992). Use of ionic and zwitterionic (Tris/BisTris and HEPES) buffers in studies on hemoglobin function. *Journal of Applied Physiology*, 72(4), 1611–1615. <https://doi.org/10.1152/jappl.1992.72.4.1611>
- Wei, G., Chen, Y., Zhou, N., Lu, Q., Xu, S., Zhang, A., Chen, K., & Ouyang, P. (2022). Chitin biopolymer mediates self-sufficient biocatalyst of pyridoxal 5'-phosphate and L-lysine decarboxylase. *Chemical Engineering Journal*, 427, 132030. <https://doi.org/10.1016/j.cej.2021.132030>
- Wei, T., Cheng, B. Y., & Liu, J. Z. (2016). Genome engineering *Escherichia coli* for L-DOPA overproduction from glucose. *Scientific Reports*, 6. <https://doi.org/10.1038/srep30080>
- Wieschalka, S., Blombach, B., Bott, M., & Eikmanns, B. J. (2013). Bio-based production of organic acids with *Corynebacterium glutamicum*. *Microbial Biotechnology*, 6(2), 87–102. <https://doi.org/10.1111/1751-7915.12013>
- Wohlgemuth, R. (2021). Biocatalysis-Key enabling tools from biocatalytic one-step and multi-step reactions to biocatalytic total synthesis. *New Biotechnol*, 60, 113–123.
- Wu, B., Zhang, S., Hong, T., Zhou, Y., Wang, H., Shi, M., Yang, H., Tian, X., Guo, J., Bian, J., Roache, J., Delgado, P., Mo, R., Fridrich, C., Gao, F., & Wang, J. (2020). Merging Biocatalysis, Flow, and Surfactant Chemistry: Innovative Synthesis of an FXI (Factor XI) Inhibitor. *Organic Process Research & Development*, 24(11), 2780–2788. <https://doi.org/10.1021/acs.oprd.0c00412>
- Wu, P., Li, G., He, Y., Luo, D., Li, L., Guo, J., Ding, P., & Yang, F. (2020). High-efficient and sustainable biodegradation of microcystin-LR using *Sphingopyxis* sp. YF1 immobilized Fe₃O₄@chitosan. *Colloids and Surfaces B: Biointerfaces*, 185, 110633. <https://doi.org/10.1016/j.colsurfb.2019.110633>
- Ye, L. J., Toh, H. H., Yang, Y., Adams, J. P., Snajdrova, R., & Li, Z. (2015). Engineering of Amine Dehydrogenase for Asymmetric Reductive Amination of Ketone by Evolving *Rhodococcus* Phenylalanine Dehydrogenase. *ACS Catalysis*, 5(2), 1119–1122. <https://doi.org/10.1021/cs501906r>
- Yoon, S., Patil, M. D., Sarak, S., Jeon, H., Kim, G., Khobragade, T. P., Sung, S., & Yun, H. (2019). Deracemization of Racemic Amines to Enantiopure (R)- and (S)-amines by Biocatalytic Cascade Employing ω -Transaminase and Amine Dehydrogenase. *ChemCatChem*, 11(7), 1898–1902. <https://doi.org/10.1002/cctc.201900080>
- Yoshitaka Hashitani, B. (1925). On the chemical constituents of malt-rootlets with special reference to Hordenine. *Journal of the College of Agriculture*, 14, 1–56.

- Zhang, B., Jiang, Y., Li, Z., Wang, F., & Wu, X.-Y. (2020). Recent Progress on Chemical Production From Non-food Renewable Feedstocks Using *Corynebacterium glutamicum*. *Frontiers in Bioengineering and Biotechnology*, *8*. <https://doi.org/10.3389/fbioe.2020.606047>
- Zhang, H., Wei, Y., Lu, Y., Wu, S., Liu, Q., Liu, J., & Jiao, Q. (2016). Three-step biocatalytic reaction using whole cells for efficient production of tyramine from keratin acid hydrolysis wastewater. *Applied Microbiology and Biotechnology*, *100*(4), 1691–1700. <https://doi.org/10.1007/s00253-015-7054-7>
- Zhang, K., & Ni, Y. (2014). Tyrosine decarboxylase from *Lactobacillus brevis*: Soluble expression and characterization. *Protein Expression and Purification*, *94*, 33–39. <https://doi.org/10.1016/j.pep.2013.10.018>
- Zhang, X., Du, L., Zhang, J., Li, C., Zhang, J., & Lv, X. (2021). Hordenine Protects Against Lipopolysaccharide-Induced Acute Lung Injury by Inhibiting Inflammation. *Frontiers in Pharmacology*, *12*, 712232. <https://doi.org/10.3389/fphar.2021.712232>
- Zhao, W., Hu, S., Huang, J., Ke, P., Yao, S., Lei, Y., Mei, L., & Wang, J. (2016). Permeabilization of *Escherichia coli* with ampicillin for a whole cell biocatalyst with enhanced glutamate decarboxylase activity. *Chinese Journal of Chemical Engineering*, *24*(7), 909–913. <https://doi.org/10.1016/j.cjche.2016.02.001>
- Zhou, F., Xu, Y., Nie, Y., & Mu, X. (2022). Substrate-Specific Engineering of Amino Acid Dehydrogenase Superfamily for Synthesis of a Variety of Chiral Amines and Amino Acids. *Catalysts*, *12*(4), 380. <https://doi.org/10.3390/catal12040380>
- Zhou, J.-W., Ruan, L.-Y., Chen, H.-J., Luo, H.-Z., Jiang, H., Wang, J.-S., & Jia, A.-Q. (2019). Inhibition of Quorum Sensing and Virulence in *Serratia marcescens* by Hordenine. *Journal of Agricultural and Food Chemistry*, *67*(3), 784–795. <https://doi.org/10.1021/acs.jafc.8b05922>
- Zhu, H., Xu, G., Zhang, K., Kong, X., Han, R., Zhou, J., & Ni, Y. (2016a). Crystal structure of tyrosine decarboxylase and identification of key residues involved in conformational swing and substrate binding. *Scientific Reports*, *6*(1), 27779. <https://doi.org/10.1038/srep27779>
- Zhu, H., Xu, G., Zhang, K., Kong, X., Han, R., Zhou, J., & Ni, Y. (2016b). Crystal structure of tyrosine decarboxylase and identification of key residues involved in conformational swing and substrate binding. *Scientific Reports*, *6*(1), 27779. <https://doi.org/10.1038/srep27779>
- Zhuang, W., Liu, H., Zhang, Y., He, J., & Wang, P. (2021). Effective asymmetric preparation of (R)-1-[3-(trifluoromethyl)phenyl]ethanol with recombinant *E. coli* whole cells in an aqueous Tween-20/natural deep eutectic solvent solution. *AMB Express*, *11*(1), 118. <https://doi.org/10.1186/s13568-021-01278-6>

4. Tailoring minimal medium composition for enhanced L-DOPA microbial fermentation

Unless explicitly stated otherwise, the research presented in this chapter is the sole and individual work of the author.

4.1 Introduction

This chapter focuses on the sustainable and cost-effective production of L-DOPA through bacterial fermentation using *E. coli* in a minimal medium, M9Y.

The primary goal was to develop a more sustainable and easily adaptable process compatible with continuous flow systems, and here a methodic strategy to simplify the fermentation medium and procedure is presented, in comparison to protocols already reported in the literature. (Fordjour et al., 2019; Muñoz et al., 2011; T. Wei et al., 2016)

The chapter explores the advantages of using D-glucose as a substrate to establish a benchmark for the efficiency, yield, and product specificity of the fermentation process. The modifications to the protocol have led to a more straightforward fermentation process that yields L-DOPA while also reducing overall costs. As previously reported, L-DOPA can be produced in resting cell biotransformations in minimal medium M9 after growing biomass in a rich medium (Muñoz et al., 2011). M9 minimal medium is a common, defined medium that contains only the essential nutrients required for microbial growth, such as carbon, nitrogen, and minerals. In comparison to LB medium (Luria Bertani medium), which is a complex medium that contains yeast extract, tryptone, and sodium chloride, M9 is often used for cell culture in flask, allowing greater control over the nutrients provided to the microorganisms. Although M9 medium is less complex than LB medium and can simplify downstream processing and analysis of the fermentation product, LB medium may be the preferred choice for cell cultivation because it is user-friendly and has a nutrient-rich composition.

Exploiting the advantages of a fermenter system for process scale-up, the goal was to sustain both cell growth and fermentation within the same minimal medium thereby maximizing L-DOPA yields and minimizing costs. Although waste feedstock has not yet been investigated as potential starting substrates, this chapter would like to set a foundation for future studies in this direction. This approach would aim to balance sustainability, cost-effectiveness, and process efficiency, ultimately contributing to the development of a streamlined fermentation process for L-DOPA production that aligns with the principles of a circular economy. However, for the sake of reproducibility and consistency in L-DOPA production, it may be more sensible to start with a defined composition of the carbon sources, such as D-glucose, rather than waste sources, especially because in this chapter L-DOPA is intended to be a starting material for a subsequent process which is realized in coupling the fermenter and flow system.

4.2 Results and discussion

4.2.1 Carbon flow for the production of L-dopa in VH33ΔtyrR_DOPA

In the genetically engineered *E. coli* strain designed for L-DOPA production, the carbon flow (Figure 4.1) starts with the uptake of D-glucose through the overexpressed galactose permease (GalP), under the control of a strong *trc* promoter. The D-glucose is then metabolized through glycolysis, generating glucose-6-phosphate (G6P), which subsequently enters the pentose phosphate pathway (PPP) via the overexpressed transketolase gene (*tktA*), enhancing the production of erythrose-4-phosphate (E4P) and phosphoenolpyruvate (PEP). These two precursors are used to synthesize aromatic amino acids through the shikimate pathway, with the feedback inhibition-resistant *aroG^{fbr}* enzyme promoting higher flux. The overexpression of *pheA_{CM}* and *tyrC* genes facilitates the conversion of chorismate to L-tyrosine.

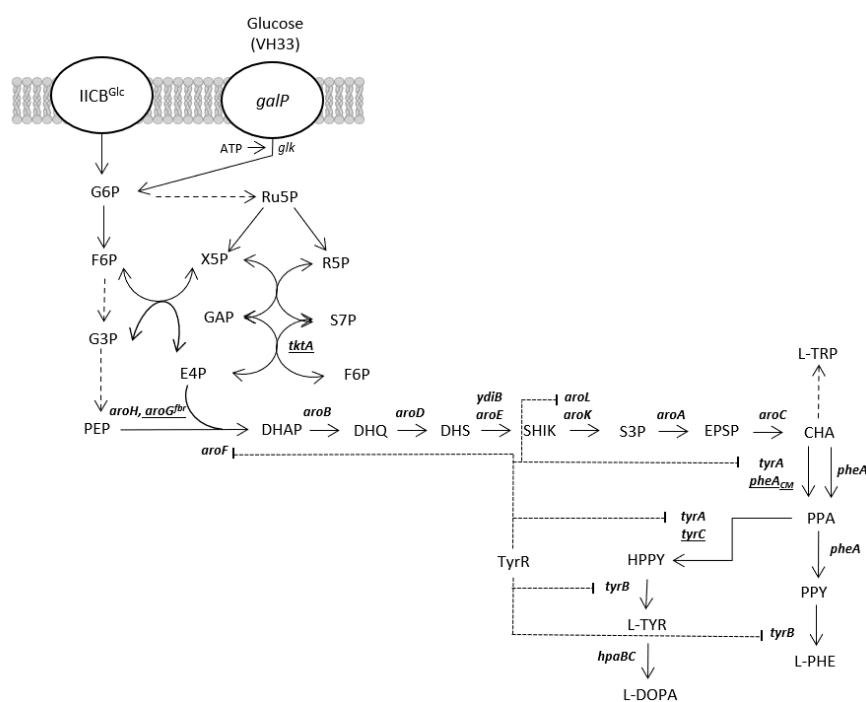


Figure 4.1: The biosynthesis of aromatic amino acids in *E. coli* involves various pathways and proteins, including glucose transport and phosphorylation. Dashed arrows represent multiple enzyme reactions, while dotted lines originating from the transcriptional regulator *TyrR* indicate the genes repression by this protein. Overexpressed genes were either from plasmids (*aroG^{fbr}*, *tktA*, *pheA_{CM}*, *tyrC*, and *hpaBC*) or the chromosome (*galP*). Enzymes involved in the biosynthesis of L-DOPA are highlighted, with corresponding gene names and pathways detailed in the figure.

The repression of the *tyrB* gene in the engineered *E. coli* strain is important for enhancing the production of L-DOPA. *TyrB* encodes an enzyme called tyrosine aminotransferase, which converts L-tyrosine to 4-hydroxyphenylpyruvate in the normal *E. coli* metabolism.

By repressing *tyrB*, the metabolic flux of L-tyrosine is redirected, preventing its conversion to 4-hydroxyphenylpyruvate and other downstream metabolites in the tyrosine degradation pathway. This strategy results in a higher intracellular concentration of L-tyrosine, which is the direct precursor for L-DOPA production via the overexpressed *hpaBC* genes. The *hpaBC* genes are overexpressed to convert L-tyrosine to L-DOPA via the 4-hydroxyphenylacetate 3-hydroxylase (HpaBC) enzyme. This carefully engineered *E. coli* strain ensures a highly efficient carbon flow towards L-DOPA production, obtaining this valuable compound from D-glucose.

4.2.2 Bacterial strain: transformed plasmids

The bacterial strain for L-DOPA fermentation, which has been engineered by modifying the phosphoenolpyruvate:sugar phosphotransferase system (PTS) and the aromatic amino acids biosynthetic pathways, was kindly provided to us by the group of Professor Guillermo Gosset (Universidad Nacional Autónoma de México, Mexico). In VH33, the bacterial strain used, PTS has been functionally replaced by GalP, controlled by the potent *trc* promoter. This modification, allowing for a constitutive import of D-glucose, confers a PTS⁻ gluc⁺ phenotype to VH33. Such an alteration has been demonstrated to yield enhanced aromatic production capacity. (Báez et al., 2001; Escalante et al., 2010; Gosset et al., 1996) Moreover, to increase L-tyrosine biosynthetic capacity, the protein TyrR, a transcriptional dual regulator that represses transcription of several genes encoding enzymes that participate in L-tyrosine biosynthesis in *E. coli*, was inactivated. In the strain, two plasmids are transformed for the overexpression of *aroG^{fbr}*, *tktA*, *pheA_{CM}*, *tyrC* and *hpaBC* (Table 4.1). Despite the absence of a provided plasmid map, the construction of the plasmids was discerned and an understanding of their functions and structures was augmented through the utilization of existing literature.

For the selection of the strain in liquid culture ampicillin, kanamycin and tetracycline were employed.

Gene	Description
<i>aroG^{fb}</i>	Mutated <i>aroG</i> gene, encodes for DAHPS enzyme, insensitive to feedback inhibition
<i>tktA</i>	Encodes for transketolase, involved in the pentose phosphate pathway
<i>pheA_{CM}</i>	Encodes for chorismate mutase domain from chorismate mutase-prephenate dehydratase
<i>tyrC</i>	Encodes for cyclohexadienyl dehydrogenase, involved in the biosynthesis of aromatic amino acids
<i>hpaBC</i>	Encodes for a native <i>E. coli</i> hydroxylase complex, HpaBC, responsible in VH33Δ <i>tyrR</i> _DOPA of the hydroxylation of L-tyrosine to L-DOPA

Table 4.1: Overview of the transformed genes of the engineered bacterial strain VH33Δ*tyrR*_DOPA for L-DOPA production, in collaboration with the group of Professor Guillerm Gosset.

aroG^{fb} is a mutated version of the *aroG* gene that encodes for the 3-deoxy-D-arabino-heptulosonate 7-phosphate synthase (DAHPS) enzyme, which is involved in the shikimate pathway of aromatic amino acid biosynthesis. The mutation makes the enzyme insensitive to feedback inhibition by the pathway's end products, allowing for increased production of aromatic amino acids.

tktA encodes for transketolase, an enzyme involved in the pentose phosphate pathway, which produces NADPH and ribose-5-phosphate for use in biosynthesis and redox reactions.

pheA_{CM} encodes for the chorismate mutase domain from the chorismate mutase-prephenate dehydratase protein, a bifunctional enzyme in the shikimate pathway that catalyzes the conversion of chorismate to prephenate.

tyrC encodes for the enzyme cyclohexadienyl dehydrogenase, which is involved in the biosynthesis of aromatic amino acids.

hpaBC encodes for two enzymatic domains of the 4-HPA 3-hydroxylase,(Chen et al., 2019; Jones et al., 2016; Prieto & Garcia, 1994) involved in the catabolism of 4-hydroxyphenylacetate (4-HPA). The expression of *hpaBC* genes from *E.coli* W in the strains VH33 *tyrR*⁻ leads to the synthesis of L-DOPA. (Figure 4.2)

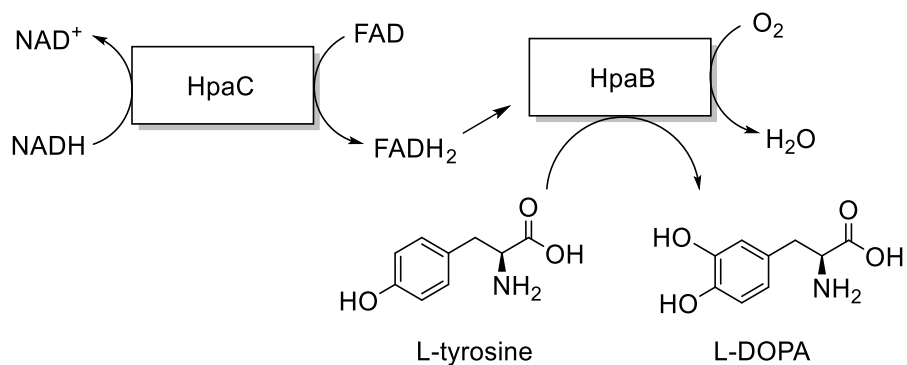


Figure 4.2: Overview of the HpaBC cofactor-dependent L-tyrosine hydroxylation. HpaBC, as flavoprotein monooxygenase, catalyzes the hydroxylation of L-tyrosine. HpaC, the flavin reductase component, provides the reduced flavin adenine dinucleotide (FADH₂) required by HpaB, the oxidase component of the system. The FADH₂ interacts with an oxygen molecule and the substrate, leading to the incorporation of a hydroxyl group in the ortho position on the aromatic ring. The oxidized FAD from this reaction is subsequently returned to HpaC for reuse in the next cycle.

4.2.3 Batch flask fermentation

For the L-dopa fermentation in shaking flasks, different protocols already reported in the literature were tested. In this study, the growth of cells in a rich and complex medium was investigated to produce sufficient biomass capable of fermenting L-DOPA directly, without performing resting cell biotransformations, therefore in one step without the need to concentrate the cells.

For this purpose, the protocols from Fordjour *et al.* (1)(Fordjour et al., 2019) and Wei *et al.* (2)(T. Wei et al., 2016) were trialed (Table 4.2).

Protocol	Medium	Carbon source	Induction
1	7 g/L yeast extract, 7.5 g/L (NH ₄) ₂ SO ₄ , 3 g/L K ₂ HPO ₄ , 2 g/L KH ₂ PO ₄ , 1 g/L MgSO ₄ ·7H ₂ O	10 g/L D-glucose, 5 g/L glycerol	0.1 mM IPTG, 3 h after the inoculum
2	Lb, 1 % trace elements ^a	14 g/L D-glucose	0.1 mM IPTG, 6 h after the inoculum

Table 4.2: (1) Fordjour *et al.* protocol. In both the protocols, the medium has been supplemented with 0.45 g/L ascorbic acid. **(2)** Wei *et al.* protocol trace elements^a: FeSO₄·7H₂O 10 g/L, ZnSO₄·7H₂O 2.2 g/L, MnSO₄·4 H₂O 0.58 g/L, CuSO₄·5 H₂O 1g/L, (NH₄)Mo₇O₂₄·4 H₂O 0.1 g/L, NaB₄O₇·10 H₂O 0.2 g/L, 10 mL HCl in 1 L.

The complex rich media were compared with the reference protocol (3) employed for the L-DOPA fermentation using this engineered strain (Table 4.3).

Protocol	Growth medium	Induction	Fermentation medium
3	Lb, 10 g/L D-glucose	0.1 mM IPTG after 1.5 h from the inoculum	M9, 10 g/L D-glucose, 0.45 g/L ascorbic acid

Table 4.3: (3) Munoz *et al.* protocol. The fermentation medium was prepared as described in material and methods (M9 medium preparation). IPTG was added in the growth medium after 1.5 h from the inoculum. The cells were harvested and resuspended in the fermentation medium with the concentration of 23 g/L after 3 hours from the induction, and IPTG was added also in the fermentation medium.

Specifically, the optical density (OD) values of cell cultures grown in three different media were measured 4.5 hours after inoculation (Table 4.4). In the case of protocol (3), after

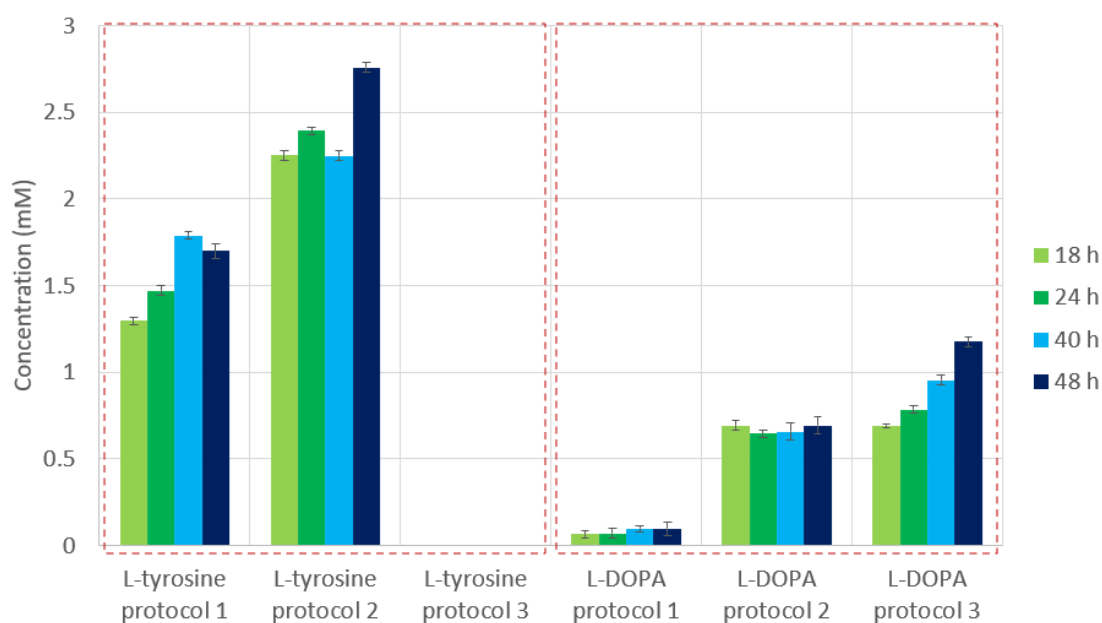
4.5 hours the cells have been concentrated to set up a resting cells culture. From the 100 mL cell culture, 0.8 ± 0.25 g of biomass was harvested to be resuspended in 35 mL of M9, 10 g/L D-glucose, 0.45 g/L ascorbic acid, 0.1 mM IPTG. After 24 h the OD values of the cell cultures for protocols (1) and (2) were, respectively, 4.7 and 4.8, while in the resting cell culture the OD was 3.6.

Protocol	Time-measurements of OD	
	4.5 h	24 h
1	1.4	4.7
2	1.5	4.8
3	0.9	3.6

Table 4.4: OD values from samples of cell cultures. The OD in protocol (3) at 24 h correspond to the one from the resting cell fermentation.

Despite the observed comparable values of OD in the three media, the maximum titer of L-DOPA obtained at 48 h was lower in the complex rich ones than that obtained in the resting cell fermentation with M9 medium, respectively 0.2 mM from protocol (1), 0.6 mM from protocol (2) and 1.2 mM from protocol (3) (Graph 4.1 and Tables 4.5).

L-DOPA and L-tyrosine production



Graph 4.1: L-tyrosine and L-DOPA concentration at different time-points in different media fermentations following the three protocols. For protocol (3), L-tyrosine, as intermediate, was not detected.

Protocol	L-DOPA titer (mM)
1	0.2 ± 0.03

2	0.6 ± 0.1
3	1.2 ± 0.08

Table 4.5: L-DOPA concentration after 24 hours from samples of different cell culture protocols.

Instead, the rich complex media were found to promote the production of L-tyrosine (Graph 4.1). In fact, while they may be effective at promoting initial cell growth, this did not seem to be the optimal choice for maximizing L-DOPA production. The experiments were performed in triplicates to ensure data consistency.

4.2.4 Fermentation in bioreactor

The 2 L fermenter was equipped with essential monitoring and control systems, including temperature, pH, dissolved oxygen, and agitation control, to ensure optimal growth conditions and L-DOPA production throughout the fermentation process.

4.2.4.1 Optimization of fermentation conditions: airflow and working volume

The optimization of L-DOPA production in the engineered *E. coli* strain necessitated a comprehensive approach, encompassing not only genetic modifications and induction timing but also the meticulous regulation of fermentation conditions, including airflow and fermenter working volume, to ensure appropriate aeration levels.

The bioreactor airflow rate was of paramount importance to provide a sufficient oxygen supply, crucial for maintaining efficient metabolic activity and optimal cell growth. Inadequate oxygen levels could adversely affect the molecular oxygen-dependent hydroxylation of L-tyrosine (Figure 4.3), which was identified to be the limiting step in L-DOPA production.

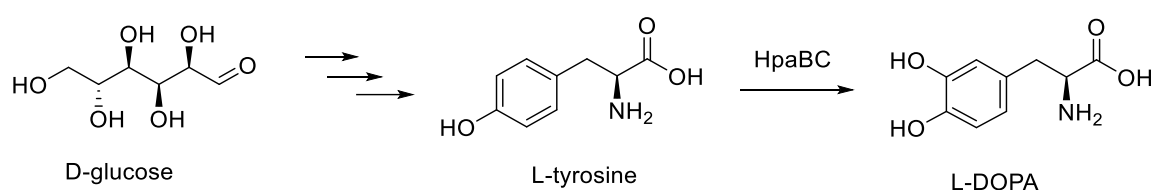


Figure 4.3: Schematic representation of the metabolic pathway illustrating the conversion of glucose to L-tyrosine and subsequent L-DOPA synthesis.

By employing an “oxygen cascade strategy” to fine-tune the airflow rate in the fermenter, an ideal balance of oxygen availability and mixing could be attained. In this strategy, oxygen was delivered to the fermentation process in a stepwise manner by controlling the dissolved oxygen concentration in the culture broth through adjusting firstly the agitation rate (see experimental for more details). This ensured that the engineered *E.*

coli cells sustained high metabolic activity and effectively converted available substrates into L-DOPA.

Another critical parameter for proper aeration in the fermenter was the working volume of the vessel. Inadequate working volume could negatively impact various aspects of the aeration process, such as oxygen transfer rate, mixing and mass transfer, subsequently affecting L-DOPA production during fermentation. The final fermentation process was carried out with a working volume of 0.65 L and an oxygen cascade ensuring the 60% oxygen saturation, striking an optimal balance to facilitate efficient L-DOPA production.

4.2.4.2 Three phases optimization to tackle induction time and carbon source loading

The optimization of L-DOPA fermentation was carried out in three distinct phases where fermentation medium, induction time and glucose concentration were respectively screened as key parameters (Table 4.6).

Optimization phase	Induction Time (OD)	Glucose Concentration (g/L)	Temperature (°C)	pH	Working Volume (L)	Stirring (rpm)	Airflow (ccm)
1	0.7	16	37	6.5	0.65	800	250
2	3.4	16	37	6.5	0.65	800	250
3	3.4	50	37	6.5	0.65	800	250

Table 4.6: Summary of fermentation conditions and parameters for the three phases of optimization in L-DOPA production. The different phases are represented by the variations in induction timing and glucose concentration, while the other parameters, such as temperature, pH, working volume, stirring, and airflow, remain consistent throughout the process.

In the first phase, VH33ΔtyrR_DOPA cells were inoculated in M9Y medium. The preculture was left in incubation at 37°C overnight in LB medium, and the starting OD for the fermentation cell culture was 0.1. The vessel volume was 2 L and the selected working volume was 1 L. The fermentation conditions were namely 37 °C, pH 6.5, 800 rpm stirring, 250 ccm (cubic centimeters per minute) air flow. The induction of proteins expression was initiated during the exponential growth phase (OD of 0.7). This approach was chosen to stimulate the production of L-DOPA when cells were in their most active state of growth. Nevertheless, the final concentration of L-DOPA achieved was poor, equal to 0.3 mM, and the fermentation conditions needed to be optimized.

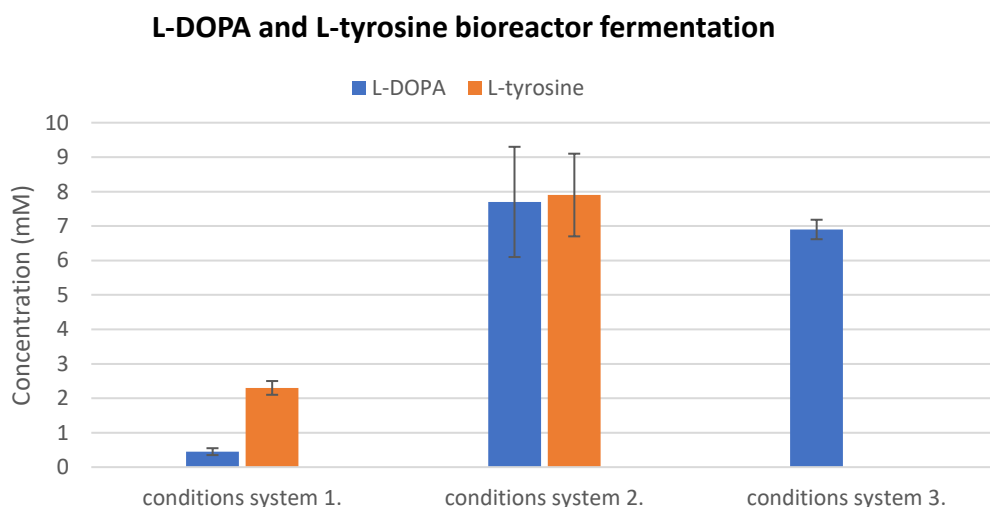
In the second phase, the induction point was shifted to the stationary phase of the cell growth, where cells reached an OD of 3.4. This modification aimed to investigate the potential benefits of inducing L-DOPA production when cells were no longer rapidly dividing.

Inducing gene expression during the late stationary phase in *E. coli* fermentation presents several advantages that can lead to improved experimental outcomes. Firstly, as the culture reaches its maximum cell density in this phase, higher overall protein yields or product formation can be achieved due to the larger number of cells available for production.

Secondly, bacteria in the late stationary phase are often more stress-tolerant, having adapted to conditions such as nutrient limitation and the accumulation of toxic by-products. This increased robustness can be beneficial when expressing foreign proteins or producing target metabolites that impose additional stress on the cells.

Thirdly, inducing expression during the late stationary phase reduces the metabolic burden associated with target production, as the cells have completed most of their growth and replication. Consequently, more energy can be allocated to the production process, potentially enhancing overall yields.

Under these conditions, an increment of the biomass during the fermentation process was observed. Although the titer of L-DOPA, namely 7.8 ± 0.8 mM, improved in the fermentation broth following a late stationary phase induction, the ratio between L-tyrosine (precursor) and L-DOPA (final product) remained close to 1 (Graph 4.2). This suggested that there is a bottleneck in the conversion of L-tyrosine to L-DOPA, possibly due to the limited enzymatic activity or expression of the HpaBC. Other factors, such as insufficient cofactor availability, could also contribute to this suboptimal conversion rate. This imbalance between L-tyrosine and L-DOPA levels indicated that further optimization of the metabolic engineering strategies and fermentation conditions was necessary to enhance L-DOPA production, by either increasing the catalytic efficiency of the HpaBC, boosting its expression, or mitigating any regulatory constraints that may limit its performance.



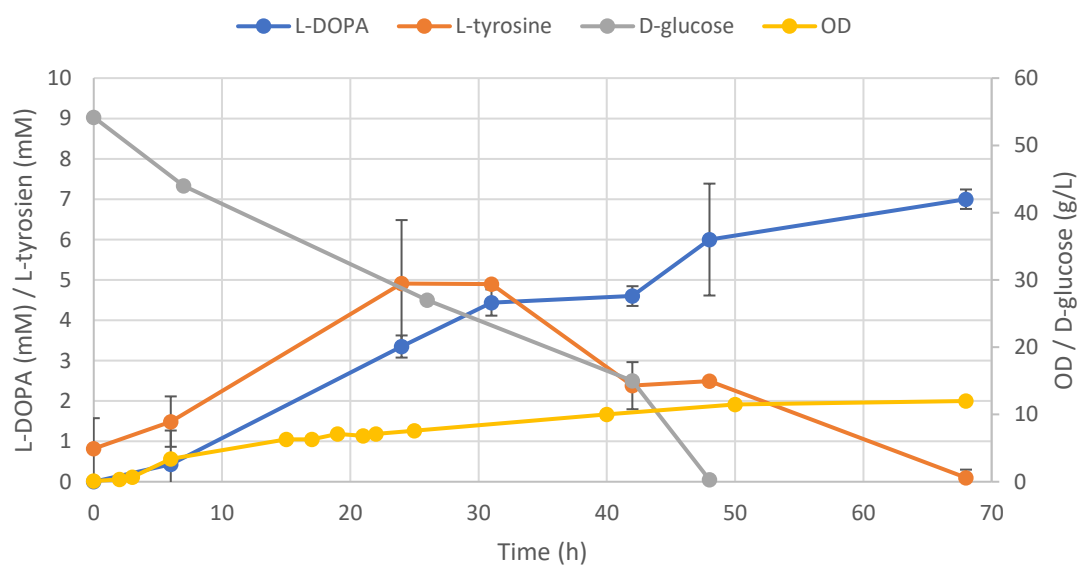
OD	4.7		12.3		22.9	
Ratio L-tyr/ L-DOPA	5		1		0	
	L-DOPA (mM)	L-tyrosine (mM)	L-DOPA (mM)	L-tyrosine (mM)	L-DOPA (mM)	L-tyrosine (mM)
	0.45	2.3	7.7	7.9	6.9	<0.1

Graph 4.2: Production of L-tyrosine and L-DOPA under the different conditions corresponding to each optimization phase, at 68 h. In the correlated table: biomass (OD) at the end of the fermentation process for each optimization phase, and ratio of intermediate L-tyrosine (L-tyr) over final product L-DOPA, with respective titers.

Following these observations, in the third phase, the carbon source for L-DOPA production was increased from 16 g/L glucose to 50 g/L. This substantial increase in glucose concentration aimed at achieving a higher biomass production, potentially enhancing L-DOPA yield and overall productivity. The cells growth and the glucose consumption were monitored (Graph 4.3). Increasing by 3-fold the carbon source indeed afforded more cells in which the HpaBC enzyme, responsible for converting L-tyrosine to L-DOPA, could be apparently more efficiently expressed as negligible amounts of L-tyrosine were detected.

As a result, the optimized fermentation conditions led to a significant improvement in L-DOPA concentration, with an average of 6.9 ± 1.2 mM being achieved (Graph 4.3). It is important to highlight how L-tyrosine has been converted completely in the last synthetic reaction step, yielding L-DOPA and removing the problematics of unwanted by-product contamination of the fermentation broth.

L-DOPA and L-tyrosine production in bioreactor from 50 g/L D-glucose



Graph 4.3: L-DOPA production in blue. L-tyrosine formation and consumption in orange. D-glucose consumption in grey. OD profile of the cell culture in the bioreactor in yellow.

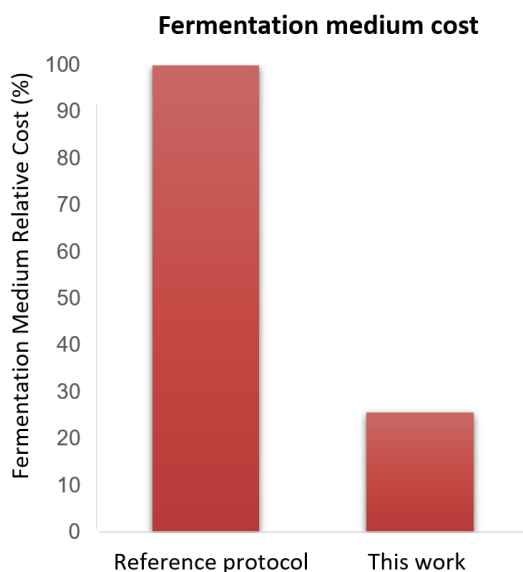
This marked increase in L-DOPA production demonstrated the effectiveness of the optimization strategies employed during the fermentation process and highlighted the potential benefits of fine-tuning the metabolic engineering approaches, carbon source concentrations, and other fermentation parameters to maximize the production of target compounds such as L-DOPA.

4.2.4.3 Stabilizing L-DOPA concentration in the fermentation broth

During the later stages of L-DOPA fermentation, particularly after 48 hours, maintaining a consistent L-DOPA concentration became challenging due to oxidation issues. Ascorbic acid can be added to mitigate this problem; however, it may be short-lived and also be oxidized as L-DOPA production continues. To store and preserve the L-DOPA concentration for a longer period, after harvesting the cell culture from the bioreactor, the fermentation broth was first centrifuged and filtered to remove any cells and impurities. The pH of the purified broth was then adjusted from 6.5 to 2 by adding 1 mL of HCl to a 50 mL Falcon tube filled with the fermentation broth sample. This acidification step helps preventing the oxidation and degradation of L-DOPA. The samples were subsequently stored frozen at -20°C (long-term storage) or kept at 4°C for shorter periods (up to one week) to maintain the L-DOPA concentration and minimize any loss due to oxidation.

4.3 Conclusion

In conclusion, this study demonstrates the successful production of L-DOPA through bacterial fermentation using a significantly more convenient and simplified medium compared to previous reports (Graph 4.4). Remarkably, the adopted synthetic medium has achieved a cost reduction of 75 % compared to the standard protocol, (Muñoz et al., 2011) considering the change of the fermentation medium, marking a significant breakthrough in cost-effective L-DOPA production. The optimal medium was identified as M9 with the addition of 2 g/L yeast extract (Table 4.7).



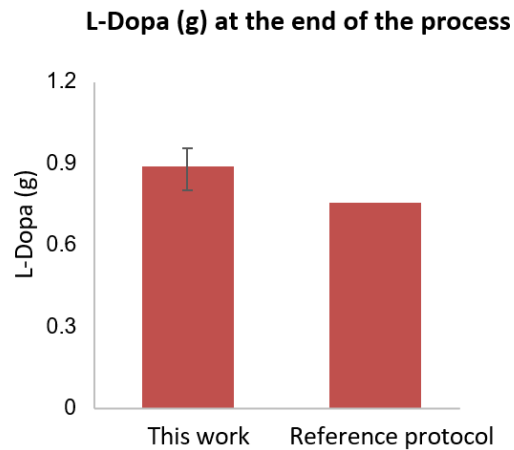
Graph 4.4: Relative cost (%) of the fermentation medium composition comparing the standard protocol from Muñoz *et al.* and this work.

Medium Composition	
This work medium (M9Y)	6 g/L Na ₂ HPO ₄ , 0.5 g/L NaCl, 3 g/L KH ₂ PO ₄ , 1 g/L NH ₄ Cl, 0.247 g/L MgSO ₄ , 0.0147 g/L CaCl ₂ , 50 g/L D-glucose, 2 g/L yeast extract, 0.45 g/L ascorbic acid
Reference protocol medium	LB medium, 0.203 g/L MgSO ₄ , 0.0147 g/L CaCl ₂ , 0.0001 g/L thiamine, 50 g/L D-glucose, 0.45 g/L ascorbic acid, 1 mL/L trace elements solution* *trace elements solution: 27 g/L FeCl ₃ , 2 g/L ZnCl ₃ , CoCl ₂ ·6H ₂ O, 2 g/L Na ₂ MoO ₄ ·2H ₂ O, 2 g/L CaCl ₂ ·2H ₂ O, 0.5 g/L H ₃ BO ₃ , 100 mL/L HCl

Table 4.7: Fermentation media compositions comparing the standard protocol from Muñoz *et al.* (Fordjour et al., 2019) and this work.

M9Y strikes a balance between a minimal and rich medium, reducing costs, streamlining broth handling, and simplifying fermentation broth composition.

By optimizing the fermentation conditions and medium composition, we have achieved a comparable if not slightly higher yield of L-DOPA while promoting a cost-effective and environmentally friendly approach (Graph 4.5).



Graph 4.5: Comparison of L-DOPA production crude yield (g) between this work and the bioreactor system of Muñoz *et al.*, respectively 0.89 g from 0.65 L fermentation broth and 0.75 g from 0.5 L.

This accomplishment not only highlights the potential of microbial fermentation as a viable method for L-DOPA production but also underscores the importance of continuous optimization in the field.

Our work paves the way for further advancements in L-DOPA production from D-glucose and contributes to the development of more accessible and sustainable products synthesis from this valuable aromatic amino acid.

4.4 Bibliography

- Abrahamson, M. J., Vázquez-Figueroa, E., Woodall, N. B., Moore, J. C., & Bommarius, A. S. (2012). Development of an Amine Dehydrogenase for Synthesis of Chiral Amines. *Angewandte Chemie International Edition*, *51*(16), 3969–3972. <https://doi.org/10.1002/anie.201107813>
- Abrahamson, M. J., Wong, J. W., & Bommarius, A. S. (2013). The Evolution of an Amine Dehydrogenase Biocatalyst for the Asymmetric Production of Chiral Amines. *Advanced Synthesis & Catalysis*, *355*(9), 1780–1786. <https://doi.org/10.1002/adsc.201201030>
- Alcántara, A. R., Domínguez de María, P., Littlechild, J. A., Schürmann, M., Sheldon, R. A., & Wohlgemuth, R. (2022). Biocatalysis as Key to Sustainable Industrial Chemistry. *ChemSusChem*, *15*(9). <https://doi.org/10.1002/cssc.202102709>
- Almud, J. J., Oliveira, M. A., Kern, A. D., Grishin, N. V., Phillips, M. A., & Hackert, M. L. (2000). Crystal structure of human ornithine decarboxylase at 2.1 Å resolution: structural insights to antizyme binding. *Journal of Molecular Biology*, *295*(1), 7–16. <https://doi.org/10.1006/jmbi.1999.3331>
- Andréll, J., Hicks, M. G., Palmer, T., Carpenter, E. P., Iwata, S., & Maher, M. J. (2009). Crystal Structure of the Acid-Induced Arginine Decarboxylase from *Escherichia coli* : Reversible Decamer Assembly Controls Enzyme Activity. *Biochemistry*, *48*(18), 3915–3927. <https://doi.org/10.1021/bi900075d>
- Anwar, S., Mohammad, T., Shamsi, A., Queen, A., Parveen, S., Luqman, S., Hasan, G. M., Alamry, K. A., Azum, N., Asiri, A. M., & Hassan, M. I. (2020). Discovery of hordenine as a potential inhibitor of pyruvate dehydrogenase kinase 3: Implication in lung cancer therapy. *Biomedicines*, *8*(5), 32–228.
- Asano, Y., Nakazawa, A., & Endo, K. (1987). Novel phenylalanine dehydrogenases from *Sporosarcina ureae* and *Bacillus sphaericus*. Purification and characterization. *The Journal of Biological Chemistry*, *262*(21), 10346–10354. <http://www.ncbi.nlm.nih.gov/pubmed/3112142>
- Báez, J. L., Bolívar, F., & Gosset, G. (2001). Determination of 3-deoxy-D- *arabino* -heptulosonate 7-phosphate productivity and yield from glucose in *Escherichia coli* devoid of the glucose phosphotransferase transport system. *Biotechnology and Bioengineering*, *73*(6), 530–535. <https://doi.org/10.1002/bit.1088>
- Bai, Z., Sun, X., Yu, X., & Li, L. (2019). Chitosan Microbeads as Supporter for *Pseudomonas putida* with Surface Displayed Laccases for Decolorization of Synthetic Dyes. *Applied Sciences*, *9*(1), 138. <https://doi.org/10.3390/app9010138>
- Baker, P. J., Turnbull, A. P., Sedelnikova, S. E., Stillman, T. J., & Rice, D. W. (1995). A role for quaternary structure in the substrate specificity of leucine dehydrogenase. *Structure*, *3*(7), 693–705. [https://doi.org/10.1016/S0969-2126\(01\)00204-0](https://doi.org/10.1016/S0969-2126(01)00204-0)
- Barwell, C. J., Basma, A. N., Lafi, M. A. K., & Leake, L. D. (2011). Deamination of hordenine by monoamine oxidase and its action on vasa deferentia of the rat. *Journal of Pharmacy and Pharmacology*, *41*(6), 421–423. <https://doi.org/10.1111/j.2042-7158.1989.tb06492.x>
- Bell, E. L., Finnigan, W., France, S. P., Green, A. P., Hayes, M. A., Hepworth, L. J., Lovelock, S. L., Niikura, H., Osuna, S., Romero, E., Ryan, K. S., Turner, N. J., & Flitsch, S. L. (2021).

- Biocatalysis. *Nature Reviews Methods Primers*, 1(1), 46. <https://doi.org/10.1038/s43586-021-00044-z>
- Benítez-Mateos, A. I., Roura Padrosa, D., & Paradisi, F. (2022). Multistep enzyme cascades as a route towards green and sustainable pharmaceutical syntheses. *Nature Chemistry*, 14(5), 489–499. <https://doi.org/10.1038/s41557-022-00931-2>
- Bennett, M., Ducrot, L., Vergne-Vaxelaire, C., & Grogan, G. (2022). Structure and Mutation of the Native Amine Dehydrogenase MATOUAmDH2. *ChemBioChem*, 23(10). <https://doi.org/10.1002/cbic.202200136>
- Berridge, M. V., Herst, P. M., & Tan, A. S. (2005). *Tetrazolium dyes as tools in cell biology: New insights into their cellular reduction* (pp. 127–152). [https://doi.org/10.1016/S1387-2656\(05\)11004-7](https://doi.org/10.1016/S1387-2656(05)11004-7)
- Bertelli, M., Kiani, A. K., Paolacci, S., Manara, E., Kurti, D., Dhuli, K., Bushati, V., Miertus, J., Pangallo, D., Baglivo, M., Beccari, T., & Michelini, S. (2020). Hydroxytyrosol: A natural compound with promising pharmacological activities. *Journal of Biotechnology*, 309, 29–33. <https://doi.org/10.1016/j.jbiotec.2019.12.016>
- Bhatia, S. K., Kim, Y. H., Kim, H. J., Seo, H.-M., Kim, J.-H., Song, H.-S., Sathiyarayanan, G., Park, S.-H., Park, K., & Yang, Y.-H. (2015). Biotransformation of lysine into cadaverine using barium alginate-immobilized *Escherichia coli* overexpressing CadA. *Bioprocess and Biosystems Engineering*, 38(12), 2315–2322. <https://doi.org/10.1007/s00449-015-1465-9>
- Bloch, D. N., Sandre, M., Ben Zichri, S., Masato, A., Kolusheva, S., Bubacco, L., & Jelinek, R. (2023). Scavenging neurotoxic aldehydes using lysine carbon dots. *Nanoscale Advances*, 5(5), 1356–1367. <https://doi.org/10.1039/D2NA00804A>
- Böhmer, W., Knaus, T., & Mutti, F. G. (2018a). Hydrogen-Borrowing Alcohol Bioamination with Coimmobilized Dehydrogenases. *ChemCatChem*, 10(4), 731–735. <https://doi.org/10.1002/cctc.201701366>
- Böhmer, W., Knaus, T., & Mutti, F. G. (2018b). Hydrogen-Borrowing Alcohol Bioamination with Coimmobilized Dehydrogenases. *ChemCatChem*, 10(4), 731–735. <https://doi.org/10.1002/cctc.201701366>
- Cai, R.-F., Liu, L., Chen, F.-F., Li, A., Xu, J.-H., & Zheng, G.-W. (2020). Reductive Amination of Biobased Levulinic Acid to Unnatural Chiral γ -Amino Acid Using an Engineered Amine Dehydrogenase. *ACS Sustainable Chemistry & Engineering*, 8(46), 17054–17061. <https://doi.org/10.1021/acssuschemeng.0c04647>
- Caparco, A. A., Bommarius, B. R., Bommarius, A. S., & Champion, J. A. (2020). Protein-inorganic calcium-phosphate supraparticles as a robust platform for enzyme co-immobilization. *Biotechnology and Bioengineering*, 117(7), 1979–1989. <https://doi.org/10.1002/bit.27348>
- Caparco, A. A., Pelletier, E., Petit, J. L., Jouenne, A., Bommarius, B. R., Berardinis, V., Zaparucha, A., Champion, J. A., Bommarius, A. S., & Vergne-Vaxelaire, C. (2020). Metagenomic Mining for Amine Dehydrogenase Discovery. *Advanced Synthesis & Catalysis*, 362(12), 2427–2436. <https://doi.org/10.1002/adsc.202000094>

- Capitani, G. (2003). Crystal structure and functional analysis of Escherichia coli glutamate decarboxylase. *The EMBO Journal*, *22*(16), 4027–4037. <https://doi.org/10.1093/emboj/cdg403>
- Cerioli, L., Planchestainer, M., Cassidy, J., Tessaro, D., & Paradisi, F. (2015). Characterization of a novel amine transaminase from Halomonas elongata. *Journal of Molecular Catalysis B: Enzymatic*, *120*, 141–150. <https://doi.org/10.1016/j.molcatb.2015.07.009>
- Chen, W., Yao, J., Meng, J., Han, W., Tao, Y., Chen, Y., Guo, Y., Shi, G., He, Y., Jin, J.-M., & Tang, S.-Y. (2019). Promiscuous enzymatic activity-aided multiple-pathway network design for metabolic flux rearrangement in hydroxytyrosol biosynthesis. *Nature Communications*, *10*(1), 960. <https://doi.org/10.1038/s41467-019-08781-2>
- Claes, L., Janssen, M., & De Vos, D. E. (2019). Organocatalytic Decarboxylation of Amino Acids as a Route to Bio-based Amines and Amides. *ChemCatChem*, *11*(17), 4297–4306. <https://doi.org/10.1002/cctc.201900800>
- Contente, M. L., & Paradisi, F. (2018). Self-sustaining closed-loop multienzyme-mediated conversion of amines into alcohols in continuous reactions. *Nature Catalysis*, *1*(6), 452–459. <https://doi.org/10.1038/s41929-018-0082-9>
- Cosenza, V. A., Navarro, D. A., & Stortz, C. A. (2011). Usage of α -picoline borane for the reductive amination of carbohydrates. *Arkivoc*, *2011*(7), 182–194. <https://doi.org/10.3998/ark.5550190.0012.716>
- Coyle, J. P., Johnson, C., Jensen, J., Farcas, M., Derk, R., Stueckle, T. A., Kornberg, T. G., Rojanasakul, Y., & Rojanasakul, L. W. (2023). Variation in pentose phosphate pathway-associated metabolism dictates cytotoxicity outcomes determined by tetrazolium reduction assays. *Scientific Reports*, *13*(1), 8220. <https://doi.org/10.1038/s41598-023-35310-5>
- DiCosimo, R., McAuliffe, J., Poulouse, A. J., & Bohlmann, G. (2013). Industrial use of immobilized enzymes. *Chemical Society Reviews*, *42*(15), 6437. <https://doi.org/10.1039/c3cs35506c>
- Ducrot, L., Bennett, M., André-Leroux, G., Elisée, E., Marynberg, S., Fossey-Jouenne, A., Zaparucha, A., Grogan, G., & Vergne-Vaxelaire, C. (2022). Expanding the Substrate Scope of Native Amine Dehydrogenases through *In Silico* Structural Exploration and Targeted Protein Engineering. *ChemCatChem*, *14*(22). <https://doi.org/10.1002/cctc.202200880>
- Ducrot, L., Bennett, M., Caparco, A. A., Champion, J. A., Bommarius, A. S., Zaparucha, A., Grogan, G., & Vergne-Vaxelaire, C. (2021). Biocatalytic Reductive Amination by Native Amine Dehydrogenases to Access Short Chiral Alkyl Amines and Amino Alcohols. *Frontiers in Catalysis*, *1*. <https://doi.org/10.3389/fctls.2021.781284>
- Eliot, A. C., & Kirsch, J. F. (2004). Pyridoxal Phosphate Enzymes: Mechanistic, Structural, and Evolutionary Considerations. *Annual Review of Biochemistry*, *73*(1), 383–415. <https://doi.org/10.1146/annurev.biochem.73.011303.074021>
- Eller, K., Henkes, E., Rossbacher, R., & Höke, H. (2000). Amines, Aliphatic. In *Ullmann's Encyclopedia of Industrial Chemistry*. Wiley-VCH Verlag GmbH & Co. KGaA. https://doi.org/10.1002/14356007.a02_001

- Escalante, A., Calderón, R., Valdivia, A., de Anda, R., Hernández, G., Ramírez, O. T., Gosset, G., & Bolívar, F. (2010). Metabolic engineering for the production of shikimic acid in an evolved *Escherichia coli* strain lacking the phosphoenolpyruvate: carbohydrate phosphotransferase system. *Microbial Cell Factories*, *9*(1), 21. <https://doi.org/10.1186/1475-2859-9-21>
- Foor, F., Morin, N., & Bostian, K. A. (1993). Production of L-dihydroxyphenylalanine in *Escherichia coli* with the tyrosine phenol-lyase gene cloned from *Erwinia herbicola*. *Applied and Environmental Microbiology*, *59*(9), 3070–3075. <https://doi.org/10.1128/aem.59.9.3070-3075.1993>
- Fordjour, E., Adipah, F. K., Zhou, S., Du, G., & Zhou, J. (2019). Metabolic engineering of *Escherichia coli* BL21 (DE3) for de novo production of l-DOPA from d-glucose. *Microbial Cell Factories*, *18*(1). <https://doi.org/10.1186/s12934-019-1122-0>
- Franklin, R. D., Whitley, J. A., Caparco, A. A., Bommarius, B. R., Champion, J. A., & Bommarius, A. S. (2021). Continuous production of a chiral amine in a packed bed reactor with co-immobilized amine dehydrogenase and formate dehydrogenase. *Chemical Engineering Journal*, *407*, 127065. <https://doi.org/10.1016/j.cej.2020.127065>
- Froidevaux, V., Negrell, C., Caillol, S., Pascault, J.-P., & Boutevin, B. (2016). Biobased Amines: From Synthesis to Polymers; Present and Future. *Chemical Reviews*, *116*(22), 14181–14224. <https://doi.org/10.1021/acs.chemrev.6b00486>
- Garg, R. P., Ma, Y., Hoyt, J. C., & Parry, R. J. (2002a). Molecular characterization and analysis of the biosynthetic gene cluster for the azoxy antibiotic valanimycin. *Molecular Microbiology*, *46*(2), 505–517. <https://doi.org/10.1046/j.1365-2958.2002.03169.x>
- Garg, R. P., Ma, Y., Hoyt, J. C., & Parry, R. J. (2002b). Molecular characterization and analysis of the biosynthetic gene cluster for the azoxy antibiotic valanimycin. *Molecular Microbiology*, *46*(2), 505–517. <https://doi.org/10.1046/j.1365-2958.2002.03169.x>
- Ghislieri, D., & Turner, N. J. (2014). Biocatalytic Approaches to the Synthesis of Enantiomerically Pure Chiral Amines. *Topics in Catalysis*, *57*(5), 284–300. <https://doi.org/10.1007/s11244-013-0184-1>
- Gianolio, S., Roura Padrosa, D., & Paradisi, F. (2022). Combined chemoenzymatic strategy for sustainable continuous synthesis of the natural product hordenine. *Green Chemistry*, *24*(21), 8434–8440. <https://doi.org/10.1039/D2GC02767D>
- Giardina, G., Montioli, R., Gianni, S., Cellini, B., Paiardini, A., Voltattorni, C. B., & Cutruzzola, F. (2011). Open conformation of human DOPA decarboxylase reveals the mechanism of PLP addition to Group II decarboxylases. *Proceedings of the National Academy of Sciences*, *108*(51), 20514–20519. <https://doi.org/10.1073/pnas.1111456108>
- Gong, X., Tao, J., Wang, Y., Wu, J., An, J., Meng, J., Wang, X., Chen, Y., & Zou, J. (2021). Total barley maiya alkaloids inhibit prolactin secretion by acting on dopamine D2 receptor and protein kinase A targets. *Journal of Ethnopharmacology*, *273*, 113994. <https://doi.org/10.1016/j.jep.2021.113994>
- Gosset, G., Yong-Xiao, J., & Berry, A. (1996). A direct comparison of approaches for increasing carbon flow to aromatic biosynthesis in *Escherichia coli*. *Journal of Industrial Microbiology*, *17*(1), 47–52. <https://doi.org/10.1007/BF01570148>

- Guisán, JoséM. (1988). Aldehyde-agarose gels as activated supports for immobilization-stabilization of enzymes. *Enzyme and Microbial Technology*, 10(6), 375–382. [https://doi.org/10.1016/0141-0229\(88\)90018-X](https://doi.org/10.1016/0141-0229(88)90018-X)
- Guo, K., Ji, C., & Li, L. (2007). Stable-Isotope Dimethylation Labeling Combined with LC–ESI MS for Quantification of Amine-Containing Metabolites in Biological Samples. *Analytical Chemistry*, 79(22), 8631–8638. <https://doi.org/10.1021/ac0704356>
- Guo, Z., Yan, N., & Lapkin, A. A. (2019). Towards circular economy: integration of bio-waste into chemical supply chain. *Current Opinion in Chemical Engineering*, 26, 148–156. <https://doi.org/10.1016/j.coche.2019.09.010>
- Gupte, A. P., Basaglia, M., Casella, S., & Favaro, L. (2022). Rice waste streams as a promising source of biofuels: feedstocks, biotechnologies and future perspectives. *Renewable and Sustainable Energy Reviews*, 167, 112673. <https://doi.org/10.1016/j.rser.2022.112673>
- Gut, H., Pennacchietti, E., John, R. A., Bossa, F., Capitani, G., De Biase, D., & Grütter, M. G. (2006). Escherichia coli acid resistance: pH-sensing, activation by chloride and autoinhibition in GadB. *The EMBO Journal*, 25(11), 2643–2651. <https://doi.org/10.1038/sj.emboj.7601107>
- H. Orrego, A., Romero-Fernández, M., Millán-Linares, M., Yust, M., Guisán, J., & Rocha-Martin, J. (2018). Stabilization of Enzymes by Multipoint Covalent Attachment on Aldehyde-Supports: 2-Picoline Borane as an Alternative Reducing Agent. *Catalysts*, 8(8), 333. <https://doi.org/10.3390/catal8080333>
- Hamid, M. H. S. A., Slatford, P. A., & Williams, J. M. J. (2007). Borrowing Hydrogen in the Activation of Alcohols. *Advanced Synthesis & Catalysis*, 349(10), 1555–1575. <https://doi.org/10.1002/adsc.200600638>
- Hapke, H. J., & Strathmann, W. (1995). [Pharmacological effects of hordenine]. *DTW. Deutsche Tierärztliche Wochenschrift*, 102(6), 228–232. <http://www.ncbi.nlm.nih.gov/pubmed/8582256>
- Harper, B. A., Barbut, S., Lim, L.-T., & Marcone, M. F. (2014). Effect of Various Gelling Cations on the Physical Properties of “Wet” Alginate Films. *Journal of Food Science*, 79(4), E562–E567. <https://doi.org/10.1111/1750-3841.12376>
- Heckmann, C. M., Gourlay, L. J., Dominguez, B., & Paradisi, F. (2020). An (R)-Selective Transaminase From *Thermomyces stellatus*: Stabilizing the Tetrameric Form. *Frontiers in Bioengineering and Biotechnology*, 8. <https://doi.org/10.3389/fbioe.2020.00707>
- Heffter, A. (1898). Ueber Pellote. *Archiv Für Experimentelle Pathologie Und Pharmakologie*, 40(5–6), 385–429. <https://doi.org/10.1007/BF01825267>
- Heydari, M., Ohshima, T., Nunoura-Kominato, N., & Sakuraba, H. (2004). Highly Stable Lysine 6-Dehydrogenase from the Thermophile *Geobacillus stearothermophilus* Isolated from a Japanese Hot Spring: Characterization, Gene Cloning and Sequencing, and Expression. *Applied and Environmental Microbiology*, 70(2), 937–942. <https://doi.org/10.1128/AEM.70.2.937-942.2004>
- Holbrook, O. T., Molligoda, B., Bushell, K. N., & Gobrogge, K. L. (2022). Behavioral consequences of the downstream products of ethanol metabolism involved in alcohol use disorder.

- Neuroscience & Biobehavioral Reviews*, 133, 104501.
<https://doi.org/10.1016/j.neubiorev.2021.12.024>
- Houwman, J. A., Knaus, T., Costa, M., & Mutti, F. G. (2019). Efficient synthesis of enantiopure amines from alcohols using resting *E. coli* cells and ammonia. *Green Chemistry*, 21(14), 3846–3857. <https://doi.org/10.1039/C9GC01059A>
- Huang, J., Mei, L., Wu, H., & Lin, D. (2007). Biosynthesis of γ -aminobutyric acid (GABA) using immobilized whole cells of *Lactobacillus brevis*. *World Journal of Microbiology and Biotechnology*, 23(6), 865–871. <https://doi.org/10.1007/s11274-006-9311-5>
- Huang, R., Chen, H., Zhong, C., Kim, J. E., & Zhang, Y.-H. P. (2016). High-Throughput Screening of Coenzyme Preference Change of Thermophilic 6-Phosphogluconate Dehydrogenase from NADP⁺ to NAD⁺. *Scientific Reports*, 6(1), 32644. <https://doi.org/10.1038/srep32644>
- Hwang, E. T., & Lee, S. (2019). Multienzymatic Cascade Reactions via Enzyme Complex by Immobilization. *ACS Catalysis*, 9(5), 4402–4425. <https://doi.org/10.1021/acscatal.8b04921>
- Jackson, D. M., Ashley, R. L., Brownfield, C. B., Morrison, D. R., & Morrison, R. W. (2015). Rapid Conventional and Microwave-Assisted Decarboxylation of L-Histidine and Other Amino Acids via Organocatalysis with R-Carvone Under Superheated Conditions. *Synthetic Communications*, 45(23), 2691–2700. <https://doi.org/10.1080/00397911.2015.1100745>
- Jansonius, J. N. (1998). Structure, evolution and action of vitamin B6-dependent enzymes. *Current Opinion in Structural Biology*, 8(6), 759–769. [https://doi.org/10.1016/S0959-440X\(98\)80096-1](https://doi.org/10.1016/S0959-440X(98)80096-1)
- Jeon, H., Yoon, S., Ahsan, M., Sung, S., Kim, G.-H., Sundaramoorthy, U., Rhee, S.-K., & Yun, H. (2017). The Kinetic Resolution of Racemic Amines Using a Whole-Cell Biocatalyst Co-Expressing Amine Dehydrogenase and NADH Oxidase. *Catalysts*, 7(9), 251. <https://doi.org/10.3390/catal7090251>
- Jiang, M., Xu, G., Ni, J., Zhang, K., Dong, J., Han, R., & Ni, Y. (2019a). Improving Soluble Expression of Tyrosine Decarboxylase from *Lactobacillus brevis* for Tyramine Synthesis with High Total Turnover Number. *Applied Biochemistry and Biotechnology*, 188(2), 436–449. <https://doi.org/10.1007/s12010-018-2925-x>
- Jiang, M., Xu, G., Ni, J., Zhang, K., Dong, J., Han, R., & Ni, Y. (2019b). Improving Soluble Expression of Tyrosine Decarboxylase from *Lactobacillus brevis* for Tyramine Synthesis with High Total Turnover Number. *Applied Biochemistry and Biotechnology*, 188(2), 436–449. <https://doi.org/10.1007/s12010-018-2925-x>
- Jones, J. A., Collins, S. M., Vernacchio, V. R., Lachance, D. M., & Koffas, M. A. G. (2016). Optimization of naringenin and *p*-coumaric acid hydroxylation using the native *E. coli* hydroxylase complex, HpaBC. *Biotechnology Progress*, 32(1), 21–25. <https://doi.org/10.1002/btpr.2185>
- Khorsand, F., Murphy, C. D., Whitehead, A. J., & Engel, P. C. (2017). Biocatalytic stereoinversion of *p*-para-bromophenylalanine in a one-pot three-enzyme reaction. *Green Chemistry*, 19(2), 503–510. <https://doi.org/10.1039/C6GC01922F>
- Kim, Baritugo, Oh, Kang, Jung, Jang, Song, Kim, Lee, Hwang, Park, Park, & Joo. (2019). High-Level Conversion of l-lysine into Cadaverine by *Escherichia coli* Whole Cell Biocatalyst Expressing

- Hafnia alvei l-lysine Decarboxylase. *Polymers*, 11(7), 1184.
<https://doi.org/10.3390/polym11071184>
- Kim, D. I., Chae, T. U., Kim, H. U., Jang, W. D., & Lee, S. Y. (2021). Microbial production of multiple short-chain primary amines via retrobiosynthesis. *Nature Communications*, 12(1), 173. <https://doi.org/10.1038/s41467-020-20423-6>
- Kim, S.-C., Lee, J.-H., Kim, M.-H., Lee, J.-A., Kim, Y. B., Jung, E., Kim, Y.-S., Lee, J., & Park, D. (2013). Hordenine, a single compound produced during barley germination, inhibits melanogenesis in human melanocytes. *Food Chemistry*, 141(1), 174–181.
<https://doi.org/10.1016/j.foodchem.2013.03.017>
- Knaus, T., Böhmer, W., & Mutti, F. G. (2017). Amine dehydrogenases: efficient biocatalysts for the reductive amination of carbonyl compounds. *Green Chemistry*, 19(2), 453–463.
<https://doi.org/10.1039/C6GC01987K>
- Knowles, W. S. (n.d.). Asymmetric Hydrogenations– The MonsantoL-Dopa Process. In *Asymmetric Catalysis on Industrial Scale* (pp. 21–38). Wiley-VCH Verlag GmbH & Co. KGaA.
<https://doi.org/10.1002/3527602151.ch1>
- Komori, H., Nitta, Y., Ueno, H., & Higuchi, Y. (2012). Structural Study Reveals That Ser-354 Determines Substrate Specificity on Human Histidine Decarboxylase. *Journal of Biological Chemistry*, 287(34), 29175–29183. <https://doi.org/10.1074/jbc.M112.381897>
- Kugler, P. (1979). A gel-sandwich technique for the qualitative and quantitative determination of dehydrogenases in the enzyme histochemistry. *Histochemistry*, 60(3), 265–293.
<https://doi.org/10.1007/BF00500656>
- Kumar, R., Vikramachakravarthi, D., & Pal, P. (2014). Production and purification of glutamic acid: A critical review towards process intensification. *Chemical Engineering and Processing: Process Intensification*, 81, 59–71. <https://doi.org/10.1016/j.cep.2014.04.012>
- Kurpejović, E., Wendisch, V. F., & Sariyar Akbulut, B. (2021). Tyrosinase-based production of l-DOPA by *Corynebacterium glutamicum*. *Applied Microbiology and Biotechnology*, 105(24), 9103–9111. <https://doi.org/10.1007/s00253-021-11681-5>
- Lapponi, M. J., Méndez, M. B., Trelles, J. A., & Rivero, C. W. (2022). Cell immobilization strategies for biotransformations. *Current Opinion in Green and Sustainable Chemistry*, 33, 100565. <https://doi.org/10.1016/j.cogsc.2021.100565>
- Lawrence, S. A. (2004). *Amines: synthesis, properties and applications*. Cambridge University Press.
- Lee, J., Michael, A. J., Martynowski, D., Goldsmith, E. J., & Phillips, M. A. (2007). Phylogenetic Diversity and the Structural Basis of Substrate Specificity in the β/α -Barrel Fold Basic Amino Acid Decarboxylases. *Journal of Biological Chemistry*, 282(37), 27115–27125.
<https://doi.org/10.1074/jbc.M704066200>
- Lee, S. Y., Kim, H. U., Chae, T. U., Cho, J. S., Kim, J. W., Shin, J. H., Kim, D. I., Ko, Y.-S., Jang, W. D., & Jang, Y.-S. (2019). A comprehensive metabolic map for production of bio-based chemicals. *Nature Catalysis*, 2(1), 18–33. <https://doi.org/10.1038/s41929-018-0212-4>

- Leuchtenberger, W., Huthmacher, K., & Drauz, K. (2005). Biotechnological production of amino acids and derivatives: current status and prospects. *Applied Microbiology and Biotechnology*, *69*(1), 1–8. <https://doi.org/10.1007/s00253-005-0155-y>
- Li, N., Chou, H., & Xu, Y. (2016). Improved cadaverine production from mutant *Klebsiella oxytoca* lysine decarboxylase. *Engineering in Life Sciences*, *16*(3), 299–305. <https://doi.org/10.1002/elsc.201500037>
- Liu, G., Zhou, N., Zhang, M., Li, S., Tian, Q., Chen, J., Chen, B., Wu, Y., & Yao, S. (2010). Hydrophobic solvent induced phase transition extraction to extract drugs from plasma for high performance liquid chromatography–mass spectrometric analysis. *Journal of Chromatography A*, *1217*(3), 243–249. <https://doi.org/10.1016/j.chroma.2009.11.037>
- Liu, J., Pang, B. Q. W., Adams, J. P., Snajdrova, R., & Li, Z. (2017). Coupled Immobilized Amine Dehydrogenase and Glucose Dehydrogenase for Asymmetric Synthesis of Amines by Reductive Amination with Cofactor Recycling. *ChemCatChem*, *9*(3), 425–431. <https://doi.org/10.1002/cctc.201601446>
- Liu, Y., Liu, P., Gao, S., Wang, Z., Luan, P., González-Sabín, J., & Jiang, Y. (2021). Construction of chemoenzymatic cascade reactions for bridging chemocatalysis and Biocatalysis: Principles, strategies and prospective. *Chemical Engineering Journal*, *420*, 127659. <https://doi.org/10.1016/j.cej.2020.127659>
- Ma, J., Wang, S., Huang, X., Geng, P., Wen, C., Zhou, Y., Yu, L., & Wang, X. (2015). Validated UPLC–MS/MS method for determination of hordenine in rat plasma and its application to pharmacokinetic study. *Journal of Pharmaceutical and Biomedical Analysis*, *111*, 131–137. <https://doi.org/10.1016/j.jpba.2015.03.032>
- Mateo, C., Grazú, V., Pessela, B. C. C., Montes, T., Palomo, J. M., Torres, R., López-Gallego, F., Fernández-Lafuente, R., & Guisán, J. M. (2007a). Advances in the design of new epoxy supports for enzyme immobilization–stabilization. *Biochemical Society Transactions*, *35*(6), 1593–1601. <https://doi.org/10.1042/BST0351593>
- Mateo, C., Grazú, V., Pessela, B. C. C., Montes, T., Palomo, J. M., Torres, R., López-Gallego, F., Fernández-Lafuente, R., & Guisán, J. M. (2007b). Advances in the design of new epoxy supports for enzyme immobilization–stabilization. *Biochemical Society Transactions*, *35*(6), 1593–1601. <https://doi.org/10.1042/BST0351593>
- Mayol, O., Bastard, K., Beloti, L., Frese, A., Turkenburg, J. P., Petit, J.-L., Mariage, A., Debard, A., Pellouin, V., Perret, A., de Berardinis, V., Zapparucha, A., Grogan, G., & Vergne-Vaxelaire, C. (2019a). A family of native amine dehydrogenases for the asymmetric reductive amination of ketones. *Nature Catalysis*, *2*(4), 324–333. <https://doi.org/10.1038/s41929-019-0249-z>
- Mayol, O., Bastard, K., Beloti, L., Frese, A., Turkenburg, J. P., Petit, J.-L., Mariage, A., Debard, A., Pellouin, V., Perret, A., de Berardinis, V., Zapparucha, A., Grogan, G., & Vergne-Vaxelaire, C. (2019b). A family of native amine dehydrogenases for the asymmetric reductive amination of ketones. *Nature Catalysis*, *2*(4), 324–333. <https://doi.org/10.1038/s41929-019-0249-z>
- Meyer, E. (1982). Separation of two distinct S-adenosylmethionine dependent N-methyltransferases involved in hordenine biosynthesis in *Hordeum vulgare*. *Plant Cell Reports*, *1*(6), 236–239. <https://doi.org/10.1007/BF00272627>

- Mi, J., Liu, S., Du, Y., Qi, H., & Zhang, L. (2022). Cofactor self-sufficient by co-immobilization of pyridoxal 5'-phosphate and lysine decarboxylase for cadaverine production. *Bioresource Technology Reports*, 17, 100939. <https://doi.org/10.1016/j.biteb.2021.100939>
- Montgomery, S. L., Mangas-Sanchez, J., Thompson, M. P., Aleku, G. A., Dominguez, B., & Turner, N. J. (2017). Direct Alkylation of Amines with Primary and Secondary Alcohols through Biocatalytic Hydrogen Borrowing. *Angewandte Chemie*, 129(35), 10627–10630. <https://doi.org/10.1002/ange.201705848>
- Mørch, Y. A., Donati, I., Strand, B. L., & Skjåk-Bræk, G. (2006). Effect of Ca²⁺, Ba²⁺, and Sr²⁺ on Alginate Microbeads. *Biomacromolecules*, 7(5), 1471–1480. <https://doi.org/10.1021/bm060010d>
- Muñoz, A. J., Hernández-Chávez, G., De Anda, R., Martínez, A., Bolívar, F., & Gosset, G. (2011). Metabolic engineering of *Escherichia coli* for improving l-3,4-dihydroxyphenylalanine (l-DOPA) synthesis from glucose. *Journal of Industrial Microbiology and Biotechnology*, 38(11), 1845–1852. <https://doi.org/10.1007/s10295-011-0973-0>
- Mutti, F. G., & Knaus, T. (2021). Enzymes Applied to the Synthesis of Amines. In *Biocatalysis for Practitioners* (pp. 143–180). Wiley. <https://doi.org/10.1002/9783527824465.ch6>
- Mutti, F. G., Knaus, T., Scrutton, N. S., Breuer, M., & Turner, N. J. (2015). Conversion of alcohols to enantiopure amines through dual-enzyme hydrogen-borrowing cascades. *Science*, 349(6255), 1525–1529. <https://doi.org/10.1126/science.aac9283>
- Nakai, T., Nakagawa, N., Maoka, N., Masui, R., Kuramitsu, S., & Kamiya, N. (2005). Structure of P-protein of the glycine cleavage system: implications for nonketotic hyperglycinemia. *The EMBO Journal*, 24(8), 1523–1536. <https://doi.org/10.1038/sj.emboj.7600632>
- Narisetty, V., Cox, R., Bommareddy, R., Agrawal, D., Ahmad, E., Pant, K. K., Chandel, A. K., Bhatia, S. K., Kumar, D., Binod, P., Gupta, V. K., & Kumar, V. (2022). Valorisation of xylose to renewable fuels and chemicals, an essential step in augmenting the commercial viability of lignocellulosic biorefineries. *Sustainable Energy & Fuels*, 6(1), 29–65. <https://doi.org/10.1039/D1SE00927C>
- Nasri, M. (2017a). *Protein Hydrolysates and Biopeptides* (pp. 109–159). <https://doi.org/10.1016/bs.afnr.2016.10.003>
- Nasri, M. (2017b). *Protein Hydrolysates and Biopeptides* (pp. 109–159). <https://doi.org/10.1016/bs.afnr.2016.10.003>
- Natte, K., Neumann, H., Jagadeesh, R. v., & Beller, M. (2017). Convenient iron-catalyzed reductive aminations without hydrogen for selective synthesis of N-methylamines. *Nature Communications*, 8(1), 1344. <https://doi.org/10.1038/s41467-017-01428-0>
- Nguyen, N. H., Truong-Thi, N.-H., Nguyen, D. T. D., Ching, Y. C., Huynh, N. T., & Nguyen, D. H. (2022). Non-ionic surfactants As co-templates to control the mesopore diameter of hollow mesoporous silica nanoparticles for drug delivery applications. *Colloids and Surfaces A: Physicochemical and Engineering Aspects*, 655, 130218. <https://doi.org/10.1016/j.colsurfa.2022.130218>
- Ohta, H., Murakami, Y., Takebe, Y., Murasaki, K., Oshima, K., Yoshihara, H., & Morimura, S. (2020). <i>N</i>-Methyltyramine, a Gastrin-releasing Factor in Beer, and

Structurally Related Compounds as Agonists for Human Trace Amine-associated Receptor 1. *Food Science and Technology Research*, 26(2), 313–317.
<https://doi.org/10.3136/fstr.26.313>

- PARADISI, F., COLLINS, S., MAGUIRE, A., & ENGEL, P. (2007). Phenylalanine dehydrogenase mutants: Efficient biocatalysts for synthesis of non-natural phenylalanine derivatives. *Journal of Biotechnology*, 128(2), 408–411. <https://doi.org/10.1016/j.jbiotec.2006.08.008>
- Park, J.-Y., Choi, M.-J., Yu, H., Choi, Y., Park, K.-M., & Chang, P.-S. (2022). Multi-functional behavior of food emulsifier erythorbyl laurate in different colloidal conditions of homogeneous oil-in-water emulsion system. *Colloids and Surfaces A: Physicochemical and Engineering Aspects*, 636, 128127. <https://doi.org/10.1016/j.colsurfa.2021.128127>
- Park, S. H., Soetyono, F., & Kim, H. K. (2017). Cadaverine Production by Using Cross-Linked Enzyme Aggregate of Escherichia coli Lysine Decarboxylase. *Journal of Microbiology and Biotechnology*, 27(2), 289–296. <https://doi.org/10.4014/jmb.1608.08033>
- Patil, M. D., Grogan, G., Bommarius, A., & Yun, H. (2018). Oxidoreductase-Catalyzed Synthesis of Chiral Amines. *ACS Catalysis*, 8(12), 10985–11015.
<https://doi.org/10.1021/acscatal.8b02924>
- Patil, M. D., Yoon, S., Jeon, H., Khobragade, T. P., Sarak, S., Pagar, A. D., Won, Y., & Yun, H. (2019). Kinetic Resolution of Racemic Amines to Enantiopure (S)-amines by a Biocatalytic Cascade Employing Amine Dehydrogenase and Alanine Dehydrogenase. *Catalysts*, 9(7), 600. <https://doi.org/10.3390/catal9070600>
- Payne, J. T., Valentic, T. R., & Smolke, C. D. (2021). Complete biosynthesis of the bisbenzylisoquinoline alkaloids guattegaumerine and berbaminine in yeast. *Proceedings of the National Academy of Sciences*, 118(51). <https://doi.org/10.1073/pnas.2112520118>
- Pelckmans, M., Renders, T., Van de Vyver, S., & Sels, B. F. (2017). Bio-based amines through sustainable heterogeneous catalysis. *Green Chemistry*, 19(22), 5303–5331.
<https://doi.org/10.1039/C7GC02299A>
- Pilkington, R. L., Dallaston, M. A., Savage, G. P., Williams, C. M., & Polyzos, A. (2021). Enone-promoted decarboxylation of *trans*-4-hydroxy-*l*-proline in flow: a side-by-side comparison to batch. *Reaction Chemistry & Engineering*, 6(3), 486–493.
<https://doi.org/10.1039/D0RE00442A>
- Planchestainer, M., Hegarty, E., Heckmann, C. M., Gourlay, L. J., & Paradisi, F. (2019). Widely applicable background depletion step enables transaminase evolution through solid-phase screening. *Chemical Science*, 10(23), 5952–5958. <https://doi.org/10.1039/C8SC05712E>
- Prieto, M. A., & Garcia, J. L. (1994). Molecular characterization of 4-hydroxyphenylacetate 3-hydroxylase of Escherichia coli. A two-protein component enzyme. *Journal of Biological Chemistry*, 269(36), 22823–22829. [https://doi.org/10.1016/S0021-9258\(17\)31719-2](https://doi.org/10.1016/S0021-9258(17)31719-2)
- Pyne, M. E., Kevvai, K., Grewal, P. S., Narcross, L., Choi, B., Bourgeois, L., Dueber, J. E., & Martin, V. J. J. (2020). A yeast platform for high-level synthesis of tetrahydroisoquinoline alkaloids. *Nature Communications*, 11(1), 3337. <https://doi.org/10.1038/s41467-020-17172-x>

- Quaglia, D., Irwin, J. A., & Paradisi, F. (2012a). Horse Liver Alcohol Dehydrogenase: New Perspectives for an Old Enzyme. *Molecular Biotechnology*, *52*(3), 244–250. <https://doi.org/10.1007/s12033-012-9542-7>
- Quaglia, D., Irwin, J. A., & Paradisi, F. (2012b). Horse Liver Alcohol Dehydrogenase: New Perspectives for an Old Enzyme. *Molecular Biotechnology*, *52*(3), 244–250. <https://doi.org/10.1007/s12033-012-9542-7>
- Ray, S. S., Bonanno, J. B., Rajashankar, K. R., Pinho, M. G., He, G., De Lencastre, H., Tomasz, A., & Burley, S. K. (2002). Cocrystal Structures of Diaminopimelate Decarboxylase. *Structure*, *10*(11), 1499–1508. [https://doi.org/10.1016/S0969-2126\(02\)00880-8](https://doi.org/10.1016/S0969-2126(02)00880-8)
- Reetz, M. T. (2013). Biocatalysis in Organic Chemistry and Biotechnology: Past, Present, and Future. *Journal of the American Chemical Society*, *135*(34), 12480–12496. <https://doi.org/10.1021/ja405051f>
- Roschangar, F., Sheldon, R. A., & Senanayake, C. H. (2015). Overcoming barriers to green chemistry in the pharmaceutical industry – the Green Aspiration Level™ concept. *Green Chemistry*, *17*(2), 752–768. <https://doi.org/10.1039/C4GC01563K>
- Ruhaak, L. R., Steenvoorden, E., Koeleman, C. A. M., Deelder, A. M., & Wuhrer, M. (2010). 2-Picoline-borane: A non-toxic reducing agent for oligosaccharide labeling by reductive amination. *Proteomics*, *10*(12), 2330–2336. <https://doi.org/10.1002/pmic.200900804>
- Sagong, H.-Y., Son, H. F., Kim, S., Kim, Y.-H., Kim, I.-K., & Kim, K.-J. (2016). Crystal Structure and Pyridoxal 5-Phosphate Binding Property of Lysine Decarboxylase from *Selenomonas ruminantium*. *PLOS ONE*, *11*(11), e0166667. <https://doi.org/10.1371/journal.pone.0166667>
- Said, A. A. E., Ali, T. F. S., Attia, E. Z., Ahmed, A.-S. F., Shehata, A. H., Abdelmohsen, U. R., & Fouad, M. A. (2021). Antidepressant potential of *Mesembryanthemum cordifolium* roots assisted by metabolomic analysis and virtual screening. *Natural Product Research*, *35*(23), 5493–5497. <https://doi.org/10.1080/14786419.2020.1788019>
- SANDMEIER, E., HALE, T. I., & CHRISTEN, P. (1994a). Multiple evolutionary origin of pyridoxal-5'-phosphate-dependent amino acid decarboxylases. *European Journal of Biochemistry*, *221*(3), 997–1002. <https://doi.org/10.1111/j.1432-1033.1994.tb18816.x>
- SANDMEIER, E., HALE, T. I., & CHRISTEN, P. (1994b). Multiple evolutionary origin of pyridoxal-5'-phosphate-dependent amino acid decarboxylases. *European Journal of Biochemistry*, *221*(3), 997–1002. <https://doi.org/10.1111/j.1432-1033.1994.tb18816.x>
- Sato, S., Sakamoto, T., Miyazawa, E., & Kikugawa, Y. (2004). One-pot reductive amination of aldehydes and ketones with α -picoline-borane in methanol, in water, and in neat conditions. *Tetrahedron*, *60*(36), 7899–7906. <https://doi.org/10.1016/j.tet.2004.06.045>
- Schoenmakers, H., & Spiegel, L. (2014). Laboratory Distillation and Scale-up. In *Distillation* (pp. 319–339). Elsevier. <https://doi.org/10.1016/B978-0-12-386878-7.00010-3>
- Seah, S. Y. K., Britton, K. L., Rice, D. W., Asano, Y., & Engel, P. C. (2002). Single Amino Acid Substitution in *Bacillus sphaericus* Phenylalanine Dehydrogenase Dramatically Increases Its Discrimination between Phenylalanine and Tyrosine Substrates. *Biochemistry*, *41*(38), 11390–11397. <https://doi.org/10.1021/bi020196a>

- Seah, S. Y. K., Linda Britton, K., Baker, P. J., Rice, D. W., Asano, Y., & Engel, P. C. (1995). Alteration in relative activities of phenylalanine dehydrogenase towards different substrates by site-directed mutagenesis. *FEBS Letters*, *370*(1–2), 93–96. [https://doi.org/10.1016/0014-5793\(95\)00804-I](https://doi.org/10.1016/0014-5793(95)00804-I)
- Sen, K. Y., & Baidurah, S. (2021). Renewable biomass feedstocks for production of sustainable biodegradable polymer. *Current Opinion in Green and Sustainable Chemistry*, *27*, 100412. <https://doi.org/10.1016/j.cogsc.2020.100412>
- Sharma, M., Mangas-Sanchez, J., Turner, N. J., & Grogan, G. (2017). NAD(P)H-Dependent Dehydrogenases for the Asymmetric Reductive Amination of Ketones: Structure, Mechanism, Evolution and Application. *Advanced Synthesis & Catalysis*, *359*(12), 2011–2025. <https://doi.org/10.1002/adsc.201700356>
- Sheldon, R. A., Basso, A., & Brady, D. (2021). New frontiers in enzyme immobilisation: robust biocatalysts for a circular bio-based economy. *Chemical Society Reviews*, *50*(10), 5850–5862. <https://doi.org/10.1039/D1CS00015B>
- Sheldon, R. A., & Brady, D. (2019). Broadening the Scope of Biocatalysis in Sustainable Organic Synthesis. *ChemSusChem*, *12*(13), 2859–2881. <https://doi.org/10.1002/cssc.201900351>
- Sheldon, R. A., & Woodley, J. M. (2018). Role of Biocatalysis in Sustainable Chemistry. *Chemical Reviews*, *118*(2), 801–838. <https://doi.org/10.1021/acs.chemrev.7b00203>
- Sommer, T., Göen, T., Budnik, N., & Pischetsrieder, M. (2020). Absorption, Biokinetics, and Metabolism of the Dopamine D2 Receptor Agonist Hordenine (*N* , *N* -Dimethyltyramine) after Beer Consumption in Humans. *Journal of Agricultural and Food Chemistry*, *68*(7), 1998–2006. <https://doi.org/10.1021/acs.jafc.9b06029>
- Song, W., Chen, X., Wu, J., Xu, J., Zhang, W., Liu, J., Chen, J., & Liu, L. (2020). Biocatalytic derivatization of proteinogenic amino acids for fine chemicals. *Biotechnology Advances*, *40*, 107496. <https://doi.org/10.1016/j.biotechadv.2019.107496>
- Stano, J., Nemeč, P., Weissová, K., Kovács, P., Kákoniová, D., & Lisková, D. (1995). Decarboxylation of l-tyrosine and l-dopa by immobilized cells of *Papaver somniferum*. *Phytochemistry*, *38*(4), 859–860. [https://doi.org/10.1016/0031-9422\(94\)00768-0](https://doi.org/10.1016/0031-9422(94)00768-0)
- Stockert, J. C., Horobin, R. W., Colombo, L. L., & Blázquez-Castro, A. (2018). Tetrazolium salts and formazan products in Cell Biology: Viability assessment, fluorescence imaging, and labeling perspectives. *Acta Histochemica*, *120*(3), 159–167. <https://doi.org/10.1016/j.acthis.2018.02.005>
- Su, Y., Liu, Y., He, D., Hu, G., Wang, H., Ye, B., He, Y., Gao, X., & Liu, D. (2022). Hordenine inhibits neuroinflammation and exerts neuroprotective effects via inhibiting NF-κB and MAPK signaling pathways in vivo and in vitro. *International Immunopharmacology*, *108*, 108694. <https://doi.org/10.1016/j.intimp.2022.108694>
- Surwase, S. N., Patil, S. A., Apine, O. A., & Jadhav, J. P. (2012). Efficient Microbial Conversion of l-Tyrosine to l-DOPA by *Brevundimonas* sp. SGJ. *Applied Biochemistry and Biotechnology*, *167*(5), 1015–1028. <https://doi.org/10.1007/s12010-012-9564-4>
- Tang, Y. Q., & Weng, N. (2013). Salting-out assisted liquid–liquid extraction for bioanalysis. *Bioanalysis*, *5*(12), 1583–1598. <https://doi.org/10.4155/bio.13.117>

- Teng, Y., Scott, E. L., van Zeeland, A. N. T., & Sanders, J. P. M. (2011). The use of l-lysine decarboxylase as a means to separate amino acids by electro dialysis. *Green Chemistry*, *13*(3), 624. <https://doi.org/10.1039/c0gc00611d>
- Thompson, M. P., Derrington, S. R., Heath, R. S., Porter, J. L., Mangas-Sanchez, J., Devine, P. N., Truppo, M. D., & Turner, N. J. (2019). A generic platform for the immobilisation of engineered biocatalysts. *Tetrahedron*, *75*(3), 327–334. <https://doi.org/10.1016/j.tet.2018.12.004>
- Thompson, M. P., & Turner, N. J. (2017a). Two-Enzyme Hydrogen-Borrowing Amination of Alcohols Enabled by a Cofactor-Switched Alcohol Dehydrogenase. *ChemCatChem*, *9*(20), 3833–3836. <https://doi.org/10.1002/cctc.201701092>
- Thompson, M. P., & Turner, N. J. (2017b). Two-Enzyme Hydrogen-Borrowing Amination of Alcohols Enabled by a Cofactor-Switched Alcohol Dehydrogenase. *ChemCatChem*, *9*(20), 3833–3836. <https://doi.org/10.1002/cctc.201701092>
- Tolbert, W. D., Graham, D. E., White, R. H., & Ealick, S. E. (2003). Pyruvoyl-Dependent Arginine Decarboxylase from *Methanococcus jannaschii*. *Structure*, *11*(3), 285–294. [https://doi.org/10.1016/S0969-2126\(03\)00026-1](https://doi.org/10.1016/S0969-2126(03)00026-1)
- Truong, C. C., Mishra, D. K., & Suh, Y. (2023). Recent Catalytic Advances on the Sustainable Production of Primary Furanic Amines from the One-Pot Reductive Amination of 5-Hydroxymethylfurfural. *ChemSusChem*, *16*(1). <https://doi.org/10.1002/cssc.202201846>
- Tseliou, V., Knaus, T., Masman, M. F., Corrado, M. L., & Mutti, F. G. (2019). Generation of amine dehydrogenases with increased catalytic performance and substrate scope from ϵ -deaminating L-Lysine dehydrogenase. *Nature Communications*, *10*(1), 3717. <https://doi.org/10.1038/s41467-019-11509-x>
- Tseliou, V., Knaus, T., Vilím, J., Masman, M. F., & Mutti, F. G. (2020). Kinetic Resolution of Racemic Primary Amines Using *Geobacillus stearothermophilus* Amine Dehydrogenase Variant. *ChemCatChem*, *12*(8), 2184–2188. <https://doi.org/10.1002/cctc.201902085>
- Tsukatani, T., Suenaga, H., Higuchi, T., Akao, T., Ishiyama, M., Ezo, K., & Matsumoto, K. (2008). Colorimetric cell proliferation assay for microorganisms in microtiter plate using water-soluble tetrazolium salts. *Journal of Microbiological Methods*, *75*(1), 109–116. <https://doi.org/10.1016/j.mimet.2008.05.016>
- Viejo, C. G., Villarreal-Lara, R., Torrico, D. D., Rodríguez-Velazco, Y. G., Escobedo-Avellaneda, Z., Ramos-Parra, P. A., Mandal, R., Singh, A. P., Hernández-Brenes, C., & Fuentes, S. (2020). Beer and consumer response using biometrics: Associations assessment of beer compounds and elicited emotions. *Foods*, *9*(6), 821.
- Vitaku, E., Smith, D. T., & Njardarson, J. T. (2014). Analysis of the Structural Diversity, Substitution Patterns, and Frequency of Nitrogen Heterocycles among U.S. FDA Approved Pharmaceuticals. *Journal of Medicinal Chemistry*, *57*(24), 10257–10274. <https://doi.org/10.1021/jm501100b>
- Wang, M., Khan, M. A., Mohsin, I., Wicks, J., Ip, A. H., Sumon, K. Z., Dinh, C.-T., Sargent, E. H., Gates, I. D., & Kibria, M. G. (2021). Can sustainable ammonia synthesis pathways compete with fossil-fuel based Haber–Bosch processes? *Energy & Environmental Science*, *14*(5), 2535–2548. <https://doi.org/10.1039/D0EE03808C>

- Wang, Q., Xin, Y., Zhang, F., Feng, Z., Fu, J., Luo, L., & Yin, Z. (2011). Enhanced γ -aminobutyric acid-forming activity of recombinant glutamate decarboxylase (*gadA*) from *Escherichia coli*. *World Journal of Microbiology and Biotechnology*, *27*(3), 693–700. <https://doi.org/10.1007/s11274-010-0508-2>
- Watanabe, Y., Tsuji, Y., Ige, H., Ohsugi, Y., & Ohta, T. (1984). Ruthenium-catalyzed N-alkylation and N-benylation of aminoarenes with alcohols. *The Journal of Organic Chemistry*, *49*(18), 3359–3363. <https://doi.org/10.1021/jo00192a021>
- Weber, R. E. (1992). Use of ionic and zwitterionic (Tris/BisTris and HEPES) buffers in studies on hemoglobin function. *Journal of Applied Physiology*, *72*(4), 1611–1615. <https://doi.org/10.1152/jappl.1992.72.4.1611>
- Wei, G., Chen, Y., Zhou, N., Lu, Q., Xu, S., Zhang, A., Chen, K., & Ouyang, P. (2022). Chitin biopolymer mediates self-sufficient biocatalyst of pyridoxal 5'-phosphate and L-lysine decarboxylase. *Chemical Engineering Journal*, *427*, 132030. <https://doi.org/10.1016/j.cej.2021.132030>
- Wei, T., Cheng, B. Y., & Liu, J. Z. (2016). Genome engineering *Escherichia coli* for L-DOPA overproduction from glucose. *Scientific Reports*, *6*. <https://doi.org/10.1038/srep30080>
- Wieschalka, S., Blombach, B., Bott, M., & Eikmanns, B. J. (2013). Bio-based production of organic acids with *Corynebacterium glutamicum*. *Microbial Biotechnology*, *6*(2), 87–102. <https://doi.org/10.1111/1751-7915.12013>
- Wohlgemuth, R. (2021). Biocatalysis-Key enabling tools from biocatalytic one-step and multi-step reactions to biocatalytic total synthesis. *New Biotechnol*, *60*, 113–123.
- Wu, B., Zhang, S., Hong, T., Zhou, Y., Wang, H., Shi, M., Yang, H., Tian, X., Guo, J., Bian, J., Roache, J., Delgado, P., Mo, R., Fridrich, C., Gao, F., & Wang, J. (2020). Merging Biocatalysis, Flow, and Surfactant Chemistry: Innovative Synthesis of an FXI (Factor XI) Inhibitor. *Organic Process Research & Development*, *24*(11), 2780–2788. <https://doi.org/10.1021/acs.oprd.0c00412>
- Wu, P., Li, G., He, Y., Luo, D., Li, L., Guo, J., Ding, P., & Yang, F. (2020). High-efficient and sustainable biodegradation of microcystin-LR using *Sphingopyxis* sp. YF1 immobilized Fe₃O₄@chitosan. *Colloids and Surfaces B: Biointerfaces*, *185*, 110633. <https://doi.org/10.1016/j.colsurfb.2019.110633>
- Ye, L. J., Toh, H. H., Yang, Y., Adams, J. P., Snajdrova, R., & Li, Z. (2015). Engineering of Amine Dehydrogenase for Asymmetric Reductive Amination of Ketone by Evolving *Rhodococcus* Phenylalanine Dehydrogenase. *ACS Catalysis*, *5*(2), 1119–1122. <https://doi.org/10.1021/cs501906r>
- Yoon, S., Patil, M. D., Sarak, S., Jeon, H., Kim, G., Khobragade, T. P., Sung, S., & Yun, H. (2019). Deracemization of Racemic Amines to Enantiopure (R)- and (S)-amines by Biocatalytic Cascade Employing ω -Transaminase and Amine Dehydrogenase. *ChemCatChem*, *11*(7), 1898–1902. <https://doi.org/10.1002/cctc.201900080>
- Yoshitaka Hashitani, B. (1925). On the chemical constituents of malt-rootlets with special reference to Hordenine. *Journal of the College of Agriculture*, *14*, 1–56.

- Zhang, B., Jiang, Y., Li, Z., Wang, F., & Wu, X.-Y. (2020). Recent Progress on Chemical Production From Non-food Renewable Feedstocks Using *Corynebacterium glutamicum*. *Frontiers in Bioengineering and Biotechnology*, *8*. <https://doi.org/10.3389/fbioe.2020.606047>
- Zhang, H., Wei, Y., Lu, Y., Wu, S., Liu, Q., Liu, J., & Jiao, Q. (2016). Three-step biocatalytic reaction using whole cells for efficient production of tyramine from keratin acid hydrolysis wastewater. *Applied Microbiology and Biotechnology*, *100*(4), 1691–1700. <https://doi.org/10.1007/s00253-015-7054-7>
- Zhang, K., & Ni, Y. (2014). Tyrosine decarboxylase from *Lactobacillus brevis*: Soluble expression and characterization. *Protein Expression and Purification*, *94*, 33–39. <https://doi.org/10.1016/j.pep.2013.10.018>
- Zhang, X., Du, L., Zhang, J., Li, C., Zhang, J., & Lv, X. (2021). Hordenine Protects Against Lipopolysaccharide-Induced Acute Lung Injury by Inhibiting Inflammation. *Frontiers in Pharmacology*, *12*, 712232. <https://doi.org/10.3389/fphar.2021.712232>
- Zhao, W., Hu, S., Huang, J., Ke, P., Yao, S., Lei, Y., Mei, L., & Wang, J. (2016). Permeabilization of *Escherichia coli* with ampicillin for a whole cell biocatalyst with enhanced glutamate decarboxylase activity. *Chinese Journal of Chemical Engineering*, *24*(7), 909–913. <https://doi.org/10.1016/j.cjche.2016.02.001>
- Zhou, F., Xu, Y., Nie, Y., & Mu, X. (2022). Substrate-Specific Engineering of Amino Acid Dehydrogenase Superfamily for Synthesis of a Variety of Chiral Amines and Amino Acids. *Catalysts*, *12*(4), 380. <https://doi.org/10.3390/catal12040380>
- Zhou, J.-W., Ruan, L.-Y., Chen, H.-J., Luo, H.-Z., Jiang, H., Wang, J.-S., & Jia, A.-Q. (2019). Inhibition of Quorum Sensing and Virulence in *Serratia marcescens* by Hordenine. *Journal of Agricultural and Food Chemistry*, *67*(3), 784–795. <https://doi.org/10.1021/acs.jafc.8b05922>
- Zhu, H., Xu, G., Zhang, K., Kong, X., Han, R., Zhou, J., & Ni, Y. (2016a). Crystal structure of tyrosine decarboxylase and identification of key residues involved in conformational swing and substrate binding. *Scientific Reports*, *6*(1), 27779. <https://doi.org/10.1038/srep27779>
- Zhu, H., Xu, G., Zhang, K., Kong, X., Han, R., Zhou, J., & Ni, Y. (2016b). Crystal structure of tyrosine decarboxylase and identification of key residues involved in conformational swing and substrate binding. *Scientific Reports*, *6*(1), 27779. <https://doi.org/10.1038/srep27779>
- Zhuang, W., Liu, H., Zhang, Y., He, J., & Wang, P. (2021). Effective asymmetric preparation of (R)-1-[3-(trifluoromethyl)phenyl]ethanol with recombinant *E. coli* whole cells in an aqueous Tween-20/natural deep eutectic solvent solution. *AMB Express*, *11*(1), 118. <https://doi.org/10.1186/s13568-021-01278-6>

5. Combined chemoenzymatic strategy for sustainable continuous synthesis of hordenine

Unless explicitly stated otherwise, the research presented in this chapter is the sole and individual work of the author and it has

been included in the following publication: S. Gianolio, D. Padrosa, F. Paradisi “*Combined chemoenzymatic strategy for sustainable continuous synthesis of the natural product hordenine*” *Green Chemistry* 2022, 24, 8434-8440.

5.1 Introduction

Hordenine (Figure 5.1) is a chemical compound that is found naturally in a variety of plants, including barley, sprouted barley, and sprouted oats.(Gong et al., 2021) It is classified as a phenethylamine, which is a class of compounds that includes a wide range of chemicals, including some that are found naturally in the human body and some that are synthesized for use in the medical and research fields.

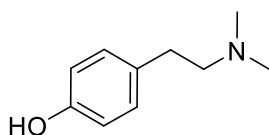


Figure 5.1: Hordenine chemical structure

As a natural product, this phenolic phytochemical has a number of potential effects on the body,(Anwar et al., 2020; Barwell et al., 2011; Hapke & Strathmann, 1995; S.-C. Kim et al., 2013; Ma et al., 2015; Ohta et al., 2020; Said et al., 2021; X. Zhang et al., 2021) including effects on the nervous system and the cardiovascular system. It has been suggested that hordenine may have some potential as a performance-enhancing supplement or weight loss aid,(Su et al., 2022) although more research is needed to confirm these effects and to determine the safety and effectiveness of hordenine for these purposes.

Hordenine chemical structure features an amino group in the form of a tertiary amine. Chemically speaking, hordenine is the N,N-dimethyl derivative of the renowned biogenic amine, tyramine, which is also its biosynthetic precursor.(Meyer, 1982)

In 1894 Arthur Heffter(Heffter, 1898) was the first to report the isolation of hordenine by extracting it from the cactus *Anhalonium fissuratus* and naming it Anhalin. Subsequently, in 1906, E. Léger isolated an alkaloid from germinated barley (*Hordeum vulgare*) seeds on his own and named it hordenine.(Yoshitaka Hashitani, 1925) Ultimately, it was confirmed that these alkaloids were the same, and the moniker 'hordenine' was preserved for this substance molecular structure.

Via barley conversion to malt, hordenine is present also in beer. Because of this, a number of research groups investigated the effects of hordenine and its biokinetic after the consumption of beer in humans.(Viejo et al., 2020) In the recent study(Sommer et al., 2020) “*Absorption, Biokinetics, and Metabolism of the Dopamine D2 Receptor Agonist Hordenine (N,N-Dimethyltyramine) after Beer Consumption in Humans*”, the plasmatic

hordenine concentration has been examined and correlated to its bioactivity as an alkaloid. Hordenine is in fact able to cross the BBB (Blood brain barrier) and work as an agonist of the Dopamine D2 receptor.

Hordenine has been studied also in the context of melanogenesis for its mechanisms of action in human epidermal melanocytes.(S.-C. Kim et al., 2013) it exhibits the capability to impede melanogenesis through the reduction of cAMP production, a critical factor in the expression of proteins associated with melanogenesis. This implies that hordenine could be a potent deterrent against hyperpigmentation.

Not only beneficial for human health, hordenine properties have been investigated also in plants.(J.-W. Zhou et al., 2019) In barley, at concentrations ranging from 0.5 to 1.0 mg mL⁻¹, hordenine inhibits the levels of acyl-homoserine lactones, negatively influencing the production of the quorum sensing (QS)-related extracellular virulence factors of *Pseudomonas aeruginosa* PAO1. Therefore, it shows activity against foodborne pathogen *Pseudomonas aeruginosa* acting as a competitive inhibitor for signaling molecules.

The conventional chemical synthesis of hordenine predominantly involves the N-dimethylation of tyramine. Goyal *et al.* (2019) introduced a method that utilized carbon-supported palladium (Pd/C) as a catalyst for N-methylation (Figure 5.2). While this approach facilitated the synthesis of a variety of N-methylamines, hordenine was produced in a moderate yield of 54%. The process was dependent on a palladium catalyst and necessitated high temperatures (130°C) over an extended reaction time (30 hours) under pressure conditions.

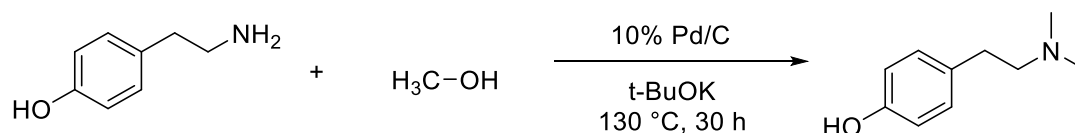


Figure 5.2: Reaction conditions: 0.5 mmol of amine, 10% Pd/C (4.7 mol % Pd, 25 mg), 2 mL of MeOH as a reagent and solvent, t-BuOK (1 mmol, 2 equiv), 30 h, 130 °C, isolated yield 54%.

In an attempt to develop a more efficient alternative, Sarki *et al.* (2021) employed RuCl₃ as a catalyst for N-methylation (Figure 5.3). Although this method was cleaner and more cost-effective than the previous approach, it continued to rely on metal catalysts and required an even longer reaction time of 60 hours at 150°C, yielding 76 % of the product.

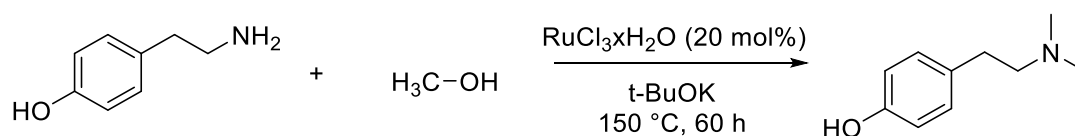


Figure 5.3: Reaction conditions: 0.5 mmol of amine, RuCl₃·xH₂O (20 mol %), KOtBu (3 equiv.), 150 °C, 60 h, isolated yield 76 %.

Further, Natte *et al.* (2017) presented a synthesis technique for N-methylamines, utilizing an iron oxide catalyst along with paraformaldehyde (Figure 5.4). This approach circumvented the need for high pressures of molecular hydrogen typically associated with reductive amination reactions. Nevertheless, despite an improved yield of 87 %, the procedure still required 24 hours of reaction time at 130°C, raising concerns regarding the environmental impact and the sustainability of this method.

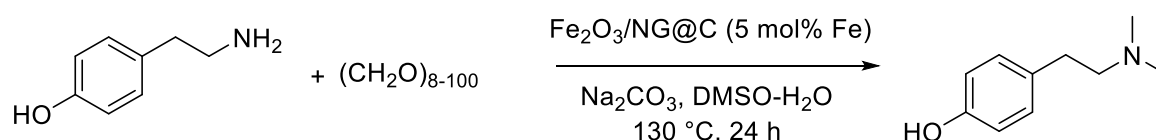


Figure 5.4: Reaction conditions: 0.5 mmol amine, 50 mg $\text{Fe}_2\text{O}_3/\text{NGr@C}$ (5 mol% Fe), 5 mmol of paraformaldehyde (150 mg), 0.5 mmol Na_2CO_3 , 2 mL DMSO-water (1:1), 130 °C, 24 h, isolated yield 87 %.

5.2 Results and discussion

5.2.1 Chemoenzymatic approach for Hordenine production

Using biocatalysis instead of metal catalysts in chemical reactions can reduce the environmental pollution and contribute to a circular economy. Biocatalytic applications have mild working conditions, use biodegradable components, and non-toxic reagents.

Aiming to adhere to the green chemistry principles, (Alcántara *et al.*, 2022; Y. Liu *et al.*, 2021; Reetz, 2013; Sheldon & Woodley, 2018) we wanted to design an alternative innovative process for the production of hordenine, (Gianolio *et al.*, 2022) that minimizes risks and environmental impact. By initiating the synthesis with L-tyrosine, an innocuous and abundant raw material, as opposed to tyramine which is hazardous to the respiratory system, tyramine is formed only as an intermediate in the process, potentially mitigating exposure. (Figure 5.5) This approach was realized through implementing a continuous flow process with enzyme immobilization technology .

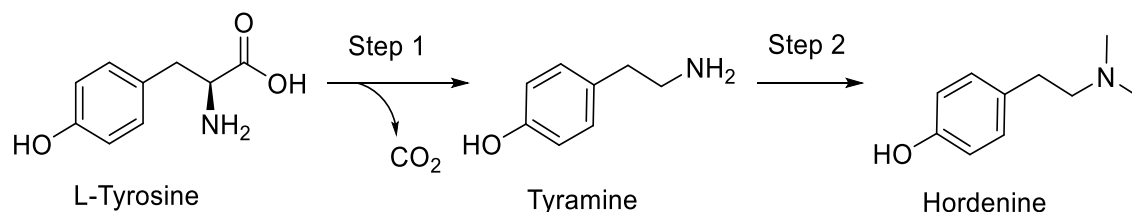


Figure 5.5: general scheme for the conversion of L-tyrosine to hordenine

5.2.2 Identification of the optimal biocatalyst

Bacterial decarboxylases are extremely efficient biocatalysts, but their expression in heterologous hosts in a soluble manner is often challenging and therefore their

applications are not as common as for other enzymes. The tyrosine decarboxylase from *Lactobacillus brevis* (*LbTDC*) has been successfully expressed in 2013,(K. Zhang & Ni, 2014) by means of a cell culture medium supplemented with 1 % of glucose. In 2016, after fine-tuning the crystallization conditions, the 3D structure of *LbTDC* was successfully determined (Figure 5.6).(Zhu et al., 2016b)



Figure 5.6: 3D *LbTDC* structure (PDB 5HSJ).

The gene for *LbTDC* (GenBank ABY71221.1) was cloned and transformed into *E. coli* BL21 (DE3) for overexpression. A culture was grown, induced with IPTG, and incubated for 5 hours (see experimental for details). Cells were harvested, washed, and stored at -20°C. *LbTDC* was purified using affinity chromatography and the protein concentration was quantified using absorbance at 280 nm (see experimental for details). The purified biocatalyst had good activity against its natural substrate (43.8 U/mg), but its volumetric yield could not be improved further than 3.5 mg $L_{culture}^{-1}$ due to cell toxicity from tyramine formation. After dialysis against phosphate buffer, the protein was quantified using absorbance at 280 nm with molar extinction coefficient estimated by ProtPram (ϵ : 115 630 $M^{-1} cm^{-1}$). The purified enzyme was obtained at a concentration of 1 mg/mL.

5.2.3 Activity assay of *LbTDC*

To measure the activity of *LbTDC*, different options were tested. Initially the activity assay was performed in 96 well plates measuring the absorbance at 475 nm of the oxidized unreacted substrate with the reaction of decarboxylation of L-DOPA to Dopamine. The problems linked to the designed colorimetric assay were the poor reproducibility of the data and the lack of selectivity in the oxidation at alkaline pH of L dopa and dopamine to the corresponding quinones (Figure 5.7).

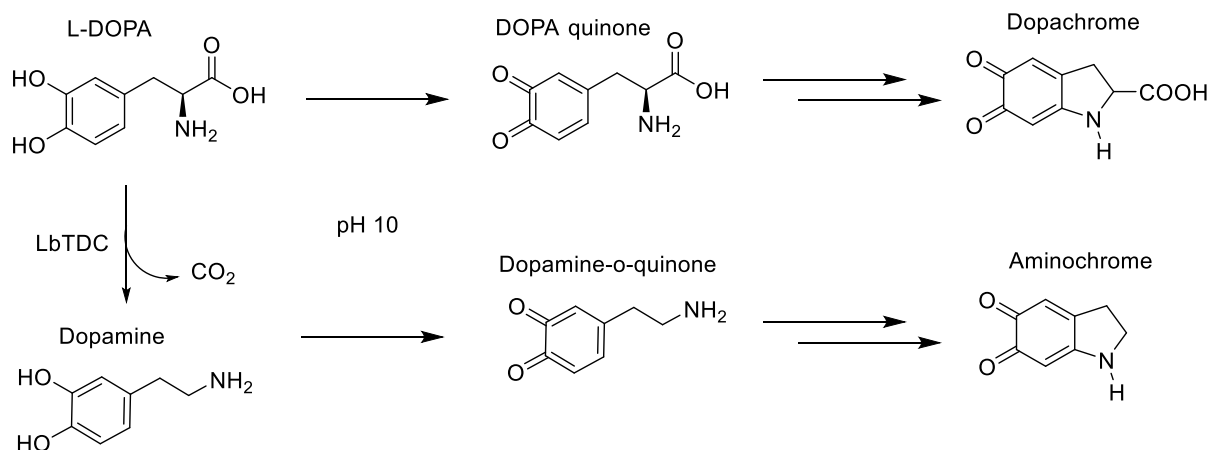


Figure 5.7: Alkaline oxidation of L-DOPA and dopamine. At 475 nm, the absorbance from dopachrome and aminochrome is detected.

Eventually, the activity assay for *LbTDC* was conducted using High-Performance Liquid Chromatography (HPLC) to measure the conversion of tyrosine to tyramine at 280 nm. This approach overcame the issues of poor reproducibility and lack of selectivity faced in the initial colorimetric assay. The details of the procedure and conditions, including elution phases and settings for the HPLC, are elaborated in the materials and methods section. This method allowed for more reliable and selective data acquisition.

5.2.4 Immobilization of *LbTDC*

The low volumetric yield of *LbTDC* expression represented a problem for the free enzyme utilization under efficiency and economic points of view. To address this issue, immobilization was identified as a practical solution. By immobilizing the enzyme on a solid support, it becomes possible to easily separate the biocatalyst from the reaction mixture and reuse it for multiple cycles. This is economically advantageous as it minimizes the necessity for frequent enzyme production.

Moreover, immobilization often enhances the enzyme's stability, preserving its structural integrity. This leads to reduced dependency on the continual expression of fresh enzyme, saving both time and resources. Furthermore, when the biocatalyst is immobilized, it becomes compatible with integration into automated flow systems. This setup allows for process intensification, maximizing enzyme efficiency in a controlled environment, making it conducive for scale-up and industrial applications. With the decision to employ immobilization as a strategy, the investigation focused on using three different methacrylic resins (EP403/S, HFA403/S, and EP400/SS) functionalized with epoxy handles for the immobilization of *LbTDC*. The process involved forming covalent bonds between the surface epoxy groups of the resin and the lysines in the protein's secondary structure, using directionality (Figure 5.8). The details of the resins used are provided in Table 5.1. Methacrylic resins are a type of polymer derived from methacrylic acid, the monomer contains an acrylic group and a methacryloyl group. These resins are known for their good

chemical resistance and mechanical properties, and they are often involved in a several applications, including coatings, adhesives, and plastics.

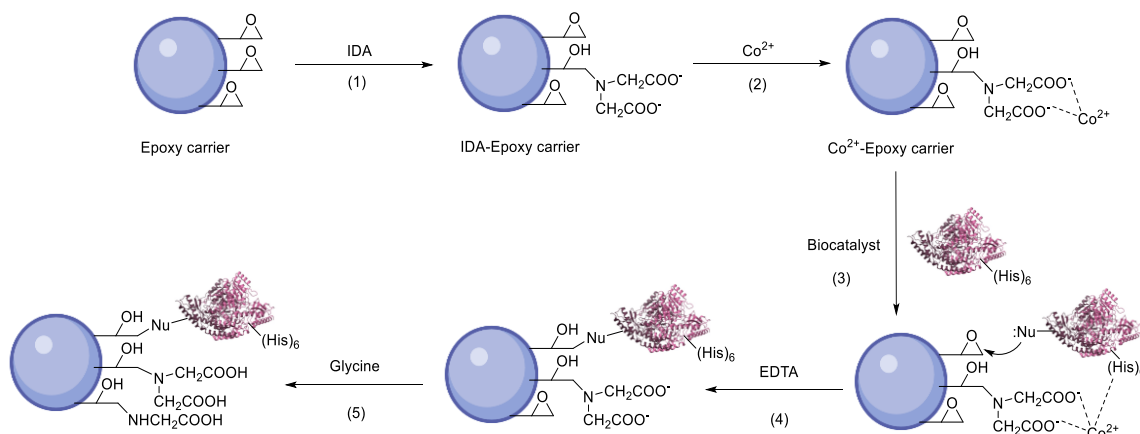


Figure 5.8: Schematic representation of enzyme immobilization on epoxy-functionalized supports. The process consists of five key steps: **(1)** support activation with iminodiacetic acid (IDA), **(2)** addition of a bivalent ion (e.g., cobalt) to form a stable complex with IDA, **(3)** docking of the enzyme containing a (His)-tag near the support, **(4)** formation of a covalent bond between nucleophilic amino acids (e.g., lysine) and epoxy groups, and **(5)** blocking of unreacted epoxy groups with glycine to prevent nonspecific binding.

The immobilization of *LbTDC* with the support through a covalent binding process was successfully performed with the protocol previously reported. (Mateo et al., 2007b)

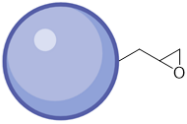
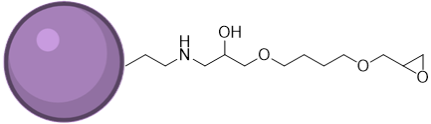
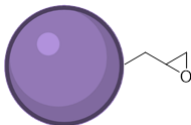
Epoxydic resin	Characteristics
EP4003/S 	Particle size: 100-300 μm \emptyset Pores: 40-60 nm
HFA403/S 	
EP400/SS 	Particle size: 50-150 μm \emptyset Pores: 40-50 nm Hydrophilic

Table 5.1: supports involved in the immobilization study.

The activity of the immobilized biocatalyst was tested by mixing it with a reaction mixture in a tube and shaking it at a specific temperature and speed. The conversion to the product was analysed every five minutes by HPLC, and the specific activity was calculated as the amount of product formed per minute for a certain amount of the immobilized support (see experimental for details). The imm-*LbTDC* specific activity (U/g) is defined as μmol of tyramine formed per minute for grams of immobilized support.

For the immobilization study, initially *LbTDC* loading on the supports was 1 mg/g. After comparing the obtained recovered activity, EP400/SS was selected for further trials where the protein loading was increased to 5 mg/g and 10 mg/g (Table 5.2).

Epoxydic Resin	Protein loading	Activity (U/g)	Recovered activity (%)	Stability (%)
EP403/S	1 mg/g	2.19	5	5
HFA403/S	1 mg/g	4.82	11	10
EP400/SS	1 mg/g	8.76	20	20
EP400/SS	5 mg/g	32.85	15	14
EP400/SS	10 mg/g	52.26	12	12

Table 5.2: immobilization study results for EP403/S, HFA403/S, and EP400/SS. Protein loading study was performed on EP400/SS as optimal support for *LbTDC* immobilization.

The results of this study showed that all three methacrylic resins were able to immobilize the biocatalyst effectively and covalently.

However, the EP403/S and HFA403/S resins showed lower levels of retained activity compared to the EP400/SS resin, suggesting that they may be less suitable for the immobilization of tyrosine decarboxylase.

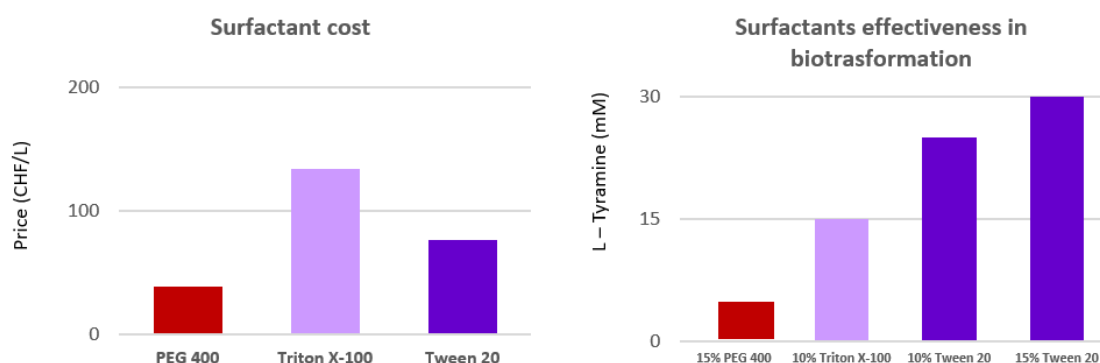
5.2.5 Biocatalytic decarboxylation of L-tyrosine with immobilized *LbTDC* in batch

The first step in our chemoenzymatic strategy is represented by the biocatalytic decarboxylation of L-tyrosine disodium salt. The optimized immobilized biocatalyst showed great stability and robustness during the batch tests. As the enzyme has high activity against L-tyrosine, a low concentration (0.006 mg mL^{-1}) of the free biocatalyst was sufficient to achieve full conversion at 2.5 mM scale in 20 minutes at 37°C. When bound to the support, *LbTDC* specific activity is reduced by approximately 5-fold. Nevertheless, in batch biotransformations at 5 mM scale, complete conversion was systematically obtained for up to five (repeated) cycles of 45 minutes, with 15 mg of *LbTDC*-EP400(SS) $5 \text{ mg}\cdot\text{g}^{-1}$, in 2 mL reaction volume. Therefore, the enzyme productivity increased from $415 \mu\text{mol}\cdot\text{mg}^{-1}$ to $670 \mu\text{mol}\cdot\text{mg}^{-1}$.

5.2.6 Batch test with immobilized enzyme and surfactant for process intensification

For the intensification of the process, we performed batch tests where the solubility of the starting material was increased by a co-solubilizer. L-tyrosine is an amino acid that is not very soluble in the reaction buffer at pH 5 and enhancing its solubility can be useful for the scale-up of the process. Jiang *et al.* screened nine different surfactants and co-solubilizers succeeding in improving the conversion to tyramine with *LbTDC* in batch. (Jiang et al., 2019b)

We investigated three different co-solubilizers (Triton-X100, Tween 20 and PEG 400) to identify the best choice in terms of cost-effectiveness, sustainability and stability impact on the immobilized biocatalyst reaction system (Graphs 5.1 and 5.2). Comparing prices from the same supplier, PEG400 was the cheapest option, while TritonX-100 was the most expensive. However, although not yielding a limpid solution, Tween 20 (15 % v/v) allowed to increase the solubility of L-tyrosine up to 30 mM, obtaining a micro-suspension and leading to full conversion to tyramine after 16 h (biotransformation condition: buffer acetate pH 5, 0.2 mM PLP and 15 % Tween 20, 0.05 mg/mL *LbTDC*) at 37°C.



Graphs 5.1 and 5.2: Comparison in terms of cost between the involved surfactants. Comparison in terms of tyramine concentration after 16 h biotransformation among the surfactants employed in the biotransformation set up.

To identify the optimal concentration of Tween 20 in the biotransformations, further experiments were performed, assessing the effectiveness of the surfactant at 10 %, 15 % and 20% v/v (Table 5.3).

L-tyrosine disodium salt (mM)	Tween 20 (% v/v)	Control M.c. (%)	M.c. (%)
10	5	73	95
30	10	39	84
40	15	34	75

Table 5.3: Batch biotransformations with the immobilized biocatalyst scaling-up the concentration of L-tyrosine disodium salt hydrate with the co-solubilizer Tween 20. The controls have been set up without adding the surfactant in the biotransformations. The biocatalyst concentration was 0.05 mg/mL and the analysis of the sample was after 16 h.

For what concerned the impact of Tween 20 on the stability of the immobilized biocatalyst, the activity of *LbTDC* was measured by the standard activity assay after the overnight biotransformations in presence of the surfactant in different concentrations (Table 5.4).

Tween 20 (% v/v)	Activity (%)
10	99
30	103
40	106

Table 5.4: Reusability of imm-*LbTDC* after 24 h biotrasformation.

Recycling the immobilized support presented the difficulty of an accurate wash of the resin, which carries residues of substrate or product on itself. Despite this, compared to the control with fresh immobilized enzyme, tests on resins from biotransformations with Tween 20 showed, like the control, complete conversion of the substrate to tyramine.

Therefore, the experiments suggested that Tween 20 did not hamper significantly the activity of the immobilized biocatalyst and contributed to a 6-fold increase in TON (Turnover Number) of the immobilized biocatalyst compared to the biotrasformations in the absence of surfactant, where the maximum L-tyrosine concentration was 5 mM.

Tween 20, also known as polysorbate 20, has already a wide range of applications in biotechnological and industrial processes. It is commonly used as a component of cell culture media to help solubilize nutrients and other compounds (Zhuang et al., 2021) and to improve the efficiency of cell growth and proliferation. It has been used as a solubilizing agent in the formulation of drugs, (Nguyen et al., 2022) including some vaccines, to improve the solubility and stability of the drug. Tween 20 is also used as an emulsifying agent (J.-Y. Park et al., 2022) in food processing to help mix together ingredients that do not normally mix well, such as oil and water. In the personal care industry, the surfactant is used in a variety of preparations, such as shampoos, conditioners, and lotions, to help improve the consistency and spreadability of the product.

However, the use of Tween 20 in industrial processes can introduce some challenges. Generally, the use of surfactants in industrial processes can become problematic, particularly for downstream work up and purification. One of the main challenges is the potential environmental impact of surfactants, as many of these compounds are synthetic and not biodegradable. They can be toxic to aquatic life and can accumulate in

the food chain, leading to potential health risks. Another important problem is the potential for product contamination, as surfactants can sometimes be difficult to remove from products and can cause contamination. This can lead to product quality issues.

The use of surfactants can also impact the efficiency of downstream processes, such as filtration or separation, and may require additional steps to remove them, which can increase the cost and complexity of the downstream step(s).

Considering this last point, the decision to employ Tween 20 for hordenine production in a chemoenzymatic system was abandoned. In addition, further issues arose with the scale-up of the experiment and the transition from batch to continuous flow systems. In fact, while a fine dispersion in solution favors the enzymatic activity in batch, over time the cloudy micro-suspension of L-tyrosine caused significant back pressure in the flow instrumentation. Therefore, the starting material concentration for the decarboxylation reaction was limited to 5 mM and further work was carried out directly in a flow system.

5.2.7 Immobilized enzyme integration into the continuous flow system

In a meso-reactor, 1 g of immobilized support with *Lb*TDC was packed to be integrated into the continuous flow system. The 1.3 mL PBR (packed bed reactor) was fed with the substrate solution (5 mM L-tyrosine in sodium acetate buffer pH 5, 0.2 mM PLP). Different protein loadings and T_R (residence time) were trialed as reported in the Table 5.5.

Protein Loading (mg/g)	T_R (min)	M.c. (%)
1	10	>99
1	5	87
5	5	>99
5	2.5	>99

Table 5.5: Experiments in flow for the conversion of L-tyrosine disodium salt to tyramine, testing the possibility to decrease the T_R exploiting the same amount of immobilized support (1 g EP400SS-*Lb*TDC).

With this PBR (1g imm-*Lb*TDC-EP400/SS 5 mg/g) it was possible to achieve complete conversion to tyramine in just 2.5 minutes T_R , at the flow rate of 0.54 mL/min.

This PBR showcased also remarkable operational stability, establishing itself as an extremely resilient system. Using 1g imm-*Lb*TDC-EP400/SS 5 mg/g, it adeptly maintained full conversion of the starting material for over 56 reaction cycles of 2.5 minutes. Notably, after 103 cycles, the system persisted in achieving conversion rates exceeding 95 %. Moreover, even after a prolonged 8-hour operation, equivalent to 192 reaction cycles, the conversion held above 90 %.

5.2.8 Optimization of the reductive amination step to convert tyramine to hordenine

After the successful set-up of the first bio-conversion step, the optimization of the reaction conditions for the chemical reductive amination was initially performed independently from the biocatalytic reaction.

As previously reported in the literature, tyramine can be dimethylated, exploiting formaldehyde and sodium cyanoborohydride (NaBH_3CN) in ammonium acetate buffer. (K. Guo et al., 2007) The possibility to achieve the complete conversion of tyramine was investigated in batch, employing less hazardous reducing agents as sodium borohydride (NaBH_4) and sodium triacetoxyborohydride (STAB) (Table 5.6). From initial batch, tests in buffer with NaBH_4 in excess were the only ones not effective.

entry	Reducing agent	Time (h)	M.c. (%)
1	Sodium borohydride	24	15
2	Sodium triacetoxyborohydride	24	95
3	Sodium cyanoborohydride	24	96

Table 5.6: Reaction mixture was 5 mM Tyramine, 50 mg of reducing agents, 100 μl acetic acid, 200 mM sodium acetate buffer pH 5. Reaction volume was 1 mL.

Due to the sodium triacetoxyborohydride instability under aqueous solvent conditions, acetonitrile (MeCN) was used as an aprotic co-solvent in the reaction to prevent its degradation and reduce the equivalents required. Different molar equivalents (eq.) of the reagents were tested to identify the minimum required for the complete conversion of tyramine to hordenine (Table 5.7). Firstly, the reductive amination was performed in batch and afterwards in continuous with a coil reactor. Despite different conditions tried, at least 50% MeCN had to be used.

Tyramine (mM)	Formaldehyde (eq.)	STAB (eq.)	MeCN (% v/v)	t (h)	M.c. (%)
5	69	12	50	1	94
5	30	7	50	1	88
15	30	7	50	1	96

Table 5.7: Optimization of the equivalents ratio in batch for hordenine production *via* reductive alkylation of tyramine with STAB.

5.2.9 Continuous flow reductive amination of tyramine in homogeneous mode

In flow the amount of formaldehyde and STAB were further reduced, and the reaction scale was increased to 40 mM tyramine (Table 5.9).

	Tyramine (mM)	Formaldehyde (Eq.)	STAB (Eq.)	MeCN (% v/v)	R _t (min)	M.c. (%)
Flow	15	25	7	50	25	>99
	15	12.5	5	50	25	95
	15	10	5	50	25	88
	15	12.5	5	75	4.62	>99
	20	12.5	5	75	4.62	>99
	30	12.5	3.3	75	4.62	>99
	40	12.5	2.5	75	4.62	82

Table 5.9: Experiments for the reductive amination of tyramine in continuous flow with STAB.

However, with the aim of coupling the two steps to establish a telescoped process, the working concentration of tyramine was again reduced to 5 mM, as this is the solubility limit of the first module.

With this condition, we identified 12.5 eq. formaldehyde and 12 eq. STAB as the optimal conditions, at room temperature, with 75 % v/v acetonitrile (Table 5.10).

	Tyramine (mM)	Formaldehyde (Eq.)	STAB (Eq.)	MeCN (% v/v)	t (min)	M.c. (%)
Batch	5	69	13	50	60	94
Flow	5	12.5	12	75	4.62	96

Table 5.10: Comparison of the experiments performed in batch and in flow at the real working concentration of 5 mM tyramine.

After the optimization tests, the PBR with the immobilised biocatalyst was coupled with two T-tubes, corresponding to the inlets for formaldehyde (62.5 mM formaldehyde, 2.5 % v/v acetic acid in acetonitrile) and for the reducing agent (60 mM STAB in acetonitrile). In line, a 10 mL flow coil reactor was connected and fed, at a flow rate of 2.16 mL/min, with the mixed solution, consisting into 25 % v/v Tyrosine solution, 25 % v/v formaldehyde solution and 50 % v/v reducing agent suspension (Scheme 5.1). This one

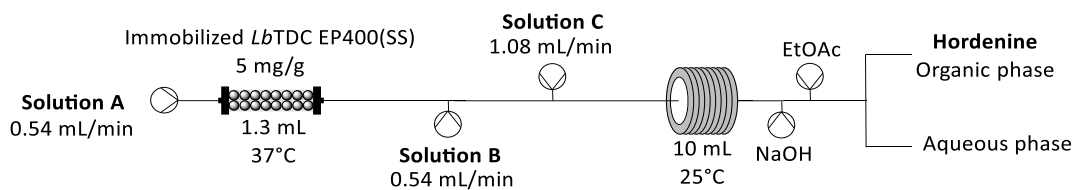
was kept under magnetic stirring of 1500 rpm in order to obtain a homogeneous suspension. We achieved almost full conversion (96 %) with the optimized reaction conditions and a R_T of 4.62 min. The temperature and pressure control of the flow chemistry coil have been investigated but the reported conversions values belong to the study case when the reaction has been performed at room temperature without any back pressure (Table 5.11).

Formaldehyde (Eq.)	STAB (Eq.)	MeCN (% v/v)	Pressure control	Temperature control	RT (min)	M.c. (%)
12.5	12	75	yes	yes	9.23	93
12.5	12	75	no	yes	9.23	83
12.5	12	75	yes	no	9.23	92
12.5	12	75	no	no	9.23	93
12.5	12	75	yes	yes	4.62	94
12.5	12	75	no	yes	4.62	87
12.5	12	75	yes	no	6.92	93
12.5	12	75	no	no	4.62	96

Table 5.11: Hordenine production starting from 5 mM tyramine (1eq), trialing different residence time under temperature (37°C) and pressure (8 bars) control.

A volume of 300 mL of final product solution was collected from the continuous flow process (Scheme 5.1) and hordenine was extracted in ethyl acetate after adjusting the pH to 9.6 (see experimental for details). Hordenine chloride was formed by the addition of an equimolar amount of HCl. The product was isolated with a yield of 90 % via precipitation and confirmed by NMR analysis.

As result of our biocatalyst productivity and of the conversion velocity, the system shows a space-time-yield (STY) of $2.68 \text{ g}_{\text{hordenine}} \cdot \text{L}^{-1} \cdot \text{h}^{-1}$, improving by 50% the best result reported to date. (Natte et al., 2017)



Scheme 5.1: Continuous flow chemoenzymatic system for the hordenine production with STAB in homogeneous mode. Solution A: 5 mM L-L-tyrosine disodium salt hydrate, 0.2 mM PLP in 200 mM sodium acetate buffer. Solution B: 62.5 mM formaldehyde, 2.5 % v/v AcOH in MeCN. Solution C: 60 mM sodium triacetoxyborohydride in MeCN. System conditions: 4.62 min residence time in the flow coil reactor volume.

5.2.10 Continuous flow reductive amination of tyramine in heterogeneous mode

Clearly, the requirement for MeCN adversely affected the sustainability of the process when using STAB as the reducing agent. Given these sustainability concerns, it was deemed necessary to seek an alternative, environmentally friendly reducing agent. Picoline borane (pic-BH₃) was initially not considered due to its significantly higher cost compared to STAB. Moreover, it was observed to efficiently reduce the imine intermediate formed from tyramine and formaldehyde only when employed in large excess in acetate buffer. Additionally, in aqueous conditions, pic-BH₃ was insoluble, making it not ideal for a homogeneous continuous flow process, where the reducing agent needed to be mixed with the in-line formed imine intermediate.

Despite these challenges, pic-BH₃ was ultimately selected for further testing as a green alternative (Table 5.11), with the understanding that a redesign of the flow process would be necessary.

Tyramine (mM)	Formaldehyde (eq.)	pic-BH ₃ (eq.)	pH	t (h)	M.c. (%)
5	30	24	4.5	1	45
5	60	24	4.5	24	99
5	60	48	4.5	1	78
5	30	24	9	1	96

Table 5.11: Optimization of the equivalents ratio in batch for hordenine production *via* reductive alkylation of tyramine with pic-BH₃.

It is noteworthy to mention that STAB was initially tested and effectively used at pH 4.5, taking inspiration from the literature, where sodium cyanoborohydride was used at acidic pH for the dimethylation of tyramine in sodium acetate buffer. (K. Guo et al., 2007)

However, during the course of my experiments, it became evident that picBH₃ displayed optimal performance under different pH conditions compared to STAB. As detailed in the tests shown in Table 8, pic-BH₃ required an alkaline environment (specifically, a pH of 9) to achieve efficient reductive alkylation of tyramine within a 1-hour timeframe.

These observations emphasize the critical role of the reaction's pH and its influence on the relative rates of the different mechanisms that can occur during reductive amination with an amine and an aldehyde.

Two different pH-dependent mechanisms of action can occur during a reductive amination reaction between an amine and an aldehyde (Figure 5.9).

Following a nucleophilic addition at acid pH, the aldehyde is the electrophile (abundant form), and the deprotonated amine is the nucleophile (limited form), attacking the carbonyl group to then form the imine intermediate. This mechanism is generally favoured when the amine is a tertiary amine, as tertiary amines are less nucleophilic and are more likely to react in presence of large amount of electrophile. This mechanism is favored at acidic pHs.

On the other hand, a nucleophilic addition at basic pH, the deprotonated amine is clearly still the nucleophile but it is now very abundant, rapidly adding to the aldehyde to generate the intermediate imine. This intermediate is then reduced to the final amine product by the reducing agent. This mechanism is generally favoured when the amine is a primary or secondary amine, as these types of amines have a more nucleophilic character. In general, the nucleophilic addition mechanism is favored at basic pH values.

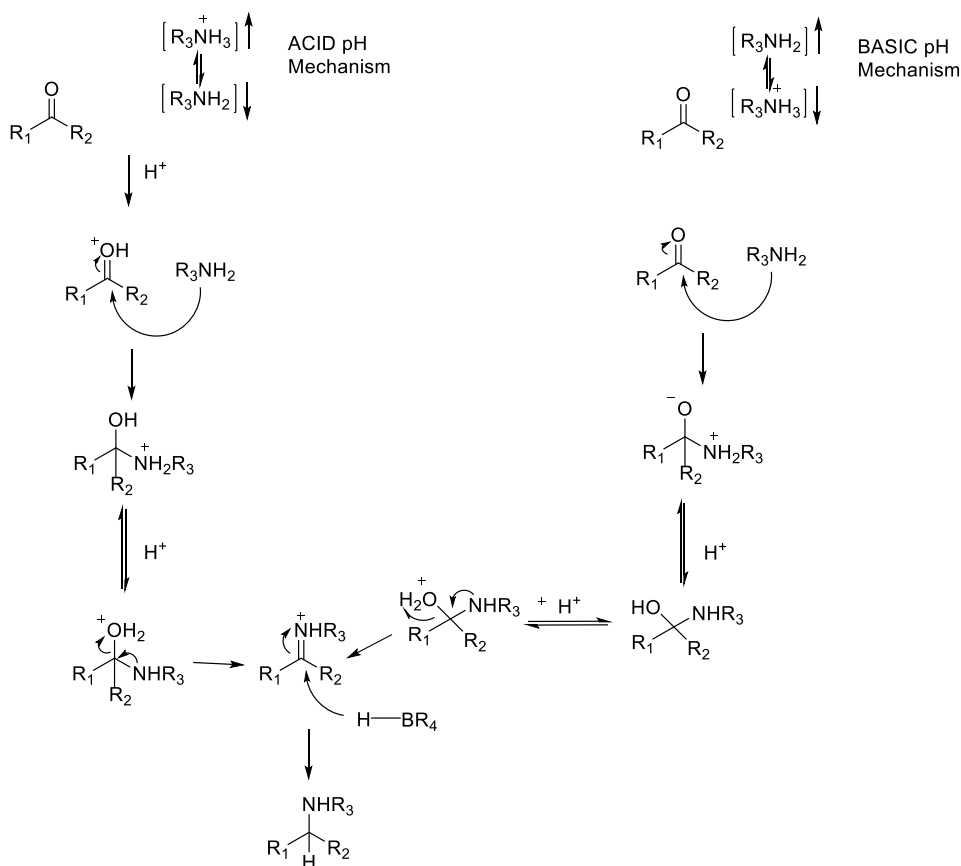
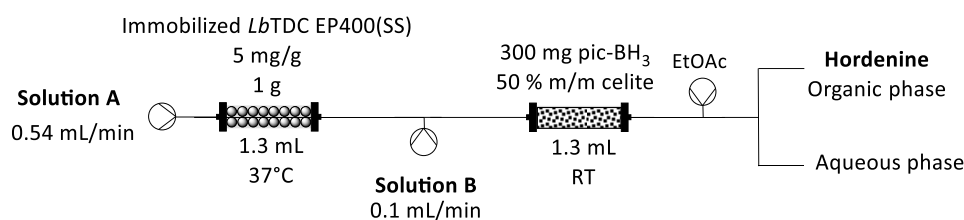


Figure 5.9: Reductive amination mechanisms at acid and basic pH.

Both mechanisms can occur, depending on the conditions of the reaction, and the relative rates of the two mechanisms can be influenced by a number of factors, such as the nature of the amine and aldehyde, the solvent, and the presence of catalysts or other reagents. Given the surprising pH-dependent differences in conversions, obtained with STAB and picBH₃, it appears plausible that the different behaviors could be indeed due to the different mechanism of action that leads to the generation of the imine intermediate and subsequent rate of reduction.

Ultimately, pic-BH₃, which is non-toxic and has been used in literature for reductive amination in water, (Cosenza et al., 2011; H. Orrego et al., 2018; Ruhaak et al., 2010; Sato et al., 2004) was proved indeed beneficial due to its solubility in various solvents and near-insolubility in water. In fact, this feature led to a strategic shift from a homogeneous to a heterogeneous flow process, making the experiment more sustainable and environmentally friendly. To utilize this characteristic, a packed bed reactor (PBR) was used in a continuous flow system with the reducing agent (300 mg) bulked up with an equivalent amount of celite (Scheme 5.2).



Scheme 5.2: Continuous flow chemoenzymatic system for the hordenine production with pic-BH₃ in heterogeneous mode. Solution A: 5 mM L-tyrosine disodium salt hydrate, 0.2 mM PLP in 200 mM sodium acetate buffer. Solution B: 202.5 mM formaldehyde, in 250 mM sodium carbonate (pH 11.5).

The previously reported batch experiments pointed out that pic-BH₃ was more efficient in reducing the imine intermediate at alkaline pH rather than acidic pH. With this assumption, a medium of 250 mM sodium carbonate (pH 11.5) was used for the formaldehyde feedstock solution, allowing for the reductive amination reaction to occur at pH 9.

With this alternative strategy 130 mL of a 5 mM feedstock solution were processed within 4 hours. The system achieved almost complete conversion using only 7.5 equivalents of formaldehyde and a residence time of 2.5 minutes. The space-time yield (STY) was determined to be 11.4 g_{hordenine}·L⁻¹·h⁻¹), representing a 4-fold improvement over the results obtained with STAB. The final product, hordenine hydrochloride, was isolated *via* liquid-liquid extraction followed by HCl titration, with an isolated yield of 77 %.

5.3 Conclusion

In this chapter an alternative method for the synthesis of the natural product hordenine was presented (Figure 5.10).

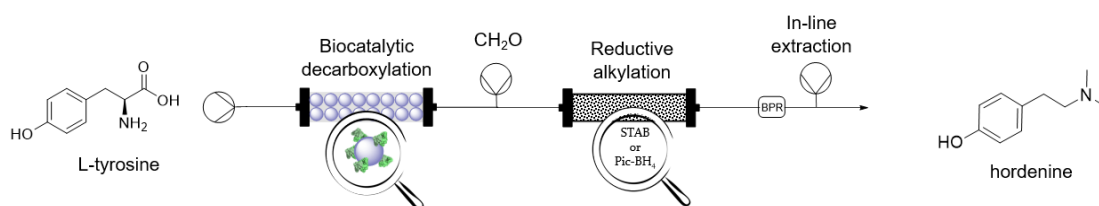


Figure 5.10: Continuous flow scheme for the conversion of L-tyrosine to hordenine. In the first reactor, the biocatalytic decarboxylation of L-tyrosine converts the amino acid into tyramine, then alkylated in the second reactor with formaldehyde by employing a reducing agent.

Through the innovative introduction of a continuous flow system that incorporates a two-step cascade process, L-tyrosine has been efficiently decarboxylated into tyramine using immobilized *LbTDC*. This is immediately followed by the in-line reductive alkylation of the

formed intermediate under mild conditions. Alternative reducing agents to replace sodium cyanoborohydride were explored; STAB and pic-BH₃ emerged as the top contenders, both offering impressive isolated yields of hordenine in remarkably short residence times, as little as 5 minutes.

What sets this method apart is the great efficiency of the biocatalytic step. It streamlines the process design by eliminating the unreacted substrate and the by-products of side reactions. In selecting the reagents, I paid special attention to their availability, environmental impact, and effectiveness. For instance, L-tyrosine is a natural amino acid that is also readily available. . Despite the loss of chirality via decarboxylation in the first step, the in situ synthesis of tyramine eliminates the safety hazards associated with handling this chemical.

While STAB is undeniably a viable and safe option, its reliance on acetonitrile detracts from the sustainability of the process. In contrast, pic-BH₃, albeit more expensive, proved to be an invaluable asset. Its seamless integration into the flow as a solid reagent in an in-line Packed Bed Reactor (PBR) was a game-changer.

In determining the environmental footprint of our system, I calculated an E-factor (a ratio representing the kilograms of waste generated per kilogram of the desired product) of 36 when using pic-BH₃ suspended in celite. This stacks up well against standard pharmaceutical processes in the same developmental stage, which generally have E-factors ranging from 25 to 100.

In essence, this process was carefully engineered to put sustainability and safety front and center. It serves as a persuasive illustration of the synergies that can be harnessed by integrating biocatalysis with chemical synthesis in continuous manufacturing. With the value of the starting material, L-tyrosine, skyrocketing by an astonishing 200-fold (from 1.72 €/g for L-tyrosine disodium salt hydrate to 382 €/g for hordenine), this approach shows how profitability and sustainability can go hand in hand in hordenine production.

5.4 Bibliography

- Abrahamson, M. J., Vázquez-Figueroa, E., Woodall, N. B., Moore, J. C., & Bommarius, A. S. (2012). Development of an Amine Dehydrogenase for Synthesis of Chiral Amines. *Angewandte Chemie International Edition*, *51*(16), 3969–3972. <https://doi.org/10.1002/anie.201107813>
- Abrahamson, M. J., Wong, J. W., & Bommarius, A. S. (2013). The Evolution of an Amine Dehydrogenase Biocatalyst for the Asymmetric Production of Chiral Amines. *Advanced Synthesis & Catalysis*, *355*(9), 1780–1786. <https://doi.org/10.1002/adsc.201201030>
- Alcántara, A. R., Domínguez de María, P., Littlechild, J. A., Schürmann, M., Sheldon, R. A., & Wohlgemuth, R. (2022). Biocatalysis as Key to Sustainable Industrial Chemistry. *ChemSusChem*, *15*(9). <https://doi.org/10.1002/cssc.202102709>
- Almrud, J. J., Oliveira, M. A., Kern, A. D., Grishin, N. V., Phillips, M. A., & Hackert, M. L. (2000). Crystal structure of human ornithine decarboxylase at 2.1 Å resolution: structural insights to antizyme binding. *Journal of Molecular Biology*, *295*(1), 7–16. <https://doi.org/10.1006/jmbi.1999.3331>
- Andréll, J., Hicks, M. G., Palmer, T., Carpenter, E. P., Iwata, S., & Maher, M. J. (2009). Crystal Structure of the Acid-Induced Arginine Decarboxylase from *Escherichia coli* : Reversible Decamer Assembly Controls Enzyme Activity. *Biochemistry*, *48*(18), 3915–3927. <https://doi.org/10.1021/bi900075d>
- Anwar, S., Mohammad, T., Shamsi, A., Queen, A., Parveen, S., Luqman, S., Hasan, G. M., Alamry, K. A., Azum, N., Asiri, A. M., & Hassan, M. I. (2020). Discovery of hordenine as a potential inhibitor of pyruvate dehydrogenase kinase 3: Implication in lung cancer therapy. *Biomedicines*, *8*(5), 32–228.
- Asano, Y., Nakazawa, A., & Endo, K. (1987). Novel phenylalanine dehydrogenases from *Sporosarcina ureae* and *Bacillus sphaericus*. Purification and characterization. *The Journal of Biological Chemistry*, *262*(21), 10346–10354. <http://www.ncbi.nlm.nih.gov/pubmed/3112142>
- Báez, J. L., Bolívar, F., & Gosset, G. (2001). Determination of 3-deoxy-D-*arabino*-heptulosonate 7-phosphate productivity and yield from glucose in *Escherichia coli* devoid of the glucose phosphotransferase transport system. *Biotechnology and Bioengineering*, *73*(6), 530–535. <https://doi.org/10.1002/bit.1088>
- Bai, Z., Sun, X., Yu, X., & Li, L. (2019). Chitosan Microbeads as Supporter for *Pseudomonas putida* with Surface Displayed Laccases for Decolorization of Synthetic Dyes. *Applied Sciences*, *9*(1), 138. <https://doi.org/10.3390/app9010138>
- Baker, P. J., Turnbull, A. P., Sedelnikova, S. E., Stillman, T. J., & Rice, D. W. (1995). A role for quaternary structure in the substrate specificity of leucine dehydrogenase. *Structure*, *3*(7), 693–705. [https://doi.org/10.1016/S0969-2126\(01\)00204-0](https://doi.org/10.1016/S0969-2126(01)00204-0)
- Barwell, C. J., Basma, A. N., Lafi, M. A. K., & Leake, L. D. (2011). Deamination of hordenine by monoamine oxidase and its action on vasa deferentia of the rat. *Journal of Pharmacy and Pharmacology*, *41*(6), 421–423. <https://doi.org/10.1111/j.2042-7158.1989.tb06492.x>

- Bell, E. L., Finnigan, W., France, S. P., Green, A. P., Hayes, M. A., Hepworth, L. J., Lovelock, S. L., Niikura, H., Osuna, S., Romero, E., Ryan, K. S., Turner, N. J., & Flitsch, S. L. (2021). Biocatalysis. *Nature Reviews Methods Primers*, 1(1), 46. <https://doi.org/10.1038/s43586-021-00044-z>
- Benítez-Mateos, A. I., Roura Padrosa, D., & Paradisi, F. (2022). Multistep enzyme cascades as a route towards green and sustainable pharmaceutical syntheses. *Nature Chemistry*, 14(5), 489–499. <https://doi.org/10.1038/s41557-022-00931-2>
- Bennett, M., Ducrot, L., Vergne-Vaxelaire, C., & Grogan, G. (2022). Structure and Mutation of the Native Amine Dehydrogenase MATOUAmDH2. *ChemBioChem*, 23(10). <https://doi.org/10.1002/cbic.202200136>
- Berridge, M. V., Herst, P. M., & Tan, A. S. (2005). *Tetrazolium dyes as tools in cell biology: New insights into their cellular reduction* (pp. 127–152). [https://doi.org/10.1016/S1387-2656\(05\)11004-7](https://doi.org/10.1016/S1387-2656(05)11004-7)
- Bertelli, M., Kiani, A. K., Paolacci, S., Manara, E., Kurti, D., Dhuli, K., Bushati, V., Miertus, J., Pangallo, D., Baglivo, M., Beccari, T., & Michelini, S. (2020). Hydroxytyrosol: A natural compound with promising pharmacological activities. *Journal of Biotechnology*, 309, 29–33. <https://doi.org/10.1016/j.jbiotec.2019.12.016>
- Bhatia, S. K., Kim, Y. H., Kim, H. J., Seo, H.-M., Kim, J.-H., Song, H.-S., Sathiyarayanan, G., Park, S.-H., Park, K., & Yang, Y.-H. (2015). Biotransformation of lysine into cadaverine using barium alginate-immobilized *Escherichia coli* overexpressing CadA. *Bioprocess and Biosystems Engineering*, 38(12), 2315–2322. <https://doi.org/10.1007/s00449-015-1465-9>
- Bloch, D. N., Sandre, M., Ben Zichri, S., Masato, A., Kolusheva, S., Bubacco, L., & Jelinek, R. (2023). Scavenging neurotoxic aldehydes using lysine carbon dots. *Nanoscale Advances*, 5(5), 1356–1367. <https://doi.org/10.1039/D2NA00804A>
- Böhmer, W., Knaus, T., & Mutti, F. G. (2018a). Hydrogen-Borrowing Alcohol Bioamination with Coimmobilized Dehydrogenases. *ChemCatChem*, 10(4), 731–735. <https://doi.org/10.1002/cctc.201701366>
- Böhmer, W., Knaus, T., & Mutti, F. G. (2018b). Hydrogen-Borrowing Alcohol Bioamination with Coimmobilized Dehydrogenases. *ChemCatChem*, 10(4), 731–735. <https://doi.org/10.1002/cctc.201701366>
- Cai, R.-F., Liu, L., Chen, F.-F., Li, A., Xu, J.-H., & Zheng, G.-W. (2020). Reductive Amination of Biobased Levulinic Acid to Unnatural Chiral γ -Amino Acid Using an Engineered Amine Dehydrogenase. *ACS Sustainable Chemistry & Engineering*, 8(46), 17054–17061. <https://doi.org/10.1021/acssuschemeng.0c04647>
- Caparco, A. A., Bommarius, B. R., Bommarius, A. S., & Champion, J. A. (2020). Protein-inorganic calcium-phosphate supraparticles as a robust platform for enzyme co-immobilization. *Biotechnology and Bioengineering*, 117(7), 1979–1989. <https://doi.org/10.1002/bit.27348>
- Caparco, A. A., Pelletier, E., Petit, J. L., Jouenne, A., Bommarius, B. R., Berardinis, V., Zaparucha, A., Champion, J. A., Bommarius, A. S., & Vergne-Vaxelaire, C. (2020). Metagenomic Mining for Amine Dehydrogenase Discovery. *Advanced Synthesis & Catalysis*, 362(12), 2427–2436. <https://doi.org/10.1002/adsc.202000094>

- Capitani, G. (2003). Crystal structure and functional analysis of Escherichia coli glutamate decarboxylase. *The EMBO Journal*, *22*(16), 4027–4037. <https://doi.org/10.1093/emboj/cdg403>
- Cerioli, L., Planchestainer, M., Cassidy, J., Tessaro, D., & Paradisi, F. (2015). Characterization of a novel amine transaminase from Halomonas elongata. *Journal of Molecular Catalysis B: Enzymatic*, *120*, 141–150. <https://doi.org/10.1016/j.molcatb.2015.07.009>
- Chen, W., Yao, J., Meng, J., Han, W., Tao, Y., Chen, Y., Guo, Y., Shi, G., He, Y., Jin, J.-M., & Tang, S.-Y. (2019). Promiscuous enzymatic activity-aided multiple-pathway network design for metabolic flux rearrangement in hydroxytyrosol biosynthesis. *Nature Communications*, *10*(1), 960. <https://doi.org/10.1038/s41467-019-08781-2>
- Claes, L., Janssen, M., & De Vos, D. E. (2019). Organocatalytic Decarboxylation of Amino Acids as a Route to Bio-based Amines and Amides. *ChemCatChem*, *11*(17), 4297–4306. <https://doi.org/10.1002/cctc.201900800>
- Contente, M. L., & Paradisi, F. (2018). Self-sustaining closed-loop multienzyme-mediated conversion of amines into alcohols in continuous reactions. *Nature Catalysis*, *1*(6), 452–459. <https://doi.org/10.1038/s41929-018-0082-9>
- Cosenza, V. A., Navarro, D. A., & Stortz, C. A. (2011). Usage of α -picoline borane for the reductive amination of carbohydrates. *Arkivoc*, *2011*(7), 182–194. <https://doi.org/10.3998/ark.5550190.0012.716>
- Coyle, J. P., Johnson, C., Jensen, J., Farcas, M., Derk, R., Stueckle, T. A., Kornberg, T. G., Rojanasakul, Y., & Rojanasakul, L. W. (2023). Variation in pentose phosphate pathway-associated metabolism dictates cytotoxicity outcomes determined by tetrazolium reduction assays. *Scientific Reports*, *13*(1), 8220. <https://doi.org/10.1038/s41598-023-35310-5>
- DiCosimo, R., McAuliffe, J., Poulouse, A. J., & Bohlmann, G. (2013). Industrial use of immobilized enzymes. *Chemical Society Reviews*, *42*(15), 6437. <https://doi.org/10.1039/c3cs35506c>
- Ducrot, L., Bennett, M., André-Leroux, G., Elisée, E., Marynberg, S., Fossey-Jouenne, A., Zaparucha, A., Grogan, G., & Vergne-Vaxelaire, C. (2022). Expanding the Substrate Scope of Native Amine Dehydrogenases through *In Silico* Structural Exploration and Targeted Protein Engineering. *ChemCatChem*, *14*(22). <https://doi.org/10.1002/cctc.202200880>
- Ducrot, L., Bennett, M., Caparco, A. A., Champion, J. A., Bommarius, A. S., Zaparucha, A., Grogan, G., & Vergne-Vaxelaire, C. (2021). Biocatalytic Reductive Amination by Native Amine Dehydrogenases to Access Short Chiral Alkyl Amines and Amino Alcohols. *Frontiers in Catalysis*, *1*. <https://doi.org/10.3389/fctls.2021.781284>
- Eliot, A. C., & Kirsch, J. F. (2004). Pyridoxal Phosphate Enzymes: Mechanistic, Structural, and Evolutionary Considerations. *Annual Review of Biochemistry*, *73*(1), 383–415. <https://doi.org/10.1146/annurev.biochem.73.011303.074021>
- Eller, K., Henkes, E., Rossbacher, R., & Höke, H. (2000). Amines, Aliphatic. In *Ullmann's Encyclopedia of Industrial Chemistry*. Wiley-VCH Verlag GmbH & Co. KGaA. https://doi.org/10.1002/14356007.a02_001

- Escalante, A., Calderón, R., Valdivia, A., de Anda, R., Hernández, G., Ramírez, O. T., Gosset, G., & Bolívar, F. (2010). Metabolic engineering for the production of shikimic acid in an evolved *Escherichia coli* strain lacking the phosphoenolpyruvate: carbohydrate phosphotransferase system. *Microbial Cell Factories*, *9*(1), 21. <https://doi.org/10.1186/1475-2859-9-21>
- Foor, F., Morin, N., & Bostian, K. A. (1993). Production of L-dihydroxyphenylalanine in *Escherichia coli* with the tyrosine phenol-lyase gene cloned from *Erwinia herbicola*. *Applied and Environmental Microbiology*, *59*(9), 3070–3075. <https://doi.org/10.1128/aem.59.9.3070-3075.1993>
- Fordjour, E., Adipah, F. K., Zhou, S., Du, G., & Zhou, J. (2019). Metabolic engineering of *Escherichia coli* BL21 (DE3) for de novo production of l-DOPA from d-glucose. *Microbial Cell Factories*, *18*(1). <https://doi.org/10.1186/s12934-019-1122-0>
- Franklin, R. D., Whitley, J. A., Caparco, A. A., Bommarius, B. R., Champion, J. A., & Bommarius, A. S. (2021). Continuous production of a chiral amine in a packed bed reactor with co-immobilized amine dehydrogenase and formate dehydrogenase. *Chemical Engineering Journal*, *407*, 127065. <https://doi.org/10.1016/j.cej.2020.127065>
- Froidevaux, V., Negrell, C., Caillol, S., Pascault, J.-P., & Boutevin, B. (2016). Biobased Amines: From Synthesis to Polymers; Present and Future. *Chemical Reviews*, *116*(22), 14181–14224. <https://doi.org/10.1021/acs.chemrev.6b00486>
- Garg, R. P., Ma, Y., Hoyt, J. C., & Parry, R. J. (2002a). Molecular characterization and analysis of the biosynthetic gene cluster for the azoxy antibiotic valanimycin. *Molecular Microbiology*, *46*(2), 505–517. <https://doi.org/10.1046/j.1365-2958.2002.03169.x>
- Garg, R. P., Ma, Y., Hoyt, J. C., & Parry, R. J. (2002b). Molecular characterization and analysis of the biosynthetic gene cluster for the azoxy antibiotic valanimycin. *Molecular Microbiology*, *46*(2), 505–517. <https://doi.org/10.1046/j.1365-2958.2002.03169.x>
- Ghislieri, D., & Turner, N. J. (2014). Biocatalytic Approaches to the Synthesis of Enantiomerically Pure Chiral Amines. *Topics in Catalysis*, *57*(5), 284–300. <https://doi.org/10.1007/s11244-013-0184-1>
- Gianolio, S., Roura Padrosa, D., & Paradisi, F. (2022). Combined chemoenzymatic strategy for sustainable continuous synthesis of the natural product hordenine. *Green Chemistry*, *24*(21), 8434–8440. <https://doi.org/10.1039/D2GC02767D>
- Giardina, G., Montioli, R., Gianni, S., Cellini, B., Paiardini, A., Voltattorni, C. B., & Cutruzzolà, F. (2011). Open conformation of human DOPA decarboxylase reveals the mechanism of PLP addition to Group II decarboxylases. *Proceedings of the National Academy of Sciences*, *108*(51), 20514–20519. <https://doi.org/10.1073/pnas.1111456108>
- Gong, X., Tao, J., Wang, Y., Wu, J., An, J., Meng, J., Wang, X., Chen, Y., & Zou, J. (2021). Total barley maiya alkaloids inhibit prolactin secretion by acting on dopamine D2 receptor and protein kinase A targets. *Journal of Ethnopharmacology*, *273*, 113994. <https://doi.org/10.1016/j.jep.2021.113994>
- Gosset, G., Yong-Xiao, J., & Berry, A. (1996). A direct comparison of approaches for increasing carbon flow to aromatic biosynthesis in *Escherichia coli*. *Journal of Industrial Microbiology*, *17*(1), 47–52. <https://doi.org/10.1007/BF01570148>

- Guisán, JoséM. (1988). Aldehyde-agarose gels as activated supports for immobilization-stabilization of enzymes. *Enzyme and Microbial Technology*, 10(6), 375–382. [https://doi.org/10.1016/0141-0229\(88\)90018-X](https://doi.org/10.1016/0141-0229(88)90018-X)
- Guo, K., Ji, C., & Li, L. (2007). Stable-Isotope Dimethylation Labeling Combined with LC–ESI MS for Quantification of Amine-Containing Metabolites in Biological Samples. *Analytical Chemistry*, 79(22), 8631–8638. <https://doi.org/10.1021/ac0704356>
- Guo, Z., Yan, N., & Lapkin, A. A. (2019). Towards circular economy: integration of bio-waste into chemical supply chain. *Current Opinion in Chemical Engineering*, 26, 148–156. <https://doi.org/10.1016/j.coche.2019.09.010>
- Gupte, A. P., Basaglia, M., Casella, S., & Favaro, L. (2022). Rice waste streams as a promising source of biofuels: feedstocks, biotechnologies and future perspectives. *Renewable and Sustainable Energy Reviews*, 167, 112673. <https://doi.org/10.1016/j.rser.2022.112673>
- Gut, H., Pennacchietti, E., John, R. A., Bossa, F., Capitani, G., De Biase, D., & Grütter, M. G. (2006). Escherichia coli acid resistance: pH-sensing, activation by chloride and autoinhibition in GadB. *The EMBO Journal*, 25(11), 2643–2651. <https://doi.org/10.1038/sj.emboj.7601107>
- H. Orrego, A., Romero-Fernández, M., Millán-Linares, M., Yust, M., Guisán, J., & Rocha-Martin, J. (2018). Stabilization of Enzymes by Multipoint Covalent Attachment on Aldehyde-Supports: 2-Picoline Borane as an Alternative Reducing Agent. *Catalysts*, 8(8), 333. <https://doi.org/10.3390/catal8080333>
- Hamid, M. H. S. A., Slatford, P. A., & Williams, J. M. J. (2007). Borrowing Hydrogen in the Activation of Alcohols. *Advanced Synthesis & Catalysis*, 349(10), 1555–1575. <https://doi.org/10.1002/adsc.200600638>
- Hapke, H. J., & Strathmann, W. (1995). [Pharmacological effects of hordenine]. *DTW. Deutsche Tierärztliche Wochenschrift*, 102(6), 228–232. <http://www.ncbi.nlm.nih.gov/pubmed/8582256>
- Harper, B. A., Barbut, S., Lim, L.-T., & Marcone, M. F. (2014). Effect of Various Gelling Cations on the Physical Properties of “Wet” Alginate Films. *Journal of Food Science*, 79(4), E562–E567. <https://doi.org/10.1111/1750-3841.12376>
- Heckmann, C. M., Gourlay, L. J., Dominguez, B., & Paradisi, F. (2020). An (R)-Selective Transaminase From *Thermomyces stellatus*: Stabilizing the Tetrameric Form. *Frontiers in Bioengineering and Biotechnology*, 8. <https://doi.org/10.3389/fbioe.2020.00707>
- Heffter, A. (1898). Ueber Pellote. *Archiv Für Experimentelle Pathologie Und Pharmakologie*, 40(5–6), 385–429. <https://doi.org/10.1007/BF01825267>
- Heydari, M., Ohshima, T., Nunoura-Kominato, N., & Sakuraba, H. (2004). Highly Stable Lysine 6-Dehydrogenase from the Thermophile *Geobacillus stearothermophilus* Isolated from a Japanese Hot Spring: Characterization, Gene Cloning and Sequencing, and Expression. *Applied and Environmental Microbiology*, 70(2), 937–942. <https://doi.org/10.1128/AEM.70.2.937-942.2004>
- Holbrook, O. T., Molligoda, B., Bushell, K. N., & Gobrogge, K. L. (2022). Behavioral consequences of the downstream products of ethanol metabolism involved in alcohol use disorder.

- Neuroscience & Biobehavioral Reviews*, 133, 104501.
<https://doi.org/10.1016/j.neubiorev.2021.12.024>
- Houwman, J. A., Knaus, T., Costa, M., & Mutti, F. G. (2019). Efficient synthesis of enantiopure amines from alcohols using resting *E. coli* cells and ammonia. *Green Chemistry*, 21(14), 3846–3857. <https://doi.org/10.1039/C9GC01059A>
- Huang, J., Mei, L., Wu, H., & Lin, D. (2007). Biosynthesis of γ -aminobutyric acid (GABA) using immobilized whole cells of *Lactobacillus brevis*. *World Journal of Microbiology and Biotechnology*, 23(6), 865–871. <https://doi.org/10.1007/s11274-006-9311-5>
- Huang, R., Chen, H., Zhong, C., Kim, J. E., & Zhang, Y.-H. P. (2016). High-Throughput Screening of Coenzyme Preference Change of Thermophilic 6-Phosphogluconate Dehydrogenase from NADP⁺ to NAD⁺. *Scientific Reports*, 6(1), 32644. <https://doi.org/10.1038/srep32644>
- Hwang, E. T., & Lee, S. (2019). Multienzymatic Cascade Reactions via Enzyme Complex by Immobilization. *ACS Catalysis*, 9(5), 4402–4425. <https://doi.org/10.1021/acscatal.8b04921>
- Jackson, D. M., Ashley, R. L., Brownfield, C. B., Morrison, D. R., & Morrison, R. W. (2015). Rapid Conventional and Microwave-Assisted Decarboxylation of L-Histidine and Other Amino Acids via Organocatalysis with R-Carvone Under Superheated Conditions. *Synthetic Communications*, 45(23), 2691–2700. <https://doi.org/10.1080/00397911.2015.1100745>
- Jansonius, J. N. (1998). Structure, evolution and action of vitamin B6-dependent enzymes. *Current Opinion in Structural Biology*, 8(6), 759–769. [https://doi.org/10.1016/S0959-440X\(98\)80096-1](https://doi.org/10.1016/S0959-440X(98)80096-1)
- Jeon, H., Yoon, S., Ahsan, M., Sung, S., Kim, G.-H., Sundaramoorthy, U., Rhee, S.-K., & Yun, H. (2017). The Kinetic Resolution of Racemic Amines Using a Whole-Cell Biocatalyst Co-Expressing Amine Dehydrogenase and NADH Oxidase. *Catalysts*, 7(9), 251. <https://doi.org/10.3390/catal7090251>
- Jiang, M., Xu, G., Ni, J., Zhang, K., Dong, J., Han, R., & Ni, Y. (2019a). Improving Soluble Expression of Tyrosine Decarboxylase from *Lactobacillus brevis* for Tyramine Synthesis with High Total Turnover Number. *Applied Biochemistry and Biotechnology*, 188(2), 436–449. <https://doi.org/10.1007/s12010-018-2925-x>
- Jiang, M., Xu, G., Ni, J., Zhang, K., Dong, J., Han, R., & Ni, Y. (2019b). Improving Soluble Expression of Tyrosine Decarboxylase from *Lactobacillus brevis* for Tyramine Synthesis with High Total Turnover Number. *Applied Biochemistry and Biotechnology*, 188(2), 436–449. <https://doi.org/10.1007/s12010-018-2925-x>
- Jones, J. A., Collins, S. M., Vernacchio, V. R., Lachance, D. M., & Koffas, M. A. G. (2016). Optimization of naringenin and *p*-coumaric acid hydroxylation using the native *E. coli* hydroxylase complex, HpaBC. *Biotechnology Progress*, 32(1), 21–25. <https://doi.org/10.1002/btpr.2185>
- Khorsand, F., Murphy, C. D., Whitehead, A. J., & Engel, P. C. (2017). Biocatalytic stereoinversion of *p*-para-bromophenylalanine in a one-pot three-enzyme reaction. *Green Chemistry*, 19(2), 503–510. <https://doi.org/10.1039/C6GC01922F>
- Kim, Baritugo, Oh, Kang, Jung, Jang, Song, Kim, Lee, Hwang, Park, Park, & Joo. (2019). High-Level Conversion of l-lysine into Cadaverine by *Escherichia coli* Whole Cell Biocatalyst Expressing

- Hafnia alvei l-lysine Decarboxylase. *Polymers*, 11(7), 1184.
<https://doi.org/10.3390/polym11071184>
- Kim, D. I., Chae, T. U., Kim, H. U., Jang, W. D., & Lee, S. Y. (2021). Microbial production of multiple short-chain primary amines via retrobiosynthesis. *Nature Communications*, 12(1), 173. <https://doi.org/10.1038/s41467-020-20423-6>
- Kim, S.-C., Lee, J.-H., Kim, M.-H., Lee, J.-A., Kim, Y. B., Jung, E., Kim, Y.-S., Lee, J., & Park, D. (2013). Hordenine, a single compound produced during barley germination, inhibits melanogenesis in human melanocytes. *Food Chemistry*, 141(1), 174–181.
<https://doi.org/10.1016/j.foodchem.2013.03.017>
- Knaus, T., Böhmer, W., & Mutti, F. G. (2017). Amine dehydrogenases: efficient biocatalysts for the reductive amination of carbonyl compounds. *Green Chemistry*, 19(2), 453–463.
<https://doi.org/10.1039/C6GC01987K>
- Knowles, W. S. (n.d.). Asymmetric Hydrogenations– The MonsantoL-Dopa Process. In *Asymmetric Catalysis on Industrial Scale* (pp. 21–38). Wiley-VCH Verlag GmbH & Co. KGaA.
<https://doi.org/10.1002/3527602151.ch1>
- Komori, H., Nitta, Y., Ueno, H., & Higuchi, Y. (2012). Structural Study Reveals That Ser-354 Determines Substrate Specificity on Human Histidine Decarboxylase. *Journal of Biological Chemistry*, 287(34), 29175–29183. <https://doi.org/10.1074/jbc.M112.381897>
- Kugler, P. (1979). A gel-sandwich technique for the qualitative and quantitative determination of dehydrogenases in the enzyme histochemistry. *Histochemistry*, 60(3), 265–293.
<https://doi.org/10.1007/BF00500656>
- Kumar, R., Vikramachakravarthi, D., & Pal, P. (2014). Production and purification of glutamic acid: A critical review towards process intensification. *Chemical Engineering and Processing: Process Intensification*, 81, 59–71. <https://doi.org/10.1016/j.cep.2014.04.012>
- Kurpejović, E., Wendisch, V. F., & Sariyar Akbulut, B. (2021). Tyrosinase-based production of l-DOPA by *Corynebacterium glutamicum*. *Applied Microbiology and Biotechnology*, 105(24), 9103–9111. <https://doi.org/10.1007/s00253-021-11681-5>
- Lapponi, M. J., Méndez, M. B., Trelles, J. A., & Rivero, C. W. (2022). Cell immobilization strategies for biotransformations. *Current Opinion in Green and Sustainable Chemistry*, 33, 100565. <https://doi.org/10.1016/j.cogsc.2021.100565>
- Lawrence, S. A. (2004). *Amines: synthesis, properties and applications*. Cambridge University Press.
- Lee, J., Michael, A. J., Martynowski, D., Goldsmith, E. J., & Phillips, M. A. (2007). Phylogenetic Diversity and the Structural Basis of Substrate Specificity in the β/α -Barrel Fold Basic Amino Acid Decarboxylases. *Journal of Biological Chemistry*, 282(37), 27115–27125.
<https://doi.org/10.1074/jbc.M704066200>
- Lee, S. Y., Kim, H. U., Chae, T. U., Cho, J. S., Kim, J. W., Shin, J. H., Kim, D. I., Ko, Y.-S., Jang, W. D., & Jang, Y.-S. (2019). A comprehensive metabolic map for production of bio-based chemicals. *Nature Catalysis*, 2(1), 18–33. <https://doi.org/10.1038/s41929-018-0212-4>

- Leuchtenberger, W., Huthmacher, K., & Drauz, K. (2005). Biotechnological production of amino acids and derivatives: current status and prospects. *Applied Microbiology and Biotechnology*, *69*(1), 1–8. <https://doi.org/10.1007/s00253-005-0155-y>
- Li, N., Chou, H., & Xu, Y. (2016). Improved cadaverine production from mutant *Klebsiella oxytoca* lysine decarboxylase. *Engineering in Life Sciences*, *16*(3), 299–305. <https://doi.org/10.1002/elsc.201500037>
- Liu, G., Zhou, N., Zhang, M., Li, S., Tian, Q., Chen, J., Chen, B., Wu, Y., & Yao, S. (2010). Hydrophobic solvent induced phase transition extraction to extract drugs from plasma for high performance liquid chromatography–mass spectrometric analysis. *Journal of Chromatography A*, *1217*(3), 243–249. <https://doi.org/10.1016/j.chroma.2009.11.037>
- Liu, J., Pang, B. Q. W., Adams, J. P., Snajdrova, R., & Li, Z. (2017). Coupled Immobilized Amine Dehydrogenase and Glucose Dehydrogenase for Asymmetric Synthesis of Amines by Reductive Amination with Cofactor Recycling. *ChemCatChem*, *9*(3), 425–431. <https://doi.org/10.1002/cctc.201601446>
- Liu, Y., Liu, P., Gao, S., Wang, Z., Luan, P., González-Sabín, J., & Jiang, Y. (2021). Construction of chemoenzymatic cascade reactions for bridging chemocatalysis and Biocatalysis: Principles, strategies and prospective. *Chemical Engineering Journal*, *420*, 127659. <https://doi.org/10.1016/j.cej.2020.127659>
- Ma, J., Wang, S., Huang, X., Geng, P., Wen, C., Zhou, Y., Yu, L., & Wang, X. (2015). Validated UPLC–MS/MS method for determination of hordenine in rat plasma and its application to pharmacokinetic study. *Journal of Pharmaceutical and Biomedical Analysis*, *111*, 131–137. <https://doi.org/10.1016/j.jpba.2015.03.032>
- Mateo, C., Grazú, V., Pessela, B. C. C., Montes, T., Palomo, J. M., Torres, R., López-Gallego, F., Fernández-Lafuente, R., & Guisán, J. M. (2007a). Advances in the design of new epoxy supports for enzyme immobilization–stabilization. *Biochemical Society Transactions*, *35*(6), 1593–1601. <https://doi.org/10.1042/BST0351593>
- Mateo, C., Grazú, V., Pessela, B. C. C., Montes, T., Palomo, J. M., Torres, R., López-Gallego, F., Fernández-Lafuente, R., & Guisán, J. M. (2007b). Advances in the design of new epoxy supports for enzyme immobilization–stabilization. *Biochemical Society Transactions*, *35*(6), 1593–1601. <https://doi.org/10.1042/BST0351593>
- Mayol, O., Bastard, K., Beloti, L., Frese, A., Turkenburg, J. P., Petit, J.-L., Mariage, A., Debard, A., Pellouin, V., Perret, A., de Berardinis, V., Zapparucha, A., Grogan, G., & Vergne-Vaxelaire, C. (2019a). A family of native amine dehydrogenases for the asymmetric reductive amination of ketones. *Nature Catalysis*, *2*(4), 324–333. <https://doi.org/10.1038/s41929-019-0249-z>
- Mayol, O., Bastard, K., Beloti, L., Frese, A., Turkenburg, J. P., Petit, J.-L., Mariage, A., Debard, A., Pellouin, V., Perret, A., de Berardinis, V., Zapparucha, A., Grogan, G., & Vergne-Vaxelaire, C. (2019b). A family of native amine dehydrogenases for the asymmetric reductive amination of ketones. *Nature Catalysis*, *2*(4), 324–333. <https://doi.org/10.1038/s41929-019-0249-z>
- Meyer, E. (1982). Separation of two distinct S-adenosylmethionine dependent N-methyltransferases involved in hordenine biosynthesis in *Hordeum vulgare*. *Plant Cell Reports*, *1*(6), 236–239. <https://doi.org/10.1007/BF00272627>

- Mi, J., Liu, S., Du, Y., Qi, H., & Zhang, L. (2022). Cofactor self-sufficient by co-immobilization of pyridoxal 5'-phosphate and lysine decarboxylase for cadaverine production. *Bioresource Technology Reports*, *17*, 100939. <https://doi.org/10.1016/j.biteb.2021.100939>
- Montgomery, S. L., Mangas-Sanchez, J., Thompson, M. P., Aleku, G. A., Dominguez, B., & Turner, N. J. (2017). Direct Alkylation of Amines with Primary and Secondary Alcohols through Biocatalytic Hydrogen Borrowing. *Angewandte Chemie*, *129*(35), 10627–10630. <https://doi.org/10.1002/ange.201705848>
- Mørch, Y. A., Donati, I., Strand, B. L., & Skjåk-Bræk, G. (2006). Effect of Ca²⁺, Ba²⁺, and Sr²⁺ on Alginate Microbeads. *Biomacromolecules*, *7*(5), 1471–1480. <https://doi.org/10.1021/bm060010d>
- Muñoz, A. J., Hernández-Chávez, G., De Anda, R., Martínez, A., Bolívar, F., & Gosset, G. (2011). Metabolic engineering of *Escherichia coli* for improving l-3,4-dihydroxyphenylalanine (l-DOPA) synthesis from glucose. *Journal of Industrial Microbiology and Biotechnology*, *38*(11), 1845–1852. <https://doi.org/10.1007/s10295-011-0973-0>
- Mutti, F. G., & Knaus, T. (2021). Enzymes Applied to the Synthesis of Amines. In *Biocatalysis for Practitioners* (pp. 143–180). Wiley. <https://doi.org/10.1002/9783527824465.ch6>
- Mutti, F. G., Knaus, T., Scrutton, N. S., Breuer, M., & Turner, N. J. (2015). Conversion of alcohols to enantiopure amines through dual-enzyme hydrogen-borrowing cascades. *Science*, *349*(6255), 1525–1529. <https://doi.org/10.1126/science.aac9283>
- Nakai, T., Nakagawa, N., Maoka, N., Masui, R., Kuramitsu, S., & Kamiya, N. (2005). Structure of P-protein of the glycine cleavage system: implications for nonketotic hyperglycinemia. *The EMBO Journal*, *24*(8), 1523–1536. <https://doi.org/10.1038/sj.emboj.7600632>
- Narisetty, V., Cox, R., Bommareddy, R., Agrawal, D., Ahmad, E., Pant, K. K., Chandel, A. K., Bhatia, S. K., Kumar, D., Binod, P., Gupta, V. K., & Kumar, V. (2022). Valorisation of xylose to renewable fuels and chemicals, an essential step in augmenting the commercial viability of lignocellulosic biorefineries. *Sustainable Energy & Fuels*, *6*(1), 29–65. <https://doi.org/10.1039/D1SE00927C>
- Nasri, M. (2017a). *Protein Hydrolysates and Biopeptides* (pp. 109–159). <https://doi.org/10.1016/bs.afnr.2016.10.003>
- Nasri, M. (2017b). *Protein Hydrolysates and Biopeptides* (pp. 109–159). <https://doi.org/10.1016/bs.afnr.2016.10.003>
- Natte, K., Neumann, H., Jagadeesh, R. v., & Beller, M. (2017). Convenient iron-catalyzed reductive aminations without hydrogen for selective synthesis of N-methylamines. *Nature Communications*, *8*(1), 1344. <https://doi.org/10.1038/s41467-017-01428-0>
- Nguyen, N. H., Truong-Thi, N.-H., Nguyen, D. T. D., Ching, Y. C., Huynh, N. T., & Nguyen, D. H. (2022). Non-ionic surfactants As co-templates to control the mesopore diameter of hollow mesoporous silica nanoparticles for drug delivery applications. *Colloids and Surfaces A: Physicochemical and Engineering Aspects*, *655*, 130218. <https://doi.org/10.1016/j.colsurfa.2022.130218>
- Ohta, H., Murakami, Y., Takebe, Y., Murasaki, K., Oshima, K., Yoshihara, H., & Morimura, S. (2020). &N-Methyltyramine, a Gastrin-releasing Factor in Beer, and

Structurally Related Compounds as Agonists for Human Trace Amine-associated Receptor 1. *Food Science and Technology Research*, 26(2), 313–317.
<https://doi.org/10.3136/fstr.26.313>

- PARADISI, F., COLLINS, S., MAGUIRE, A., & ENGEL, P. (2007). Phenylalanine dehydrogenase mutants: Efficient biocatalysts for synthesis of non-natural phenylalanine derivatives. *Journal of Biotechnology*, 128(2), 408–411. <https://doi.org/10.1016/j.jbiotec.2006.08.008>
- Park, J.-Y., Choi, M.-J., Yu, H., Choi, Y., Park, K.-M., & Chang, P.-S. (2022). Multi-functional behavior of food emulsifier erythorbyl laurate in different colloidal conditions of homogeneous oil-in-water emulsion system. *Colloids and Surfaces A: Physicochemical and Engineering Aspects*, 636, 128127. <https://doi.org/10.1016/j.colsurfa.2021.128127>
- Park, S. H., Soetyono, F., & Kim, H. K. (2017). Cadaverine Production by Using Cross-Linked Enzyme Aggregate of Escherichia coli Lysine Decarboxylase. *Journal of Microbiology and Biotechnology*, 27(2), 289–296. <https://doi.org/10.4014/jmb.1608.08033>
- Patil, M. D., Grogan, G., Bommarius, A., & Yun, H. (2018). Oxidoreductase-Catalyzed Synthesis of Chiral Amines. *ACS Catalysis*, 8(12), 10985–11015.
<https://doi.org/10.1021/acscatal.8b02924>
- Patil, M. D., Yoon, S., Jeon, H., Khobragade, T. P., Sarak, S., Pagar, A. D., Won, Y., & Yun, H. (2019). Kinetic Resolution of Racemic Amines to Enantiopure (S)-amines by a Biocatalytic Cascade Employing Amine Dehydrogenase and Alanine Dehydrogenase. *Catalysts*, 9(7), 600. <https://doi.org/10.3390/catal9070600>
- Payne, J. T., Valentic, T. R., & Smolke, C. D. (2021). Complete biosynthesis of the bisbenzylisoquinoline alkaloids guattegaumerine and berbaminine in yeast. *Proceedings of the National Academy of Sciences*, 118(51). <https://doi.org/10.1073/pnas.2112520118>
- Pelckmans, M., Renders, T., Van de Vyver, S., & Sels, B. F. (2017). Bio-based amines through sustainable heterogeneous catalysis. *Green Chemistry*, 19(22), 5303–5331.
<https://doi.org/10.1039/C7GC02299A>
- Pilkington, R. L., Dallaston, M. A., Savage, G. P., Williams, C. M., & Polyzos, A. (2021). Enone-promoted decarboxylation of *trans*-4-hydroxy-*l*-proline in flow: a side-by-side comparison to batch. *Reaction Chemistry & Engineering*, 6(3), 486–493.
<https://doi.org/10.1039/D0RE00442A>
- Planchestainer, M., Hegarty, E., Heckmann, C. M., Gourlay, L. J., & Paradisi, F. (2019). Widely applicable background depletion step enables transaminase evolution through solid-phase screening. *Chemical Science*, 10(23), 5952–5958. <https://doi.org/10.1039/C8SC05712E>
- Prieto, M. A., & Garcia, J. L. (1994). Molecular characterization of 4-hydroxyphenylacetate 3-hydroxylase of Escherichia coli. A two-protein component enzyme. *Journal of Biological Chemistry*, 269(36), 22823–22829. [https://doi.org/10.1016/S0021-9258\(17\)31719-2](https://doi.org/10.1016/S0021-9258(17)31719-2)
- Pyne, M. E., Kevvai, K., Grewal, P. S., Narcross, L., Choi, B., Bourgeois, L., Dueber, J. E., & Martin, V. J. J. (2020). A yeast platform for high-level synthesis of tetrahydroisoquinoline alkaloids. *Nature Communications*, 11(1), 3337. <https://doi.org/10.1038/s41467-020-17172-x>

- Quaglia, D., Irwin, J. A., & Paradisi, F. (2012a). Horse Liver Alcohol Dehydrogenase: New Perspectives for an Old Enzyme. *Molecular Biotechnology*, 52(3), 244–250. <https://doi.org/10.1007/s12033-012-9542-7>
- Quaglia, D., Irwin, J. A., & Paradisi, F. (2012b). Horse Liver Alcohol Dehydrogenase: New Perspectives for an Old Enzyme. *Molecular Biotechnology*, 52(3), 244–250. <https://doi.org/10.1007/s12033-012-9542-7>
- Ray, S. S., Bonanno, J. B., Rajashankar, K. R., Pinho, M. G., He, G., De Lencastre, H., Tomasz, A., & Burley, S. K. (2002). Cocrystal Structures of Diaminopimelate Decarboxylase. *Structure*, 10(11), 1499–1508. [https://doi.org/10.1016/S0969-2126\(02\)00880-8](https://doi.org/10.1016/S0969-2126(02)00880-8)
- Reetz, M. T. (2013). Biocatalysis in Organic Chemistry and Biotechnology: Past, Present, and Future. *Journal of the American Chemical Society*, 135(34), 12480–12496. <https://doi.org/10.1021/ja405051f>
- Roschangar, F., Sheldon, R. A., & Senanayake, C. H. (2015). Overcoming barriers to green chemistry in the pharmaceutical industry – the Green Aspiration Level™ concept. *Green Chemistry*, 17(2), 752–768. <https://doi.org/10.1039/C4GC01563K>
- Ruhaak, L. R., Steenvoorden, E., Koeleman, C. A. M., Deelder, A. M., & Wuhrer, M. (2010). 2-Picoline-borane: A non-toxic reducing agent for oligosaccharide labeling by reductive amination. *Proteomics*, 10(12), 2330–2336. <https://doi.org/10.1002/pmic.200900804>
- Sagong, H.-Y., Son, H. F., Kim, S., Kim, Y.-H., Kim, I.-K., & Kim, K.-J. (2016). Crystal Structure and Pyridoxal 5-Phosphate Binding Property of Lysine Decarboxylase from *Selenomonas ruminantium*. *PLOS ONE*, 11(11), e0166667. <https://doi.org/10.1371/journal.pone.0166667>
- Said, A. A. E., Ali, T. F. S., Attia, E. Z., Ahmed, A.-S. F., Shehata, A. H., Abdelmohsen, U. R., & Fouad, M. A. (2021). Antidepressant potential of *Mesembryanthemum cordifolium* roots assisted by metabolomic analysis and virtual screening. *Natural Product Research*, 35(23), 5493–5497. <https://doi.org/10.1080/14786419.2020.1788019>
- SANDMEIER, E., HALE, T. I., & CHRISTEN, P. (1994a). Multiple evolutionary origin of pyridoxal-5'-phosphate-dependent amino acid decarboxylases. *European Journal of Biochemistry*, 221(3), 997–1002. <https://doi.org/10.1111/j.1432-1033.1994.tb18816.x>
- SANDMEIER, E., HALE, T. I., & CHRISTEN, P. (1994b). Multiple evolutionary origin of pyridoxal-5'-phosphate-dependent amino acid decarboxylases. *European Journal of Biochemistry*, 221(3), 997–1002. <https://doi.org/10.1111/j.1432-1033.1994.tb18816.x>
- Sato, S., Sakamoto, T., Miyazawa, E., & Kikugawa, Y. (2004). One-pot reductive amination of aldehydes and ketones with α -picoline-borane in methanol, in water, and in neat conditions. *Tetrahedron*, 60(36), 7899–7906. <https://doi.org/10.1016/j.tet.2004.06.045>
- Schoenmakers, H., & Spiegel, L. (2014). Laboratory Distillation and Scale-up. In *Distillation* (pp. 319–339). Elsevier. <https://doi.org/10.1016/B978-0-12-386878-7.00010-3>
- Seah, S. Y. K., Britton, K. L., Rice, D. W., Asano, Y., & Engel, P. C. (2002). Single Amino Acid Substitution in *Bacillus sphaericus* Phenylalanine Dehydrogenase Dramatically Increases Its Discrimination between Phenylalanine and Tyrosine Substrates. *Biochemistry*, 41(38), 11390–11397. <https://doi.org/10.1021/bi020196a>

- Seah, S. Y. K., Linda Britton, K., Baker, P. J., Rice, D. W., Asano, Y., & Engel, P. C. (1995). Alteration in relative activities of phenylalanine dehydrogenase towards different substrates by site-directed mutagenesis. *FEBS Letters*, *370*(1–2), 93–96. [https://doi.org/10.1016/0014-5793\(95\)00804-I](https://doi.org/10.1016/0014-5793(95)00804-I)
- Sen, K. Y., & Baidurah, S. (2021). Renewable biomass feedstocks for production of sustainable biodegradable polymer. *Current Opinion in Green and Sustainable Chemistry*, *27*, 100412. <https://doi.org/10.1016/j.cogsc.2020.100412>
- Sharma, M., Mangas-Sanchez, J., Turner, N. J., & Grogan, G. (2017). NAD(P)H-Dependent Dehydrogenases for the Asymmetric Reductive Amination of Ketones: Structure, Mechanism, Evolution and Application. *Advanced Synthesis & Catalysis*, *359*(12), 2011–2025. <https://doi.org/10.1002/adsc.201700356>
- Sheldon, R. A., Basso, A., & Brady, D. (2021). New frontiers in enzyme immobilisation: robust biocatalysts for a circular bio-based economy. *Chemical Society Reviews*, *50*(10), 5850–5862. <https://doi.org/10.1039/D1CS00015B>
- Sheldon, R. A., & Brady, D. (2019). Broadening the Scope of Biocatalysis in Sustainable Organic Synthesis. *ChemSusChem*, *12*(13), 2859–2881. <https://doi.org/10.1002/cssc.201900351>
- Sheldon, R. A., & Woodley, J. M. (2018). Role of Biocatalysis in Sustainable Chemistry. *Chemical Reviews*, *118*(2), 801–838. <https://doi.org/10.1021/acs.chemrev.7b00203>
- Sommer, T., Göen, T., Budnik, N., & Pischetsrieder, M. (2020). Absorption, Biokinetics, and Metabolism of the Dopamine D2 Receptor Agonist Hordenine (*N, N*-Dimethyltyramine) after Beer Consumption in Humans. *Journal of Agricultural and Food Chemistry*, *68*(7), 1998–2006. <https://doi.org/10.1021/acs.jafc.9b06029>
- Song, W., Chen, X., Wu, J., Xu, J., Zhang, W., Liu, J., Chen, J., & Liu, L. (2020). Biocatalytic derivatization of proteinogenic amino acids for fine chemicals. *Biotechnology Advances*, *40*, 107496. <https://doi.org/10.1016/j.biotechadv.2019.107496>
- Stano, J., Nemeč, P., Weissová, K., Kovács, P., Kákoniová, D., & Lisková, D. (1995). Decarboxylation of l-tyrosine and l-dopa by immobilized cells of *Papaver somniferum*. *Phytochemistry*, *38*(4), 859–860. [https://doi.org/10.1016/0031-9422\(94\)00768-0](https://doi.org/10.1016/0031-9422(94)00768-0)
- Stockert, J. C., Horobin, R. W., Colombo, L. L., & Blázquez-Castro, A. (2018). Tetrazolium salts and formazan products in Cell Biology: Viability assessment, fluorescence imaging, and labeling perspectives. *Acta Histochemica*, *120*(3), 159–167. <https://doi.org/10.1016/j.acthis.2018.02.005>
- Su, Y., Liu, Y., He, D., Hu, G., Wang, H., Ye, B., He, Y., Gao, X., & Liu, D. (2022). Hordenine inhibits neuroinflammation and exerts neuroprotective effects via inhibiting NF- κ B and MAPK signaling pathways in vivo and in vitro. *International Immunopharmacology*, *108*, 108694. <https://doi.org/10.1016/j.intimp.2022.108694>
- Surwase, S. N., Patil, S. A., Apine, O. A., & Jadhav, J. P. (2012). Efficient Microbial Conversion of l-Tyrosine to l-DOPA by *Brevundimonas* sp. SGJ. *Applied Biochemistry and Biotechnology*, *167*(5), 1015–1028. <https://doi.org/10.1007/s12010-012-9564-4>
- Tang, Y. Q., & Weng, N. (2013). Salting-out assisted liquid–liquid extraction for bioanalysis. *Bioanalysis*, *5*(12), 1583–1598. <https://doi.org/10.4155/bio.13.117>

- Teng, Y., Scott, E. L., van Zeeland, A. N. T., & Sanders, J. P. M. (2011). The use of l-lysine decarboxylase as a means to separate amino acids by electro dialysis. *Green Chemistry*, *13*(3), 624. <https://doi.org/10.1039/c0gc00611d>
- Thompson, M. P., Derrington, S. R., Heath, R. S., Porter, J. L., Mangas-Sanchez, J., Devine, P. N., Truppo, M. D., & Turner, N. J. (2019). A generic platform for the immobilisation of engineered biocatalysts. *Tetrahedron*, *75*(3), 327–334. <https://doi.org/10.1016/j.tet.2018.12.004>
- Thompson, M. P., & Turner, N. J. (2017a). Two-Enzyme Hydrogen-Borrowing Amination of Alcohols Enabled by a Cofactor-Switched Alcohol Dehydrogenase. *ChemCatChem*, *9*(20), 3833–3836. <https://doi.org/10.1002/cctc.201701092>
- Thompson, M. P., & Turner, N. J. (2017b). Two-Enzyme Hydrogen-Borrowing Amination of Alcohols Enabled by a Cofactor-Switched Alcohol Dehydrogenase. *ChemCatChem*, *9*(20), 3833–3836. <https://doi.org/10.1002/cctc.201701092>
- Tolbert, W. D., Graham, D. E., White, R. H., & Ealick, S. E. (2003). Pyruvoyl-Dependent Arginine Decarboxylase from *Methanococcus jannaschii*. *Structure*, *11*(3), 285–294. [https://doi.org/10.1016/S0969-2126\(03\)00026-1](https://doi.org/10.1016/S0969-2126(03)00026-1)
- Truong, C. C., Mishra, D. K., & Suh, Y. (2023). Recent Catalytic Advances on the Sustainable Production of Primary Furanic Amines from the One-Pot Reductive Amination of 5-Hydroxymethylfurfural. *ChemSusChem*, *16*(1). <https://doi.org/10.1002/cssc.202201846>
- Tseliou, V., Knaus, T., Masman, M. F., Corrado, M. L., & Mutti, F. G. (2019). Generation of amine dehydrogenases with increased catalytic performance and substrate scope from ϵ -deaminating L-Lysine dehydrogenase. *Nature Communications*, *10*(1), 3717. <https://doi.org/10.1038/s41467-019-11509-x>
- Tseliou, V., Knaus, T., Vilím, J., Masman, M. F., & Mutti, F. G. (2020). Kinetic Resolution of Racemic Primary Amines Using *Geobacillus stearothermophilus* Amine Dehydrogenase Variant. *ChemCatChem*, *12*(8), 2184–2188. <https://doi.org/10.1002/cctc.201902085>
- Tsukatani, T., Suenaga, H., Higuchi, T., Akao, T., Ishiyama, M., Ezo, K., & Matsumoto, K. (2008). Colorimetric cell proliferation assay for microorganisms in microtiter plate using water-soluble tetrazolium salts. *Journal of Microbiological Methods*, *75*(1), 109–116. <https://doi.org/10.1016/j.mimet.2008.05.016>
- Viejo, C. G., Villarreal-Lara, R., Torrico, D. D., Rodríguez-Velazco, Y. G., Escobedo-Avellaneda, Z., Ramos-Parra, P. A., Mandal, R., Singh, A. P., Hernández-Brenes, C., & Fuentes, S. (2020). Beer and consumer response using biometrics: Associations assessment of beer compounds and elicited emotions. *Foods*, *9*(6), 821.
- Vitaku, E., Smith, D. T., & Njardarson, J. T. (2014). Analysis of the Structural Diversity, Substitution Patterns, and Frequency of Nitrogen Heterocycles among U.S. FDA Approved Pharmaceuticals. *Journal of Medicinal Chemistry*, *57*(24), 10257–10274. <https://doi.org/10.1021/jm501100b>
- Wang, M., Khan, M. A., Mohsin, I., Wicks, J., Ip, A. H., Sumon, K. Z., Dinh, C.-T., Sargent, E. H., Gates, I. D., & Kibria, M. G. (2021). Can sustainable ammonia synthesis pathways compete with fossil-fuel based Haber–Bosch processes? *Energy & Environmental Science*, *14*(5), 2535–2548. <https://doi.org/10.1039/D0EE03808C>

- Wang, Q., Xin, Y., Zhang, F., Feng, Z., Fu, J., Luo, L., & Yin, Z. (2011). Enhanced γ -aminobutyric acid-forming activity of recombinant glutamate decarboxylase (*gadA*) from *Escherichia coli*. *World Journal of Microbiology and Biotechnology*, *27*(3), 693–700. <https://doi.org/10.1007/s11274-010-0508-2>
- Watanabe, Y., Tsuji, Y., Ige, H., Ohsugi, Y., & Ohta, T. (1984). Ruthenium-catalyzed N-alkylation and N-benylation of aminoarenes with alcohols. *The Journal of Organic Chemistry*, *49*(18), 3359–3363. <https://doi.org/10.1021/jo00192a021>
- Weber, R. E. (1992). Use of ionic and zwitterionic (Tris/BisTris and HEPES) buffers in studies on hemoglobin function. *Journal of Applied Physiology*, *72*(4), 1611–1615. <https://doi.org/10.1152/jappl.1992.72.4.1611>
- Wei, G., Chen, Y., Zhou, N., Lu, Q., Xu, S., Zhang, A., Chen, K., & Ouyang, P. (2022). Chitin biopolymer mediates self-sufficient biocatalyst of pyridoxal 5'-phosphate and L-lysine decarboxylase. *Chemical Engineering Journal*, *427*, 132030. <https://doi.org/10.1016/j.cej.2021.132030>
- Wei, T., Cheng, B. Y., & Liu, J. Z. (2016). Genome engineering *Escherichia coli* for L-DOPA overproduction from glucose. *Scientific Reports*, *6*. <https://doi.org/10.1038/srep30080>
- Wieschalka, S., Blombach, B., Bott, M., & Eikmanns, B. J. (2013). Bio-based production of organic acids with *Corynebacterium glutamicum*. *Microbial Biotechnology*, *6*(2), 87–102. <https://doi.org/10.1111/1751-7915.12013>
- Wohlgemuth, R. (2021). Biocatalysis-Key enabling tools from biocatalytic one-step and multi-step reactions to biocatalytic total synthesis. *New Biotechnol*, *60*, 113–123.
- Wu, B., Zhang, S., Hong, T., Zhou, Y., Wang, H., Shi, M., Yang, H., Tian, X., Guo, J., Bian, J., Roache, J., Delgado, P., Mo, R., Fridrich, C., Gao, F., & Wang, J. (2020). Merging Biocatalysis, Flow, and Surfactant Chemistry: Innovative Synthesis of an FXI (Factor XI) Inhibitor. *Organic Process Research & Development*, *24*(11), 2780–2788. <https://doi.org/10.1021/acs.oprd.0c00412>
- Wu, P., Li, G., He, Y., Luo, D., Li, L., Guo, J., Ding, P., & Yang, F. (2020). High-efficient and sustainable biodegradation of microcystin-LR using *Sphingopyxis* sp. YF1 immobilized Fe₃O₄@chitosan. *Colloids and Surfaces B: Biointerfaces*, *185*, 110633. <https://doi.org/10.1016/j.colsurfb.2019.110633>
- Ye, L. J., Toh, H. H., Yang, Y., Adams, J. P., Snajdrova, R., & Li, Z. (2015). Engineering of Amine Dehydrogenase for Asymmetric Reductive Amination of Ketone by Evolving *Rhodococcus* Phenylalanine Dehydrogenase. *ACS Catalysis*, *5*(2), 1119–1122. <https://doi.org/10.1021/cs501906r>
- Yoon, S., Patil, M. D., Sarak, S., Jeon, H., Kim, G., Khobragade, T. P., Sung, S., & Yun, H. (2019). Deracemization of Racemic Amines to Enantiopure (R)- and (S)-amines by Biocatalytic Cascade Employing ω -Transaminase and Amine Dehydrogenase. *ChemCatChem*, *11*(7), 1898–1902. <https://doi.org/10.1002/cctc.201900080>
- Yoshitaka Hashitani, B. (1925). On the chemical constituents of malt-rootlets with special reference to Hordenine. *Journal of the College of Agriculture*, *14*, 1–56.

- Zhang, B., Jiang, Y., Li, Z., Wang, F., & Wu, X.-Y. (2020). Recent Progress on Chemical Production From Non-food Renewable Feedstocks Using *Corynebacterium glutamicum*. *Frontiers in Bioengineering and Biotechnology*, *8*. <https://doi.org/10.3389/fbioe.2020.606047>
- Zhang, H., Wei, Y., Lu, Y., Wu, S., Liu, Q., Liu, J., & Jiao, Q. (2016). Three-step biocatalytic reaction using whole cells for efficient production of tyramine from keratin acid hydrolysis wastewater. *Applied Microbiology and Biotechnology*, *100*(4), 1691–1700. <https://doi.org/10.1007/s00253-015-7054-7>
- Zhang, K., & Ni, Y. (2014). Tyrosine decarboxylase from *Lactobacillus brevis*: Soluble expression and characterization. *Protein Expression and Purification*, *94*, 33–39. <https://doi.org/10.1016/j.pep.2013.10.018>
- Zhang, X., Du, L., Zhang, J., Li, C., Zhang, J., & Lv, X. (2021). Hordenine Protects Against Lipopolysaccharide-Induced Acute Lung Injury by Inhibiting Inflammation. *Frontiers in Pharmacology*, *12*, 712232. <https://doi.org/10.3389/fphar.2021.712232>
- Zhao, W., Hu, S., Huang, J., Ke, P., Yao, S., Lei, Y., Mei, L., & Wang, J. (2016). Permeabilization of *Escherichia coli* with ampicillin for a whole cell biocatalyst with enhanced glutamate decarboxylase activity. *Chinese Journal of Chemical Engineering*, *24*(7), 909–913. <https://doi.org/10.1016/j.cjche.2016.02.001>
- Zhou, F., Xu, Y., Nie, Y., & Mu, X. (2022). Substrate-Specific Engineering of Amino Acid Dehydrogenase Superfamily for Synthesis of a Variety of Chiral Amines and Amino Acids. *Catalysts*, *12*(4), 380. <https://doi.org/10.3390/catal12040380>
- Zhou, J.-W., Ruan, L.-Y., Chen, H.-J., Luo, H.-Z., Jiang, H., Wang, J.-S., & Jia, A.-Q. (2019). Inhibition of Quorum Sensing and Virulence in *Serratia marcescens* by Hordenine. *Journal of Agricultural and Food Chemistry*, *67*(3), 784–795. <https://doi.org/10.1021/acs.jafc.8b05922>
- Zhu, H., Xu, G., Zhang, K., Kong, X., Han, R., Zhou, J., & Ni, Y. (2016a). Crystal structure of tyrosine decarboxylase and identification of key residues involved in conformational swing and substrate binding. *Scientific Reports*, *6*(1), 27779. <https://doi.org/10.1038/srep27779>
- Zhu, H., Xu, G., Zhang, K., Kong, X., Han, R., Zhou, J., & Ni, Y. (2016b). Crystal structure of tyrosine decarboxylase and identification of key residues involved in conformational swing and substrate binding. *Scientific Reports*, *6*(1), 27779. <https://doi.org/10.1038/srep27779>
- Zhuang, W., Liu, H., Zhang, Y., He, J., & Wang, P. (2021). Effective asymmetric preparation of (R)-1-[3-(trifluoromethyl)phenyl]ethanol with recombinant *E. coli* whole cells in an aqueous Tween-20/natural deep eutectic solvent solution. *AMB Express*, *11*(1), 118. <https://doi.org/10.1186/s13568-021-01278-6>

6. Production of short chain primary amines with immobilized valine decarboxylase

Unless explicitly stated otherwise, the research presented in this chapter is the sole and individual work of the author.

6.1 Introduction

In line with the global shift towards sustainable and green practices, our investigation also seeks to contribute to environmentally responsible strategies for the production of amines, which are currently derived from petroleum cracking processes or produced by dehydrating appropriate alcohols with ammonia using a catalyst under a harsh condition. (Eller et al., 2000) The aim is to support this sector by offering a more ecologically sound alternative that leverages the efficiency of biocatalysis. By doing so, not only the scientific understanding of these processes is going to increase, but also a more sustainable enzymatic method is fostered, as alternative to the chemical production.

To this end, the bioconversion of abundantly available natural molecules, such as amino acids, presents significant potential. (Z. Guo et al., 2019; Pelckmans et al., 2017; Sen & Baidurah, 2021) This chapter focuses on the biocatalyst L-valine decarboxylase from *Streptomyces viridifaciens*. (Garg et al., 2002b) This exploration delves into the enzyme substrate scope, investigating its catalytic activity and the prospects of expanding its use. Moreover, the possibility of immobilizing this biocatalyst is examined, to potentially set up the way for its effective and recurrent use in industrial applications.

6.2 Results and discussion

6.2.1 VImD expression and purification

The expression of L-valine decarboxylase, known as VImD, has previously been achieved with satisfactory volumetric yields based on established literature protocols. (D. I. Kim et al., 2021) However, through refinement of the expression conditions, this yield has been successfully enhanced (Table 6.1). The important adjustments involved modifying the post-induction incubation temperature and duration. By reducing the temperature from 37 to 20 °C and extending the incubation period from 5 hours to 24 hours post-induction, the volumetric yield of VImD effectively increased, going from 180 mg/L to 300 mg/L. Initially, the results of the expression conditions were evaluated through protein electrophoresis using a gel (Figure 6.1). Even though the gel analysis was normalized based on the amount of buffer used for sonication of the pellet from each condition, the result did not clearly highlight the improvement due to the modified condition. At the same time, no toxic effects from protein expression were identified in the biomass. This means that no cell lysis was detected, and the OD levels were not diminished compared to the standard cell culture condition, indicating that the cells were not suffering. Subsequently, the obtained pellets were utilized for protein purification and the VImD volumetric yield were compared (Table 6.1).

Expression condition	Expression time (h)	Temperature (°C)	Culture volume (L)	Biomass (g)	Biomass yield (g/L)	Volumetric yield (mg/L)
1	5	37	0.3	1.3	4.3	175
2	24	20	0.3	1.9	6.3	300

Table 6.1: Comparison of expression conditions for VImD.

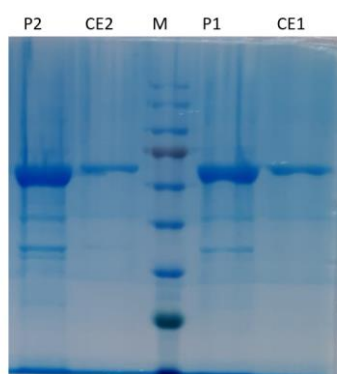


Figure 6.1: Gel electrophoresis (SDS-PAGE) showing two conditions in the expression study for VImD. Despite suboptimal sonication efficiency, a comparative analysis of soluble and insoluble fractions under two conditions((**1**) 5-hour protein expression from LB cell culture at 37 °C and (**2**) 24-hour protein expression from LB cell culture at 20 °C) exhibits minimal variation. **P1**: insoluble fraction from condition 1; **CE1**: soluble fraction from condition 1; **M**: marker; **P2**: insoluble fraction from condition 2; **CE2**: soluble fraction from condition 2.

In the process of purifying VImD using the ÄKTA purification system, a 5 mL column was employed. However, during the purification process, it was observed that the His-tagged protein did not show strong affinity for the Ni-NTA resin. To mitigate potential loss of VImD during the purification step, a buffer solution with a relatively low concentration of imidazole, 7.5 mM, was used (Buffer A). Only this buffer was then utilized for washing the resin to remove aspecific protein interactions, post-loading of the crude extract, showed a minimization of the His-tagged protein loss during the process. Expression and purification were controlled by SDS-PAGE (Figure 6.2). The specific activity measurements of the enzyme against L-valine, conducted according to the protocols outlined in the Materials and Methods section, shown that the enzyme exhibited a specific activity of 4.7 U/mg.

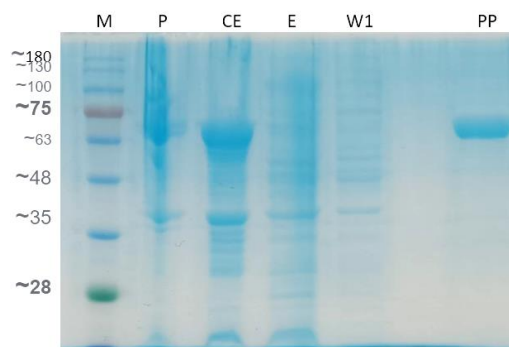


Figure 6.2: Gel Electrophoresis (SDS-PAGE) depicting the expression and purification stages of VImD. Distinct bands correspond to the targeted protein VImD, demonstrating successful expression and subsequent purification. **M:** marker; **P:** insoluble fraction; **CE:** soluble fraction; **E:** eluted crude extract; **W1:** wash with buffer A (50 mM phosphate buffer, 300 mM NaCl, 7.5 mM imidazole, pH 7.5); **PP:** purified protein

Addressing the point concerning the potential influence of protein structure on the observed lower affinity of the His-tag for the nickel resin, *in silico* visualization was used for further insights. Upon examination of the protein structure, no evidence of structural impediments were apparent (Figure 6.3). Specifically, the His-tag at the N-terminal did not appear to be obscured or hidden within the protein tertiary structure, which would otherwise have hindered its interaction with the nickel ions.

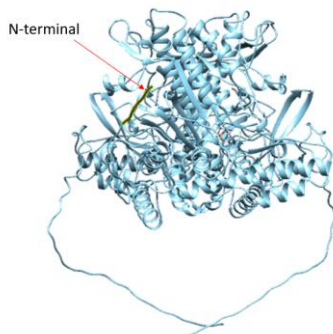


Figure 6.3: This image showcases the structural models of VImD obtained through AlphaFold prediction. In the picture, the N-terminal is highlighted in red indicating the His-tag location.

6.2.2 Enzyme biotransformations with free enzyme

During biotransformation experiments using the free enzyme, various aliphatic amino acids were tested as substrates (Table 6.2). The concentration of biocatalyst, after optimization tests, was maintained at a consistent level of 1.5 mg/mL, and each biotransformation reaction was carried out with 0.1 M substrate in a total volume of 1 mL. The result for this initial trial of biotransformation is shown in Graph 6.1.

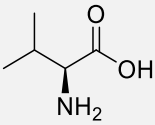
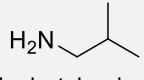
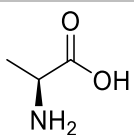
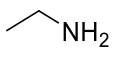
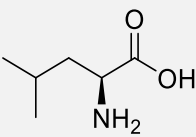
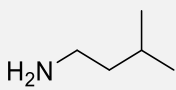
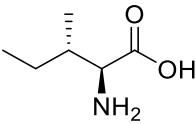
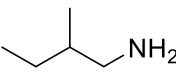
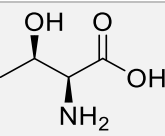
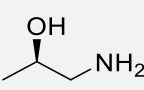
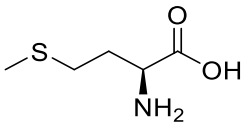
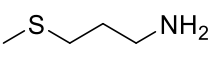
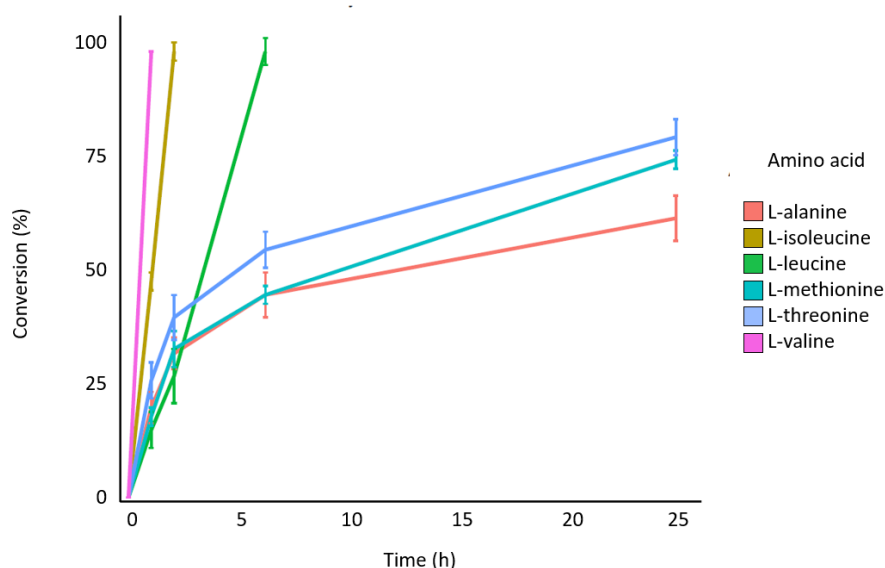
Entry	Amino acid - substrate	Amine - product
1	 L-valine	 isobutylamine
2	 L-alanine	 ethylamine
3	 L-leucine	 isoamylamine
4	 L-isoleucine	 2-methylbutylamine
5	 L-threonine	 1-amino-2-propanol
6	 L-methionine	 3-(methylthio)propanamine

Table 6.2: Substrates and corresponding products for VImD biotransformations.

L-valine, L-leucine, and L-isoleucine, at a scale of 0.1 M, achieved a complete conversion in relatively short times, specifically 1 hour for L-valine, 2 hours for L-isoleucine and 6 hours for L-leucine. L-alanine exhibited a slightly lower conversion of 61 % over a duration of 24 hours. L-threonine and L-methionine had maximum conversions of 80 % and 75 %, respectively, over the same duration of 24 hours. This data implies that certain amino acids, notably L-valine, L-leucine, and L-isoleucine, can be converted with greater efficiency in relatively short timeframes. However, it is also evident that with a stable enzyme, substantial conversions can be achieved over extended periods for a broader range of substrates. L-alanine, being smaller, may not form strong interactions in the enzyme catalytic pocket, possibly limiting its decarboxylation. Conversely, amino acids with polar functional groups, as L-threonine and L-methionine, may form additional

hydrogen bonds in the active site, potentially enhancing their stability and conversion rates.

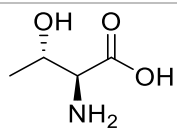
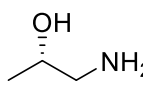
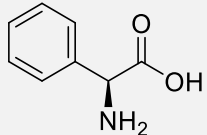
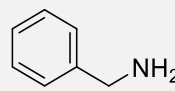
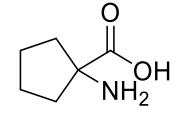
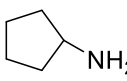
Batch biotransformations at 0.1 M scale with free VImD



Graph 6.1: Conversions of the various amino acids to their corresponding products, calculated using the corresponding product calibration curves. The sole exception is for the product of L-isoleucine, which is calculated based on substrate depletion. This comprehensive representation provides an overview of the biotransformation efficiencies for each tested amino acid.

While expanding the substrate scope, other amino acids such as L-serine, *allo*-threonine, L-2-phenylglycine and 1-amino-cyclopentanecarboxylic acid were also evaluated (Table 6.3). Among these compounds, the last two were already tested in previous work. (D. I. Kim et al., 2021) However, these substrates did not yield particularly promising results for potential scale-up applications and, because of factors such as poor solubility, low conversion rates, or lack of bioavailability, they were not further considered in the context of this study.

Amino acid - substrate	Amine - product	Problematics
<chem>NC(CO)C(=O)O</chem> L-serine	<chem>CCO</chem> ethanolamine	low conversion

 <i>Allo</i> -threonine	 1-amino-2-propanol	lack of bioavailability
 L-2-Phenylglycine	 benzylamine	poor solubility, lack of bioavailability
 1-amino cyclopentanecarboxylic acid	 cyclopentylamine	lack of bioavailability, toxicity

Table

6.3:

Summary of additional substrates tested for VImD biotransformation scope. These substrates were found to be less relevant for the objectives of the project.

6.2.3 Covalent immobilization on inert supports

Efforts were undertaken to covalently immobilize VImD to an inert carrier. The supports evaluated in this study included EP400/SS, HFA 403/S, and agarose, as shown in Table 6.4.

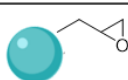
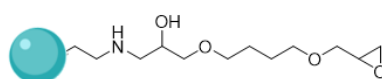
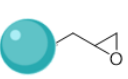
Support	Resin decoration	Properties
EP400/SS		\emptyset pores: 40 – 60 nm Particle size: 100 – 300 μ m
HFA403/S		
Agarose		\emptyset pores: \sim 200 nm Particle size: 50-150 μ m

Table 6.4: Comprehensive overview of the various immobilization supports trialed in this study, along with their specific properties including particle pore diameters and particle sizes.

Initial trials utilized agarose and EP400/SS for immobilization, exploiting the chemistry of immobilization where the protein is docked onto the support surface by the cobalt rapid interaction and directionality. These experiments indicated a higher recovered activity when using agarose as a support. However, methacrylic resins with a linker were also

considered due to their potential suitability. Table 6.5 highlights VImD performance for different hydrophobic and hydrophilic carriers.

Protein loading (mg/g)	Support	Immobilization yield before desorption (%)	Immobilization yield (%)	Recovered activity (%)	Expressed activity (U/g)
2.5	EP400/SS	>99	95	6 %	0.7
2.5	HFA403/S	96	41	<1 %	n.d.
2.5	Agarose	>99	>99	28 %	3.3

Table 6.5: This table summarizes the initial trial conducted with different immobilization supports for VImD, with the protein loading of 2.5 mg/g, detailing each support performance in terms of enzyme immobilization efficiency and recovered activity of the immobilized biocatalyst. The free enzyme VImD activity was 4.7 U/mg.

Experiments for the immobilization of VImD were conducted both at room temperature and at 4°C. Lowering the temperature to 4°C has been found to enhance enzyme stability, thereby preserving its activity, especially in those cases where longer immobilization times are required. In fact, the immobilization time for methacrylic resins was 6 hours, while the experiment with agarose was carried out overnight for 16 hours.

VImD appeared to have a greater affinity for hydrophilic supports. Interestingly, with the HFA403/S resin, close to complete immobilization was obtained after 6 hours. Yet, following the desorption procedure involving the specific buffer (50 mM EDTA, 500 mM NaCl in 50 mM phosphate buffer pH 7) to remove the Co²⁺ metal ion, important in directing the protein towards the support surface, the immobilization yield declined to 41 %. This suggests that VImD may primarily be adhering to the resin via hydrophobic interactions.

Upon increasing the protein loading, it was observed that this approach beneficially contributed to the immobilization of a greater amount of units (U) per g of hydrophilic supports, such as agarose and EP400/SS, generating a more active resin (Table 6.6).

Protein loading (mg/g)	Support	Immobilization yield (%)	Recovered activity (%)	Expressed activity (U/g)
5	EP400SS	95	8	1.8
5	Agarose	>99	24	5.4
20	EP400SS	80	5	3.7
20	Agarose	72	23	16.2

Table 6.6: Effect of increased protein loadings on the immobilization efficiency.

Considering an alternative to covalent immobilization, the physical entrapment of whole cells within alginate beads was explored as a potentially feasible strategy. This decision came from the fact that VImD demonstrated robust expression, making space to the prospect of circumventing the purification step before the immobilization. Moreover, this alternative could potentially avoid the observed activity loss associated with covalent immobilization. Finally, as far as the cost-effectiveness of the process, this second type of immobilization strategy has lower costs, making it particularly attractive for the purpose of scaling up the biotransformations.

While quantifying the concentration of leaked protein, an investigation was also carried out to assess the activity of the leaked biocatalyst. To achieve this, a 200 μL sample of the reaction solution from the SpinChem[®] system, which was used for the decarboxylation of L-threonine, was collected 8 hours into the process. This sample was then incubated in a 1.5 mL Eppendorf tube at 37 °C for 16 hours. Following this incubation period, the concentration of 1-amino-2-propanol in this small sample was compared to that in the main SpinChem[®] system. Compared to the product concentration at the 8-hour point, the conversion in the incubated sample increased by 10%, resulting in just under two-thirds of the total consumption of the starting material. However, it did not achieve the nearly complete conversion that was observed at the end of the process in the main SpinChem[®] system. Thus, it can be concluded that the VImD that leaked from the alginate matrix retains only a reduced part of its activity, after being released into the solution.

6.2.4 Alginates production with Ca^{+2} and Ba^{+2}

Alginate, an unbranched anionic polysaccharide primarily sourced from brown algae (Phaeophyta), is built from two main units: a-L-guluronic acid and b-D-mannuronic acid (Figure 6.4.) These units are linked in a 1-4 fashion and form structures of homopolymeric blocks (blocks of the same unit, either GGG or MMM) or heteropolymeric blocks (blocks containing alternating units, referred to as MGM).

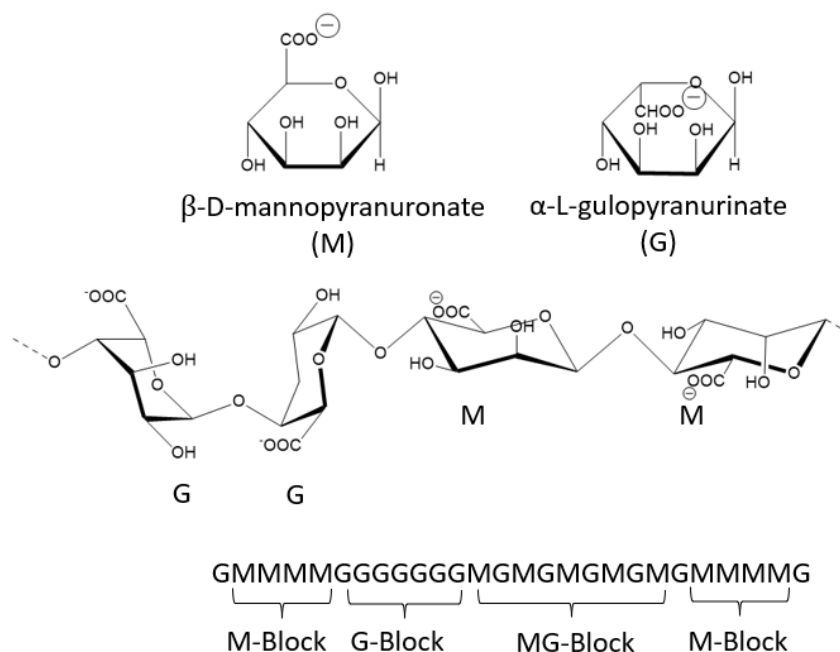


Figure 6.4: Alginate structure.

Alginate beads present an effective medium for immobilizing amino acid decarboxylases due to their unique gel-forming capability with divalent cations. (Bhatia et al., 2015; J. Huang et al., 2007; Q. Wang et al., 2011; Zhao et al., 2016) This simple yet proficient process encapsulates whole cells within the bead matrix, allowing substrate and product diffusion. The approach simplifies immobilization by avoiding enzyme purification and potentially enhancing biocatalyst stability.

In order to produce VImD whole cell alginate beads, after protein expression, the biomass was harvested and mixed with 5 % sodium alginate solution in a 1:1 ratio. The cell suspension was pumped drop-by-drop into a solution containing a divalent positive ion using a peristaltic pump. For 25 mL of mixture of cells and alginate, 500 mL of ions solution was used. This divalent cations (Ca^{+2} or Ba^{+2}) plays a crucial role in the polymerization of alginate by enabling the formation of ionic bonds with the carboxylic groups present on the alginate matrix (Figure 6.5). This process allows the immobilization of the cells within the solidified alginate polymeric structure. Initially the cell-alginate suspension was pumped into a solution of 200 mM calcium chloride to form alginate beads .

However, these beads were found to be degrading during batch biotransformation with L-valine to isobutylamine at 0.1 M scale, lasting only about an hour. The instability was evidenced by the noticeable dissolution of the alginate matrix following product formation (Figure 6.6).

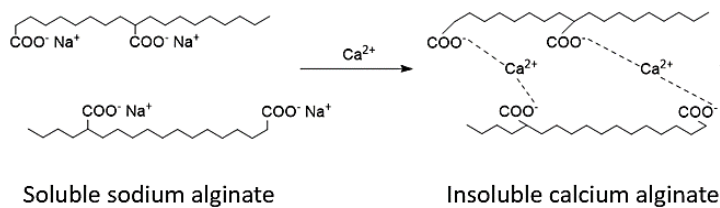


Figure 6.5: Schematic depiction of the ionotropic gelation process of sodium alginate. Upon the addition of a divalent ion such as Ca^{2+} , ionic cross-linking occurs, leading to the formation of a gel matrix.

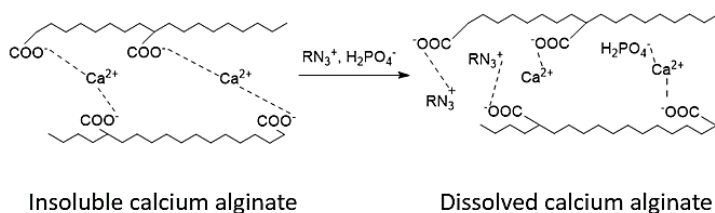
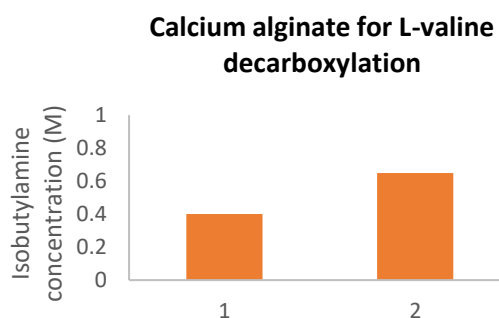


Figure 6.6: Calcium alginate beads dissolution. The illustration demonstrates how the addition of positively and negatively charged species can disrupt or weaken the ionic bonds between the carboxyl groups of alginate and Ca^{2+} ions, resulting in the dissolution of the solid matrix.

This dissolution was attributed to the displacement of calcium ions by the newly formed isobutylamine. At pH 7, isobutylamine carries a positive charge on the amino group, allowing it to disrupt the ionic interactions between calcium ions and the carboxylic groups on the alginate matrix, thereby leading to the breakdown of the beads. To further investigate this phenomenon, a proof-of-concept experiment was carried out. A volume of 2 mL of degraded alginate beads solution was collected after biotransformation and aliquoted into two microcentrifuge tubes. One of them was treated with the same volume of 200 mM CaCl_2 solution, while the other one, serving as a control, was added with water. Interestingly, the concentration of isobutylamine was found to be higher in the sample to which CaCl_2 was added.



Graph 6.2: Variation of isobutylamine concentration. (1) Sample from dissolved calcium alginate supplemented with water; (2) sample supplemented with 200 mM calcium chloride solution.

This observation suggested a reversible mechanism of competition between positively charged species, further supporting the hypothesis that isobutylamine can displace calcium ions from the alginate matrix, and that the addition of more calcium ions can partially reverse this process.

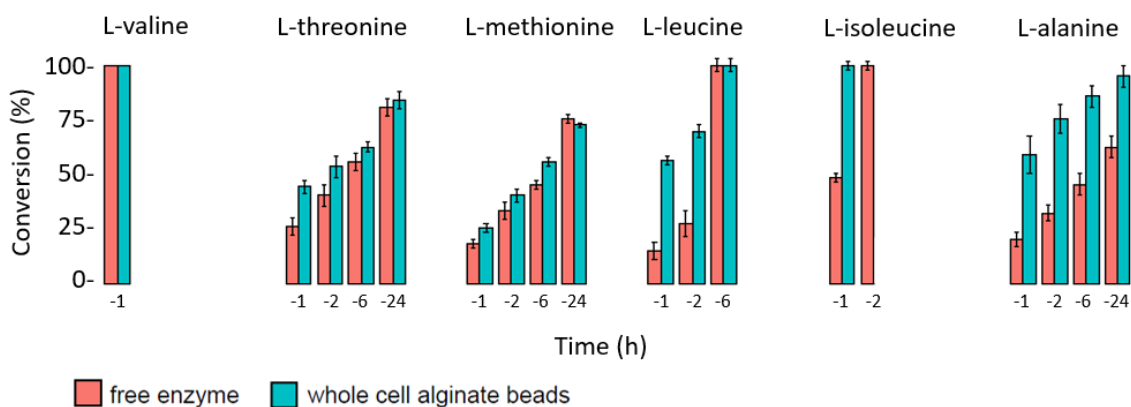
Upon encountering the issue of bead instability and decrease in activity increasing the CaCl_2 (up to 800 mM concentration), a promising alternative was found in substituting Ca^{2+} with Ba^{2+} as the divalent cation in the solution. Indeed, this improved the rigidity of the alginate beads. (Harper et al., 2014; Mørch et al., 2006) According to the literature, barium is capable of forming stronger ionic bonds, thus increasing the stiffness of the beads and enhancing the polymerization process. This change made the beads more resilient and less susceptible to dissolution. (Harper et al., 2014)

Another approach to enhance the stability of the alginate beads involved revisiting the choice of catalytic buffer for the reaction. Specifically, the phosphate buffer, which carries negative charges, was replaced with HEPES. This change was made because HEPES, being a zwitterionic buffer, (Weber, 1992) is less likely to interfere with the ionic cross-linking that gives the alginate beads their structure and stability.

6.2.5 Small batch biotransformations (0.1 M scale)

Performing batch biotransformations with barium alginate beads, it became evident that the VImD can operate efficiently even within the cell system entrapped in the polymeric matrix of alginate. As shown by the Graph 6.3, comparing the performance of the free enzyme and the use of whole cells in alginate beads, no detrimental effect on the conversions is observed regarding the immobilized biocatalyst. In fact, all the recorded conversions are comparable between the two systems, which reinforces the viability of the alginate beads approach as sustainable production method.

Comparison of batch biotransformations at 0.1 M substrate scale: free enzyme vs whole cell alginate beads



Graph 6.3: Comparative analysis of biotransformations at 0.1 M scale (free enzyme vs whole cell alginate beads).

For an estimation of the biocatalyst concentration in the biotransformations conducted with whole cell alginate beads, and to compare those with the free enzyme ones, a correlation was drawn between the pellet used for alginate production and the potential purified protein yield derived from that biomass (Table 6.7). Further, by considering the weight of produced beads from that specific biomass, it was possible to calculate the quantity of enzyme, in mg, per g of alginate beads. This approach provided a more accurate representation of the biocatalyst concentration in the two different types of biotransformations, thus facilitating a more robust comparison.

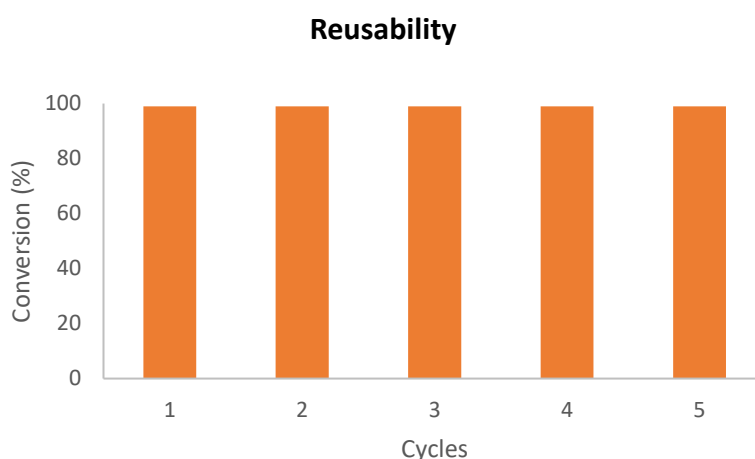
Parameter	Value
Biomass used for alginate preparation [g]	4
Purified protein yield [$\text{mg}_{\text{protein}}/\text{g}_{\text{biomass}}$]	47.4
Alginate yield [g]	15
Protein per alginate [mg/g]	$= \frac{47.4 \cdot 4}{15} = 12.5 \text{ [mg}_{\text{protein}}/\text{g}_{\text{alginate}}]$

Table 6.7: Estimation of enzyme concentration in whole cell alginate beads. This table illustrates the calculations utilized to estimate the amount of VImD enzyme encapsulated within alginate beads when using whole cell preparations. The approximation is based on the purified protein yield from biomass and the resultant weight of the produced alginate beads.

While these results offer an indication of the amount of VImD inside the whole-cell alginate beads, it should be noted that the calculations do not take into account the protein quantity remaining in the insoluble fraction after sonication during the purification process. Therefore, it is acknowledged that the effective protein concentration within the alginate beads may be inaccurate, if part of the enzyme is in inclusion bodies or, on the other hand, fully soluble. Consequently, the estimated concentration of 2.5 mg/mL of enzyme in the whole cell alginate beads batch biotransformations, where 200 mg of beads were employed, is just a ballpark figure.

6.2.6 Reusability and stability of free purified enzyme and whole cell alginate bead systems

The reusability of VImD in whole-cell alginate beads was examined in small batch biotransformations, using L-valine as the substrate, on a scale of 0.1 M. Prior to each new biotransformation, the biocatalyst was carefully washed with water. The same 200 mg of alginate beads were successfully reused for five consecutive cycles, consistently yielding complete conversion to the product after just one hour of biotransformation in each cycle (Graph 6.4).



Graph 6.4: Reusability of the immobilized biocatalyst as whole cell barium alginate beads. Each cycle was performed with 200 mg of alginates beads for the conversion of L-valine at 0.1 M concentration.

Afterwards the stability of the different biocatalyst versions was investigated. The stability of the free enzyme and the whole cells alginate beads was assessed after 10 days of storage at 4°C. This was achieved by comparing the conversion efficiency after the storage period with the original performance under the same biotransformation conditions (Table 6.8).

Biocatalyst system	Relative stability after 10 days at 4°C (%)
Free Enzyme	44
Alginate with Whole Cells	98

Table 6.8: Comparative stability of different biocatalyst systems after 10 days at 4 °C. The relative stability is presented as a percentage of initial activity.

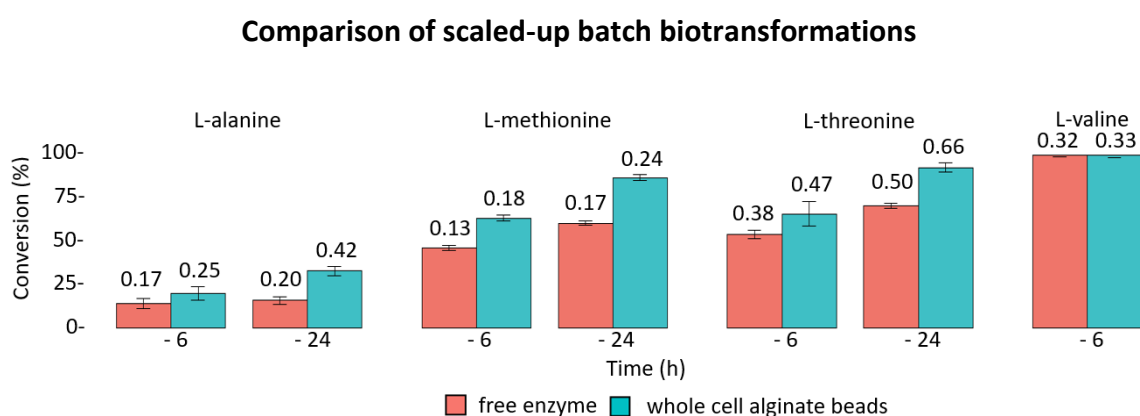
This result suggests a superior preservation of enzyme function within the whole cell alginate beads, possibly due to additional protective effects conferred by the cellular environment.

6.2.7 Scale-up of whole cell alginate bead biotransformations

Following the promising results obtained from the batch biotransformations, the scale up the reaction was set up, pushing the biotransformation towards its limit by operating close to the maximum substrate solubility level (Table 6.9 and Graph 6.5).

	Biocatalyst	Concentration (M)	Time (h)	Maximum Conversion (%)
L-alanine	free enzyme	1.28	6	15
	alginate beads		24	33
L-methionine	free enzyme	0.28	24	61
	alginate beads		24	86
L-threonine	free enzyme	0.71	24	70
	alginate beads		24	93
L-valine	free enzyme	0.32	6	99
	alginate beads		6	99

Table 6.9: Scale-up biotransformations using free enzyme (VImD concentration 1.5 mg/mL) and whole cell alginate beads (VImD ~2.5 mg/mL). This table shows the substrate concentrations, reaction times, and maximum conversions for the substrate where the concentration level was possible to be increased above 0.1 M.



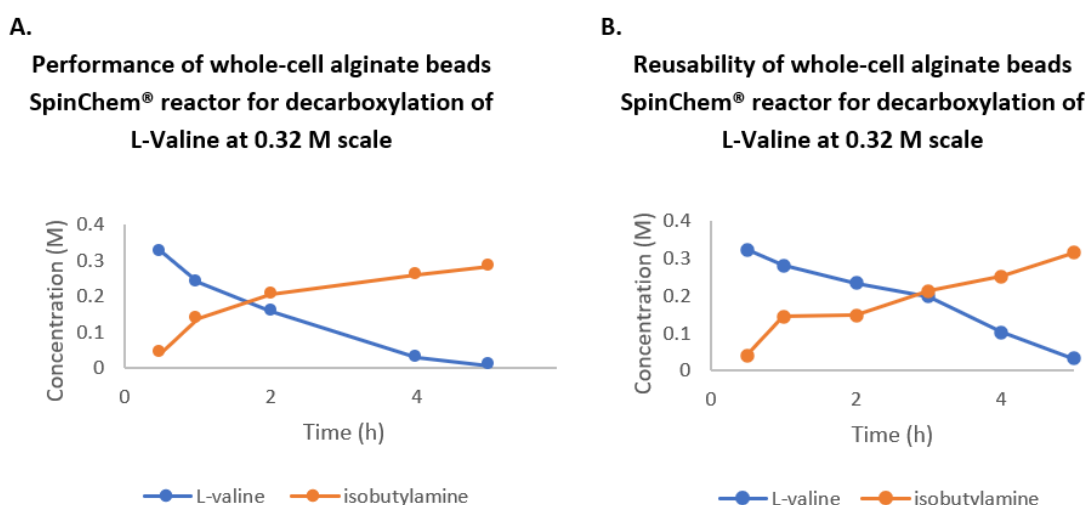
Graph 6.5: Conversions to primary amine in scale-up condition for the selected substrates at 6 and 24 hours using the free version of VImD or entrapped whole cell in alginate

beads. The labels above the graph bars indicate the achieved mean concentration values in molarity (M).

When working with significantly higher substrate concentrations, particularly in the cases where there is a slower reaction time, it was observed that the alginate beads with whole cells consistently yielded better conversions at 24 h (Graph 6.5). This improved performance can likely be attributed to enhanced biocatalyst stability within the whole-cell system, that therefore does not allow enzyme inactivation or precipitation.

6.2.8 SpinChem[®] system with whole cell alginate beads

The feasibility of implementing them in the SpinChem[®] system with a rotating bed reactor was then examined. For the scale-up in the SpinChem[®], three substrates from the substrate scope were selected for investigation: L-valine, L-threonine, and L-methionine. With L-valine, the natural substrate of VImD, the reusability of the immobilized biocatalyst was particularly explored. Impressively, the same batch of whole cell alginate beads was successfully reused for two separate SpinChem[®] batch biotransformation, each consisting of 200 mL of 0.32 M L-valine (Graph 6.6, A and B). In both instances, the biotransformation achieved excellent conversions after 5 h, demonstrating the robustness and recyclability of the whole-cell alginate bead system in the scaled-up process.

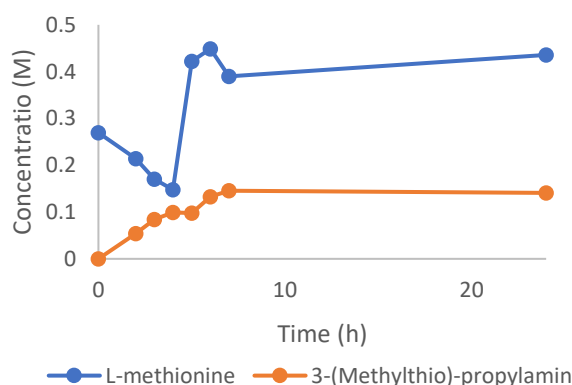


Graph 6.6: **A.** Performance of whole cell alginate beads in SpinChem[®] reactor for decarboxylation of L-Valine. **B.** Reusability after one cycle of whole cell alginate beads in SpinChem[®] reactor for decarboxylation of L-Valine.

Compared to L-valine, L-methionine has a similar maximum solubility level at pH 7.5. In order to enhance the productivity of the biocatalyst, and therefore the amount of product which is possible to obtain from the biotransformation, conducting consecutive additions of L-methionine as a solid powder to the reaction vessel was trialed, in order to increase the substrate concentration while the decarboxylation reaction was depleting it. In this

way it was possible to investigate the biocatalyst performance in a heterogeneous reaction environment inside the SpinChem®. However, this experiment was not successful, as the attempt to enhance the solubility of L-methionine through multiple additions did not yield the desired outcome (Graph 6.7). In this case, the maximum conversion reached was only 25 % (0.18 M) after a 24-hour period. The process started with an initial substrate concentration of 0.25 M. Subsequently, L-methionine, in powder, was added in two separate times at the 5-hour and 7-hour, resulting in doubling and tripling the initial substrate concentration, respectively. After the first initial addition, L-methionine appeared to dissolve almost entirely. However, subsequent attempts to offer more substrate to the system resulted in a suspension which did not dissolve, even after 16 hours of stirring at 37 °C. Continuing the experiment without complete dissolution of the substrate in the reaction mixture complicated the monitoring of substrate consumption. In fact, the measurement of L-methionine concentration via HPLC was incomplete, as the undissolved amino acid was filtered out prior to the analysis. Eventually, after 24 hours, while cleaning the SpinChem®, a solid residue was observed accumulated within the inner cavity of the metal reactor. This residue, which was L-methionine, as the HPLC analysis confirmed, had absorbed part of the reaction solution, which contributed to an underestimation of the final conversion to product.

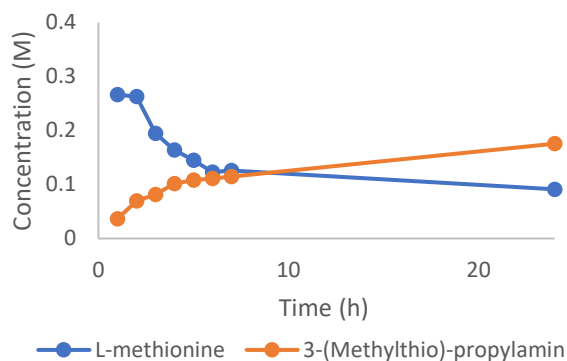
Performance of whole-cell alginate beads in SpinChem® reactor for decarboxylation of L-methionine in heterogeneous phase



Graph 6.7: Performance of whole-cell alginate beads in the SpinChem® reactor for the decarboxylation of L-methionine.

Due to the difficulties with L-methionine solubility at higher concentrations, the approach was adjusted. The initial substrate concentration was lowered to 0.30 M, which resulted in a homogenous reaction environment. Over a 24-hour period, the conversion improved to 54% reaching again a maximum product concentration of 0.18 M (Graph 6.8).

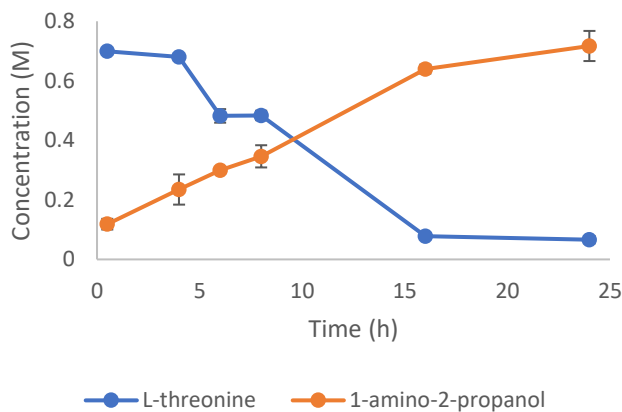
Performance of whole-cell alginate beads in SpinChem® reactor for decarboxylation of L-methionine at 0.30 M scale



Graph 6.8: Decarboxylation of L-methionine with whole-cell alginate beads in the SpinChem® reactor with a substrate solution at 0.33 M scale.

Looking at the third amino acid involved in the scale-up in the SpinChem® reactor, the decarboxylation process for L-threonine yielded promising results. Benefiting from L-threonine high solubility at pH 7.5, we were able to set up the reactor in a similar fashion to the L-valine setup, but with an initial substrate concentration of 0.71 M. Over a 24-hour monitoring period, the decarboxylation of L-threonine in the SpinChem® system resulted in a 90% conversion (Graph 6.9). This consistently high yield, obtained in duplicate, underscores the efficacy of utilizing whole cell barium alginate beads in this batch mode and clearly established the robustness of this platform for such biocatalytic processes.

Performance of whole-cell alginate beads in SpinChem® reactor for decarboxylation of L-threonine at 0.71 M scale



Graph 6.9: Performance of whole-cell alginate beads in the SpinChem® reactor for the decarboxylation of L-threonine.

6.2.9 Purified VImD barium alginate beads

An attempt was also made to immobilize the purified VImD in barium alginate beads. This was accomplished by combining the purified enzyme solution with sodium alginate at a v/v of 1:3, resulting in a final VImD concentration in the alginate of 2.5 mg/mL. Although

the performance of these beads was mostly similar to that of the whole cell alginate on a scale of 0.1 M substrate (data not shown), protein precipitation was evident in the biotransformation supernatant. As confirmed by the SDS gel, after 24 hours of incubation at 37 °C with shaking, the enzyme was observed to be leaking from the beads in most of the biotransformations (Figure 6.7).

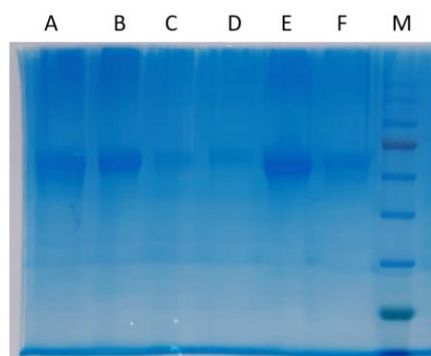


Figure 6.7: Gel electrophoresis (SDS-PAGE) of biotransformation supernatants. **A.** supernatant from L-isoleucine biotransformation; **B.** supernatant from L-leucine biotransformation; **C.** supernatant from L-alanine biotransformation; **D.** supernatant from L-threonine biotransformation; **E.** supernatant from L-valine biotransformation; **F.** supernatant from L-methionine biotransformation; **M.** ladder.

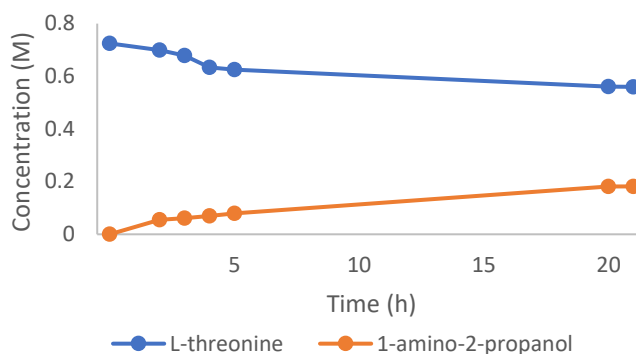
Given these results, the advantage of reusability inherent to immobilized biocatalysts in continuous mode operation could not be tested as the enzyme leaks continuously during the experiment, and the potential reuse would be significantly compromised.

6.2.10 SpinChem[®] system with cell crude extract in dialysis membrane

To evaluate the system and explore alternative scale-up methods to the use of immobilized biocatalysts, a modification was made to the rotating packed bed reactor, where the whole cell barium alginate beads were replaced with crude cell extract. For this procedure, 3 g of wet cell pellet from cells stored at -20 °C were resuspended in 50 mM phosphate buffer containing 100 mM NaCl at pH 7.5. Following sonication, centrifugation, and filtration, the supernatant (10 mL) was utilized to fill four dialysis bags within the SpinChem reactor, equating to a total protein load of approximately 150 mg of VImD. This estimate was derived from the protein quantification in the crude extract at 280 nm with the EPOC. Despite the protein not being purely isolated in the solution, VImD was evidently overexpressed, as confirmed by previous SDS gel analysis. This supports the conclusion that the concentration measured at 208 nm in the crude extract offers a reliable estimate of the actual protein concentration. The enzyme activity of the crude extract was also evaluated, comparing it to that of the free form of the enzyme. The activity assay showed that the crude extract maintained approximately 70 % of the activity level of the purified protein. However, when compared to the SpinChem[®] system that employed whole cell alginate, this conditions were not as satisfactory as anticipated,

primarily because the biocatalyst loading within the reactor did not match. Nevertheless, we proceeded to set up the SpinChem® system for the decarboxylation of L-threonine, noting that the biocatalyst concentration was approximately 60 % of what was used in the whole cell barium alginate beads SpinChem®. After 24 hours, the conversion to 1-amino-2-propanol was 25 %, which appeared significantly lower compared to the 85 % conversion achieved with the previously set up immobilized biocatalyst system (Graph 6.10). Moreover, the protein solution in the dialysis bag was significantly cloudy indicating enzyme precipitation.

SpinChem with Crude Extract in dialysis bags



Graph 6.10: Performance of crude extract beads in the SpinChem® reactor for the decarboxylation of L-threonine.

6.2.11 Downstream for the isolation of the products

For the downstream processing of the amine production from the scaled-up biotransformations, where the chosen amino acids underwent decarboxylation using whole cells entrapped in alginate beads, various strategies were explored, each tailored to the specific reaction substrate. With the intention of further manipulating the amino product, the objective of the purification process was to yield the product in its pure amino form, avoiding its conversion into a salt form.

6.2.11.1 Isobutylamine isolation

For the L-valine biotransformation, distillation emerged as the method of choice due to the physical properties of the product, isobutylamine. According to literature, isobutylamine has a boiling point ranging between 64 and 71 °C, making it readily separable from the aqueous solvent medium and the substrate. The significantly higher boiling point of L-valine at 213 °C further simplifies this separation.

Distillation is a purification technique widely employed in industry, offering the advantage of avoiding processes like filtration and chromatography, which are less preferred due to their lower scalability and efficiency. Focusing on the efficiency, on the other hand, a lab scale set up is always less efficient in terms of yield compared to large industrial scale. This is normally attributed to excessive wall heat loss in a small

apparatus.(Schoenmakers & Spiegel, 2014) As such, it was expected that the yield of purified isobutylamine from the SpinChem® system would be limited. In this experiment, 200 mL product solution was introduced into a 500 mL round-bottom flask together with a magnetic stirrer, and heated up with an oil bath (Figure 6.8). This system took around 3 hours to reach a uniform temperature and initiate evaporation within the distillation column. After continuous heating the round-bottom flask at 110°C, the heat began to propagate to the column. To minimize heat loss from the glass walls, aluminium foil was wrapped around the column.



Figure 6.8: Distillation set up for the purification of isobutylamine from the SpinChem® system.

After collecting the distilled isobutylamine in a weighed round-bottom flask, the gravimetric yield was calculated to be 30%. An NMR analysis was then performed and confirmed the purity of the product.

For the other amino products, namely 1-amino-2-propanol and 3-(methylthio)-propylamine, derived from L-threonine and L-methionine respectively, distillation was not a suitable strategy for their purification and isolation from the aqueous reaction medium. This is due to the high boiling points of these products, which are 159 °C for 1-amino-2-propanol and 169 °C for 3-(methylthio)-propylamine, making distillation impractical for their recovery.

6.2.11.2 Liquid-liquid extraction for 1-amino-2-propanol and 3-(methylthio)-propylamine

To isolate and purify the products derived from L-threonine and L-methionine, the strategy of liquid-liquid extraction was attempted. This technique takes advantage of the differential solubility of substances in two immiscible liquid phases, typically water and an organic solvent, to separate and concentrate the desired product. With amine products, it is usually sufficient to raise the pH above the corresponding pK_a , in order to have the amino group predominantly not protonated, and extract the basified solution

with an apolar solvent. However, this approach proved to be ineffective in this case, specifically dealing with 1-amino-2-propanol (pK_a value of 9). Due to its chemical structure, the molecule is hydrophilic and does not migrate easily to the organic phase, even at $pH > 9$. In a small-scale setup, various organic solvents including dichloromethane (DCM), ethyl acetate, heptane, methyl tert-butyl ether (MTBE), and diethyl ether were tested, but none resulted in a satisfactory extraction upon checking on TLC with ninidrine.

An additional challenge arose when attempting the liquid-liquid extraction approach with an aliquot of the product solution from the scaled-up system. When the solution was basified to $pH 10$, precipitation occurred in the aqueous phase. Further investigation confirmed that the precipitate was the VImD biocatalyst, which had leaked into the reaction bulk in the SpinChem[®] system. (Figure 6.9).

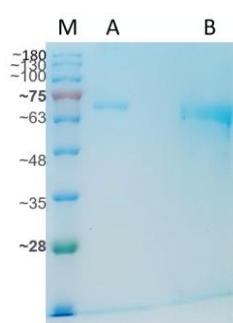


Figure 6.9: Gel electrophoresis (SDS-PAGE) of scaled-up system solution and resulting precipitate. **(A)** Sample of the initial solution from the scaled-up system. **(B)** Resuspended pellet, harvested following the basification of the aqueous phase.

After unsuccessful attempts of extracting 1-amino-2-propanol, salting-out assisted liquid-liquid extraction (SALLE) was trialed as an alternative strategy. (Tang & Weng, 2013) In this case, the ionic strength of the aqueous phase is increased by adding NaCl, which lowers the solubility of less polar compounds in water and thus encourages their partitioning into the organic phase, which was acetonitrile (MeCN) in this case. MeCN, a polar aprotic solvent, is capable of dissolving a broad spectrum of polar and non-polar compounds. Its miscibility with water decreases as the ionic strength of the solution rises, enabling it to serve as an effective extracting phase. As an added benefit, MeCN exhibits low toxicity, is relatively inexpensive, and can be easily removed by evaporation.

As in previous work, the addition of a small amount of hydrophobic solvent to the acetonitrile-water system was adopted to enhance phase separation. (G. Liu et al., 2010) In this case, hexane was added in a volume ratio 1 to 20 to the acetonitrile directly in the separatory funnel. After drying with sodium sulphate and filtering the organic phase, the organic solvent was removed at the rotavapor. For 1-amino-2-propanol, despite different attempts, the gravimetric yield was always lower than 5 %, while with and 3-(methylthio)-propylamine, 54 % yield was obtained. The isolated products were also submitted for NMR analysis, which confirmed in both cases the identity with the products. The isolated

materials were also subjected to NMR analysis which confirmed the purity of the products.

6.2.11.3 Trituration of 1-amino-2-propanol

An alternative strategy to isolate 1-amino-2-propanol was *via* trituration. To do so, lyophilization of the product solution and selective solubilization of 1-amino-2-propanol in organic solvent were performed. Two approaches were employed for the lyophilization step. In the first approach, the aqueous solution (a 50 mL aliquot) was directly frozen in a round bottom flask using liquid nitrogen. Alternatively, in the second approach, the freezing of the product solution was performed only after the hydrochloride salt of the amine was generated. The hydrochloride salt was obtained by adjusting the solution pH to 1, using 37 % HCl. The second approach was hypothesized to reduce the impact of lyophilization on the final yield, thereby reducing the likelihood of product loss during the process. However, for the product to be solubilized in the organic phase, the free form of 1-amino-2-propanol was necessary. Consequently, solid NaOH was added to the round bottom flask with a minimal volume (2 mL) water post-lyophilization. The organic solvents used in the experiments were MeCN and DCM. Spotting the solvent on TLC and staining with ninhydrin revealed that the product in the organic phase was not pure. After evaporating the solvent under vacuum, yields were disappointingly low, under 5 %.

6.2.12 Quantification of the leaked protein in the SpinChem[®] product solution

Although the alginate beads did not show visible signs of damage following the SpinChem[®] batch biotransformation, and the harvested product solution was clear, evidence of protein contamination became apparent during the downstream handling steps for the decarboxylation products of L-threonine and L-methionine. In fact, this deduction was based on the product solution foamy appearance during the liquid-liquid extractions, where it formed an emulsion with the organic phase. Additionally, protein precipitation occurred upon adjustment of the solutions pH. This precipitated protein was subsequently identified as VImD *via* SDS gel analysis. The determination of VImD leakage from the whole cell barium alginate beads into the product solution was conducted using a calibration curve on an SDS gel (Figure 6.10). The concentration of leaked VImD in the 200 mL biotransformation volume within the SpinChem[®] system was determined to be 0.10 mg/mL and 0.16 mg/mL, measured at 8 hours and 16 hours after the start of the process, respectively. These samplings were conducted on the scale-up decarboxylation of L-threonine.

While quantifying the leaked protein concentration, an investigation was also carried out to assess the activity of the leaked biocatalyst. To achieve this, a 200 μ L sample of the reaction solution from the SpinChem[®] system, which was used for the 24-hour decarboxylation of L-threonine, was collected 8 hours after the process started. This

sample was then incubated in a 1.5 mL Eppendorf tube at 37 °C for 16 hours. Afterwards, the concentration of 1-amino-2-propanol in this small sample was compared to that in the SpinChem® system. Compared to the product concentration at the 8-hour point, the conversion achieved in the incubated sample increased by 10%, while at the end of the process in the SpinChem® system, nearly complete conversion was observed. Thus, it can be concluded that the VImD that leaked from the alginate matrix retained at least part of its activity, after being released into the solution.

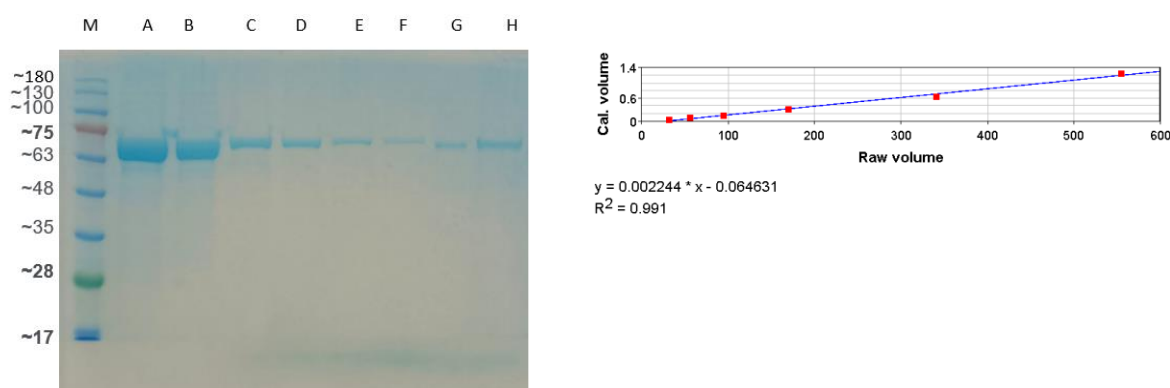


Figure 6.10: Calibration curve of VImD protein derived from SDS gel analysis. The gel image (left) displays varying concentrations of VImD for calibration purposes, along with samples from the product solution harvested from the SpinChem® system. The graph (right) illustrates the derived calibration curve, used to quantify the amount of VImD protein leaked into the product solution. **M.** Marker; **A.** 1.23 mg/mL; **B.** 0.62 mg/mL; **C.** 0.31 mg/mL; **D.** 0.15 mg/mL; **E.** 0.07 mg/mL; **F.** 0.04 mg/mL; **G.** Whole cell barium alginate beads SpinChem 8h sample; **H.** Whole cell barium alginate beads SpinChem 16h sample.

6.3 Conclusion

The successful immobilization of VImD using two distinct strategies was performed. Covalent immobilization of the purified enzyme form and physical entrapment within barium alginate of whole cells expressing VImD proved to be valid strategies to be investigated. Both techniques proved promising, yet the latter, being more time- and cost-efficient, was extensively optimized. Subsequently, it was incorporated within the SpinChem® rotating packed bed reactor to foster a sustainable and carbon-free production of primary amines. These amines have diverse industrial applications: for instance, iso-butylamine and amylamine serve as food additives, the latter also being used for drilling applications alongside other isomers. Ethylamine, on the other hand, is a key precursor for several herbicides and a stabilizer for chlorine in swimming pools.

Moreover, the scope of enzyme substrates has been expanded to incorporate new amino acids like L-threonine and L-methionine. Together with L-valine, these novel starting materials have been successfully decarboxylated in scaled-up biotransformations. A substantial enhancement in the system productivity was realized with L-valine, achieved

through the reuse of the immobilized biocatalyst. This resulted in an increase in the process Space-Time Yield (STY) by a factor of 6, reaching 2.3 g/L/h, as compared to the system with VImD previously reported in the literature for isobutylamine. (D. I. Kim et al., 2021)

However, throughout the study, an unexpected leaching of the enzyme from the whole cell alginate beads was identified. This discovery prompts further exploration into the potential impact of this phenomenon on the process. Specifically, it raises questions regarding the reusability of the immobilized biocatalyst, which proved to be particularly effective for L-valine. Indeed, L-valine, being a particularly favorable substrate, required significantly shorter biotransformation times, suggesting that the concentration of the immobilized biocatalyst needed for full conversion into isobutylamine is also lower compared to other substrates. This could be the reason why the reusability of the SpinChem reactor was possible over two consecutive cycles, even with the observed leakage of VImD into the reaction solution. It's important to note that the leakage of VImD appears to be time-dependent; however, whether this leakage is influenced by different substrates/products has not yet been explored. Understanding the factors affecting enzyme leakage is critical for optimizing the process to ensure the efficiency and reusability of the immobilized biocatalyst.

6.4 Bibliography

- Abrahamson, M. J., Vázquez-Figueroa, E., Woodall, N. B., Moore, J. C., & Bommarius, A. S. (2012). Development of an Amine Dehydrogenase for Synthesis of Chiral Amines. *Angewandte Chemie International Edition*, 51(16), 3969–3972. <https://doi.org/10.1002/anie.201107813>
- Abrahamson, M. J., Wong, J. W., & Bommarius, A. S. (2013). The Evolution of an Amine Dehydrogenase Biocatalyst for the Asymmetric Production of Chiral Amines. *Advanced Synthesis & Catalysis*, 355(9), 1780–1786. <https://doi.org/10.1002/adsc.201201030>
- Alcántara, A. R., Domínguez de María, P., Littlechild, J. A., Schürmann, M., Sheldon, R. A., & Wohlgemuth, R. (2022). Biocatalysis as Key to Sustainable Industrial Chemistry. *ChemSusChem*, 15(9). <https://doi.org/10.1002/cssc.202102709>
- Almud, J. J., Oliveira, M. A., Kern, A. D., Grishin, N. V., Phillips, M. A., & Hackert, M. L. (2000). Crystal structure of human ornithine decarboxylase at 2.1 Å resolution: structural insights to antizyme binding. *Journal of Molecular Biology*, 295(1), 7–16. <https://doi.org/10.1006/jmbi.1999.3331>
- Andréll, J., Hicks, M. G., Palmer, T., Carpenter, E. P., Iwata, S., & Maher, M. J. (2009). Crystal Structure of the Acid-Induced Arginine Decarboxylase from *Escherichia coli*: Reversible Decamer Assembly Controls Enzyme Activity. *Biochemistry*, 48(18), 3915–3927. <https://doi.org/10.1021/bi900075d>

- Anwar, S., Mohammad, T., Shamsi, A., Queen, A., Parveen, S., Luqman, S., Hasan, G. M., Alamry, K. A., Azum, N., Asiri, A. M., & Hassan, M. I. (2020). Discovery of hordenine as a potential inhibitor of pyruvate dehydrogenase kinase 3: Implication in lung cancer therapy. *Biomedicines*, *8*(5), 32–228.
- Asano, Y., Nakazawa, A., & Endo, K. (1987). Novel phenylalanine dehydrogenases from *Sporosarcina ureae* and *Bacillus sphaericus*. Purification and characterization. *The Journal of Biological Chemistry*, *262*(21), 10346–10354.
<http://www.ncbi.nlm.nih.gov/pubmed/3112142>
- Báez, J. L., Bolívar, F., & Gosset, G. (2001). Determination of 3-deoxy-D- *arabino* -heptulosonate 7-phosphate productivity and yield from glucose in *Escherichia coli* devoid of the glucose phosphotransferase transport system. *Biotechnology and Bioengineering*, *73*(6), 530–535.
<https://doi.org/10.1002/bit.1088>
- Bai, Z., Sun, X., Yu, X., & Li, L. (2019). Chitosan Microbeads as Supporter for *Pseudomonas putida* with Surface Displayed Laccases for Decolorization of Synthetic Dyes. *Applied Sciences*, *9*(1), 138. <https://doi.org/10.3390/app9010138>
- Baker, P. J., Turnbull, A. P., Sedelnikova, S. E., Stillman, T. J., & Rice, D. W. (1995). A role for quaternary structure in the substrate specificity of leucine dehydrogenase. *Structure*, *3*(7), 693–705. [https://doi.org/10.1016/S0969-2126\(01\)00204-0](https://doi.org/10.1016/S0969-2126(01)00204-0)
- Barwell, C. J., Basma, A. N., Lafi, M. A. K., & Leake, L. D. (2011). Deamination of hordenine by monoamine oxidase and its action on vasa deferentia of the rat. *Journal of Pharmacy and Pharmacology*, *41*(6), 421–423. <https://doi.org/10.1111/j.2042-7158.1989.tb06492.x>
- Bell, E. L., Finnigan, W., France, S. P., Green, A. P., Hayes, M. A., Hepworth, L. J., Lovelock, S. L., Niiikura, H., Osuna, S., Romero, E., Ryan, K. S., Turner, N. J., & Flitsch, S. L. (2021). Biocatalysis. *Nature Reviews Methods Primers*, *1*(1), 46. <https://doi.org/10.1038/s43586-021-00044-z>
- Benítez-Mateos, A. I., Roura Padrosa, D., & Paradisi, F. (2022). Multistep enzyme cascades as a route towards green and sustainable pharmaceutical syntheses. *Nature Chemistry*, *14*(5), 489–499. <https://doi.org/10.1038/s41557-022-00931-2>
- Bennett, M., Ducrot, L., Vergne-Vaxelaire, C., & Grogan, G. (2022). Structure and Mutation of the Native Amine Dehydrogenase MATOUAmDH2. *ChemBioChem*, *23*(10).
<https://doi.org/10.1002/cbic.202200136>
- Berridge, M. V., Herst, P. M., & Tan, A. S. (2005). *Tetrazolium dyes as tools in cell biology: New insights into their cellular reduction* (pp. 127–152). [https://doi.org/10.1016/S1387-2656\(05\)11004-7](https://doi.org/10.1016/S1387-2656(05)11004-7)
- Bertelli, M., Kiani, A. K., Paolacci, S., Manara, E., Kurti, D., Dhuli, K., Bushati, V., Miertus, J., Pangallo, D., Baglivo, M., Beccari, T., & Michelini, S. (2020). Hydroxytyrosol: A natural compound with promising pharmacological activities. *Journal of Biotechnology*, *309*, 29–33. <https://doi.org/10.1016/j.jbiotec.2019.12.016>
- Bhatia, S. K., Kim, Y. H., Kim, H. J., Seo, H.-M., Kim, J.-H., Song, H.-S., Sathiyarayanan, G., Park, S.-H., Park, K., & Yang, Y.-H. (2015). Biotransformation of lysine into cadaverine using barium alginate-immobilized *Escherichia coli* overexpressing CadA. *Bioprocess and Biosystems Engineering*, *38*(12), 2315–2322. <https://doi.org/10.1007/s00449-015-1465-9>

- Bloch, D. N., Sandre, M., Ben Zichri, S., Masato, A., Kolusheva, S., Bubacco, L., & Jelinek, R. (2023). Scavenging neurotoxic aldehydes using lysine carbon dots. *Nanoscale Advances*, 5(5), 1356–1367. <https://doi.org/10.1039/D2NA00804A>
- Böhmer, W., Knaus, T., & Mutti, F. G. (2018a). Hydrogen-Borrowing Alcohol Bioamination with Coimmobilized Dehydrogenases. *ChemCatChem*, 10(4), 731–735. <https://doi.org/10.1002/cctc.201701366>
- Böhmer, W., Knaus, T., & Mutti, F. G. (2018b). Hydrogen-Borrowing Alcohol Bioamination with Coimmobilized Dehydrogenases. *ChemCatChem*, 10(4), 731–735. <https://doi.org/10.1002/cctc.201701366>
- Cai, R.-F., Liu, L., Chen, F.-F., Li, A., Xu, J.-H., & Zheng, G.-W. (2020). Reductive Amination of Biobased Levulinic Acid to Unnatural Chiral γ -Amino Acid Using an Engineered Amine Dehydrogenase. *ACS Sustainable Chemistry & Engineering*, 8(46), 17054–17061. <https://doi.org/10.1021/acssuschemeng.0c04647>
- Caparco, A. A., Bommarius, B. R., Bommarius, A. S., & Champion, J. A. (2020). Protein-inorganic calcium-phosphate supraparticles as a robust platform for enzyme co-immobilization. *Biotechnology and Bioengineering*, 117(7), 1979–1989. <https://doi.org/10.1002/bit.27348>
- Caparco, A. A., Pelletier, E., Petit, J. L., Jouenne, A., Bommarius, B. R., Berardinis, V., Zapparucha, A., Champion, J. A., Bommarius, A. S., & Vergne-Vaxelaire, C. (2020). Metagenomic Mining for Amine Dehydrogenase Discovery. *Advanced Synthesis & Catalysis*, 362(12), 2427–2436. <https://doi.org/10.1002/adsc.202000094>
- Capitani, G. (2003). Crystal structure and functional analysis of Escherichia coli glutamate decarboxylase. *The EMBO Journal*, 22(16), 4027–4037. <https://doi.org/10.1093/emboj/cdg403>
- Cerioli, L., Planchestainer, M., Cassidy, J., Tessaro, D., & Paradisi, F. (2015). Characterization of a novel amine transaminase from Halomonas elongata. *Journal of Molecular Catalysis B: Enzymatic*, 120, 141–150. <https://doi.org/10.1016/j.molcatb.2015.07.009>
- Chen, W., Yao, J., Meng, J., Han, W., Tao, Y., Chen, Y., Guo, Y., Shi, G., He, Y., Jin, J.-M., & Tang, S.-Y. (2019). Promiscuous enzymatic activity-aided multiple-pathway network design for metabolic flux rearrangement in hydroxytyrosol biosynthesis. *Nature Communications*, 10(1), 960. <https://doi.org/10.1038/s41467-019-08781-2>
- Claes, L., Janssen, M., & De Vos, D. E. (2019). Organocatalytic Decarboxylation of Amino Acids as a Route to Bio-based Amines and Amides. *ChemCatChem*, 11(17), 4297–4306. <https://doi.org/10.1002/cctc.201900800>
- Contente, M. L., & Paradisi, F. (2018). Self-sustaining closed-loop multienzyme-mediated conversion of amines into alcohols in continuous reactions. *Nature Catalysis*, 1(6), 452–459. <https://doi.org/10.1038/s41929-018-0082-9>
- Cosenza, V. A., Navarro, D. A., & Stortz, C. A. (2011). Usage of α -picoline borane for the reductive amination of carbohydrates. *Arkivoc*, 2011(7), 182–194. <https://doi.org/10.3998/ark.5550190.0012.716>
- Coyle, J. P., Johnson, C., Jensen, J., Farcas, M., Derk, R., Stueckle, T. A., Kornberg, T. G., Rojanasakul, Y., & Rojanasakul, L. W. (2023). Variation in pentose phosphate pathway-

- associated metabolism dictates cytotoxicity outcomes determined by tetrazolium reduction assays. *Scientific Reports*, 13(1), 8220. <https://doi.org/10.1038/s41598-023-35310-5>
- DiCosimo, R., McAuliffe, J., Poulouse, A. J., & Bohlmann, G. (2013). Industrial use of immobilized enzymes. *Chemical Society Reviews*, 42(15), 6437. <https://doi.org/10.1039/c3cs35506c>
- Ducrot, L., Bennett, M., André-Leroux, G., Elisée, E., Marynberg, S., Fossey-Jouenne, A., Zaparucha, A., Grogan, G., & Vergne-Vaxelaire, C. (2022). Expanding the Substrate Scope of Native Amine Dehydrogenases through *In Silico* Structural Exploration and Targeted Protein Engineering. *ChemCatChem*, 14(22). <https://doi.org/10.1002/cctc.202200880>
- Ducrot, L., Bennett, M., Caparco, A. A., Champion, J. A., Bommarius, A. S., Zaparucha, A., Grogan, G., & Vergne-Vaxelaire, C. (2021). Biocatalytic Reductive Amination by Native Amine Dehydrogenases to Access Short Chiral Alkyl Amines and Amino Alcohols. *Frontiers in Catalysis*, 1. <https://doi.org/10.3389/fctls.2021.781284>
- Eliot, A. C., & Kirsch, J. F. (2004). Pyridoxal Phosphate Enzymes: Mechanistic, Structural, and Evolutionary Considerations. *Annual Review of Biochemistry*, 73(1), 383–415. <https://doi.org/10.1146/annurev.biochem.73.011303.074021>
- Eller, K., Henkes, E., Rossbacher, R., & Höke, H. (2000). Amines, Aliphatic. In *Ullmann's Encyclopedia of Industrial Chemistry*. Wiley-VCH Verlag GmbH & Co. KGaA. https://doi.org/10.1002/14356007.a02_001
- Escalante, A., Calderón, R., Valdivia, A., de Anda, R., Hernández, G., Ramírez, O. T., Gosset, G., & Bolívar, F. (2010). Metabolic engineering for the production of shikimic acid in an evolved *Escherichia coli* strain lacking the phosphoenolpyruvate: carbohydrate phosphotransferase system. *Microbial Cell Factories*, 9(1), 21. <https://doi.org/10.1186/1475-2859-9-21>
- Foor, F., Morin, N., & Bostian, K. A. (1993). Production of L-dihydroxyphenylalanine in *Escherichia coli* with the tyrosine phenol-lyase gene cloned from *Erwinia herbicola*. *Applied and Environmental Microbiology*, 59(9), 3070–3075. <https://doi.org/10.1128/aem.59.9.3070-3075.1993>
- Fordjour, E., Adipah, F. K., Zhou, S., Du, G., & Zhou, J. (2019). Metabolic engineering of *Escherichia coli* BL21 (DE3) for de novo production of l-DOPA from d-glucose. *Microbial Cell Factories*, 18(1). <https://doi.org/10.1186/s12934-019-1122-0>
- Franklin, R. D., Whitley, J. A., Caparco, A. A., Bommarius, B. R., Champion, J. A., & Bommarius, A. S. (2021). Continuous production of a chiral amine in a packed bed reactor with co-immobilized amine dehydrogenase and formate dehydrogenase. *Chemical Engineering Journal*, 407, 127065. <https://doi.org/10.1016/j.cej.2020.127065>
- Froidevaux, V., Negrell, C., Caillol, S., Pascault, J.-P., & Boutevin, B. (2016). Biobased Amines: From Synthesis to Polymers; Present and Future. *Chemical Reviews*, 116(22), 14181–14224. <https://doi.org/10.1021/acs.chemrev.6b00486>
- Garg, R. P., Ma, Y., Hoyt, J. C., & Parry, R. J. (2002a). Molecular characterization and analysis of the biosynthetic gene cluster for the azoxy antibiotic valanimycin. *Molecular Microbiology*, 46(2), 505–517. <https://doi.org/10.1046/j.1365-2958.2002.03169.x>

- Garg, R. P., Ma, Y., Hoyt, J. C., & Parry, R. J. (2002b). Molecular characterization and analysis of the biosynthetic gene cluster for the azoxy antibiotic valanimycin. *Molecular Microbiology*, *46*(2), 505–517. <https://doi.org/10.1046/j.1365-2958.2002.03169.x>
- Ghislieri, D., & Turner, N. J. (2014). Biocatalytic Approaches to the Synthesis of Enantiomerically Pure Chiral Amines. *Topics in Catalysis*, *57*(5), 284–300. <https://doi.org/10.1007/s11244-013-0184-1>
- Gianolio, S., Roura Padrosa, D., & Paradisi, F. (2022). Combined chemoenzymatic strategy for sustainable continuous synthesis of the natural product hordenine. *Green Chemistry*, *24*(21), 8434–8440. <https://doi.org/10.1039/D2GC02767D>
- Giardina, G., Montioli, R., Gianni, S., Cellini, B., Paiardini, A., Voltattorni, C. B., & Cutruzzolà, F. (2011). Open conformation of human DOPA decarboxylase reveals the mechanism of PLP addition to Group II decarboxylases. *Proceedings of the National Academy of Sciences*, *108*(51), 20514–20519. <https://doi.org/10.1073/pnas.1111456108>
- Gong, X., Tao, J., Wang, Y., Wu, J., An, J., Meng, J., Wang, X., Chen, Y., & Zou, J. (2021). Total barley maiya alkaloids inhibit prolactin secretion by acting on dopamine D2 receptor and protein kinase A targets. *Journal of Ethnopharmacology*, *273*, 113994. <https://doi.org/10.1016/j.jep.2021.113994>
- Gosset, G., Yong-Xiao, J., & Berry, A. (1996). A direct comparison of approaches for increasing carbon flow to aromatic biosynthesis in *Escherichia coli*. *Journal of Industrial Microbiology*, *17*(1), 47–52. <https://doi.org/10.1007/BF01570148>
- Guisán, JoséM. (1988). Aldehyde-agarose gels as activated supports for immobilization-stabilization of enzymes. *Enzyme and Microbial Technology*, *10*(6), 375–382. [https://doi.org/10.1016/0141-0229\(88\)90018-X](https://doi.org/10.1016/0141-0229(88)90018-X)
- Guo, K., Ji, C., & Li, L. (2007). Stable-Isotope Dimethylation Labeling Combined with LC–ESI MS for Quantification of Amine-Containing Metabolites in Biological Samples. *Analytical Chemistry*, *79*(22), 8631–8638. <https://doi.org/10.1021/ac0704356>
- Guo, Z., Yan, N., & Lapkin, A. A. (2019). Towards circular economy: integration of bio-waste into chemical supply chain. *Current Opinion in Chemical Engineering*, *26*, 148–156. <https://doi.org/10.1016/j.coche.2019.09.010>
- Gupte, A. P., Basaglia, M., Casella, S., & Favaro, L. (2022). Rice waste streams as a promising source of biofuels: feedstocks, biotechnologies and future perspectives. *Renewable and Sustainable Energy Reviews*, *167*, 112673. <https://doi.org/10.1016/j.rser.2022.112673>
- Gut, H., Pennacchietti, E., John, R. A., Bossa, F., Capitani, G., De Biase, D., & Grütter, M. G. (2006). *Escherichia coli* acid resistance: pH-sensing, activation by chloride and autoinhibition in GadB. *The EMBO Journal*, *25*(11), 2643–2651. <https://doi.org/10.1038/sj.emboj.7601107>
- H. Orrego, A., Romero-Fernández, M., Millán-Linares, M., Yust, M., Guisán, J., & Rocha-Martin, J. (2018). Stabilization of Enzymes by Multipoint Covalent Attachment on Aldehyde-Supports: 2-Picoline Borane as an Alternative Reducing Agent. *Catalysts*, *8*(8), 333. <https://doi.org/10.3390/catal8080333>

- Hamid, M. H. S. A., Slatford, P. A., & Williams, J. M. J. (2007). Borrowing Hydrogen in the Activation of Alcohols. *Advanced Synthesis & Catalysis*, 349(10), 1555–1575. <https://doi.org/10.1002/adsc.200600638>
- Hapke, H. J., & Strathmann, W. (1995). [Pharmacological effects of hordenine]. *DTW. Deutsche Tierärztliche Wochenschrift*, 102(6), 228–232. <http://www.ncbi.nlm.nih.gov/pubmed/8582256>
- Harper, B. A., Barbut, S., Lim, L.-T., & Marcone, M. F. (2014). Effect of Various Gelling Cations on the Physical Properties of “Wet” Alginate Films. *Journal of Food Science*, 79(4), E562–E567. <https://doi.org/10.1111/1750-3841.12376>
- Heckmann, C. M., Gourlay, L. J., Dominguez, B., & Paradisi, F. (2020). An (R)-Selective Transaminase From *Thermomyces stellatus*: Stabilizing the Tetrameric Form. *Frontiers in Bioengineering and Biotechnology*, 8. <https://doi.org/10.3389/fbioe.2020.00707>
- Heffter, A. (1898). Ueber Pellote. *Archiv Für Experimentelle Pathologie Und Pharmakologie*, 40(5–6), 385–429. <https://doi.org/10.1007/BF01825267>
- Heydari, M., Ohshima, T., Nunoura-Kominato, N., & Sakuraba, H. (2004). Highly Stable Lysine 6-Dehydrogenase from the Thermophile *Geobacillus stearothermophilus* Isolated from a Japanese Hot Spring: Characterization, Gene Cloning and Sequencing, and Expression. *Applied and Environmental Microbiology*, 70(2), 937–942. <https://doi.org/10.1128/AEM.70.2.937-942.2004>
- Holbrook, O. T., Molligoda, B., Bushell, K. N., & Gobrogge, K. L. (2022). Behavioral consequences of the downstream products of ethanol metabolism involved in alcohol use disorder. *Neuroscience & Biobehavioral Reviews*, 133, 104501. <https://doi.org/10.1016/j.neubiorev.2021.12.024>
- Houwman, J. A., Knaus, T., Costa, M., & Mutti, F. G. (2019). Efficient synthesis of enantiopure amines from alcohols using resting *E. coli* cells and ammonia. *Green Chemistry*, 21(14), 3846–3857. <https://doi.org/10.1039/C9GC01059A>
- Huang, J., Mei, L., Wu, H., & Lin, D. (2007). Biosynthesis of γ -aminobutyric acid (GABA) using immobilized whole cells of *Lactobacillus brevis*. *World Journal of Microbiology and Biotechnology*, 23(6), 865–871. <https://doi.org/10.1007/s11274-006-9311-5>
- Huang, R., Chen, H., Zhong, C., Kim, J. E., & Zhang, Y.-H. P. (2016). High-Throughput Screening of Coenzyme Preference Change of Thermophilic 6-Phosphogluconate Dehydrogenase from NADP⁺ to NAD⁺. *Scientific Reports*, 6(1), 32644. <https://doi.org/10.1038/srep32644>
- Hwang, E. T., & Lee, S. (2019). Multienzymatic Cascade Reactions via Enzyme Complex by Immobilization. *ACS Catalysis*, 9(5), 4402–4425. <https://doi.org/10.1021/acscatal.8b04921>
- Jackson, D. M., Ashley, R. L., Brownfield, C. B., Morrison, D. R., & Morrison, R. W. (2015). Rapid Conventional and Microwave-Assisted Decarboxylation of L-Histidine and Other Amino Acids via Organocatalysis with R-Carvone Under Superheated Conditions. *Synthetic Communications*, 45(23), 2691–2700. <https://doi.org/10.1080/00397911.2015.1100745>
- Jansonius, J. N. (1998). Structure, evolution and action of vitamin B6-dependent enzymes. *Current Opinion in Structural Biology*, 8(6), 759–769. [https://doi.org/10.1016/S0959-440X\(98\)80096-1](https://doi.org/10.1016/S0959-440X(98)80096-1)

- Jeon, H., Yoon, S., Ahsan, M., Sung, S., Kim, G.-H., Sundaramoorthy, U., Rhee, S.-K., & Yun, H. (2017). The Kinetic Resolution of Racemic Amines Using a Whole-Cell Biocatalyst Co-Expressing Amine Dehydrogenase and NADH Oxidase. *Catalysts*, 7(9), 251. <https://doi.org/10.3390/catal7090251>
- Jiang, M., Xu, G., Ni, J., Zhang, K., Dong, J., Han, R., & Ni, Y. (2019a). Improving Soluble Expression of Tyrosine Decarboxylase from *Lactobacillus brevis* for Tyramine Synthesis with High Total Turnover Number. *Applied Biochemistry and Biotechnology*, 188(2), 436–449. <https://doi.org/10.1007/s12010-018-2925-x>
- Jiang, M., Xu, G., Ni, J., Zhang, K., Dong, J., Han, R., & Ni, Y. (2019b). Improving Soluble Expression of Tyrosine Decarboxylase from *Lactobacillus brevis* for Tyramine Synthesis with High Total Turnover Number. *Applied Biochemistry and Biotechnology*, 188(2), 436–449. <https://doi.org/10.1007/s12010-018-2925-x>
- Jones, J. A., Collins, S. M., Vernacchio, V. R., Lachance, D. M., & Koffas, M. A. G. (2016). Optimization of naringenin and *p*-coumaric acid hydroxylation using the native *E. coli* hydroxylase complex, HpaBC. *Biotechnology Progress*, 32(1), 21–25. <https://doi.org/10.1002/btpr.2185>
- Khorsand, F., Murphy, C. D., Whitehead, A. J., & Engel, P. C. (2017). Biocatalytic stereoinversion of *p*-para-bromophenylalanine in a one-pot three-enzyme reaction. *Green Chemistry*, 19(2), 503–510. <https://doi.org/10.1039/C6GC01922F>
- Kim, Baritugo, Oh, Kang, Jung, Jang, Song, Kim, Lee, Hwang, Park, Park, & Joo. (2019). High-Level Conversion of l-lysine into Cadaverine by *Escherichia coli* Whole Cell Biocatalyst Expressing *Hafnia alvei* l-lysine Decarboxylase. *Polymers*, 11(7), 1184. <https://doi.org/10.3390/polym11071184>
- Kim, D. I., Chae, T. U., Kim, H. U., Jang, W. D., & Lee, S. Y. (2021). Microbial production of multiple short-chain primary amines via retrobiosynthesis. *Nature Communications*, 12(1), 173. <https://doi.org/10.1038/s41467-020-20423-6>
- Kim, S.-C., Lee, J.-H., Kim, M.-H., Lee, J.-A., Kim, Y. B., Jung, E., Kim, Y.-S., Lee, J., & Park, D. (2013). Hordenine, a single compound produced during barley germination, inhibits melanogenesis in human melanocytes. *Food Chemistry*, 141(1), 174–181. <https://doi.org/10.1016/j.foodchem.2013.03.017>
- Knaus, T., Böhmer, W., & Mutti, F. G. (2017). Amine dehydrogenases: efficient biocatalysts for the reductive amination of carbonyl compounds. *Green Chemistry*, 19(2), 453–463. <https://doi.org/10.1039/C6GC01987K>
- Knowles, W. S. (n.d.). Asymmetric Hydrogenations—The MonsantoL-Dopa Process. In *Asymmetric Catalysis on Industrial Scale* (pp. 21–38). Wiley-VCH Verlag GmbH & Co. KGaA. <https://doi.org/10.1002/3527602151.ch1>
- Komori, H., Nitta, Y., Ueno, H., & Higuchi, Y. (2012). Structural Study Reveals That Ser-354 Determines Substrate Specificity on Human Histidine Decarboxylase. *Journal of Biological Chemistry*, 287(34), 29175–29183. <https://doi.org/10.1074/jbc.M112.381897>
- Kugler, P. (1979). A gel-sandwich technique for the qualitative and quantitative determination of dehydrogenases in the enzyme histochemistry. *Histochemistry*, 60(3), 265–293. <https://doi.org/10.1007/BF00500656>

- Kumar, R., Vikramachakravarthi, D., & Pal, P. (2014). Production and purification of glutamic acid: A critical review towards process intensification. *Chemical Engineering and Processing: Process Intensification*, *81*, 59–71. <https://doi.org/10.1016/j.cep.2014.04.012>
- Kurpejović, E., Wendisch, V. F., & Sariyar Akbulut, B. (2021). Tyrosinase-based production of L-DOPA by *Corynebacterium glutamicum*. *Applied Microbiology and Biotechnology*, *105*(24), 9103–9111. <https://doi.org/10.1007/s00253-021-11681-5>
- Lapponi, M. J., Méndez, M. B., Trelles, J. A., & Rivero, C. W. (2022). Cell immobilization strategies for biotransformations. *Current Opinion in Green and Sustainable Chemistry*, *33*, 100565. <https://doi.org/10.1016/j.cogsc.2021.100565>
- Lawrence, S. A. (2004). *Amines: synthesis, properties and applications*. Cambridge University Press.
- Lee, J., Michael, A. J., Martynowski, D., Goldsmith, E. J., & Phillips, M. A. (2007). Phylogenetic Diversity and the Structural Basis of Substrate Specificity in the β/α -Barrel Fold Basic Amino Acid Decarboxylases. *Journal of Biological Chemistry*, *282*(37), 27115–27125. <https://doi.org/10.1074/jbc.M704066200>
- Lee, S. Y., Kim, H. U., Chae, T. U., Cho, J. S., Kim, J. W., Shin, J. H., Kim, D. I., Ko, Y.-S., Jang, W. D., & Jang, Y.-S. (2019). A comprehensive metabolic map for production of bio-based chemicals. *Nature Catalysis*, *2*(1), 18–33. <https://doi.org/10.1038/s41929-018-0212-4>
- Leuchtenberger, W., Huthmacher, K., & Drauz, K. (2005). Biotechnological production of amino acids and derivatives: current status and prospects. *Applied Microbiology and Biotechnology*, *69*(1), 1–8. <https://doi.org/10.1007/s00253-005-0155-y>
- Li, N., Chou, H., & Xu, Y. (2016). Improved cadaverine production from mutant *Klebsiella oxytoca* lysine decarboxylase. *Engineering in Life Sciences*, *16*(3), 299–305. <https://doi.org/10.1002/elsc.201500037>
- Liu, G., Zhou, N., Zhang, M., Li, S., Tian, Q., Chen, J., Chen, B., Wu, Y., & Yao, S. (2010). Hydrophobic solvent induced phase transition extraction to extract drugs from plasma for high performance liquid chromatography–mass spectrometric analysis. *Journal of Chromatography A*, *1217*(3), 243–249. <https://doi.org/10.1016/j.chroma.2009.11.037>
- Liu, J., Pang, B. Q. W., Adams, J. P., Snajdrova, R., & Li, Z. (2017). Coupled Immobilized Amine Dehydrogenase and Glucose Dehydrogenase for Asymmetric Synthesis of Amines by Reductive Amination with Cofactor Recycling. *ChemCatChem*, *9*(3), 425–431. <https://doi.org/10.1002/cctc.201601446>
- Liu, Y., Liu, P., Gao, S., Wang, Z., Luan, P., González-Sabín, J., & Jiang, Y. (2021). Construction of chemoenzymatic cascade reactions for bridging chemocatalysis and Biocatalysis: Principles, strategies and prospective. *Chemical Engineering Journal*, *420*, 127659. <https://doi.org/10.1016/j.cej.2020.127659>
- Ma, J., Wang, S., Huang, X., Geng, P., Wen, C., Zhou, Y., Yu, L., & Wang, X. (2015). Validated UPLC–MS/MS method for determination of hordenine in rat plasma and its application to pharmacokinetic study. *Journal of Pharmaceutical and Biomedical Analysis*, *111*, 131–137. <https://doi.org/10.1016/j.jpba.2015.03.032>

- Mateo, C., Grazú, V., Pessela, B. C. C., Montes, T., Palomo, J. M., Torres, R., López-Gallego, F., Fernández-Lafuente, R., & Guisán, J. M. (2007a). Advances in the design of new epoxy supports for enzyme immobilization–stabilization. *Biochemical Society Transactions*, 35(6), 1593–1601. <https://doi.org/10.1042/BST0351593>
- Mateo, C., Grazú, V., Pessela, B. C. C., Montes, T., Palomo, J. M., Torres, R., López-Gallego, F., Fernández-Lafuente, R., & Guisán, J. M. (2007b). Advances in the design of new epoxy supports for enzyme immobilization–stabilization. *Biochemical Society Transactions*, 35(6), 1593–1601. <https://doi.org/10.1042/BST0351593>
- Mayol, O., Bastard, K., Beloti, L., Frese, A., Turkenburg, J. P., Petit, J.-L., Mariage, A., Debard, A., Pellouin, V., Perret, A., de Berardinis, V., Zaparucha, A., Grogan, G., & Vergne-Vaxelaire, C. (2019a). A family of native amine dehydrogenases for the asymmetric reductive amination of ketones. *Nature Catalysis*, 2(4), 324–333. <https://doi.org/10.1038/s41929-019-0249-z>
- Mayol, O., Bastard, K., Beloti, L., Frese, A., Turkenburg, J. P., Petit, J.-L., Mariage, A., Debard, A., Pellouin, V., Perret, A., de Berardinis, V., Zaparucha, A., Grogan, G., & Vergne-Vaxelaire, C. (2019b). A family of native amine dehydrogenases for the asymmetric reductive amination of ketones. *Nature Catalysis*, 2(4), 324–333. <https://doi.org/10.1038/s41929-019-0249-z>
- Meyer, E. (1982). Separation of two distinct S-adenosylmethionine dependent N-methyltransferases involved in hordenine biosynthesis in *Hordeum vulgare*. *Plant Cell Reports*, 1(6), 236–239. <https://doi.org/10.1007/BF00272627>
- Mi, J., Liu, S., Du, Y., Qi, H., & Zhang, L. (2022). Cofactor self-sufficient by co-immobilization of pyridoxal 5'-phosphate and lysine decarboxylase for cadaverine production. *Bioresource Technology Reports*, 17, 100939. <https://doi.org/10.1016/j.biteb.2021.100939>
- Montgomery, S. L., Mangas-Sanchez, J., Thompson, M. P., Aleku, G. A., Dominguez, B., & Turner, N. J. (2017). Direct Alkylation of Amines with Primary and Secondary Alcohols through Biocatalytic Hydrogen Borrowing. *Angewandte Chemie*, 129(35), 10627–10630. <https://doi.org/10.1002/ange.201705848>
- Mørch, Y. A., Donati, I., Strand, B. L., & Skjåk-Bræk, G. (2006). Effect of Ca²⁺, Ba²⁺, and Sr²⁺ on Alginate Microbeads. *Biomacromolecules*, 7(5), 1471–1480. <https://doi.org/10.1021/bm060010d>
- Muñoz, A. J., Hernández-Chávez, G., De Anda, R., Martínez, A., Bolívar, F., & Gosset, G. (2011). Metabolic engineering of *Escherichia coli* for improving l-3,4-dihydroxyphenylalanine (l-DOPA) synthesis from glucose. *Journal of Industrial Microbiology and Biotechnology*, 38(11), 1845–1852. <https://doi.org/10.1007/s10295-011-0973-0>
- Mutti, F. G., & Knaus, T. (2021). Enzymes Applied to the Synthesis of Amines. In *Biocatalysis for Practitioners* (pp. 143–180). Wiley. <https://doi.org/10.1002/9783527824465.ch6>
- Mutti, F. G., Knaus, T., Scrutton, N. S., Breuer, M., & Turner, N. J. (2015). Conversion of alcohols to enantiopure amines through dual-enzyme hydrogen-borrowing cascades. *Science*, 349(6255), 1525–1529. <https://doi.org/10.1126/science.aac9283>
- Nakai, T., Nakagawa, N., Maoka, N., Masui, R., Kuramitsu, S., & Kamiya, N. (2005). Structure of P-protein of the glycine cleavage system: implications for nonketotic hyperglycinemia. *The EMBO Journal*, 24(8), 1523–1536. <https://doi.org/10.1038/sj.emboj.7600632>

- Narisetty, V., Cox, R., Bommareddy, R., Agrawal, D., Ahmad, E., Pant, K. K., Chandel, A. K., Bhatia, S. K., Kumar, D., Binod, P., Gupta, V. K., & Kumar, V. (2022). Valorisation of xylose to renewable fuels and chemicals, an essential step in augmenting the commercial viability of lignocellulosic biorefineries. *Sustainable Energy & Fuels*, *6*(1), 29–65. <https://doi.org/10.1039/D1SE00927C>
- Nasri, M. (2017a). *Protein Hydrolysates and Biopeptides* (pp. 109–159). <https://doi.org/10.1016/bs.afnr.2016.10.003>
- Nasri, M. (2017b). *Protein Hydrolysates and Biopeptides* (pp. 109–159). <https://doi.org/10.1016/bs.afnr.2016.10.003>
- Natte, K., Neumann, H., Jagadeesh, R. v., & Beller, M. (2017). Convenient iron-catalyzed reductive aminations without hydrogen for selective synthesis of N-methylamines. *Nature Communications*, *8*(1), 1344. <https://doi.org/10.1038/s41467-017-01428-0>
- Nguyen, N. H., Truong-Thi, N.-H., Nguyen, D. T. D., Ching, Y. C., Huynh, N. T., & Nguyen, D. H. (2022). Non-ionic surfactants As co-templates to control the mesopore diameter of hollow mesoporous silica nanoparticles for drug delivery applications. *Colloids and Surfaces A: Physicochemical and Engineering Aspects*, *655*, 130218. <https://doi.org/10.1016/j.colsurfa.2022.130218>
- Ohta, H., Murakami, Y., Takebe, Y., Murasaki, K., Oshima, K., Yoshihara, H., & Morimura, S. (2020). Ñ-Methyltyramine, a Gastrin-releasing Factor in Beer, and Structurally Related Compounds as Agonists for Human Trace Amine-associated Receptor 1. *Food Science and Technology Research*, *26*(2), 313–317. <https://doi.org/10.3136/fstr.26.313>
- PARADISI, F., COLLINS, S., MAGUIRE, A., & ENGEL, P. (2007). Phenylalanine dehydrogenase mutants: Efficient biocatalysts for synthesis of non-natural phenylalanine derivatives. *Journal of Biotechnology*, *128*(2), 408–411. <https://doi.org/10.1016/j.jbiotec.2006.08.008>
- Park, J.-Y., Choi, M.-J., Yu, H., Choi, Y., Park, K.-M., & Chang, P.-S. (2022). Multi-functional behavior of food emulsifier erythorbyl laurate in different colloidal conditions of homogeneous oil-in-water emulsion system. *Colloids and Surfaces A: Physicochemical and Engineering Aspects*, *636*, 128127. <https://doi.org/10.1016/j.colsurfa.2021.128127>
- Park, S. H., Soetyono, F., & Kim, H. K. (2017). Cadaverine Production by Using Cross-Linked Enzyme Aggregate of Escherichia coli Lysine Decarboxylase. *Journal of Microbiology and Biotechnology*, *27*(2), 289–296. <https://doi.org/10.4014/jmb.1608.08033>
- Patil, M. D., Grogan, G., Bommarius, A., & Yun, H. (2018). Oxidoreductase-Catalyzed Synthesis of Chiral Amines. *ACS Catalysis*, *8*(12), 10985–11015. <https://doi.org/10.1021/acscatal.8b02924>
- Patil, M. D., Yoon, S., Jeon, H., Khobragade, T. P., Sarak, S., Pagar, A. D., Won, Y., & Yun, H. (2019). Kinetic Resolution of Racemic Amines to Enantiopure (S)-amines by a Biocatalytic Cascade Employing Amine Dehydrogenase and Alanine Dehydrogenase. *Catalysts*, *9*(7), 600. <https://doi.org/10.3390/catal9070600>
- Payne, J. T., Valentic, T. R., & Smolke, C. D. (2021). Complete biosynthesis of the bisbenzylisoquinoline alkaloids guattegaumerine and berbamunine in yeast. *Proceedings of the National Academy of Sciences*, *118*(51). <https://doi.org/10.1073/pnas.2112520118>

- Pelckmans, M., Renders, T., Van de Vyver, S., & Sels, B. F. (2017). Bio-based amines through sustainable heterogeneous catalysis. *Green Chemistry*, *19*(22), 5303–5331. <https://doi.org/10.1039/C7GC02299A>
- Pilkington, R. L., Dallaston, M. A., Savage, G. P., Williams, C. M., & Polyzos, A. (2021). Enone-promoted decarboxylation of *trans*-4-hydroxy-*l*-proline in flow: a side-by-side comparison to batch. *Reaction Chemistry & Engineering*, *6*(3), 486–493. <https://doi.org/10.1039/D0RE00442A>
- Planchestainer, M., Hegarty, E., Heckmann, C. M., Gourlay, L. J., & Paradisi, F. (2019). Widely applicable background depletion step enables transaminase evolution through solid-phase screening. *Chemical Science*, *10*(23), 5952–5958. <https://doi.org/10.1039/C8SC05712E>
- Prieto, M. A., & Garcia, J. L. (1994). Molecular characterization of 4-hydroxyphenylacetate 3-hydroxylase of *Escherichia coli*. A two-protein component enzyme. *Journal of Biological Chemistry*, *269*(36), 22823–22829. [https://doi.org/10.1016/S0021-9258\(17\)31719-2](https://doi.org/10.1016/S0021-9258(17)31719-2)
- Pyne, M. E., Kevvai, K., Grewal, P. S., Narcross, L., Choi, B., Bourgeois, L., Dueber, J. E., & Martin, V. J. J. (2020). A yeast platform for high-level synthesis of tetrahydroisoquinoline alkaloids. *Nature Communications*, *11*(1), 3337. <https://doi.org/10.1038/s41467-020-17172-x>
- Quaglia, D., Irwin, J. A., & Paradisi, F. (2012a). Horse Liver Alcohol Dehydrogenase: New Perspectives for an Old Enzyme. *Molecular Biotechnology*, *52*(3), 244–250. <https://doi.org/10.1007/s12033-012-9542-7>
- Quaglia, D., Irwin, J. A., & Paradisi, F. (2012b). Horse Liver Alcohol Dehydrogenase: New Perspectives for an Old Enzyme. *Molecular Biotechnology*, *52*(3), 244–250. <https://doi.org/10.1007/s12033-012-9542-7>
- Ray, S. S., Bonanno, J. B., Rajashankar, K. R., Pinho, M. G., He, G., De Lencastre, H., Tomasz, A., & Burley, S. K. (2002). Cocrystal Structures of Diaminopimelate Decarboxylase. *Structure*, *10*(11), 1499–1508. [https://doi.org/10.1016/S0969-2126\(02\)00880-8](https://doi.org/10.1016/S0969-2126(02)00880-8)
- Reetz, M. T. (2013). Biocatalysis in Organic Chemistry and Biotechnology: Past, Present, and Future. *Journal of the American Chemical Society*, *135*(34), 12480–12496. <https://doi.org/10.1021/ja405051f>
- Roschangar, F., Sheldon, R. A., & Senanayake, C. H. (2015). Overcoming barriers to green chemistry in the pharmaceutical industry – the Green Aspiration Level™ concept. *Green Chemistry*, *17*(2), 752–768. <https://doi.org/10.1039/C4GC01563K>
- Ruhaak, L. R., Steenvoorden, E., Koeleman, C. A. M., Deelder, A. M., & Wuhrer, M. (2010). 2-Picoline-borane: A non-toxic reducing agent for oligosaccharide labeling by reductive amination. *Proteomics*, *10*(12), 2330–2336. <https://doi.org/10.1002/pmic.200900804>
- Sagong, H.-Y., Son, H. F., Kim, S., Kim, Y.-H., Kim, I.-K., & Kim, K.-J. (2016). Crystal Structure and Pyridoxal 5-Phosphate Binding Property of Lysine Decarboxylase from *Selenomonas ruminantium*. *PLOS ONE*, *11*(11), e0166667. <https://doi.org/10.1371/journal.pone.0166667>
- Said, A. A. E., Ali, T. F. S., Attia, E. Z., Ahmed, A.-S. F., Shehata, A. H., Abdelmohsen, U. R., & Fouad, M. A. (2021). Antidepressant potential of *Mesembryanthemum cordifolium* roots

- assisted by metabolomic analysis and virtual screening. *Natural Product Research*, 35(23), 5493–5497. <https://doi.org/10.1080/14786419.2020.1788019>
- SANDMEIER, E., HALE, T. I., & CHRISTEN, P. (1994a). Multiple evolutionary origin of pyridoxal-5'-phosphate-dependent amino acid decarboxylases. *European Journal of Biochemistry*, 221(3), 997–1002. <https://doi.org/10.1111/j.1432-1033.1994.tb18816.x>
- SANDMEIER, E., HALE, T. I., & CHRISTEN, P. (1994b). Multiple evolutionary origin of pyridoxal-5'-phosphate-dependent amino acid decarboxylases. *European Journal of Biochemistry*, 221(3), 997–1002. <https://doi.org/10.1111/j.1432-1033.1994.tb18816.x>
- Sato, S., Sakamoto, T., Miyazawa, E., & Kikugawa, Y. (2004). One-pot reductive amination of aldehydes and ketones with α -picoline-borane in methanol, in water, and in neat conditions. *Tetrahedron*, 60(36), 7899–7906. <https://doi.org/10.1016/j.tet.2004.06.045>
- Schoenmakers, H., & Spiegel, L. (2014). Laboratory Distillation and Scale-up. In *Distillation* (pp. 319–339). Elsevier. <https://doi.org/10.1016/B978-0-12-386878-7.00010-3>
- Seah, S. Y. K., Britton, K. L., Rice, D. W., Asano, Y., & Engel, P. C. (2002). Single Amino Acid Substitution in *Bacillus sphaericus* Phenylalanine Dehydrogenase Dramatically Increases Its Discrimination between Phenylalanine and Tyrosine Substrates. *Biochemistry*, 41(38), 11390–11397. <https://doi.org/10.1021/bi020196a>
- Seah, S. Y. K., Linda Britton, K., Baker, P. J., Rice, D. W., Asano, Y., & Engel, P. C. (1995). Alteration in relative activities of phenylalanine dehydrogenase towards different substrates by site-directed mutagenesis. *FEBS Letters*, 370(1–2), 93–96. [https://doi.org/10.1016/0014-5793\(95\)00804-I](https://doi.org/10.1016/0014-5793(95)00804-I)
- Sen, K. Y., & Baidurah, S. (2021). Renewable biomass feedstocks for production of sustainable biodegradable polymer. *Current Opinion in Green and Sustainable Chemistry*, 27, 100412. <https://doi.org/10.1016/j.cogsc.2020.100412>
- Sharma, M., Mangas-Sanchez, J., Turner, N. J., & Grogan, G. (2017). NAD(P)H-Dependent Dehydrogenases for the Asymmetric Reductive Amination of Ketones: Structure, Mechanism, Evolution and Application. *Advanced Synthesis & Catalysis*, 359(12), 2011–2025. <https://doi.org/10.1002/adsc.201700356>
- Sheldon, R. A., Basso, A., & Brady, D. (2021). New frontiers in enzyme immobilisation: robust biocatalysts for a circular bio-based economy. *Chemical Society Reviews*, 50(10), 5850–5862. <https://doi.org/10.1039/D1CS00015B>
- Sheldon, R. A., & Brady, D. (2019). Broadening the Scope of Biocatalysis in Sustainable Organic Synthesis. *ChemSusChem*, 12(13), 2859–2881. <https://doi.org/10.1002/cssc.201900351>
- Sheldon, R. A., & Woodley, J. M. (2018). Role of Biocatalysis in Sustainable Chemistry. *Chemical Reviews*, 118(2), 801–838. <https://doi.org/10.1021/acs.chemrev.7b00203>
- Sommer, T., Göen, T., Budnik, N., & Pischetsrieder, M. (2020). Absorption, Biokinetics, and Metabolism of the Dopamine D2 Receptor Agonist Hordenine (N, N-Dimethyltyramine) after Beer Consumption in Humans. *Journal of Agricultural and Food Chemistry*, 68(7), 1998–2006. <https://doi.org/10.1021/acs.jafc.9b06029>

- Song, W., Chen, X., Wu, J., Xu, J., Zhang, W., Liu, J., Chen, J., & Liu, L. (2020). Biocatalytic derivatization of proteinogenic amino acids for fine chemicals. *Biotechnology Advances*, *40*, 107496. <https://doi.org/10.1016/j.biotechadv.2019.107496>
- Stano, J., Nemeč, P., Weissová, K., Kovács, P., Kákoniová, D., & Lisková, D. (1995). Decarboxylation of l-tyrosine and l-dopa by immobilized cells of *Papaver somniferum*. *Phytochemistry*, *38*(4), 859–860. [https://doi.org/10.1016/0031-9422\(94\)00768-0](https://doi.org/10.1016/0031-9422(94)00768-0)
- Stockert, J. C., Horobin, R. W., Colombo, L. L., & Blázquez-Castro, A. (2018). Tetrazolium salts and formazan products in Cell Biology: Viability assessment, fluorescence imaging, and labeling perspectives. *Acta Histochemica*, *120*(3), 159–167. <https://doi.org/10.1016/j.acthis.2018.02.005>
- Su, Y., Liu, Y., He, D., Hu, G., Wang, H., Ye, B., He, Y., Gao, X., & Liu, D. (2022). Hordenine inhibits neuroinflammation and exerts neuroprotective effects via inhibiting NF- κ B and MAPK signaling pathways in vivo and in vitro. *International Immunopharmacology*, *108*, 108694. <https://doi.org/10.1016/j.intimp.2022.108694>
- Surwase, S. N., Patil, S. A., Apine, O. A., & Jadhav, J. P. (2012). Efficient Microbial Conversion of l-Tyrosine to l-DOPA by *Brevundimonas* sp. SGJ. *Applied Biochemistry and Biotechnology*, *167*(5), 1015–1028. <https://doi.org/10.1007/s12010-012-9564-4>
- Tang, Y. Q., & Weng, N. (2013). Salting-out assisted liquid–liquid extraction for bioanalysis. *Bioanalysis*, *5*(12), 1583–1598. <https://doi.org/10.4155/bio.13.117>
- Teng, Y., Scott, E. L., van Zeeland, A. N. T., & Sanders, J. P. M. (2011). The use of l-lysine decarboxylase as a means to separate amino acids by electrodialysis. *Green Chemistry*, *13*(3), 624. <https://doi.org/10.1039/c0gc00611d>
- Thompson, M. P., Derrington, S. R., Heath, R. S., Porter, J. L., Mangas-Sanchez, J., Devine, P. N., Truppo, M. D., & Turner, N. J. (2019). A generic platform for the immobilisation of engineered biocatalysts. *Tetrahedron*, *75*(3), 327–334. <https://doi.org/10.1016/j.tet.2018.12.004>
- Thompson, M. P., & Turner, N. J. (2017a). Two-Enzyme Hydrogen-Borrowing Amination of Alcohols Enabled by a Cofactor-Switched Alcohol Dehydrogenase. *ChemCatChem*, *9*(20), 3833–3836. <https://doi.org/10.1002/cctc.201701092>
- Thompson, M. P., & Turner, N. J. (2017b). Two-Enzyme Hydrogen-Borrowing Amination of Alcohols Enabled by a Cofactor-Switched Alcohol Dehydrogenase. *ChemCatChem*, *9*(20), 3833–3836. <https://doi.org/10.1002/cctc.201701092>
- Tolbert, W. D., Graham, D. E., White, R. H., & Ealick, S. E. (2003). Pyruvoyl-Dependent Arginine Decarboxylase from *Methanococcus jannaschii*. *Structure*, *11*(3), 285–294. [https://doi.org/10.1016/S0969-2126\(03\)00026-1](https://doi.org/10.1016/S0969-2126(03)00026-1)
- Truong, C. C., Mishra, D. K., & Suh, Y. (2023). Recent Catalytic Advances on the Sustainable Production of Primary Furanic Amines from the One-Pot Reductive Amination of 5-Hydroxymethylfurfural. *ChemSusChem*, *16*(1). <https://doi.org/10.1002/cssc.202201846>
- Tseliou, V., Knaus, T., Masman, M. F., Corrado, M. L., & Mutti, F. G. (2019). Generation of amine dehydrogenases with increased catalytic performance and substrate scope from ϵ -

- deaminating L-Lysine dehydrogenase. *Nature Communications*, *10*(1), 3717.
<https://doi.org/10.1038/s41467-019-11509-x>
- Tseliou, V., Knaus, T., Vilím, J., Masman, M. F., & Mutti, F. G. (2020). Kinetic Resolution of Racemic Primary Amines Using *Geobacillus stearothermophilus* Amine Dehydrogenase Variant. *ChemCatChem*, *12*(8), 2184–2188. <https://doi.org/10.1002/cctc.201902085>
- Tsukatani, T., Suenaga, H., Higuchi, T., Akao, T., Ishiyama, M., Ezoe, K., & Matsumoto, K. (2008). Colorimetric cell proliferation assay for microorganisms in microtiter plate using water-soluble tetrazolium salts. *Journal of Microbiological Methods*, *75*(1), 109–116.
<https://doi.org/10.1016/j.mimet.2008.05.016>
- Viejo, C. G., Villarreal-Lara, R., Torrico, D. D., Rodríguez-Velazco, Y. G., Escobedo-Avellaneda, Z., Ramos-Parra, P. A., Mandal, R., Singh, A. P., Hernández-Brenes, C., & Fuentes, S. (2020). Beer and consumer response using biometrics: Associations assessment of beer compounds and elicited emotions. *Foods*, *9*(6), 821.
- Vitaku, E., Smith, D. T., & Njardarson, J. T. (2014). Analysis of the Structural Diversity, Substitution Patterns, and Frequency of Nitrogen Heterocycles among U.S. FDA Approved Pharmaceuticals. *Journal of Medicinal Chemistry*, *57*(24), 10257–10274.
<https://doi.org/10.1021/jm501100b>
- Wang, M., Khan, M. A., Mohsin, I., Wicks, J., Ip, A. H., Sumon, K. Z., Dinh, C.-T., Sargent, E. H., Gates, I. D., & Kibria, M. G. (2021). Can sustainable ammonia synthesis pathways compete with fossil-fuel based Haber–Bosch processes? *Energy & Environmental Science*, *14*(5), 2535–2548. <https://doi.org/10.1039/D0EE03808C>
- Wang, Q., Xin, Y., Zhang, F., Feng, Z., Fu, J., Luo, L., & Yin, Z. (2011). Enhanced γ -aminobutyric acid-forming activity of recombinant glutamate decarboxylase (gadA) from *Escherichia coli*. *World Journal of Microbiology and Biotechnology*, *27*(3), 693–700.
<https://doi.org/10.1007/s11274-010-0508-2>
- Watanabe, Y., Tsuji, Y., Ige, H., Ohsugi, Y., & Ohta, T. (1984). Ruthenium-catalyzed N-alkylation and N-benzylation of aminoarenes with alcohols. *The Journal of Organic Chemistry*, *49*(18), 3359–3363. <https://doi.org/10.1021/jo00192a021>
- Weber, R. E. (1992). Use of ionic and zwitterionic (Tris/BisTris and HEPES) buffers in studies on hemoglobin function. *Journal of Applied Physiology*, *72*(4), 1611–1615.
<https://doi.org/10.1152/jappl.1992.72.4.1611>
- Wei, G., Chen, Y., Zhou, N., Lu, Q., Xu, S., Zhang, A., Chen, K., & Ouyang, P. (2022). Chitin biopolymer mediates self-sufficient biocatalyst of pyridoxal 5'-phosphate and L-lysine decarboxylase. *Chemical Engineering Journal*, *427*, 132030.
<https://doi.org/10.1016/j.cej.2021.132030>
- Wei, T., Cheng, B. Y., & Liu, J. Z. (2016). Genome engineering *Escherichia coli* for L-DOPA overproduction from glucose. *Scientific Reports*, *6*. <https://doi.org/10.1038/srep30080>
- Wieschalka, S., Blombach, B., Bott, M., & Eikmanns, B. J. (2013). Bio-based production of organic acids with *Corynebacterium glutamicum*. *Microbial Biotechnology*, *6*(2), 87–102.
<https://doi.org/10.1111/1751-7915.12013>

- Wohlgemuth, R. (2021). Biocatalysis-Key enabling tools from biocatalytic one-step and multi-step reactions to biocatalytic total synthesis. *New Biotechnol*, *60*, 113–123.
- Wu, B., Zhang, S., Hong, T., Zhou, Y., Wang, H., Shi, M., Yang, H., Tian, X., Guo, J., Bian, J., Roache, J., Delgado, P., Mo, R., Fridrich, C., Gao, F., & Wang, J. (2020). Merging Biocatalysis, Flow, and Surfactant Chemistry: Innovative Synthesis of an FXI (Factor XI) Inhibitor. *Organic Process Research & Development*, *24*(11), 2780–2788. <https://doi.org/10.1021/acs.oprd.0c00412>
- Wu, P., Li, G., He, Y., Luo, D., Li, L., Guo, J., Ding, P., & Yang, F. (2020). High-efficient and sustainable biodegradation of microcystin-LR using *Sphingopyxis* sp. YF1 immobilized Fe₃O₄@chitosan. *Colloids and Surfaces B: Biointerfaces*, *185*, 110633. <https://doi.org/10.1016/j.colsurfb.2019.110633>
- Ye, L. J., Toh, H. H., Yang, Y., Adams, J. P., Snajdrova, R., & Li, Z. (2015). Engineering of Amine Dehydrogenase for Asymmetric Reductive Amination of Ketone by Evolving *Rhodococcus* Phenylalanine Dehydrogenase. *ACS Catalysis*, *5*(2), 1119–1122. <https://doi.org/10.1021/cs501906r>
- Yoon, S., Patil, M. D., Sarak, S., Jeon, H., Kim, G., Khobragade, T. P., Sung, S., & Yun, H. (2019). Deracemization of Racemic Amines to Enantiopure (*R*)- and (*S*)-amines by Biocatalytic Cascade Employing ω -Transaminase and Amine Dehydrogenase. *ChemCatChem*, *11*(7), 1898–1902. <https://doi.org/10.1002/cctc.201900080>
- Yoshitaka Hashitani, B. (1925). On the chemical constituents of malt-rootlets with special reference to Hordenine. *Journal of the College of Agriculture*, *14*, 1–56.
- Zhang, B., Jiang, Y., Li, Z., Wang, F., & Wu, X.-Y. (2020). Recent Progress on Chemical Production From Non-food Renewable Feedstocks Using *Corynebacterium glutamicum*. *Frontiers in Bioengineering and Biotechnology*, *8*. <https://doi.org/10.3389/fbioe.2020.606047>
- Zhang, H., Wei, Y., Lu, Y., Wu, S., Liu, Q., Liu, J., & Jiao, Q. (2016). Three-step biocatalytic reaction using whole cells for efficient production of tyramine from keratin acid hydrolysis wastewater. *Applied Microbiology and Biotechnology*, *100*(4), 1691–1700. <https://doi.org/10.1007/s00253-015-7054-7>
- Zhang, K., & Ni, Y. (2014). Tyrosine decarboxylase from *Lactobacillus brevis*: Soluble expression and characterization. *Protein Expression and Purification*, *94*, 33–39. <https://doi.org/10.1016/j.pep.2013.10.018>
- Zhang, X., Du, L., Zhang, J., Li, C., Zhang, J., & Lv, X. (2021). Hordenine Protects Against Lipopolysaccharide-Induced Acute Lung Injury by Inhibiting Inflammation. *Frontiers in Pharmacology*, *12*, 712232. <https://doi.org/10.3389/fphar.2021.712232>
- Zhao, W., Hu, S., Huang, J., Ke, P., Yao, S., Lei, Y., Mei, L., & Wang, J. (2016). Permeabilization of *Escherichia coli* with ampicillin for a whole cell biocatalyst with enhanced glutamate decarboxylase activity. *Chinese Journal of Chemical Engineering*, *24*(7), 909–913. <https://doi.org/10.1016/j.cjche.2016.02.001>
- Zhou, F., Xu, Y., Nie, Y., & Mu, X. (2022). Substrate-Specific Engineering of Amino Acid Dehydrogenase Superfamily for Synthesis of a Variety of Chiral Amines and Amino Acids. *Catalysts*, *12*(4), 380. <https://doi.org/10.3390/catal12040380>

- Zhou, J.-W., Ruan, L.-Y., Chen, H.-J., Luo, H.-Z., Jiang, H., Wang, J.-S., & Jia, A.-Q. (2019). Inhibition of Quorum Sensing and Virulence in *Serratia marcescens* by Hordenine. *Journal of Agricultural and Food Chemistry*, *67*(3), 784–795. <https://doi.org/10.1021/acs.jafc.8b05922>
- Zhu, H., Xu, G., Zhang, K., Kong, X., Han, R., Zhou, J., & Ni, Y. (2016a). Crystal structure of tyrosine decarboxylase and identification of key residues involved in conformational swing and substrate binding. *Scientific Reports*, *6*(1), 27779. <https://doi.org/10.1038/srep27779>
- Zhu, H., Xu, G., Zhang, K., Kong, X., Han, R., Zhou, J., & Ni, Y. (2016b). Crystal structure of tyrosine decarboxylase and identification of key residues involved in conformational swing and substrate binding. *Scientific Reports*, *6*(1), 27779. <https://doi.org/10.1038/srep27779>
- Zhuang, W., Liu, H., Zhang, Y., He, J., & Wang, P. (2021). Effective asymmetric preparation of (R)-1-[3-(trifluoromethyl)phenyl]ethanol with recombinant *E. coli* whole cells in an aqueous Tween-20/natural deep eutectic solvent solution. *AMB Express*, *11*(1), 118. <https://doi.org/10.1186/s13568-021-01278-6>

7. Exploring the potential of amine dehydrogenases in oxidative deamination for aldehyde production

Unless explicitly stated otherwise, the research presented in this chapter is the sole and individual work of the author.

7.1 Introduction

Hydrogen borrowing is a synthetic strategy that entails the internal transfer of hydrogen atoms within a molecule or a pair of molecules during a sequence of reactions. In the context of biocatalysis, this could involve the cooperation of two enzymes, where one performs an oxidation (hydrogen removal) and the other performs a reduction (hydrogen addition), essentially 'borrowing' and 'returning' the hydrogen atom.

The term "hydrogen borrowing" comes from the strategy used in synthetic chemistry where a hydrogen atom is "borrowed" from a molecule, used in a first reaction, and then returned to the molecule.

For example, in the context of the amination of alcohols (Figure 7.1), this term can be explained through a three-step reaction process: oxidation, imine formation and reduction. (Hamid et al., 2007)

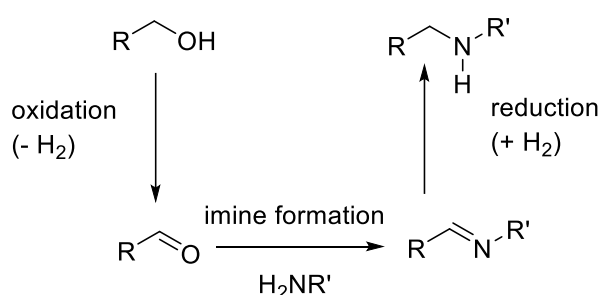


Figure 7.1: Conversion of alcohols into amines by hydrogen borrowing.

In the first step, an alcohol is activated via oxidation to a carbonyl compound using a transition metal catalyst. In this step, a hydrogen atom is removed from the alcohol molecule, which is then held (or "borrowed") by the catalyst. Afterwards, the carbonyl compound reacts with an amine, leading to the formation of an imine. Finally, the imine is reduced back to an amine by the same transition metal catalyst and during this reduction, the hydrogen that was "borrowed" in the first step is returned to the carbonyl compound.

A standard instance is shown in Figure 7.2, where the aniline (**1**) undergoes alkylation, predominantly producing the secondary amines (**2**) together with some tertiary amine, which is also produced due to dialkylation. (Watanabe et al., 1984)

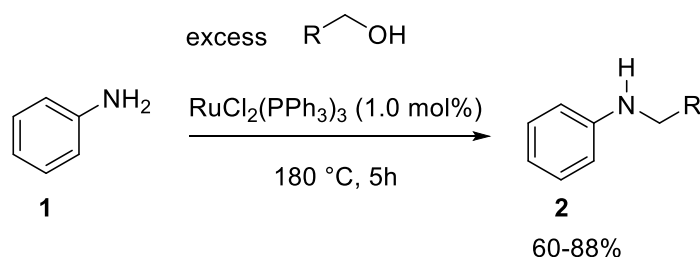


Figure 7.2: Ruthenium catalyzed N-alkylation of amines.

The net result is the transformation of alcohols into amines, all without the need for external hydrogen sources. This internal transfer of hydrogen allows for more efficient and sustainable catalysis, which is why the concept of "hydrogen borrowing" is so attractive in chemistry and subsequently translated into biocatalytic applications.

The hydrogen borrowing strategy is indeed an efficient solution for catalyzing desired biotransformations involving dehydrogenases, recycling the cofactor simultaneously, because it allows for the conservation of the reducing equivalents in the system. This occurs by coupling an oxidation reaction, where the cofactor is reduced (gaining electrons, or in this case, a hydride), with a subsequent reduction reaction, where the cofactor is oxidized (losing electrons). This interplay between two reactions essentially borrows hydrogen atoms from the starting material and returns them to the end product, enabling the recycling of the cofactor NAD(P)H within the same enzymatic system without the need for additional input.

In the work from Mutti *et al.*, a highly enantioselective hydrogen-borrowing amination method for both primary and secondary alcohols was presented, involving two biocatalysts, an Alcohol Dehydrogenase (ADH) and an Amine Dehydrogenase (AmDH) (Figure 7.3). (Mutti *et al.*, 2015) The reaction cascade utilizes successfully NADH in catalytic amounts to transport the hydride from the oxidation phase to the reduction phase.

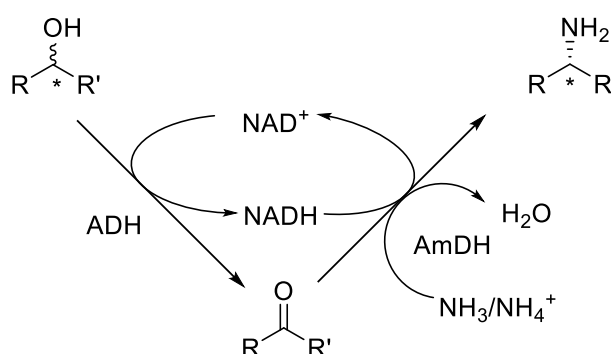


Figure 7.3: Two-enzymes system employed for the hydrogen borrowing amination of alcohols. In the initial oxidation phase, ADHs from *Aromatoleum sp.*, *Lactobacillus sp.*, or *Bacillus sp.* were utilized for the conversion of the alcohol substrates. In the subsequent reduction step, AmDH yields the production of (R)-configured amines.

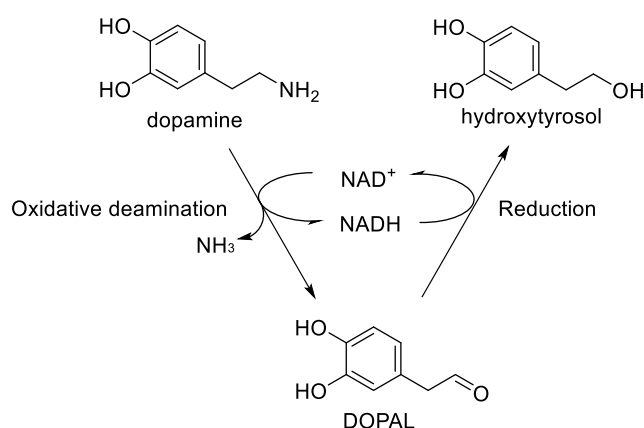
Important to consider is that for a successful implementation of this hydrogen borrowing strategy, the ADH should be aselective, and additionally, the cofactor preference for both the oxidizing and reducing enzymes should be the same. (Thompson & Turner, 2017b)

An example of a novel potential application for the hydrogen borrowing strategy can be seen in the specific context of the hydroxytyrosol cascade. (Contente & Paradisi, 2018) The novelty in this instance stems from the exploration of AmDH catalysis in the direction of oxidative deamination. As was highlighted in the introduction chapter, this direction has

remained largely unexplored up to now, suggesting that this approach could open up new avenues for research and application.

In this case, this approach could be applied to convert dopamine, the catecholamine deriving from the decarboxylation of L-DOPA, into DOPAL, the corresponding aldehyde, via an oxidative deamination reaction that is NADH-dependent (Figure 7.4 A). In this step, an amine dehydrogenase could catalyze the deamination of dopamine, generating DOPAL, reducing NAD^+ to NADH. This would be followed by the conversion of the DOPAL intermediate into the final product, hydroxytyrosol, a valuable antioxidant, generating an economic profit where the value increases by a factor of 1000 from substrate to product. This reduction could be catalyzed by an alcohol dehydrogenase such as horse liver alcohol dehydrogenase (HLADH),(Quaglia et al., 2012b) as reported in previous work. The reduced cofactor NADH from the previous reaction would be oxidized back to NAD^+ , transferring its hydrogen atoms to DOPAL, and thus recycling the cofactor within an enzymatic cascade. This could represent an efficient in-line process, streamlining the conversion of dopamine to hydroxytyrosol with minimal loss of energy and resources, thus highlighting the potential of hydrogen borrowing in biocatalysis. This approach could serve as an alternative to the established enzymatic flow cascade for hydroxytyrosol production (Figure 7.4 B). In the existing process, the ω -transaminase from *Halomonas elongata* (HeWT),(Cerioli et al., 2015) which catalyzes the transamination reaction converting dopamine to the corresponding aldehyde, is coupled with HLADH. The proposed method could eliminate the need for pyruvate as an amino acceptor and for ethanol as a co-substrate for NADH regeneration.

A



B

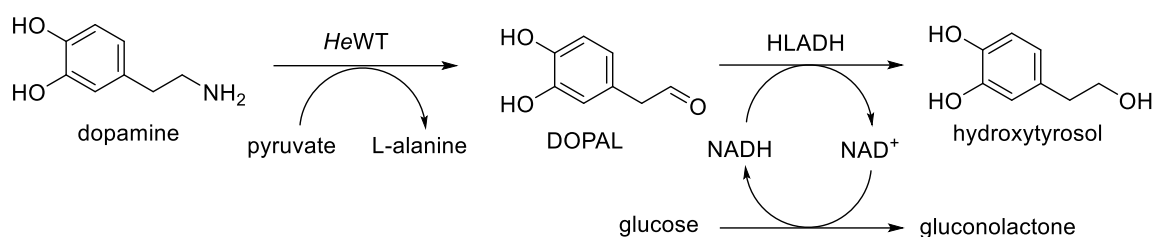


Figure 7.4: A. Schematic representation of the proposed hydrogen-borrowing strategy for the enzymatic hydroxytyrosol cascade. The cycle illustrates the interconversion of the cofactors NADH and NAD⁺, fueling the biocatalytic transformations; **B.** Telescoped enzymatic cascade for hydroxytyrosol synthesis. The cascade involves the ω -transaminase from *Halomonas elongata* (HeWT) catalyzing the transamination reaction between dopamine and pyruvate, followed by horse liver alcohol dehydrogenase (HLADH) reducing DOPAL to the final product, hydroxytyrosol.

Amine Dehydrogenases (AmDHs) and Amino Acid Dehydrogenases (AADHs) are two classes of enzymes that hold substantial potential in biocatalysis due to their unique catalytic capabilities.

AmDHs are enzymes that catalyze the NAD(P)H-dependent asymmetric reductive amination of aldehyde and ketone substrates, with concurrent reduction or oxidation of the cofactor.(Ghislieri & Turner, 2014; Patil et al., 2018) These enzymes typically demonstrate high substrate specificity and excellent enantioselectivity, enabling them to generate optically pure amino products.

AADHs, on the other hand, are involved in the oxidation L-amino acids and the reversible reductive amination of the corresponding α -keto acids using NAD(P)H as cofactor.(F. Zhou et al., 2022) Like AmDHs, they too show high substrate specificity and enantioselectivity. With their inherent properties, these enzymes have been further harnessed through engineering methods and the resultant engineered amine dehydrogenases perform a symmetric synthesis of a range of chiral amines.

So far, there have been no scientific studies showing that AmDHs or AADHs can exploit their capabilities in oxidative deamination of primary amines to produce aldehydes, and only a few works have investigated the direction of oxidative deamination from secondary amines.(Abrahamson et al., 2012; Tseliou et al., 2020) This lack of reported evidence suggests a gap in our current understanding of these enzymes potential catalytic functions and emphasizes the need for further research in this area.

To date, there has been a significant expansion in the substrate scope of a number of amine dehydrogenases.(Ducrot et al., 2022)

*Cfus*AmDH (6IAU), *Micro*AmDH (C3UMY1), MATOUAmDH2 (7ZBO) were the AmDHs examined in this chapter (Figure 7.5).(Mayol et al., 2019b)

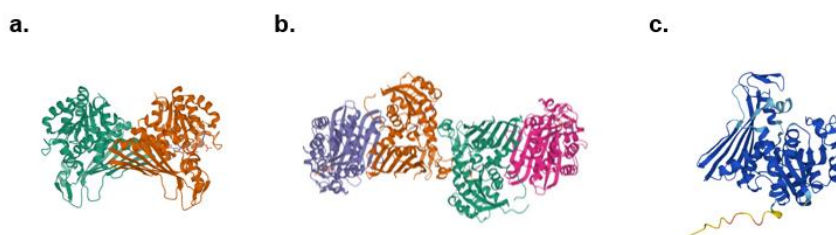


Figure 7.5: 3D structural representations of the AmDHs involved in the screening for the oxidative deamination reaction. **a.** *CfusAmDH*, **b.** MATOUAmDH, **c.** *MicroAmDH*.

By engineering the active sites of these enzymes, the groups of Gideon Grogan and Carine Vergne-Vaxelaire broadened their substrate scope to accept various aldehydes into their catalytic repertoire. (Ducrot et al., 2022; Mayol et al., 2019b) Long chain aldehydes such as pentanal, hexanal, heptanal, octanal, nonanal and decanal can now be successfully aminated by these biocatalysts. Additionally, aldehydes with branched or aromatic structures, such as 2-methylbutanal, 2-methylpropanal, and benzaldehyde are also accepted. Of particular interest for the topic of this chapter, the substrate scope of these AmDHs has been expanded further to include also 4-phenylbutan-2-one. This starting material has a greater similarity to dopamine, in comparison with the previously mentioned aldehydes. *CfusAmDH*-W145A mutant has shown great efficacy in this reaction, achieving a conversion of 52.5 % into S-4-phenylbutan-2-amine (ee=99.6 %) (Figure 7.6). (Ducrot et al., 2022)

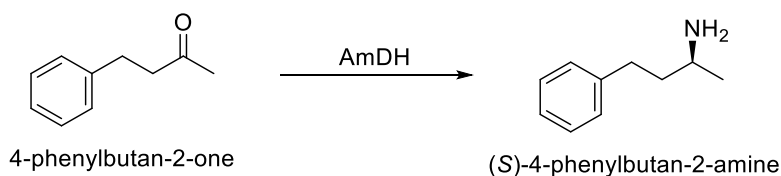


Figure 7.6: Conversion of 4-phenylbutan-2-one into its S-enantiomeric amine, catalyzed by the mutant Amine Dehydrogenase *CfusAmDH* W145A. The figure demonstrates the enzyme's ability to facilitate the reductive amination reaction, showcasing its potential in its expanded substrate scope.

7.2 Results and discussion

7.2.1 AmDHs expression and purification

AmDHs were expressed following the protocol outlined in the Materials and Methods section. Upon reaching optimal growth, AmDH expression was induced and the cells were harvested and lysed to release the recombinant protein. The crude extract was clarified and the AmDH was isolated using Ni-NTA affinity chromatography (Figure 7.7).

CfusAmDH

MATOUAmDH

MicroAmDH

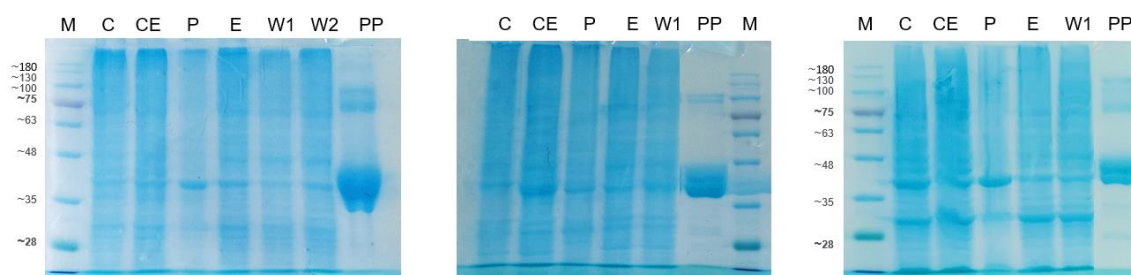


Figure 7.7: SDS-PAGE gels displaying the purification stages of the AmdHs, specifically *CfusAmdH*, MATOUAmdH2, and *MicroAmdH*. The gels provide a visual representation of protein purity across different purification steps, confirming the successful isolation of the target AmdH enzymes. **M**: marker; **C**: cell lysate; **CE**: crude extract; **P**: pellet; **E**: eluted flow through; **W1**: wash with buffer A; **W2**: wash with 10% buffer B; **PP**: purified protein (38 kDa). Buffer A: 100 mM phosphate, 50 mM NaCl, 10 % glycerol, 30 mM imidazole, pH 7.5. Buffer B: 100 mM phosphate, 50 mM NaCl, 10 % glycerol, 250 mM imidazole, pH 7.5.

The biomass production, indicating the cell growth, was consistent across all three AmdH variants, *CfusAmdH*, MATOUAmdH2 and *MicroAmdH*, with a measurement of approximately 3 g/L. The volumetric yield, representing the total amount of the AmdH produced in the bacterial culture, was determined for each variant. Finally, the protein concentration of the AmdH after dialysis was determined. These results are summarized in Table 7.1.

AmdH Variant	Biomass (g/L)	Volumetric Yield (mg/L)	Protein Concentration After Dialysis (mg/mL)
<i>CfusAmdH</i>	~3	37.5 mg/L	5
MATOUAmdH2	~3	22.5 mg/L	2.5
<i>MicroAmdH</i>	~3	20.3 mg/L	1.4

Table 7.1: Compilation of key expression parameters for each amine dehydrogenase (AmdH) involved in the study.

7.2.2 AmdHs screening for oxidative deamination activity

The investigation into the activity of amine dehydrogenases (AmdHs) was methodically conducted in two stages. In the initial stage, the enzymatic activity of *CfusAmdH*, MATOUAmdH2, and *MicroAmdH* against substrates 2-phenylethylamine, isobutylamine, and pentylamine was assessed via a spectrofluorometer (Figure 7.8).

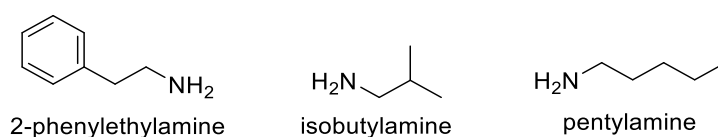
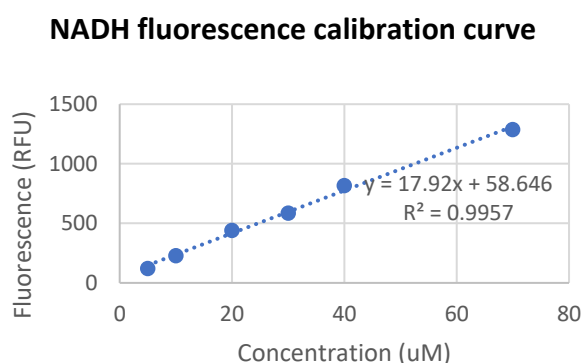


Figure 7.8: Substrates for AmdH oxidative deamination activity monitoring NADH fluorescence.

This technique facilitated real-time monitoring of the reaction by recording the emission from the NADH product every 10 seconds over a 10-minute period. The fluorescence of the cofactor was excited at a wavelength of 351 ± 9 nm and the emission was measured at 450 ± 30 nm. The experiments were conducted under varying enzyme concentrations and pHs to determine their impact on enzymatic performance (Table 7.2 -4).

To ensure accurate quantification of NADH, a calibration curve was generated prior to the activity measurements, confirming a linear correlation between NADH concentration (μM) and fluorescence intensity (relative fluorescence units, RFU) (Graph 7.1).



Graph 7.1: Calibration curve for the measurement of fluorescence of different NADH concentrations in the range of 5 and 70 μM .

Table 7.2

Enzyme	Substrate	Enzyme concentration (mg/mL)	pH	Activity (mU/mg)
<i>CfusAmDH</i>	isobutylamine	1.5	9.0	<i>n.d.</i>
<i>CfusAmDH</i>	isobutylamine	1.5	9.5	200 ± 0.015
<i>CfusAmDH</i>	isobutylamine	0.16	9.5	<i>n.d.</i>
<i>CfusAmDH</i>	pentylamine	1.5	9.0	<i>n.d.</i>
<i>CfusAmDH</i>	pentylamine	1.5	9.5	<i>n.d.</i>
<i>CfusAmDH</i>	pentylamine	0.16	9.5	<i>n.d.</i>
<i>CfusAmDH</i>	2-phenylethylamine	1.5	9.0	<i>n.d.</i>
<i>CfusAmDH</i>	2-phenylethylamine	1.5	9.5	<i>n.d.</i>
<i>CfusAmDH</i>	2-phenylethylamine	0.16	9.5	<i>n.d.</i>

Table 7.3

Enzyme	Substrate	Enzyme concentration (mg/mL)	pH	Activity (mU/mg)
MATOUAmDH2	isobutylamine	1.25	9.0	<i>n.d.</i>

MATOUAmDH2	isobutylamine	1.25	9.5	85 ± 0.031
MATOUAmDH2	isobutylamine	0.16	9.5	<i>n.d.</i>
MATOUAmDH2	pentylamine	1.25	9.0	<i>n.d.</i>
MATOUAmDH2	pentylamine	1.25	9.5	<i>n.d.</i>
MATOUAmDH2	pentylamine	0.16	9.5	<i>n.d.</i>
MATOUAmDH2	2-phenylethylamine	1.25	9.0	<i>n.d.</i>
MATOUAmDH2	2-phenylethylamine	1.25	9.5	<i>n.d.</i>
MATOUAmDH2	2-phenylethylamine	0.16	9.5	<i>n.d.</i>

Table 7.4

Enzyme	Substrate	Enzyme concentration (mg/mL)	pH	Activity (mU/mg)
<i>MicroAmDH</i>	isobutylamine	0.30	9.0	<i>n.d.</i>
<i>MicroAmDH</i>	isobutylamine	0.30	9.5	7 ± 0.001
<i>MicroAmDH</i>	isobutylamine	0.16	9.5	10 ± 0.001
<i>MicroAmDH</i>	pentylamine	0.30	9.0	<i>n.d.</i>
<i>MicroAmDH</i>	pentylamine	0.30	9.5	<i>n.d.</i>
<i>MicroAmDH</i>	pentylamine	0.16	9.5	<i>n.d.</i>
<i>MicroAmDH</i>	2-phenylethylamine	0.30	9.0	<i>n.d.</i>
<i>MicroAmDH</i>	2-phenylethylamine	0.30	9.5	<i>n.d.</i>
<i>MicroAmDH</i>	2-phenylethylamine	0.16	9.5	<i>n.d.</i>

Table 7.2-4: Summary of the results from the activity screening at the spectrofluorometer of AmDHs against range of substrates under varying experimental conditions. Each table reports the enzymatic activity, unless not detected (*n.d.*), monitoring the fluorescence of NADH at 450 ± 3 nm.

The data gathered from the spectrofluorometer during the screening process did not provide a consistent pattern to conclusively determine the activity of the AmDHs. In fact, the inconsistencies in the data prevented the identification of robust trends or clear interpretations (Figure 7.9).

Assessment of oxidative deamination activity *via* NADH formation measurement

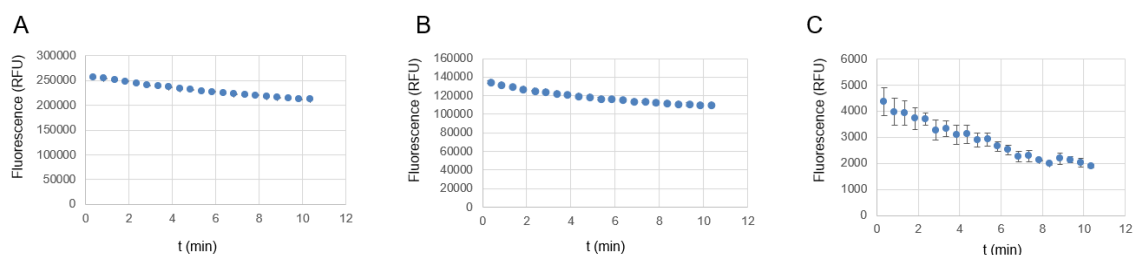
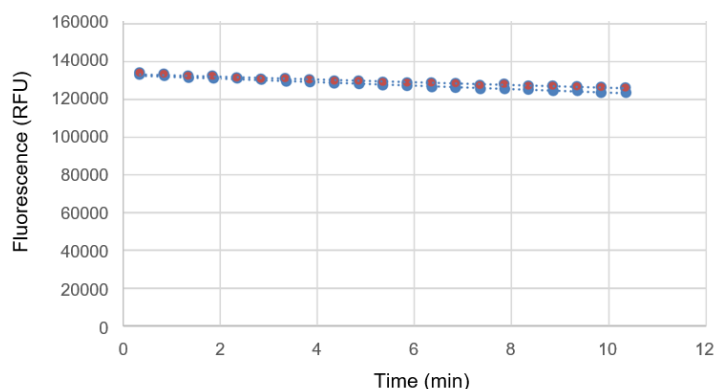


Figure 7.9: Activity measurements of *Cfus*AmDH (A), MATOUAmDH2 (B), *Micro*AmDH (C) against pentylamine. Conditions: 50 mM pentylamine, 0.1 mM NAD⁺ in 200 μ l sodium carbonate buffer 100 mM, pH 9.5. The biocatalyst concentration used varies depending from the enzyme: 1.25 mg/mL *Cfus*AmDH, 1.25 mg/mL MATOUAmDH2, 0.30 mg/mL *Micro*AmDH.

One notable inconsistency was the variation in fluorescence values, at time 0, on the Y-axis across different amines and enzymes components assays. This discrepancy suggested that there were other factors influencing the fluorescence measurements besides the intended variables. A consistent starting point value between the sample measurement and the blank was observed (Graph 7.2). This consistency suggests that the high level of fluorescence is not attributable to the addition of the enzyme solution. Given the high level of relative fluorescence units (RFU) on the Y-axis, there is a strong possibility that the signal might have reached saturation. This could potentially hinder the effective monitoring of NADH formation. Notably, these levels substantially exceeded those within the range of the calibration curve, which further complicates accurate interpretation and measurement of NADH formation. As far as the reproducibility, the activities values recorded in specific for *Cfus*AmDH and MATOUAmDH2 against isobutylamine did not consistently correlate with the variations in enzyme concentration. As such, these results were discarded and needed to be reassessed.

Furthermore, the alkaline pH required for catalysis raised concerns regarding the stability of the cofactor (NADH) over time at pH 9.5. An alkaline pH might not have promoted the stability of the cofactor, potentially impacting the reliability of the results obtained. (Knaus et al., 2017) With this hypothesis, these alkaline buffer condition could possibly account for the observed negative trendlines in the experiments, which may be a manifestation of cofactor degradation. However, it is worth noting that the perceived negative trendline might in fact be flat and only appears negative when the scale on the Y-axis is magnified.

MATOUAmDH2 oxidative deamination activity measurements



Graph 7.2: Time-dependent fluorescence comparison of blank (enzyme-free sample) and MATOUAmDH2 activity against pentylamine. The blue dots and trendline represent the

blank with a slope of -947.41, while the red dots and trendline depict the activity assay, derived from duplicate experiments, with a slope of -743.27.

Following the unsuccessful attempt to identify a positive slope for the monitored activity using the initial method, an alternative approach was tested. A UV spectrophotometer was employed to continuously monitor the signal of NADH absorbance at 340 nm. All three AmDHs, namely *Cfus*AmDH, MATOUAmDH2 and *Micro*AmDH were re-tested. The trial focused on the enzymes activity against isobutylamine, 3-amino-2-propanol, pentylamine, butylamine, and 4-amino-1-butanol (Figure 7.10). This shift in substrates aimed to explore the potential of AmDHs in catalyzing the oxidative deamination reaction, in line with prior studies that reported specific activity of AmDHs against aldehydes.(Mayol et al., 2019b)

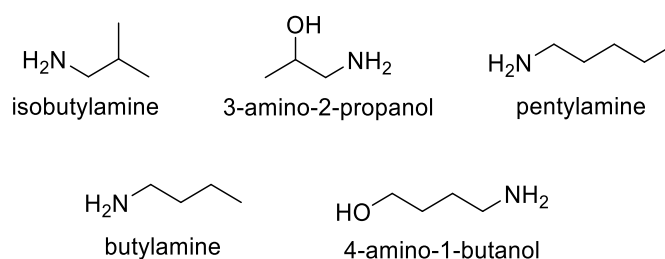


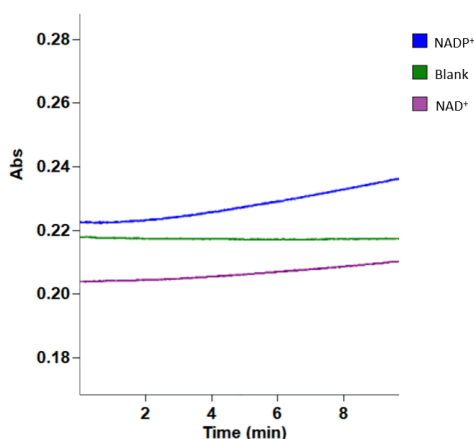
Figure 7.10: Substrate scope for investigating AmDH oxidative deamination activity monitoring NADH formation at 340 nm.

The results of the UV activity screening were also unsuccessful. All measurable slopes approximated the blank line slope, resulting in low specific activities (below 2 U/mg) measured in milliunits per milligram.

To exclude the possibility that the enzymes may have a different preference for NADH and NADPH, the cofactor preference of each enzyme was evaluated through the oxidative deamination of isobutylamine. The evaluation of the cofactor preference was a critical step undertaken to ensure that the assay was able to capture the maximum potential enzymatic activity. This assessment ensured that each enzyme was tested under its optimal conditions, facilitating a fair and accurate comparison across different AmDHs.

Notably, *Cfus*AmDH exhibited a higher activity with NADP⁺ than with NAD⁺, demonstrating respective activity levels of 1.5 mU/mg and 0.7 mU/mg (Graph 7.3). Comparing these results with those reported in previous literature seemed to be challenging, as existing studies on this particular AmDH do not clearly establish a preference for one cofactor over another. Moreover, it appears that the cofactor preference may vary depending on the substrate used in the reaction.

Cofactor Preference of *Cfus*AmDH monitored via UV Absorbance



Graph 7.3: Time-dependent UV absorbance monitoring at 340 nm of the reaction catalyzed by *CfusAmDH* with isobutylamine as the substrate. This experiment investigates the enzyme preference between the cofactors NAD⁺ and NADP⁺. In green color is the blank trendline (slope -0.0040), in violet color is the NAD⁺ reaction (slope 0.0010) and in blue color is the NADP⁺ trendline reaction (0.0021). Reaction conditions: *CfusAmDH* 0.25 mg/mL, 30 mM isobutylamine, 1 mM NAD(P)⁺ in 1 mL final volume of 100 mM buffer sodium carbonate pH 9.5. Time monitoring: 10 min.

For MATOUAmDH2 and *MicroAmDH*, NAD⁺ emerged as the preferred cofactor, because no difference from the blank trendline was detected with NADP⁺ in the trialed reaction with isobutylamine (Table 7.5).

Specific Activity vs isobutylamine (mU/mg)		
AmDH	NAD ⁺	NADP ⁺
<i>CfusAmDH</i>	0.7	1.5
MATOUAmDH2	1.8	<i>n.d.</i>
<i>MicroAmDH</i>	0.7	<i>n.d.</i>

Table 7.5: Cofactor preference of AmDHs. Reaction conditions: *CfusAmDH* 0.25 mg/mL, MATOUAmDH2 0.25 mg/mL, *MicroAmDH* 0.45 mg/mL, 30 mM isobutylamine, 1 mM NAD(P)⁺ in 1 mL final volume of 100 mM buffer sodium carbonate pH 9.5. Time monitoring: 10 min. In the table, 'n.d.' indicates that activity was not detected with the corresponding cofactor.

Unfortunately, repeating the experiments, minimal activity values were reported (Table 7.6), suggesting that the biocatalysts under consideration for the hydrogen borrowing strategy, in the targeted enzymatic application, could not meet the anticipated performance levels.

Enzyme	Substrate	Enzyme concentration (mg/mL)	Cofactor	pH	Activity (mU/mg)
<i>Cfus</i> AmDH	isobutylamine	0.25	NADP ⁺	9.5	1.5 ± 0.0009
<i>Micro</i> AmDH	isobutylamine	0.45	NAD ⁺	9.5	0.7 ± 0.0010
<i>Micro</i> AmDH	pentylamine	0.45	NAD ⁺	9.5	0.9 ± 0.0012
<i>Micro</i> AmDH	4-amino-2-propanol	0.45	NAD ⁺	9.5	0.4 ± 0.0020
MATOUAmDH2	isobutylamine	0.25	NAD ⁺	9.5	1.8 ± 0.0021
MATOUAmDH2	butylamine	0.25	NAD ⁺	9.5	1.5 ± 0.0019
MATOUAmDH2	4-amino-1-butanol	0.25	NAD ⁺	9.5	1.5 ± 0.0006

Table 7.6: Results of the AmDHs activity screening utilizing the Cary60 UV-Vis Spectrophotometer. The table presents the enzymatic activities as determined by monitoring the absorbance of NADH at 340 nm.

The results underline the importance of enzyme selection in biocatalysis and suggest the need for further exploration and optimization of other potential biocatalysts for the hydrogen borrowing strategy between dopamine oxidation to DOPAL and DOPAL reduction to hydroxytyrosol.

In a final attempt to prove the system, despite evidence suggesting that the selected AmDHs were incapable of converting amine to aldehyde, a series of biotransformation experiments were conducted with changes in pH (8.5 and 9.5), and type of cofactor used

(NAD⁺ or NADP⁺). The reactions were also performed both with the individual AmDH enzymes (*CfusAmDH*, MATOUAmDH2, *MicroAmDH*) and in a bienzymatic biotransformation setup with HLADH. The goal of these experiments was to fully assess the potential of this strategy and explore any conditions where the biocatalysts activity might be favoured. Unfortunately, neither aldehydes nor alcohols from isobutylamine, pentylamine, butylamine, and 4-amino-1-butanol were detected under any of the tested conditions up to 48 h (data not shown).

Eventually, the last attempt to find an appropriate biocatalyst capable of converting an aromatic primary amine, such as dopamine, into its corresponding aldehyde, was performed with the mutated version of *CfusAmDH*.(Ducrot et al., 2022) This mutation involved a single residue at position 145, changing a tryptophan (W) into an alanine (A). This allowed the enzyme (*CfusAmDH* W145A) to convert, as previously mentioned, 4-phenylbutan-2-one into the corresponding aromatic secondary amines *via* reductive amination, expanding the scope of substrates that could be effectively transformed.(Ducrot et al., 2022)

7.2.3 Optimization of expression and purification for *CfusAmDH* W145A mutant

The expression and purification process of the mutant *CfusAmDH* W145A involved some key optimizations in comparison to the standard protocol. Traditionally, protein expression was induced at an OD of 0.7 with 1 mM IPTG and the expression was carried out at 16 °C. In the revised protocol, induction was performed at a higher OD of 1.2 but with a reduced IPTG concentration of 0.5 mM, and the expression temperature was raised to 20 °C (Figure 7.11). This new methodology provided significant improvements in protein yield, with the concentration of the purified protein at 280 nm reaching 10.4 mg/mL and a volumetric yield of 125 mg/L.

CfusAmDH W145A

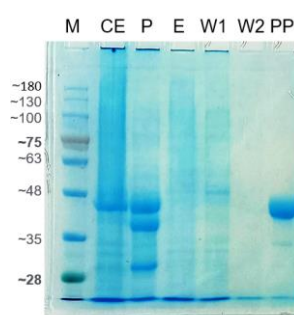


Figure 7.11: SDS-PAGE gel of *CfusAmDH* W145A purification stages. **M:** marker; **C:** cell lysate, **CE:** crude extract; **P:** pellet; **E:** eluted; **W1:** wash with buffer A; **W2:** wash with 10% buffer B; **PP:** purified protein. Buffer A: 100 mM phosphate, 50 mM NaCl, 10 % glycerol, 30 mM imidazole, pH 7.5. Buffer B: 100 mM phosphate, 50 mM NaCl, 10 % glycerol, 250 mM imidazole, pH 7.5.

7.2.4 Screening of *Cfus*AmDH W145A activity

A series of experiments were conducted to evaluate the enzymatic activity of the *Cfus*AmDH W145A mutant. Initial tests were carried out with 2-phenylethylamine at a concentration of 25 mM. In these trials, various enzyme concentrations (0.1 -1.1 - 2.2 mg/mL) were used in combination with 1 mM NADP⁺, the preferred cofactor as suggested by previous literature for this mutated variant.(Ducrot et al., 2022) The reactions were buffered using carbonate at pH 9.5 and were monitored continuously over a period of 10 minutes at temperatures of both 30°C and 37°C. The outcomes showed only a minor degree of activity, ranging from 1-3 mU/mg.

To confirm the enzyme activity against a known substrate from the literature, a subsequent activity assay was performed using 4-phenyl-2-butanone as the substrate. Conditions for this trial were as follows: 10 mM 4-phenyl-2-butanone, 0.1 mg/mL enzyme concentration, 0.2 mM NADPH, and 2 M NH₄HCO₂ buffer at pH 8.5, 30°C. This experiment yielded a more promising result of 33 mU/mg, indicating a good negative slope, aligning well with results reported in the literature.(Ducrot et al., 2022)

Further testing was conducted using octanal as a substrate to corroborate the enzyme activity against a known substrate from the literature. The experimental conditions mirrored the previous tests, and the activity observed was in line with reported values, yielding an activity of 511 mU/mg, which compares favorably to the 483 mU/mg cited in the literature.(Ducrot et al., 2022) These results conclusively dispelled any concerns regarding the performance of the biocatalyst, firmly establishing its functionality and effectiveness.

7.3 Conclusion

In this initial screening of the selected natural AmDHs (*Cfus*AmDH , MATOUAmDH2, and *Micro*AmDH), no significant activity was reported in the oxidative deamination direction. This suggests that the reaction is not intrinsically favorable, and that significant engineering of the biocatalysts would be necessary to create an active site favorable to this specific catalysis. Unfortunately, the ambitious goal of finding an AmDH active against dopamine, to involve in the hydroxytyrosol cascade, was not achieved in this stage. Dopamine was not included as a substrate in this screening due to its tendency to oxidize at the catechol moiety under the employed alkaline pH conditions. Initially, 2-phenylethylamine was chosen as a substrate instead, due to its structural similarity to both dopamine and 4-phenyl-2-butanone, yet the experimental outcomes did not yield positive results. Future investigations will need to address these challenges to expand the utility of AmDHs in oxidative deamination.

7.4 Bibliography

- Abrahamson, M. J., Vázquez-Figueroa, E., Woodall, N. B., Moore, J. C., & Bommarius, A. S. (2012). Development of an Amine Dehydrogenase for Synthesis of Chiral Amines. *Angewandte Chemie International Edition*, *51*(16), 3969–3972. <https://doi.org/10.1002/anie.201107813>
- Abrahamson, M. J., Wong, J. W., & Bommarius, A. S. (2013). The Evolution of an Amine Dehydrogenase Biocatalyst for the Asymmetric Production of Chiral Amines. *Advanced Synthesis & Catalysis*, *355*(9), 1780–1786. <https://doi.org/10.1002/adsc.201201030>
- Alcántara, A. R., Domínguez de María, P., Littlechild, J. A., Schürmann, M., Sheldon, R. A., & Wohlgemuth, R. (2022). Biocatalysis as Key to Sustainable Industrial Chemistry. *ChemSusChem*, *15*(9). <https://doi.org/10.1002/cssc.202102709>
- Almud, J. J., Oliveira, M. A., Kern, A. D., Grishin, N. V., Phillips, M. A., & Hackert, M. L. (2000). Crystal structure of human ornithine decarboxylase at 2.1 Å resolution: structural insights to antizyme binding. *Journal of Molecular Biology*, *295*(1), 7–16. <https://doi.org/10.1006/jmbi.1999.3331>
- Andréll, J., Hicks, M. G., Palmer, T., Carpenter, E. P., Iwata, S., & Maher, M. J. (2009). Crystal Structure of the Acid-Induced Arginine Decarboxylase from *Escherichia coli* : Reversible Decamer Assembly Controls Enzyme Activity. *Biochemistry*, *48*(18), 3915–3927. <https://doi.org/10.1021/bi900075d>
- Anwar, S., Mohammad, T., Shamsi, A., Queen, A., Parveen, S., Luqman, S., Hasan, G. M., Alamry, K. A., Azum, N., Asiri, A. M., & Hassan, M. I. (2020). Discovery of hordenine as a potential inhibitor of pyruvate dehydrogenase kinase 3: Implication in lung cancer therapy. *Biomedicines*, *8*(5), 32–228.
- Asano, Y., Nakazawa, A., & Endo, K. (1987). Novel phenylalanine dehydrogenases from *Sporosarcina ureae* and *Bacillus sphaericus*. Purification and characterization. *The Journal of Biological Chemistry*, *262*(21), 10346–10354. <http://www.ncbi.nlm.nih.gov/pubmed/3112142>
- Báez, J. L., Bolívar, F., & Gosset, G. (2001). Determination of 3-deoxy-D- *arabino* -heptulosonate 7-phosphate productivity and yield from glucose in *Escherichia coli* devoid of the glucose

- phosphotransferase transport system. *Biotechnology and Bioengineering*, 73(6), 530–535. <https://doi.org/10.1002/bit.1088>
- Bai, Z., Sun, X., Yu, X., & Li, L. (2019). Chitosan Microbeads as Supporter for *Pseudomonas putida* with Surface Displayed Laccases for Decolorization of Synthetic Dyes. *Applied Sciences*, 9(1), 138. <https://doi.org/10.3390/app9010138>
- Baker, P. J., Turnbull, A. P., Sedelnikova, S. E., Stillman, T. J., & Rice, D. W. (1995). A role for quaternary structure in the substrate specificity of leucine dehydrogenase. *Structure*, 3(7), 693–705. [https://doi.org/10.1016/S0969-2126\(01\)00204-0](https://doi.org/10.1016/S0969-2126(01)00204-0)
- Barwell, C. J., Basma, A. N., Lafi, M. A. K., & Leake, L. D. (2011). Deamination of hordenine by monoamine oxidase and its action on vasa deferentia of the rat. *Journal of Pharmacy and Pharmacology*, 41(6), 421–423. <https://doi.org/10.1111/j.2042-7158.1989.tb06492.x>
- Bell, E. L., Finnigan, W., France, S. P., Green, A. P., Hayes, M. A., Hepworth, L. J., Lovelock, S. L., Niiikura, H., Osuna, S., Romero, E., Ryan, K. S., Turner, N. J., & Flitsch, S. L. (2021). Biocatalysis. *Nature Reviews Methods Primers*, 1(1), 46. <https://doi.org/10.1038/s43586-021-00044-z>
- Benítez-Mateos, A. I., Roura Padrosa, D., & Paradisi, F. (2022). Multistep enzyme cascades as a route towards green and sustainable pharmaceutical syntheses. *Nature Chemistry*, 14(5), 489–499. <https://doi.org/10.1038/s41557-022-00931-2>
- Bennett, M., Ducrot, L., Vergne-Vaxelaire, C., & Grogan, G. (2022). Structure and Mutation of the Native Amine Dehydrogenase MATOUAmDH2. *ChemBioChem*, 23(10). <https://doi.org/10.1002/cbic.202200136>
- Berridge, M. V., Herst, P. M., & Tan, A. S. (2005). *Tetrazolium dyes as tools in cell biology: New insights into their cellular reduction* (pp. 127–152). [https://doi.org/10.1016/S1387-2656\(05\)11004-7](https://doi.org/10.1016/S1387-2656(05)11004-7)
- Bertelli, M., Kiani, A. K., Paolacci, S., Manara, E., Kurti, D., Dhuli, K., Bushati, V., Miertus, J., Pangallo, D., Baglivo, M., Beccari, T., & Michelini, S. (2020). Hydroxytyrosol: A natural compound with promising pharmacological activities. *Journal of Biotechnology*, 309, 29–33. <https://doi.org/10.1016/j.jbiotec.2019.12.016>
- Bhatia, S. K., Kim, Y. H., Kim, H. J., Seo, H.-M., Kim, J.-H., Song, H.-S., Sathiyarayanan, G., Park, S.-H., Park, K., & Yang, Y.-H. (2015). Biotransformation of lysine into cadaverine using barium alginate-immobilized *Escherichia coli* overexpressing CadA. *Bioprocess and Biosystems Engineering*, 38(12), 2315–2322. <https://doi.org/10.1007/s00449-015-1465-9>
- Bloch, D. N., Sandre, M., Ben Zichri, S., Masato, A., Kolusheva, S., Bubacco, L., & Jelinek, R. (2023). Scavenging neurotoxic aldehydes using lysine carbon dots. *Nanoscale Advances*, 5(5), 1356–1367. <https://doi.org/10.1039/D2NA00804A>
- Böhmer, W., Knaus, T., & Mutti, F. G. (2018a). Hydrogen-Borrowing Alcohol Bioamination with Coimmobilized Dehydrogenases. *ChemCatChem*, 10(4), 731–735. <https://doi.org/10.1002/cctc.201701366>
- Böhmer, W., Knaus, T., & Mutti, F. G. (2018b). Hydrogen-Borrowing Alcohol Bioamination with Coimmobilized Dehydrogenases. *ChemCatChem*, 10(4), 731–735. <https://doi.org/10.1002/cctc.201701366>

- Cai, R.-F., Liu, L., Chen, F.-F., Li, A., Xu, J.-H., & Zheng, G.-W. (2020). Reductive Amination of Biobased Levulinic Acid to Unnatural Chiral γ -Amino Acid Using an Engineered Amine Dehydrogenase. *ACS Sustainable Chemistry & Engineering*, 8(46), 17054–17061. <https://doi.org/10.1021/acssuschemeng.0c04647>
- Caparco, A. A., Bommarius, B. R., Bommarius, A. S., & Champion, J. A. (2020). Protein-inorganic calcium-phosphate supraparticles as a robust platform for enzyme co-immobilization. *Biotechnology and Bioengineering*, 117(7), 1979–1989. <https://doi.org/10.1002/bit.27348>
- Caparco, A. A., Pelletier, E., Petit, J. L., Jouenne, A., Bommarius, B. R., Berardinis, V., Zaparucha, A., Champion, J. A., Bommarius, A. S., & Vergne-Vaxelaire, C. (2020). Metagenomic Mining for Amine Dehydrogenase Discovery. *Advanced Synthesis & Catalysis*, 362(12), 2427–2436. <https://doi.org/10.1002/adsc.202000094>
- Capitani, G. (2003). Crystal structure and functional analysis of Escherichia coli glutamate decarboxylase. *The EMBO Journal*, 22(16), 4027–4037. <https://doi.org/10.1093/emboj/cdg403>
- Ceroli, L., Planchestainer, M., Cassidy, J., Tessaro, D., & Paradisi, F. (2015). Characterization of a novel amine transaminase from Halomonas elongata. *Journal of Molecular Catalysis B: Enzymatic*, 120, 141–150. <https://doi.org/10.1016/j.molcatb.2015.07.009>
- Chen, W., Yao, J., Meng, J., Han, W., Tao, Y., Chen, Y., Guo, Y., Shi, G., He, Y., Jin, J.-M., & Tang, S.-Y. (2019). Promiscuous enzymatic activity-aided multiple-pathway network design for metabolic flux rearrangement in hydroxytyrosol biosynthesis. *Nature Communications*, 10(1), 960. <https://doi.org/10.1038/s41467-019-08781-2>
- Claes, L., Janssen, M., & De Vos, D. E. (2019). Organocatalytic Decarboxylation of Amino Acids as a Route to Bio-based Amines and Amides. *ChemCatChem*, 11(17), 4297–4306. <https://doi.org/10.1002/cctc.201900800>
- Contente, M. L., & Paradisi, F. (2018). Self-sustaining closed-loop multienzyme-mediated conversion of amines into alcohols in continuous reactions. *Nature Catalysis*, 1(6), 452–459. <https://doi.org/10.1038/s41929-018-0082-9>
- Cosenza, V. A., Navarro, D. A., & Stortz, C. A. (2011). Usage of α -picoline borane for the reductive amination of carbohydrates. *Arkivoc*, 2011(7), 182–194. <https://doi.org/10.3998/ark.5550190.0012.716>
- Coyle, J. P., Johnson, C., Jensen, J., Farcas, M., Derk, R., Stueckle, T. A., Kornberg, T. G., Rojanasakul, Y., & Rojanasakul, L. W. (2023). Variation in pentose phosphate pathway-associated metabolism dictates cytotoxicity outcomes determined by tetrazolium reduction assays. *Scientific Reports*, 13(1), 8220. <https://doi.org/10.1038/s41598-023-35310-5>
- DiCosimo, R., McAuliffe, J., Poulou, A. J., & Bohlmann, G. (2013). Industrial use of immobilized enzymes. *Chemical Society Reviews*, 42(15), 6437. <https://doi.org/10.1039/c3cs35506c>
- Ducrot, L., Bennett, M., André-Leroux, G., Elisée, E., Marynberg, S., Fossey-Jouenne, A., Zaparucha, A., Grogan, G., & Vergne-Vaxelaire, C. (2022). Expanding the Substrate Scope of Native Amine Dehydrogenases through *In Silico* Structural Exploration and Targeted Protein Engineering. *ChemCatChem*, 14(22). <https://doi.org/10.1002/cctc.202200880>

- Ducrot, L., Bennett, M., Caparco, A. A., Champion, J. A., Bommarius, A. S., Zaparucha, A., Grogan, G., & Vergne-Vaxelaire, C. (2021). Biocatalytic Reductive Amination by Native Amine Dehydrogenases to Access Short Chiral Alkyl Amines and Amino Alcohols. *Frontiers in Catalysis*, 1. <https://doi.org/10.3389/fctls.2021.781284>
- Eliot, A. C., & Kirsch, J. F. (2004). Pyridoxal Phosphate Enzymes: Mechanistic, Structural, and Evolutionary Considerations. *Annual Review of Biochemistry*, 73(1), 383–415. <https://doi.org/10.1146/annurev.biochem.73.011303.074021>
- Eller, K., Henkes, E., Rossbacher, R., & Höke, H. (2000). Amines, Aliphatic. In *Ullmann's Encyclopedia of Industrial Chemistry*. Wiley-VCH Verlag GmbH & Co. KGaA. https://doi.org/10.1002/14356007.a02_001
- Escalante, A., Calderón, R., Valdivia, A., de Anda, R., Hernández, G., Ramírez, O. T., Gosset, G., & Bolívar, F. (2010). Metabolic engineering for the production of shikimic acid in an evolved *Escherichia coli* strain lacking the phosphoenolpyruvate: carbohydrate phosphotransferase system. *Microbial Cell Factories*, 9(1), 21. <https://doi.org/10.1186/1475-2859-9-21>
- Foor, F., Morin, N., & Bostian, K. A. (1993). Production of L-dihydroxyphenylalanine in *Escherichia coli* with the tyrosine phenol-lyase gene cloned from *Erwinia herbicola*. *Applied and Environmental Microbiology*, 59(9), 3070–3075. <https://doi.org/10.1128/aem.59.9.3070-3075.1993>
- Fordjour, E., Adipah, F. K., Zhou, S., Du, G., & Zhou, J. (2019). Metabolic engineering of *Escherichia coli* BL21 (DE3) for de novo production of l-DOPA from d-glucose. *Microbial Cell Factories*, 18(1). <https://doi.org/10.1186/s12934-019-1122-0>
- Franklin, R. D., Whitley, J. A., Caparco, A. A., Bommarius, B. R., Champion, J. A., & Bommarius, A. S. (2021). Continuous production of a chiral amine in a packed bed reactor with co-immobilized amine dehydrogenase and formate dehydrogenase. *Chemical Engineering Journal*, 407, 127065. <https://doi.org/10.1016/j.cej.2020.127065>
- Froidevaux, V., Negrell, C., Caillol, S., Pascault, J.-P., & Boutevin, B. (2016). Biobased Amines: From Synthesis to Polymers; Present and Future. *Chemical Reviews*, 116(22), 14181–14224. <https://doi.org/10.1021/acs.chemrev.6b00486>
- Garg, R. P., Ma, Y., Hoyt, J. C., & Parry, R. J. (2002a). Molecular characterization and analysis of the biosynthetic gene cluster for the azoxy antibiotic valanimycin. *Molecular Microbiology*, 46(2), 505–517. <https://doi.org/10.1046/j.1365-2958.2002.03169.x>
- Garg, R. P., Ma, Y., Hoyt, J. C., & Parry, R. J. (2002b). Molecular characterization and analysis of the biosynthetic gene cluster for the azoxy antibiotic valanimycin. *Molecular Microbiology*, 46(2), 505–517. <https://doi.org/10.1046/j.1365-2958.2002.03169.x>
- Ghislieri, D., & Turner, N. J. (2014). Biocatalytic Approaches to the Synthesis of Enantiomerically Pure Chiral Amines. *Topics in Catalysis*, 57(5), 284–300. <https://doi.org/10.1007/s11244-013-0184-1>
- Gianolio, S., Roura Padrosa, D., & Paradisi, F. (2022). Combined chemoenzymatic strategy for sustainable continuous synthesis of the natural product hordenine. *Green Chemistry*, 24(21), 8434–8440. <https://doi.org/10.1039/D2GC02767D>

- Giardina, G., Montioli, R., Gianni, S., Cellini, B., Paiardini, A., Voltattorni, C. B., & Cutruzzolà, F. (2011). Open conformation of human DOPA decarboxylase reveals the mechanism of PLP addition to Group II decarboxylases. *Proceedings of the National Academy of Sciences*, *108*(51), 20514–20519. <https://doi.org/10.1073/pnas.1111456108>
- Gong, X., Tao, J., Wang, Y., Wu, J., An, J., Meng, J., Wang, X., Chen, Y., & Zou, J. (2021). Total barley maiya alkaloids inhibit prolactin secretion by acting on dopamine D2 receptor and protein kinase A targets. *Journal of Ethnopharmacology*, *273*, 113994. <https://doi.org/10.1016/j.jep.2021.113994>
- Gosset, G., Yong-Xiao, J., & Berry, A. (1996). A direct comparison of approaches for increasing carbon flow to aromatic biosynthesis in *Escherichia coli*. *Journal of Industrial Microbiology*, *17*(1), 47–52. <https://doi.org/10.1007/BF01570148>
- Guisán, JoséM. (1988). Aldehyde-agarose gels as activated supports for immobilization-stabilization of enzymes. *Enzyme and Microbial Technology*, *10*(6), 375–382. [https://doi.org/10.1016/0141-0229\(88\)90018-X](https://doi.org/10.1016/0141-0229(88)90018-X)
- Guo, K., Ji, C., & Li, L. (2007). Stable-Isotope Dimethylation Labeling Combined with LC–ESI MS for Quantification of Amine-Containing Metabolites in Biological Samples. *Analytical Chemistry*, *79*(22), 8631–8638. <https://doi.org/10.1021/ac0704356>
- Guo, Z., Yan, N., & Lapkin, A. A. (2019). Towards circular economy: integration of bio-waste into chemical supply chain. *Current Opinion in Chemical Engineering*, *26*, 148–156. <https://doi.org/10.1016/j.coche.2019.09.010>
- Gupte, A. P., Basaglia, M., Casella, S., & Favaro, L. (2022). Rice waste streams as a promising source of biofuels: feedstocks, biotechnologies and future perspectives. *Renewable and Sustainable Energy Reviews*, *167*, 112673. <https://doi.org/10.1016/j.rser.2022.112673>
- Gut, H., Pennacchietti, E., John, R. A., Bossa, F., Capitani, G., De Biase, D., & Grütter, M. G. (2006). *Escherichia coli* acid resistance: pH-sensing, activation by chloride and autoinhibition in GadB. *The EMBO Journal*, *25*(11), 2643–2651. <https://doi.org/10.1038/sj.emboj.7601107>
- H. Orrego, A., Romero-Fernández, M., Millán-Linares, M., Yust, M., Guisán, J., & Rocha-Martin, J. (2018). Stabilization of Enzymes by Multipoint Covalent Attachment on Aldehyde-Supports: 2-Picoline Borane as an Alternative Reducing Agent. *Catalysts*, *8*(8), 333. <https://doi.org/10.3390/catal8080333>
- Hamid, M. H. S. A., Slatford, P. A., & Williams, J. M. J. (2007). Borrowing Hydrogen in the Activation of Alcohols. *Advanced Synthesis & Catalysis*, *349*(10), 1555–1575. <https://doi.org/10.1002/adsc.200600638>
- Hapke, H. J., & Strathmann, W. (1995). [Pharmacological effects of hordenine]. *DTW. Deutsche Tierärztliche Wochenschrift*, *102*(6), 228–232. <http://www.ncbi.nlm.nih.gov/pubmed/8582256>
- Harper, B. A., Barbut, S., Lim, L.-T., & Marcone, M. F. (2014). Effect of Various Gelling Cations on the Physical Properties of “Wet” Alginate Films. *Journal of Food Science*, *79*(4), E562–E567. <https://doi.org/10.1111/1750-3841.12376>

- Heckmann, C. M., Gourlay, L. J., Dominguez, B., & Paradisi, F. (2020). An (R)-Selective Transaminase From *Thermomyces stellatus*: Stabilizing the Tetrameric Form. *Frontiers in Bioengineering and Biotechnology*, *8*. <https://doi.org/10.3389/fbioe.2020.00707>
- Heffter, A. (1898). Ueber Pellote. *Archiv Für Experimentelle Pathologie Und Pharmakologie*, *40*(5–6), 385–429. <https://doi.org/10.1007/BF01825267>
- Heydari, M., Ohshima, T., Nunoura-Kominato, N., & Sakuraba, H. (2004). Highly Stable Lysine 6-Dehydrogenase from the Thermophile *Geobacillus stearothermophilus* Isolated from a Japanese Hot Spring: Characterization, Gene Cloning and Sequencing, and Expression. *Applied and Environmental Microbiology*, *70*(2), 937–942. <https://doi.org/10.1128/AEM.70.2.937-942.2004>
- Holbrook, O. T., Molligoda, B., Bushell, K. N., & Gobrogge, K. L. (2022). Behavioral consequences of the downstream products of ethanol metabolism involved in alcohol use disorder. *Neuroscience & Biobehavioral Reviews*, *133*, 104501. <https://doi.org/10.1016/j.neubiorev.2021.12.024>
- Houwman, J. A., Knaus, T., Costa, M., & Mutti, F. G. (2019). Efficient synthesis of enantiopure amines from alcohols using resting *E. coli* cells and ammonia. *Green Chemistry*, *21*(14), 3846–3857. <https://doi.org/10.1039/C9GC01059A>
- Huang, J., Mei, L., Wu, H., & Lin, D. (2007). Biosynthesis of γ -aminobutyric acid (GABA) using immobilized whole cells of *Lactobacillus brevis*. *World Journal of Microbiology and Biotechnology*, *23*(6), 865–871. <https://doi.org/10.1007/s11274-006-9311-5>
- Huang, R., Chen, H., Zhong, C., Kim, J. E., & Zhang, Y.-H. P. (2016). High-Throughput Screening of Coenzyme Preference Change of Thermophilic 6-Phosphogluconate Dehydrogenase from NADP⁺ to NAD⁺. *Scientific Reports*, *6*(1), 32644. <https://doi.org/10.1038/srep32644>
- Hwang, E. T., & Lee, S. (2019). Multienzymatic Cascade Reactions via Enzyme Complex by Immobilization. *ACS Catalysis*, *9*(5), 4402–4425. <https://doi.org/10.1021/acscatal.8b04921>
- Jackson, D. M., Ashley, R. L., Brownfield, C. B., Morrison, D. R., & Morrison, R. W. (2015). Rapid Conventional and Microwave-Assisted Decarboxylation of L-Histidine and Other Amino Acids via Organocatalysis with R-Carvone Under Superheated Conditions. *Synthetic Communications*, *45*(23), 2691–2700. <https://doi.org/10.1080/00397911.2015.1100745>
- Jansonius, J. N. (1998). Structure, evolution and action of vitamin B6-dependent enzymes. *Current Opinion in Structural Biology*, *8*(6), 759–769. [https://doi.org/10.1016/S0959-440X\(98\)80096-1](https://doi.org/10.1016/S0959-440X(98)80096-1)
- Jeon, H., Yoon, S., Ahsan, M., Sung, S., Kim, G.-H., Sundaramoorthy, U., Rhee, S.-K., & Yun, H. (2017). The Kinetic Resolution of Racemic Amines Using a Whole-Cell Biocatalyst Co-Expressing Amine Dehydrogenase and NADH Oxidase. *Catalysts*, *7*(9), 251. <https://doi.org/10.3390/catal7090251>
- Jiang, M., Xu, G., Ni, J., Zhang, K., Dong, J., Han, R., & Ni, Y. (2019a). Improving Soluble Expression of Tyrosine Decarboxylase from *Lactobacillus brevis* for Tyramine Synthesis with High Total Turnover Number. *Applied Biochemistry and Biotechnology*, *188*(2), 436–449. <https://doi.org/10.1007/s12010-018-2925-x>

- Jiang, M., Xu, G., Ni, J., Zhang, K., Dong, J., Han, R., & Ni, Y. (2019b). Improving Soluble Expression of Tyrosine Decarboxylase from *Lactobacillus brevis* for Tyramine Synthesis with High Total Turnover Number. *Applied Biochemistry and Biotechnology*, *188*(2), 436–449. <https://doi.org/10.1007/s12010-018-2925-x>
- Jones, J. A., Collins, S. M., Vernacchio, V. R., Lachance, D. M., & Koffas, M. A. G. (2016). Optimization of naringenin and *p*-coumaric acid hydroxylation using the native *E. coli* hydroxylase complex, HpaBC. *Biotechnology Progress*, *32*(1), 21–25. <https://doi.org/10.1002/btpr.2185>
- Khorsand, F., Murphy, C. D., Whitehead, A. J., & Engel, P. C. (2017). Biocatalytic stereoinversion of *p*-para-bromophenylalanine in a one-pot three-enzyme reaction. *Green Chemistry*, *19*(2), 503–510. <https://doi.org/10.1039/C6GC01922F>
- Kim, Baritugo, Oh, Kang, Jung, Jang, Song, Kim, Lee, Hwang, Park, Park, & Joo. (2019). High-Level Conversion of l-lysine into Cadaverine by *Escherichia coli* Whole Cell Biocatalyst Expressing *Hafnia alvei* l-lysine Decarboxylase. *Polymers*, *11*(7), 1184. <https://doi.org/10.3390/polym11071184>
- Kim, D. I., Chae, T. U., Kim, H. U., Jang, W. D., & Lee, S. Y. (2021). Microbial production of multiple short-chain primary amines via retrobiosynthesis. *Nature Communications*, *12*(1), 173. <https://doi.org/10.1038/s41467-020-20423-6>
- Kim, S.-C., Lee, J.-H., Kim, M.-H., Lee, J.-A., Kim, Y. B., Jung, E., Kim, Y.-S., Lee, J., & Park, D. (2013). Hordenine, a single compound produced during barley germination, inhibits melanogenesis in human melanocytes. *Food Chemistry*, *141*(1), 174–181. <https://doi.org/10.1016/j.foodchem.2013.03.017>
- Knaus, T., Böhmer, W., & Mutti, F. G. (2017). Amine dehydrogenases: efficient biocatalysts for the reductive amination of carbonyl compounds. *Green Chemistry*, *19*(2), 453–463. <https://doi.org/10.1039/C6GC01987K>
- Knowles, W. S. (n.d.). Asymmetric Hydrogenations– The MonsantoL-Dopa Process. In *Asymmetric Catalysis on Industrial Scale* (pp. 21–38). Wiley-VCH Verlag GmbH & Co. KGaA. <https://doi.org/10.1002/3527602151.ch1>
- Komori, H., Nitta, Y., Ueno, H., & Higuchi, Y. (2012). Structural Study Reveals That Ser-354 Determines Substrate Specificity on Human Histidine Decarboxylase. *Journal of Biological Chemistry*, *287*(34), 29175–29183. <https://doi.org/10.1074/jbc.M112.381897>
- Kugler, P. (1979). A gel-sandwich technique for the qualitative and quantitative determination of dehydrogenases in the enzyme histochemistry. *Histochemistry*, *60*(3), 265–293. <https://doi.org/10.1007/BF00500656>
- Kumar, R., Vikramachakravarthi, D., & Pal, P. (2014). Production and purification of glutamic acid: A critical review towards process intensification. *Chemical Engineering and Processing: Process Intensification*, *81*, 59–71. <https://doi.org/10.1016/j.cep.2014.04.012>
- Kurpejović, E., Wendisch, V. F., & Sariyar Akbulut, B. (2021). Tyrosinase-based production of l-DOPA by *Corynebacterium glutamicum*. *Applied Microbiology and Biotechnology*, *105*(24), 9103–9111. <https://doi.org/10.1007/s00253-021-11681-5>

- Lapponi, M. J., Méndez, M. B., Trelles, J. A., & Rivero, C. W. (2022). Cell immobilization strategies for biotransformations. *Current Opinion in Green and Sustainable Chemistry*, 33, 100565. <https://doi.org/10.1016/j.cogsc.2021.100565>
- Lawrence, S. A. (2004). *Amines: synthesis, properties and applications*. Cambridge University Press.
- Lee, J., Michael, A. J., Martynowski, D., Goldsmith, E. J., & Phillips, M. A. (2007). Phylogenetic Diversity and the Structural Basis of Substrate Specificity in the β/α -Barrel Fold Basic Amino Acid Decarboxylases. *Journal of Biological Chemistry*, 282(37), 27115–27125. <https://doi.org/10.1074/jbc.M704066200>
- Lee, S. Y., Kim, H. U., Chae, T. U., Cho, J. S., Kim, J. W., Shin, J. H., Kim, D. I., Ko, Y.-S., Jang, W. D., & Jang, Y.-S. (2019). A comprehensive metabolic map for production of bio-based chemicals. *Nature Catalysis*, 2(1), 18–33. <https://doi.org/10.1038/s41929-018-0212-4>
- Leuchtenberger, W., Huthmacher, K., & Drauz, K. (2005). Biotechnological production of amino acids and derivatives: current status and prospects. *Applied Microbiology and Biotechnology*, 69(1), 1–8. <https://doi.org/10.1007/s00253-005-0155-y>
- Li, N., Chou, H., & Xu, Y. (2016). Improved cadaverine production from mutant *Klebsiella oxytoca* lysine decarboxylase. *Engineering in Life Sciences*, 16(3), 299–305. <https://doi.org/10.1002/elsc.201500037>
- Liu, G., Zhou, N., Zhang, M., Li, S., Tian, Q., Chen, J., Chen, B., Wu, Y., & Yao, S. (2010). Hydrophobic solvent induced phase transition extraction to extract drugs from plasma for high performance liquid chromatography–mass spectrometric analysis. *Journal of Chromatography A*, 1217(3), 243–249. <https://doi.org/10.1016/j.chroma.2009.11.037>
- Liu, J., Pang, B. Q. W., Adams, J. P., Snajdrova, R., & Li, Z. (2017). Coupled Immobilized Amine Dehydrogenase and Glucose Dehydrogenase for Asymmetric Synthesis of Amines by Reductive Amination with Cofactor Recycling. *ChemCatChem*, 9(3), 425–431. <https://doi.org/10.1002/cctc.201601446>
- Liu, Y., Liu, P., Gao, S., Wang, Z., Luan, P., González-Sabín, J., & Jiang, Y. (2021). Construction of chemoenzymatic cascade reactions for bridging chemocatalysis and Biocatalysis: Principles, strategies and prospective. *Chemical Engineering Journal*, 420, 127659. <https://doi.org/10.1016/j.cej.2020.127659>
- Ma, J., Wang, S., Huang, X., Geng, P., Wen, C., Zhou, Y., Yu, L., & Wang, X. (2015). Validated UPLC–MS/MS method for determination of hordenine in rat plasma and its application to pharmacokinetic study. *Journal of Pharmaceutical and Biomedical Analysis*, 111, 131–137. <https://doi.org/10.1016/j.jpba.2015.03.032>
- Mateo, C., Grazú, V., Pessela, B. C. C., Montes, T., Palomo, J. M., Torres, R., López-Gallego, F., Fernández-Lafuente, R., & Guisán, J. M. (2007a). Advances in the design of new epoxy supports for enzyme immobilization–stabilization. *Biochemical Society Transactions*, 35(6), 1593–1601. <https://doi.org/10.1042/BST0351593>
- Mateo, C., Grazú, V., Pessela, B. C. C., Montes, T., Palomo, J. M., Torres, R., López-Gallego, F., Fernández-Lafuente, R., & Guisán, J. M. (2007b). Advances in the design of new epoxy supports for enzyme immobilization–stabilization. *Biochemical Society Transactions*, 35(6), 1593–1601. <https://doi.org/10.1042/BST0351593>

- Mayol, O., Bastard, K., Beloti, L., Frese, A., Turkenburg, J. P., Petit, J.-L., Mariage, A., Debard, A., Pellouin, V., Perret, A., de Berardinis, V., Zaparucha, A., Grogan, G., & Vergne-Vaxelaire, C. (2019a). A family of native amine dehydrogenases for the asymmetric reductive amination of ketones. *Nature Catalysis*, 2(4), 324–333. <https://doi.org/10.1038/s41929-019-0249-z>
- Mayol, O., Bastard, K., Beloti, L., Frese, A., Turkenburg, J. P., Petit, J.-L., Mariage, A., Debard, A., Pellouin, V., Perret, A., de Berardinis, V., Zaparucha, A., Grogan, G., & Vergne-Vaxelaire, C. (2019b). A family of native amine dehydrogenases for the asymmetric reductive amination of ketones. *Nature Catalysis*, 2(4), 324–333. <https://doi.org/10.1038/s41929-019-0249-z>
- Meyer, E. (1982). Separation of two distinct S-adenosylmethionine dependent N-methyltransferases involved in hordenine biosynthesis in *Hordeum vulgare*. *Plant Cell Reports*, 1(6), 236–239. <https://doi.org/10.1007/BF00272627>
- Mi, J., Liu, S., Du, Y., Qi, H., & Zhang, L. (2022). Cofactor self-sufficient by co-immobilization of pyridoxal 5'-phosphate and lysine decarboxylase for cadaverine production. *Bioresource Technology Reports*, 17, 100939. <https://doi.org/10.1016/j.biteb.2021.100939>
- Montgomery, S. L., Mangas-Sanchez, J., Thompson, M. P., Aleku, G. A., Dominguez, B., & Turner, N. J. (2017). Direct Alkylation of Amines with Primary and Secondary Alcohols through Biocatalytic Hydrogen Borrowing. *Angewandte Chemie*, 129(35), 10627–10630. <https://doi.org/10.1002/ange.201705848>
- Mørch, Y. A., Donati, I., Strand, B. L., & Skjåk-Bræk, G. (2006). Effect of Ca²⁺, Ba²⁺, and Sr²⁺ on Alginate Microbeads. *Biomacromolecules*, 7(5), 1471–1480. <https://doi.org/10.1021/bm060010d>
- Muñoz, A. J., Hernández-Chávez, G., De Anda, R., Martínez, A., Bolívar, F., & Gosset, G. (2011). Metabolic engineering of *Escherichia coli* for improving l-3,4-dihydroxyphenylalanine (l-DOPA) synthesis from glucose. *Journal of Industrial Microbiology and Biotechnology*, 38(11), 1845–1852. <https://doi.org/10.1007/s10295-011-0973-0>
- Mutti, F. G., & Knaus, T. (2021). Enzymes Applied to the Synthesis of Amines. In *Biocatalysis for Practitioners* (pp. 143–180). Wiley. <https://doi.org/10.1002/9783527824465.ch6>
- Mutti, F. G., Knaus, T., Scrutton, N. S., Breuer, M., & Turner, N. J. (2015). Conversion of alcohols to enantiopure amines through dual-enzyme hydrogen-borrowing cascades. *Science*, 349(6255), 1525–1529. <https://doi.org/10.1126/science.aac9283>
- Nakai, T., Nakagawa, N., Maoka, N., Masui, R., Kuramitsu, S., & Kamiya, N. (2005). Structure of P-protein of the glycine cleavage system: implications for nonketotic hyperglycinemia. *The EMBO Journal*, 24(8), 1523–1536. <https://doi.org/10.1038/sj.emboj.7600632>
- Narisetty, V., Cox, R., Bommareddy, R., Agrawal, D., Ahmad, E., Pant, K. K., Chandel, A. K., Bhatia, S. K., Kumar, D., Binod, P., Gupta, V. K., & Kumar, V. (2022). Valorisation of xylose to renewable fuels and chemicals, an essential step in augmenting the commercial viability of lignocellulosic biorefineries. *Sustainable Energy & Fuels*, 6(1), 29–65. <https://doi.org/10.1039/D1SE00927C>
- Nasri, M. (2017a). *Protein Hydrolysates and Biopeptides* (pp. 109–159). <https://doi.org/10.1016/bs.afnr.2016.10.003>

- Nasri, M. (2017b). *Protein Hydrolysates and Biopeptides* (pp. 109–159).
<https://doi.org/10.1016/bs.afnr.2016.10.003>
- Natte, K., Neumann, H., Jagadeesh, R. v., & Beller, M. (2017). Convenient iron-catalyzed reductive aminations without hydrogen for selective synthesis of N-methylamines. *Nature Communications*, 8(1), 1344. <https://doi.org/10.1038/s41467-017-01428-0>
- Nguyen, N. H., Truong-Thi, N.-H., Nguyen, D. T. D., Ching, Y. C., Huynh, N. T., & Nguyen, D. H. (2022). Non-ionic surfactants As co-templates to control the mesopore diameter of hollow mesoporous silica nanoparticles for drug delivery applications. *Colloids and Surfaces A: Physicochemical and Engineering Aspects*, 655, 130218.
<https://doi.org/10.1016/j.colsurfa.2022.130218>
- Ohta, H., Murakami, Y., Takebe, Y., Murasaki, K., Oshima, K., Yoshihara, H., & Morimura, S. (2020). <i>N</i>-Methyltyramine, a Gastrin-releasing Factor in Beer, and Structurally Related Compounds as Agonists for Human Trace Amine-associated Receptor 1. *Food Science and Technology Research*, 26(2), 313–317.
<https://doi.org/10.3136/fstr.26.313>
- PARADISI, F., COLLINS, S., MAGUIRE, A., & ENGEL, P. (2007). Phenylalanine dehydrogenase mutants: Efficient biocatalysts for synthesis of non-natural phenylalanine derivatives. *Journal of Biotechnology*, 128(2), 408–411. <https://doi.org/10.1016/j.jbiotec.2006.08.008>
- Park, J.-Y., Choi, M.-J., Yu, H., Choi, Y., Park, K.-M., & Chang, P.-S. (2022). Multi-functional behavior of food emulsifier erythorbyl laurate in different colloidal conditions of homogeneous oil-in-water emulsion system. *Colloids and Surfaces A: Physicochemical and Engineering Aspects*, 636, 128127. <https://doi.org/10.1016/j.colsurfa.2021.128127>
- Park, S. H., Soetyono, F., & Kim, H. K. (2017). Cadaverine Production by Using Cross-Linked Enzyme Aggregate of Escherichia coli Lysine Decarboxylase. *Journal of Microbiology and Biotechnology*, 27(2), 289–296. <https://doi.org/10.4014/jmb.1608.08033>
- Patil, M. D., Grogan, G., Bommarius, A., & Yun, H. (2018). Oxidoreductase-Catalyzed Synthesis of Chiral Amines. *ACS Catalysis*, 8(12), 10985–11015.
<https://doi.org/10.1021/acscatal.8b02924>
- Patil, M. D., Yoon, S., Jeon, H., Khobragade, T. P., Sarak, S., Pagar, A. D., Won, Y., & Yun, H. (2019). Kinetic Resolution of Racemic Amines to Enantiopure (S)-amines by a Biocatalytic Cascade Employing Amine Dehydrogenase and Alanine Dehydrogenase. *Catalysts*, 9(7), 600. <https://doi.org/10.3390/catal9070600>
- Payne, J. T., Valentic, T. R., & Smolke, C. D. (2021). Complete biosynthesis of the bisbenzylisoquinoline alkaloids guattegaumerine and berbaminine in yeast. *Proceedings of the National Academy of Sciences*, 118(51). <https://doi.org/10.1073/pnas.2112520118>
- Pelckmans, M., Renders, T., Van de Vyver, S., & Sels, B. F. (2017). Bio-based amines through sustainable heterogeneous catalysis. *Green Chemistry*, 19(22), 5303–5331.
<https://doi.org/10.1039/C7GC02299A>
- Pilkington, R. L., Dallaston, M. A., Savage, G. P., Williams, C. M., & Polyzos, A. (2021). Enone-promoted decarboxylation of *trans*-4-hydroxy- <sc>l</sc>-proline in flow: a side-by-side comparison to batch. *Reaction Chemistry & Engineering*, 6(3), 486–493.
<https://doi.org/10.1039/D0RE00442A>

- Planchestainer, M., Hegarty, E., Heckmann, C. M., Gourlay, L. J., & Paradisi, F. (2019). Widely applicable background depletion step enables transaminase evolution through solid-phase screening. *Chemical Science*, *10*(23), 5952–5958. <https://doi.org/10.1039/C8SC05712E>
- Prieto, M. A., & Garcia, J. L. (1994). Molecular characterization of 4-hydroxyphenylacetate 3-hydroxylase of *Escherichia coli*. A two-protein component enzyme. *Journal of Biological Chemistry*, *269*(36), 22823–22829. [https://doi.org/10.1016/S0021-9258\(17\)31719-2](https://doi.org/10.1016/S0021-9258(17)31719-2)
- Pyne, M. E., Kevvai, K., Grewal, P. S., Narcross, L., Choi, B., Bourgeois, L., Dueber, J. E., & Martin, V. J. J. (2020). A yeast platform for high-level synthesis of tetrahydroisoquinoline alkaloids. *Nature Communications*, *11*(1), 3337. <https://doi.org/10.1038/s41467-020-17172-x>
- Quaglia, D., Irwin, J. A., & Paradisi, F. (2012a). Horse Liver Alcohol Dehydrogenase: New Perspectives for an Old Enzyme. *Molecular Biotechnology*, *52*(3), 244–250. <https://doi.org/10.1007/s12033-012-9542-7>
- Quaglia, D., Irwin, J. A., & Paradisi, F. (2012b). Horse Liver Alcohol Dehydrogenase: New Perspectives for an Old Enzyme. *Molecular Biotechnology*, *52*(3), 244–250. <https://doi.org/10.1007/s12033-012-9542-7>
- Ray, S. S., Bonanno, J. B., Rajashankar, K. R., Pinho, M. G., He, G., De Lencastre, H., Tomasz, A., & Burley, S. K. (2002). Cocrystal Structures of Diaminopimelate Decarboxylase. *Structure*, *10*(11), 1499–1508. [https://doi.org/10.1016/S0969-2126\(02\)00880-8](https://doi.org/10.1016/S0969-2126(02)00880-8)
- Reetz, M. T. (2013). Biocatalysis in Organic Chemistry and Biotechnology: Past, Present, and Future. *Journal of the American Chemical Society*, *135*(34), 12480–12496. <https://doi.org/10.1021/ja405051f>
- Roschangar, F., Sheldon, R. A., & Senanayake, C. H. (2015). Overcoming barriers to green chemistry in the pharmaceutical industry – the Green Aspiration Level™ concept. *Green Chemistry*, *17*(2), 752–768. <https://doi.org/10.1039/C4GC01563K>
- Ruhaak, L. R., Steenvoorden, E., Koeleman, C. A. M., Deelder, A. M., & Wuhrer, M. (2010). 2-Picoline-borane: A non-toxic reducing agent for oligosaccharide labeling by reductive amination. *Proteomics*, *10*(12), 2330–2336. <https://doi.org/10.1002/pmic.200900804>
- Sagong, H.-Y., Son, H. F., Kim, S., Kim, Y.-H., Kim, I.-K., & Kim, K.-J. (2016). Crystal Structure and Pyridoxal 5-Phosphate Binding Property of Lysine Decarboxylase from *Selenomonas ruminantium*. *PLOS ONE*, *11*(11), e0166667. <https://doi.org/10.1371/journal.pone.0166667>
- Said, A. A. E., Ali, T. F. S., Attia, E. Z., Ahmed, A.-S. F., Shehata, A. H., Abdelmohsen, U. R., & Fouad, M. A. (2021). Antidepressant potential of *Mesembryanthemum cordifolium* roots assisted by metabolomic analysis and virtual screening. *Natural Product Research*, *35*(23), 5493–5497. <https://doi.org/10.1080/14786419.2020.1788019>
- SANDMEIER, E., HALE, T. I., & CHRISTEN, P. (1994a). Multiple evolutionary origin of pyridoxal-5'-phosphate-dependent amino acid decarboxylases. *European Journal of Biochemistry*, *221*(3), 997–1002. <https://doi.org/10.1111/j.1432-1033.1994.tb18816.x>
- SANDMEIER, E., HALE, T. I., & CHRISTEN, P. (1994b). Multiple evolutionary origin of pyridoxal-5'-phosphate-dependent amino acid decarboxylases. *European Journal of Biochemistry*, *221*(3), 997–1002. <https://doi.org/10.1111/j.1432-1033.1994.tb18816.x>

- Sato, S., Sakamoto, T., Miyazawa, E., & Kikugawa, Y. (2004). One-pot reductive amination of aldehydes and ketones with α -picoline-borane in methanol, in water, and in neat conditions. *Tetrahedron*, *60*(36), 7899–7906. <https://doi.org/10.1016/j.tet.2004.06.045>
- Schoenmakers, H., & Spiegel, L. (2014). Laboratory Distillation and Scale-up. In *Distillation* (pp. 319–339). Elsevier. <https://doi.org/10.1016/B978-0-12-386878-7.00010-3>
- Seah, S. Y. K., Britton, K. L., Rice, D. W., Asano, Y., & Engel, P. C. (2002). Single Amino Acid Substitution in *Bacillus sphaericus* Phenylalanine Dehydrogenase Dramatically Increases Its Discrimination between Phenylalanine and Tyrosine Substrates. *Biochemistry*, *41*(38), 11390–11397. <https://doi.org/10.1021/bi020196a>
- Seah, S. Y. K., Linda Britton, K., Baker, P. J., Rice, D. W., Asano, Y., & Engel, P. C. (1995). Alteration in relative activities of phenylalanine dehydrogenase towards different substrates by site-directed mutagenesis. *FEBS Letters*, *370*(1–2), 93–96. [https://doi.org/10.1016/0014-5793\(95\)00804-I](https://doi.org/10.1016/0014-5793(95)00804-I)
- Sen, K. Y., & Baidurah, S. (2021). Renewable biomass feedstocks for production of sustainable biodegradable polymer. *Current Opinion in Green and Sustainable Chemistry*, *27*, 100412. <https://doi.org/10.1016/j.cogsc.2020.100412>
- Sharma, M., Mangas-Sanchez, J., Turner, N. J., & Grogan, G. (2017). NAD(P)H-Dependent Dehydrogenases for the Asymmetric Reductive Amination of Ketones: Structure, Mechanism, Evolution and Application. *Advanced Synthesis & Catalysis*, *359*(12), 2011–2025. <https://doi.org/10.1002/adsc.201700356>
- Sheldon, R. A., Basso, A., & Brady, D. (2021). New frontiers in enzyme immobilisation: robust biocatalysts for a circular bio-based economy. *Chemical Society Reviews*, *50*(10), 5850–5862. <https://doi.org/10.1039/D1CS00015B>
- Sheldon, R. A., & Brady, D. (2019). Broadening the Scope of Biocatalysis in Sustainable Organic Synthesis. *ChemSusChem*, *12*(13), 2859–2881. <https://doi.org/10.1002/cssc.201900351>
- Sheldon, R. A., & Woodley, J. M. (2018). Role of Biocatalysis in Sustainable Chemistry. *Chemical Reviews*, *118*(2), 801–838. <https://doi.org/10.1021/acs.chemrev.7b00203>
- Sommer, T., Göen, T., Budnik, N., & Pischetsrieder, M. (2020). Absorption, Biokinetics, and Metabolism of the Dopamine D2 Receptor Agonist Hordenine (N, N-Dimethyltyramine) after Beer Consumption in Humans. *Journal of Agricultural and Food Chemistry*, *68*(7), 1998–2006. <https://doi.org/10.1021/acs.jafc.9b06029>
- Song, W., Chen, X., Wu, J., Xu, J., Zhang, W., Liu, J., Chen, J., & Liu, L. (2020). Biocatalytic derivatization of proteinogenic amino acids for fine chemicals. *Biotechnology Advances*, *40*, 107496. <https://doi.org/10.1016/j.biotechadv.2019.107496>
- Stano, J., Nemeč, P., Weissová, K., Kovács, P., Kákoniová, D., & Lisková, D. (1995). Decarboxylation of l-tyrosine and l-dopa by immobilized cells of *Papaver somniferum*. *Phytochemistry*, *38*(4), 859–860. [https://doi.org/10.1016/0031-9422\(94\)00768-O](https://doi.org/10.1016/0031-9422(94)00768-O)
- Stockert, J. C., Horobin, R. W., Colombo, L. L., & Blázquez-Castro, A. (2018). Tetrazolium salts and formazan products in Cell Biology: Viability assessment, fluorescence imaging, and labeling perspectives. *Acta Histochemica*, *120*(3), 159–167. <https://doi.org/10.1016/j.acthis.2018.02.005>

- Su, Y., Liu, Y., He, D., Hu, G., Wang, H., Ye, B., He, Y., Gao, X., & Liu, D. (2022). Hordenine inhibits neuroinflammation and exerts neuroprotective effects via inhibiting NF- κ B and MAPK signaling pathways in vivo and in vitro. *International Immunopharmacology*, *108*, 108694. <https://doi.org/10.1016/j.intimp.2022.108694>
- Surwase, S. N., Patil, S. A., Apine, O. A., & Jadhav, J. P. (2012). Efficient Microbial Conversion of L-Tyrosine to L-DOPA by *Brevundimonas* sp. SGJ. *Applied Biochemistry and Biotechnology*, *167*(5), 1015–1028. <https://doi.org/10.1007/s12010-012-9564-4>
- Tang, Y. Q., & Weng, N. (2013). Salting-out assisted liquid–liquid extraction for bioanalysis. *Bioanalysis*, *5*(12), 1583–1598. <https://doi.org/10.4155/bio.13.117>
- Teng, Y., Scott, E. L., van Zeeland, A. N. T., & Sanders, J. P. M. (2011). The use of L-lysine decarboxylase as a means to separate amino acids by electrodialysis. *Green Chemistry*, *13*(3), 624. <https://doi.org/10.1039/c0gc00611d>
- Thompson, M. P., Derrington, S. R., Heath, R. S., Porter, J. L., Mangas-Sanchez, J., Devine, P. N., Truppo, M. D., & Turner, N. J. (2019). A generic platform for the immobilisation of engineered biocatalysts. *Tetrahedron*, *75*(3), 327–334. <https://doi.org/10.1016/j.tet.2018.12.004>
- Thompson, M. P., & Turner, N. J. (2017a). Two-Enzyme Hydrogen-Borrowing Amination of Alcohols Enabled by a Cofactor-Switched Alcohol Dehydrogenase. *ChemCatChem*, *9*(20), 3833–3836. <https://doi.org/10.1002/cctc.201701092>
- Thompson, M. P., & Turner, N. J. (2017b). Two-Enzyme Hydrogen-Borrowing Amination of Alcohols Enabled by a Cofactor-Switched Alcohol Dehydrogenase. *ChemCatChem*, *9*(20), 3833–3836. <https://doi.org/10.1002/cctc.201701092>
- Tolbert, W. D., Graham, D. E., White, R. H., & Ealick, S. E. (2003). Pyruvoyl-Dependent Arginine Decarboxylase from *Methanococcus jannaschii*. *Structure*, *11*(3), 285–294. [https://doi.org/10.1016/S0969-2126\(03\)00026-1](https://doi.org/10.1016/S0969-2126(03)00026-1)
- Truong, C. C., Mishra, D. K., & Suh, Y. (2023). Recent Catalytic Advances on the Sustainable Production of Primary Furanic Amines from the One-Pot Reductive Amination of 5-Hydroxymethylfurfural. *ChemSusChem*, *16*(1). <https://doi.org/10.1002/cssc.202201846>
- Tseliou, V., Knaus, T., Masman, M. F., Corrado, M. L., & Mutti, F. G. (2019). Generation of amine dehydrogenases with increased catalytic performance and substrate scope from ϵ -deaminating L-Lysine dehydrogenase. *Nature Communications*, *10*(1), 3717. <https://doi.org/10.1038/s41467-019-11509-x>
- Tseliou, V., Knaus, T., Vilím, J., Masman, M. F., & Mutti, F. G. (2020). Kinetic Resolution of Racemic Primary Amines Using *Geobacillus stearothermophilus* Amine Dehydrogenase Variant. *ChemCatChem*, *12*(8), 2184–2188. <https://doi.org/10.1002/cctc.201902085>
- Tsukatani, T., Suenaga, H., Higuchi, T., Akao, T., Ishiyama, M., Ezo, K., & Matsumoto, K. (2008). Colorimetric cell proliferation assay for microorganisms in microtiter plate using water-soluble tetrazolium salts. *Journal of Microbiological Methods*, *75*(1), 109–116. <https://doi.org/10.1016/j.mimet.2008.05.016>
- Viejo, C. G., Villarreal-Lara, R., Torrico, D. D., Rodríguez-Velazco, Y. G., Escobedo-Avellaneda, Z., Ramos-Parra, P. A., Mandal, R., Singh, A. P., Hernández-Brenes, C., & Fuentes, S. (2020).

- Beer and consumer response using biometrics: Associations assessment of beer compounds and elicited emotions. *Foods*, 9(6), 821.
- Vitaku, E., Smith, D. T., & Njardarson, J. T. (2014). Analysis of the Structural Diversity, Substitution Patterns, and Frequency of Nitrogen Heterocycles among U.S. FDA Approved Pharmaceuticals. *Journal of Medicinal Chemistry*, 57(24), 10257–10274. <https://doi.org/10.1021/jm501100b>
- Wang, M., Khan, M. A., Mohsin, I., Wicks, J., Ip, A. H., Sumon, K. Z., Dinh, C.-T., Sargent, E. H., Gates, I. D., & Kibria, M. G. (2021). Can sustainable ammonia synthesis pathways compete with fossil-fuel based Haber–Bosch processes? *Energy & Environmental Science*, 14(5), 2535–2548. <https://doi.org/10.1039/D0EE03808C>
- Wang, Q., Xin, Y., Zhang, F., Feng, Z., Fu, J., Luo, L., & Yin, Z. (2011). Enhanced γ -aminobutyric acid-forming activity of recombinant glutamate decarboxylase (gadA) from *Escherichia coli*. *World Journal of Microbiology and Biotechnology*, 27(3), 693–700. <https://doi.org/10.1007/s11274-010-0508-2>
- Watanabe, Y., Tsuji, Y., Ige, H., Ohsugi, Y., & Ohta, T. (1984). Ruthenium-catalyzed N-alkylation and N-benzylation of aminoarenes with alcohols. *The Journal of Organic Chemistry*, 49(18), 3359–3363. <https://doi.org/10.1021/jo00192a021>
- Weber, R. E. (1992). Use of ionic and zwitterionic (Tris/BisTris and HEPES) buffers in studies on hemoglobin function. *Journal of Applied Physiology*, 72(4), 1611–1615. <https://doi.org/10.1152/jappl.1992.72.4.1611>
- Wei, G., Chen, Y., Zhou, N., Lu, Q., Xu, S., Zhang, A., Chen, K., & Ouyang, P. (2022). Chitin biopolymer mediates self-sufficient biocatalyst of pyridoxal 5'-phosphate and L-lysine decarboxylase. *Chemical Engineering Journal*, 427, 132030. <https://doi.org/10.1016/j.cej.2021.132030>
- Wei, T., Cheng, B. Y., & Liu, J. Z. (2016). Genome engineering *Escherichia coli* for L-DOPA overproduction from glucose. *Scientific Reports*, 6. <https://doi.org/10.1038/srep30080>
- Wieschalka, S., Blombach, B., Bott, M., & Eikmanns, B. J. (2013). Bio-based production of organic acids with *Corynebacterium glutamicum*. *Microbial Biotechnology*, 6(2), 87–102. <https://doi.org/10.1111/1751-7915.12013>
- Wohlgemuth, R. (2021). Biocatalysis-Key enabling tools from biocatalytic one-step and multi-step reactions to biocatalytic total synthesis. *New Biotechnol*, 60, 113–123.
- Wu, B., Zhang, S., Hong, T., Zhou, Y., Wang, H., Shi, M., Yang, H., Tian, X., Guo, J., Bian, J., Roache, J., Delgado, P., Mo, R., Fridrich, C., Gao, F., & Wang, J. (2020). Merging Biocatalysis, Flow, and Surfactant Chemistry: Innovative Synthesis of an FXI (Factor XI) Inhibitor. *Organic Process Research & Development*, 24(11), 2780–2788. <https://doi.org/10.1021/acs.oprd.0c00412>
- Wu, P., Li, G., He, Y., Luo, D., Li, L., Guo, J., Ding, P., & Yang, F. (2020). High-efficient and sustainable biodegradation of microcystin-LR using *Sphingopyxis* sp. YF1 immobilized Fe₃O₄@chitosan. *Colloids and Surfaces B: Biointerfaces*, 185, 110633. <https://doi.org/10.1016/j.colsurfb.2019.110633>

- Ye, L. J., Toh, H. H., Yang, Y., Adams, J. P., Snajdrova, R., & Li, Z. (2015). Engineering of Amine Dehydrogenase for Asymmetric Reductive Amination of Ketone by Evolving *Rhodococcus* Phenylalanine Dehydrogenase. *ACS Catalysis*, *5*(2), 1119–1122. <https://doi.org/10.1021/cs501906r>
- Yoon, S., Patil, M. D., Sarak, S., Jeon, H., Kim, G., Khobragade, T. P., Sung, S., & Yun, H. (2019). Deracemization of Racemic Amines to Enantiopure (*R*)- and (*S*)-amines by Biocatalytic Cascade Employing ω -Transaminase and Amine Dehydrogenase. *ChemCatChem*, *11*(7), 1898–1902. <https://doi.org/10.1002/cctc.201900080>
- Yoshitaka Hashitani, B. (1925). On the chemical constituents of malt-rootlets with special reference to Hordenine. *Journal of the College of Agriculture*, *14*, 1–56.
- Zhang, B., Jiang, Y., Li, Z., Wang, F., & Wu, X.-Y. (2020). Recent Progress on Chemical Production From Non-food Renewable Feedstocks Using *Corynebacterium glutamicum*. *Frontiers in Bioengineering and Biotechnology*, *8*. <https://doi.org/10.3389/fbioe.2020.606047>
- Zhang, H., Wei, Y., Lu, Y., Wu, S., Liu, Q., Liu, J., & Jiao, Q. (2016). Three-step biocatalytic reaction using whole cells for efficient production of tyramine from keratin acid hydrolysis wastewater. *Applied Microbiology and Biotechnology*, *100*(4), 1691–1700. <https://doi.org/10.1007/s00253-015-7054-7>
- Zhang, K., & Ni, Y. (2014). Tyrosine decarboxylase from *Lactobacillus brevis*: Soluble expression and characterization. *Protein Expression and Purification*, *94*, 33–39. <https://doi.org/10.1016/j.pep.2013.10.018>
- Zhang, X., Du, L., Zhang, J., Li, C., Zhang, J., & Lv, X. (2021). Hordenine Protects Against Lipopolysaccharide-Induced Acute Lung Injury by Inhibiting Inflammation. *Frontiers in Pharmacology*, *12*, 712232. <https://doi.org/10.3389/fphar.2021.712232>
- Zhao, W., Hu, S., Huang, J., Ke, P., Yao, S., Lei, Y., Mei, L., & Wang, J. (2016). Permeabilization of *Escherichia coli* with ampicillin for a whole cell biocatalyst with enhanced glutamate decarboxylase activity. *Chinese Journal of Chemical Engineering*, *24*(7), 909–913. <https://doi.org/10.1016/j.cjche.2016.02.001>
- Zhou, F., Xu, Y., Nie, Y., & Mu, X. (2022). Substrate-Specific Engineering of Amino Acid Dehydrogenase Superfamily for Synthesis of a Variety of Chiral Amines and Amino Acids. *Catalysts*, *12*(4), 380. <https://doi.org/10.3390/catal12040380>
- Zhou, J.-W., Ruan, L.-Y., Chen, H.-J., Luo, H.-Z., Jiang, H., Wang, J.-S., & Jia, A.-Q. (2019). Inhibition of Quorum Sensing and Virulence in *Serratia marcescens* by Hordenine. *Journal of Agricultural and Food Chemistry*, *67*(3), 784–795. <https://doi.org/10.1021/acs.jafc.8b05922>
- Zhu, H., Xu, G., Zhang, K., Kong, X., Han, R., Zhou, J., & Ni, Y. (2016a). Crystal structure of tyrosine decarboxylase and identification of key residues involved in conformational swing and substrate binding. *Scientific Reports*, *6*(1), 27779. <https://doi.org/10.1038/srep27779>
- Zhu, H., Xu, G., Zhang, K., Kong, X., Han, R., Zhou, J., & Ni, Y. (2016b). Crystal structure of tyrosine decarboxylase and identification of key residues involved in conformational swing and substrate binding. *Scientific Reports*, *6*(1), 27779. <https://doi.org/10.1038/srep27779>

Zhuang, W., Liu, H., Zhang, Y., He, J., & Wang, P. (2021). Effective asymmetric preparation of (R)-1-[3-(trifluoromethyl)phenyl]ethanol with recombinant *E. coli* whole cells in an aqueous Tween-20/natural deep eutectic solvent solution. *AMB Express*, *11*(1), 118.
<https://doi.org/10.1186/s13568-021-01278-6>

Appendix A: Additional related studies

A.1 Screening of engineered amino acid dehydrogenases for oxidative deamination reaction

Unless explicitly stated otherwise, the research presented in this chapter is the sole and individual work of the author.

A.1.1 Background

In addition to naturally occurring Amine Dehydrogenases (AmDHs), engineered Aromatic Amino Acid Dehydrogenases (AADHs) represent another intriguing class of biocatalysts that could potentially facilitate the oxidative deamination of primary amines. AADHs have been effectively manipulated to act on ketones, bypassing the need for a carboxylic group typically required by these enzymes. (Abrahamson et al., 2012; Tseliou et al., 2019; Ye et al., 2015) This feature expands the substrate scope of these enzymes, potentially enabling new synthetic pathways.

Presented in this appendix is the investigation concerning two specific Amino Acid Dehydrogenases (AADHs), Phenylalanine Dehydrogenase (*BsPheDH*) from *Bacillus sphaericus* (Asano et al., 1987) and Lysine ϵ -Dehydrogenase (*LysEDH*) from *Geobacillus stearothermophilus*. (Tseliou et al., 2019) The goal was to harness the considerable potential of these enzymes and adapt them for the oxidative deamination reaction, expanding their substrate scope to primary aromatic amines. Specifically, similar to the approach outlined in chapter 7, these enzymes were aimed to be incorporated within a hydrogen-borrowing system for the enzymatic cascade of hydroxytyrosol (Figure A1.1). Coupled with horse liver alcohol dehydrogenase (HLADH), this system would facilitate the conversion of dopamine to hydroxytyrosol, ensuring efficient recycling of the NADH cofactor.

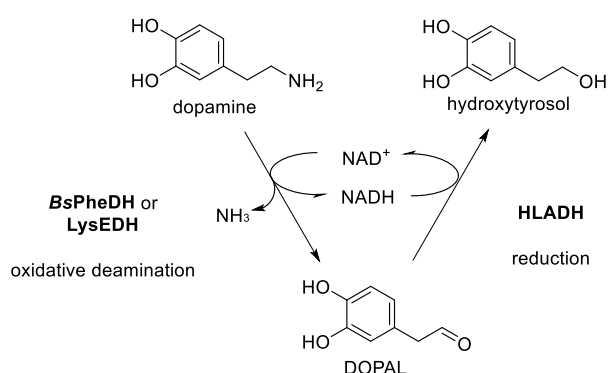


Figure A1.1: Hydrogen borrowing strategy with AADHs and HLADH in the hydroxytyrosol cascade application.

Selection of AADHs for oxidative deamination reaction towards aromatic primary amines

The selection of the two AADHs, *BsPheDH* and *LysEDH*, was primarily driven by their previously described substrate scopes.

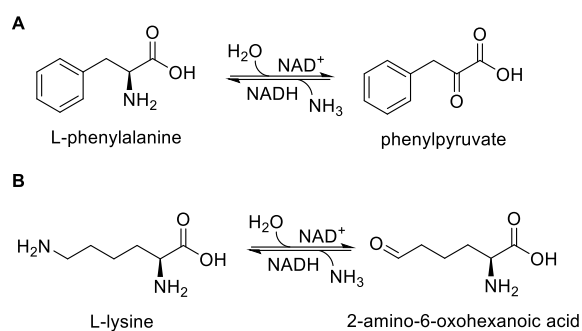


Figure A1.2: Schematic representation of the reactions undergone by the natural substrates for BsPheDH (**A**) and LysEDH (**B**).

BsPheDH is structured as an octamer, with each of its eight subunits weighing 42 kDa and consisting of 381 amino acids. Over time, various mutations have been made at different positions in the active site to enhance our understanding of its functions. (Asano et al., 1987; Khorsand et al., 2017; PARADISI et al., 2007; Seah et al., 1995) This enzyme exhibits an uncommon characteristic in its class, as it demonstrates similar activities towards L-phenylalanine and L-tyrosine. The asparagine (N) at position 145, unique to *B. sphaericus*, appears to interact favorably with the hydroxyl group of a tyrosine substrate, as suggested by modeling studies, leading to the promiscuous activity. (Seah et al., 2002) This biocatalyst showed promise for further engineering, given its observed activity towards L-DOPA as well.

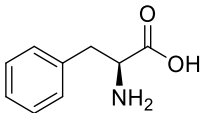
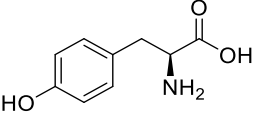
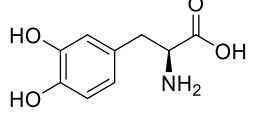
Substrate	Activity (U/mg)
L-phenylalanine 	87.5
L-tyrosine 	50.1
L-dopa 	12.3

Table A1.1: Specific activities of His-tagged BsPheDH towards L-phenylalanine, L-tyrosine and L-DOPA measuring NADH formation at 340 nm. Conditions: 5 mM substrate, 1 mM NAD⁺, 0.007 mg/mL BsPheDH, in 0.1 M glycine-KOH, 100 mM KCl, pH 10.4, 1 mL final volume.

On the other hand, LysEDH possesses a unique ability to act on the epsilon amino group of its natural substrate, lysine. This feature makes LysEDH particularly interesting as it already demonstrates the capability to target primary amines without the presence of the carboxylic group in alpha position, converting L-lysine into 2-Amino-6-oxohexanoic acid.(Tseliou et al., 2019) The activity of LysEDH was measured to be 0.5 U/mg, assessed under the conditions outlined in the materials and methods section.

By leveraging this peculiarity and exploring the potential of LysEDH to act on a broader range of primary amines, the aim was to exploit the inherent versatility of these enzymes and develop them into valuable biocatalysts for various applications.

A1.2 Findings

Expression and purification of PheDH and LysEDH

The expressions of both PheDH and LysEDH were executed following the procedures delineated in the Materials and Methods section. The gene for PheDH was subcloned from the plasmid ptac85 into the pRSETb plasmid, obtaining the His-tagged enzyme for easier purification. It was ensured that this modification to the protein sequence did not affect the protein expression, solubility, or activity. In fact SDS-PAGE analysis confirmed successful expression and no adverse effects from the introduction of the His-tag.

BsPheDH was expressed in Autoinduction medium (Figure A1.3) while LysEDH in LB medium (Figure A1.4).

In the case of PheDH, protein precipitation was encountered during the dialysis process, particularly when a 0.05 M phosphate buffer at pH 8 with 0.1 M KCl was used. However, this issue was effectively resolved by switching to a TRIS-HCl buffer. This modification ensured a successful dialysis process and resulted in the final yield of a purified PheDH preparation, underscoring the significance of careful buffer selection in preserving protein stability during purification procedures.

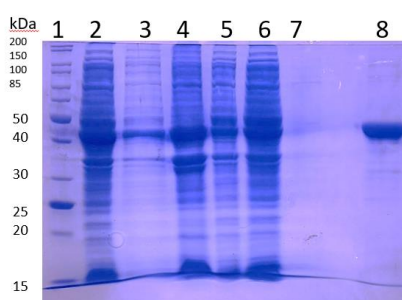


Figure A1.3: SDS-PAGE analysis of different stages of PheDH purification. Lanes are as follows: (1) Marker; (2) Crude cell extract; (3) Diluted crude extract (1:10); (4) Pellet; (5) Wash buffer A; (6) Flowthrough; (7) Wash with 10% buffer B; (8) Purified protein (1.6 mg/mL). Buffer A: 50 mM potassium phosphate buffer, 100 mM NaCl, 30 mM imidazole,

pH 8. Buffer B: 50 mM potassium phosphate buffer, 100 mM NaCl, 300 mM imidazole, pH 8.

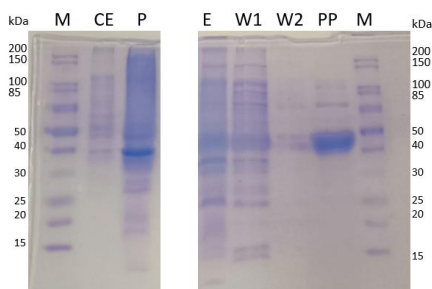


Figure A1.4: SDS-PAGE analysis of the expression and purification of LysEDH. **M.** Marker; **CE.** Crude cell extract; **P.** Pellet; **E.** Flowthrough; **W1.** Wash with buffer A; **W2.** Wash with 10 % of buffer B; **PP.** Purified protein. Buffer A: 50 mM potassium phosphate buffer, 100 mM NaCl, 30 mM imidazole, pH 8. Buffer B: 50 mM potassium phosphate buffer, 100 mM NaCl, 300 mM imidazole, pH 8.

Screening of AADHs for oxidative deamination reaction

Both wild-type and mutant versions of the AADHs were screened measuring the activity of the purified enzymes. The activity was monitored by either tracking the absorbance of NADH at 340 nm or by following the formation of cofactor with fluorescence using a spectrofluorometer.

As expected, the wild-type versions of both *BsPheDH* and LysEDH could not convert the targeted substrates, 2-phenylethylamine and tyramine, into its corresponding aldehyde. This presented the necessity of engineering these biocatalysts to enhance their performance for the desired reaction. 2-phenylethylamine and tyramine were the primary amine utilized in the screening, because dopamine can easily oxidase under the alkaline pH reaction conditions.

Engineered AADHs for oxidative deamination of aromatic primary amines

From a collaboration with the group of Professor Mutti, from Amsterdam University, the mutant LysEDH F173A was tested against 2-phenylethylamine.(Tseliou et al., 2019) In fact, among the variants generated by Tseliou *et al.* , LysEDH F173A emerged as the most promising candidate for our specific goal, because of its activity towards aromatic ketones, such as acetophenone and propiophenone (Figure A1.5).

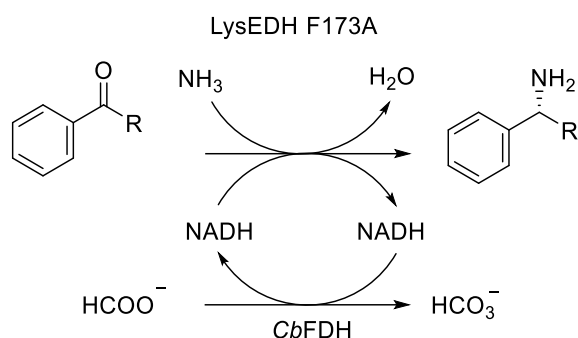


Figure A1.5: Scheme of the biocatalytic reductive amination performed by LysEDH F173A variant towards acetophenone (R = H) and propiophenone (R = CH₃).

For *BsPheDH*, a targeted approach was used for mutagenesis, which was guided by in silico visualizations and docking experiments. To implement the strategy of transposing mutagenesis, various examples from the literature were examined. From these works, it was noted that an effective strategy involved altering the lysine (K) and asparagine (N) residues, which establish ionic interactions with the carboxylic acid present in the substrates.

One example is the work by Ye *et al.*, who performed the engineering of PheDH from *Rhodococcus sp.* M4. (Ye *et al.*, 2015) This enzyme shares 35.33 % identity and 52 % similarity with PheDH from *Bacillus sphaericus*. In their work, mutations were introduced at positions K66 and N262, which resulted in a superior triple mutant (K66Q/S149G/N262C). This mutant showed activity (8.8 mU/mg) with the substrates phenylacetone and 4-phenyl-2-butanone, thereby expanding the substrate scope beyond alpha-keto acids through the removal of the carboxyl moiety.

Other significant examples were provided by the works of Bommarius *et al.* on PheDH from *Bacillus badius* (Abrahamson *et al.*, 2013) and Leucine dehydrogenase (*BsLeuDH*) from *Bacillus stearothermophilus*. (Abrahamson *et al.*, 2012)

The mutant PheDH-AmDH (K77S/N276L) was able to carry out the oxidative deamination of 1,3-dimethyl butyl amine (1,3-DMBA) with an activity of 166.3 mU/mg, in 0.1 M glycine buffer, pH 10 with 1 mM NAD⁺, at 25 °C.

On the other hand, the engineered LeuDH variant K68S/E114V/N261L/V291Cm completely loses its activity on its natural substrate, L-Leucine, but was active in the oxidative deamination direction against (R)-methylbenzylamine (586.3 mU/mg) and cyclohexylamine (56 mU/mg), in 250 mM Na₂CO₃ buffer at pH 10 with 1 mM NAD⁺.

With the 52 % identity and 68 % similarity between *BsLeuDH* and *BsPheDH*, the corresponding amino acid residues lysine (K) and asparagine (N) were targeted for mutagenesis in *BsPheDH* (Figure A1.3). The aim was to adapt its active site to accommodate the desired aromatic primary amine.

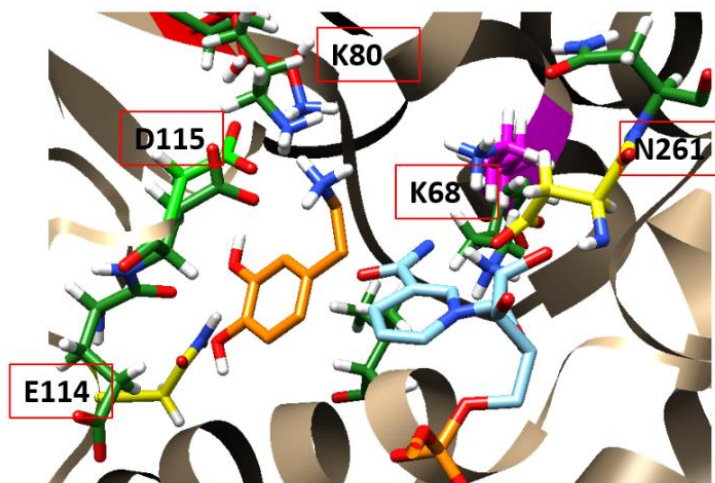


Figure A1.6: Model of the active site of *BsPhe* with PLP (light blue), where dopamine (orange) has been docked. The labeled residues in dark green are from *BsLeuDH* and are superimposed over the homology model sequence of *BsPheDH*, obtained with Protein Homology/analogy Recognition Engine V 2.0 (Phyre²). *BsPhe* active site catalytic residues are D126 (light green) and K91 (red). The target residue for mutagenesis were K79 (violet) and N277 (yellow).

In the case of K79, a variety of strategic rationales were employed to guide the mutation of the lysine residue. This amino acid, with its positively charged side chain, plays a critical role in coordinating the carboxylic group in the enzyme natural substrates. As part of this mutagenesis experiment, three different mutants were generated at position 79: K79Q, K79E, and K79M.

The rationale behind the K79Q mutation involved replacing the lysine with glutamine, an amino acid with a polar uncharged side chain. This modification was expected to enhance the enzyme adaptability to substrates that are smaller and have higher hydrophobicity, such as the corresponding primary amines of L-phenylalanine, L-tyrosine, or L-DOPA, due to the absence of a carboxylic moiety.

The K79E mutation, on the other hand, followed a different rationale. Here, lysine was replaced with glutamic acid, which has a negatively charged side chain. This mutation was expected to improve coordination of the positively charged amino group of the primary aromatic amine substrates in the active site, due to the potential electrostatic interaction with the negatively charged side chain of glutamic acid.

Lastly, the rationale for the K79M mutation was based on the fact that L-methionine, with its long aliphatic hydrophobic side chains, could increase the overall hydrophobicity of the active site pocket, enabling better accommodation for substrates with increased hydrophobicity. This change aimed to increase the overall hydrophobicity of the active site pocket, promoting better accommodation of the targeted aromatic primary amines.

In silico visualization of the mutations using Chimera and PyMol programs revealed how the mutants interacted with L-dopamine. Furthermore, the expression of the three *BsPheDH* mutants targeting K68 was examined, and SDS-PAGE analysis confirmed that these proteins were present in the soluble fraction following centrifugation of the cell lysate.

Screening the activity of purified mutants by monitoring cofactor formation at 340 nm

The approach of monitoring NADH formation at 340 nm using the Cary 60 for the activity assay with 2-phenylethylamine and tyramine yielded no positive results for all the mutants tested, which included the three mutants of *BsPheDH* and the *LysEDH* F173A mutant. The used conditions are described in the section 3.2.10.3 of materials and methods. Furthermore, for the mutants derived from direct mutagenesis of K79 in *BsPheDH*, activity towards L-phenylalanine was also lost. This raised the question of whether the mutations that targeted this particular amino acid residue had completely disrupted the enzymatic activity, in both reaction directions. To investigate this, the activity towards phenylpyruvate was assessed. While the mutations had a significantly negative impact on enzyme activity, the enzyme retained some activity, with a measured activity of 0.1 U/mg. For investigating *BsPheDH* activity towards phenylpyruvate 5 mM substrate was employed with 1 mM NADH in 50 mM Tris-HCl buffer, 100 mM KCl, 400 mM NH₄Cl, pH 8.

Screening of the activity of purified mutants at the spectrofluorometer

The strategy to monitor the formation of NADH from the oxidative deamination reaction with 2-phenylethylamine using a spectrofluorometer yielded positive results during the screening of *BsPheDH* mutants (Figure A1.7). This promising outcome set also the foundation for further mutations targeting the N277 residue. As shown in the Table A1.2, the mutant K79Q scored the best result in terms of specific activity over the other single mutant versions, with 93 mU/mg.

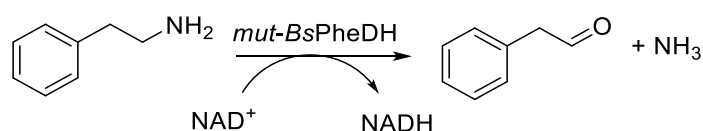


Figure A1.7: Reaction scheme for the oxidative deamination reaction of 2-phenylethylamine in the screening for *BsPheDH* mutants.

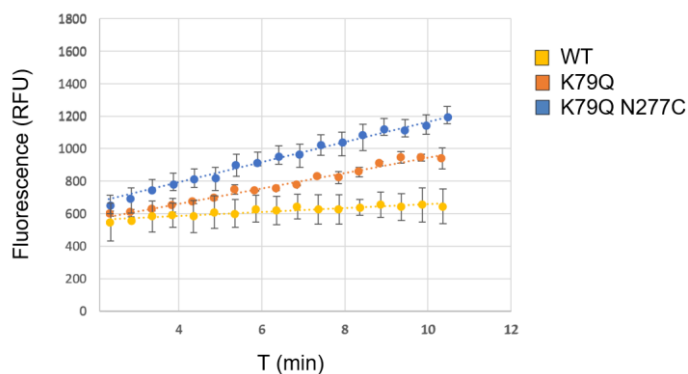
As per existing literature, coordinated mutation of residues involved in carboxylic acid binding, specifically, for *BsPheDH*, K79 and N277, can result in a combined beneficial effect, unlocking the capacity of the enzyme to function as an AmDH. Hence, in the direct mutagenesis approach, also the N277 residue was considered. In the selection of an amino acid replacement for N277, references from the literature were taken into consideration, (Abrahamson et al., 2013; Ye et al., 2015) where cysteine (C) and leucine

(L) were employed. These amino acids are known to provide a comparable influence in terms of steric hindrance and hydrophobicity.

From the monitoring of the activity at the spectrofluorometer, the double mutant showed an improved activity of 124 mU/mg (Table A1.2 and Graph A1.1)

Biocatalyst	Activity (mU/mg)
WT	24
K79Q	93
K79E	3
K79M	17
K79Q N277C	124

Table A1.2: Specific activity of the purified wt and mutated versions of PheDH towards 2-phenylethylamine. Conditions: 0.16 mg/mL of enzyme, 20 mM 2-phenylethylamine, and 0.1 mM NAD⁺, total volume of 200 μ L. Readings were taken every 30 seconds over a period of 10 minutes, exciting the NADH at 351 \pm 9 nm and recording its emissions at 450 \pm 30 nm.



Graph A.1.1: Specific activity measurements of the single mutant PheDH K79Q and of the double mutant PheDH K79Q N277C, compared with *Bs*PheDH wt. Assay conditions as in Table A1.2.

Biotransformations with PheDH K79Q N277C

The double mutant PheDH K79Q N277C was tested in biotransformations involving 2-phenylethylamine. Multiple strategies were explored, initially incorporating a stoichiometric amount of NAD⁺ at a 20 mM scale. The reaction pH was adjusted, trying different values as pH 8, 9, and 9.5, alongside varying the biocatalyst concentrations (0.3, 0.6, 1, and 1.5 mg/mL). A biphasic system containing 25 % toluene was also attempted with 1 mg/mL of PheDH K79Q N277C, with the aim of driving the reaction equilibrium

towards the product by extracting the formed 2-phenylacetaldehyde into the organic phase. The lack of significant conversion led to the hypothesis that the absence of a driving force, provided by a recycling system, might play a critical role in achieving a successful outcome in the biotransformation. A different strategy, the hydrogen borrowing method, was then employed. The biotransformation was coupled with HLADH in a bienzymatic system, using a ratio of 1 to 3 between the amount of mutant and HLADH, at a concentration of 0.15 mg/mL for the mutant, at pH of 9, and a 20 mM substrate scale. Despite these modifications, the biotransformations did not yield the expected results.

Colony screening of *BsPheDH* mutants

As the strategy of site-directed mutagenesis did not yield an active biocatalyst for dopamine-like primary amines, the approach of random mutagenesis was considered as a potential solution. In order to do this, a screening assay should have been set up.

The screening of mutants was planned to be conducted directly from the agar plates where the transformed cells with the mutated PheDH gene would grow. The aim was to differentiate colonies based on their ability to produce NADH after receiving the reaction solution containing 2-phenylethylamine and NAD⁺.

For the sake of convenience in subsequent procedures, the colonies were placed onto a nitrocellulose membrane, enabling easy transfer from one plate to another. For instance, to induce protein expression, the membrane hosting the transformed cells was subsequently shifted onto another agar plate that contained 1 mM IPTG.

To measure the formation of the reduced cofactor NADH, tetrazolium salts, which are known to correlate with cellular metabolic activity, were utilized. (Berridge et al., 2005; Coyle et al., 2023; Stockert et al., 2018; Tsukatani et al., 2008) The process involves the conversion of tetrazolium salts from colourless or lightly coloured aqueous solutions into intensely dark coloured formazans. This change has been widely used as a marker of redox metabolism and effective in quantifying NADH production. MTT (2-(4,5-dimethyl-2-thiazolyl)-3,5-diphenyl-2H-tetrazolium bromide) and WST-1 (2-(4-Iodophenyl)-3-(4-nitrophenyl)-5-(2,4-disulfophenyl)-2H-tetrazolium), were the tetrazolium salts considered in this screening assay (Figure A1.8). The MTT, possessing a net positive charge, is typically absorbed by cells through the plasma membrane potential, whereas WST-1, a second-generation tetrazolium dye, because of its negatively charged groups, rendering it mostly impermeable to cells, forms water-soluble formazans. In our solid phase cell screening, the presence of intracellular insoluble formazan crystals was advantageous. In fact, unlike many applications of this dye, there was no necessity to solubilize it in a 96-well plate to read the absorbance in a spectrophotometer. Along with the tetrazolium salt, PMS (1-methoxy-5-methyl-phenazinium methyl sulfate) was also offered to the cell colonies. PMS is used as an intermediate electron carrier from the production of NADH or NADPH to the reduction of tetrazolium salts to colored formazans.

WST-1, which is more stable in the presence of PMS than MTT, can be purchased in a ready-to-use kit (CCK-8) where both substances are pre-solubilized.

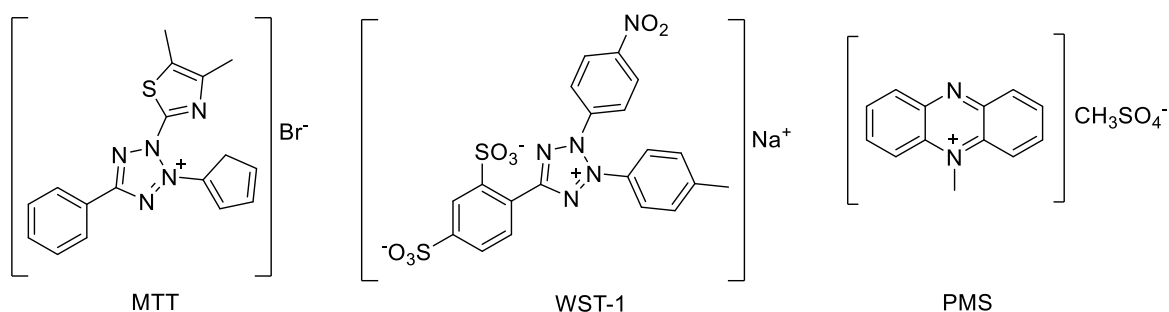


Figure A1.8: Molecular structure of the used tetrazolium salts, MTT and WST-1, and of the intermediate electron acceptor PMS.

In the designed screening process, the transformed colonies on the agar plate were first sprayed with the reaction solution (10 mM Phenylalanine, 1 mM NAD⁺ in 0.1 M glycine-KOH buffer, pH 10.4). Subsequently, either the MTT and PMS solutions were applied sequentially, or the CCK-8 kit solution containing WST-1 and PMS was used in a single step. Following this, the transformed plates were incubated for a period of 2 to 4 hours, in the dark.

In the preliminary phase of the screening assay design, BL21 *E. coli* cells were transformed with the wild-type gene of BsPheDH. The experiment aimed to serve as a proof of concept for the next steps of the direct evolution. Regrettably, when the control plate (transformed with an empty plasmid) was compared, there was no visible difference indicating that colonies expressing BsPheDH had an increased concentration of NADH after receiving the reaction solution.

This observation led to the identification of two issues: firstly, the spraying of the reaction solution, which was either followed immediately, or after a 30-minute incubation, by the tetrazolium salt, resulted in a partial dissolution of the colonies and presented difficulties in volume dosing. Secondly, an evident issue arose from the background signal given by the NADH already present in the cells, which also darkened the control plate colonies.

In an attempt to resolve the first issue, the reaction solution, tetrazolium salts, and PMS were mixed with agarose for electrophoresis (0.8 %), for a final volume of 10 mL, to facilitate the screening using a gel-sandwich technique. (R. Huang et al., 2016; Kugler, 1979)

The gel-sandwich technique is a methodology designed to overcome the drawbacks associated with applying liquid reagents directly onto colonies. The concept is straightforward: the colonies on the agar plate are sandwiched between two layers; one is gel containing the necessary reagents for the screening assay, and one is the agar layer itself. This creates a more stable, controlled environment for reagents to interact with the colonies. By encapsulating the colonies between these two layers of gel, we ensure

the uniform distribution of reagents, limiting any potential damage or displacement of the colonies.

Importantly, care was required when combining the components with the melted agarose solution. It was a compromise between mixing while the agarose was still in a liquid state, and being mindful of the temperature of the agarose solution to avoid thermal degradation of the reaction components.

Because of this overcomplicated part of the agarose handling, eventually the reaction reagent solution was offered to the colonies on the plate using a paper filter, matching the diameter of the agar plate. This filter was soaked with the specific volume of reaction solution (6 mL) and was then transferred from its soaking petri dish onto the dish containing the cell colonies.

Regrettably, an effective strategy to mitigate the problem of background signal interference from endogenous NADH was not found. Nevertheless, an attempt was made to design a multi-step system, which incorporated a step to deplete endogenous NADH prior to conducting the screening assay (Figure A1.9). Two distinct strategies were attempted following the scheme in Figure A1.10.

In the first approach, the CCK-8 kit was initially employed with the aim of converting all existing NADH in the cells to its oxidized form, NAD^+ , by facilitating a reaction with PMS to form formazan from WST-1. After performing three washing cycles, by transferring the nitrocellulose membrane with the colonies to new petri dishes with buffer until the orange coloration was entirely removed, the screening was executed. The screening involved adding the reagent solution and subsequently the MTT and PMS, thereby revealing the NADH specifically produced from the oxidative deamination of L-phenylalanine.

In the second strategy, the reaction solution initially added contained phenylpyruvate (10 mM phenylpyruvate, 400 mM NH_4Cl , 100 mM KCl in 50 mM Tris HCl , pH 8). The aim was to utilize the endogenous NADH in the reductive amination of the alpha-keto acid to synthesize phenylalanine. Similar to the first strategy, washing in buffer was performed to remove reagents and products, followed by conducting the screening as previously described with MTT and PMS.

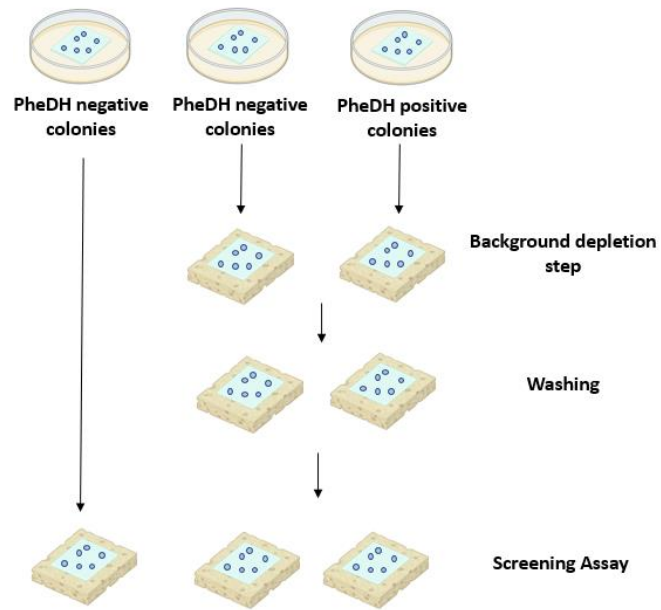


Figure A1.9: Schematic overview of the in solido screening assay for the random mutagenesis of PheDH.

A

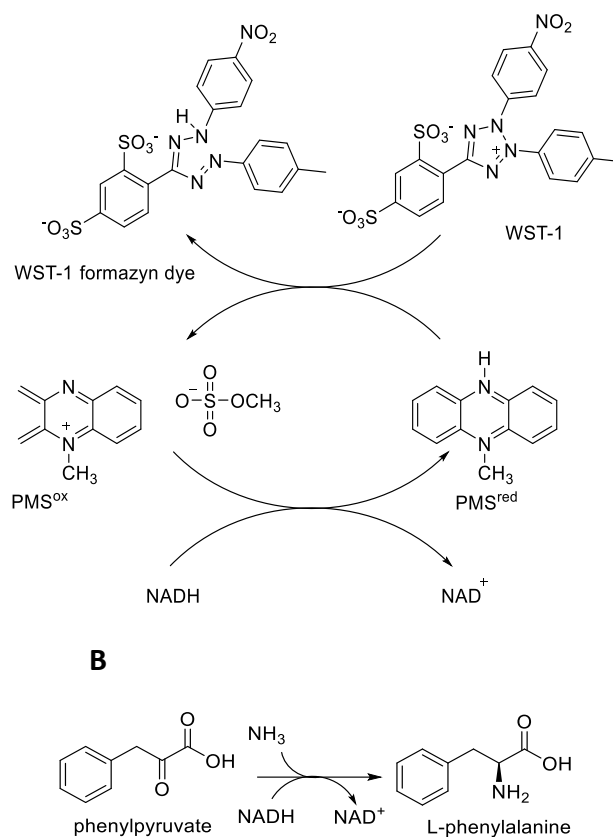


Figure A1.10: Schematic reaction schemes applied for the depletion of the endogenous NADH in cells for the elimination of the background signal in the colonies screening assay. **A.** NADH is oxidized to NAD⁺, reacting with PMS. The reduction of PMS is followed by the formation of WST-1 formazan dye. **B.** NADH is used in the reductive amination of phenylpyruvate.

The in-situ screening project was ultimately discontinued following numerous attempts, due primarily to the persistent challenge of mitigating interference from background signals. Notably, when utilizing a 96-well plate setup with purified enzymes, the CCK-8 kit effectively discriminated between the reaction wells (which contained *BsPheDH* or *LysEDHm*, their natural substrate and NAD⁺) and both the blank and negative control wells. However, while this approach was successful, the use of purified enzymes would not be a feasible strategy for the high-throughput screening needed for the assessment of random mutagenesis mutants.

Conclusion

The experimental focus on *BsPheDH* and *LysEDH* proved challenging, and unfortunately, the discussed attempts did not succeed in generating active mutants for the desired oxidative deamination reaction towards dopamine. While these results were not fruitful, they lay an essential groundwork for future research. With the incorporation of advanced bioinformatics tools and the development of an effective high-throughput screening

method, there is promising potential to overcome the obstacles which were met in this study. Hopefully, different future strategies could lead to the beneficial expansion of the substrate scope of these biocatalysts, opening new avenues for innovation and practical application in the field.

Bibliography

- Abrahamson, M. J., Vázquez-Figueroa, E., Woodall, N. B., Moore, J. C., & Bommarius, A. S. (2012). Development of an Amine Dehydrogenase for Synthesis of Chiral Amines. *Angewandte Chemie International Edition*, *51*(16), 3969–3972. <https://doi.org/10.1002/anie.201107813>
- Abrahamson, M. J., Wong, J. W., & Bommarius, A. S. (2013). The Evolution of an Amine Dehydrogenase Biocatalyst for the Asymmetric Production of Chiral Amines. *Advanced Synthesis & Catalysis*, *355*(9), 1780–1786. <https://doi.org/10.1002/adsc.201201030>
- Alcántara, A. R., Domínguez de María, P., Littlechild, J. A., Schürmann, M., Sheldon, R. A., & Wohlgemuth, R. (2022). Biocatalysis as Key to Sustainable Industrial Chemistry. *ChemSusChem*, *15*(9). <https://doi.org/10.1002/cssc.202102709>
- Almud, J. J., Oliveira, M. A., Kern, A. D., Grishin, N. V., Phillips, M. A., & Hackert, M. L. (2000). Crystal structure of human ornithine decarboxylase at 2.1 Å resolution: structural insights to antizyme binding. *Journal of Molecular Biology*, *295*(1), 7–16. <https://doi.org/10.1006/jmbi.1999.3331>
- Andréll, J., Hicks, M. G., Palmer, T., Carpenter, E. P., Iwata, S., & Maher, M. J. (2009). Crystal Structure of the Acid-Induced Arginine Decarboxylase from *Escherichia coli* : Reversible Decamer Assembly Controls Enzyme Activity. *Biochemistry*, *48*(18), 3915–3927. <https://doi.org/10.1021/bi900075d>
- Anwar, S., Mohammad, T., Shamsi, A., Queen, A., Parveen, S., Luqman, S., Hasan, G. M., Alamry, K. A., Azum, N., Asiri, A. M., & Hassan, M. I. (2020). Discovery of hordenine as a potential inhibitor of pyruvate dehydrogenase kinase 3: Implication in lung cancer therapy. *Biomedicines*, *8*(5), 32–228.
- Asano, Y., Nakazawa, A., & Endo, K. (1987). Novel phenylalanine dehydrogenases from *Sporosarcina ureae* and *Bacillus sphaericus*. Purification and characterization. *The Journal of Biological Chemistry*, *262*(21), 10346–10354. <http://www.ncbi.nlm.nih.gov/pubmed/3112142>
- Báez, J. L., Bolívar, F., & Gosset, G. (2001). Determination of 3-deoxy-D- *arabino* -heptulosonate 7-phosphate productivity and yield from glucose in *Escherichia coli* devoid of the glucose phosphotransferase transport system. *Biotechnology and Bioengineering*, *73*(6), 530–535. <https://doi.org/10.1002/bit.1088>
- Bai, Z., Sun, X., Yu, X., & Li, L. (2019). Chitosan Microbeads as Supporter for *Pseudomonas putida* with Surface Displayed Laccases for Decolorization of Synthetic Dyes. *Applied Sciences*, *9*(1), 138. <https://doi.org/10.3390/app9010138>
- Baker, P. J., Turnbull, A. P., Sedelnikova, S. E., Stillman, T. J., & Rice, D. W. (1995). A role for quaternary structure in the substrate specificity of leucine dehydrogenase. *Structure*, *3*(7), 693–705. [https://doi.org/10.1016/S0969-2126\(01\)00204-0](https://doi.org/10.1016/S0969-2126(01)00204-0)
- Barwell, C. J., Basma, A. N., Lafi, M. A. K., & Leake, L. D. (2011). Deamination of hordenine by monoamine oxidase and its action on vasa deferentia of the rat. *Journal of Pharmacy and Pharmacology*, *41*(6), 421–423. <https://doi.org/10.1111/j.2042-7158.1989.tb06492.x>
- Bell, E. L., Finnigan, W., France, S. P., Green, A. P., Hayes, M. A., Hepworth, L. J., Lovelock, S. L., Niikura, H., Osuna, S., Romero, E., Ryan, K. S., Turner, N. J., & Flitsch, S. L. (2021).

- Biocatalysis. *Nature Reviews Methods Primers*, 1(1), 46. <https://doi.org/10.1038/s43586-021-00044-z>
- Benítez-Mateos, A. I., Roura Padrosa, D., & Paradisi, F. (2022). Multistep enzyme cascades as a route towards green and sustainable pharmaceutical syntheses. *Nature Chemistry*, 14(5), 489–499. <https://doi.org/10.1038/s41557-022-00931-2>
- Bennett, M., Ducrot, L., Vergne-Vaxelaire, C., & Grogan, G. (2022). Structure and Mutation of the Native Amine Dehydrogenase MATOUAmDH2. *ChemBioChem*, 23(10). <https://doi.org/10.1002/cbic.202200136>
- Berridge, M. V., Herst, P. M., & Tan, A. S. (2005). *Tetrazolium dyes as tools in cell biology: New insights into their cellular reduction* (pp. 127–152). [https://doi.org/10.1016/S1387-2656\(05\)11004-7](https://doi.org/10.1016/S1387-2656(05)11004-7)
- Bertelli, M., Kiani, A. K., Paolacci, S., Manara, E., Kurti, D., Dhuli, K., Bushati, V., Miertus, J., Pangallo, D., Baglivo, M., Beccari, T., & Michelini, S. (2020). Hydroxytyrosol: A natural compound with promising pharmacological activities. *Journal of Biotechnology*, 309, 29–33. <https://doi.org/10.1016/j.jbiotec.2019.12.016>
- Bhatia, S. K., Kim, Y. H., Kim, H. J., Seo, H.-M., Kim, J.-H., Song, H.-S., Sathiyarayanan, G., Park, S.-H., Park, K., & Yang, Y.-H. (2015). Biotransformation of lysine into cadaverine using barium alginate-immobilized *Escherichia coli* overexpressing CadA. *Bioprocess and Biosystems Engineering*, 38(12), 2315–2322. <https://doi.org/10.1007/s00449-015-1465-9>
- Bloch, D. N., Sandre, M., Ben Zichri, S., Masato, A., Kolusheva, S., Bubacco, L., & Jelinek, R. (2023). Scavenging neurotoxic aldehydes using lysine carbon dots. *Nanoscale Advances*, 5(5), 1356–1367. <https://doi.org/10.1039/D2NA00804A>
- Böhmer, W., Knaus, T., & Mutti, F. G. (2018a). Hydrogen-Borrowing Alcohol Bioamination with Coimmobilized Dehydrogenases. *ChemCatChem*, 10(4), 731–735. <https://doi.org/10.1002/cctc.201701366>
- Böhmer, W., Knaus, T., & Mutti, F. G. (2018b). Hydrogen-Borrowing Alcohol Bioamination with Coimmobilized Dehydrogenases. *ChemCatChem*, 10(4), 731–735. <https://doi.org/10.1002/cctc.201701366>
- Cai, R.-F., Liu, L., Chen, F.-F., Li, A., Xu, J.-H., & Zheng, G.-W. (2020). Reductive Amination of Biobased Levulinic Acid to Unnatural Chiral γ -Amino Acid Using an Engineered Amine Dehydrogenase. *ACS Sustainable Chemistry & Engineering*, 8(46), 17054–17061. <https://doi.org/10.1021/acssuschemeng.0c04647>
- Caparco, A. A., Bommarius, B. R., Bommarius, A. S., & Champion, J. A. (2020). Protein-inorganic calcium-phosphate supraparticles as a robust platform for enzyme co-immobilization. *Biotechnology and Bioengineering*, 117(7), 1979–1989. <https://doi.org/10.1002/bit.27348>
- Caparco, A. A., Pelletier, E., Petit, J. L., Jouenne, A., Bommarius, B. R., Berardinis, V., Zaparucha, A., Champion, J. A., Bommarius, A. S., & Vergne-Vaxelaire, C. (2020). Metagenomic Mining for Amine Dehydrogenase Discovery. *Advanced Synthesis & Catalysis*, 362(12), 2427–2436. <https://doi.org/10.1002/adsc.202000094>

- Capitani, G. (2003). Crystal structure and functional analysis of Escherichia coli glutamate decarboxylase. *The EMBO Journal*, *22*(16), 4027–4037. <https://doi.org/10.1093/emboj/cdg403>
- Cerioli, L., Planchestainer, M., Cassidy, J., Tessaro, D., & Paradisi, F. (2015). Characterization of a novel amine transaminase from Halomonas elongata. *Journal of Molecular Catalysis B: Enzymatic*, *120*, 141–150. <https://doi.org/10.1016/j.molcatb.2015.07.009>
- Chen, W., Yao, J., Meng, J., Han, W., Tao, Y., Chen, Y., Guo, Y., Shi, G., He, Y., Jin, J.-M., & Tang, S.-Y. (2019). Promiscuous enzymatic activity-aided multiple-pathway network design for metabolic flux rearrangement in hydroxytyrosol biosynthesis. *Nature Communications*, *10*(1), 960. <https://doi.org/10.1038/s41467-019-08781-2>
- Claes, L., Janssen, M., & De Vos, D. E. (2019). Organocatalytic Decarboxylation of Amino Acids as a Route to Bio-based Amines and Amides. *ChemCatChem*, *11*(17), 4297–4306. <https://doi.org/10.1002/cctc.201900800>
- Contente, M. L., & Paradisi, F. (2018). Self-sustaining closed-loop multienzyme-mediated conversion of amines into alcohols in continuous reactions. *Nature Catalysis*, *1*(6), 452–459. <https://doi.org/10.1038/s41929-018-0082-9>
- Cosenza, V. A., Navarro, D. A., & Stortz, C. A. (2011). Usage of α -picoline borane for the reductive amination of carbohydrates. *Arkivoc*, *2011*(7), 182–194. <https://doi.org/10.3998/ark.5550190.0012.716>
- Coyle, J. P., Johnson, C., Jensen, J., Farcas, M., Derk, R., Stueckle, T. A., Kornberg, T. G., Rojanasakul, Y., & Rojanasakul, L. W. (2023). Variation in pentose phosphate pathway-associated metabolism dictates cytotoxicity outcomes determined by tetrazolium reduction assays. *Scientific Reports*, *13*(1), 8220. <https://doi.org/10.1038/s41598-023-35310-5>
- DiCosimo, R., McAuliffe, J., Poulouse, A. J., & Bohlmann, G. (2013). Industrial use of immobilized enzymes. *Chemical Society Reviews*, *42*(15), 6437. <https://doi.org/10.1039/c3cs35506c>
- Ducrot, L., Bennett, M., André-Leroux, G., Elisée, E., Marynberg, S., Fossey-Jouenne, A., Zaparucha, A., Grogan, G., & Vergne-Vaxelaire, C. (2022). Expanding the Substrate Scope of Native Amine Dehydrogenases through *In Silico* Structural Exploration and Targeted Protein Engineering. *ChemCatChem*, *14*(22). <https://doi.org/10.1002/cctc.202200880>
- Ducrot, L., Bennett, M., Caparco, A. A., Champion, J. A., Bommarius, A. S., Zaparucha, A., Grogan, G., & Vergne-Vaxelaire, C. (2021). Biocatalytic Reductive Amination by Native Amine Dehydrogenases to Access Short Chiral Alkyl Amines and Amino Alcohols. *Frontiers in Catalysis*, *1*. <https://doi.org/10.3389/fctls.2021.781284>
- Eliot, A. C., & Kirsch, J. F. (2004). Pyridoxal Phosphate Enzymes: Mechanistic, Structural, and Evolutionary Considerations. *Annual Review of Biochemistry*, *73*(1), 383–415. <https://doi.org/10.1146/annurev.biochem.73.011303.074021>
- Eller, K., Henkes, E., Rossbacher, R., & Höke, H. (2000). Amines, Aliphatic. In *Ullmann's Encyclopedia of Industrial Chemistry*. Wiley-VCH Verlag GmbH & Co. KGaA. https://doi.org/10.1002/14356007.a02_001

- Escalante, A., Calderón, R., Valdivia, A., de Anda, R., Hernández, G., Ramírez, O. T., Gosset, G., & Bolívar, F. (2010). Metabolic engineering for the production of shikimic acid in an evolved *Escherichia coli* strain lacking the phosphoenolpyruvate: carbohydrate phosphotransferase system. *Microbial Cell Factories*, *9*(1), 21. <https://doi.org/10.1186/1475-2859-9-21>
- Foor, F., Morin, N., & Bostian, K. A. (1993). Production of L-dihydroxyphenylalanine in *Escherichia coli* with the tyrosine phenol-lyase gene cloned from *Erwinia herbicola*. *Applied and Environmental Microbiology*, *59*(9), 3070–3075. <https://doi.org/10.1128/aem.59.9.3070-3075.1993>
- Fordjour, E., Adipah, F. K., Zhou, S., Du, G., & Zhou, J. (2019). Metabolic engineering of *Escherichia coli* BL21 (DE3) for de novo production of l-DOPA from d-glucose. *Microbial Cell Factories*, *18*(1). <https://doi.org/10.1186/s12934-019-1122-0>
- Franklin, R. D., Whitley, J. A., Caparco, A. A., Bommarius, B. R., Champion, J. A., & Bommarius, A. S. (2021). Continuous production of a chiral amine in a packed bed reactor with co-immobilized amine dehydrogenase and formate dehydrogenase. *Chemical Engineering Journal*, *407*, 127065. <https://doi.org/10.1016/j.cej.2020.127065>
- Froidevaux, V., Negrell, C., Caillol, S., Pascault, J.-P., & Boutevin, B. (2016). Biobased Amines: From Synthesis to Polymers; Present and Future. *Chemical Reviews*, *116*(22), 14181–14224. <https://doi.org/10.1021/acs.chemrev.6b00486>
- Garg, R. P., Ma, Y., Hoyt, J. C., & Parry, R. J. (2002a). Molecular characterization and analysis of the biosynthetic gene cluster for the azoxy antibiotic valanimycin. *Molecular Microbiology*, *46*(2), 505–517. <https://doi.org/10.1046/j.1365-2958.2002.03169.x>
- Garg, R. P., Ma, Y., Hoyt, J. C., & Parry, R. J. (2002b). Molecular characterization and analysis of the biosynthetic gene cluster for the azoxy antibiotic valanimycin. *Molecular Microbiology*, *46*(2), 505–517. <https://doi.org/10.1046/j.1365-2958.2002.03169.x>
- Ghislieri, D., & Turner, N. J. (2014). Biocatalytic Approaches to the Synthesis of Enantiomerically Pure Chiral Amines. *Topics in Catalysis*, *57*(5), 284–300. <https://doi.org/10.1007/s11244-013-0184-1>
- Gianolio, S., Roura Padrosa, D., & Paradisi, F. (2022). Combined chemoenzymatic strategy for sustainable continuous synthesis of the natural product hordenine. *Green Chemistry*, *24*(21), 8434–8440. <https://doi.org/10.1039/D2GC02767D>
- Giardina, G., Montioli, R., Gianni, S., Cellini, B., Paiardini, A., Voltattorni, C. B., & Cutruzzola, F. (2011). Open conformation of human DOPA decarboxylase reveals the mechanism of PLP addition to Group II decarboxylases. *Proceedings of the National Academy of Sciences*, *108*(51), 20514–20519. <https://doi.org/10.1073/pnas.1111456108>
- Gong, X., Tao, J., Wang, Y., Wu, J., An, J., Meng, J., Wang, X., Chen, Y., & Zou, J. (2021). Total barley maiya alkaloids inhibit prolactin secretion by acting on dopamine D2 receptor and protein kinase A targets. *Journal of Ethnopharmacology*, *273*, 113994. <https://doi.org/10.1016/j.jep.2021.113994>
- Gosset, G., Yong-Xiao, J., & Berry, A. (1996). A direct comparison of approaches for increasing carbon flow to aromatic biosynthesis in *Escherichia coli*. *Journal of Industrial Microbiology*, *17*(1), 47–52. <https://doi.org/10.1007/BF01570148>

- Guisán, JoséM. (1988). Aldehyde-agarose gels as activated supports for immobilization-stabilization of enzymes. *Enzyme and Microbial Technology*, 10(6), 375–382. [https://doi.org/10.1016/0141-0229\(88\)90018-X](https://doi.org/10.1016/0141-0229(88)90018-X)
- Guo, K., Ji, C., & Li, L. (2007). Stable-Isotope Dimethylation Labeling Combined with LC–ESI MS for Quantification of Amine-Containing Metabolites in Biological Samples. *Analytical Chemistry*, 79(22), 8631–8638. <https://doi.org/10.1021/ac0704356>
- Guo, Z., Yan, N., & Lapkin, A. A. (2019). Towards circular economy: integration of bio-waste into chemical supply chain. *Current Opinion in Chemical Engineering*, 26, 148–156. <https://doi.org/10.1016/j.coche.2019.09.010>
- Gupte, A. P., Basaglia, M., Casella, S., & Favaro, L. (2022). Rice waste streams as a promising source of biofuels: feedstocks, biotechnologies and future perspectives. *Renewable and Sustainable Energy Reviews*, 167, 112673. <https://doi.org/10.1016/j.rser.2022.112673>
- Gut, H., Pennacchietti, E., John, R. A., Bossa, F., Capitani, G., De Biase, D., & Grütter, M. G. (2006). Escherichia coli acid resistance: pH-sensing, activation by chloride and autoinhibition in GadB. *The EMBO Journal*, 25(11), 2643–2651. <https://doi.org/10.1038/sj.emboj.7601107>
- H. Orrego, A., Romero-Fernández, M., Millán-Linares, M., Yust, M., Guisán, J., & Rocha-Martin, J. (2018). Stabilization of Enzymes by Multipoint Covalent Attachment on Aldehyde-Supports: 2-Picoline Borane as an Alternative Reducing Agent. *Catalysts*, 8(8), 333. <https://doi.org/10.3390/catal8080333>
- Hamid, M. H. S. A., Slatford, P. A., & Williams, J. M. J. (2007). Borrowing Hydrogen in the Activation of Alcohols. *Advanced Synthesis & Catalysis*, 349(10), 1555–1575. <https://doi.org/10.1002/adsc.200600638>
- Hapke, H. J., & Strathmann, W. (1995). [Pharmacological effects of hordenine]. *DTW. Deutsche Tierärztliche Wochenschrift*, 102(6), 228–232. <http://www.ncbi.nlm.nih.gov/pubmed/8582256>
- Harper, B. A., Barbut, S., Lim, L.-T., & Marcone, M. F. (2014). Effect of Various Gelling Cations on the Physical Properties of “Wet” Alginate Films. *Journal of Food Science*, 79(4), E562–E567. <https://doi.org/10.1111/1750-3841.12376>
- Heckmann, C. M., Gourlay, L. J., Dominguez, B., & Paradisi, F. (2020). An (R)-Selective Transaminase From *Thermomyces stellatus*: Stabilizing the Tetrameric Form. *Frontiers in Bioengineering and Biotechnology*, 8. <https://doi.org/10.3389/fbioe.2020.00707>
- Heffter, A. (1898). Ueber Pellote. *Archiv Für Experimentelle Pathologie Und Pharmakologie*, 40(5–6), 385–429. <https://doi.org/10.1007/BF01825267>
- Heydari, M., Ohshima, T., Nunoura-Kominato, N., & Sakuraba, H. (2004). Highly Stable Lysine 6-Dehydrogenase from the Thermophile *Geobacillus stearothermophilus* Isolated from a Japanese Hot Spring: Characterization, Gene Cloning and Sequencing, and Expression. *Applied and Environmental Microbiology*, 70(2), 937–942. <https://doi.org/10.1128/AEM.70.2.937-942.2004>
- Holbrook, O. T., Molligoda, B., Bushell, K. N., & Gobrogge, K. L. (2022). Behavioral consequences of the downstream products of ethanol metabolism involved in alcohol use disorder.

- Neuroscience & Biobehavioral Reviews*, 133, 104501.
<https://doi.org/10.1016/j.neubiorev.2021.12.024>
- Houwman, J. A., Knaus, T., Costa, M., & Mutti, F. G. (2019). Efficient synthesis of enantiopure amines from alcohols using resting *E. coli* cells and ammonia. *Green Chemistry*, 21(14), 3846–3857. <https://doi.org/10.1039/C9GC01059A>
- Huang, J., Mei, L., Wu, H., & Lin, D. (2007). Biosynthesis of γ -aminobutyric acid (GABA) using immobilized whole cells of *Lactobacillus brevis*. *World Journal of Microbiology and Biotechnology*, 23(6), 865–871. <https://doi.org/10.1007/s11274-006-9311-5>
- Huang, R., Chen, H., Zhong, C., Kim, J. E., & Zhang, Y.-H. P. (2016). High-Throughput Screening of Coenzyme Preference Change of Thermophilic 6-Phosphogluconate Dehydrogenase from NADP⁺ to NAD⁺. *Scientific Reports*, 6(1), 32644. <https://doi.org/10.1038/srep32644>
- Hwang, E. T., & Lee, S. (2019). Multienzymatic Cascade Reactions via Enzyme Complex by Immobilization. *ACS Catalysis*, 9(5), 4402–4425. <https://doi.org/10.1021/acscatal.8b04921>
- Jackson, D. M., Ashley, R. L., Brownfield, C. B., Morrison, D. R., & Morrison, R. W. (2015). Rapid Conventional and Microwave-Assisted Decarboxylation of L-Histidine and Other Amino Acids via Organocatalysis with R-Carvone Under Superheated Conditions. *Synthetic Communications*, 45(23), 2691–2700. <https://doi.org/10.1080/00397911.2015.1100745>
- Jansonius, J. N. (1998). Structure, evolution and action of vitamin B6-dependent enzymes. *Current Opinion in Structural Biology*, 8(6), 759–769. [https://doi.org/10.1016/S0959-440X\(98\)80096-1](https://doi.org/10.1016/S0959-440X(98)80096-1)
- Jeon, H., Yoon, S., Ahsan, M., Sung, S., Kim, G.-H., Sundaramoorthy, U., Rhee, S.-K., & Yun, H. (2017). The Kinetic Resolution of Racemic Amines Using a Whole-Cell Biocatalyst Co-Expressing Amine Dehydrogenase and NADH Oxidase. *Catalysts*, 7(9), 251. <https://doi.org/10.3390/catal7090251>
- Jiang, M., Xu, G., Ni, J., Zhang, K., Dong, J., Han, R., & Ni, Y. (2019a). Improving Soluble Expression of Tyrosine Decarboxylase from *Lactobacillus brevis* for Tyramine Synthesis with High Total Turnover Number. *Applied Biochemistry and Biotechnology*, 188(2), 436–449. <https://doi.org/10.1007/s12010-018-2925-x>
- Jiang, M., Xu, G., Ni, J., Zhang, K., Dong, J., Han, R., & Ni, Y. (2019b). Improving Soluble Expression of Tyrosine Decarboxylase from *Lactobacillus brevis* for Tyramine Synthesis with High Total Turnover Number. *Applied Biochemistry and Biotechnology*, 188(2), 436–449. <https://doi.org/10.1007/s12010-018-2925-x>
- Jones, J. A., Collins, S. M., Vernacchio, V. R., Lachance, D. M., & Koffas, M. A. G. (2016). Optimization of naringenin and *p*-coumaric acid hydroxylation using the native *E. coli* hydroxylase complex, HpaBC. *Biotechnology Progress*, 32(1), 21–25. <https://doi.org/10.1002/btpr.2185>
- Khorsand, F., Murphy, C. D., Whitehead, A. J., & Engel, P. C. (2017). Biocatalytic stereoinversion of *p*-para-bromophenylalanine in a one-pot three-enzyme reaction. *Green Chemistry*, 19(2), 503–510. <https://doi.org/10.1039/C6GC01922F>
- Kim, Baritugo, Oh, Kang, Jung, Jang, Song, Kim, Lee, Hwang, Park, Park, & Joo. (2019). High-Level Conversion of l-lysine into Cadaverine by *Escherichia coli* Whole Cell Biocatalyst Expressing

- Hafnia alvei l-lysine Decarboxylase. *Polymers*, 11(7), 1184.
<https://doi.org/10.3390/polym11071184>
- Kim, D. I., Chae, T. U., Kim, H. U., Jang, W. D., & Lee, S. Y. (2021). Microbial production of multiple short-chain primary amines via retrobiosynthesis. *Nature Communications*, 12(1), 173. <https://doi.org/10.1038/s41467-020-20423-6>
- Kim, S.-C., Lee, J.-H., Kim, M.-H., Lee, J.-A., Kim, Y. B., Jung, E., Kim, Y.-S., Lee, J., & Park, D. (2013). Hordenine, a single compound produced during barley germination, inhibits melanogenesis in human melanocytes. *Food Chemistry*, 141(1), 174–181.
<https://doi.org/10.1016/j.foodchem.2013.03.017>
- Knaus, T., Böhmer, W., & Mutti, F. G. (2017). Amine dehydrogenases: efficient biocatalysts for the reductive amination of carbonyl compounds. *Green Chemistry*, 19(2), 453–463.
<https://doi.org/10.1039/C6GC01987K>
- Knowles, W. S. (n.d.). Asymmetric Hydrogenations– The MonsantoL-Dopa Process. In *Asymmetric Catalysis on Industrial Scale* (pp. 21–38). Wiley-VCH Verlag GmbH & Co. KGaA.
<https://doi.org/10.1002/3527602151.ch1>
- Komori, H., Nitta, Y., Ueno, H., & Higuchi, Y. (2012). Structural Study Reveals That Ser-354 Determines Substrate Specificity on Human Histidine Decarboxylase. *Journal of Biological Chemistry*, 287(34), 29175–29183. <https://doi.org/10.1074/jbc.M112.381897>
- Kugler, P. (1979). A gel-sandwich technique for the qualitative and quantitative determination of dehydrogenases in the enzyme histochemistry. *Histochemistry*, 60(3), 265–293.
<https://doi.org/10.1007/BF00500656>
- Kumar, R., Vikramachakravarthi, D., & Pal, P. (2014). Production and purification of glutamic acid: A critical review towards process intensification. *Chemical Engineering and Processing: Process Intensification*, 81, 59–71. <https://doi.org/10.1016/j.cep.2014.04.012>
- Kurpejović, E., Wendisch, V. F., & Sariyar Akbulut, B. (2021). Tyrosinase-based production of l-DOPA by *Corynebacterium glutamicum*. *Applied Microbiology and Biotechnology*, 105(24), 9103–9111. <https://doi.org/10.1007/s00253-021-11681-5>
- Lapponi, M. J., Méndez, M. B., Trelles, J. A., & Rivero, C. W. (2022). Cell immobilization strategies for biotransformations. *Current Opinion in Green and Sustainable Chemistry*, 33, 100565. <https://doi.org/10.1016/j.cogsc.2021.100565>
- Lawrence, S. A. (2004). *Amines: synthesis, properties and applications*. Cambridge University Press.
- Lee, J., Michael, A. J., Martynowski, D., Goldsmith, E. J., & Phillips, M. A. (2007). Phylogenetic Diversity and the Structural Basis of Substrate Specificity in the β/α -Barrel Fold Basic Amino Acid Decarboxylases. *Journal of Biological Chemistry*, 282(37), 27115–27125.
<https://doi.org/10.1074/jbc.M704066200>
- Lee, S. Y., Kim, H. U., Chae, T. U., Cho, J. S., Kim, J. W., Shin, J. H., Kim, D. I., Ko, Y.-S., Jang, W. D., & Jang, Y.-S. (2019). A comprehensive metabolic map for production of bio-based chemicals. *Nature Catalysis*, 2(1), 18–33. <https://doi.org/10.1038/s41929-018-0212-4>

- Leuchtenberger, W., Huthmacher, K., & Drauz, K. (2005). Biotechnological production of amino acids and derivatives: current status and prospects. *Applied Microbiology and Biotechnology*, *69*(1), 1–8. <https://doi.org/10.1007/s00253-005-0155-y>
- Li, N., Chou, H., & Xu, Y. (2016). Improved cadaverine production from mutant *Klebsiella oxytoca* lysine decarboxylase. *Engineering in Life Sciences*, *16*(3), 299–305. <https://doi.org/10.1002/elsc.201500037>
- Liu, G., Zhou, N., Zhang, M., Li, S., Tian, Q., Chen, J., Chen, B., Wu, Y., & Yao, S. (2010). Hydrophobic solvent induced phase transition extraction to extract drugs from plasma for high performance liquid chromatography–mass spectrometric analysis. *Journal of Chromatography A*, *1217*(3), 243–249. <https://doi.org/10.1016/j.chroma.2009.11.037>
- Liu, J., Pang, B. Q. W., Adams, J. P., Snajdrova, R., & Li, Z. (2017). Coupled Immobilized Amine Dehydrogenase and Glucose Dehydrogenase for Asymmetric Synthesis of Amines by Reductive Amination with Cofactor Recycling. *ChemCatChem*, *9*(3), 425–431. <https://doi.org/10.1002/cctc.201601446>
- Liu, Y., Liu, P., Gao, S., Wang, Z., Luan, P., González-Sabín, J., & Jiang, Y. (2021). Construction of chemoenzymatic cascade reactions for bridging chemocatalysis and Biocatalysis: Principles, strategies and prospective. *Chemical Engineering Journal*, *420*, 127659. <https://doi.org/10.1016/j.cej.2020.127659>
- Ma, J., Wang, S., Huang, X., Geng, P., Wen, C., Zhou, Y., Yu, L., & Wang, X. (2015). Validated UPLC–MS/MS method for determination of hordenine in rat plasma and its application to pharmacokinetic study. *Journal of Pharmaceutical and Biomedical Analysis*, *111*, 131–137. <https://doi.org/10.1016/j.jpba.2015.03.032>
- Mateo, C., Grazú, V., Pessela, B. C. C., Montes, T., Palomo, J. M., Torres, R., López-Gallego, F., Fernández-Lafuente, R., & Guisán, J. M. (2007a). Advances in the design of new epoxy supports for enzyme immobilization–stabilization. *Biochemical Society Transactions*, *35*(6), 1593–1601. <https://doi.org/10.1042/BST0351593>
- Mateo, C., Grazú, V., Pessela, B. C. C., Montes, T., Palomo, J. M., Torres, R., López-Gallego, F., Fernández-Lafuente, R., & Guisán, J. M. (2007b). Advances in the design of new epoxy supports for enzyme immobilization–stabilization. *Biochemical Society Transactions*, *35*(6), 1593–1601. <https://doi.org/10.1042/BST0351593>
- Mayol, O., Bastard, K., Beloti, L., Frese, A., Turkenburg, J. P., Petit, J.-L., Mariage, A., Debard, A., Pellouin, V., Perret, A., de Berardinis, V., Zapparucha, A., Grogan, G., & Vergne-Vaxelaire, C. (2019a). A family of native amine dehydrogenases for the asymmetric reductive amination of ketones. *Nature Catalysis*, *2*(4), 324–333. <https://doi.org/10.1038/s41929-019-0249-z>
- Mayol, O., Bastard, K., Beloti, L., Frese, A., Turkenburg, J. P., Petit, J.-L., Mariage, A., Debard, A., Pellouin, V., Perret, A., de Berardinis, V., Zapparucha, A., Grogan, G., & Vergne-Vaxelaire, C. (2019b). A family of native amine dehydrogenases for the asymmetric reductive amination of ketones. *Nature Catalysis*, *2*(4), 324–333. <https://doi.org/10.1038/s41929-019-0249-z>
- Meyer, E. (1982). Separation of two distinct S-adenosylmethionine dependent N-methyltransferases involved in hordenine biosynthesis in *Hordeum vulgare*. *Plant Cell Reports*, *1*(6), 236–239. <https://doi.org/10.1007/BF00272627>

- Mi, J., Liu, S., Du, Y., Qi, H., & Zhang, L. (2022). Cofactor self-sufficient by co-immobilization of pyridoxal 5'-phosphate and lysine decarboxylase for cadaverine production. *Bioresource Technology Reports*, *17*, 100939. <https://doi.org/10.1016/j.biteb.2021.100939>
- Montgomery, S. L., Mangas-Sanchez, J., Thompson, M. P., Aleku, G. A., Dominguez, B., & Turner, N. J. (2017). Direct Alkylation of Amines with Primary and Secondary Alcohols through Biocatalytic Hydrogen Borrowing. *Angewandte Chemie*, *129*(35), 10627–10630. <https://doi.org/10.1002/ange.201705848>
- Mørch, Y. A., Donati, I., Strand, B. L., & Skjåk-Bræk, G. (2006). Effect of Ca²⁺, Ba²⁺, and Sr²⁺ on Alginate Microbeads. *Biomacromolecules*, *7*(5), 1471–1480. <https://doi.org/10.1021/bm060010d>
- Muñoz, A. J., Hernández-Chávez, G., De Anda, R., Martínez, A., Bolívar, F., & Gosset, G. (2011). Metabolic engineering of *Escherichia coli* for improving l-3,4-dihydroxyphenylalanine (l-DOPA) synthesis from glucose. *Journal of Industrial Microbiology and Biotechnology*, *38*(11), 1845–1852. <https://doi.org/10.1007/s10295-011-0973-0>
- Mutti, F. G., & Knaus, T. (2021). Enzymes Applied to the Synthesis of Amines. In *Biocatalysis for Practitioners* (pp. 143–180). Wiley. <https://doi.org/10.1002/9783527824465.ch6>
- Mutti, F. G., Knaus, T., Scrutton, N. S., Breuer, M., & Turner, N. J. (2015). Conversion of alcohols to enantiopure amines through dual-enzyme hydrogen-borrowing cascades. *Science*, *349*(6255), 1525–1529. <https://doi.org/10.1126/science.aac9283>
- Nakai, T., Nakagawa, N., Maoka, N., Masui, R., Kuramitsu, S., & Kamiya, N. (2005). Structure of P-protein of the glycine cleavage system: implications for nonketotic hyperglycinemia. *The EMBO Journal*, *24*(8), 1523–1536. <https://doi.org/10.1038/sj.emboj.7600632>
- Narisetty, V., Cox, R., Bommareddy, R., Agrawal, D., Ahmad, E., Pant, K. K., Chandel, A. K., Bhatia, S. K., Kumar, D., Binod, P., Gupta, V. K., & Kumar, V. (2022). Valorisation of xylose to renewable fuels and chemicals, an essential step in augmenting the commercial viability of lignocellulosic biorefineries. *Sustainable Energy & Fuels*, *6*(1), 29–65. <https://doi.org/10.1039/D1SE00927C>
- Nasri, M. (2017a). *Protein Hydrolysates and Biopeptides* (pp. 109–159). <https://doi.org/10.1016/bs.afnr.2016.10.003>
- Nasri, M. (2017b). *Protein Hydrolysates and Biopeptides* (pp. 109–159). <https://doi.org/10.1016/bs.afnr.2016.10.003>
- Natte, K., Neumann, H., Jagadeesh, R. v., & Beller, M. (2017). Convenient iron-catalyzed reductive aminations without hydrogen for selective synthesis of N-methylamines. *Nature Communications*, *8*(1), 1344. <https://doi.org/10.1038/s41467-017-01428-0>
- Nguyen, N. H., Truong-Thi, N.-H., Nguyen, D. T. D., Ching, Y. C., Huynh, N. T., & Nguyen, D. H. (2022). Non-ionic surfactants As co-templates to control the mesopore diameter of hollow mesoporous silica nanoparticles for drug delivery applications. *Colloids and Surfaces A: Physicochemical and Engineering Aspects*, *655*, 130218. <https://doi.org/10.1016/j.colsurfa.2022.130218>
- Ohta, H., Murakami, Y., Takebe, Y., Murasaki, K., Oshima, K., Yoshihara, H., & Morimura, S. (2020). &N-Methyltyramine, a Gastrin-releasing Factor in Beer, and

Structurally Related Compounds as Agonists for Human Trace Amine-associated Receptor 1. *Food Science and Technology Research*, 26(2), 313–317.
<https://doi.org/10.3136/fstr.26.313>

- PARADISI, F., COLLINS, S., MAGUIRE, A., & ENGEL, P. (2007). Phenylalanine dehydrogenase mutants: Efficient biocatalysts for synthesis of non-natural phenylalanine derivatives. *Journal of Biotechnology*, 128(2), 408–411. <https://doi.org/10.1016/j.jbiotec.2006.08.008>
- Park, J.-Y., Choi, M.-J., Yu, H., Choi, Y., Park, K.-M., & Chang, P.-S. (2022). Multi-functional behavior of food emulsifier erythorbyl laurate in different colloidal conditions of homogeneous oil-in-water emulsion system. *Colloids and Surfaces A: Physicochemical and Engineering Aspects*, 636, 128127. <https://doi.org/10.1016/j.colsurfa.2021.128127>
- Park, S. H., Soetyono, F., & Kim, H. K. (2017). Cadaverine Production by Using Cross-Linked Enzyme Aggregate of Escherichia coli Lysine Decarboxylase. *Journal of Microbiology and Biotechnology*, 27(2), 289–296. <https://doi.org/10.4014/jmb.1608.08033>
- Patil, M. D., Grogan, G., Bommarius, A., & Yun, H. (2018). Oxidoreductase-Catalyzed Synthesis of Chiral Amines. *ACS Catalysis*, 8(12), 10985–11015.
<https://doi.org/10.1021/acscatal.8b02924>
- Patil, M. D., Yoon, S., Jeon, H., Khobragade, T. P., Sarak, S., Pagar, A. D., Won, Y., & Yun, H. (2019). Kinetic Resolution of Racemic Amines to Enantiopure (S)-amines by a Biocatalytic Cascade Employing Amine Dehydrogenase and Alanine Dehydrogenase. *Catalysts*, 9(7), 600. <https://doi.org/10.3390/catal9070600>
- Payne, J. T., Valentic, T. R., & Smolke, C. D. (2021). Complete biosynthesis of the bisbenzylisoquinoline alkaloids guattegaumerine and berbaminine in yeast. *Proceedings of the National Academy of Sciences*, 118(51). <https://doi.org/10.1073/pnas.2112520118>
- Pelckmans, M., Renders, T., Van de Vyver, S., & Sels, B. F. (2017). Bio-based amines through sustainable heterogeneous catalysis. *Green Chemistry*, 19(22), 5303–5331.
<https://doi.org/10.1039/C7GC02299A>
- Pilkington, R. L., Dallaston, M. A., Savage, G. P., Williams, C. M., & Polyzos, A. (2021). Enone-promoted decarboxylation of *trans*-4-hydroxy-*l*-proline in flow: a side-by-side comparison to batch. *Reaction Chemistry & Engineering*, 6(3), 486–493.
<https://doi.org/10.1039/D0RE00442A>
- Planchestainer, M., Hegarty, E., Heckmann, C. M., Gourlay, L. J., & Paradisi, F. (2019). Widely applicable background depletion step enables transaminase evolution through solid-phase screening. *Chemical Science*, 10(23), 5952–5958. <https://doi.org/10.1039/C8SC05712E>
- Prieto, M. A., & Garcia, J. L. (1994). Molecular characterization of 4-hydroxyphenylacetate 3-hydroxylase of Escherichia coli. A two-protein component enzyme. *Journal of Biological Chemistry*, 269(36), 22823–22829. [https://doi.org/10.1016/S0021-9258\(17\)31719-2](https://doi.org/10.1016/S0021-9258(17)31719-2)
- Pyne, M. E., Kevvai, K., Grewal, P. S., Narcross, L., Choi, B., Bourgeois, L., Dueber, J. E., & Martin, V. J. J. (2020). A yeast platform for high-level synthesis of tetrahydroisoquinoline alkaloids. *Nature Communications*, 11(1), 3337. <https://doi.org/10.1038/s41467-020-17172-x>

- Quaglia, D., Irwin, J. A., & Paradisi, F. (2012a). Horse Liver Alcohol Dehydrogenase: New Perspectives for an Old Enzyme. *Molecular Biotechnology*, *52*(3), 244–250. <https://doi.org/10.1007/s12033-012-9542-7>
- Quaglia, D., Irwin, J. A., & Paradisi, F. (2012b). Horse Liver Alcohol Dehydrogenase: New Perspectives for an Old Enzyme. *Molecular Biotechnology*, *52*(3), 244–250. <https://doi.org/10.1007/s12033-012-9542-7>
- Ray, S. S., Bonanno, J. B., Rajashankar, K. R., Pinho, M. G., He, G., De Lencastre, H., Tomasz, A., & Burley, S. K. (2002). Cocrystal Structures of Diaminopimelate Decarboxylase. *Structure*, *10*(11), 1499–1508. [https://doi.org/10.1016/S0969-2126\(02\)00880-8](https://doi.org/10.1016/S0969-2126(02)00880-8)
- Reetz, M. T. (2013). Biocatalysis in Organic Chemistry and Biotechnology: Past, Present, and Future. *Journal of the American Chemical Society*, *135*(34), 12480–12496. <https://doi.org/10.1021/ja405051f>
- Roschangar, F., Sheldon, R. A., & Senanayake, C. H. (2015). Overcoming barriers to green chemistry in the pharmaceutical industry – the Green Aspiration Level™ concept. *Green Chemistry*, *17*(2), 752–768. <https://doi.org/10.1039/C4GC01563K>
- Ruhaak, L. R., Steenvoorden, E., Koeleman, C. A. M., Deelder, A. M., & Wuhrer, M. (2010). 2-Picoline-borane: A non-toxic reducing agent for oligosaccharide labeling by reductive amination. *Proteomics*, *10*(12), 2330–2336. <https://doi.org/10.1002/pmic.200900804>
- Sagong, H.-Y., Son, H. F., Kim, S., Kim, Y.-H., Kim, I.-K., & Kim, K.-J. (2016). Crystal Structure and Pyridoxal 5-Phosphate Binding Property of Lysine Decarboxylase from *Selenomonas ruminantium*. *PLOS ONE*, *11*(11), e0166667. <https://doi.org/10.1371/journal.pone.0166667>
- Said, A. A. E., Ali, T. F. S., Attia, E. Z., Ahmed, A.-S. F., Shehata, A. H., Abdelmohsen, U. R., & Fouad, M. A. (2021). Antidepressant potential of *Mesembryanthemum cordifolium* roots assisted by metabolomic analysis and virtual screening. *Natural Product Research*, *35*(23), 5493–5497. <https://doi.org/10.1080/14786419.2020.1788019>
- SANDMEIER, E., HALE, T. I., & CHRISTEN, P. (1994a). Multiple evolutionary origin of pyridoxal-5'-phosphate-dependent amino acid decarboxylases. *European Journal of Biochemistry*, *221*(3), 997–1002. <https://doi.org/10.1111/j.1432-1033.1994.tb18816.x>
- SANDMEIER, E., HALE, T. I., & CHRISTEN, P. (1994b). Multiple evolutionary origin of pyridoxal-5'-phosphate-dependent amino acid decarboxylases. *European Journal of Biochemistry*, *221*(3), 997–1002. <https://doi.org/10.1111/j.1432-1033.1994.tb18816.x>
- Sato, S., Sakamoto, T., Miyazawa, E., & Kikugawa, Y. (2004). One-pot reductive amination of aldehydes and ketones with α -picoline-borane in methanol, in water, and in neat conditions. *Tetrahedron*, *60*(36), 7899–7906. <https://doi.org/10.1016/j.tet.2004.06.045>
- Schoenmakers, H., & Spiegel, L. (2014). Laboratory Distillation and Scale-up. In *Distillation* (pp. 319–339). Elsevier. <https://doi.org/10.1016/B978-0-12-386878-7.00010-3>
- Seah, S. Y. K., Britton, K. L., Rice, D. W., Asano, Y., & Engel, P. C. (2002). Single Amino Acid Substitution in *Bacillus sphaericus* Phenylalanine Dehydrogenase Dramatically Increases Its Discrimination between Phenylalanine and Tyrosine Substrates. *Biochemistry*, *41*(38), 11390–11397. <https://doi.org/10.1021/bi020196a>

- Seah, S. Y. K., Linda Britton, K., Baker, P. J., Rice, D. W., Asano, Y., & Engel, P. C. (1995). Alteration in relative activities of phenylalanine dehydrogenase towards different substrates by site-directed mutagenesis. *FEBS Letters*, *370*(1–2), 93–96. [https://doi.org/10.1016/0014-5793\(95\)00804-I](https://doi.org/10.1016/0014-5793(95)00804-I)
- Sen, K. Y., & Baidurah, S. (2021). Renewable biomass feedstocks for production of sustainable biodegradable polymer. *Current Opinion in Green and Sustainable Chemistry*, *27*, 100412. <https://doi.org/10.1016/j.cogsc.2020.100412>
- Sharma, M., Mangas-Sanchez, J., Turner, N. J., & Grogan, G. (2017). NAD(P)H-Dependent Dehydrogenases for the Asymmetric Reductive Amination of Ketones: Structure, Mechanism, Evolution and Application. *Advanced Synthesis & Catalysis*, *359*(12), 2011–2025. <https://doi.org/10.1002/adsc.201700356>
- Sheldon, R. A., Basso, A., & Brady, D. (2021). New frontiers in enzyme immobilisation: robust biocatalysts for a circular bio-based economy. *Chemical Society Reviews*, *50*(10), 5850–5862. <https://doi.org/10.1039/D1CS00015B>
- Sheldon, R. A., & Brady, D. (2019). Broadening the Scope of Biocatalysis in Sustainable Organic Synthesis. *ChemSusChem*, *12*(13), 2859–2881. <https://doi.org/10.1002/cssc.201900351>
- Sheldon, R. A., & Woodley, J. M. (2018). Role of Biocatalysis in Sustainable Chemistry. *Chemical Reviews*, *118*(2), 801–838. <https://doi.org/10.1021/acs.chemrev.7b00203>
- Sommer, T., Göen, T., Budnik, N., & Pischetsrieder, M. (2020). Absorption, Biokinetics, and Metabolism of the Dopamine D2 Receptor Agonist Hordenine (*N,N*-Dimethyltyramine) after Beer Consumption in Humans. *Journal of Agricultural and Food Chemistry*, *68*(7), 1998–2006. <https://doi.org/10.1021/acs.jafc.9b06029>
- Song, W., Chen, X., Wu, J., Xu, J., Zhang, W., Liu, J., Chen, J., & Liu, L. (2020). Biocatalytic derivatization of proteinogenic amino acids for fine chemicals. *Biotechnology Advances*, *40*, 107496. <https://doi.org/10.1016/j.biotechadv.2019.107496>
- Stano, J., Nemeč, P., Weissová, K., Kovács, P., Kákoniová, D., & Lisková, D. (1995). Decarboxylation of l-tyrosine and l-dopa by immobilized cells of *Papaver somniferum*. *Phytochemistry*, *38*(4), 859–860. [https://doi.org/10.1016/0031-9422\(94\)00768-0](https://doi.org/10.1016/0031-9422(94)00768-0)
- Stockert, J. C., Horobin, R. W., Colombo, L. L., & Blázquez-Castro, A. (2018). Tetrazolium salts and formazan products in Cell Biology: Viability assessment, fluorescence imaging, and labeling perspectives. *Acta Histochemica*, *120*(3), 159–167. <https://doi.org/10.1016/j.acthis.2018.02.005>
- Su, Y., Liu, Y., He, D., Hu, G., Wang, H., Ye, B., He, Y., Gao, X., & Liu, D. (2022). Hordenine inhibits neuroinflammation and exerts neuroprotective effects via inhibiting NF- κ B and MAPK signaling pathways in vivo and in vitro. *International Immunopharmacology*, *108*, 108694. <https://doi.org/10.1016/j.intimp.2022.108694>
- Surwase, S. N., Patil, S. A., Apine, O. A., & Jadhav, J. P. (2012). Efficient Microbial Conversion of l-Tyrosine to l-DOPA by *Brevundimonas* sp. SGJ. *Applied Biochemistry and Biotechnology*, *167*(5), 1015–1028. <https://doi.org/10.1007/s12010-012-9564-4>
- Tang, Y. Q., & Weng, N. (2013). Salting-out assisted liquid–liquid extraction for bioanalysis. *Bioanalysis*, *5*(12), 1583–1598. <https://doi.org/10.4155/bio.13.117>

- Teng, Y., Scott, E. L., van Zeeland, A. N. T., & Sanders, J. P. M. (2011). The use of l-lysine decarboxylase as a means to separate amino acids by electro dialysis. *Green Chemistry*, *13*(3), 624. <https://doi.org/10.1039/c0gc00611d>
- Thompson, M. P., Derrington, S. R., Heath, R. S., Porter, J. L., Mangas-Sanchez, J., Devine, P. N., Truppo, M. D., & Turner, N. J. (2019). A generic platform for the immobilisation of engineered biocatalysts. *Tetrahedron*, *75*(3), 327–334. <https://doi.org/10.1016/j.tet.2018.12.004>
- Thompson, M. P., & Turner, N. J. (2017a). Two-Enzyme Hydrogen-Borrowing Amination of Alcohols Enabled by a Cofactor-Switched Alcohol Dehydrogenase. *ChemCatChem*, *9*(20), 3833–3836. <https://doi.org/10.1002/cctc.201701092>
- Thompson, M. P., & Turner, N. J. (2017b). Two-Enzyme Hydrogen-Borrowing Amination of Alcohols Enabled by a Cofactor-Switched Alcohol Dehydrogenase. *ChemCatChem*, *9*(20), 3833–3836. <https://doi.org/10.1002/cctc.201701092>
- Tolbert, W. D., Graham, D. E., White, R. H., & Ealick, S. E. (2003). Pyruvoyl-Dependent Arginine Decarboxylase from *Methanococcus jannaschii*. *Structure*, *11*(3), 285–294. [https://doi.org/10.1016/S0969-2126\(03\)00026-1](https://doi.org/10.1016/S0969-2126(03)00026-1)
- Truong, C. C., Mishra, D. K., & Suh, Y. (2023). Recent Catalytic Advances on the Sustainable Production of Primary Furanic Amines from the One-Pot Reductive Amination of 5-Hydroxymethylfurfural. *ChemSusChem*, *16*(1). <https://doi.org/10.1002/cssc.202201846>
- Tseliou, V., Knaus, T., Masman, M. F., Corrado, M. L., & Mutti, F. G. (2019). Generation of amine dehydrogenases with increased catalytic performance and substrate scope from ϵ -deaminating L-Lysine dehydrogenase. *Nature Communications*, *10*(1), 3717. <https://doi.org/10.1038/s41467-019-11509-x>
- Tseliou, V., Knaus, T., Vilím, J., Masman, M. F., & Mutti, F. G. (2020). Kinetic Resolution of Racemic Primary Amines Using *Geobacillus stearothermophilus* Amine Dehydrogenase Variant. *ChemCatChem*, *12*(8), 2184–2188. <https://doi.org/10.1002/cctc.201902085>
- Tsukatani, T., Suenaga, H., Higuchi, T., Akao, T., Ishiyama, M., Ezo, K., & Matsumoto, K. (2008). Colorimetric cell proliferation assay for microorganisms in microtiter plate using water-soluble tetrazolium salts. *Journal of Microbiological Methods*, *75*(1), 109–116. <https://doi.org/10.1016/j.mimet.2008.05.016>
- Viejo, C. G., Villarreal-Lara, R., Torrico, D. D., Rodríguez-Velazco, Y. G., Escobedo-Avellaneda, Z., Ramos-Parra, P. A., Mandal, R., Singh, A. P., Hernández-Brenes, C., & Fuentes, S. (2020). Beer and consumer response using biometrics: Associations assessment of beer compounds and elicited emotions. *Foods*, *9*(6), 821.
- Vitaku, E., Smith, D. T., & Njardarson, J. T. (2014). Analysis of the Structural Diversity, Substitution Patterns, and Frequency of Nitrogen Heterocycles among U.S. FDA Approved Pharmaceuticals. *Journal of Medicinal Chemistry*, *57*(24), 10257–10274. <https://doi.org/10.1021/jm501100b>
- Wang, M., Khan, M. A., Mohsin, I., Wicks, J., Ip, A. H., Sumon, K. Z., Dinh, C.-T., Sargent, E. H., Gates, I. D., & Kibria, M. G. (2021). Can sustainable ammonia synthesis pathways compete with fossil-fuel based Haber–Bosch processes? *Energy & Environmental Science*, *14*(5), 2535–2548. <https://doi.org/10.1039/D0EE03808C>

- Wang, Q., Xin, Y., Zhang, F., Feng, Z., Fu, J., Luo, L., & Yin, Z. (2011). Enhanced γ -aminobutyric acid-forming activity of recombinant glutamate decarboxylase (*gadA*) from *Escherichia coli*. *World Journal of Microbiology and Biotechnology*, *27*(3), 693–700. <https://doi.org/10.1007/s11274-010-0508-2>
- Watanabe, Y., Tsuji, Y., Ige, H., Ohsugi, Y., & Ohta, T. (1984). Ruthenium-catalyzed N-alkylation and N-benzoylation of aminoarenes with alcohols. *The Journal of Organic Chemistry*, *49*(18), 3359–3363. <https://doi.org/10.1021/jo00192a021>
- Weber, R. E. (1992). Use of ionic and zwitterionic (Tris/BisTris and HEPES) buffers in studies on hemoglobin function. *Journal of Applied Physiology*, *72*(4), 1611–1615. <https://doi.org/10.1152/jappl.1992.72.4.1611>
- Wei, G., Chen, Y., Zhou, N., Lu, Q., Xu, S., Zhang, A., Chen, K., & Ouyang, P. (2022). Chitin biopolymer mediates self-sufficient biocatalyst of pyridoxal 5'-phosphate and L-lysine decarboxylase. *Chemical Engineering Journal*, *427*, 132030. <https://doi.org/10.1016/j.cej.2021.132030>
- Wei, T., Cheng, B. Y., & Liu, J. Z. (2016). Genome engineering *Escherichia coli* for L-DOPA overproduction from glucose. *Scientific Reports*, *6*. <https://doi.org/10.1038/srep30080>
- Wieschalka, S., Blombach, B., Bott, M., & Eikmanns, B. J. (2013). Bio-based production of organic acids with *Corynebacterium glutamicum*. *Microbial Biotechnology*, *6*(2), 87–102. <https://doi.org/10.1111/1751-7915.12013>
- Wohlgenuth, R. (2021). Biocatalysis-Key enabling tools from biocatalytic one-step and multi-step reactions to biocatalytic total synthesis. *New Biotechnol*, *60*, 113–123.
- Wu, B., Zhang, S., Hong, T., Zhou, Y., Wang, H., Shi, M., Yang, H., Tian, X., Guo, J., Bian, J., Roache, J., Delgado, P., Mo, R., Fridrich, C., Gao, F., & Wang, J. (2020). Merging Biocatalysis, Flow, and Surfactant Chemistry: Innovative Synthesis of an FXI (Factor XI) Inhibitor. *Organic Process Research & Development*, *24*(11), 2780–2788. <https://doi.org/10.1021/acs.oprd.0c00412>
- Wu, P., Li, G., He, Y., Luo, D., Li, L., Guo, J., Ding, P., & Yang, F. (2020). High-efficient and sustainable biodegradation of microcystin-LR using *Sphingopyxis* sp. YF1 immobilized Fe₃O₄@chitosan. *Colloids and Surfaces B: Biointerfaces*, *185*, 110633. <https://doi.org/10.1016/j.colsurfb.2019.110633>
- Ye, L. J., Toh, H. H., Yang, Y., Adams, J. P., Snajdrova, R., & Li, Z. (2015). Engineering of Amine Dehydrogenase for Asymmetric Reductive Amination of Ketone by Evolving *Rhodococcus* Phenylalanine Dehydrogenase. *ACS Catalysis*, *5*(2), 1119–1122. <https://doi.org/10.1021/cs501906r>
- Yoon, S., Patil, M. D., Sarak, S., Jeon, H., Kim, G., Khobragade, T. P., Sung, S., & Yun, H. (2019). Deracemization of Racemic Amines to Enantiopure (R)- and (S)-amines by Biocatalytic Cascade Employing ω -Transaminase and Amine Dehydrogenase. *ChemCatChem*, *11*(7), 1898–1902. <https://doi.org/10.1002/cctc.201900080>
- Yoshitaka Hashitani, B. (1925). On the chemical constituents of malt-rootlets with special reference to Hordenine. *Journal of the College of Agriculture*, *14*, 1–56.

- Zhang, B., Jiang, Y., Li, Z., Wang, F., & Wu, X.-Y. (2020). Recent Progress on Chemical Production From Non-food Renewable Feedstocks Using *Corynebacterium glutamicum*. *Frontiers in Bioengineering and Biotechnology*, *8*. <https://doi.org/10.3389/fbioe.2020.606047>
- Zhang, H., Wei, Y., Lu, Y., Wu, S., Liu, Q., Liu, J., & Jiao, Q. (2016). Three-step biocatalytic reaction using whole cells for efficient production of tyramine from keratin acid hydrolysis wastewater. *Applied Microbiology and Biotechnology*, *100*(4), 1691–1700. <https://doi.org/10.1007/s00253-015-7054-7>
- Zhang, K., & Ni, Y. (2014). Tyrosine decarboxylase from *Lactobacillus brevis*: Soluble expression and characterization. *Protein Expression and Purification*, *94*, 33–39. <https://doi.org/10.1016/j.pep.2013.10.018>
- Zhang, X., Du, L., Zhang, J., Li, C., Zhang, J., & Lv, X. (2021). Hordenine Protects Against Lipopolysaccharide-Induced Acute Lung Injury by Inhibiting Inflammation. *Frontiers in Pharmacology*, *12*, 712232. <https://doi.org/10.3389/fphar.2021.712232>
- Zhao, W., Hu, S., Huang, J., Ke, P., Yao, S., Lei, Y., Mei, L., & Wang, J. (2016). Permeabilization of *Escherichia coli* with ampicillin for a whole cell biocatalyst with enhanced glutamate decarboxylase activity. *Chinese Journal of Chemical Engineering*, *24*(7), 909–913. <https://doi.org/10.1016/j.cjche.2016.02.001>
- Zhou, F., Xu, Y., Nie, Y., & Mu, X. (2022). Substrate-Specific Engineering of Amino Acid Dehydrogenase Superfamily for Synthesis of a Variety of Chiral Amines and Amino Acids. *Catalysts*, *12*(4), 380. <https://doi.org/10.3390/catal12040380>
- Zhou, J.-W., Ruan, L.-Y., Chen, H.-J., Luo, H.-Z., Jiang, H., Wang, J.-S., & Jia, A.-Q. (2019). Inhibition of Quorum Sensing and Virulence in *Serratia marcescens* by Hordenine. *Journal of Agricultural and Food Chemistry*, *67*(3), 784–795. <https://doi.org/10.1021/acs.jafc.8b05922>
- Zhu, H., Xu, G., Zhang, K., Kong, X., Han, R., Zhou, J., & Ni, Y. (2016a). Crystal structure of tyrosine decarboxylase and identification of key residues involved in conformational swing and substrate binding. *Scientific Reports*, *6*(1), 27779. <https://doi.org/10.1038/srep27779>
- Zhu, H., Xu, G., Zhang, K., Kong, X., Han, R., Zhou, J., & Ni, Y. (2016b). Crystal structure of tyrosine decarboxylase and identification of key residues involved in conformational swing and substrate binding. *Scientific Reports*, *6*(1), 27779. <https://doi.org/10.1038/srep27779>
- Zhuang, W., Liu, H., Zhang, Y., He, J., & Wang, P. (2021). Effective asymmetric preparation of (R)-1-[3-(trifluoromethyl)phenyl]ethanol with recombinant *E. coli* whole cells in an aqueous Tween-20/natural deep eutectic solvent solution. *AMB Express*, *11*(1), 118. <https://doi.org/10.1186/s13568-021-01278-6>

A.2 Hydroxytyrosol multi-enzymatic cascade

Unless explicitly stated otherwise, the research presented in this chapter is the sole and individual work of the author.

A.2.1 Background

Multi-enzymatic cascades have emerged as a promising approach for producing high-value products in a sustainable and eco-friendly manner. (Benítez-Mateos et al., 2022; Chen et al., 2019; Hwang & Lee, 2019; Wohlgemuth, 2021) This method involves the sequential arrangement of enzymes that work together to convert substrates into final products, providing enhanced control and flexibility to customize enzymatic reactions for specific purposes. The use of immobilized purified enzymes has been identified as a key strategy for optimizing these external pathways, as it significantly improves enzyme stability and reusability, resulting in a more efficient and cost-effective process.

One challenge in constructing multi-enzymatic cascades is balancing the diverse requirements of different enzymes, which may have varying optimal pH, temperature, or substrate concentrations for their activity. However, this challenge can be addressed through careful optimization and fine-tuning of reaction conditions, which is possible through immobilized biocatalysts compartmentalization in bioreactors. This approach offers great promise for enhancing the efficiency and sustainability of industrial processes.

In this appendix the efforts to successfully synthesizing hydroxytyrosol, (Bertelli et al., 2020) an antioxidant of great value that is challenging to obtain from natural sources extraction, are described. The cascade was designed to employ a series of enzymes, starting with *LbTDC*, (K. Zhang & Ni, 2014) which is responsible for the decarboxylation of L-DOPA, the initial substrate. Subsequently, the process proceeded with a transaminase, *TsRTA*, (Heckmann et al., 2020) which was introduced as a substitute for the enzyme *HeWT*, (Cerioli et al., 2015) already applied in previous literature. (Contente & Paradisi, 2018) The final stage involved the use of *HLADH* (Quaglia et al., 2012a) to reduce DOPAL, ultimately yielding hydroxytyrosol. This multi-enzyme cascade aims to provide a cost-effective, environmentally friendly, and efficient method for producing hydroxytyrosol (Figure A2.1). This approach can be particularly beneficial given that the natural sources extraction yields are typically low and require significant quantities of organic solvents. Hydroxytyrosol has notable applications in the pharmaceutical, nutraceutical, and cosmetic sectors.

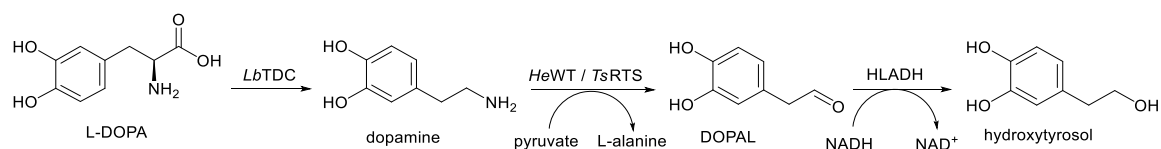


Figure A2.1: Hydroxytyrosol multi-enzymatic cascade.

One of the most challenging steps in this cascade was the production of DOPAL, which is an extremely reactive intermediate. (Bloch et al., 2023) The conversion of dopamine to DOPAL is catalysed by *HeWT*, and it is a critical step in this synthesis because the intermediate is highly unstable and prone to oxidation, which can result in the formation

of by-products. Further, the performance of a different transaminase, *TsRTA*, was investigated for catalyse this step.

The main by-product from the reactivity of DOPAL is given from Pictet-Spengler condensation of DOPAL with dopamine, leading to the formation of unwanted side products as tetrahydropapaveroline (Figure A2.2).(Holbrook et al., 2022)

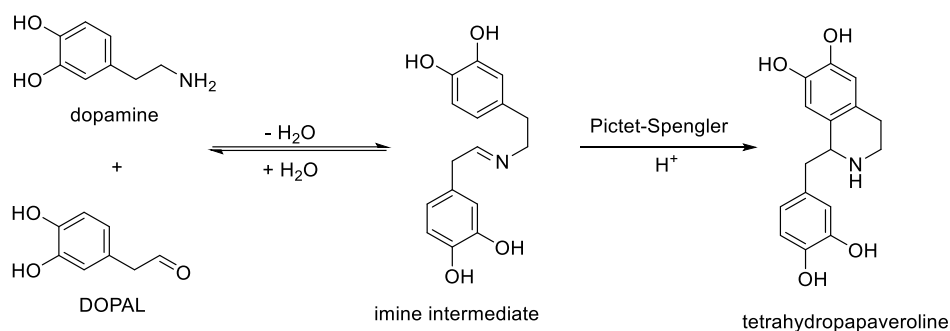


Figure A2.2: Formation of the by-product tetrahydropapaveroline from the Pictet-Spengler condensation between DOPAL and dopamine

To overcome this challenge, HLADH is expected to rapidly reduce DOPAL to hydroxytyrosol, limiting its exposure to the reaction environment. Another reported key strategy for effectively exploiting the reactive intermediate DOPAL was the implementation of a segmented flow with aqueous buffer and toluene.(Contente & Paradisi, 2018) This was based on the principle that separating the reaction mixture into two immiscible phases (water and toluene) inside the flow system line, allows for the isolation of the reactive intermediate, DOPAL, from the other components in the reaction mixture, and leads to effective stripping of this apolar aldehyde from the hydrophobic supports used for the immobilization. In order to exploit the segmented flow with toluene, the stability of the biocatalysts had to be guaranteed in organic phase, therefore the enzymatic immobilization became essential for the successful result of the synthesis even in batch.

A.2.2 Findings

Enzymes immobilization

The selection of L-tyrosine decarboxylase from *Bacillus brevis* (*LbTDC*), *Thermomyces stellatus* R-selective transaminase (*TsRTA*), and horse liver alcohol dehydrogenase (HLADH) for the hydroxytyrosol synthesis cascade was based on their specific roles in the pathway, their substrate scope and their availability for purification.

The immobilization of *LbTDC* and *TsRTA* was achieved using covalent immobilization on an epoxy support with cobalt directionality. Because PLP (pyridoxal 5'-phosphate) is the cofactor required for the activity of both *LbTDC* and *TsRTA* enzymes, the immobilization of these biocatalysts on the support was attempted with the co-immobilization of the cofactor on the support.

The immobilization of HLADH was performed on glyoxyl supports exploiting the covalent bond formation between support aldehydes handles and enzyme amino groups.

Immobilization of *LbTDC*

In the immobilization study for *LbTDC*, EP403/s, HFA403/S, EP400/SS, were the methacrylic support investigated. The results for the immobilization with this resin is described in Chapter 5. An additional support trialed for *LbTDC* was epoxy-agarose (Table A2.1). The coating with PEI 60 kDa was successfully applied to EP400/SS and epoxy-agarose to retain the cofactor PLP ionically and by Schiff base bond.

Support	Protein loading	Specific activity (U/mg)	Support Activity (U/g)	Recovered activity (%)	Stability (%)
Epoxy-agarose	1	6.8	6.8	16	15
Coimm-PLP-EP400/SS	1	2.8	2.8	7	4
Coimm-PLP-Epoxy-agarose-	1	5.6	5.6	13	10

Table A2.1 : Immobilization experiments of *LbTDC* on different supports. The protein was covalently immobilized through epoxy handles with Co²⁺ directionality. The specific activity of the free enzyme *LbTDC* was 43 U/mg. The stability test shows the recoved activity of the immobilized biocatalyst after 1 week storage at 4 °C.

The immobilization buffer used was 100 mM phosphate buffer, 0.1 mM PLP, pH 7.4. When the support was coated with PEI, the buffer employed was 10 mM phosphate buffer, pH 7.4. After washing the co-immobilized enzyme with the cofactor, the retained PLP was above the 90 % for both supports.

Immobilization of *TsRTA* and *HeWT*

In the immobilization study for *HeWT*, EP403/S, EP400/SS, and epoxy-agarose were used as carriers. Additionally, EP403/S and epoxy-agarose were coated with PEI. The protein loadings tested were 5 mg/mL and 10 mg/mL.

The resin-to-volume ratio in the immobilization experiment was maintained at 1:10. The immobilization process typically occurred within 6 hours, leading to full immobilization yield. The immobilization buffer used was 100 mM phosphate at pH 8. When the support was coated with PEI, the buffer employed was 10 mM phosphate, 0.1 mM PLP, pH 8. After washing the co-immobilized enzyme with the cofactor, the retained PLP was around 85 % in the case of EP400/SS and 90% for epoxy-agarose.

Starting from a *HeWT* with an initial specific activity of 1.1 ± 0.3 U/mg, the different supports and protein loadings yielded the values reported in Table A2.2.

Support	Protein loading	Specific activity (U/mg)	Support Activity (U/g)	Recovered activity (%)
Coimm-PLP-EP403/S	10	0.7	7	45
EP400/SS	5	0.34	1.7	35
Coimm-PLP-Agarose	5	0.33	1.65	30

Table A2.2: Immobilization experiments of *HeWT* on different supports. The protein was covalently immobilized through epoxy handles with directionality. The specific activity of the free *HeWT* was 1.1 U/mg.

To address the issue of the observed low activity on the supports (< 45 % recovered activity) in the *HeWT* immobilization, an immobilization study using *TsRTA* was conducted as an alternative TA. In this study, EP400/SS and EP403/S were selected as the supports to investigate, with and without co-immobilization of the cofactor. Striking for a high number of units of activity on support the protein loading trialed were 10 mg/g and 20 mg/g (Table A2.3).

Support	Protein loading (mg/g)	Specific activity (U/mg)	Expressed activity (U/g)	Recovered activity (%)
Coimm-PLP-EP403/S	10	2.05	20.53	91
Coimm-PLP-EP403/S	20	1.97	39.76	88
EP403/S	10	2.23	22.58	99
EP403/S	20	1.89	37.74	84
EP400/SS	10	2.1	21.0	95

Table A2.3 : Immobilization experiments of *TsRTA* on different supports. The protein was covalently immobilized through epoxy handles with directionality. The specific activity of the free *TsRTA* was 2.25 U/mg.

The resin-to-volume ratio in the immobilization experiment was maintained at 1:10. The immobilization buffer used was 100 mM phosphate at pH 8. The immobilization reached completion after 6 hours of incubation at room temperature and mild shaking. When the support was coated with PEI, the buffer employed was 10 mM phosphate, 0.1 mM PLP, pH 8. After washing the co-immobilized enzyme with the cofactor, the retained PLP was around 80 % for EP400/SS and 85 % for agarose.

Immobilization of HLADH

In the immobilization study for HLADH, which features a strep-tag at the N-terminus rather than a His-tag, the chemistry employed was based on imine bond formation. This was achieved by reacting the aldehydic handles on the support with the nucleophilic amino groups present in the protein structure. The imine bonds were then reduced to stable covalent bonds using sodium borohydride.

The different protein loading trialed were 5 and 10 mg/g. The supports of choice were EP403/S and EP400/SS, which were promising in previous immobilization experiments as well for TsRTA. The procedure for the immobilization in this case was previously described in the paragraph “Covalent immobilization on glyoxyl support” in the Materials and methods section.

Support	Protein loading (mg/g)	Specific activity (U/mg)	Support Activity (U/g)	Recovered activity (%)
EP403/S	5	1.1	5.5	74
EP403/S	10	0.8	8.0	60
EP400/SS	5	0.7	3.5	47
EP400/SS	10	0.6	6.0	41

Table A2.4 : Immobilization experiments of HLADH on different supports. The protein was covalently immobilized through aldehydic handles. The specific activity of the free HLADH was 1.48 U/mg.

Enzymes stability in organic solvents

The enzymes stability in biphasic systems with toluene was already reported for *HeWT* and *HLADH*.(Contente & Paradisi, 2018) The stability in organic solvents was then investigated only for *TsRTA* (Tables A2.5 A,B) and *LbTDC* (Table A2.6), involving ethyl acetate (EtOAc) and toluene in the experiments. After the incubation, performed in 1 mL glass vials, the resin was recovered by filtering the solution, and an activity test was subsequently performed.

Stability in organic solvent system of 20 mg/g imm-*TsRTA*-EP403/S

EtOAc (%)	Recovered activity (%)
10	69
20	70
30	68

Table A2.5 A

Toluene (%)	Recovered activity (%)
10	98
20	97
30	90

Table A2.5 B

Tables A2.5 A, B: Recovered activity for 20 mg/g imm-*TsRTA*-EP403/S after 4 hours incubation time under agitation at 37 °C, with different percentages of (A) EtOAc and (B) toluene.

Stability in toluene of 5 mg/g imm-*LbTDC* -EP400/SS

Toluene (%)	Recovered activity (%)
10	49
20	52
30	49

Tables A2.6: Recovered activity for 5 mg/g imm-*LbTDC*-EP400/SS after 4 hours incubation time under agitation at 37 °C, with different percentages of toluene.

It was anticipated that ethyl acetate, despite representing a greener alternative, being a much more polar solvent than toluene and partially soluble in water, would have a greater impact on enzyme activity. This is because ethyl acetate can strip water molecules away from the protein surface, potentially leading to the denaturation of the protein

structure. Thus, for the selection of the organic solvent to be used in the segmented continuous flow, toluene remained the chosen option.

Batch enzyme biotransformations

The experimental setup for the batch biotransformation involved the use of the immobilized transaminase and alcohol dehydrogenase to study the conversion of dopamine to hydroxytyrosol, as well as the conversion of tyramine and 2-phenylethylamine to tyrosol and 2-phenylethanol, respectively.

The selection of tyramine and 2-phenylethylamine as substrates for the batch biotransformation optimization phase aimed to test the enzymatic cascade using compounds with a chemical structure similar to dopamine, while avoiding the formation of the highly reactive intermediate, DOPAL. This experimental design allowed for the evaluation of the efficiency and selectivity of the biocatalysts in a controlled environment before moving on to the targeted substrate.

To investigate the performance of the immobilized *TsRTA* in batch with tyramine and 2-phenylethylamine, a biphasic batch biotransformation was conducted (Figure A2.3). The experiment was carried out with 20 mM substrate, 40 mM pyruvate (2 eq.) as amino acceptor, 2 mg/mL of *TsRTA* (50 mg of EP400/SS with protein loading 20 mg/g), for a total volume of 0.5 mL. Toluene, for the organic phase, was also added at 20% v/v.

The reactions were monitored up to 24 hours by thin-layer chromatography (TLC) analyzing both the aqueous and organic phases. The TLC solvent systems used were *n*-butanol/acetic acid/water in a ratio 7:2:1 or hexane/ethyl acetate in a ratio 7:3.

Ninhydrin was used as the revealing agent, which allowed for the detection of alanine formation and substrate depletion in the aqueous phase. However, no aldehyde formation was detected under UV or spotting the TLC with iodine. During the analysis, the standard for 4-hydroxy-phenylacetaldehyde, the corresponding product of tyramine, was not available, while the standard for 2-phenylacetaldehyde, the corresponding product of 2-phenylethylamine, was.

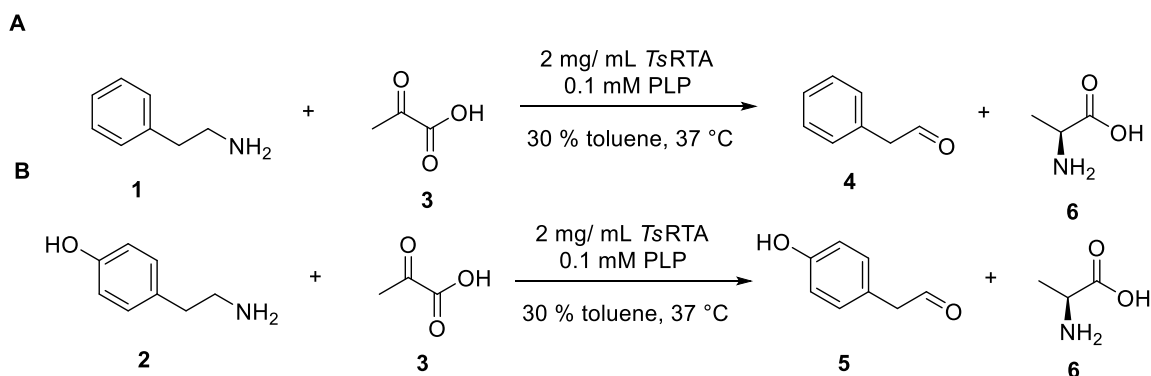


Figure A2.3: Schematic transamination reactions for the conversion of 2-phenylethylamine (**1**) and tyramine (**2**) into 2-phenylacetaldehyde (**4**) and 4-hydroxy-phenylacetaldehyde (**5**). The amino acceptor used was pyruvic acid (**3**), which was transformed into alanine (**6**). The reactions were monitored at 4 and 24 hours

To monitor the transamination reaction from dopamine, the biotransformation setup was modified to shift even more the equilibrium towards DOPAL formation, using 5 mM substrate, 50 equivalents of amino acceptor (pyruvate), 0.1 mM PLP, 2.5 mM ascorbic acid, and 2 mg/mL TsRTA for a final volume of 3 mL in a glass screw-top vial.

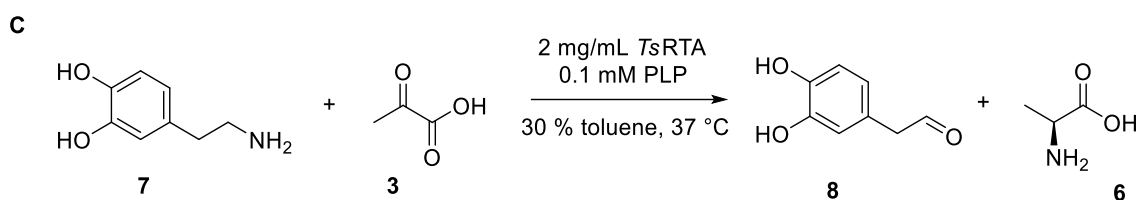


Figure A2.4: Schematic transamination reactions for the conversion of dopamine (**7**) to DOPAL (**8**). The amino acceptor used was pyruvic acid (**3**), which was transformed into alanine (**6**).

Also in this case, the detection of alanine formation and substrate depletion in the aqueous phase was observed on TLC, but no aldehyde product could be identified. An attempt was made to use FMOC derivatization of alanine to estimate the conversion of the starting material to the product after 24 hours of biotransformations. However, the results were not conducted in duplicate and did not display a logical or consistent trend.

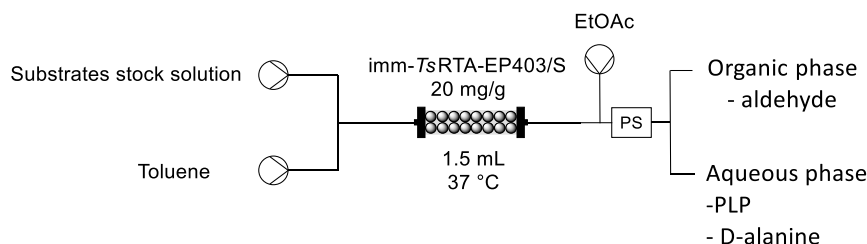
It is possible that the lack of observation of the aldehyde product or of the corresponding by-products, resulting from the condensation of the starting material with DOPAL, was due to the stickiness of the compounds on the resin.

Unfortunately, it was observed that the immobilized TsRTA was almost completely deactivated after overnight incubation with the reaction solution or with a solution of the product (10 mM phenylacetaldehyde in buffer). This raised concerns in terms of the immobilized biocatalyst reusability.

Flow multi-enzyme biotransformations

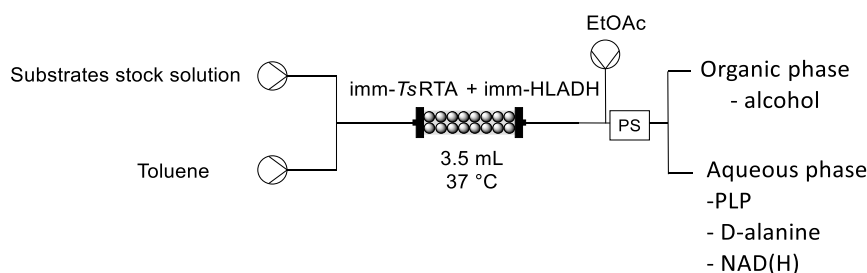
The implementation of the transamination reaction in a continuous flow system was expected to improve the outcome of the biotransformation compared to the batch mode. In fact, in a continuous flow setup, the product would be effectively stripped from the support in the reactor, with a favorable impact on the lifetime of the immobilized biocatalyst. With this consideration in mind, a preliminary attempt was made to carry out the transamination reaction of dopamine to the corresponding aldehyde, DOPAL, in the flow system shown in Scheme A2.1. Unfortunately, the results did not differ from the batch biotransformation, where alanine formation could be detected along with

substrate depletion, but no traces of the product were found in the organic phase. The immobilized biocatalyst thou retained almost all the activity after 4 hours of reaction. To achieve a minimum volume of organic phase that the phase separator (PS) was able to separate, an inlet with EtOAc was connected downstream of the packed-bed reactor (PBR). To pump the substrate solution (20 mM dopamine, 40 mM pyruvate, 0.1 mM PLP, 2.5 mM ascorbic acid in 100 mM phosphate buffer, pH 8) and the organic phase (30 % v/v), achieving a residence time of 30 minutes in the PRB, HPLC pumps were used to generate a flow rate of 0.05 mL/min.



Scheme A2.1: Continuous flow system for the transamination reaction catalysed by *TsRTA*, to convert dopamine into DOPAL. The segmented flow was created by combining aqueous phase and toluene through a T-shaped tube in a ratio of 70:30. Substrate stock solution: 20 mM dopamine, 40 mM pyruvate, 0.1 mM PLP, 2.5 mM ascorbic acid in 100 mM phosphate buffer, pH 8. PS: phase separator.

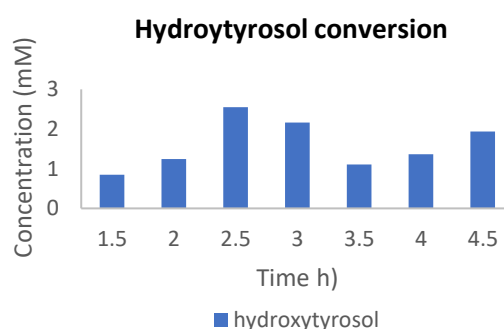
Another attempt, with optimized conditions, was made using the less challenging substrate 2-phenylethylamine, on a smaller scale of 5 mM. The equivalents of amino acceptor were increased from 2 to 10. In a 3.5 mL PBR, 2.25 g of resin were packed, mixing together *TsRTA* and *HLADH* in a mass ratio (mg/mg) of 1:8, corresponding to a units of activity ratio of 1:1.5 (Scheme A2.2). The resin time was kept at 30 minutes. In this case, the conversion to 2-phenylethanol was complete, and the final product was recovered in the organic phase.



Scheme A2.2: Continuous flow system for the bienzymatic reaction catalysed by *TsRTA* and *HLADH*, to convert 2-phenylethylamine into 2-phenylethanol. The segmented flow was created by combining aqueous phase and toluene through a T-shaped tube in a ratio of 70:30. Substrate stock solution: 5 mM substrate, 50 mM pyruvate, 0.1 mM PLP, 5 mM NADH in 100 mM phosphate buffer, pH 8. PS: phase separator.

The rationale behind housing both immobilized biocatalysts in one reactor followed different reasons. It aimed to readily convert the reactive intermediate, thereby streamlining the reaction pathway and pushing the transamination reaction equilibrium in favour of the product, improving overall reaction efficiency. Moreover, this approach could also mitigate the reactivity of the aldehyde, which might otherwise affect the substrate/product itself, the enzyme, or the resin, turning it into the corresponding alcohol.

With a similar setup, mimicking the conditions reported above, substituting dopamine for 2-phenylethylamine, and adding the final product hydroxytyrosol was finally detected in the HPLC. However, it was not found, as anticipated, in the organic phase, but rather in the water phase. In fact, the LogP value of hydroxytyrosol is 0.13, according to ALOGPS. This value, which is close to zero, indicates the relative solubility of the compound in both water and non-polar phases. While monitoring the conversion to hydroxytyrosol and the consumption of the starting material, dopamine, fluctuations were observed across the seven cycles of 30-minute fractions that were collected in flow. This could indicate that equilibrium within the reactor was not achieved although this was unexpected, as equilibrium has typically been assessed after the third fraction in similar setups.

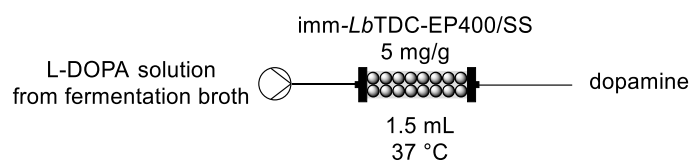


Graph A2.1: Conversions of hydroxytyrosol in continuous flow with dopamine as starting material. The transamination and the reduction were realized in the same PBR with the conditions described in Scheme A2.2.

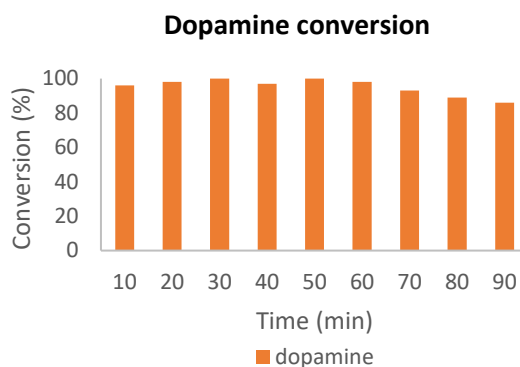
Despite various attempts to scale the dopamine concentration to 10 mM, the conversion of the product consistently remained within the range of 1 to 2 mM. The experiments were not further continued with the multi-enzymatic cascade in flow.

Instead, a flow reaction was set up solely for the decarboxylation of L-dopa, produced from the bioreactor in minimal medium. A 1.5 mL packed-bed reactor (PBR) containing 5 mg/g imm-LbTDC-EP400/SS was employed (Scheme A2.3), which was able to convert over 85 % of the amino acid starting material to dopamine. This conversion was achieved with a residence time of 10 minutes and was maintained consistently over 10 cycles (Graph A2.2). This result confirmed the feasibility of coupling the bioreactor L-DOPA solution, obtained as described in Chapter 4, with the hydroxytyrosol cascade. Notably, the pH of the L-DOPA solution did not require adjustment from the pH in the bioreactor

to be fed into the PBR with *LbTDC*. This is an aspect that, on the contrary, would need to be addressed with a NaOH feed for the connection between the decarboxylation step, performed at pH 5.5, and the transamination step, performed at pH 8.



Scheme A2.3: Continuous flow system for the decarboxylation reaction of L-DOPA with *LbTDC*. The flow rate was set at 0.15 mL/min to achieve a residence time of 10 minutes. The L-DOPA solution, consisting of 6 mM L-DOPA at pH 5.6, was obtained from the fermentation broth after centrifugation and filtration of the bioreactor fermentation medium. Additionally, 0.1 mM PLP and 0.45 g/L ascorbic acid were added to the solution.



Graph A2.2: Conversions of dopamine in continuous flow from L-DOPA, obtained *via* bacterial fermentation in bioreactor.

Conclusion

In conclusion, the performance of the multi-enzymatic cascade in the hydroxytyrosol project did not meet expectations and could not be achieved at the same level of productivity as reported in existing literature. This outcome, although disappointing, should not overshadow the several efforts spent for advancing the process. Tackling the modular design of the cascade, the introduction of novel biocatalyst has been attempted, in regards to the use of *LbTDC* and *TsRTA*. Moreover, the concept of feeding the cascade with L-DOPA and in-line producing dopamine, which is prone to oxidation at the pH 8 required for the transamination step, emerged as a beneficial strategy for both sustainability and cost-effectiveness of the process. Importantly, L-dopa can be fermented from the ubiquitous and bioavailable starting material glucose, making it a sustainable feed for the antioxidant cascade production. The inclusion of *LbTDC* as an additional module to the cascade could further enhance this approach.

Bibliography

- Abrahamson, M. J., Vázquez-Figueroa, E., Woodall, N. B., Moore, J. C., & Bommarius, A. S. (2012). Development of an Amine Dehydrogenase for Synthesis of Chiral Amines. *Angewandte Chemie International Edition*, 51(16), 3969–3972. <https://doi.org/10.1002/anie.201107813>
- Abrahamson, M. J., Wong, J. W., & Bommarius, A. S. (2013). The Evolution of an Amine Dehydrogenase Biocatalyst for the Asymmetric Production of Chiral Amines. *Advanced Synthesis & Catalysis*, 355(9), 1780–1786. <https://doi.org/10.1002/adsc.201201030>
- Alcántara, A. R., Domínguez de María, P., Littlechild, J. A., Schürmann, M., Sheldon, R. A., & Wohlgemuth, R. (2022). Biocatalysis as Key to Sustainable Industrial Chemistry. *ChemSusChem*, 15(9). <https://doi.org/10.1002/cssc.202102709>
- Almud, J. J., Oliveira, M. A., Kern, A. D., Grishin, N. V., Phillips, M. A., & Hackert, M. L. (2000). Crystal structure of human ornithine decarboxylase at 2.1 Å resolution: structural insights to antizyme binding. *Journal of Molecular Biology*, 295(1), 7–16. <https://doi.org/10.1006/jmbi.1999.3331>
- Andréll, J., Hicks, M. G., Palmer, T., Carpenter, E. P., Iwata, S., & Maher, M. J. (2009). Crystal Structure of the Acid-Induced Arginine Decarboxylase from *Escherichia coli* : Reversible Decamer Assembly Controls Enzyme Activity. *Biochemistry*, 48(18), 3915–3927. <https://doi.org/10.1021/bi900075d>
- Anwar, S., Mohammad, T., Shamsi, A., Queen, A., Parveen, S., Luqman, S., Hasan, G. M., Alamry, K. A., Azum, N., Asiri, A. M., & Hassan, M. I. (2020). Discovery of hordenine as a potential inhibitor of pyruvate dehydrogenase kinase 3: Implication in lung cancer therapy. *Biomedicines*, 8(5), 32–228.
- Asano, Y., Nakazawa, A., & Endo, K. (1987). Novel phenylalanine dehydrogenases from *Sporosarcina ureae* and *Bacillus sphaericus*. Purification and characterization. *The Journal of Biological Chemistry*, 262(21), 10346–10354. <http://www.ncbi.nlm.nih.gov/pubmed/3112142>
- Báez, J. L., Bolívar, F., & Gosset, G. (2001). Determination of 3-deoxy-D-*arabino*-heptulosonate 7-phosphate productivity and yield from glucose in *Escherichia coli* devoid of the glucose phosphotransferase transport system. *Biotechnology and Bioengineering*, 73(6), 530–535. <https://doi.org/10.1002/bit.1088>
- Bai, Z., Sun, X., Yu, X., & Li, L. (2019). Chitosan Microbeads as Supporter for *Pseudomonas putida* with Surface Displayed Laccases for Decolorization of Synthetic Dyes. *Applied Sciences*, 9(1), 138. <https://doi.org/10.3390/app9010138>
- Baker, P. J., Turnbull, A. P., Sedelnikova, S. E., Stillman, T. J., & Rice, D. W. (1995). A role for quaternary structure in the substrate specificity of leucine dehydrogenase. *Structure*, 3(7), 693–705. [https://doi.org/10.1016/S0969-2126\(01\)00204-0](https://doi.org/10.1016/S0969-2126(01)00204-0)

- Barwell, C. J., Basma, A. N., Lafi, M. A. K., & Leake, L. D. (2011). Deamination of hordenine by monoamine oxidase and its action on vasa deferentia of the rat. *Journal of Pharmacy and Pharmacology*, *41*(6), 421–423. <https://doi.org/10.1111/j.2042-7158.1989.tb06492.x>
- Bell, E. L., Finnigan, W., France, S. P., Green, A. P., Hayes, M. A., Hepworth, L. J., Lovelock, S. L., Niikura, H., Osuna, S., Romero, E., Ryan, K. S., Turner, N. J., & Flitsch, S. L. (2021). Biocatalysis. *Nature Reviews Methods Primers*, *1*(1), 46. <https://doi.org/10.1038/s43586-021-00044-z>
- Benítez-Mateos, A. I., Roura Padrosa, D., & Paradisi, F. (2022). Multistep enzyme cascades as a route towards green and sustainable pharmaceutical syntheses. *Nature Chemistry*, *14*(5), 489–499. <https://doi.org/10.1038/s41557-022-00931-2>
- Bennett, M., Ducrot, L., Vergne-Vaxelaire, C., & Grogan, G. (2022). Structure and Mutation of the Native Amine Dehydrogenase MATOUAmDH2. *ChemBioChem*, *23*(10). <https://doi.org/10.1002/cbic.202200136>
- Berridge, M. V., Herst, P. M., & Tan, A. S. (2005). *Tetrazolium dyes as tools in cell biology: New insights into their cellular reduction* (pp. 127–152). [https://doi.org/10.1016/S1387-2656\(05\)11004-7](https://doi.org/10.1016/S1387-2656(05)11004-7)
- Bertelli, M., Kiani, A. K., Paolacci, S., Manara, E., Kurti, D., Dhuli, K., Bushati, V., Miertus, J., Pangallo, D., Baglivo, M., Beccari, T., & Michelini, S. (2020). Hydroxytyrosol: A natural compound with promising pharmacological activities. *Journal of Biotechnology*, *309*, 29–33. <https://doi.org/10.1016/j.jbiotec.2019.12.016>
- Bhatia, S. K., Kim, Y. H., Kim, H. J., Seo, H.-M., Kim, J.-H., Song, H.-S., Sathiyarayanan, G., Park, S.-H., Park, K., & Yang, Y.-H. (2015). Biotransformation of lysine into cadaverine using barium alginate-immobilized Escherichia coli overexpressing CadA. *Bioprocess and Biosystems Engineering*, *38*(12), 2315–2322. <https://doi.org/10.1007/s00449-015-1465-9>
- Bloch, D. N., Sandre, M., Ben Zichri, S., Masato, A., Kolusheva, S., Bubacco, L., & Jelinek, R. (2023). Scavenging neurotoxic aldehydes using lysine carbon dots. *Nanoscale Advances*, *5*(5), 1356–1367. <https://doi.org/10.1039/D2NA00804A>
- Böhmer, W., Knaus, T., & Mutti, F. G. (2018a). Hydrogen-Borrowing Alcohol Bioamination with Coimmobilized Dehydrogenases. *ChemCatChem*, *10*(4), 731–735. <https://doi.org/10.1002/cctc.201701366>
- Böhmer, W., Knaus, T., & Mutti, F. G. (2018b). Hydrogen-Borrowing Alcohol Bioamination with Coimmobilized Dehydrogenases. *ChemCatChem*, *10*(4), 731–735. <https://doi.org/10.1002/cctc.201701366>
- Cai, R.-F., Liu, L., Chen, F.-F., Li, A., Xu, J.-H., & Zheng, G.-W. (2020). Reductive Amination of Biobased Levulinic Acid to Unnatural Chiral γ -Amino Acid Using an Engineered Amine Dehydrogenase. *ACS Sustainable Chemistry & Engineering*, *8*(46), 17054–17061. <https://doi.org/10.1021/acssuschemeng.0c04647>
- Caparco, A. A., Bommarius, B. R., Bommarius, A. S., & Champion, J. A. (2020). Protein-inorganic calcium-phosphate supraparticles as a robust platform for enzyme co-immobilization. *Biotechnology and Bioengineering*, *117*(7), 1979–1989. <https://doi.org/10.1002/bit.27348>

- Caparco, A. A., Pelletier, E., Petit, J. L., Jouenne, A., Bommarius, B. R., Berardinis, V., Zaparucha, A., Champion, J. A., Bommarius, A. S., & Vergne-Vaxelaire, C. (2020). Metagenomic Mining for Amine Dehydrogenase Discovery. *Advanced Synthesis & Catalysis*, *362*(12), 2427–2436. <https://doi.org/10.1002/adsc.202000094>
- Capitani, G. (2003). Crystal structure and functional analysis of Escherichia coli glutamate decarboxylase. *The EMBO Journal*, *22*(16), 4027–4037. <https://doi.org/10.1093/emboj/cdg403>
- Ceroli, L., Planchestainer, M., Cassidy, J., Tessaro, D., & Paradisi, F. (2015). Characterization of a novel amine transaminase from Halomonas elongata. *Journal of Molecular Catalysis B: Enzymatic*, *120*, 141–150. <https://doi.org/10.1016/j.molcatb.2015.07.009>
- Chen, W., Yao, J., Meng, J., Han, W., Tao, Y., Chen, Y., Guo, Y., Shi, G., He, Y., Jin, J.-M., & Tang, S.-Y. (2019). Promiscuous enzymatic activity-aided multiple-pathway network design for metabolic flux rearrangement in hydroxytyrosol biosynthesis. *Nature Communications*, *10*(1), 960. <https://doi.org/10.1038/s41467-019-08781-2>
- Claes, L., Janssen, M., & De Vos, D. E. (2019). Organocatalytic Decarboxylation of Amino Acids as a Route to Bio-based Amines and Amides. *ChemCatChem*, *11*(17), 4297–4306. <https://doi.org/10.1002/cctc.201900800>
- Contente, M. L., & Paradisi, F. (2018). Self-sustaining closed-loop multienzyme-mediated conversion of amines into alcohols in continuous reactions. *Nature Catalysis*, *1*(6), 452–459. <https://doi.org/10.1038/s41929-018-0082-9>
- Cosenza, V. A., Navarro, D. A., & Stortz, C. A. (2011). Usage of α -picoline borane for the reductive amination of carbohydrates. *Arkivoc*, *2011*(7), 182–194. <https://doi.org/10.3998/ark.5550190.0012.716>
- Coyle, J. P., Johnson, C., Jensen, J., Farcas, M., Derk, R., Stueckle, T. A., Kornberg, T. G., Rojanasakul, Y., & Rojanasakul, L. W. (2023). Variation in pentose phosphate pathway-associated metabolism dictates cytotoxicity outcomes determined by tetrazolium reduction assays. *Scientific Reports*, *13*(1), 8220. <https://doi.org/10.1038/s41598-023-35310-5>
- DiCosimo, R., McAuliffe, J., Poulouse, A. J., & Bohlmann, G. (2013). Industrial use of immobilized enzymes. *Chemical Society Reviews*, *42*(15), 6437. <https://doi.org/10.1039/c3cs35506c>
- Ducrot, L., Bennett, M., André-Leroux, G., Elisée, E., Marynberg, S., Fossey-Jouenne, A., Zaparucha, A., Grogan, G., & Vergne-Vaxelaire, C. (2022). Expanding the Substrate Scope of Native Amine Dehydrogenases through *In Silico* Structural Exploration and Targeted Protein Engineering. *ChemCatChem*, *14*(22). <https://doi.org/10.1002/cctc.202200880>
- Ducrot, L., Bennett, M., Caparco, A. A., Champion, J. A., Bommarius, A. S., Zaparucha, A., Grogan, G., & Vergne-Vaxelaire, C. (2021). Biocatalytic Reductive Amination by Native Amine Dehydrogenases to Access Short Chiral Alkyl Amines and Amino Alcohols. *Frontiers in Catalysis*, *1*. <https://doi.org/10.3389/fctls.2021.781284>
- Eliot, A. C., & Kirsch, J. F. (2004). Pyridoxal Phosphate Enzymes: Mechanistic, Structural, and Evolutionary Considerations. *Annual Review of Biochemistry*, *73*(1), 383–415. <https://doi.org/10.1146/annurev.biochem.73.011303.074021>

- Eller, K., Henkes, E., Rossbacher, R., & Höke, H. (2000). Amines, Aliphatic. In *Ullmann's Encyclopedia of Industrial Chemistry*. Wiley-VCH Verlag GmbH & Co. KGaA. https://doi.org/10.1002/14356007.a02_001
- Escalante, A., Calderón, R., Valdivia, A., de Anda, R., Hernández, G., Ramírez, O. T., Gosset, G., & Bolívar, F. (2010). Metabolic engineering for the production of shikimic acid in an evolved *Escherichia coli* strain lacking the phosphoenolpyruvate: carbohydrate phosphotransferase system. *Microbial Cell Factories*, 9(1), 21. <https://doi.org/10.1186/1475-2859-9-21>
- Foor, F., Morin, N., & Bostian, K. A. (1993). Production of L-dihydroxyphenylalanine in *Escherichia coli* with the tyrosine phenol-lyase gene cloned from *Erwinia herbicola*. *Applied and Environmental Microbiology*, 59(9), 3070–3075. <https://doi.org/10.1128/aem.59.9.3070-3075.1993>
- Fordjour, E., Adipah, F. K., Zhou, S., Du, G., & Zhou, J. (2019). Metabolic engineering of *Escherichia coli* BL21 (DE3) for de novo production of l-DOPA from d-glucose. *Microbial Cell Factories*, 18(1). <https://doi.org/10.1186/s12934-019-1122-0>
- Franklin, R. D., Whitley, J. A., Caparco, A. A., Bommarius, B. R., Champion, J. A., & Bommarius, A. S. (2021). Continuous production of a chiral amine in a packed bed reactor with co-immobilized amine dehydrogenase and formate dehydrogenase. *Chemical Engineering Journal*, 407, 127065. <https://doi.org/10.1016/j.cej.2020.127065>
- Froidevaux, V., Negrell, C., Caillol, S., Pascault, J.-P., & Boutevin, B. (2016). Biobased Amines: From Synthesis to Polymers; Present and Future. *Chemical Reviews*, 116(22), 14181–14224. <https://doi.org/10.1021/acs.chemrev.6b00486>
- Garg, R. P., Ma, Y., Hoyt, J. C., & Parry, R. J. (2002a). Molecular characterization and analysis of the biosynthetic gene cluster for the azoxy antibiotic valanimycin. *Molecular Microbiology*, 46(2), 505–517. <https://doi.org/10.1046/j.1365-2958.2002.03169.x>
- Garg, R. P., Ma, Y., Hoyt, J. C., & Parry, R. J. (2002b). Molecular characterization and analysis of the biosynthetic gene cluster for the azoxy antibiotic valanimycin. *Molecular Microbiology*, 46(2), 505–517. <https://doi.org/10.1046/j.1365-2958.2002.03169.x>
- Ghislieri, D., & Turner, N. J. (2014). Biocatalytic Approaches to the Synthesis of Enantiomerically Pure Chiral Amines. *Topics in Catalysis*, 57(5), 284–300. <https://doi.org/10.1007/s11244-013-0184-1>
- Gianolio, S., Roura Padrosa, D., & Paradisi, F. (2022). Combined chemoenzymatic strategy for sustainable continuous synthesis of the natural product hordenine. *Green Chemistry*, 24(21), 8434–8440. <https://doi.org/10.1039/D2GC02767D>
- Giardina, G., Montioli, R., Gianni, S., Cellini, B., Paiardini, A., Voltattorni, C. B., & Cutruzzolà, F. (2011). Open conformation of human DOPA decarboxylase reveals the mechanism of PLP addition to Group II decarboxylases. *Proceedings of the National Academy of Sciences*, 108(51), 20514–20519. <https://doi.org/10.1073/pnas.1111456108>
- Gong, X., Tao, J., Wang, Y., Wu, J., An, J., Meng, J., Wang, X., Chen, Y., & Zou, J. (2021). Total barley maiya alkaloids inhibit prolactin secretion by acting on dopamine D2 receptor and protein kinase A targets. *Journal of Ethnopharmacology*, 273, 113994. <https://doi.org/10.1016/j.jep.2021.113994>

- Gosset, G., Yong-Xiao, J., & Berry, A. (1996). A direct comparison of approaches for increasing carbon flow to aromatic biosynthesis in *Escherichia coli*. *Journal of Industrial Microbiology*, *17*(1), 47–52. <https://doi.org/10.1007/BF01570148>
- Guisán, JoséM. (1988). Aldehyde-agarose gels as activated supports for immobilization-stabilization of enzymes. *Enzyme and Microbial Technology*, *10*(6), 375–382. [https://doi.org/10.1016/0141-0229\(88\)90018-X](https://doi.org/10.1016/0141-0229(88)90018-X)
- Guo, K., Ji, C., & Li, L. (2007). Stable-Isotope Dimethylation Labeling Combined with LC-ESI MS for Quantification of Amine-Containing Metabolites in Biological Samples. *Analytical Chemistry*, *79*(22), 8631–8638. <https://doi.org/10.1021/ac0704356>
- Guo, Z., Yan, N., & Lapkin, A. A. (2019). Towards circular economy: integration of bio-waste into chemical supply chain. *Current Opinion in Chemical Engineering*, *26*, 148–156. <https://doi.org/10.1016/j.coche.2019.09.010>
- Gupte, A. P., Basaglia, M., Casella, S., & Favaro, L. (2022). Rice waste streams as a promising source of biofuels: feedstocks, biotechnologies and future perspectives. *Renewable and Sustainable Energy Reviews*, *167*, 112673. <https://doi.org/10.1016/j.rser.2022.112673>
- Gut, H., Pennacchietti, E., John, R. A., Bossa, F., Capitani, G., De Biase, D., & Grütter, M. G. (2006). *Escherichia coli* acid resistance: pH-sensing, activation by chloride and autoinhibition in GadB. *The EMBO Journal*, *25*(11), 2643–2651. <https://doi.org/10.1038/sj.emboj.7601107>
- H. Orrego, A., Romero-Fernández, M., Millán-Linares, M., Yust, M., Guisán, J., & Rocha-Martin, J. (2018). Stabilization of Enzymes by Multipoint Covalent Attachment on Aldehyde-Supports: 2-Picoline Borane as an Alternative Reducing Agent. *Catalysts*, *8*(8), 333. <https://doi.org/10.3390/catal8080333>
- Hamid, M. H. S. A., Slatford, P. A., & Williams, J. M. J. (2007). Borrowing Hydrogen in the Activation of Alcohols. *Advanced Synthesis & Catalysis*, *349*(10), 1555–1575. <https://doi.org/10.1002/adsc.200600638>
- Hapke, H. J., & Strathmann, W. (1995). [Pharmacological effects of hordenine]. *DTW. Deutsche Tierärztliche Wochenschrift*, *102*(6), 228–232. <http://www.ncbi.nlm.nih.gov/pubmed/8582256>
- Harper, B. A., Barbut, S., Lim, L.-T., & Marcone, M. F. (2014). Effect of Various Gelling Cations on the Physical Properties of “Wet” Alginate Films. *Journal of Food Science*, *79*(4), E562–E567. <https://doi.org/10.1111/1750-3841.12376>
- Heckmann, C. M., Gourlay, L. J., Dominguez, B., & Paradisi, F. (2020). An (R)-Selective Transaminase From *Thermomyces stellatus*: Stabilizing the Tetrameric Form. *Frontiers in Bioengineering and Biotechnology*, *8*. <https://doi.org/10.3389/fbioe.2020.00707>
- Heffter, A. (1898). Ueber Pellote. *Archiv Für Experimentelle Pathologie Und Pharmakologie*, *40*(5–6), 385–429. <https://doi.org/10.1007/BF01825267>
- Heydari, M., Ohshima, T., Nunoura-Kominato, N., & Sakuraba, H. (2004). Highly Stable Lysine 6-Dehydrogenase from the Thermophile *Geobacillus stearothermophilus* Isolated from a Japanese Hot Spring: Characterization, Gene Cloning

- and Sequencing, and Expression. *Applied and Environmental Microbiology*, 70(2), 937–942. <https://doi.org/10.1128/AEM.70.2.937-942.2004>
- Holbrook, O. T., Molligoda, B., Bushell, K. N., & Gobrogge, K. L. (2022). Behavioral consequences of the downstream products of ethanol metabolism involved in alcohol use disorder. *Neuroscience & Biobehavioral Reviews*, 133, 104501. <https://doi.org/10.1016/j.neubiorev.2021.12.024>
- Houwman, J. A., Knaus, T., Costa, M., & Mutti, F. G. (2019). Efficient synthesis of enantiopure amines from alcohols using resting *E. coli* cells and ammonia. *Green Chemistry*, 21(14), 3846–3857. <https://doi.org/10.1039/C9GC01059A>
- Huang, J., Mei, L., Wu, H., & Lin, D. (2007). Biosynthesis of γ -aminobutyric acid (GABA) using immobilized whole cells of *Lactobacillus brevis*. *World Journal of Microbiology and Biotechnology*, 23(6), 865–871. <https://doi.org/10.1007/s11274-006-9311-5>
- Huang, R., Chen, H., Zhong, C., Kim, J. E., & Zhang, Y.-H. P. (2016). High-Throughput Screening of Coenzyme Preference Change of Thermophilic 6-Phosphogluconate Dehydrogenase from NADP⁺ to NAD⁺. *Scientific Reports*, 6(1), 32644. <https://doi.org/10.1038/srep32644>
- Hwang, E. T., & Lee, S. (2019). Multienzymatic Cascade Reactions via Enzyme Complex by Immobilization. *ACS Catalysis*, 9(5), 4402–4425. <https://doi.org/10.1021/acscatal.8b04921>
- Jackson, D. M., Ashley, R. L., Brownfield, C. B., Morrison, D. R., & Morrison, R. W. (2015). Rapid Conventional and Microwave-Assisted Decarboxylation of L-Histidine and Other Amino Acids via Organocatalysis with R-Carvone Under Superheated Conditions. *Synthetic Communications*, 45(23), 2691–2700. <https://doi.org/10.1080/00397911.2015.1100745>
- Jansonius, J. N. (1998). Structure, evolution and action of vitamin B6-dependent enzymes. *Current Opinion in Structural Biology*, 8(6), 759–769. [https://doi.org/10.1016/S0959-440X\(98\)80096-1](https://doi.org/10.1016/S0959-440X(98)80096-1)
- Jeon, H., Yoon, S., Ahsan, M., Sung, S., Kim, G.-H., Sundaramoorthy, U., Rhee, S.-K., & Yun, H. (2017). The Kinetic Resolution of Racemic Amines Using a Whole-Cell Biocatalyst Co-Expressing Amine Dehydrogenase and NADH Oxidase. *Catalysts*, 7(9), 251. <https://doi.org/10.3390/catal7090251>
- Jiang, M., Xu, G., Ni, J., Zhang, K., Dong, J., Han, R., & Ni, Y. (2019a). Improving Soluble Expression of Tyrosine Decarboxylase from *Lactobacillus brevis* for Tyramine Synthesis with High Total Turnover Number. *Applied Biochemistry and Biotechnology*, 188(2), 436–449. <https://doi.org/10.1007/s12010-018-2925-x>
- Jiang, M., Xu, G., Ni, J., Zhang, K., Dong, J., Han, R., & Ni, Y. (2019b). Improving Soluble Expression of Tyrosine Decarboxylase from *Lactobacillus brevis* for Tyramine Synthesis with High Total Turnover Number. *Applied Biochemistry and Biotechnology*, 188(2), 436–449. <https://doi.org/10.1007/s12010-018-2925-x>
- Jones, J. A., Collins, S. M., Vernacchio, V. R., Lachance, D. M., & Koffas, M. A. G. (2016). Optimization of naringenin and *p*-coumaric acid hydroxylation using the native *E. coli* hydroxylase complex, HpaBC. *Biotechnology Progress*, 32(1), 21–25. <https://doi.org/10.1002/btpr.2185>

- Khorsand, F., Murphy, C. D., Whitehead, A. J., & Engel, P. C. (2017). Biocatalytic stereoinversion of α -para-bromophenylalanine in a one-pot three-enzyme reaction. *Green Chemistry*, *19*(2), 503–510. <https://doi.org/10.1039/C6GC01922F>
- Kim, Baritugo, Oh, Kang, Jung, Jang, Song, Kim, Lee, Hwang, Park, Park, & Joo. (2019). High-Level Conversion of l-lysine into Cadaverine by *Escherichia coli* Whole Cell Biocatalyst Expressing *Hafnia alvei* l-lysine Decarboxylase. *Polymers*, *11*(7), 1184. <https://doi.org/10.3390/polym11071184>
- Kim, D. I., Chae, T. U., Kim, H. U., Jang, W. D., & Lee, S. Y. (2021). Microbial production of multiple short-chain primary amines via retrobiosynthesis. *Nature Communications*, *12*(1), 173. <https://doi.org/10.1038/s41467-020-20423-6>
- Kim, S.-C., Lee, J.-H., Kim, M.-H., Lee, J.-A., Kim, Y. B., Jung, E., Kim, Y.-S., Lee, J., & Park, D. (2013). Hordenine, a single compound produced during barley germination, inhibits melanogenesis in human melanocytes. *Food Chemistry*, *141*(1), 174–181. <https://doi.org/10.1016/j.foodchem.2013.03.017>
- Knaus, T., Böhmer, W., & Mutti, F. G. (2017). Amine dehydrogenases: efficient biocatalysts for the reductive amination of carbonyl compounds. *Green Chemistry*, *19*(2), 453–463. <https://doi.org/10.1039/C6GC01987K>
- Knowles, W. S. (n.d.). Asymmetric Hydrogenations– The MonsantoL-Dopa Process. In *Asymmetric Catalysis on Industrial Scale* (pp. 21–38). Wiley-VCH Verlag GmbH & Co. KGaA. <https://doi.org/10.1002/3527602151.ch1>
- Komori, H., Nitta, Y., Ueno, H., & Higuchi, Y. (2012). Structural Study Reveals That Ser-354 Determines Substrate Specificity on Human Histidine Decarboxylase. *Journal of Biological Chemistry*, *287*(34), 29175–29183. <https://doi.org/10.1074/jbc.M112.381897>
- Kugler, P. (1979). A gel-sandwich technique for the qualitative and quantitative determination of dehydrogenases in the enzyme histochemistry. *Histochemistry*, *60*(3), 265–293. <https://doi.org/10.1007/BF00500656>
- Kumar, R., Vikramachakravarthi, D., & Pal, P. (2014). Production and purification of glutamic acid: A critical review towards process intensification. *Chemical Engineering and Processing: Process Intensification*, *81*, 59–71. <https://doi.org/10.1016/j.cep.2014.04.012>
- Kurpejović, E., Wendisch, V. F., & Sariyar Akbulut, B. (2021). Tyrosinase-based production of l-DOPA by *Corynebacterium glutamicum*. *Applied Microbiology and Biotechnology*, *105*(24), 9103–9111. <https://doi.org/10.1007/s00253-021-11681-5>
- Lapponi, M. J., Méndez, M. B., Trelles, J. A., & Rivero, C. W. (2022). Cell immobilization strategies for biotransformations. *Current Opinion in Green and Sustainable Chemistry*, *33*, 100565. <https://doi.org/10.1016/j.cogsc.2021.100565>
- Lawrence, S. A. (2004). *Amines: synthesis, properties and applications*. Cambridge University Press.
- Lee, J., Michael, A. J., Martynowski, D., Goldsmith, E. J., & Phillips, M. A. (2007). Phylogenetic Diversity and the Structural Basis of Substrate Specificity in the β/α -Barrel Fold Basic Amino Acid Decarboxylases. *Journal of Biological Chemistry*, *282*(37), 27115–27125. <https://doi.org/10.1074/jbc.M704066200>

- Lee, S. Y., Kim, H. U., Chae, T. U., Cho, J. S., Kim, J. W., Shin, J. H., Kim, D. I., Ko, Y.-S., Jang, W. D., & Jang, Y.-S. (2019). A comprehensive metabolic map for production of bio-based chemicals. *Nature Catalysis*, *2*(1), 18–33. <https://doi.org/10.1038/s41929-018-0212-4>
- Leuchtenberger, W., Huthmacher, K., & Drauz, K. (2005). Biotechnological production of amino acids and derivatives: current status and prospects. *Applied Microbiology and Biotechnology*, *69*(1), 1–8. <https://doi.org/10.1007/s00253-005-0155-y>
- Li, N., Chou, H., & Xu, Y. (2016). Improved cadaverine production from mutant *Klebsiella oxytoca* lysine decarboxylase. *Engineering in Life Sciences*, *16*(3), 299–305. <https://doi.org/10.1002/elsc.201500037>
- Liu, G., Zhou, N., Zhang, M., Li, S., Tian, Q., Chen, J., Chen, B., Wu, Y., & Yao, S. (2010). Hydrophobic solvent induced phase transition extraction to extract drugs from plasma for high performance liquid chromatography–mass spectrometric analysis. *Journal of Chromatography A*, *1217*(3), 243–249. <https://doi.org/10.1016/j.chroma.2009.11.037>
- Liu, J., Pang, B. Q. W., Adams, J. P., Snajdrova, R., & Li, Z. (2017). Coupled Immobilized Amine Dehydrogenase and Glucose Dehydrogenase for Asymmetric Synthesis of Amines by Reductive Amination with Cofactor Recycling. *ChemCatChem*, *9*(3), 425–431. <https://doi.org/10.1002/cctc.201601446>
- Liu, Y., Liu, P., Gao, S., Wang, Z., Luan, P., González-Sabín, J., & Jiang, Y. (2021). Construction of chemoenzymatic cascade reactions for bridging chemocatalysis and Biocatalysis: Principles, strategies and prospective. *Chemical Engineering Journal*, *420*, 127659. <https://doi.org/10.1016/j.cej.2020.127659>
- Ma, J., Wang, S., Huang, X., Geng, P., Wen, C., Zhou, Y., Yu, L., & Wang, X. (2015). Validated UPLC–MS/MS method for determination of hordenine in rat plasma and its application to pharmacokinetic study. *Journal of Pharmaceutical and Biomedical Analysis*, *111*, 131–137. <https://doi.org/10.1016/j.jpba.2015.03.032>
- Mateo, C., Grazú, V., Pessela, B. C. C., Montes, T., Palomo, J. M., Torres, R., López-Gallego, F., Fernández-Lafuente, R., & Guisán, J. M. (2007a). Advances in the design of new epoxy supports for enzyme immobilization–stabilization. *Biochemical Society Transactions*, *35*(6), 1593–1601. <https://doi.org/10.1042/BST0351593>
- Mateo, C., Grazú, V., Pessela, B. C. C., Montes, T., Palomo, J. M., Torres, R., López-Gallego, F., Fernández-Lafuente, R., & Guisán, J. M. (2007b). Advances in the design of new epoxy supports for enzyme immobilization–stabilization. *Biochemical Society Transactions*, *35*(6), 1593–1601. <https://doi.org/10.1042/BST0351593>
- Mayol, O., Bastard, K., Beloti, L., Frese, A., Turkenburg, J. P., Petit, J.-L., Mariage, A., Debard, A., Pellouin, V., Perret, A., de Berardinis, V., Zaparucha, A., Grogan, G., & Vergne-Vaxelaire, C. (2019a). A family of native amine dehydrogenases for the asymmetric reductive amination of ketones. *Nature Catalysis*, *2*(4), 324–333. <https://doi.org/10.1038/s41929-019-0249-z>
- Mayol, O., Bastard, K., Beloti, L., Frese, A., Turkenburg, J. P., Petit, J.-L., Mariage, A., Debard, A., Pellouin, V., Perret, A., de Berardinis, V., Zaparucha, A., Grogan, G., & Vergne-Vaxelaire, C. (2019b). A family of native amine dehydrogenases for the asymmetric reductive amination of ketones. *Nature Catalysis*, *2*(4), 324–333. <https://doi.org/10.1038/s41929-019-0249-z>

- Meyer, E. (1982). Separation of two distinct S-adenosylmethionine dependent N-methyltransferases involved in hordenine biosynthesis in *Hordeum vulgare*. *Plant Cell Reports*, 1(6), 236–239. <https://doi.org/10.1007/BF00272627>
- Mi, J., Liu, S., Du, Y., Qi, H., & Zhang, L. (2022). Cofactor self-sufficient by co-immobilization of pyridoxal 5'-phosphate and lysine decarboxylase for cadaverine production. *Bioresource Technology Reports*, 17, 100939. <https://doi.org/10.1016/j.biteb.2021.100939>
- Montgomery, S. L., Mangas-Sanchez, J., Thompson, M. P., Aleku, G. A., Dominguez, B., & Turner, N. J. (2017). Direct Alkylation of Amines with Primary and Secondary Alcohols through Biocatalytic Hydrogen Borrowing. *Angewandte Chemie*, 129(35), 10627–10630. <https://doi.org/10.1002/ange.201705848>
- Mørch, Ý. A., Donati, I., Strand, B. L., & Skjåk-Bræk, G. (2006). Effect of Ca²⁺, Ba²⁺, and Sr²⁺ on Alginate Microbeads. *Biomacromolecules*, 7(5), 1471–1480. <https://doi.org/10.1021/bm060010d>
- Muñoz, A. J., Hernández-Chávez, G., De Anda, R., Martínez, A., Bolívar, F., & Gosset, G. (2011). Metabolic engineering of *Escherichia coli* for improving l-3,4-dihydroxyphenylalanine (l-DOPA) synthesis from glucose. *Journal of Industrial Microbiology and Biotechnology*, 38(11), 1845–1852. <https://doi.org/10.1007/s10295-011-0973-0>
- Mutti, F. G., & Knaus, T. (2021). Enzymes Applied to the Synthesis of Amines. In *Biocatalysis for Practitioners* (pp. 143–180). Wiley. <https://doi.org/10.1002/9783527824465.ch6>
- Mutti, F. G., Knaus, T., Scrutton, N. S., Breuer, M., & Turner, N. J. (2015). Conversion of alcohols to enantiopure amines through dual-enzyme hydrogen-borrowing cascades. *Science*, 349(6255), 1525–1529. <https://doi.org/10.1126/science.aac9283>
- Nakai, T., Nakagawa, N., Maoka, N., Masui, R., Kuramitsu, S., & Kamiya, N. (2005). Structure of P-protein of the glycine cleavage system: implications for nonketotic hyperglycinemia. *The EMBO Journal*, 24(8), 1523–1536. <https://doi.org/10.1038/sj.emboj.7600632>
- Narisetty, V., Cox, R., Bommareddy, R., Agrawal, D., Ahmad, E., Pant, K. K., Chandel, A. K., Bhatia, S. K., Kumar, D., Binod, P., Gupta, V. K., & Kumar, V. (2022). Valorisation of xylose to renewable fuels and chemicals, an essential step in augmenting the commercial viability of lignocellulosic biorefineries. *Sustainable Energy & Fuels*, 6(1), 29–65. <https://doi.org/10.1039/D1SE00927C>
- Nasri, M. (2017a). *Protein Hydrolysates and Biopeptides* (pp. 109–159). <https://doi.org/10.1016/bs.afnr.2016.10.003>
- Nasri, M. (2017b). *Protein Hydrolysates and Biopeptides* (pp. 109–159). <https://doi.org/10.1016/bs.afnr.2016.10.003>
- Natte, K., Neumann, H., Jagadeesh, R. v., & Beller, M. (2017). Convenient iron-catalyzed reductive aminations without hydrogen for selective synthesis of N-methylamines. *Nature Communications*, 8(1), 1344. <https://doi.org/10.1038/s41467-017-01428-0>
- Nguyen, N. H., Truong-Thi, N.-H., Nguyen, D. T. D., Ching, Y. C., Huynh, N. T., & Nguyen, D. H. (2022). Non-ionic surfactants As co-templates to control the mesopore diameter of hollow mesoporous silica nanoparticles for drug delivery applications. *Colloids and Surfaces A*:

Physicochemical and Engineering Aspects, 655, 130218.
<https://doi.org/10.1016/j.colsurfa.2022.130218>

- Ohta, H., Murakami, Y., Takebe, Y., Murasaki, K., Oshima, K., Yoshihara, H., & Morimura, S. (2020). Ñ-Methyltyramine, a Gastrin-releasing Factor in Beer, and Structurally Related Compounds as Agonists for Human Trace Amine-associated Receptor 1. *Food Science and Technology Research*, 26(2), 313–317.
<https://doi.org/10.3136/fstr.26.313>
- PARADISI, F., COLLINS, S., MAGUIRE, A., & ENGEL, P. (2007). Phenylalanine dehydrogenase mutants: Efficient biocatalysts for synthesis of non-natural phenylalanine derivatives. *Journal of Biotechnology*, 128(2), 408–411. <https://doi.org/10.1016/j.jbiotec.2006.08.008>
- Park, J.-Y., Choi, M.-J., Yu, H., Choi, Y., Park, K.-M., & Chang, P.-S. (2022). Multi-functional behavior of food emulsifier erythorbyl laurate in different colloidal conditions of homogeneous oil-in-water emulsion system. *Colloids and Surfaces A: Physicochemical and Engineering Aspects*, 636, 128127. <https://doi.org/10.1016/j.colsurfa.2021.128127>
- Park, S. H., Soetyono, F., & Kim, H. K. (2017). Cadaverine Production by Using Cross-Linked Enzyme Aggregate of Escherichia coli Lysine Decarboxylase. *Journal of Microbiology and Biotechnology*, 27(2), 289–296. <https://doi.org/10.4014/jmb.1608.08033>
- Patil, M. D., Grogan, G., Bommarius, A., & Yun, H. (2018). Oxidoreductase-Catalyzed Synthesis of Chiral Amines. *ACS Catalysis*, 8(12), 10985–11015.
<https://doi.org/10.1021/acscatal.8b02924>
- Patil, M. D., Yoon, S., Jeon, H., Khobragade, T. P., Sarak, S., Pagar, A. D., Won, Y., & Yun, H. (2019). Kinetic Resolution of Racemic Amines to Enantiopure (S)-amines by a Biocatalytic Cascade Employing Amine Dehydrogenase and Alanine Dehydrogenase. *Catalysts*, 9(7), 600. <https://doi.org/10.3390/catal9070600>
- Payne, J. T., Valentic, T. R., & Smolke, C. D. (2021). Complete biosynthesis of the bisbenzylisoquinoline alkaloids guattegaumerine and berbamunine in yeast. *Proceedings of the National Academy of Sciences*, 118(51). <https://doi.org/10.1073/pnas.2112520118>
- Pelckmans, M., Renders, T., Van de Vyver, S., & Sels, B. F. (2017). Bio-based amines through sustainable heterogeneous catalysis. *Green Chemistry*, 19(22), 5303–5331.
<https://doi.org/10.1039/C7GC02299A>
- Pilkington, R. L., Dallaston, M. A., Savage, G. P., Williams, C. M., & Polyzos, A. (2021). Enone-promoted decarboxylation of *trans*-4-hydroxy-*l*-proline in flow: a side-by-side comparison to batch. *Reaction Chemistry & Engineering*, 6(3), 486–493.
<https://doi.org/10.1039/D0RE00442A>
- Planchestainer, M., Hegarty, E., Heckmann, C. M., Gourlay, L. J., & Paradisi, F. (2019). Widely applicable background depletion step enables transaminase evolution through solid-phase screening. *Chemical Science*, 10(23), 5952–5958. <https://doi.org/10.1039/C8SC05712E>
- Prieto, M. A., & Garcia, J. L. (1994). Molecular characterization of 4-hydroxyphenylacetate 3-hydroxylase of Escherichia coli. A two-protein component enzyme. *Journal of Biological Chemistry*, 269(36), 22823–22829. [https://doi.org/10.1016/S0021-9258\(17\)31719-2](https://doi.org/10.1016/S0021-9258(17)31719-2)

- Pyne, M. E., Kevvai, K., Grewal, P. S., Narcross, L., Choi, B., Bourgeois, L., Dueber, J. E., & Martin, V. J. J. (2020). A yeast platform for high-level synthesis of tetrahydroisoquinoline alkaloids. *Nature Communications*, *11*(1), 3337. <https://doi.org/10.1038/s41467-020-17172-x>
- Quaglia, D., Irwin, J. A., & Paradisi, F. (2012a). Horse Liver Alcohol Dehydrogenase: New Perspectives for an Old Enzyme. *Molecular Biotechnology*, *52*(3), 244–250. <https://doi.org/10.1007/s12033-012-9542-7>
- Quaglia, D., Irwin, J. A., & Paradisi, F. (2012b). Horse Liver Alcohol Dehydrogenase: New Perspectives for an Old Enzyme. *Molecular Biotechnology*, *52*(3), 244–250. <https://doi.org/10.1007/s12033-012-9542-7>
- Ray, S. S., Bonanno, J. B., Rajashankar, K. R., Pinho, M. G., He, G., De Lencastre, H., Tomasz, A., & Burley, S. K. (2002). Cocrystal Structures of Diaminopimelate Decarboxylase. *Structure*, *10*(11), 1499–1508. [https://doi.org/10.1016/S0969-2126\(02\)00880-8](https://doi.org/10.1016/S0969-2126(02)00880-8)
- Reetz, M. T. (2013). Biocatalysis in Organic Chemistry and Biotechnology: Past, Present, and Future. *Journal of the American Chemical Society*, *135*(34), 12480–12496. <https://doi.org/10.1021/ja405051f>
- Roschangar, F., Sheldon, R. A., & Senanayake, C. H. (2015). Overcoming barriers to green chemistry in the pharmaceutical industry – the Green Aspiration Level™ concept. *Green Chemistry*, *17*(2), 752–768. <https://doi.org/10.1039/C4GC01563K>
- Ruhaak, L. R., Steenvoorden, E., Koeleman, C. A. M., Deelder, A. M., & Wuhrer, M. (2010). 2-Picoline-borane: A non-toxic reducing agent for oligosaccharide labeling by reductive amination. *Proteomics*, *10*(12), 2330–2336. <https://doi.org/10.1002/pmic.200900804>
- Sagong, H.-Y., Son, H. F., Kim, S., Kim, Y.-H., Kim, I.-K., & Kim, K.-J. (2016). Crystal Structure and Pyridoxal 5-Phosphate Binding Property of Lysine Decarboxylase from *Selenomonas ruminantium*. *PLOS ONE*, *11*(11), e0166667. <https://doi.org/10.1371/journal.pone.0166667>
- Said, A. A. E., Ali, T. F. S., Attia, E. Z., Ahmed, A.-S. F., Shehata, A. H., Abdelmohsen, U. R., & Fouad, M. A. (2021). Antidepressant potential of *Mesembryanthemum cordifolium* roots assisted by metabolomic analysis and virtual screening. *Natural Product Research*, *35*(23), 5493–5497. <https://doi.org/10.1080/14786419.2020.1788019>
- SANDMEIER, E., HALE, T. I., & CHRISTEN, P. (1994a). Multiple evolutionary origin of pyridoxal-5'-phosphate-dependent amino acid decarboxylases. *European Journal of Biochemistry*, *221*(3), 997–1002. <https://doi.org/10.1111/j.1432-1033.1994.tb18816.x>
- SANDMEIER, E., HALE, T. I., & CHRISTEN, P. (1994b). Multiple evolutionary origin of pyridoxal-5'-phosphate-dependent amino acid decarboxylases. *European Journal of Biochemistry*, *221*(3), 997–1002. <https://doi.org/10.1111/j.1432-1033.1994.tb18816.x>
- Sato, S., Sakamoto, T., Miyazawa, E., & Kikugawa, Y. (2004). One-pot reductive amination of aldehydes and ketones with α -picoline-borane in methanol, in water, and in neat conditions. *Tetrahedron*, *60*(36), 7899–7906. <https://doi.org/10.1016/j.tet.2004.06.045>
- Schoenmakers, H., & Spiegel, L. (2014). Laboratory Distillation and Scale-up. In *Distillation* (pp. 319–339). Elsevier. <https://doi.org/10.1016/B978-0-12-386878-7.00010-3>

- Seah, S. Y. K., Britton, K. L., Rice, D. W., Asano, Y., & Engel, P. C. (2002). Single Amino Acid Substitution in *Bacillus sphaericus* Phenylalanine Dehydrogenase Dramatically Increases Its Discrimination between Phenylalanine and Tyrosine Substrates. *Biochemistry*, *41*(38), 11390–11397. <https://doi.org/10.1021/bi020196a>
- Seah, S. Y. K., Linda Britton, K., Baker, P. J., Rice, D. W., Asano, Y., & Engel, P. C. (1995). Alteration in relative activities of phenylalanine dehydrogenase towards different substrates by site-directed mutagenesis. *FEBS Letters*, *370*(1–2), 93–96. [https://doi.org/10.1016/0014-5793\(95\)00804-I](https://doi.org/10.1016/0014-5793(95)00804-I)
- Sen, K. Y., & Baidurah, S. (2021). Renewable biomass feedstocks for production of sustainable biodegradable polymer. *Current Opinion in Green and Sustainable Chemistry*, *27*, 100412. <https://doi.org/10.1016/j.cogsc.2020.100412>
- Sharma, M., Mangas-Sanchez, J., Turner, N. J., & Grogan, G. (2017). NAD(P)H-Dependent Dehydrogenases for the Asymmetric Reductive Amination of Ketones: Structure, Mechanism, Evolution and Application. *Advanced Synthesis & Catalysis*, *359*(12), 2011–2025. <https://doi.org/10.1002/adsc.201700356>
- Sheldon, R. A., Basso, A., & Brady, D. (2021). New frontiers in enzyme immobilisation: robust biocatalysts for a circular bio-based economy. *Chemical Society Reviews*, *50*(10), 5850–5862. <https://doi.org/10.1039/D1CS00015B>
- Sheldon, R. A., & Brady, D. (2019). Broadening the Scope of Biocatalysis in Sustainable Organic Synthesis. *ChemSusChem*, *12*(13), 2859–2881. <https://doi.org/10.1002/cssc.201900351>
- Sheldon, R. A., & Woodley, J. M. (2018). Role of Biocatalysis in Sustainable Chemistry. *Chemical Reviews*, *118*(2), 801–838. <https://doi.org/10.1021/acs.chemrev.7b00203>
- Sommer, T., Göen, T., Budnik, N., & Pischetsrieder, M. (2020). Absorption, Biokinetics, and Metabolism of the Dopamine D2 Receptor Agonist Hordenine (*N*, *N*-Dimethyltyramine) after Beer Consumption in Humans. *Journal of Agricultural and Food Chemistry*, *68*(7), 1998–2006. <https://doi.org/10.1021/acs.jafc.9b06029>
- Song, W., Chen, X., Wu, J., Xu, J., Zhang, W., Liu, J., Chen, J., & Liu, L. (2020). Biocatalytic derivatization of proteinogenic amino acids for fine chemicals. *Biotechnology Advances*, *40*, 107496. <https://doi.org/10.1016/j.biotechadv.2019.107496>
- Stano, J., Nemeč, P., Weissová, K., Kovács, P., Kákoniová, D., & Lisková, D. (1995). Decarboxylation of l-tyrosine and l-dopa by immobilized cells of *Papaver somniferum*. *Phytochemistry*, *38*(4), 859–860. [https://doi.org/10.1016/0031-9422\(94\)00768-O](https://doi.org/10.1016/0031-9422(94)00768-O)
- Stockert, J. C., Horobin, R. W., Colombo, L. L., & Blázquez-Castro, A. (2018). Tetrazolium salts and formazan products in Cell Biology: Viability assessment, fluorescence imaging, and labeling perspectives. *Acta Histochemica*, *120*(3), 159–167. <https://doi.org/10.1016/j.acthis.2018.02.005>
- Su, Y., Liu, Y., He, D., Hu, G., Wang, H., Ye, B., He, Y., Gao, X., & Liu, D. (2022). Hordenine inhibits neuroinflammation and exerts neuroprotective effects via inhibiting NF-κB and MAPK signaling pathways in vivo and in vitro. *International Immunopharmacology*, *108*, 108694. <https://doi.org/10.1016/j.intimp.2022.108694>

- Surwase, S. N., Patil, S. A., Apine, O. A., & Jadhav, J. P. (2012). Efficient Microbial Conversion of L-Tyrosine to L-DOPA by *Brevundimonas* sp. SGJ. *Applied Biochemistry and Biotechnology*, *167*(5), 1015–1028. <https://doi.org/10.1007/s12010-012-9564-4>
- Tang, Y. Q., & Weng, N. (2013). Salting-out assisted liquid–liquid extraction for bioanalysis. *Bioanalysis*, *5*(12), 1583–1598. <https://doi.org/10.4155/bio.13.117>
- Teng, Y., Scott, E. L., van Zeeland, A. N. T., & Sanders, J. P. M. (2011). The use of L-lysine decarboxylase as a means to separate amino acids by electrodialysis. *Green Chemistry*, *13*(3), 624. <https://doi.org/10.1039/c0gc00611d>
- Thompson, M. P., Derrington, S. R., Heath, R. S., Porter, J. L., Mangas-Sanchez, J., Devine, P. N., Truppo, M. D., & Turner, N. J. (2019). A generic platform for the immobilisation of engineered biocatalysts. *Tetrahedron*, *75*(3), 327–334. <https://doi.org/10.1016/j.tet.2018.12.004>
- Thompson, M. P., & Turner, N. J. (2017a). Two-Enzyme Hydrogen-Borrowing Amination of Alcohols Enabled by a Cofactor-Switched Alcohol Dehydrogenase. *ChemCatChem*, *9*(20), 3833–3836. <https://doi.org/10.1002/cctc.201701092>
- Thompson, M. P., & Turner, N. J. (2017b). Two-Enzyme Hydrogen-Borrowing Amination of Alcohols Enabled by a Cofactor-Switched Alcohol Dehydrogenase. *ChemCatChem*, *9*(20), 3833–3836. <https://doi.org/10.1002/cctc.201701092>
- Tolbert, W. D., Graham, D. E., White, R. H., & Ealick, S. E. (2003). Pyruvoyl-Dependent Arginine Decarboxylase from *Methanococcus jannaschii*. *Structure*, *11*(3), 285–294. [https://doi.org/10.1016/S0969-2126\(03\)00026-1](https://doi.org/10.1016/S0969-2126(03)00026-1)
- Truong, C. C., Mishra, D. K., & Suh, Y. (2023). Recent Catalytic Advances on the Sustainable Production of Primary Furanic Amines from the One-Pot Reductive Amination of 5-Hydroxymethylfurfural. *ChemSusChem*, *16*(1). <https://doi.org/10.1002/cssc.202201846>
- Tseliou, V., Knaus, T., Masman, M. F., Corrado, M. L., & Mutti, F. G. (2019). Generation of amine dehydrogenases with increased catalytic performance and substrate scope from ϵ -deaminating L-Lysine dehydrogenase. *Nature Communications*, *10*(1), 3717. <https://doi.org/10.1038/s41467-019-11509-x>
- Tseliou, V., Knaus, T., Vilím, J., Masman, M. F., & Mutti, F. G. (2020). Kinetic Resolution of Racemic Primary Amines Using *Geobacillus stearothermophilus* Amine Dehydrogenase Variant. *ChemCatChem*, *12*(8), 2184–2188. <https://doi.org/10.1002/cctc.201902085>
- Tsukatani, T., Suenaga, H., Higuchi, T., Akao, T., Ishiyama, M., Ezo, K., & Matsumoto, K. (2008). Colorimetric cell proliferation assay for microorganisms in microtiter plate using water-soluble tetrazolium salts. *Journal of Microbiological Methods*, *75*(1), 109–116. <https://doi.org/10.1016/j.mimet.2008.05.016>
- Viejo, C. G., Villarreal-Lara, R., Torrico, D. D., Rodríguez-Velazco, Y. G., Escobedo-Avellaneda, Z., Ramos-Parra, P. A., Mandal, R., Singh, A. P., Hernández-Brenes, C., & Fuentes, S. (2020). Beer and consumer response using biometrics: Associations assessment of beer compounds and elicited emotions. *Foods*, *9*(6), 821.
- Vitaku, E., Smith, D. T., & Njardarson, J. T. (2014). Analysis of the Structural Diversity, Substitution Patterns, and Frequency of Nitrogen Heterocycles among U.S. FDA Approved

- Pharmaceuticals. *Journal of Medicinal Chemistry*, 57(24), 10257–10274.
<https://doi.org/10.1021/jm501100b>
- Wang, M., Khan, M. A., Mohsin, I., Wicks, J., Ip, A. H., Sumon, K. Z., Dinh, C.-T., Sargent, E. H., Gates, I. D., & Kibria, M. G. (2021). Can sustainable ammonia synthesis pathways compete with fossil-fuel based Haber–Bosch processes? *Energy & Environmental Science*, 14(5), 2535–2548. <https://doi.org/10.1039/D0EE03808C>
- Wang, Q., Xin, Y., Zhang, F., Feng, Z., Fu, J., Luo, L., & Yin, Z. (2011). Enhanced γ -aminobutyric acid-forming activity of recombinant glutamate decarboxylase (gadA) from *Escherichia coli*. *World Journal of Microbiology and Biotechnology*, 27(3), 693–700.
<https://doi.org/10.1007/s11274-010-0508-2>
- Watanabe, Y., Tsuji, Y., Ige, H., Ohsugi, Y., & Ohta, T. (1984). Ruthenium-catalyzed N-alkylation and N-benzoylation of aminoarenes with alcohols. *The Journal of Organic Chemistry*, 49(18), 3359–3363. <https://doi.org/10.1021/jo00192a021>
- Weber, R. E. (1992). Use of ionic and zwitterionic (Tris/BisTris and HEPES) buffers in studies on hemoglobin function. *Journal of Applied Physiology*, 72(4), 1611–1615.
<https://doi.org/10.1152/jappl.1992.72.4.1611>
- Wei, G., Chen, Y., Zhou, N., Lu, Q., Xu, S., Zhang, A., Chen, K., & Ouyang, P. (2022). Chitin biopolymer mediates self-sufficient biocatalyst of pyridoxal 5'-phosphate and L-lysine decarboxylase. *Chemical Engineering Journal*, 427, 132030.
<https://doi.org/10.1016/j.cej.2021.132030>
- Wei, T., Cheng, B. Y., & Liu, J. Z. (2016). Genome engineering *Escherichia coli* for L-DOPA overproduction from glucose. *Scientific Reports*, 6. <https://doi.org/10.1038/srep30080>
- Wieschalka, S., Blombach, B., Bott, M., & Eikmanns, B. J. (2013). Bio-based production of organic acids with *Corynebacterium glutamicum*. *Microbial Biotechnology*, 6(2), 87–102.
<https://doi.org/10.1111/1751-7915.12013>
- Wohlgemuth, R. (2021). Biocatalysis-Key enabling tools from biocatalytic one-step and multi-step reactions to biocatalytic total synthesis. *New Biotechnol*, 60, 113–123.
- Wu, B., Zhang, S., Hong, T., Zhou, Y., Wang, H., Shi, M., Yang, H., Tian, X., Guo, J., Bian, J., Roache, J., Delgado, P., Mo, R., Fridrich, C., Gao, F., & Wang, J. (2020). Merging Biocatalysis, Flow, and Surfactant Chemistry: Innovative Synthesis of an FXI (Factor XI) Inhibitor. *Organic Process Research & Development*, 24(11), 2780–2788.
<https://doi.org/10.1021/acs.oprd.0c00412>
- Wu, P., Li, G., He, Y., Luo, D., Li, L., Guo, J., Ding, P., & Yang, F. (2020). High-efficient and sustainable biodegradation of microcystin-LR using *Sphingopyxis* sp. YF1 immobilized Fe₃O₄@chitosan. *Colloids and Surfaces B: Biointerfaces*, 185, 110633.
<https://doi.org/10.1016/j.colsurfb.2019.110633>
- Ye, L. J., Toh, H. H., Yang, Y., Adams, J. P., Snajdrova, R., & Li, Z. (2015). Engineering of Amine Dehydrogenase for Asymmetric Reductive Amination of Ketone by Evolving *Rhodococcus* Phenylalanine Dehydrogenase. *ACS Catalysis*, 5(2), 1119–1122.
<https://doi.org/10.1021/cs501906r>

- Yoon, S., Patil, M. D., Sarak, S., Jeon, H., Kim, G., Khobragade, T. P., Sung, S., & Yun, H. (2019). Deracemization of Racemic Amines to Enantiopure (R)- and (S)-amines by Biocatalytic Cascade Employing ω -Transaminase and Amine Dehydrogenase. *ChemCatChem*, *11*(7), 1898–1902. <https://doi.org/10.1002/cctc.201900080>
- Yoshitaka Hashitani, B. (1925). On the chemical constituents of malt-rootlets with special reference to Hordenine. *Journal of the College of Agriculture*, *14*, 1–56.
- Zhang, B., Jiang, Y., Li, Z., Wang, F., & Wu, X.-Y. (2020). Recent Progress on Chemical Production From Non-food Renewable Feedstocks Using *Corynebacterium glutamicum*. *Frontiers in Bioengineering and Biotechnology*, *8*. <https://doi.org/10.3389/fbioe.2020.606047>
- Zhang, H., Wei, Y., Lu, Y., Wu, S., Liu, Q., Liu, J., & Jiao, Q. (2016). Three-step biocatalytic reaction using whole cells for efficient production of tyramine from keratin acid hydrolysis wastewater. *Applied Microbiology and Biotechnology*, *100*(4), 1691–1700. <https://doi.org/10.1007/s00253-015-7054-7>
- Zhang, K., & Ni, Y. (2014). Tyrosine decarboxylase from *Lactobacillus brevis*: Soluble expression and characterization. *Protein Expression and Purification*, *94*, 33–39. <https://doi.org/10.1016/j.pep.2013.10.018>
- Zhang, X., Du, L., Zhang, J., Li, C., Zhang, J., & Lv, X. (2021). Hordenine Protects Against Lipopolysaccharide-Induced Acute Lung Injury by Inhibiting Inflammation. *Frontiers in Pharmacology*, *12*, 712232. <https://doi.org/10.3389/fphar.2021.712232>
- Zhao, W., Hu, S., Huang, J., Ke, P., Yao, S., Lei, Y., Mei, L., & Wang, J. (2016). Permeabilization of *Escherichia coli* with ampicillin for a whole cell biocatalyst with enhanced glutamate decarboxylase activity. *Chinese Journal of Chemical Engineering*, *24*(7), 909–913. <https://doi.org/10.1016/j.cjche.2016.02.001>
- Zhou, F., Xu, Y., Nie, Y., & Mu, X. (2022). Substrate-Specific Engineering of Amino Acid Dehydrogenase Superfamily for Synthesis of a Variety of Chiral Amines and Amino Acids. *Catalysts*, *12*(4), 380. <https://doi.org/10.3390/catal12040380>
- Zhou, J.-W., Ruan, L.-Y., Chen, H.-J., Luo, H.-Z., Jiang, H., Wang, J.-S., & Jia, A.-Q. (2019). Inhibition of Quorum Sensing and Virulence in *Serratia marcescens* by Hordenine. *Journal of Agricultural and Food Chemistry*, *67*(3), 784–795. <https://doi.org/10.1021/acs.jafc.8b05922>
- Zhu, H., Xu, G., Zhang, K., Kong, X., Han, R., Zhou, J., & Ni, Y. (2016a). Crystal structure of tyrosine decarboxylase and identification of key residues involved in conformational swing and substrate binding. *Scientific Reports*, *6*(1), 27779. <https://doi.org/10.1038/srep27779>
- Zhu, H., Xu, G., Zhang, K., Kong, X., Han, R., Zhou, J., & Ni, Y. (2016b). Crystal structure of tyrosine decarboxylase and identification of key residues involved in conformational swing and substrate binding. *Scientific Reports*, *6*(1), 27779. <https://doi.org/10.1038/srep27779>
- Zhuang, W., Liu, H., Zhang, Y., He, J., & Wang, P. (2021). Effective asymmetric preparation of (R)-1-[3-(trifluoromethyl)phenyl]ethanol with recombinant *E. coli* whole cells in an aqueous Tween-20/natural deep eutectic solvent solution. *AMB Express*, *11*(1), 118. <https://doi.org/10.1186/s13568-021-01278-6>

Appendix B: NMR spectra

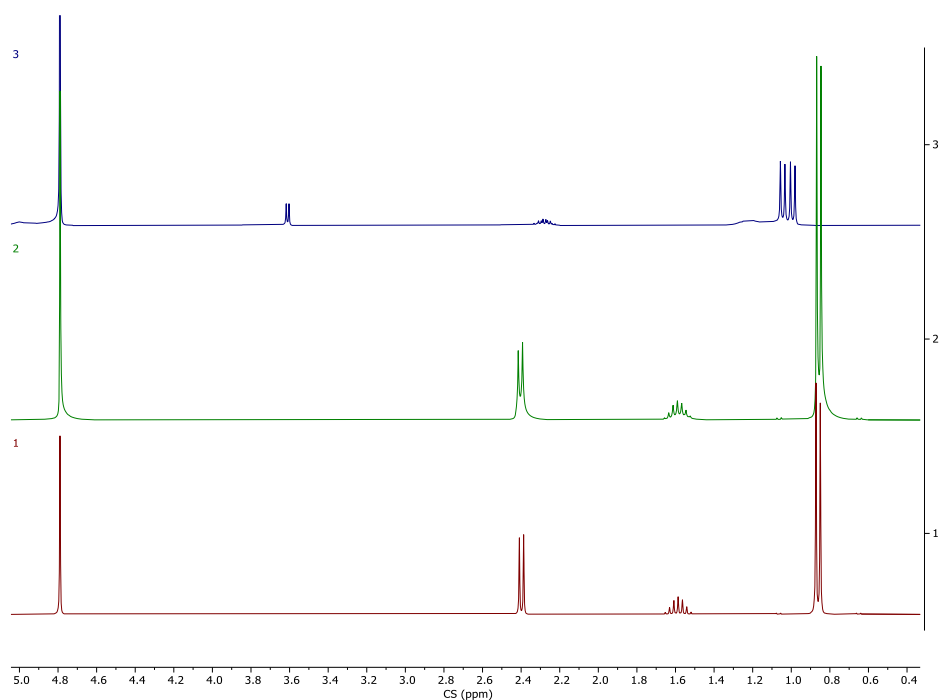


Figure A3.1: Stacked NMR spectra for L-valine and isobutylamine comparison. **(3)** L-Valine in deuterated water, serving as the substrate reference. **(2)** Standard isobutylamine spectrum in deuterated water. **(1)** Distilled isobutylamine fraction, analyzed in deuterated water to determine product purity post-distillation

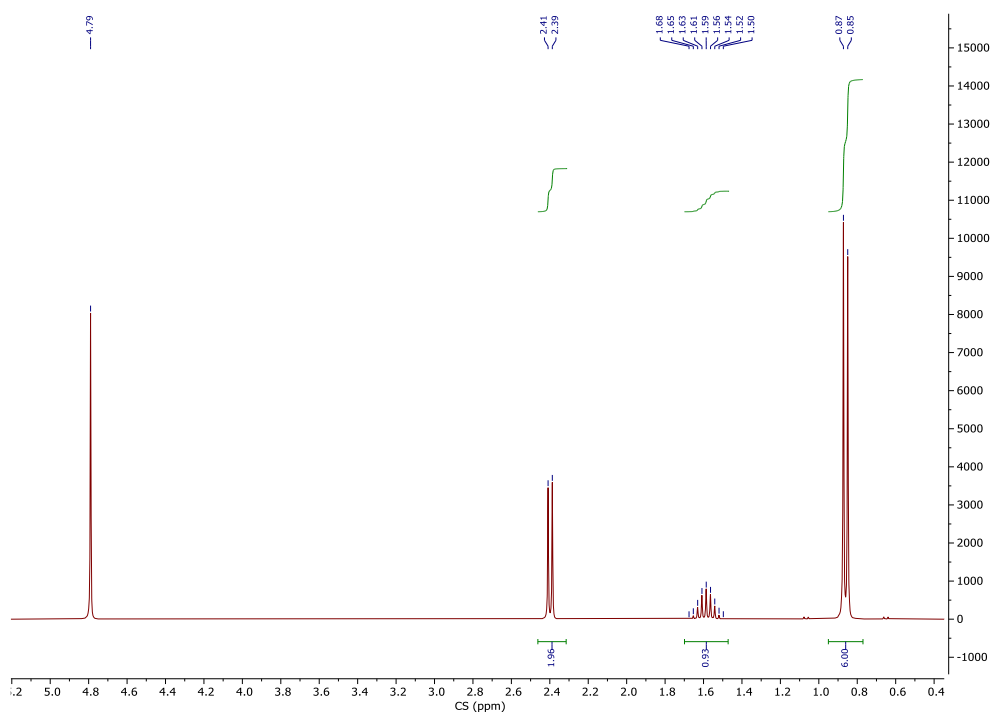


Figure A3.2: NMR spectrum for isolated isobutylamine *via* distillation.

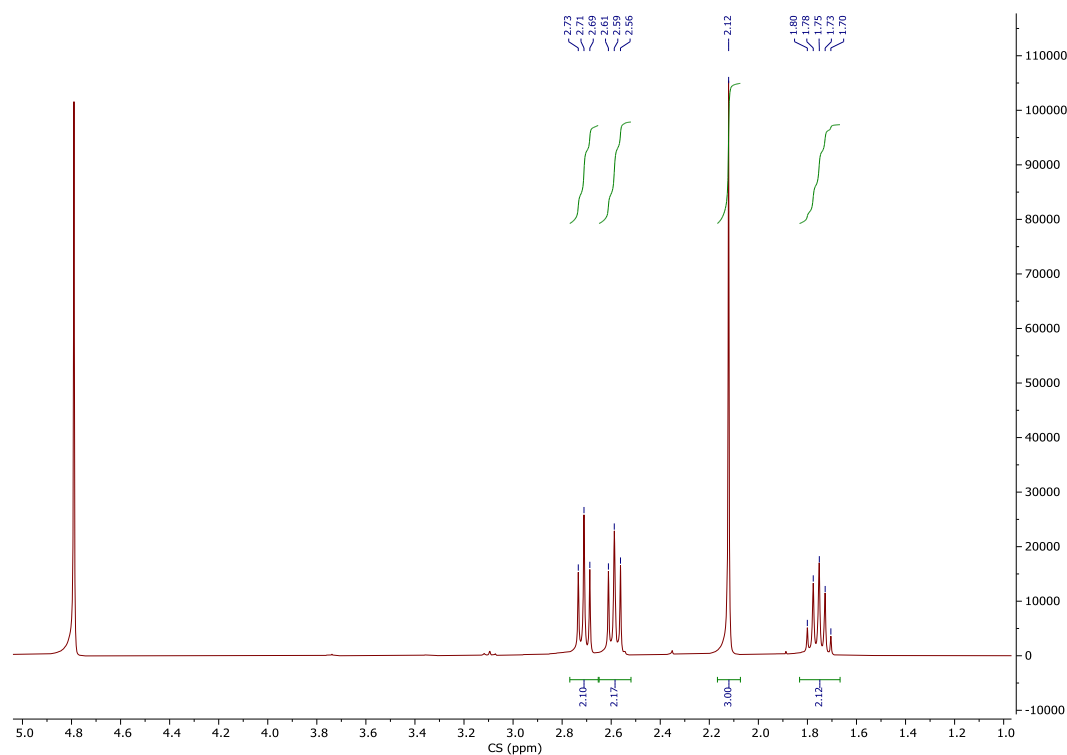


Figure A3.3: NMR spectrum for isolated 3-(methylthio)-propylamine *via* SALLE.

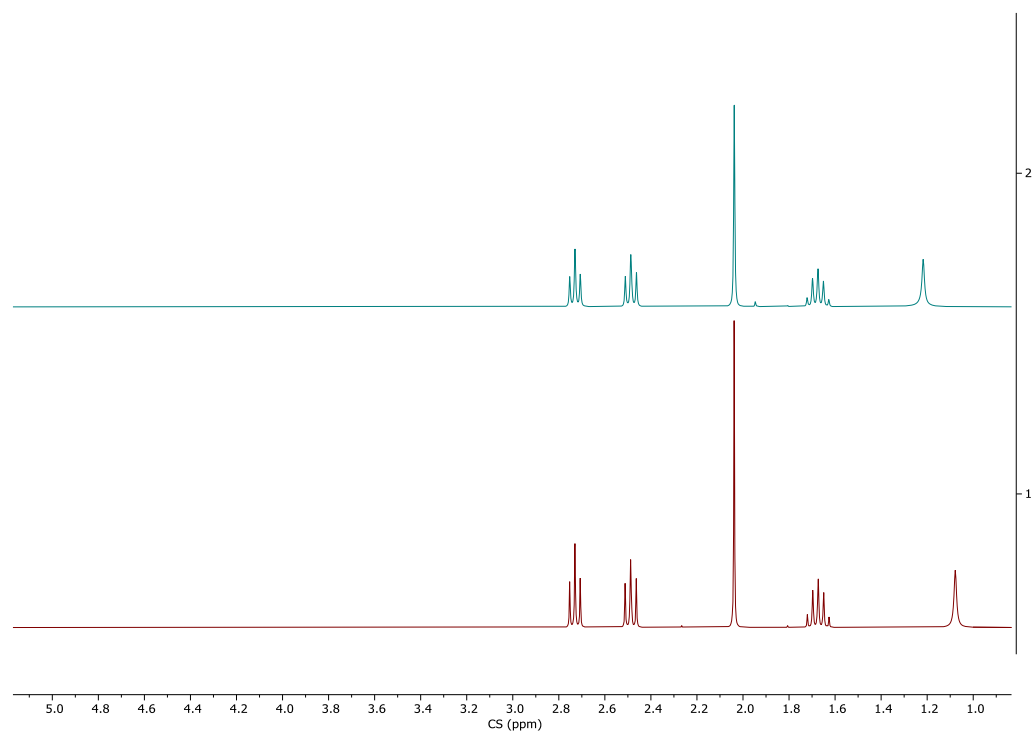


Figure A3.4: Stacked NMR spectra for the comparison of the L-methionine decarboxylation product with its standard. **(1)** L-methionine decarboxylation product, 3-(methylthio)-propylamine, in deuterated chloroform. **(2)** Standard 3-(methylthio)-propylamine spectrum in deuterated chloroform.

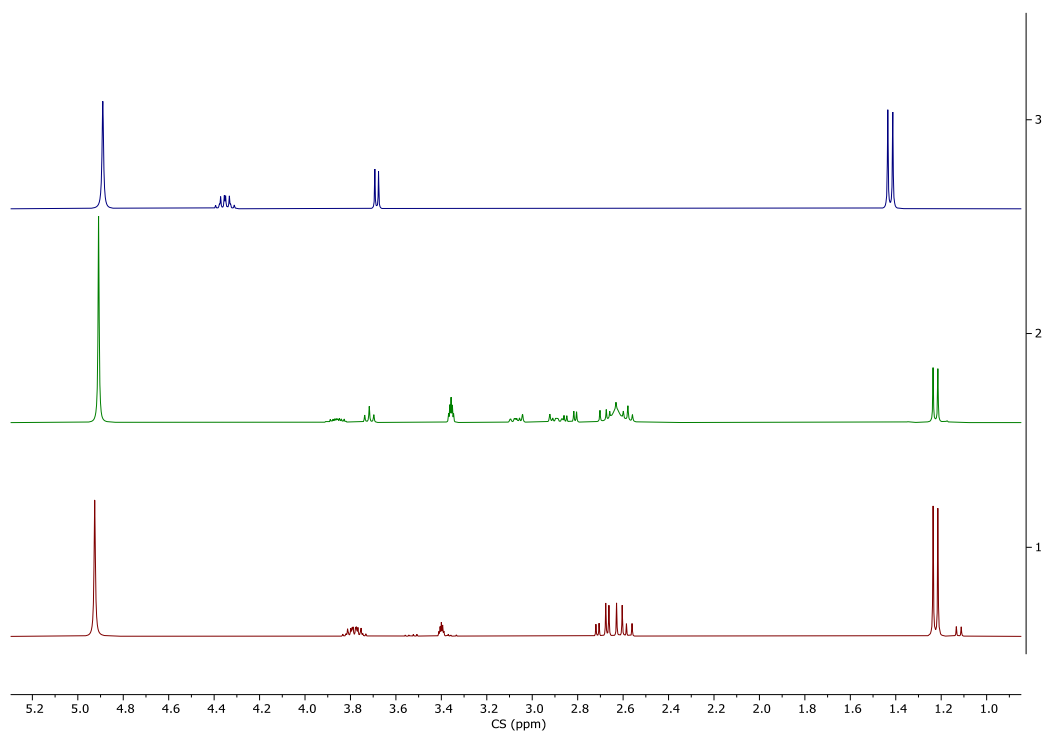


Figure A3.5: Stacked NMR spectra for the comparison of the L-threonine decarboxylation product with its standard and its starting material. **(1)** Standard of L-threonine; **(2)** 1-amino-2-propanol from trituration with DCM; **(3)** Standard of 1-amino-2-propanol.

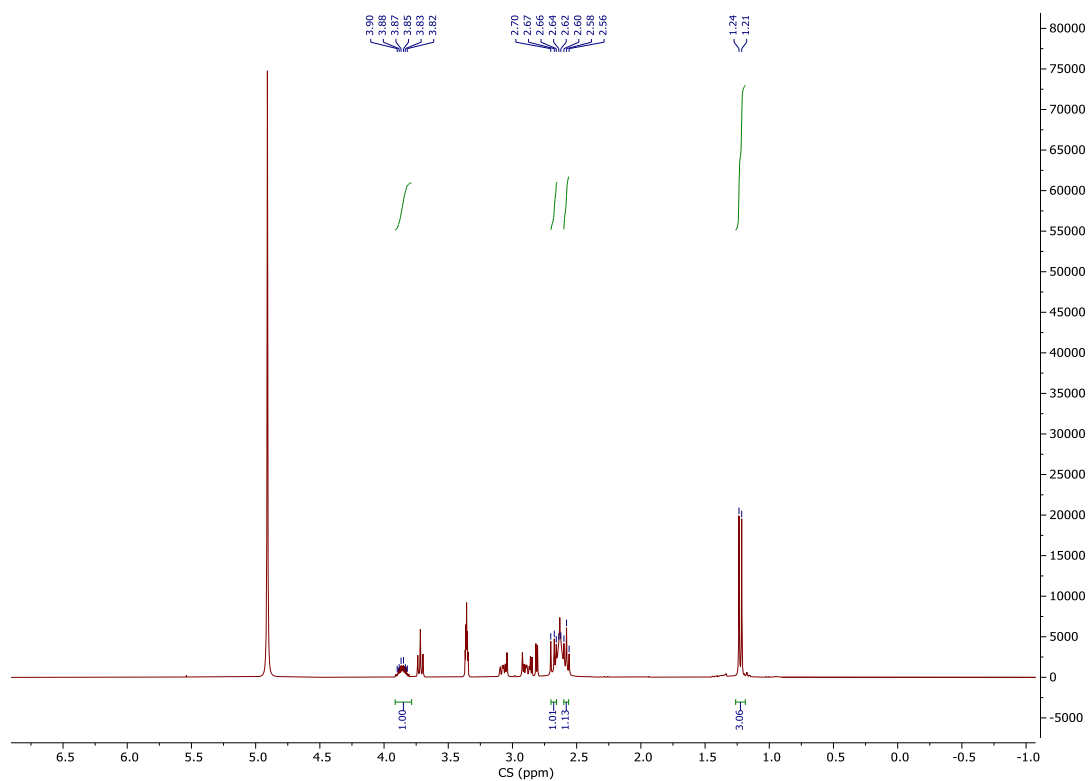


Figure A3.6: NMR spectrum for isolated 1-amino-2-propanol *via* trituration with DCM.

Acknowledgements

This thesis, marking the conclusion of my doctoral journey, and these past four years, would not have been possible without Professor Francesca Paradisi, or Fran as those of us in her group call her. I owe her my deepest gratitude for giving me the opportunity to join her team and embark on what this thesis now concludes in Bern.

I thank her for being there, having faith in me throughout this journey, and for her support during those challenging times which raised both my professional and personal growth.

It is so important for me to thank my parents. Even from my hometown, they continue to look after me. I know I can always turn to them with any doubts or challenges I face. They are my rock, and I'm deeply grateful for their unconditioned support.

I also want to thank all my colleagues who have patiently tolerated me throughout this long journey, those with whom I've been able to open and discuss with. Honestly, also without their support, I cannot imagine how different my PhD would have been, and I am grateful for having them by my side.

A loud and clear thank you goes to Lucia, who has been both a colleague and more importantly, a friend and anchor for me. But I've been truly lucky, and she was not the only one! Besides my entire group, with my fellow PhD colleagues Beatrice, Pablo, Keir, and Lauriane, I want to thank Davey for his extraordinary patience and availability. He is one of the kindest people I know; and Laura for always keeping me grounded in reality.

Thank you to Manos for remaining my desk neighbor, even when it often felt like being in the middle of an Italian theater, which surely taught you a few phrases in my language. I am also very thankful for the time we shared outside the lab with you and Iris!

I have been incredibly fortunate for all those who passed through the lab, visiting our group for short or long durations. I remember these people as I reflect on these years and I am feeling again very lucky: thank you Sofia! thank you Amalie! thank you Martina! thank you, Silvia and Federica!!! Things would not have been the same without each one of you.

Eimear, who was my housemate during the initial years of my PhD, and who has since become my colleague and friend too, deserves a big thank you. Settling down in Bern was made so much easier with her by my side. She made me feel at home and was incredibly supportive during the pandemic.

I have the feeling I am missing someone in this acknowledgment section, and if so, I apologize for it. I am genuinely grateful for all the help and support I have received here in Bern. While I have tried to express my thanks here, the depth of appreciation and the mutual support exchanged during this journey cannot be fully encapsulated in these words. In fact, the actual personal experiences and genuine connections surpassed what is captured in these words.